frontiers | Research Topics

The Philippine seas: Biodiversity and ecological impacts of natural and anthropogenic stressors in tropical reef systems,

2nd edition

Edited by
Michael Yu Roleda and Yehuda Benayahu

Published in
Frontiers in Marine Science

ISSN 1664-8714
ISBN 978-2-8325-4821-9
DOI 10.3389/978-2-8325-4821-9

About Frontiers

Frontiers is more than just an open access publisher of scholarly articles: it is a pioneering approach to the world of academia, radically improving the way scholarly research is managed. The grand vision of Frontiers is a world where all people have an equal opportunity to seek, share and generate knowledge. Frontiers provides immediate and permanent online open access to all its publications, but this alone is not enough to realize our grand goals.

Frontiers journal series

The Frontiers journal series is a multi-tier and interdisciplinary set of open-access, online journals, promising a paradigm shift from the current review, selection and dissemination processes in academic publishing. All Frontiers journals are driven by researchers for researchers; therefore, they constitute a service to the scholarly community. At the same time, the *Frontiers journal series* operates on a revolutionary invention, the tiered publishing system, initially addressing specific communities of scholars, and gradually climbing up to broader public understanding, thus serving the interests of the lay society, too.

Dedication to quality

Each Frontiers article is a landmark of the highest quality, thanks to genuinely collaborative interactions between authors and review editors, who include some of the world's best academicians. Research must be certified by peers before entering a stream of knowledge that may eventually reach the public - and shape society; therefore, Frontiers only applies the most rigorous and unbiased reviews. Frontiers revolutionizes research publishing by freely delivering the most outstanding research, evaluated with no bias from both the academic and social point of view. By applying the most advanced information technologies, Frontiers is catapulting scholarly publishing into a new generation.

What are Frontiers Research Topics?

Frontiers Research Topics are very popular trademarks of the *Frontiers journals series*: they are collections of at least ten articles, all centered on a particular subject. With their unique mix of varied contributions from Original Research to Review Articles, Frontiers Research Topics unify the most influential researchers, the latest key findings and historical advances in a hot research area.

Find out more on how to host your own Frontiers Research Topic or contribute to one as an author by contacting the Frontiers editorial office: frontiersin.org/about/contact

The Philippine seas: Biodiversity and ecological impacts of natural and anthropogenic stressors in tropical reef systems, 2nd edition

Topic editors
Michael Yu Roleda — University of the Philippines Diliman, Philippines
Yehuda Benayahu — Tel Aviv University, Israel

Citation
Roleda, M. Y., Benayahu, Y., eds. (2024). *The Philippine seas: Biodiversity and ecological impacts of natural and anthropogenic stressors in tropical reef systems, 2nd edition*. Lausanne: Frontiers Media SA. doi: 10.3389/978-2-8325-4821-9

Publisher's note: This is a 2nd edition due to an article mistakenly added to the ebook.

Table of contents

frontiers
in Marine Science

ORIGINAL RESEARCH
published: 18 August 2021
doi: 10.3389/fmars.2021.702071

Through the Boundaries: Environmental Factors Affecting Reef Benthic Cover in Marine Protected Areas in the Philippines

Fleurdeliz M. Panga[1,2]*, *Jonathan A. Anticamara*[2], *Miledel Christine C. Quibilan*[1], *Michael P. Atrigenio*[1] and *Porfirio M. Aliño*[1]

[1] *Community Ecology Laboratory, Marine Science Institute, University of the Philippines, Quezon City, Philippines,* [2] *UP Diliman Invertebrate Museum, Institute of Biology, University of the Philippines, Quezon City, Philippines*

Philippine coral reefs have been on the decline since the 1970s, and this degradation has posed a risk to biodiversity, food security, and livelihood in the country. In an effort to arrest this degradation, marine protected areas (MPAs) were established across the country. MPAs are known to improve fish biomass, but their effect on live coral cover and other benthos is not yet well documented and understood. In this study, 28 MPAs across the Philippines were surveyed comparing benthic cover and indices between protected reefs and adjacent unprotected reefs. No consistent differences were found between reefs inside and outside MPAs through all the benthic categories and reef health indices considered that are indicative of protection effects or recovery within MPAs. However, there were notable site-specific differences in benthic cover across the study MPAs-suggesting that factors other than protection play important roles in influencing benthic cover inside and outside of MPAs. Storm frequency and proximity to rivers, as a proxy for siltation, were the strongest negative correlates to live coral cover. Also, high coastal population, a proxy for pollution, and occurrence of blast and poison fishing positively correlated with high dead coral cover. The lack of significant difference in benthic cover between reefs inside and outside MPAs suggests that protection does not necessarily guarantee immediate improvement in benthic condition. Correlations between benthic condition and storm frequency, siltation, and pollution suggest that it is necessary to augment MPAs with other management strategies that will address the multiple stressors that are usually indiscriminate of MPA boundaries. Supplementing long-term and systematic monitoring of benthic cover and biodiversity inside and outside of MPAs with data on other important environmental and human impact variables will help improve understanding of benthic cover and biodiversity dynamics inside and outside of MPA boundaries.

Keywords: Philippines, marine protected areas, protection effects, health indices, coral reef benthos

Edited by:
Yehuda Benayahu,
Tel Aviv University, Israel

Reviewed by:
Susannah Leahy,
Queensland Department of Agriculture and Fisheries, Australia
Guillermo Diaz-Pulido,
Griffith University, Australia

***Correspondence:**
Fleurdeliz M. Panga
fleurpanga@gmail.com

Specialty section:
This article was submitted to Marine Ecosystem Ecology, a section of the journal Frontiers in Marine Science

Received: *29 April 2021*
Accepted: *14 July 2021*
Published: *18 August 2021*

Citation:
Panga FM, Anticamara JA, Quibilan MCC, Atrigenio MP and Aliño PM (2021) Through the Boundaries: Environmental Factors Affecting Reef Benthic Cover in Marine Protected Areas in the Philippines. Front. Mar. Sci. 8:702071. doi: 10.3389/fmars.2021.702071

INTRODUCTION

The Philippine coral reefs have been on a decline since the first national assessment in the 1970s. At that time, Gomez and Alcala (1979) found only 30% of the reefs having more than 50% coral cover. Years of overfishing, destructive fishing methods, and siltation has brought this percentage even lower, where currently only 10% of the reefs had more than 50% coral cover (Wilkinson, 2008; Licuanan et al., 2017). With the demand for fish still increasing, destructive fishing methods are still rampant, and the effects of climate change now being realized, this decline is expected to continue unless more comprehensive actions are taken (Burke et al., 2011).

The Philippines, however, cannot risk further reef decline. The country is at the apex of the Coral Triangle and its reefs support the highest concentration of marine species per unit area (Licuanan and Gomez, 2000; Carpenter and Springer, 2005; Burke et al., 2011; Sanciangco et al., 2013). The demise of habitat forming species such as corals will bring about a cascade that will result in considerable marine biodiversity loss (Jones et al., 2004; Bruno and Selig, 2007). Furthermore, at least one-third of Filipinos directly utilize reef-derived food and services (Briones et al., 2004; SCTR-Philippines, 2012; Cabral et al., 2013).

The popular management action to arrest reef decline is the establishment of marine protected areas (MPAs) (Russ et al., 2004). These are areas of managed access where fishing and other activities are regulated (Alcala, 1998). MPAs have been shown to rapidly recover fish abundance and biomass after a few years of effective implementation (Alcala, 1998; Russ et al., 2004; Abesamis and Russ, 2005; Maliao et al., 2009). However, the effect of MPAs on benthic cover is not as straightforward. The immediate positive influence of protection on coral cover is not conclusive. Coral cover was found to increase inside the MPAs in the Bahamas (Mumby et al., 2007), in the Seychelles (Wilson et al., 2012), and even in the Philippines (Magdaong et al., 2013). The massive protection efforts in the Great Barrier Reef also led to the improvement in coral cover (McCook et al., 2010). In contrast, Selig and Bruno (2010) found no increase in coral cover within MPAs, although coral cover is declining in unprotected reefs. Declines in coral cover despite protection has been reported in another global study by Selig et al. (2012), in a regional scale studies in the Caribbean (Huntington et al., 2011), the Great Barrier Reef (De'ath et al., 2012), and in specific locations in the Florida Keys (Toth et al., 2014) and Papua New Guinea (Jones et al., 2004).

In this study, 28 MPAs (inside and adjacent) were evaluated to determine the effect of protection based on benthic cover attributes and reef health indices. The relative contribution of environmental factors other than protection was explored using multivariate analyses to determine their contribution to the observed the variation in benthic cover attributes. Insights from this study, will help reevaluate the effectiveness of MPAs in terms of metrics, and reorient management options toward increasing MPA management effectiveness and actions that will accelerate recovery of degraded reefs.

The main objectives of this paper are as follows: (1) To evaluate the differences in measured benthic cover variables and indices inside and outside MPAs across 28 study sites across the Philippines, and (2) To evaluate how variations in environmental variables across the study sites correlate with benthic cover attributes and reef health indices. The insights from these analyses may help inform expectations on how we define and improve impacts management interventions such as those of MPAs.

MATERIALS AND METHODS

Study Sites

Benthic surveys were conducted inside and outside 28 MPAs across 12 provinces in the Philippines (**Figure 1**). The surveys on 15 MPAs were done from April to May 2012, while surveys on the other 13 MPAs were conducted from April to May 2014. The MPAs were all managed by their respective local government units and have different management levels at the time of survey. The ages of the MPAs at time of survey ranged from 0–21 years (mean = 8 years, median = 7 years) and core areas ranged from 9 to 453.25 ha (mean = 62.7 ha).

In each MPA, coral reef assessment was done using five replicate 50-m transects within the MPA no-take zone, and five replicate 50-m transects outside the MPA. Transects outside MPAs were at least 200 m away from the MPA boundaries. Depending on the extent of coral reef area, the actual number of transects laid within and outside MPAs were varied-, ranging from 2 to 7. But on average, the number of transects sampled is five inside and five outside MPAs. These transects were laid parallel to the shore, following the contour of the upper reef slope at depths ranging between 5 and 10 m.

Data Collection

Benthic cover was determined *via* the line intercept transect (LIT) method (English et al., 1997) on 50-m transects. The benthic categories were aggregated into five major benthic groupings (HC, live hard coral; DC/A, dead coral/with algae; AL, algae; OT, other benthic organisms; AB, abiotic components), and cover was expressed as percent cover.

The following reef health indices were calculated: Mortality Index (MI) (Gomez et al., 1994), Reef development index (DI), condition index (CI), and succession (by algae) index (SI) (Manthachitra, 1994), using the equations below. Note that the equation for the SI has been modified to take into consideration growing algae on dead coral, which are abundant in many sites:

$$MI = \frac{\%\text{ dead coral cover }(DC + DCA)}{\%\text{ hard coral cover }(HC) + \%\text{ dead coral cover}}$$

$$DI = \log\left[\frac{(HC + SC + DC + DCA + AL + OT)}{AB}\right]$$

$$CI = \log\left[\frac{HC}{(SC + DC + DCA + AL + OT)}\right]$$

$$SI(\text{by algae}) = \log\left[\frac{AL + DCA}{(SC + DC + OT)}\right]$$

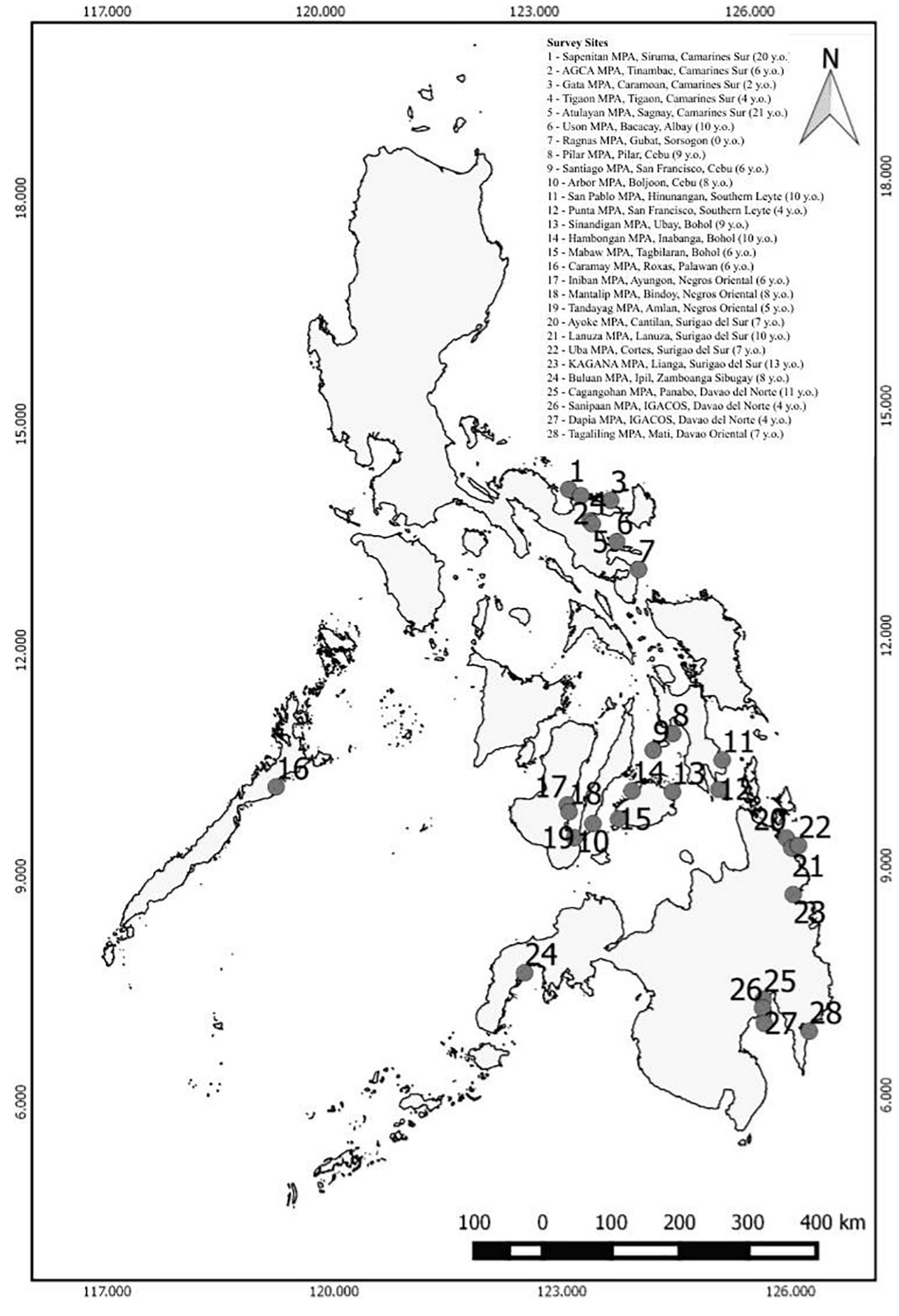

FIGURE 1 | Survey sites with MPA age at time of survey.

To explore possible drivers of variation in benthic cover and reef health indices, the following environmental data were gathered: proximity to rivers, fisher density, coastal population, occurrence of poison fishing, occurrence of blast fishing, storm frequency, and relative exposure index. Proximity to rivers was chosen as a proxy for siltation as it is assumed that terrigenous materials are conveyed to the reef through river runoff (Gomez et al., 1994). Fisher density (number of fishers per square kilometer municipal water) was chosen as a proxy for overfishing which if unmanaged can translate to degradation of the reefs (Teh et al., 2013). Coastal population was chosen as a proxy for human activities and/or pollution (Gjertsen, 2005). Occurrences of poison and blast fishing were chosen as they led to coral mortality and destruction of the reef structure (Rubec, 1986; McManus et al., 1997). Storm frequency (number of storms from 1980 to 2000) and relative exposure index (to wind, factoring in wind speed and fetch, Villanoy et al., 2013) were also used to depict natural or climate-related factors (Brown, 1997).

As some of these data were discrete, while others had categorical measurement (e.g., occurrence of poison and blast fishing were from the surveys measured as low, moderate, and high), all environmental data were categorized from 1 to 3, with 1 being the lowest score and 3 being the highest.

Data Analyses

The biotic and environmental data obtained did not satisfy the assumptions of parametric tests despite transformation, hence comparisons and correlations were conducted through non-parametric univariate and multivariate data analyses.

Non-parametric Kruskal–Wallis test was implemented to compare transects inside and outside MPAs and across all study MPAs for various benthic variables (HC, AL, DCA, OT, and AB) and the reef health indices (development, condition, mortality, and succession indices) using SPSS Statistics 21 (IBM Corp, 2012).

Multivariate analyses approach (using PERMANOVA) was implemented to determine significant differences in benthic communities inside and outside the MPA, and across the 28 MPAs (Clarke and Gorley, 2006; Anderson et al., 2008). In running the PERMANOVA, Bray-Curtis resemblance matrix (using square root-transformed five categories of raw percent cover benthic data) was applied, and then using MPA locations and MPA status (inside/outside) as factors—*P*-values generated through 9,999 permutations. Pairwise PERMANOVA was also done to compare the individual MPAs, and see if there are significant differences inside and outside each MPAs in terms of the benthic community.

In addition, multivariate matrix correlation approach (BIO-ENV/BEST) in Primer 6 (Clarke and Gorley, 2006) was used to perform a Spearman correlation between the resemblance matrices of the benthic cover or reef health indices, and the environmental resemblance matrix, to determine which environmental factor best correlated to the biotic pattern observed.

Moreover, a Principal Coordinates analysis (PCO) plot was constructed to visualize the benthic variation across MPAs. This plot was overlaid with vectors that represent the Spearman correlation between benthic cover and environmental data, where the proximity of each data point (transect) to a certain vector (benthic cover or environmental factor) represents stronger correlation between that transect to the vector.

RESULTS

No Clear Effects of Protection on Benthic Cover and Indices

We found no significant differences in benthic cover and reef health indices inside and outside the MPAs. Kruskal–Wallis tests did not show significant univariate differences in hard coral cover ($P = 0.738$), dead coral cover ($P = 0.705$), algal cover ($P = 0.217$), cover of other benthic organisms ($P = 0.828$), and abiotic components ($P = 0.845$). Likewise, no significant differences were observed inside and outside MPAs in terms of DI ($P = 0.368$), CI ($P = 0.516$), mortality index ($P = 0.639$), and succession index ($P = 0.957$).

Averaging the data (presented as mean ± SE) from the 267 transects surveyed (**Figure 2**), the live hard coral cover was at 41.9 ± 1.2% inside the MPAs and 42.7 ± 1.2% outside the MPAs. Reefs were generally dominated by massive and branching *Porites,* branching and tabular *Acropora*, and encrusting *Montipora.* The cover of dead coral was at 30.8 ± 1.1% inside the MPA and 30.3 ± 1.1% outside. Dead corals (except for a few recently killed colonies) were covered with short filamentous or matting algae. Larger fleshy macroalgae, calcifying algae (i.e., *Halimeda*), coralline algae, other turf algae, and indistinct algal assemblages collectively covered an average of 11.8 ± 1.1% of the reef bottom inside the MPA and 11.7 ± 1.0% outside. Benthic organisms other than corals and algae covered an average of 6.3 ± 0.5% both inside and outside the MPA. Abiotic components such as rock, rubble, and sand, made up 9.1 ± 0.7% and 9.0 ± 0.7% of the benthos inside and outside the MPA, respectively.

In terms of the reef health indices, we observed that the reefs were highly developed and relatively coral dominated, but with high mortality and a high proportion of algae. The average DI was within Manthachitra's "very good" category at 2.03 ± 0.20 inside

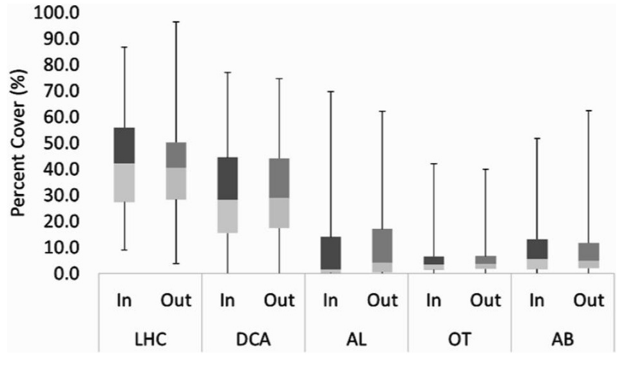

FIGURE 2 | Mean benthic cover inside and outside all MPAs surveyed.

the MPA and 1.88 ± 0.18 outside, indicating that these reefs were well developed, with the spaces in the reefs being inhabited or are habitable by benthic organisms, in contrast to poorly developed reefs which were mostly sand or silt. The average CI was within Manthachitra's "fair" category at −0.06 ± 0.04 inside the MPA and −0.70 ± 0.04 outside, implying that the reefs were fairly coral-dominated. On the other hand, the average mortality index was at 0.41 ± 0.02 inside the MPA and 0.42 ± 0.02 outside. Lastly, the average succession index was also within Manthachitra's "very good" category, at 1.22 ± 0.10 inside the MPA and 1.29 ± 0.12 outside, suggesting substantial algal cover and that algae are likely to succeed corals in dominance among other benthic organisms.

PERMANOVA results comparing sites inside and outside the MPAs also did not yield significant differences ($P = 0.4774$), suggesting that cover of the five benthic categories were generally the same regardless of protection. The interaction term for the multivariate analysis (MPA location × MPA status) was significant ($P = 0.0117$). Pairwise tests revealed that the benthic cover multivariate varied significantly in five out of the 28 sites, which may be attributed to site-specific factors.

Site-Specific Variations in Environmental Variables That Correlated With Benthic Cover and Indices

Benthic cover and reef health indices varied; however, when compared across the 28 MPA locations (**Figure 3**). Kruskal–Wallis results yielded a P-value of less than 0.001 when MPA locations were univariately compared using each of the benthic categories and reef health indices tested. PERMANOVA results across MPA locations also gave a P-value of 0.001. As mentioned earlier, the interaction term (MPA location × MPA status) was also significant.

The resemblance matrix did not present a clear and consistent pattern in terms of benthic cover. The PCO plot (**Figure 4**) showed a wide data spread with no tight, distinct groupings either for MPA location or MPA status (inside/outside). The 70% similarity clusters showed overlaps and no clear spatial geographic patterns. The two axes of the PCO plot already jointly explain 76.7% of the variation, with a third axis (not illustrated) explaining a further 16.5%.

The correlation results with the individual major benthic groups overlaid on the PCO plot showed a rough divide. Axis 1 separated the transects by algae ($r = 0.806$), while axis 2 showed gradients in dead coral ($r = 0.516$) and hard coral cover ($r = -0.929$). Most of the transects in the Pacific Seaboard (e.g., Tinambac, Gubat, Caramoan, Bacacay, Lianga, and Lanuza) were correlated with high algal cover, while the transects in internal seas (mostly in the Visayas Region) correlated with dead coral and abiotic components.

To explore if any of the environmental proxies may help explain spatial variation across MPA locations, we looked at the relationship of the resemblance matrices of benthic cover and reef health indices with that of environmental correlates identified. Bio-ENV results showed a weak yet significant correlation between the resemblance matrices of benthic cover and environmental factors ($\rho = 0.151$, $P = 0.01$). The same was also observed between the resemblance matrices of the reef health indices and the environmental factors ($\rho = 0.097$, $P = 0.01$).

Storm frequency was the strongest correlate among the environmental factors (**Figure 5**), followed by the combination of storm frequency and proximity to rivers. These two factors correlated more with transects in the Pacific Seaboard, which were also the sites with high algal cover. On the other hand, transects in the internal seas were less correlated with these two factors, but instead were more affected by anthropogenic factors such as high coastal population (which is a proxy for pollution and human activity), and high occurrences of blast and poison fishing. These were also the sites correlated with higher dead coral cover, which was rather intuitive, since these anthropogenic factors were often implicated in coral mortality.

DISCUSSION

The Status of Benthos and the Lack of Clear Protection Effects on Benthic Cover Across the MPA Study Sites

The average hard coral cover reported in this study is significantly higher (more than 40%) compared to what has been previously reported as national average (Magdaong et al., 2013; Licuanan et al., 2019). It is easy to assume that reefs are in better condition now, although care should be taken in saying this increase was a direct effect of conservation and management efforts. The transects surveyed here were within or adjacent to MPAs, in contrast to previous studies that were not as selective. More often, the reefs with good coral cover are chosen for protection as they fit the criteria recommended for MPA establishment (Roberts, 2000; Roberts et al., 2003), hence it is likely that we are averaging hard coral cover values from the best parts of the reefs in the surveyed areas. This may also explain why previous meta-analyses on the Philippine reefs were able to detect significantly higher coral cover inside MPAs than in reefs that were not protected (Magdaong et al., 2013). The non-protected areas surveyed here are adjacent to MPAs and may still have benefited from local management efforts (such as reduced destructive fishing methods), in contrast to areas that may not have any degree of management at all.

The average c oral mortality index is also higher in this study than previously reported. Despite transects in this study being within or adjacent to MPAs, the average mortality index was at 0.4 ± 0.01, while the national coral mortality index in 1994 was at 0.2 ± 0.03 (Gomez et al., 1994). Gomez et al. (1994) also indicated that the primary cause of coral mortality was siltation. Other causes of mortality include overfishing and destructive fishing methods (Burke et al., 2011; Magdaong et al., 2013). In many sites we surveyed, illegal and destructive fishing activities were still rampant (Muallil et al., 2014), and siltation was observed in varying degrees. Many of the reefs were also highly exposed to storms and waves, and without proper planning, these reefs are vulnerable, especially to the exacerbating effects of climate change. In fact, in 2010, a mass bleaching event occurred through many of the reefs in the Philippines (Philippine

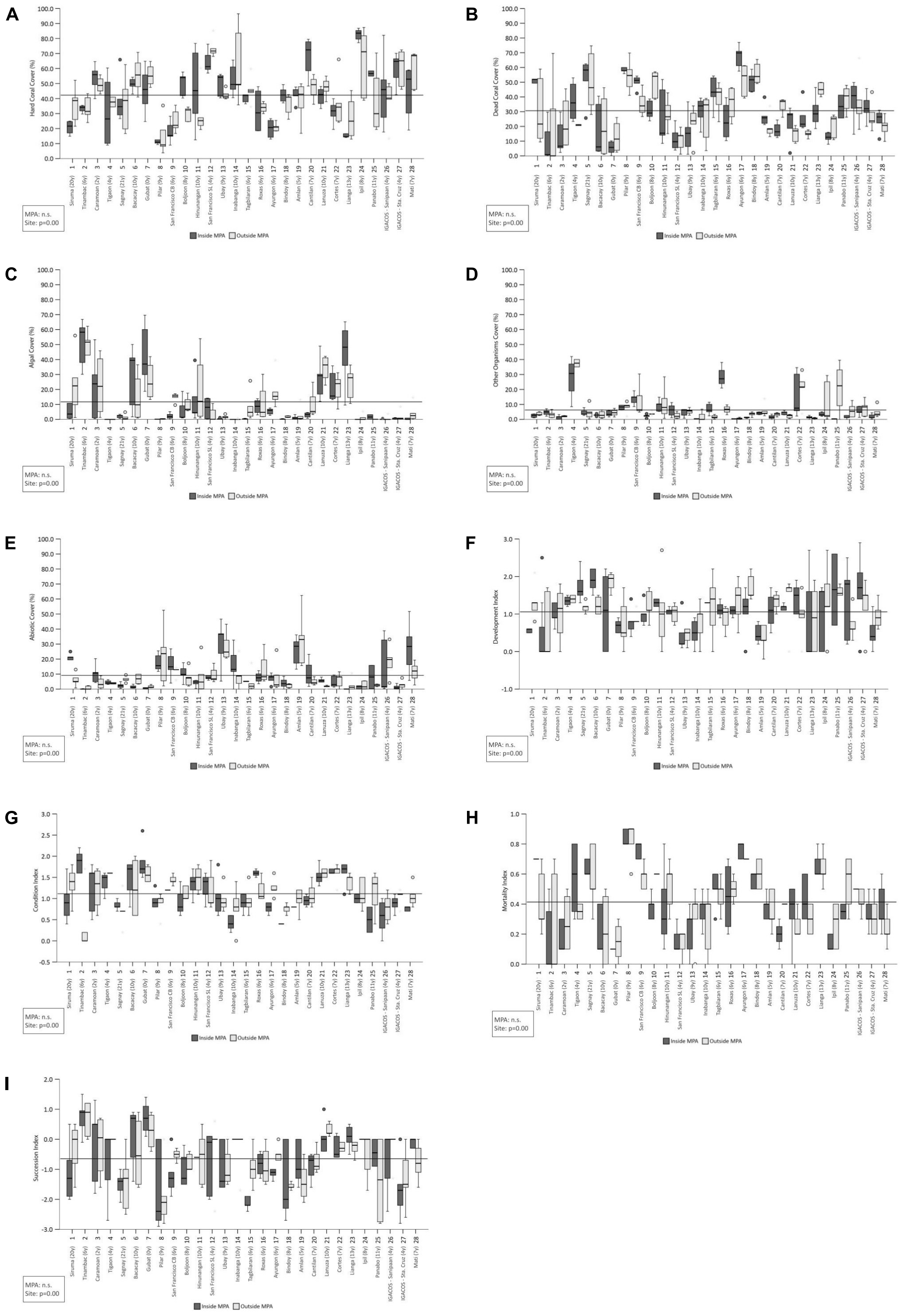

FIGURE 3 | Variation of benthic condition across MPA locations in terms of **(A)** hard coral cover, **(B)** dead coral cover, **(C)** algal cover, **(D)** cover of other benthic organisms, **(E)** abiotic cover, **(F)** development index, **(G)** condition index, **(H)** mortality index, and **(I)** succession by algae index.

Coral Bleach Watch, unpublished), and though we have not looked into the bleaching history of each of the 28 MPAs, this event would have contributed to coral mortality in the reefs. It is, however, important to note that reef decline is a process (Bellwood et al., 2004). The extent of coral mortality is but a snapshot that indicates how much we have already lost, but a

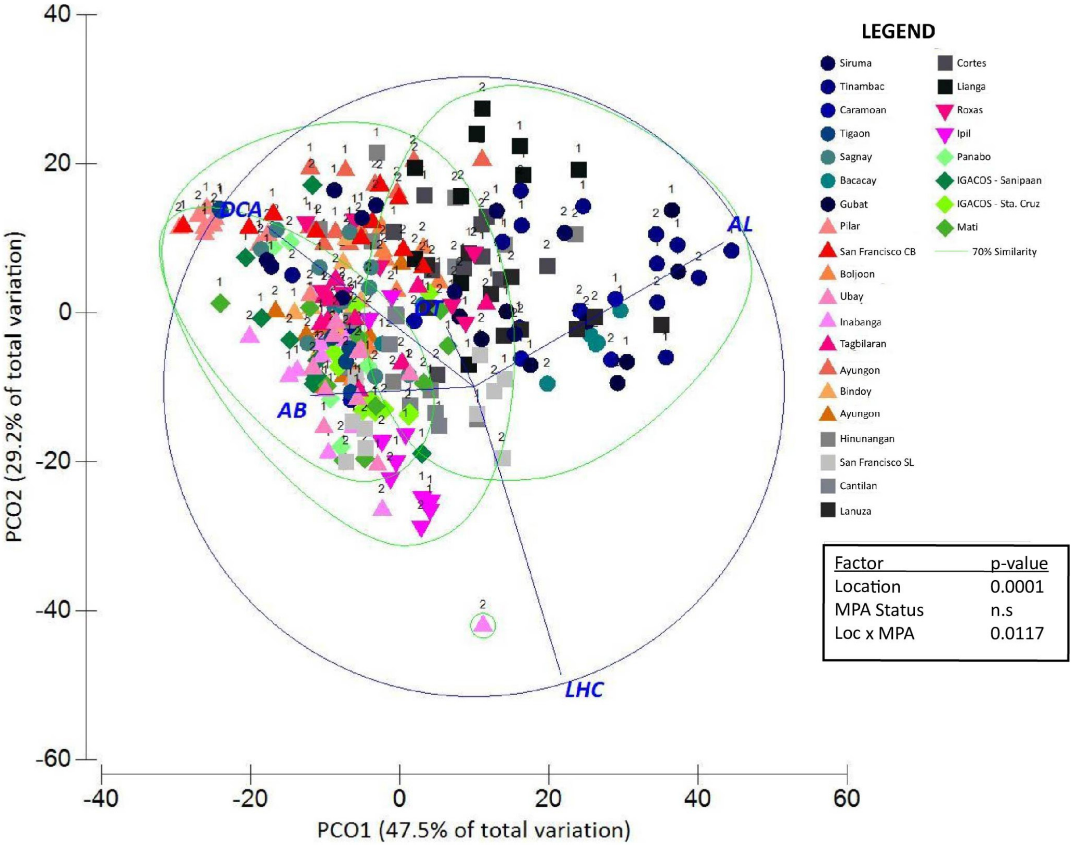

Factor	p-value
Location	0.0001
MPA Status	n.s
Loc x MPA	0.0117

FIGURE 4 | PCO Plot showing the distances between the locations according to differences in the multivariate benthic cover, with vectors depicting Spearman correlation with the different benthic groups. 1, inside MPA; 2, outside MPA.

long-term closely-monitored study will be necessary to establish causal relationships.

The Site-Specific Variations in Environmental Variables That Correlated With Benthos Cover, and Their Implications

A commentary by Knowlton (2021a) on a paper by Donovan et al. (2021) on the ability of sea urchin and macroalgae abundance to amplify the impact of bleaching in corals, suggest and infer that local management can play an important role in mitigating climate impacts. Knowlton's position, also related to her recent paper (Knowlton, 2021b), argues for optimism in marine conservation, despite the larger problems that the marine environment is facing—from large scale overfishing to climate change impacts. This is a call to change the narrative of gloom and doom in ocean conservation, similar to other offerings of hope for the ocean by 2050 if right actions are made (Duarte et al., 2020), as supported by increasing trends in numbers of established MPAs, and emerging efforts on coral restoration.

To date, however, the actual effects of MPAs on benthic and coral cover appear mixed and paradoxical (Howarth et al., 2015; Bates et al., 2019), and more often show coral reef benthos being greatly and negatively impacted by disturbances such as bleaching due to ocean warming (Huntington et al., 2011; Toth et al., 2014), reduced water quality—turbidity, siltation, nutrient loading, and pollution (Wenger et al., 2015), prior degradation before protection, and a lack of enforcement in many MPAs. In contrast, a global analysis of coral cover inside and outside MPAs (Selig and Bruno, 2010) showed that from 1969 to 2006, surveyed coral reefs showed more stable coral cover inside MPAs compared to declining coral cover in fished grounds, suggesting that in the long term, the MPAs may offer more benefits to coral reefs than no protection at all. Given these mixed results and a growing body of literature showing empirically that many benthic communities and corals failed to recover inside MPAs due to local stressors and larger disturbances ongoing despite the removal of fishing (Jones et al., 2004; Coelho and Manfrino, 2007; Carassou et al., 2013; Anderson et al., 2014; McClure et al., 2020), there is, indeed, a need to tease apart hierarchical or interacting effects of these multiple disturbances as well as management efforts inside and outside the MPAs, to understand ways to improve benthic and coral recovery.

The results of our study showed that, like majority of papers, coral reefs in the Philippines are not showing clear trends of recovery inside MPAs, but instead are somewhat related to the degrees of other disturbances such as siltation, possible nutrient

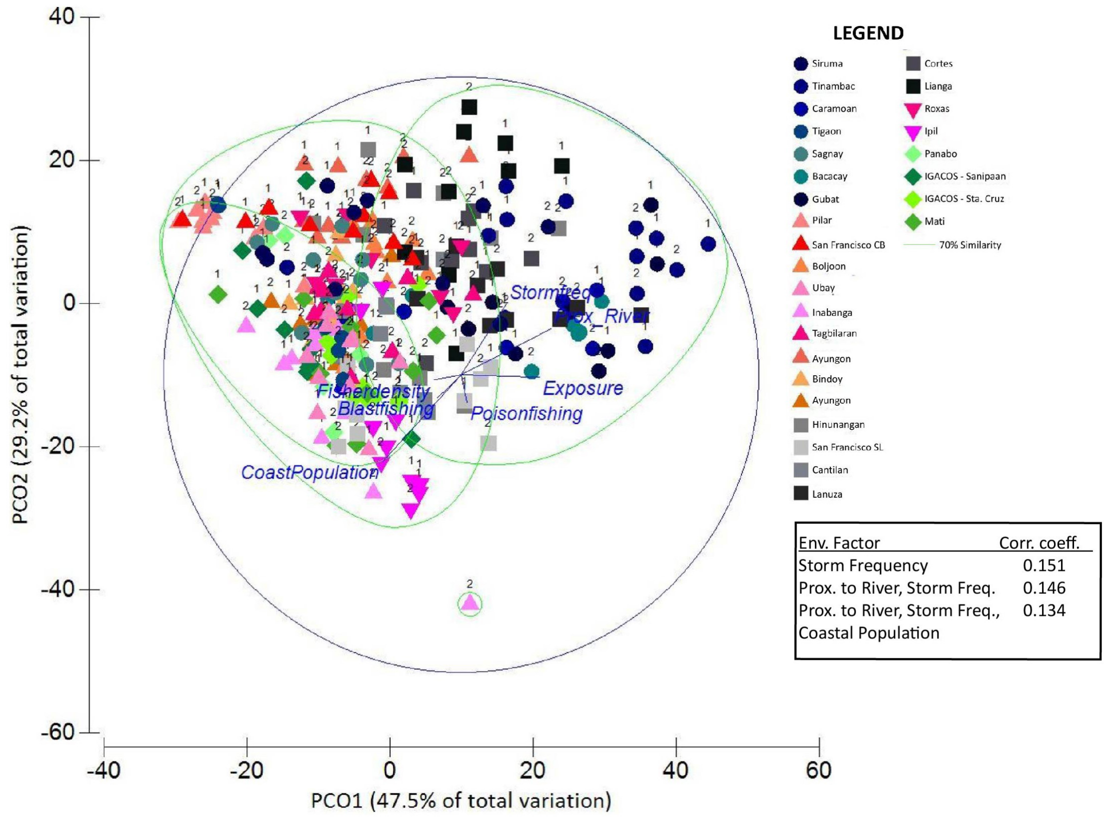

Env. Factor	Corr. coeff.
Storm Frequency	0.151
Prox. to River, Storm Freq.	0.146
Prox. to River, Storm Freq., Coastal Population	0.134

FIGURE 5 | PCO Plot showing the distances between the locations according to differences in the multivariate benthic cover, with vectors depicting Spearman correlation with the environmental factors. 1, inside MPA; 2, outside MPA.

loading, and impacts of storms that are causing coral degradation inside the MPA boundaries. Corals are slow-growing, sessile reef-building organisms, and as such, their growth and recovery rates could easily be overwhelmed and affected by stressors acting at a prolonged scale (Hughes and Connell, 1999; Carilli et al., 2009). What MPAs can directly do for corals is to prevent damage by excluding human activities such as trampling, anchoring, and fishing (Selig and Bruno, 2010). MPAs can also bring about a top-down trophic cascade, where protection will lead to an increase in abundance and biomass of fish, which in turn will help regulate algal growth, prevent outbreaks of coral predators, and lower prevalence of coral disease (Stockwell et al., 2000; Hughes et al., 2007; Mumby et al., 2007; Sweatman, 2008; Raymundo et al., 2009). However, the top-down effect of MPAs on coral communities is indirect and sometimes the mechanisms are not well established. The reduction of predator crown-of-thorns starfish, for example, has been greatly implicated in the improvement of coral cover in the protected Great Barrier Reef, although how protection actually reduces starfish outbreaks is still unclear (McCook et al., 2010). Furthermore, the stressors that drive coral decline such as frequent damage from storms, chronic siltation, and coral bleaching cannot be excluded by the boundaries of MPAs, hence these will continue to negatively affect the reefs unless they are addressed (Selig et al., 2012; Eakin et al., 2019).

In fact, half of the MPAs in this survey were about 5–10 years old, with two MPAs at least 20 years old, and still no consistent differences in benthic cover inside and outside the MPAs were observed. In some MPA locations, coral cover is high both inside and outside, suggesting that management efforts (such as constant patrolling) may be benefiting non-protected reefs as well. However, some of the MPA locations still suffer from poor water quality, pollution, and destructive fishing methods, problems that need other interventions such as water quality management, waste management, and fishery law enforcement, before coral conditions (regardless of protection) are expected to improve. Indeed, MPAs are not a "silver bullet" that can rapidly bring about an observable increase in coral cover and a decrease in algal cover (Gilby et al., 2015). The reef benthos will not be able to recover as rapidly so long as the threats that limit them in the first place are not eliminated (Burke et al., 2011). In addition, acute environmental disturbances can devastate reefs regardless of protection. The Apo Island No-Take Marine Reserve, for example, was not spared from back-to-back typhoons from 2010 to 2012, where coral cover dropped to ∼1%, a significant reduction compared to the more sheltered fished reefs outside the reserve (Russ et al., 2021).

MPAs as an approach addresses stressors at a single scale, while the different environmental factors such as those correlated in this study occur at different scales. The apparent spatial variation across MPA locations, despite the lack of significant difference in the MPA level (inside and outside) suggest that factors driving variation are in scales large enough to surpass the functional size of the MPA and thus affect the benthic communities protected and unprotected alike (Selig et al., 2012).

It is, indeed, important to match the scale of the intervention to the stressor. The Great Barrier Reef, for example, for the length of time it has been protected, the considerable management efforts, and the massiveness of the functional size of the protected area (especially when compared to locally-managed MPAs), have not been immune degradation, and what is being looked at as the "best bet" is really to manage the local stressors and to help improve local management in the face of large-scale disturbances that reefs and marine environment are experiencing beyond the impacts and removal of fishing (in the case of MPAs) (Knowlton, 2012).

This, however, does not reduce the need for MPAs for managing and conserving the reefs as they still function and provide valuable ecosystem goods and services (as safe refuge for fishes from fishing). The strong implementation of MPAs has been proven to be effective in improving fish abundance and biomass (Alcala, 1998; Maliao et al., 2009) important for food and livelihood security. Russ et al. (2004) have even shown a threefold increase in the biomass of commercially important fish inside the Apo Reef Marine Reserve. Even if the effects of MPAs on reef benthic communities are rather indirect, the establishment of MPAs is a good entry point in coastal resource management (Christie et al., 2002). The process of setting up and maintaining MPAs will guide the local management through the different considerations in conservation, such as the presence of local stressors, and threats to sustainability of management efforts (Roberts, 2000; Maypa et al., 2012). In this regard, MPAs can be considered as "canaries in the coal mine" (Tabor and Aguirre, 2004), where their deterioration despite strong protection will signal a need to reevaluate the MPA design, objectives or management strategies. Furthermore, excluding fishing can also assist coral reef recovery after disturbances such as coral bleaching (Wilson et al., 2012).

As most of the stressors that drive reef benthic variation occur in larger scales than the MPAs, there is need to augment MPAs with other management approaches that can address the stressors in their respective scales to "cover all bases" and provide a more holistic protection of the reefs (Agardy et al., 2011). This prevents stressors from overwhelming the benefits of protection (e.g., trophic cascades) and render the efforts in improving the reef benthic community in the MPAs futile (Huntington et al., 2011; Selig et al., 2012; Anderson et al., 2014). For example, MPAs that are often damaged because they are along the pathway of storms or other disturbances may be repositioned to more sheltered locations (Roberts et al., 2003) and need to be replicated in other areas for redundancy. MPAs that are degraded by heavy siltation from rivers may be moved farther from the river mouth, and activities upland such as agriculture are to be strictly managed to prevent terrigenous sedimentation from smothering the reefs (Gomez et al., 1994; Kroon et al., 2016; van Grieken et al., 2019). Regulations in areas overwhelmed by algae may be adjusted to control fishing of herbivores and reduce nutrient loading (Carassou et al., 2013). Indeed, the establishment and maintenance of MPAs should always be accompanied by adaptive measures to eliminate anthropogenic threats and keep the MPAs out of harm's way (Roberts et al., 2003). These will ensure that the benthic communities are productive and resilient despite climate-related threats (Burke et al., 2011; Selig et al., 2012). Furthermore, networking of MPAs may be considered to provide ample representativeness, replication, and redundancy (Roberts et al., 2001; Eisma-Osorio et al., 2009) and evaluated as to their functions and multiple objectives.

We think that there is still a need to expand current analyses of the impacts of MPAs on sessile and benthic organisms, and explore the ongoing ecological processes inside and outside of MPA boundaries. While comparing biotic communities inside and outside the MPAs are necessary to monitor MPA health and effectiveness, this may be too simplistic, and should be analyzed within the frame of its environment and present stressors to provide clearer conditions, and management intervention needs. It may be interesting to also consider the morphology of the corals and algae, structural complexity, coral recruitment, and metrics other than benthic cover to gain more insights on reef condition. Consistent reef monitoring and analysis of trends will help investigate the effects of protection in decreasing coral loss (if not necessarily coral cover improvement), similar to what Selig and Bruno (2010) has found in their global analyses. These types of studies can further be aligned to the objectives of the MPAs to have a better handle of success (Edinger and Risk, 2000; Strain et al., 2019). Furthermore, an improved understanding of ecological interactions can also improve local management efforts in dealing with disturbances other than fishing. These in-depth analyses and management considerations will hopefully enhance local efforts and bring promising results, and contribute to the ocean conservation optimism that Knowlton and Duarte are proposing in the face of large-scale and long-term degradation and threats to marine biodiversity in the anthropocene.

DATA AVAILABILITY STATEMENT

The raw data supporting the conclusions of this article will be made available by the authors, without undue reservation.

AUTHOR CONTRIBUTIONS

FP collected and analyzed the data, discussed the results, and wrote the manuscript with support from all authors. JA contributed in data analysis and manuscript writing and revision. MQ contributed in data analysis, results discussion, and the manuscript revision. MA contributed in study design, data collection, results discussion, and the manuscript revision. PA contributed in study design, data analysis, and results discussion. All authors contributed to the article and approved the submitted version.

FUNDING

This study was made possible through funding from RARE Philippines and USAID, in collaboration with the Marine Environment and Resources Foundation (MERF).

ACKNOWLEDGMENTS

We would like to thank RARE Philippines and USAID, in collaboration with the Marine Environment and Resources Foundation (MERF), for research funding, coordination, and support in the execution of this research. We would also like to thank the RARE Conservation Fellows and Local Government Units for logistical support and coordination on all of the MPAs studied. We would also like to thank the Fisheries team of the MSI Community Laboratory for the municipal profile data, and the MSI Physical Oceanography Laboratory for the storm frequency and relative exposure index used in the environmental correlation. We would also like to thank the rest of the MERF-RARE Team/MSI Community Ecology Laboratory who joined and supported the many months of data gathering, encoding, and data analysis.

SUPPLEMENTARY MATERIAL

The Supplementary Material for this article can be found online at: https://www.frontiersin.org/articles/10.3389/fmars.2021.702071/full#supplementary-material

REFERENCES

Abesamis, R. A., and Russ, G. R. (2005). Density-dependent spillover from a marine reserve: long-term evidence. *Ecol. Appl.* 15, 1798–1812. doi: 10.1890/05-0174

Agardy, T., di Sciara, G. N., and Christie, P. (2011). Mind the gap: addressing the shortcomings of marine protected areas through large scale marine spatial planning. *Mar. Policy* 35, 226–232. doi: 10.1016/j.marpol.2010.10.006

Alcala, A. C. (1998). Community-based coastal resource management in the Philippines: a case study. *Ocean Coast. Manag.* 38, 179–186. doi: 10.1016/s0964-5691(97)00072-0

Anderson, M. J., Gorley, R. N., and Clarke, K. R. (2008). *PERMANOVA + for PRIMER: Guide to Software and Statistical Methods*. Plymouth: PRIMER-E Ltd.

Anderson, R., Morrall, C., Jossart, J., Nimrod, S., Bolda, E., Musser, K., et al. (2014). Marine protected area monitoring in the nearshore waters of Grenada, Eastern Caribbean: benthic cover and fish populations. *Int. J. Trop. Biol.* 62, 273–286.

Bates, A. E., Cook, R. S. C., Duncan, M. I., Edgar, G. J., Bruno, J. F., Benedetti-Cecchi, L., et al. (2019). Climate resilience in marine protected areas and the 'Protection Paradox'. *Biol. Conserv.* 236, 305–314.

Bellwood, D. R., Hughes, T. P., Folke, C., and Nystrom, M. (2004). Confronting the coral reef crisis. *Nature* 492, 827–833. doi: 10.1038/nature02691

Briones, M., Dey, M. M., and Ahmed, M. (2004). The future for fish in the food and livelihoods of the poor in Asia. *NAGA WorldFish Center Quarterly* 27(3–4), 48–50.

Brown, B. E. (1997). "Disturbances to reefs in recent times," in *Life and Death of Coral Reefs*, ed. C. Birkeland (New York, NY: Chapman and Hall), 354–378. doi: 10.1007/978-1-4615-5995-5_15

Bruno, J. F., and Selig, E. R. (2007). Regional decline of coral cover in the Indo-Pacific: timing, extent, and subregional comparisons. *PLoS One* 2:e711. doi: 10.1371/journal.pone.0000711

Burke, L., Reytar, K., Spalding, M., and Perry, A. (2011). *Reefs at Risk Revisited*. Washington, DC: World Resources Institute.

Cabral, R., Cruz-Trinidad, A., Geronimo, R., Napitupulu, L., Lokani, P., Boso, D., et al. (2013). Crisis sentinel indicators: averting a potential meltdown in the Coral Triangle. *Mar. Policy* 39, 241–247. doi: 10.1016/j.marpol.2012.10.012

Carassou, L., Leopold, M., Guillemot, N., Wantiez, L., and Kulbicki, M. (2013). Does herbivorous fish protection really improve coral reef resilience? A case study from New Caledonia. *PLoS One* 8:e60564. doi: 10.1371/journal.pone.0060564

Carilli, J. E., Norris, R. D., Black, B. A., Walsh, S. M., and McField, M. (2009). Local stressors reduce coral resilience to bleaching. *PLoS One* 4:e6324. doi: 10.1371/journal.pone.0006324

Carpenter, K. E., and Springer, V. G. (2005). The center of the center of marine shore fish biodiversity: the Philippine Islands. *Environ. Biol. Fish.* 72, 467–480. doi: 10.1007/s10641-004-3154-4

Christie, P., White, A., and Deguit, E. (2002). Starting point or solution? Community-based marine protected areas in the Philippines. *J. Environ. Manage.* 66, 441–451. doi: 10.1006/jema.2002.0595

Clarke, K. R., and Gorley, R. N. (2006). *PRIMER v6: User Manual/Tutorial*. Plymouth: PRIMER-E.

Coelho, V. R., and Manfrino, C. (2007). Coral community decline at a remote Carribean island: marine no-take reserves are not enough. *Aquat. Conserv.* 17, 666–685. doi: 10.1002/aqc.822

De'ath, G., Fabricius, K. E., Sweatman, H., and Puotinen, M. (2012). The 27-year decline of coral cover on the Great Barrier Reef and its causes. *Proc. Natl. Acad. Sci. U. S. A.* 109, 17995–17999. doi: 10.1073/pnas.1208909109

Donovan, M. K., Burkepile, D. E., Kratochwill, C., Shesinger, T., Sully, S., Oliver, T. A., et al. (2021). Local conditions magnify coral loss after marine heatwaves. *Science* 72, 977–980. doi: 10.1126/science.abd9464

Duarte, C. M., Agusti, S., Barbier, E., Britten, G. L., Castilla, J. C., Gattusso, J., et al. (2020). Rebuilding marine life. *Nature* 280, 39–51.

Eakin, C. M., Sweatman, H. P. A., and Brainard, R. E. (2019). The 2014–2017 global-scale coral bleaching event: insights and impacts. *Coral Reefs* 38, 539–545. doi: 10.1007/s00338-019-01844-2

Edinger, E. N., and Risk, M. J. (2000). Reef classification by coral morphology predicts coral reef conservation value. *Biol. Conserv.* 92, 1–13. doi: 10.1016/s0006-3207(99)00067-1

Eisma-Osorio, R.-L., Amolo, R. C., Maypa, A. P., White, A. T., and Christie, P. (2009). Scaling up local government initiatives toward ecosystem-based fisheries management in Southeast Cebu Island, Philippines. *Coast. Manag.* 37, 291–207. doi: 10.1080/08920750902851237

English, S., Wilkinson, C., and Baker, V. (1997). *Survey Manual for Tropical Marine Resources*. Townsville, QLD: Australian Institute of Marine Science.

Gilby, B. L., Maxwell, P. S., Tibbetts, I. R., and Stevens, T. (2015). Bottom-up factors for algal productivity outweigh no-fishing marine protected area effects in a marginal coral reef system. *Ecosystems* 18, 1056–1069. doi: 10.1007/s10021-015-9883-8

Gjertsen, H. (2005). Can habitat protection lead to improvements in human well-being? Evidence from marine protected areas in the Philippines. *World Dev.* 33, 199–217. doi: 10.1016/j.worlddev.2004.07.009

Gomez, E. D., and Alcala, A. C. (1979). "Status of Philippine Coral Reefs – 1978," in *Proceedings of the International Symposium on Marine Biogeography and Evolution in the Southern Hemisphere*, Auckland, 663–669.

Gomez, E. D., Aliño, P. M., Yap, H. T., and Licuanan, W. Y. (1994). A review of the status of Philippine Reefs. *Mar. Pollut. Bull.* 29, 62–68. doi: 10.1016/0025-326x(94)90427-8

Howarth, L. M., Pickup, S. E., Evans, L. E., Cross, T. J., Hawkins, J. P., Roberts, C. M., et al. (2015). Sessile and mobile components of a benthic ecosystem display mixed trends within a temperate marine reserve. *Mar. Environ. Res.* 107:8e23.

Hughes, T. P., and Connell, J. H. (1999). Multiple stressors on coral reefs: a long-term perspective. *Limnol. Oceanogr.* 44, 932–940. doi: 10.4319/lo.1999.44.3_part_2.0932

Hughes, T. P., Rodrigues, M. J., Bellwood, D. R., Ceccarelli, D., Hoegh-Guldberg, O., McCook, L., et al. (2007). Phase shifts, herbivory, and the resilience of coral reefs to climate change. *Curr. Biol.* 17, 360–365. doi: 10.1016/j.cub.2006.12.049

Huntington, B. E., Karnauskas, M., and Lirman, D. (2011). Corals fail to recover at a Caribbean marine reserve despite ten years of reserve designation. *Coral Reefs* 30, 1077–1085. doi: 10.1007/s00338-011-0809-4

IBM Corp (2012). *IBM SPSS Statistics for Windows, Version 21.0*. Armonk, NY: IBM Corp.

Jones, G. P., McCormick, M. I., Srinivasan, M., and Eagle, J. V. (2004). Coral decline threatens fish biodiversity in marine reserves. *Proc. Natl. Acad. Sci. U. S. A.* 101, 8251–8253. doi: 10.1073/pnas.0401277101

Knowlton, N. (2012). Iconic coral reef degraded despite substantial protection. *Proc. Natl. Acad. Sci. U. S. A.* 109, 17734–17735. doi: 10.1073/pnas.1215836109

Knowlton, N. (2021a). Local management matters for coral reefs. *Science* 372, 908–909. doi: 10.1126/science.abi7286

Knowlton, N. (2021b). Ocean optimism: moving beyond the obituaries in marine conservation. *Annu. Rev. Mar. Sci.* 13, 479–499. doi: 10.1146/annurev-marine-040220-101608

Kroon, F. J., Thorburn, P., Schaffelke, B., and Whitten, S. (2016). Towards protecting the Great Barrier Reef from land-based pollution. *Glob. Change Biol.* 22, 1985–2002. doi: 10.1111/gcb.13262

Licuanan, A. M., Reyes, M. Z., Luzon, K. S., Chan, M. A., and Licuanan, W. Y. (2017). Initial findings of the nationwide assessment of Philippine coral reefs. *Philipp. J. Sci.* 146, 177–185.

Licuanan, W. Y., and Gomez, E. D. (2000). *Philippine Coral Reefs, Reef Fishes, and associated Fisheries: Status and Recommendations to Improve Their Management*. Gland: Global Coral Reef Monitoring Network (GCRMN).

Licuanan, W. Y., Robles, R., and Reyes, M. (2019). Status and recent trends in coral reefs of the Philippines. *Mari. Pollut. Bull.* 142, 544–550. doi: 10.1016/j.marpolbul.2019.04.013

Magdaong, E. T., Fujii, M., Yamano, H., Licuanan, W. Y., Maypa, A., Campos, W. L., et al. (2013). Long-term change in coral cover and the effectiveness of marine protected areas in the Philippines: a meta-analysis. *Hydrobiologia* 733, 5–17. doi: 10.1007/s10750-013-1720-5

Maliao, R. J., White, A. T., Maypa, A. P., and Turingan, R. G. (2009). Trajectories and magnitude of change in coral reef fish populations in Philippine marine reserves: a meta-analysis. *Coral Reefs* 28, 809–822. doi: 10.1007/s00338-009-0532-6

Manthachitra, V. (1994). "Indices assessing the status of coral reef assemblage: formulated from benthic lifeform transect data," in *Proceedings of the Third ASEAN-Australia Symposium on Living Coastal Resources. 2: Research Papers*, eds S. Sudara, C. R. Wilkinson, and L. M. Chou (Bangkok: Chulalongkorn University), 41–50.

Maypa, A. P., White, A. T., Canares, E., Martinez, R., Eisma-Osorio, R., Alino, P., et al. (2012). Marine protected area management effectiveness: progress and lessons in the Philippines. *Coast. Manage.* 40, 510–524. doi: 10.1080/08920753.2012.709465

McClure, E. C., Sieversa, K. T., Abesamis, R. A., Hoeyb, A. S., Alcala, A. C., and Russ, G. R. (2020). Higher fish biomass inside than outside marine protected areas despite typhoon impacts in a complex reefscape. *Biol. Conserv.* 241:108354. doi: 10.1016/j.biocon.2019.108354

McCook, L. J., Ayling, T., Cappo, M., Choat, J. H., Evans, R. D., De Freitas, D. M., et al. (2010). Adaptive management of the Great Barrier Reef: a globally significant demonstration of the benefits of networks of marine reserves. *Proc. Natl. Acad. Sci. U. S. A.* 107, 18278–18285. doi: 10.1073/pnas.0909335107

McManus, J. W., Reyes, R., and Nanola, C. (1997). Effects of some destructive fishing methods on coral cover and potential rates of recovery. *Environ. Manage.* 21, 69–78. doi: 10.1007/s002679900006

Muallil, R. N., Mamauag, S. S., Cabral, R. B., Celeste-Dizon, E. O., and Alino, P. M. (2014). Status, trends and challenges in the sustainability of small-scale fisheries in the Philippines: insights from FISHDA (Fishing Industries' Support in Handling Decisions Application) Model. *Mar. Policy* 44, 212–221. doi: 10.1016/j.marpol.2013.08.026

Mumby, P. J., Harborne, A. R., Williams, J., Kappel, C. V., Brumbaugh, D. R., Micheli, F., et al. (2007). Trophic cascade facilitates coral recruitment in a marine reserve. *Proc. Natl. Acad. Sci. U. S. A.* 104, 8362–8367. doi: 10.1073/pnas.0702602104

Raymundo, L. J., Halford, A. R., Maypa, A. P., and Kerr, A. M. (2009). Functionally diverse reef-fish communities ameliorate coral disease. *Proc. Natl. Acad. Sci.* 106, 17067–17070. doi: 10.3354/meps08150

Roberts, C. M. (2000). Selecting marine reserve locations: optimality versus opportunism. *Bull. Mar. Sci.* 66, 581–592.

Roberts, C. M., Andelman, S., Branch, G., Bustamante, R. H., Castilla, J., Dugan, J., et al. (2003). Ecological criteria for evaluating candidate sites for marine reserves. *Ecol. Appl.* 13, S199–S214.

Roberts, C. M., Halpern, B., Palumbi, S. R., and Warner, R. R. (2001). Designing marine reserve networks: why small, isolated protected areas are not enough. *Summer* 2, 1–8. doi: 10.1002/9781119075806.ch1

Rubec, P. J. (1986). "The effects of sodium cyanide on coral reefs and marine fish in the Philippines," in *The First Asian Fisheries Forum*, eds J. L. Maclean, L. B. Dizon, and L. V. Hosillos (Manila: Asian Fisheries Society), 297–302.

Russ, G. R., Alcala, A. C., Maypa, A. P., Calumpong, H. P., and White, A. T. (2004). Marine reserve benefits local fisheries. *Ecol. Appl.* 14, 587–606.

Russ, G. R., Rizzari, J. R., Abesamis, R. A., and Alcala, A. C. (2021). Coral cover a stronger driver of reef fish trophic biomass than fishing. *Ecol. Appl.* 31:e02224.

Sanciangco, J. C., Carpenter, K. E., Etnoyer, P. J., and Moretzsohn, F. (2013). Habitat availability and heterogeneity and the indo-pacific warm pool as predictors of marine species richness in the tropical indo-pacific. 8:e56245. doi: 10.1371/journal.pone.0056245

SCTR-Philippines (2012). *State of the Coral Triangle Report – Philippines*. Manado: Coral Triangle Initiative.

Selig, E. R., and Bruno, J. F. (2010). A global analysis of the effectiveness of marine protected areas in preventing coral loss. *PLoS One* 5:e9278. doi: 10.1371/journal.pone.00009278

Selig, E. R., Casey, K. S., and Bruno, J. F. (2012). Temperature-driven coral decline: the role of marine protected areas. *Glob. Change Biol.* 18, 1561–1570. doi: 10.1111/j.1365-2486.2012.02658.x

Stockwell, B., Jadloc, C. L., Abesamis, R. A., Alcala, A. C., and Russ, G. R. (2000). Trophic and benthic responses to no-take marine reserve protection in the Philippines. *Mar. Ecol. Prog. Ser.* 389, 1–15. doi: 10.3354/meps08150

Strain, E. M. A., Edgar, G. J., Ceccarelli, D., Stuart-Smith, R. D., Hosack, G. R., and Thomson, R. J. (2019). A global assessment of the direct and indirect benefits of marine protected areas for coral reef conservation. *Divers. Distrib.* 25, 9–20. doi: 10.1111/ddi.12838

Sweatman, H. (2008). No-take reserves protect coral reefs from predatory starfish. *Curr. Biol.* 18, R598–R599. doi: 10.1016/j.cub.2008.05.033

Tabor, G. M., and Aguirre, A. A. (2004). Ecosystem health and sentinel species: adding an ecological element to the proverbial "canary in the mineshaft". *EcoHealth* 1, 226–228.

Teh, L. S., Teh, L. C., and Sumalia, R. U. (2013). A global estimate of the number of coral reef fishers. *PLoS One* 8:e65397. doi: 10.1371/journal.pone.0065397

Toth, L. T., van Woesik, R., Murdoch, T. T., Smith, S. R., Ogden, J. C., Precht, W. F., et al. (2014). Do no-take reserves benefit Florida's corals? 14 years of change and stasis in the Florida Keys National Marine Sanctuary. *Coral Reefs* 33, 565–577. doi: 10.1007/s00338-014-1158-x

van Grieken, M. E., Roebeling, P. C., Bohnet, I. C., Whitten, S. M., Webster, A. J., Poggio, M., et al. (2019). Adoption of agricultural management for Great Barrier Reef water quality improvement in heterogeneous farming communities. *Agric. Syst.* 170, 1–8. doi: 10.1016/j.agsy.2018.12.003

Villanoy, C. L., Salamante, E., and Cabrera, O. (2013). "Chapter 3: exposure: waves and storm surges," in *MERF. (2013). Vulnerability Assessment Tools for Coastal Ecosystems: A Guidebook*. R. C. Geronimo, N. M. G. Follosco, M. C. C. Quibilan, M. S. Samson, and M. G. J. P. Tiquio (Quezon City: Marine Environment and Resources Foundation, Inc.), 162.

Wenger, A. S., Williamson, D. H., da Silva, E. T., Ceccarelli, D. M., Browne, N. K., Petus, C., et al. (2015). Effects of reduced water quality on coral reefs in and out of no-take marine reserves. *Conserv. Biol.* 30, 142–153. doi: 10.1111/cobi.12576

Wilkinson, C. (2008). *Status of Coral Reefs of the World: 2008*. Townsville, QLD: Global Coral Reef Monitoring Network and Reef and Rainforest Research Centre.

Wilson, S. K., Graham, N. A., Fisher, R., Robinson, J., Nash, K., Chong-Seng, K., et al. (2012). Effect of macroalgal expansion and marine protected areas on coral recovery following a climatic disturbance. *Conserv. Biol.* 26, 995–1004. doi: 10.1111/j.1523-1739.2012.01926.x

Conflict of Interest: The authors declare that the research was conducted in the absence of any commercial or financial relationships that could be construed as a potential conflict of interest.

frontiers in Marine Science

ORIGINAL RESEARCH
published: 09 September 2021
doi: 10.3389/fmars.2021.704487

Individual and Interactive Effects of Ocean Warming and Acidification on Adult *Favites colemani*

Mikhael Clotilde S. Tañedo[1]*, Ronald D. Villanueva[1†], Andrew F. Torres[1,2], Rachel Ravago-Gotanco[1] and Maria Lourdes San Diego-McGlone[1]

[1] Marine Science Institute, University of the Philippines, Quezon City, Philippines, [2] Department of Earth Sciences, National History Museum, London, United Kingdom

Tropical coral reefs are threatened by local-scale stressors that are exacerbated by global ocean warming and acidification from the post-industrial increase of atmospheric CO_2 levels. Despite their observed decline in the past four decades, little is known on how Philippine coral reefs will respond to ocean warming and acidification. This study explored individual and synergistic effects of present-day (pH 8.0, 28°C) and near-future (pH 7.7, 32°C) scenarios of ocean temperature and pH on the adult *Favites colemani*, a common massive reef-building coral in Bolinao-Anda, Philippines. Changes in seawater temperature drive the physiological responses of *F. colemani,* whereas changes in pH create an additive effect on survival, growth, and photosynthetic efficiency. Under near-future scenarios, *F. colemani* showed sustained photosynthetic competency despite the decline in growth rate and zooxanthellae density. *F. colemani* exhibited specificity with the *Cladocopium* clade C3u. This coral experienced lower growth rates but survived projected near-future ocean warming and acidification scenarios. Its pH-thermal stress threshold is possibly a consequence of acclimation and adaptation to local environmental conditions and past bleaching events. This research highlights the importance of examining the susceptibility and resilience of Philippine corals to climate-driven stressors for future conservation and restoration efforts in the changing ocean.

Keywords: ocean warming, ocean acidification, tropical coral, growth, zooxanthellae

Edited by:
Yehuda Benayahu,
Tel Aviv University, Israel

Reviewed by:
Christopher Edward Cornwall,
Victoria University of Wellington,
New Zealand
Christopher Paul Jury,
University of Hawai'i at Mānoa,
United States

****Correspondence:***
Mikhael Clotilde S. Tañedo
mctanedo@gmail.com

†Deceased

Specialty section:
This article was submitted to
Marine Ecosystem Ecology,
a section of the journal
Frontiers in Marine Science

Received: *03 May 2021*
Accepted: *10 August 2021*
Published: *09 September 2021*

Citation:
Tañedo MCS, Villanueva RD, Torres AF, Ravago-Gotanco R and San Diego-McGlone ML (2021) Individual and Interactive Effects of Ocean Warming and Acidification on Adult Favites colemani. Front. Mar. Sci. 8:704487. doi: 10.3389/fmars.2021.704487

INTRODUCTION

Global warming and ocean acidification due to the unprecedented increase in anthropogenic CO_2 emissions pose a serious threat to coral reefs worldwide (Hoegh-Guldberg et al., 2007). The ocean's storage of 90% accumulated excess energy in the climate system over the past century led to a $0.6 \pm 0.2°C$ increase in global sea surface temperatures (IPCC, 2001; Hoegh-Guldberg et al., 2007). The average oceanic uptake of CO_2 from anthropogenic emissions is 31%, with uptake rate in 1994–2007 increasing in proportion to the rise in atmospheric CO_2 (Gruber et al., 2019). Oceanic uptake may have slowed down the accumulation of CO_2 in the atmosphere, but it has resulted in ocean acidification (Sabine et al., 2004; Doney et al., 2009). Under business-as-usual scenarios of atmospheric CO_2 emission levels, global sea surface temperatures are projected to increase another 0.3–4.8°C, and sea surface pH to further decrease by 0.06–0.32 pH units by the end of the twenty-first century (IPCC, 2014). With the climate-driven changes in the ocean, coral reefs worldwide are forecast to rapidly degrade over the next 20 years (Hoegh-Guldberg et al., 2017). Record-breaking highs in global surface temperatures (from 2014 to at least 2016) have resulted in the longest global coral bleaching event on record (NOAA, 2015).

Maximum habitat temperatures are close to the upper thermal limits of most tropical corals (Somero, 2010). Changes in habitat pH and temperature may influence the coral's ability to survive, thrive, and to build and maintain massive complex reef structures (Kleypas and Langdon, 2006; Hoegh-Guldberg et al., 2007). High sea surface temperatures (1°C above average summer value) have been strongly associated with mass coral bleaching (Glynn, 1993; Hoegh-Guldberg et al., 2007; Gattuso et al., 2014). Bleached and/or thermally stressed corals may exhibit decline in growth/calcification rates (Cooper et al., 2008; Tanzil et al., 2009; Cantin et al., 2010), in protein content (Grottoli et al., 2004), and in tissue regeneration capacities (Meesters and Bak, 1993). Inability of corals to recover from bleaching may lead to mortality depending on the severity of the heat stress (Goreau et al., 2000; Kavousi et al., 2015). Further, ocean acidification may affect $CaCO_3$ forming ability of corals through induced calcium carbonate precipitation (Doney et al., 2009) and increased calcium carbonate dissolution rates (Andersson and Gledhill, 2013). Thus, the predicted interaction of ocean warming and acidification may negatively affect coral reef global distribution and their existence in the future. While most studies focused on individual effects, combined ocean warming and acidification effects on corals are scarcely explored (Reynaud et al., 2003; Ogawa et al., 2013; Kavousi et al., 2015).

Coral reef ecosystems are of immense biological, economical, and societal importance (Roth, 2014). Philippine reefs are among the most productive and diverse in the world. The country's 25,000 km^2 of total reef area (Gomez et al., 1994) contribute about US $4.94 billion annually (Cruz-Trinidad et al., 2011) to the nation's economy in the form of fisheries, tourism, and coastal protection (Conservation International, 2008). A recent nationwide coral reef assessment (2014–2018) estimated that over the past decade, the country lost about a third of its coral reefs (Licuanan et al., 2019). This decline in the local reefs due to both natural and manmade threats (Roberts et al., 2002; Burke et al., 2011) may be amplified by impending global climate driven stressors. Nonetheless, little is known on the effects of low pH and a combination of low pH and high temperature on Philippine corals (Baria, 2016).

The 1997–1998 bleaching event that occurred during a decade of warmest average temperatures saw the highest decline in live coral reef cover (up to 46%) in the Philippines (Arceo et al., 2001; NOAA, 2015). It was during this time that 80% of corals in the Bolinao-Anda Reef Complex (BARC, northwestern Philippines) bleached including the more tolerant massive corals (Arceo et al., 2001; Chou et al., 2002). Further, fish farming of *Chanos chanos* along the Guiguiwanen channel in Bolinao led to ∼0.2–0.3 decrease in seawater pH in the mariculture area (San Diego-McGlone et al., 2008; Escobar et al., 2013; Lagumen, 2017). Effluent from the mariculture area may adversely affect the adjacent reefs and exacerbate effects of future scenarios of ocean warming and acidification. Interestingly, *Favites colemani* corals still thrive in the Lucero reef in BARC, which is near Guiguiwanen channel. Could this be a consequence of acclimation and adaptation to local environmental conditions? To address this, we focused our work on this encrusting, submassive to massive reef-building coral *F. colemani* (Family *Faviidae*) commonly found in the Philippines (Veron, 2000; Maboloc et al., 2015). This study aims to explore physiological responses of adult *F. colemani* from Lucero reef to near-future scenarios of ocean warming and acidification.

MATERIALS AND METHODS

Coral Collection and Acclimatization

Five non-gravid adult *Favites colemani* colonies (>15 cm), with no pigmented oocytes, were collected in January 2016 at depths of 3–5 m in Lucero, Bolinao (16°24′43.2″ N 119°54′12.2″ E; Garmin Montana 680). Although genotype validation was not conducted, colonies were collected at least 15 m apart horizontally to minimize the chances of incidentally sampling clones. Coral collection was done by chipping the substrate where the colonies were attached. All five colonies were collected during one dive. The coral colonies were placed in aerated seawater tanks in the research boat, and immediately transported to the UP Marine Science Institute Bolinao Laboratory (UPMSI BML) that was a 10–15 min boat ride away from the site.

Fifteen to eighteen explants (6–9 cm^2) were fragmented from each colony and attached to plastic screws using cyanoacrylate adhesive (Mighty Bond Xtreme, Pioneer). Explants were tagged and pre-conditioned for 1 month in indoor experimental tanks in a ∼24°C temperature-controlled room with flow-through seawater maintained at 28 ± 0.7°C and under artificial photosynthetic photon flux density of ∼90 $\mu mol\ m^{-2}\ s^{-1}$ on a 12:12 light-dark cycle. This enabled coral explants to recover from handling stress and acclimate to the conditions in the experiment control tanks. Similar to other studies, coral explants had positive growth, no mortality and no bleaching under relatively lower light intensity than the natural environment (Ohki et al., 2013; Kavousi et al., 2015; Da-Anoy et al., 2019; Manullang et al., 2020).

Experiment Setup

Ocean acidification-thermal stress experiments were conducted in 17 L tanks in a flow through seawater system (**Figure 1**). Filtered (10 μm) seawater maintained at 28 ± 0.7°C (HC1000A, Hailea) was pumped into each experiment tank from a 45 L mixing tank at a flow rate of ∼2–3 $L\ h^{-1}$. Seawater inside each mixing tank was either adjusted to a lower pH value using the mass-flow controlled (Sev-E40, Horibastec) CO_2 dosing, or maintained at control pH value through bubbling aeration. Additional mixing in the experiment tanks was provided by a 285 $L\ h^{-1}$ submersible water pump (HX800, Hailea). Each experimental tank was placed in 45 L thermal bath with submersible thermostat heater (Eheim, Germany). Four pH-temperature treatments were used: Control (C: pH 8.0, 28°C), ocean acidification (OA: pH 7.7, 28°C), ocean warming (T: pH 8.0, 32°C), and ocean acidification with warming (OAT: pH 7.7, 32°C). pH conditions of 7.7 and 8.0 were chosen as present day (study site pH range ∼8.0–8.1), and IPCC projected seawater pH (based on Representative Concentration Pathway 8.5) by the end of this century (IPCC, 2014) scenarios, respectively. We chose 28°C as control temperature, which represents annual seawater temperature in Bolinao (28.89 ± 0.90°C; Guzman and Conaco, 2016), and 32°C as stress temperature, which represents increases of 4°C from mean annual and 2°C from warmest monthly mean seawater temperatures (30.64 ± 0.79°C; Maboloc et al., 2015) in Bolinao. Seawater temperature inside the experiment tanks were kept stable by using thermal baths with thermostat heaters, and by maintaining the temperatures in the mixing tanks (∼28°C) and the experiment room (∼24°C). Three independent replicate experimental tanks were used for each pH-temperature treatment. No two pH-temperature replicates were dependent on the same treatment water source. Treatment replicates were randomly interspersed in the system (Cornwall and Hurd, 2015). Experimental tanks were illuminated under artificial light with photosynthetic photon flux density of ∼90 μmol $m^{-2}s^{-1}$ (Onset HOBO) on a 12:12 light-dark cycle to avoid light stress. Temperature and pH in each experimental tank were recorded thrice a day (8:00 a.m., 12:00 p.m., 6:00 p.m.) using pH/conductivity meter (SevenGo, Mettler Toledo) calibrated using NBS buffer solutions. Experimental tank water temperatures were also recorded every 15 min using data logger (UA-002-64, Onset HOBO). The seawater salinity was 32.9 ppt. Seawater samples were collected every week and analyzed using a Total Alkalinity titrator (Kimoto, ATT-05, Japan) calibrated with certified reference material (CRM) for ocean CO_2 measurements. The partial pressure of carbon dioxide (pCO_2) and aragonite saturation (Ωa) were calculated using the CO_2SYS program (Lewis and Wallace, 1998), utilizing K1 and K2 dissociation constants (Mehrbach et al., 1973).

Physiological Analyses

Fifteen coral explants were exposed under each pH-temperature treatment (one explant per colony in each experiment tank replicate) for 28 days. The explants were monitored daily for bleaching (Siebeck et al., 2006) and survival (McClanahan, 2004). *F. colemani* explants that were both bleached and necrosed (no visible living coral tissue) were recorded as "dead" (**Figure 2**). Quantification of the growth (calcification) rate was done through buoyant weight method. Growth rate (% d^{-1}) was determined using the equation $G = (\Delta W_a/\Delta t) \times 100$; where ΔW_a is change in final and initial dry coral weight, and Δt is length of experiment (28 days). Dry coral weight (W_a) was calculated using the equation $W_a = W_w/(1–(\rho_w/\rho_s))$; where W_w is buoyant weight of coral explant, ρ_w (g cm^{-3}) is density of water used for buoyant weight measurement, and ρ_s (∼2.94 g cm^{-3}) is density of pure aragonite (Jokiel et al., 1978; Davies, 1989; Langdon et al., 2010; Takahashi and Kurihara, 2013). The maximum photosynthetic efficiency of the photosystem II of zooxanthellae, Fv/Fm, was measured weekly (at days 0, 7, 14, 21, 28) through pulse-amplitude modulated (Diving PAM; Walz, Effeltrich, Germany) fluorometry (Schreiber et al., 1986). The explants were dark acclimated for 60 min prior to measurement (Ohki et al., 2013). To quantify zooxanthellae density ($\times 10^6$ cell cm^{-2}) (Nakamura et al., 2005), coral tissue was obtained from each explant through the water-pik method using 50 mL 0.2 μm filtered seawater (Johannes and Wiebe, 1970). A Neubauer hemocytometer (LeGresley and McDermott, 2010) was used to count zooxanthellae cells under a microscope. Only healthy-looking zooxanthellae were counted, while irregular-shaped and pale-colored cells were excluded. Cell counts were normalized to slurry volume (50 mL), and explant surface area was determined using the paraffin wax method (Stimson and Kinzie, 1991; Veal et al., 2010).

Zooxanthellae Collection and Identification

Prior to the start of the experiment, three explants per *F. colemani* colony were sampled, preserved in salt saturated DMSO (SSD) buffer (Gaither et al., 2011), and stored at 4°C. At the end of the experiment, explant tissue slurries (1–2 explant per colony per treatment) were pelletized and preserved in SSD. Zooxanthellae diversity was characterized through DGGE fingerprinting. Holobiont DNA was extracted using a modified organic DNA extraction method (Mieog et al., 2009). Following the touchdown thermal cycle protocol of LaJeunesse (2002), the zooxanthella-specific primers *ITSintfor2* and the GC-attached *ITS2clamp* were used to amplify the internal transcribed spacer 2 region (ITS2, ∼350 bp) for downstream DGGE fingerprinting. All ITS2 PCR products (7 μL) were loaded 1:1 with 0.05% bromophenol blue-xylene cyanol solution into an 8% polyacrylamide (37.5:1 acrylamide/bis) denaturing gel with an internal gradient (30–60%) of denaturants (urea and formamide) and were separated by electrophoresis using DCode Universal Mutation Detection System (Bio-Rad) for 18 h at 100 V with a constant tank buffer temperature of 60°C. The acrylamide gels were post-stained with 1 × SYBR Green in 1 × TAE buffer for 30 min and photographed under UV illumination. A subset of prominent bands and likely heteroduplexes from randomly sampled explants were excised and incubated overnight with 500 μL nuclease-free water. Eluates were used as template for re-amplification of the ITS2 using the oligonucleotide primers *ITSintfor2* and *ITS2reverse* following a similar thermal cycling protocol but without the touchdown cycles (LaJeunesse et al., 2010). Bidirectional DNA sequencing was performed (First Base Laboratories, Malaysia) and individual ITS2 sequences were manually trimmed, checked, and aligned using Geneious 6.1.8. Sequences were queried through BLAST (Altschul et al., 1990) in a custom zooxanthellae database from GeoSymbio (Franklin et al., 2012) and additional unique sequences obtained from GenBank (query: "Symbiodiniaceae" "ITS2") via the NCBI portal[1].

Statistical Analyses

All data were tested for homogeneity of variances (Levene's test) and normality (Shapiro-Wilk Test). On each pH-temperature treatment, differences in physico-chemical values between tank replicates were analyzed. The Kruskal-Wallis test was utilized for pH and temperature, and one-way analysis of

---

[1] http://blast.ncbi.nlm.gov/Blast.cgi

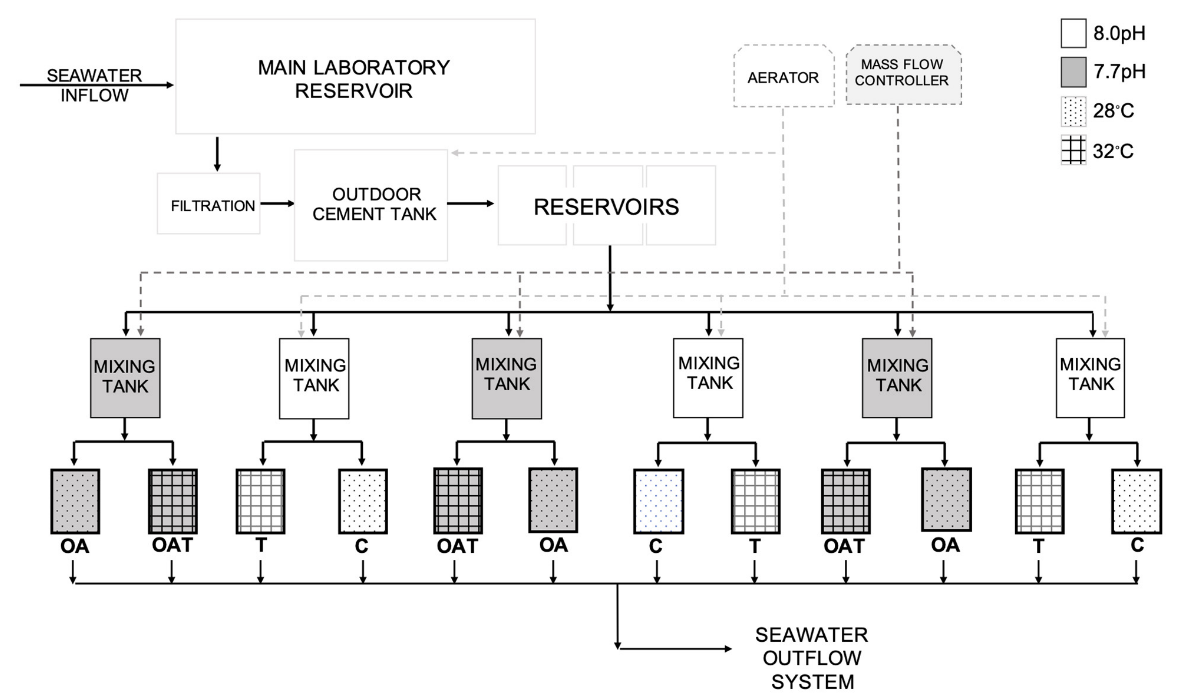

FIGURE 1 | Schematic diagram of ocean acidification-thermal stress system set-up at UPMSI BML. Solid arrows are seawater flow paths as it enters and exits the system. Dashed arrows are inputs of air and CO_2 to the system.

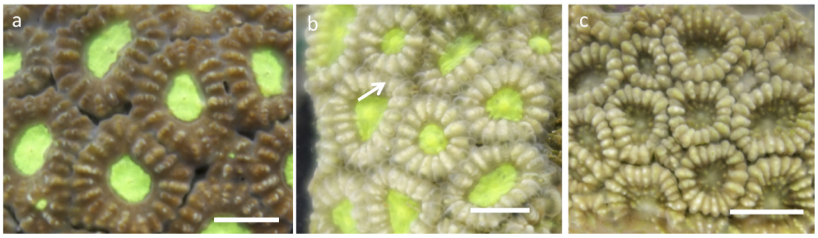

FIGURE 2 | Survival of *favites colemani* explants: **(a)** alive: Unbleached with coral tissue, **(b)** alive: Bleached with coral tissue **(c)** dead: Bleached and necrosed (no coral tissue, skeleton exposed). Scale = 0.5 cm.

variance (ANOVA) for pCO_2 and aragonite saturation levels (Ω_a). Kaplan–Meier model (Lee, 1992) survival analysis was used to investigate survival of *F. colemani* explants under pH-temperature treatments for 4 weeks. Pairwise comparisons of the survival curves were done using log-rank test (Mantel-Haenszel Test). RStudio (version 0.98.1102) software was used in the analyses. Permutational analysis of variance (PERMANOVA, Anderson, 2001) was used to investigate effects of pH-temperature treatments on growth rate, zooxanthellae density, and maximum photosynthetic efficiency of *F. colemani* explants. Two-way PERMANOVA was used on growth rates and zooxanthellae densities. The fixed factors in the design were pH (two levels), and temperature (two levels). Three-way PERMANOVA was used on maximum photosynthetic efficiencies. Fixed factors were pH (two levels), temperature (two levels), and time (five levels). Euclidean distances were used for all permutational analyses. Analyses were followed by *a posteriori* pairwise test when significant values were obtained. This was done to determine differences between levels within a factor. PRIMER 7 and PERMANOVA + 1 version 7.0.11 software were used for these statistical analyses.

RESULTS

Physico-Chemical Parameters

Seawater mean pH and temperature values measured during the experiment are given in **Table 1** for the following treatments: C (pH 8.02 ± 0.05, 27.91 ± 0.61°C), OA (pH 7.74 ± 0.05, 27.91 ± 0.60°C), T (pH 8.00 ± 0.05, 32.01 ± 0.43°C), and OAT (pH 7.72 ± 0.05, 32.00 ± 0.45°C). The pCO_2 increased, and aragonite saturation levels (Ω_a) decreased at low pH in all temperature treatments. pH, temperature, pCO_2, and Ω_a

TABLE 1 | Physico-chemical values (mean ± SD) of pH-temperature treatments for 28 days; pH (n = 255), temperature (n = 8064), partial pressure of carbon dioxide (pCO_2; n = 15), aragonite saturation levels (Ω_a; n = 15).

Treatment	pH	Temperature (°C)	Carbonate Chemistry		
			TA (μmol/kg)	pCO_2 (μatm)	Ω_a
C	8.02 ± 0.05	27.91 ± 0.61	2244.63 ± 24.31	520.13 ± 44.86	2.81 ± 0.12
OA	7.74 ± 0.05	27.91 ± 0.60	2234.61 ± 49.92	1049.63 ± 201.54	1.62 ± 0.16
T	8.00 ± 0.05	32.01 ± 0.43	2250.97 ± 28.69	526.58 ± 85.47	2.74 ± 0.12
OAT	7.72 ± 0.05	32.00 ± 0.45	2249.14 ± 47.61	1008.67 ± 177.53	1.74 ± 0.21

showed non-significant differences between replicates in each pH-temperature treatment (**Supplementary Table 1**).

Survival

The survival of *F. colemani* explants after 28 days of exposure under both C and OA treatments was 100 ± 0%. Bleaching was only observed under T and OAT treatments. The survival of coral explants under both T and OAT treatments was 66.7 ± 12.17% (**Figure 3** and **Supplementary Table 2**), and mortalities were observed on the 3rd and 4th weeks of exposure. Temperature (χ^2 = 11.8; $P < 0.001$) significantly influenced coral survival. Coral survival was also affected by a decrease in seawater pH but only when this co-occurred with elevated temperature (χ^2 = 11.8; $P < 0.001$) and longer exposure (χ^2 = 59.1; $P < 0.001$) (**Table 2**).

Effect on Growth Rate

The growth rate of *F. colemani* explants after 28 days of exposure under C was 0.071 ± 0.031% d^{-1}. Growth rates under both OA (0.038 ± 0.036% d^{-1}) and T (0.047 ± 0.011% d^{-1}) treatments were lower compared to C. The lowest growth rate was seen under OAT (0.010 ± 0.051% d^{-1}) treatment (**Figure 3** and **Supplementary Table 2**). Based on PERMOVA, pH [$F_{(1,\ 46)}$ = 12.069, P = 0.002] and temperature [$F_{(1,\ 46)}$ = 6.6978, P = 0.016] significantly affected *F. colemani*'s growth rate, however, the synergistic effect of pH and temperature [$F_{(1,\ 46)}$ = 0.0570, P = 0.808] was non-significant (**Table 2**). *Posteriori* pairwise test showed a significant decline in growth rate under treatments with either increased temperature alone (P = 0.001) or in combination with decreased pH (P = 0.002) (**Supplementary Table 3**).

Effect on Maximum Photosynthetic Efficiency (Fv/Fm)

The maximum photosynthetic efficiency of *F. colemani* explants after 28 days of exposure to OA (0.735 ± 0.045, mean ± SD) was comparable to C (0.713 ± 0.058), but lower values were observed under T (0.642 ± 0.079) and OAT (0.517 ± 0.129) (**Figure 3** and **Supplementary Table 2**). Based on three-way PERMANOVA, the Fv/Fm of the coral explants was significantly affected by pH [$F_{(1,\ 265)}$ = 5.8584, P = 0017], temperature [$F_{(1,\ 265)}$ = 87.233, P = 0.001], and duration of exposure to treatments [$F_{(4,\ 46)}$ = 14.093, P = 0.001; **Table 2**]. Significant decline in Fv/Fm was observed starting week 2 for T (P = 0.001) and OAT (P = 0.001). This significant decline persisted in week 3 (T: P = 0.001, OAT T: P = 0.001) to week 4 (T: P = 0.002, OAT T: P = 0.001) (**Supplementary Table 3**). The maximum photosynthetic efficiencies of the coral explants were above 0.5 and remained photosynthetically competent even after exposure to stress treatments (>0.5; Kavousi et al., 2015).

Zooxanthellae Density and Diversity

The zooxanthellae density of *F. colemani* explants after 28 days of exposure under control conditions was 4.211 ± 2.743 × 10^6 cells cm^{-2} (mean ± SD). Decline in zooxanthellae densities was observed under OA (3.208 ± 2.146 × 10^6 cells cm^{-2}), T (0.492 ± 1.122 × 10^6 cells cm^{-2}), and OAT (0.476 ± 0.280 × 10^6 cells cm^{-2}) treatments (**Figure 3** and **Supplementary Table 2**). Based on two-way PERMANOVA, zooxanthellae density was not significantly affected by pH alone [$F_{(1,\ 46)}$ = 0.0861, P = 0.744], and by interaction of pH and temperature [$F_{(1,\ 46)}$ = 1.1486, P = 0.291] but by seawater temperature [$F_{(1,\ 46)}$ = 42.706, P = 0.001; **Table 2**]. *Posteriori* pairwise test showed a significant decline in zooxanthellae density under treatments with increased temperature (P = 0.001) (**Supplementary Table 3**). All pre- and post-experiment explants processed for zooxanthellae clade identification showed the occurrence and possible dominance of *Cladocopium* sp. clade C3u (formerly a subclade of *Symbiodinium*) in all *F. colemani* samples (GenBank Accession Nos. MN031741–MN031752; **Supplementary Figure 1**).

DISCUSSION

Tropical corals exist in marine environments where natural habitat temperature variabilities are close to their physiological limits. Further increase in temperatures of up to 2°C due to climate change could therefore be intolerable for these organisms and pose "dangerous" climatic and ecological consequences (Somero, 2010; Hennige et al., 2014; Elder and Seibel, 2015). Coral bleaching is highly associated with increase in seawater temperatures (Glynn, 1993; McClanahan, 2004; Hoegh-Guldberg et al., 2007; Gattuso et al., 2014). During 1997–1998 El Niño event, 80% of BARC reefs bleached following a prolonged exposure (7 months) to a major "hotspot" (>1 thermal anomaly above expected max monthly mean SST) in the region, which included submassive and massive corals that are generalized as less susceptible to bleaching (Arceo et al., 2001). Although signaling events that lead to bleaching are partially understood, there is strong evidence that oxidative stress plays a critical role in the host-bleaching cascade (Weis, 2008). However, bleaching may not occur if the coral is able to recover from

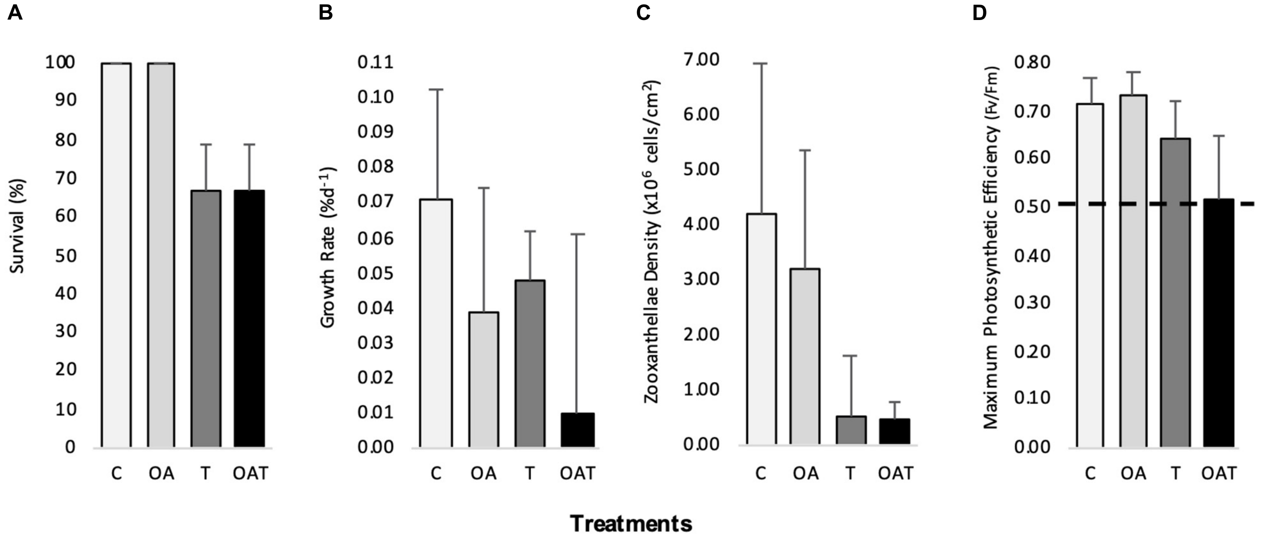

FIGURE 3 | Physiological response (mean ±SD) of Favites colemani after 28 days exposure to pH-temperature stress. **(A)** survival **(B)** growth rate **(C)** zooxanthellae density **(D)** maximum photosynthetic efficiency (values above horizontal dashed line mean photosynthetically competent). (*n* = 15 for survival in OA, T, OAT; *n* = 15 for growth rate, zooanthellae density, maximum photosynthetic efficiency in C, OA, and *n* = 10 in T, OAT).

stress (Goreau et al., 2000; Kavousi et al., 2015). *Favites* spp. colonies in Kenya (McClanahan, 2004), and *F. colemani* colonies in BARC (Maboloc et al., 2015) both exhibited post-bleaching survival after the 1997–1998 El Niño event. The survival of *F. colemani* in this study was also high (66.7 ± 12.3%) under both T and OAT treatments, where the temperature used was 4°C above the annual mean, and 2°C above the maximum monthly mean (30.64 ± 0.79°C; Maboloc et al., 2015) SST in Bolinao. This was also observed during the 2016 thermal bleaching event where no *F. colemani* colonies in the study site was recorded to have bleached. The 2016 thermal stress began around mid-April to May and peaked during the months of June to July. During this event, sea surface temperatures (SST) in Bolinao rose to 1–2°C above the maximum monthly mean SST (29–30°C). Degree Heating Weeks (DHW) since the onset of warming lasted for about 11–12 weeks. This event caused coral bleaching but with low prevalence (<25%) at the BARC where majority (77%) of the corals comprise five genera (*Dipsastrea, Porites, Fungia, Seriatopora, and Montipora*) (Quimpo et al., 2020).

Facing the South China Sea, reefs in the BARC experience high temperature variations (Peñaflor et al., 2009; Guzman and Conaco, 2016). Annual mean seawater temperature in Bolinao is 28–29°C (Guzman and Conaco, 2016), while max monthly mean in the Lucero reef can reach 30–31°C (Maboloc et al., 2015). Dry-warm months in the Philippines occur in April–May. Monthly seawater temperatures from December to March (dry-cold months) range from 27 to 28°C. *In situ* spawning of *F. colemani* occurs between full moon and last quarter of May, the warmest month of the year (Maboloc et al., 2015). Lucero reef is adjacent to the Guiguiwanen channel, a designated mariculture area where fish farming of *Chanos chanos* has intensified since it started in the 1990s (San Diego-McGlone et al., 2008). The reef may be exposed to seawater with lower pH levels due to seasonal outflow of mariculture effluent from the channel. Lagumen (2017) observed that expansion of fish farming activities caused a decrease of seawater pH by ∼0.2–0.3 units in the mariculture area. The diurnal pH range in the reef adjacent to the channel (mariculture area) was lower during dry (pH 7.78–8.22, pCO_2 235–849) compared to the wet (pH 7.96–8.14, pCO_2 305–518) periods. Prior *in situ* exposure of *F. colemani* to lowered pH and elevated temperature could be the reason why explants had no mortality after a 28-days exposure to C and OA treatments, which suggests that they may have locally adapted to wide pH and thermal limits.

Corals' ability to sustain calcification rates that can withstand natural forces of biological and physical erosion is a fundamental aspect in maintenance of reef ecosystems. However, this ability may be compromised by exposure to warmer and acidified waters (Doney et al., 2012; Lough and Cantin, 2014). Our understanding of factors that drive coral calcification is still rudimentary (Tambutte et al., 2011). In this study, *F. colemani* growth rates significantly declined under OA and T treatments. Some studies suggest that coral growth rates may be adversely affected by seawater pH decrease (Anthony et al., 2008; Doney et al., 2009; Feely et al., 2009; Tanzil et al., 2009), and seawater temperature increase (Leder et al., 1991; Tanzil et al., 2009; Cantin et al., 2010). Scleractinian tropical corals existing near low-pH springs (e.g., Hawaii) or submarine groundwater discharge (Mexico) experience lower tissue density and higher bioerosion rates (Crook et al., 2012; Lubarsky et al., 2018). The decline in growth rate under the OA and T treatments seen in this study may be due to mechanisms that trade off calcification processes in favor of generating more tissue biomass and energy reserves (Strahl et al., 2016). The coral's capability to retain calcification rates may be affected by stress-induced damages that occur inside coral cell (mitochondria) and zooxanthellae (chloroplast). This further leads to high production of reactive oxygen species (ROS) and reactive nitrogen species (RNS) that may overwhelm oxygen-handling pathways (Venn et al., 2008; Weis, 2008). Consequently, host DNA (Lesser and Farrell, 2004), protein, and membrane (Richier et al., 2005) become damaged. Increased concentrations of the RNS nitric oxide may also initiate an apoptotic cascade leading to coral bleaching (Perez and Weis, 2006). While ocean acidification may be associated to decline in coral calcification, the mechanisms underlying its influence on coral growth remain unclear (Venn et al., 2013). Corals have ectodermis and gastrodermis tissue layers that fold over each other to form the gastrovascular cavity known as coelenteron. Among these extra- and intracellular coral compartments, there is wide carbon chemistry and pH variability (Barott et al., 2017). For instance, the coral ectodermis has pH ranging between 7.9 and 8.3, the gastrodermal cells symbiosome has a pH of around 4, the sub-calicoblastic medium (SCM) has pH ranging between 8.2 and 10, and the coelenteron has pH ranging between 6.6 and 8.5 (Al-Horani et al., 2003; Agostini et al., 2011; McCulloch et al., 2012; Cai et al., 2016). Corals and other coral reef organisms modulate the chemistry of their calcifying fluids (CF) and may override changes in the chemistry of the seawater source to the site of calcification (Cohen and Holcomb, 2009; Cohen et al., 2009). One hypothesis (Kaniewska et al., 2012) suggests that exposure to low pH may overwhelm the coral's acid-base regulation and cell membrane transporters and may lead to cell acidosis. This pH imbalance then causes damage to both the coral cell and its algal symbiont, leading to increase in ROS and RNS and the disruption of symbiosis. Another consequence of this acidosis is calcium ion (Ca^{2+}) imbalance resulting from an increase in ROS and Ca^{2+} ion storage disruption in the endoplasmic reticulum. This may then lead to changes in the extracellular matrix, cytoskeletal remodeling, changes in cytoskeletal interactions, disruptions in cell reception and signaling potential, and increased cell death. A study on *Stylophora pistillata* colonies (Venn et al., 2013) saw reductions in calcification rate only when pH was significantly low in the calcifying cells in addition to the SCM. This highlights the roles of SCM pH regulation and calcifying cell pH homeostasis in the coral's response to ocean acidification. According to McCulloch et al. (2017), carbonate saturation state in the calcifying fluid (O$_{CF}$) which is the key driver of calcification, is maintained elevated but at near-constant levels by seasonally varying supply of summer-enhanced metabolic dissolved inorganic carbon (DIC$_{CF}$), and dynamic out-of-phase upregulation of pH$_{CF}$. In the advent of extreme thermal stress, O$_{CF}$ becomes unstable, and this leads to termination of calcification. As observed in this study, *F. colemani* exhibited lower growth rates under OA, T, and OAT treatments, and decline in zooxanthellae densities were likewise recorded.

Coral growth rates after bleaching events may decline, experience setbacks, or cease altogether (Cooper et al., 2008; Carilli et al., 2009), but the surviving corals may still recover to pre-bleaching growth rates after some years (Lough and Cantin, 2014). Based on the study by Ogawa et al. (2013), corals exhibit differential expression of candidate calcification genes after prolonged exposure to combined pH-temperature stress. In this study, decreased pH and increased seawater temperature have additive adverse effect on *F. colemani*'s growth rates, with lowest values observed under OAT. This suggests that while *F. colemani* exhibited post-bleaching recovery in the past (McClanahan, 2004; Maboloc et al., 2015), adverse effects on its growth, distribution, and post-bleaching recovery may be aggravated in a future scenario of co-occurring ocean warming and acidification.

The divergent responses of corals under stressed scenarios are likely reflective of the holobiont's stress response machinery, as well as the variable interactions between the host and its symbionts. It is probable that the coral's stress response is influenced by its zooxanthellae and their photosynthetic capacity. The disruption of the coral-zooxanthellae relationship and reduction in its photochemical efficiencies are potentially driven by decline in seawater pH and are highly correlated with elevated temperatures (McClanahan, 2004; Hoegh-Guldberg et al., 2007; Anthony et al., 2008; Weis, 2008; Gattuso et al.,

TABLE 2 | Summary of statistical analyses on *Favites colemani* physiological response under pH-temperature treatments for 28 days.

Survival

Mantel-haenszel test	df	χ^2	*p*-value
pH	1	0	0.976
Temperature	1	11.8	**<0.001**
Time	1	59	**<0.001**
pH × temperature	3	11.8	**<0.001**
Temperature × time	2	62.4	**<0.001**
pH × Time	3	59.1	**<0.001**
pH × temperature × time	5	62.5	**<0.001**

Growth rate

Two-way PERMANOVA	df	Pseudo-*F*(1,46)	P(perm)
pH	1	12.069	**<0.01**
Temperature	1	6.6978	**<0.05**
pH × temperature	1	0.056974	0.808

Zooxanthellae density

Two-way PERMANOVA	df	Pseudo-*F*(1,46)	P(perm)
pH	1	0.086067	0.744
Temperature	1	42.706	**<0.01**
pH × temperature	1	1.1486	0.291

Maximum photosynthetic efficiency

Three-way PERMANOVA	df	Pseudo-*F*(df, 265)	P(perm)
pH	1	5.8584	**<0.05**
Temperature	1	87.233	**<0.01**
Time	4	14.093	**<0.01**
pH × Temperature	1	0.69676	0.376
Temperature × time	4	14.535	**<0.01**
pH × Time	4	1.8639	0.134
pH × Temperature × time	4	7.3448	**<0.01**

Factors include pH, temperature, and time.
Significant differences are shown in bold.

2014; Davies et al., 2018). In this study, seawater temperature dominantly influenced *F. colemani*'s zooxanthellae density. Cell damage and death may occur due to increase in ROS and RNS during thermal stress and cell acidosis (Richier et al., 2005; Weis, 2008; Kaniewska et al., 2012). High temperatures may cause damage to zooxanthellae's photosynthetic apparatus at photosystem II, the thylakoid membranes, and the Calvin cycle (Lesser, 1996; Weis, 2008). As a stress defense mechanism, the observed decline in zooxanthellae densities under T, and OAT treatments may have resulted from the coral's active digestion and selective expulsion of damaged or incompetent symbiont cells (Lesser, 1996, 1997; Downs et al., 2002; Smith et al., 2005; Venn et al., 2008; Weis, 2008). Similarly, seawater pH and temperature additively affected Fv/Fm of *F. colemani* explants. Despite the recorded decline in zooxanthellae density, *F. colemani* explants remained photosynthetically competent (>0.5; Kavousi et al., 2015) under T, and OAT treatments. Corals expel and digest damaged cells also as a regulatory means to maintain constant symbiont density and stable carbon concentration within their tissues (Downs et al., 2009; Fujise et al., 2014). In some cases, corals under stressed treatments may also expel morphologically normal but photosynthetically incompetent/damaged symbiont cells as a stress coping mechanism (Lesser, 1997; Fujise et al., 2014). One study revealed that under elevated temperatures, two species of scleractinian corals (*Acroporidae*) sustained high maximum photosynthetic efficiency (Fv/Fm) values and expelled zooxanthellae cells that are morphologically normal with low Fv/Fm values (Fujise et al., 2014). Massive corals such as *F. colemani* may likely be provided with photoprotection by its thicker tissues and high levels of stored energy (Thornhill et al., 2011; Grottoli et al., 2014; Strahl et al., 2016).

Coral-zooxanthellae associations can influence the adaptation of corals and the maintenance of coral reefs. For instance, bleaching presents an opportunity for some coral taxa to undergo "shuffling" of dominant zooxanthellae types to more tolerant species as an adaptation to current environmental conditions (Gates and Edmunds, 1999; Kinzie, 1999). Some corals can improve their thermal tolerance through switching their dominant symbiont type from *Cladocopium* sp. to the generally more tolerant *Durusdinium* sp. (Fabricius et al., 2004; LaJeunesse et al., 2004; Berkelmans and van Oppen, 2006; Stat and Gates, 2011). In this study, however, no "shuffling" of dominant symbionts was observed, as *F. colemani* colonies maintained their hosting *Cladocopium* clade C3u before and after a 28-day exposure to pH-temperature treatments. While it is possible that the DGGE may have not detected rare symbionts (Da-Anoy et al., 2019), one likely reason for this response is its probable adaptation to environmental changes via other mechanisms. For one, host genotype may play a key role on varying physiological responses (Parkinson et al., 2015). In the same way, different zooxanthellae species or clades, as they are sometimes physiologically adapted to certain environments, may likewise vary in response to a stressor (Fabricius et al., 2004; Jones et al., 2008; Brading et al., 2011). Highly stable coral-zooxanthellae symbiotic associations could be observed in some coral species throughout bleaching events, after transplantation, and over wide geographical and temperature ranges (LaJeunesse et al., 2004; Stat et al., 2009). For instance, the *Cladocopium* clade C15 was hosted by *Porites lobata* colonies found on both fore reefs and warmer more variable back reefs in American Samoa (Barshis et al., 2010). *Cladocopium thermophilum* (C3-Gulf) dominated corals found in Persian/Arabian Gulf, one of the hottest environments in the world (Hume et al., 2013). Clade C1 also exhibits local adaptation to high temperatures (Howells et al., 2011) and thermal stress resistance due to acclimation of the coral holobiont (Bellantuono et al., 2012; Palumbi et al., 2014). Another study has also observed *F. colemani* hosting C3u symbionts but showed less apparent reduction in Fv/Fm and symbiont density after a 72-h exposure to thermal stress (Da-Anoy et al., 2019). In this current study, that *F. colemani* harbors *Cladocopium* clade C3u through the month-long experiment could either indicate the coral host's sufficient physiological adaptation to local environmental temperature and pH variations (Berkelmans and van Oppen, 2006; Noonan et al., 2013) as a result of recurring exposure to local stress (Thornhill et al., 2011; Grottoli et al., 2014), or the zooxanthellae clade's resistance to the stressors being investigated. Either way, more genetic and physiological investigations are still needed to unveil host and host-symbiont responses as well as other adaptive mechanisms to ocean warming and acidification.

CONCLUSION

The physiological responses of *F. colemani* in this study indicate that this coral may have lower growth rates and yet still survive projected near-future ocean warming and acidification scenarios. This supports the hypothesis that *F. colemani*'s pH-thermal stress tolerance is a result of possible acclimation and adaptation to local environmental conditions and past bleaching events. This study adds to the limited knowledge on how Philippine corals would respond to independent and interactive effects of pH and temperature stress. The study highlights the significance of exploring individual and integrative effects of climate-driven stressors on Philippine reef building corals as a guide for future conservation and restoration efforts in the changing ocean. Studies on coral physiological responses at earlier life stages and finer genetic investigations on the host and its symbionts are warranted to better understand local acclimation, adaptation, and stress tolerance to ocean warming and acidification.

DATA AVAILABILITY STATEMENT

The sequence data that support the findings of this study have been deposited in GenBank with the accession numbers: MN031741–MN031752.

AUTHOR CONTRIBUTIONS

MT, RV, RR-G, and MS-M contributed to conception and design of the study. MT and AT performed the experiments. MT and MS-M analyzed the data. RV, RR-G, and MS-M provided supervision. MT wrote the original draft of the manuscript. MT, AT, RR-G, and MS-M reviewed and edited the manuscript. All authors contributed to the article and approved the submitted version.

FUNDING

This study was supported by the Department of Science and Technology—Philippine Council for Agriculture, Aquatic, and Natural Resource Research and Development (DOST-PCAARRD) through the project "Identifying resilient coral species" under the program on *Molecular genetic and genomic studies of coral resilience in support of coral restoration and rehabilitation efforts* (Project Code: QSR-MR-COR.02.01).

ACKNOWLEDGMENTS

We are grateful to the Marine Biogeochemistry Laboratory and Bolinao Marine Laboratory of the Marine Science Institute, University of the Philippines for the valuable logistical and laboratory support provided. We would also like to thank Drs. Haruko Kurihara, Atsushi Watanabe, and Toshihiro Miyajima for the design of the mass flow controller used in the experiments. This is UP-MSI contribution number 484.

SUPPLEMENTARY MATERIAL

The Supplementary Material for this article can be found online at: https://www.frontiersin.org/articles/10.3389/fmars.2021.704487/full#supplementary-material

REFERENCES

Agostini, S., Suzuki, Y., Higuchi, T., Casareto, B. E., Yoshinaga, K., Nakano, Y., et al. (2011). Biological and chemical characteristics of the coral gastric cavity. *Coral Reefs* 31, 147–156. doi: 10.1007/ s00338-011-0831-6

Al-Horani, F. A., Al-Moghrabi, S. M., and De Beer, D. (2003). The mechanism of calcification and its relation to photosynthesis and respiration in the scleractinian coral *Galaxea fascicularis*. *Mar. Biol.* 142, 419–426. doi: 10.1007/s00227-002-0981-8

Altschul, S. F., Gish, W., Miller, W., Myers, E. W., and Lipman, D. J. (1990). Basic local alignment search tool. *J. Mol. Biol.* 215, 403–410.

Anderson, M. J. (2001). A new method for non-parametric multivariate analysis of variance. *Austral. Ecol.* 26, 32–46. doi: 10.1111/j.1442-9993.2001.01070.pp.x

Andersson, A. J., and Gledhill, D. (2013). Ocean acidification and coral reefs: effects on breakdown, dissolution, and net ecosystem calcification. *Annu. Rev. Mar. Sci.* 5, 321–348. doi: 10.1146/annurev-marine-121211-172241

Anthony, K. R. N., Kline, D. I., Díaz-Pulido, G., Dove, S., and Hoegh-Guldberg, O. (2008). Ocean acidification causes bleaching and productivity loss in coral reef builders. *Proc. Natl. Acad. Sci.* 105, 17442–17446. doi: 10.1073/pnas.0804478105

Arceo, H. O., Quibilan, M. C., Aliño, P. M., Lim, G., and Licuanan, W. Y. (2001). Coral bleaching in Philippine reefs: Coincident evidences with meso-scale thermal anomalies. *B. Mar. Sci.* 69, 579–593.

Baria, M. V. B. (2016). *The impacts of elevated temperature and ocean acidification on spawning and early life stages of corals*. PhD Ryukyus: University of Ryukyus.

Barott, K. L., Barron, M. E., and Tresguerres, M. (2017). Identification of a molecular pH sensor in coral. *P. Roy. Soc. B.* 284:1866. doi: 10.1098/rspb.2017.1769

Barshis, D. J., Stillman, J. H., Toonen, R. J., Smith, L. W., and Birkeland, C. (2010). Protein expression and genetic structure of the coral *Porites lobata* in an environmentally extreme Samoan back reef: does host genotype limit phenotypic plasticity? *Mol. Ecol.* 19, 1705–1720. doi: 10.1111/j.1365-294X.2010.04574.x

Bellantuono, A. J., Hoegh-Guldberg, O., and Rodriguez-Lanetty, M. (2012). Resistance to thermal stress in corals without changes in symbiont composition. *Proc. R. Soc. B* 279, 1100–1107. doi: 10.1098/rspb.2011.1780

Berkelmans, R., and van Oppen, M. J. H. (2006). The role of zooxanthellae in the thermal tolerance of corals: a "nugget of hope" for coral reefs in an era of climate change. *Proc. Royal Soc. B.* 273, 2305–2312. doi: 10.1098/rspb.2006.3567

Brading, P., Warner, M. E., Davey, P., Smith, D. J., Achterberg, E. P., and Suggett, D. J. (2011). Differential effects of ocean acidification on growth and photosynthesis among phylotypes of *Symbiodinium* (*Dinophyceae*). *Limnol. Oceanogr.* 56, 927–938. doi: 10.4319/lo.2012.57.4.1255

Burke, L., Reytar, K., Spalding, M., and Perry, A. (2011). *Reefs at risk revisited*. Washington, DC: World Resources Institute, 114.

Cai, W. J., Ma, Y., Hopkinson, B. M., Grottoli, A. G., Warner, M. E., Ding, Q., et al. (2016). Microelectrode characterization of coral daytime interior pH and carbonate chemistry. *Nat. Commun.* 7:11144. doi: 10.1038/ ncomms11144

Cantin, N. E., Cohen, A. L., Karnauskas, K. B., Tarrant, A. M., and McCorkle, D. C. (2010). Ocean warming slows coral growth in the central Red Sea. *Science* 329, 322–325. doi: 10.1126/science.1190182

Carilli, J. E., Norris, R. D., Black, B. A., Walsh, S. M., and McField, M. (2009). Local stressors reduce coral resilience to bleaching. *PLoS One* 4:e6324. doi: 10.1371/journal.pone.0006324

Chou, L. M., Tuan, V. S., Philreefs, Yeemin, T., Cabanban, A., Suharsono, et al. (2002). "Status of Southeast Asia coral reefs," in *Status of Coral Reefs of the World. GCRMN Report*, Vol. 7, ed. C. R. Wilkinson (Townsville: Australian Institute of Marine Science), 123–152.

Cohen, A. L., and Holcomb, M. (2009). Why corals care about ocean acidification: uncovering the mechanism. *Oceanography* 22, 118–127. doi: 10.5670/oceanog.2009.102

Cohen, A. L., McCorkle, D. C., de Putron, S., Gaetani, G. A., and Rose, K. A. (2009). Morphological and compositional changes in the skeletons of new coral recruits reared in acidified seawater: insights into the biomineralization response to ocean acidification. *Geochem. Geophy. Geosy.* 10:Q07005. doi: 10.1029/2009GC002411

Conservation International. (2008). *Economic values of coral reefs, mangroves, and seagrasses: a global compilation*. Arlington, VA: Center for Applied Biodiversity Science, Conservation International.

Cooper, T. F., De'Ath, G., Fabricius, K. E., and Lough, J. M. (2008). Declining coral calcification in massive Porites in two nearshore regions of the northern Great Barrier Reef. *Glob. Change. Biol.* 14, 529–538. doi: 10.1111/j.1365-2486.2007.01520.x

Cornwall, E. C., and Hurd, C. L. (2015). Experimental design in ocean acidification research: problems and solutions. *ICES J. Mar. Sci.* 73, 572–581. doi: 10.1093/icesjms/fsv118

Cruz-Trinidad, A., Geronimo, R. C., Cabral, R. B., and Aliño, P. M. (2011). How much are the Bolinao-Anda coral reefs worth? *Ocean. Coast. Manag.* 54, 696–705. doi: 10.1016/j.ocecoaman.2011.07.002

Crook, E. D., Potts, D., Rebolledo-Vieyra, M., Hernandez, L., and Paytan, A. (2012). Calcifying coral abundance near low-pH springs: implications for future ocean acidification. *Coral Reefs* 31, 239–245. doi: 10.1007/s00338-011-0839-y

Da-Anoy, J. P., Cabaitan, P. C., and Conaco, C. (2019). Species variability in the response to elevated temperature of select corals in north-western Philippines. *J. Mar. Biol. Assoc.* 2019, 1–7. doi: 10.1017/S0025315419000158

Davies, P. S. (1989). Short-term growth measurements of corals using an accurate buoyant weighing technique. *Mar. Biol.* 101, 389–395. doi: 10.1007/BF00428135

Davies, S. W., Ries, J. B., Marchetti, A., and Castillo, K. D. (2018). Symbiodinium functional diversity in the coral *Siderastrea siderea* is influenced by thermal stress and reef environment, but not ocean acidification. *Front. Mar. Sci.* 5:150. doi: 10.3389/fmars.2018.00150

Doney, S. C., Fabry, V. J., Feely, R. A., and Kleypas, J. A. (2009). Ocean acidification: the other CO_2 problem. *Annu. Rev. Mar. Sci.* 1, 169–192. doi: 10.1146/annurev.marine.010908.163834

Doney, S. C., Ruckelshaus, M., Duffy, J. E., Barry, J. P., Chan, F., English, C. A., et al. (2012). Climate change impacts on marine ecosystems. *Annu. Rev. Mar. Sci.* 4, 11–37. doi: 10.1146/annurev-marine-041911-111611

Downs, C. A., Fauth, J. E., Halas, J. C., Dustan, P., Bemiss, J., and Woodley, C. M. (2002). Oxidative stress and seasonal coral bleaching. *Free. Radical. Biol. Med.* 33, 533–543. doi: 10.1016/S0891-5849(02)00907-3

Downs, C. A., Kramarsky-Winter, E., Martinez, J., Kushmaro, A., Woodley, C. M., Loya, Y., et al. (2009). Symbiophagy as a cellular mechanism for coral bleaching. *Autophagy* 5, 211–216. doi: 10.4161/auto.5.2.7405

Elder, L. E., and Seibel, B. A. (2015). The thermal stress response to diel vertical migration in the hyperiid amphipod *Phronimase dentaria*. *Comp. Biochem. Physiol., Part A Mol. Integr. Physiol.* 187, 20–26. doi: 10.1016/j.cbpa.2015.04.008

Escobar, M. T. L., Sotto, L. P. A., Jacinto, G. S., Benico, G. A., San Diego-McGlone, M. L., and Azanza, R. V. (2013). Eutrophic conditions during the 2010 fish kill in Bolinao and Anda, Pangasinan, Philippines. *J. Environ. Sci. Manag. Spec. Issue.* 1, 29–35.

Fabricius, K. E., Mieog, J. C., Colin, P. L., Idip, D., and van Oppen, M. J. H. (2004). Identity and diversity of coral endosymbionts (zooxanthellae) from three Palauan reefs with contrasting bleaching, temperature and shading histories. *Mol. Ecol.* 13, 2445–2458. doi: 10.1111/j.1365-294X.2004.02230.x

Feely, R. A., Doney, S. C., and Cooley, S. R. (2009). Ocean acidification: present conditions and future changes in a high-CO_2 world. *Oceanography.* 22:4. doi: 10.5670/oceanog.2009.95

Franklin, E. C., Stat, M., Pochon, X., Putnam, H. M., and Gates, R. D. (2012). GeoSymbio: a hybrid, cloud−based web application of global geospatial bioinformatics and ecoinformatics for Symbiodinium–host symbioses. *Mol. Ecol. Resour.* 12, 369–373. doi: 10.1111/j.1755-0998.2011.03081.x

Fujise, L., Yamashita, H., Suzuki, G., Sasaki, K., Liao, L. M., and Koike, K. (2014). Moderate thermal stress causes active and immediate expulsion of photosynthetically damaged zooxanthellae (*Symbiodinium*) from corals. *PLoS One* 9:e114321. doi: 10.1371/journal.pone.0114321

Gaither, M. R., Szabó, Z., Crepeau, M. W., Bird, C. E., and Toonen, R. J. (2011). Preservation of corals in salt-saturated DMSO buffer is superior to ethanol for PCR experiments. *Coral Reefs* 30, 329–333. doi: 10.1007/s00338-010-0687-1

Gates, R. D., and Edmunds, P. J. (1999). The physiological mechanisms of acclimatization in tropical reef corals. *Am. Zool.* 39, 30–43. doi: 10.1093/icb/39.1.30

Gattuso, J. P., Hoegh-Guldberg, O., and Pörtner, H. O. (2014). "Cross-chapter box on coral reefs," in *Climate Change 2014: Impacts, Adaptation, and Vulnerability Part A: Global and Sectoral Aspects Contribution of Working Group II to the Fifth Assessment Report of the Intergovernmental Panel of Climate Change*, eds C. B. Field, V. R. Barros, D. J. Dokken, K. J. Mach, M. D. Mastrandrea, and T. E. Bilir (New York, NY: Cambridge University Press), 97–100.

Glynn, P. W. (1993). Coral reef bleaching: ecological perspectives. *Coral Reefs* 12, 1–17. doi: 10.1007/BF00303779

Gomez, E. D., Aliño, P. M., Yap, H. T., and Licuanan, W. Y. (1994). A review of the status of Philippine reefs. *Mar. Pollut. Bull.* 29, 62–68. doi: 10.1016/0025-326X(94)90427- 8

Goreau, T., McClanahan, T., Hayes, R., and Strong, A. L. (2000). Conservation of coral reefs after the 1998 global bleaching event. *Conserv. Biol.* 14, 5–15. doi: 10.1046/j.1523-1739.2000.00011.x

Grottoli, A. G., Rodrigues, L. J., and Juarez, C. (2004). Lipids and stable carbon isotopes in two species of Hawaiian corals, *Porites compressa* and *Montipora verrucosa*, following a bleaching event. *Mar. Biol.* 145, 621–631. doi: 10.1007/s00227-004-1337-3

Grottoli, A. G., Warner, M. E., Levas, S. J., Aschaffenburg, M. D., Schoepf, V., Baumann, J., et al. (2014). The cumulative impact of annual coral bleaching can turn some coral species winners into losers. *Glob. Chang. Biol.* 20, 3823–3833. doi: 10.1111/gcb.12658

Gruber, N., Clement, D., Carter, B. R., Feely, R. A., van Heuven, S., Hoppema, M., et al. (2019). The oceanic sink for anthropogenic CO_2 from 1994 to 2007. *Science* 363, 1193–1199. doi: 10.1126/science.aau5153

Guzman, C., and Conaco, C. (2016). Gene expression dynamics accompanying the sponge thermal stress response. *PLoS One* 11:e0165368. doi: 10.1371/journal.pone.0165368

Hennige, S., Roberts, J. M., and Williamson, P. (eds) (2014). *An updated synthesis of the impacts of ocean acidification on marine biodiversity*. Technical Series No. 75, Montreal: Secretariat of the Convention on Biological Diversity, 99.

Hoegh-Guldberg, O., Mumby, P. J., Hooten, A. J., Steneck, R. S., Greenfield, P., Gomez, E., et al. (2007). Coral reefs under rapid climate change and ocean acidification. *Science* 318, 1737–1742. doi: 10.1126/science.1152509

Hoegh-Guldberg, O., Poloczanska, E. S., Skirving, W., and Dove, S. (2017). Coral reef ecosystems under climate change and ocean acidification. *Front. Mar. Sci.* 4:158. doi: 10.3389/fmars.2017.00158

Howells, J. E., Beltran, V. H., Larsen, N. W., Bay, L. K., Willis, B. L., and van Oppen, M. J. H. (2011). Coral thermal tolerance shaped by local adaptation of photosymbionts. *Nat. Clim. Change.* 2, 116–120. doi: 10.1038/nclimate1330

Hume, B., D'Angelo, C., Burt, J., Baker, A. C., Riegl, B., and Wiedenmann, J. (2013). Corals from the Persian/Arabian Gulf as models for thermotolerant reef-builders: Prevalence of clade C3 *Symbiodinium,* host fluorescence and ex situ temperature tolerance. *Mar. Poll. Bull.* 72, 313–322. doi: 10.1016/j.marpolbul.2012.11.032

IPCC (2001). *Climate Change 2001: Synthesis Report. A Contribution of Working Groups I, II, and III to the Third Assessment Report of the Intergovernmental Panel on Climate Change*, eds R. T. Watson and Core Writing Team (Cambridge: Cambridge University Press), 398.

IPCC (2014). "Climate change 2014: synthesis report," in *part B: regional aspects. Contribution of working groups I, II and III to the fifth assessment report of the Intergovernmental Panel on Climate Change*, eds R. K. Pachauri and L. A. Meyer (Geneva: IPCC), 151.

Johannes, R. E., and Wiebe, W. J. (1970). Method for determination of coral tissue biomass Composition. *Limnol. Oceanogr.* 15, 822–824. doi: 10.4319/lo.1970.15.5.0822

Jokiel, P. L., Maragos, J. E., and Franzisket, L. (1978). "Coral growth: buoyant weight technique," in *Coral Reefs: Research Methods*, eds D. R. Stoddart and R. E. Johannes (Paris: UNESCO monographs on oceanographic methodology), 529–542.

Jones, A. M., Berkelmans, R., van Oppen, M. J. H., Mieog, J. C., and Sinclair, W. (2008). A community change in the algal endosymbionts of a scleractinian coral following a natural bleaching event: field evidence of acclimatization. *Proc. Royal Soc. B.* 275, 1359–1365. doi: 10.1098/rspb.2008.0069

Kaniewska, P., Campbell, P. R., Kline, D. I., Rodriguez-Lanetty, M., Miller, D. J., Dove, S., et al. (2012). Major cellular and physiological impacts of ocean acidification on a reef building coral. *PLoS One* 7:e34659. doi: 10.1371/journal.pone.0034659

Kavousi, J., Reimer, J. D., Tanaka, Y., and Nakamura, T. (2015). Colony-specific investigations reveal highly variable responses among individual corals to ocean acidification and warming. *Mar. Environ. Res.* 109, 9–20. doi: 10.1016/j.marenvres.2015.05.004

Kinzie, R. A. (1999). Sex, symbiosis and coral communities. *Am. Zool.* 39, 80–91. doi: 10.1093/ICB/39.1.80

Kleypas, J. A., and Langdon, C. (2006). Coral reefs and changing seawater chemistry in Coral reefs and climate change: science and management. AGU monograph series, coastal and estuarine studies. *Am. Geophys.* 61, 73–110. doi: 10.1029/61CE06

Langdon, C., Gattuso, J. P., and Andersson, A. (2010). "Measurements of calcification and dissolution of benthic organisms and communities," in *Guide to Best Practices for Ocean Acidification Research and Data Reporting*, eds U. Riebesell, V. J. Fabry, L. Hansson, and J.-P. Gattuso (Luxembourg: Publications Office of the European Union), 213–232. doi: 10.7717/peerj.411

Lubarsky, K. A., Silbiger, N. J., and Donahue, M. J. (2018). Effects of submarine groundwater discharge on coral accretion and bioerosion on two shallow reef flats. *Limnol. Oceanogr.* 63, 1660–1676. doi: 10.1002/lno.10799

Lagumen, M. C. T. (2017). *Spatial and Temporal Variability of Carbonate Parameters in Bolinao-Anda, Pangasinan*. MSc, Philippines: University of the Philippines.

LaJeunesse, T. C. (2002). Diversity and community structure of symbiotic dinoflagellates from Caribbean coral reefs. *Mar. Biol.* 141, 387–400. doi: 10.1007/s00227-002-0829-2

LaJeunesse, T. C., Bhagooli, R., Hidaka, M., DeVantier, L., Done, T., Schmidt, G. W., et al. (2004). Closely related *Symbiodinium* spp. differ in relative dominance in coral reef host communities across environmental, latitudinal and biogeographic gradients. *Mar. Ecol. Progr. Ser.* 284, 147–161. doi: 10.3354/meps284147

LaJeunesse, T. C., Pettay, D. T., Sampayo, E. M., Phongsuwan, N., Brown, B., Obura, D. O., et al. (2010). Long-standing environmental conditions, geographic isolation and hostsymbiont specificity influence the relative ecological dominace and genetic diversification of coral endosymbionts in the genus *Symbiodinium*. *J. Biogeogr.* 37, 785–800. doi: 10.1111/j.1365-2699.2010.02273.x

Leder, J. J., Szmant, A. M., and Swart, P. K. (1991). The effect of prolonged 'bleaching' on skeletal banding and stable isotopic composition in *Montastrea annularis*. *Coral Reefs* 10, 19–27. doi: 10.1007/BF00301902

Lee, E. T. (1992). *Statistical Methods for Survival Data Analysis*, 2nd Edn. New York, NY: John Wiley & Sons.

LeGresley, M., and McDermott, G. (2010). "Counting chamber methods for quantitative phytoplankton analysis – haemocytometer, Palmer-Maloney cell and Sedgewick-Rafter cell," in *Microscopic and Molecular Methods for Quantitative Phytoplankton Analysis*, eds B. Karlson, C. Cusack, and E. Bresnan (Paris: UNESCO), 25–30.

Lesser, M. P. (1996). Elevated temperatures and ultraviolet radiation cause oxidative stress and inhibit photosynthesis in symbiotic dinoflagellates. *Limnol. Oceanogr.* 41, 271–283. doi: 10.4319/LO.1996.41.2.0271

Lesser, M. P. (1997). Oxidative stress causes coral bleaching during exposure to elevated temperatures. *Coral Reefs* 16, 187–192. doi: 10.1007/s003380050073

Lesser, M. P., and Farrell, J. H. (2004). Exposure to solar radiation increases damage to both host tissues and algal symbionts of corals during thermal stress. *Coral Reefs* 23, 367–377. doi: 10.1007/s00338-004-0392-z

Lewis, E., and Wallace, D. W. R. (1998). *Program developed for CO_2 system calculations. Carbon Dioxide Information Analysis Center, Oak Ridge National Laboratory*. Oak Ridge, TN: U.S. Dept. of Energy, doi: 10.15485/1464255

Licuanan, W. Y., Robles, R., and Reyes, M. (2019). Status and recent trends in coral reefs of the Philippines. *Mar. Pollut. Bull.* 142, 544–550. doi: 10 1016/j.marpolbul.2019.04.013

Lough, J. M., and Cantin, N. E. (2014). Perspectives on massive coral growth rates in a changing ocean. *Biol. Bull.* 226, 187–202. doi: 10.1086/BBLv226n3p187

Maboloc, E. A., Jamodiong, E. A., and Villanueva, R. D. (2015). Reproductive biology and larval development of the scleractinian corals *F. colemani* and *F. abdita* (Faviidae) in northwestern Philippines. *Invertebr. Reprod. Dev.* 60, 1–11. doi: 10.1080/07924259.2015.1086829

Manullang, C., Millyaningrum, I. H., Iguchi, A., Miyagi, A., Tanaka, Y., Nojiri, Y., et al. (2020). Responses of branching reef corals *Acropora digitifera* and *Montipora digitata* to elevated temperature and pCO_2. *Peer J.* 8:e10562. doi: 10.7717/peerj.10562

McClanahan, T. R. (2004). The relationship between bleaching and mortality of common corals. *Mar. Biol.* 144, 1239–1245. doi: 10.1007/s00227-003-1271-9

McCulloch, M., D'Olivo, J., Falter, J., Holcomb, M., and Trotter, J. A. (2017). Coral calcification in a changing World and the interactive dynamics of pH and DIC upregulation. *Nat. Commun.* 8:15686. doi: 10.1038/ncomms15686

McCulloch, M., Falter, J., Trotter, J., and Montagna, P. (2012). Coral resilience to ocean acidification and global warming through pH up-regulation. *Nat. Clim. Change* 2, 623–627. doi: 10.1038/nclimate1473

Meesters, E. H., and Bak, R. P. M. (1993). Effects of coral bleaching on tissue regeneration potential and colony survival. *Mar. Ecol. Progr. Ser.* 96, 189–198. doi: 10.3354/meps096189

Mehrbach, C., Culberson, C. H., Hawley, J. E., and Pytkowicz, R. N. (1973). Measurement of the apparent dissociation constants of carbonic acid in seawater at atmospheric pressure. *Limnol. Oceanogr.* 18, 897–907. doi: 10.4319/lo.1973.18.6.0897

Mieog, J. C., van Oppen, M. J. H., Berkelmans, R., Stam, W. T., and Olsen, J. L. (2009). Quantification of algal endosymbionts (*Symbiodinium*) in coral tissue using real-time PCR. *Mol. Ecol. Res.* 9, 74–82. doi: 10.1111/j.1755-0998.2008.02222.x

Nakamura, T., Van Woesik, R., and Yamasaki, H. (2005). Photoinhibition of photosynthesis is reduced by water flow in the reef-building coral *Acropora digitifera*. *Mar. Ecol. Prog. Ser.* 301, 109–118. doi: 10.3354/meps301109

NOAA (2015). *National Centers for Environmental Information, State of the Climate: Global Analysis for Annual 2015*. Available online at: http://www.ncdc.noaa.gov/sotc/global/201513

Noonan, S. H. C., Fabricius, K. E., and Humphrey, C. (2013). *Symbiodinium* community composition in scleractinian corals is not affected by life-long exposure to elevated carbon dioxide. *PLoS One* 8:e63985. doi: 10.1371/journal.pone.0063985

Ogawa, D., Bobeszko, T., Ainsworth, T., and Leggat, W. (2013). The combined effects of temperature and CO_2 lead to altered gene expression in *Acropora aspera*. *Coral Reefs* 32, 895–907. doi: 10.1007/s00338-013-1046-9

Ohki, S., Irie, T., Inoue, M., Shinmen, K., Kawahata, H., Nakamura, T., et al. (2013). Symbiosis increases coral tolerance to ocean acidification. *Biogeosci. Discuss.* 10, 7013–7030. doi: 10.5194/bgd-10-7013-2013

Palumbi, S. R., Barshis, D. J., Traylor-Knowles, N., and Bay, R. A. (2014). Mechanisms of reef coral resistance to future climate change. *Science* 344, 895–898. doi: 10.1126/science.1251336

Parkinson, J. E., Banaszak, A. T., Altman, N. S., LaJeunesse, T. C., and Baums, I. B. (2015). Intraspecific diversity among partners drives functional variation in coral symbioses. *Sci. Rep.* 5:15667. doi: 10.1038/srep15667

Peñaflor, E. L., Skirving, W. J., Strong, A. E., Heron, S. F., and David, L. T. (2009). Sea-surface temperature and thermal stress in the Coral Triangle over the past two decades. *Coral Reefs* 28:841. doi: 10.1007/s00338-009-0522-8

Perez, S., and Weis, V. M. (2006). Nitric oxide and cnidarian bleaching: an eviction notice mediates the breakdown of symbiosis. *J. Exp. Biol.* 209, 2804–2810. doi: 10.1242/jeb.02309

Quimpo, T. J. R., Requilme, J. N. C., Gomez, E. J., Sayco, S. L. G., Tolentino, M. P. S., and Cabaitan, P. C. (2020). Low coral bleaching prevalence at the Bolinao-Anda Reef Complex, northwestern Philippines during the 2016 thermal stress event. *Mar. Pollut. Bull.* 160:111567. doi: 10.1016/j.marpolbul.2020.111567

Reynaud, S., Leclercq, N., Romaine-Lioud, S., Ferrier-Pagès, C., Jaubert, J., and Gattuso, J. P. (2003). Interacting effects of CO_2 partial pressure and temperature on photosynthesis and calcification in a scleractinian coral. *Glob. Change Biol.* 9, 1660–1668. doi: 10.1046/j.1365-2486.2003.00678.x

Richier, S., Furla, P., Plantivaux, A., Merle, P.-L., and Allemand, D. (2005). Symbiosis-induced adaptation to oxidative stress. *J. Exp. Biol.* 208, 277–285. doi: 10.1242/jeb.01368

Roberts, C. M., McClean, C. J., Veron, J. E. N., Hawkins, J. P., Allen, G. R., McAllister, D. E., et al. (2002). Marine biodiversity hotspots and conservation priorities for tropical reefs. *Science* 295, 1280–1284. doi: 10.1126/science.1067728

Roth, M. S. (2014). The engine of the reef: photobiology of the coral-algal symbiosis. *Front. Microbiol.* 5:422. doi: 10.3389/fmicb.2014.00422

Sabine, L., Feely, R. A., Gruber, N., Key, R. M., Lee, K., Bullister, J. L., et al. (2004). The oceanic sink for anthropogenic CO_2. *Science* 305:367. doi: 10.1126/science.1097403

San Diego-McGlone, M. L., Azanza, R. V., Villanoy, C. L., and Jacinto, G. S. (2008). Eutrophic waters, algal bloom and fish kill in fish farming areas in Bolinao, Pangasinan, Philippines. *Mar. Poll. Bull.* 57, 295–301. doi: 10.1016/j.marpolbul.2008.03.028

Schreiber, U., Schliwa, U., and Bilger, W. (1986). Continuous recording of photochemical and non-photochemical chlorophyll fluorescence quenching with a new type of modulation fluorometer. *Photosyn. Res.* 10, 51–62. doi: 10.1007/BF00024185

Siebeck, U. E., Marshall, N. J., Klüter, A., and Hoegh-Guldberg, O. (2006). Monitoring coral bleaching using a colour reference card. *Coral Reefs* 25, 453–460. doi: 10.1007/s00338-006-0123-8

Smith, D. J., Suggett, D. J., and Baker, N. R. (2005). Is photoinhibition of zooxanthellae photosynthesis the primary cause of thermal bleaching in corals? *Glob. Chang. Biol.* 11, 1–11. doi: 10.1111/j.1529-8817.2003.00895.x

Somero, G. N. (2010). The physiology of climate change: how potentials for acclimatization and genetic adaptation will determine "winners" and "losers". *J. Exp. Biol.* 213, 912–920. doi: 10.1242/jeb.037473

Stat, M., and Gates, R. D. (2011). Clade D *Symbiodinium* in scleractinian corals: a "nugget" of hope, a selfish opportunist, an ominous sign, or all of the above. *J. Mar. Biol.* 730, 1–9. doi: 10.1155/2011/730715

Stat, M., Loh, W. K. W., LaJeunesse, T. C., Hoegh-Guldberg, O., and Carter, D. A. (2009). Stability of coral–endosymbiont associations during and after a thermal stress event in the southern Great Barrier Reef. *Coral Reefs* 28, 709–713. doi: 10.1007/s00338-009-0509-5

Stimson, J., and Kinzie, R. A. I. I. I. (1991). The temporal pattern and rate of release of zooxanthellae from the reef coral *Pocillopora damicornis* (Linnaeus) under nitrogen enrichment and control conditions. *J. Exp. Mar. Biol. Ecol.* 153, 63–74. doi: 10.1016/S0022-0981(05)80006-1

Strahl, J., Francis, D., Doyle, J., Humphrey, C., and Fabricius, K. (2016). Biochemical responses to ocean acidification contrast between tropical corals with high and low abundances at volcanic carbon dioxide seeps. *ICES. J. Mar. Sci.* 73, 897–909. doi: 10.1093/icesjms/fsv194

Takahashi, A., and Kurihara, H. (2013). Ocean acidification does not affect the physiology of the tropical coral *Acropora digitifera* during a 5-week experiment. *Coral Reefs* 32, 305–314. doi: 10.1007/s00338-012-0979-8

Tambutte, S., Holcomb, M., Ferrier-Pages, C., Reynaud, S., Tambutte, E., Zoccola, D., et al. (2011). Coral biomineralization: from the gene to the environment. *J. Exp. Mar. Biol. Ecol.* 408, 58–78. doi: 10.1016/j.jembe.2011.07.026

Tanzil, J. T. I., Brown, B. E., Tudhope, A. W., and Dunne, R. P. (2009). Decline in skeletal growth of the coral *Porites lutea* from the Andaman Sea, South Thailand between 1984 and 2005. *Coral Reefs* 28, 519–528. doi: 10.1007/s00338-008-0457-5

Thornhill, D. J., Rotjan, R. D., Todd, B. D., Chilcoat, G. C., Iglesias-Prieto, R., Kemp, D. W., et al. (2011). A connection between colony biomass and death in Caribbean reef-building corals. *PLoS One* 6:e29535. doi: 10.1371/journal.pone.0029535

Veal, C. J., Carmi, M., Fine, M., and Hoegh-Guldberg, O. (2010). Increasing the accuracy of surface area estimation using single wax dipping of coral fragments. *Coral Reefs* 29, 893–897. doi: 10.1007/s00338-010-0647-9

Venn, A. A., Loram, J. E., and Douglas, A. E. (2008). Photosynthetic symbioses in animals. *J. Exp. Bot.* 59, 1069–1080. doi: 10.1093/jxb/erm328

Venn, A. A., Tambutté, E., Holcomb, M., Laurent, J., Allemand, D., and Tambutte, S. (2013). Impact of seawater acidification on pH at the tissue-skeleton interface and calcification in reef corals. *Proc. Nat. Acad. Sci.* 110, 1634–1639. doi: 10.1073/pnas.1216153110

Veron, J. E. N. (2000). *Corals of the world*. Townsville: Australian Institute of Marine Science Australia.

Weis, V. (2008). Cellular mechanisms of Cnidarian bleaching: stress causes the collapse of symbiosis. *J. Exp. Biol.* 211, 3059–3066. doi: 10.1242/jeb.009597

Conflict of Interest: The authors declare that the research was conducted in the absence of any commercial or financial relationships that could be construed as a potential conflict of interest.

frontiers
in Marine Science

ORIGINAL RESEARCH
published: 06 October 2021
doi: 10.3389/fmars.2021.719691

Spatial Planning Insights for Philippine Coral Reef Conservation Using Larval Connectivity Networks

***Patrick R. Pata*[1,2,3]* *and Aletta T. Yñiguez*[1]**

[1] Marine Science Institute, University of the Philippines Diliman, Quezon City, Philippines, [2] Institute for the Oceans and Fisheries, University of British Columbia, Vancouver, BC, Canada, [3] Department of Earth, Ocean and Atmospheric Sciences, University of British Columbia, Vancouver, BC, Canada

The marine habitats of the Philippines are recognized to be some of the most biodiverse systems globally yet only 1.7% of its seas are designated as marine protected areas (MPAs) with varying levels of implementation. Many of these MPAs were established based on local-scale conservation and fisheries objectives without considering larger-scale ecological connections. The connectivity of reefs through larval dispersal is important in the regional-scale resilience against anthropogenic disturbances and is considered a significant criterion in planning for MPAs. In this study, we provide insights into the delineation of ecologically connected MPA networks using larval dispersal modeling and network analysis. We characterized the network properties of the Philippine coral reefs, organized as 252 reef nodes, based on the larval connectivity networks of a branching coral, sea urchin, and grouper. We then evaluated the distribution of the existing 1,060 MPAs relative to the connectivity patterns. All reef nodes were found to be highly interconnected with a mean shortest path ranging from 1.96 to 4.06. Reef nodes were then ranked according to their relative importance in regional connectivity based on five connectivity indices. Despite the between-organism and between-index variability in rankings, there were reefs nodes, mostly located offshore and at major straits, which consistently ranked high. We found that the distribution of existing MPAs partially capture some of the regional connectivity functions but there is a spatial mismatch between the primarily coastal MPAs and the high-ranking reef nodes. Furthermore, network partitioning identified subnetworks and dispersal barriers. The existing MPAs were found to be disproportionately distributed to a few subnetworks and that the largest subnetworks do not contain the greatest number of MPAs. Considering these gaps, we suggest expanding the coverage of protected areas especially in underrepresented reef networks to meaningfully capture national-scale connectivity and meet global conservation objectives.

Keywords: connectivity, MPA network, coral reefs, conservation, graph theory

Edited by:
Yehuda Benayahu,
Tel Aviv University, Israel

Reviewed by:
Jorge MS. Gonçalves,
University of Algarve, Portugal
Tommaso Russo,
University of Rome Tor Vergata, Italy

****Correspondence:***
Patrick R. Pata
p.pata@oceans.ubc.ca

Specialty section:
This article was submitted to Marine Ecosystem Ecology, a section of the journal Frontiers in Marine Science

Received: *02 June 2021*
Accepted: *08 September 2021*
Published: *06 October 2021*

Citation:
Pata PR and Yñiguez AT (2021) Spatial Planning Insights for Philippine Coral Reef Conservation Using Larval Connectivity Networks. Front. Mar. Sci. 8:719691. doi: 10.3389/fmars.2021.719691

INTRODUCTION

Global biodiversity targets aim for the protection of at least 10% of coastal and marine areas particularly those providing important biodiversity and ecosystem services by the year 2020 (CTI-CFF [Coral Triangle Initiative on Coral reefs, Fisheries and Food Security], 2009; CBD [Convention on Biological Diversity], 2010). A key part of this is the establishment of marine protected areas (MPAs) which are actively managed areas at various levels of protection from extractive and destructive activities (TNC-WWF-CI-WCS [The Nature Conservancy, World Wildlife Fund, Conservation International and Wildlife Conservation Society], 2008). MPAs play an important role in ensuring ecological and social resilience with two general objectives of biodiversity conservation and increasing fisheries stocks (Almany et al., 2009; Harrison et al., 2012).

The Philippines house a large coral reef area (Spalding et al., 2001) that provides various ecosystem services (Burke et al., 2012; Ferrario et al., 2014). It is one of the most biodiverse systems globally (Carpenter and Springer, 2005; Gaither and Rocha, 2013; DeVantier and Turak, 2017) that can be reserves of coral reef resilience and functions (Briggs, 2005; McWilliam et al., 2018). Establishing MPAs has been a common approach in conservation and management of coral reefs in the Philippines to address declines in fish stocks (Horigue et al., 2012). In the past 30 years, over 1,800 MPAs have been designated (Cabral et al., 2014) although most of these were locally established, less than 1 km^2 in area, and not designed to be part of regional-scale ecological networks (Weeks et al., 2010; Horigue et al., 2015). Only 1.7% of the exclusive economic zone and territorial seas of the Philippines are designated as MPAs (MPAtlas, 2021) and 2.7–3.4% of coral reefs are protected in MPAs (Weeks et al., 2010). The year 2020 has passed without reaching the 10% protection goal, which may actually still be insufficient (O'Leary et al., 2016). Expanding the coverage of protection is now more than ever an urgent endeavor considering the rapid decline in coral cover in the Philippines and its importance for global biodiversity (Licuanan et al., 2019). Importantly, determining which areas to protect should ideally be systematically guided by a set of ecological indicators in order to increase the likelihood of contributing to conservation objectives. These include habitat quality, habitat representativeness, biodiversity, special interest species, ecological connectivity, social connectivity, coastal resource usage, current and future threats, social acceptance, and potential ecosystem services (White et al., 2006; Kininmonth et al., 2011; Cabral et al., 2015, 2016; Horigue et al., 2015).

A key criterion in marine conservation is ecological connectivity (Parsons et al., 2014) through the dispersal of larval organisms between distant populations (Cowen and Sponaugle, 2009; Jones et al., 2009). Connectivity is especially important in promoting regional-scale resilience against anthropogenic disturbances (Hock et al., 2017; O'Leary et al., 2017). Despite this, connectivity is the least understood aspect and is seldom considered in designing MPAs in practice (Botsford et al., 2009). Such is the case for the Philippines where there is available regional information on habitat coverage and habitat quality to aid the siting of reserves (Cabral et al., 2015), but there is a knowledge gap regarding connectivity. Some studies have utilized connectivity information to provide insights on protection within subregions in the Philippines (Abesamis et al., 2016; Deauna et al., 2021) but a national-scale assessment is still needed.

The principal bottleneck in obtaining connectivity information is the difficulty in observing and estimating connectivity itself because eggs and larvae are microscopic and pre-recruitment mortality is high (Cowen and Sponaugle, 2009; Peck and Hufnagl, 2012). Empirical methods provide valuable observations of realized connectivity (Botsford et al., 2009; Cowen and Sponaugle, 2009) but these tend to span spatial and temporal scales that may not be sufficient for regional-scale reserve siting (Botsford et al., 2009; McCook et al., 2009; Berumen et al., 2012). Biophysical modeling of larval dispersal provides a complementary method (Werner et al., 2007; Botsford et al., 2009; Cowen and Sponaugle, 2009) through simulating the general dynamics of connectivity of large spatial domains for several different organisms.

A graph theoretical approach, i.e., network analysis, of connectivity model results has been useful in nominating potential areas for protection (Kininmonth et al., 2011; Holstein et al., 2014; Deauna et al., 2021). The regional benefits of connectivity are asymmetric (Munguia-Vega et al., 2014) and various indices derived from characteristics of connectivity networks help to quantify different ecological functions of connectivity (Betancur et al., 2011; Grorud-Colvert et al., 2014). Additionally, connectivity networks can be partitioned into subnetworks of more strongly ecologically interconnected reefs that more likely share the regional benefits of protection (Thomas et al., 2014). A network analysis of connectivity is appropriate for Philippine coral reefs which have a complex spatial distribution (Licuanan et al., 2019). These reefs are found in multiple basins separated by narrow straits and subjected to seasonally variable circulation patterns resulting in the asymmetric dispersal of larvae (Melbourne-Thomas et al., 2011; Pata and Yñiguez, 2019). In this study, we aimed to characterize the regional connectivity properties of the Philippine coral reef network and delineate interconnected subnetworks. Furthermore, we evaluated the distribution of currently designated MPAs with regards to regional ecological connectivity and identified potential areas where protection can be expanded.

METHODOLOGY

Data Sources

The connectivity data used was derived from a biophysical dispersal model of the larger domain of the North Indo-West Pacific coral reefs (Pata and Yñiguez, 2019). The model was driven by the surface circulation of the global Hybrid Coordinate Modeling System (Chassignet et al., 2007). Three larval coral reef organisms were simulated: a broadcast-spawning branching coral (*Acropora millepora*), a reef-associated sea urchin (*Tripneustes gratilla*), and a predatory grouper (*Epinephelus* sp.). All three organisms vary in early life-history characteristics and are ecologically and economically important in Philippine coral reefs. The branching coral larva has a shorter pelagic larval duration (PLD) than the other organisms. The branching coral and sea urchin larva were simulated to be passive drifters. The grouper larva was simulated to have a swimming behavior directed toward reefs after reaching their flexion age. The connectivity data was validated to have dispersal kernels within the range of empirical estimates and have connectivity ranges concordant with inferred dispersal barriers from population genetic studies (Pata and Yñiguez, 2019).

The raw settlement probability matrices for this analysis represent averages across the spawning period of each organism and three simulation years (2011, 2013, 2015). The reef cells were further averaged based on the clustering of covarying regional spatiotemporal patterns (Pata and Yñiguez, 2019) resulting in 406 reef nodes within the North Indo-West Pacific. A subset of 252 reef nodes found inside the Philippine exclusive economic zone and territorial seas (Flanders Marine Institute, 2019) were used in this analysis (**Figure 1**). The 252 × 252-node settlement probability matrices were transformed to a network by dividing the rows of the matrix with the horizontal sum, i.e., the total settlement probability of each reef node. The network edges thus represent the proportion of successfully settling larvae from a source node arriving at a sink node. The previous analysis of this dataset has demonstrated that there is high seasonal and interannual variability in connectivity patterns but the relative spatial patterns are similar between closely located reefs within each node (Pata and Yñiguez, 2019). As this study used weighted network edges, this variability was reflected in the relative edge strength between nodes.

MPA data was obtained from the MPA Support Network database (Cabral et al., 2014) in March 2017. Only MPAs with known geographic locations were included in the analysis. We also excluded MPAs around the Tañon Strait in the central Philippines because this area was not resolved in the connectivity model (Pata and Yñiguez, 2019). This resulted in 1,060 MPAs out of the 1,893 MPAs recorded in the database.

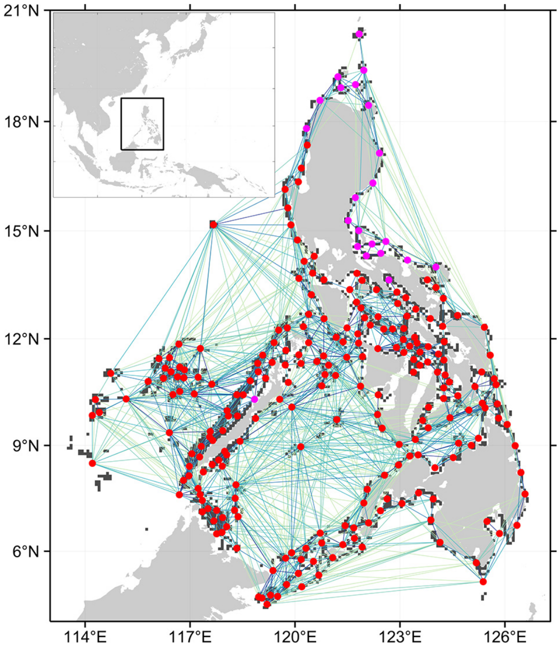

FIGURE 1 | Connectivity network for branching coral. Only the top 50% of connections are shown, darker lines are stronger connections. Circles represent the centroids of the 252 reef nodes within the Philippine EEZ. Red circles are nodes that are part of the largest strongly connected component (SCC) when the weakest 50% of connections are removed. Purple circles are nodes that are unidirectionally connected to the main SCC.

Network Topology

Descriptive network properties on strongly connected components (SCC), shortest paths, and network diameter were calculated for each of the organism networks. SCCs are the group of nodes in which there is a path to and from each node in the network (Holstein et al., 2014). A region in which all nodes are connected will have an SCC of 1. If more than 1 SCC is found, potential dispersal barriers may exist as the other SCCs may either be fully disconnected or unidirectionally connected to the main SCC containing the greatest number of nodes. Within an SCC, shortest paths are the minimum number of edges which connect two nodes. The longest shortest path is the diameter of an SCC. The shortest path represents the most efficient and probable path connecting a source node to a sink node. The diameter represents the minimum number of steps that can connect any two nodes in the network. Shorter mean shortest paths and diameters indicate a more interconnected network. We recalculated the network topology after retaining the top 75 and 50% of the strongest connections in each network as a sensitivity analysis on the connectedness of the nodes.

Connectivity Indices

The connectivity indices calculated for the reef nodes within the network are betweenness centrality, source-sink index, source diversity, and sink diversity. This is a similar set of indices used in the analysis of a Caribbean coral reef network (Holstein et al., 2014). For comparison with the other indices, we also calculated the local retention, or the proportion of larvae spawned from each node that settled in the same node.

Betweenness centrality (BC) accounts for the number of shortest paths passing through each node (Treml et al., 2008). This quantifies the importance of the reef node in maintaining the integrity of the network (Kough and Paris, 2015). In this study, the edges were weighted by the strength of the connection and consequently, the shortest path was then transformed to the most reliable path (MRP). The MRP was identified as the highest value of the product notation of all weighted paths connecting two nodes (Hock and Mumby, 2015). The BC of a node i was calculated from,

$$BC_i = \frac{\sigma(i)}{\sigma}, \tag{1}$$

in which $\sigma(i)$ is the sum of all MRPs that pass through node i and σ is the total number of most reliable paths connecting all pairs of nodes (Holstein et al., 2014). Nodes which are central to the network are efficient stepping stones or corridors in larval dispersal (Munguia-Vega et al., 2014) making these ideal areas for protection to preserve network functioning (Kininmonth et al., 2011).

The source-sink index (SSI) of a node i was calculated from,

$$SSI_i = \frac{P_{exp} - P_{imp}}{P_{exp} + P_{imp}}, \tag{2}$$

in which P_{exp} is the summation of all outgoing edge weights from node i and P_{imp} is the summation of all incoming edge weights to node i (Holstein et al., 2014). Thus, a positive SSI indicates that the node is a net source. Conversely, a negative SSI indicates that the node is a net sink. Areas which disproportionately act as strong sources could provide subsidies to other areas making them ideal candidates for protection (Almany et al., 2009) since protection benefits would likely extend beyond the local domain. Disproportionate sinks receive more larvae than it provides suggesting that population growth may be more of a function of external larval supply. In this analysis, we considered a positive SSI as more ideal. The SSI is not able to account for the range of the exports and imports of each node (e.g., a strong source node providing large subsidies to a single node). Thus, calculating source and sink diversity complements the source-sink index.

The source diversity (SoD) of a node accounts for the richness and evenness of its source nodes computed from a modified Shannon's diversity index (Holstein et al., 2014). Thus, the SoD of the sink node *si* was calculated from,

$$SoD_{si} = -\sum_{i=1}^{so} p_i \ln p_i, \tag{3}$$

in which *so* are all the source nodes connected to node *si* and p_i is the weight of each incoming edge to node *si* normalized with the sum of all its incoming edges. Areas which have multiple larval sources, i.e., have high SoD, are more likely to be resilient due to the resulting high genetic diversity and thus is more likely to experience the rescue effect compared to areas with low SoD which are more likely sensitive to local population disruptions (Holstein et al., 2014; Dorman et al., 2016).

The sink diversity (SiD) was calculated using the inverse edge directions wherein,

$$SiD_{so} = -\sum_{j=1}^{si} p_j \ln p_j, \tag{4}$$

in which p_j is the weight of each outgoing edge from node *so* normalized with the sum of all its outgoing edges. The SiD index tries to identify sources that maximize the spread of successfully settling larvae to the greatest number of areas in terms of richness and evenness. Areas which subsidize more reefs likely contribute more to the network since connectivity benefits would be spread out.

The connectivity index scores were compared between the three organism networks using Pearson's correlation to identify similarities in network importance across larval types. To identify associations in index scores, Pearson's correlation was also used for pairwise comparisons between connectivity indices for each organism network. Reef nodes were then ranked for each organism network and connectivity index. The overall reef rankings were determined by calculating the mean and standard deviation of rankings.

Deriving Reef Subnetworks

Subnetworks which represent ecologically interconnected reefs were identified by applying the Leiden Algorithm (Traag et al., 2018) using the Constant Potts Model (CPM) (Traag et al., 2013). A multiplex approach that combines networks with similar nodes but with different layers of edges (Mucha et al., 2010; Traag et al., 2018) was used to determine the subnetworks that are consistent across the three organism networks. The advantage of using CPM is that it provides a natural interpretation where nodes within the same community or subnetwork have an average dispersal probability greater than a threshold resolution parameter, while nodes from different subnetworks are connected by less than that resolution parameter (Thomas et al., 2014). The resulting subnetworks represent ecologically separate reef communities, based on the likelihood of larval dispersal, which are more internally interconnected with each other than with reefs outside the subnetwork. The size of the subnetworks is dependent on the resolution parameter used to partition the network. The appropriate resolution parameter was determined using bisection profiles (Traag et al., 2013) in which plateaus in the proportion of connections between subnetworks indicate local optima in partitioning. A sensitivity analysis of the partitioning was done by deriving eight bisection profiles based on the multiplex network for each of the three organism networks, and when using unweighted and weighted network edges. Network topology properties were recalculated to characterize and compare the subnetworks.

Comparing Marine Protected Area Locations With Network Features

The 1,060 MPAs were matched with reef nodes through a nearest neighbor search between the MPA longitude and latitude positions and the reef cell centroids. Many of the MPAs do not have information on the MPA area. Thus, MPAs were analyzed as individual sites and the relative sizes of the MPAs were not accounted for. We assumed that the spatial density of individual MPAs reflect management efforts for different areas. The distribution of the MPAs were then evaluated in relation to each connectivity index and network, and then to the overall ranking of reef nodes. The number of MPAs were also tallied for each of the subnetworks to determine the proportional distribution of the MPAs across subnetworks and discern if there are regional gaps in the distribution of MPAs.

The CPM was analyzed in Python 3.6 using the leidenalg package (Traag et al., 2018). All other numerical analyses were done in MATLAB 2019a.

RESULTS

Philippine Network Topology

The SCC of the full network for each organism is one (**Table 1**) which indicates that there is a path connecting all nodes in the network. The coral network has a longer mean shortest path and diameter compared to the other networks. This implies that it takes longer for coral larvae spawned at any node to reach farther nodes. The urchin and grouper networks have similar topologies with the grouper network having a slightly shorter mean shortest path. All three networks were robust to the removal of lower probability connections based on the sensitivity analysis. When only the top 75% of connections were analyzed, a single node was excluded in the main SCC of the coral network. This is similar to the SCC of the sea urchin and grouper networks when the top 50% of connections were analyzed. The coral network

TABLE 1 | Topology of the three organism-specific networks.

	Full network			Top 75% of connections			Top 50% of connections		
Network properties	***C***	***U***	***G***	***C***	***U***	***G***	***C***	***U***	***G***
Number of strongly connected components (SCC)	1	1	1	2	1	1	7	2	2
Number of nodes in main SCC	252	252	252	251	252	252	230	251	251
Mean shortest path of the main SCC	4.06	2.11	1.96	4.82	2.41	2.26	5.42	3.03	2.77
Standard deviation of shortest paths	2.13	0.92	0.85	2.81	1.10	1.05	3.07	1.52	1.35
Longest shortest path (diameter)	12.00	6.00	6.00	17.00	8.00	7.00	18.00	10.00	9.00

The full network means that all connections were retained in the analysis. The results were reanalyzed by retaining the top 75 and 50% strongest connections in each organism network. ***C****, Branching coral;* ***U****, Sea urchin;* ***G****, Grouper.*

TABLE 2 | Pearson coefficient of determination (r^2) between pairs of organism networks for each index.

Networks compared	Betweenness centrality (BC)	Source strength (+SSI)	Source diversity (SoD)	Sink diversity (SiD)	Local retention (LR)
Branching coral vs. Sea urchin	0.177	0.514	0.634	0.717	0.632
Branching coral vs. Grouper	0.142	0.451	0.603	0.702	0.501
Sea urchin vs. Grouper	0.646	0.884	0.958	0.968	0.881

All relationships are significant ($p < 0.001$).

further excluded 21 nodes found at the northeastern Philippines at 50% connections (**Figure 1**). The mean shortest paths and the diameter values did not greatly increase when the weaker connections were excluded.

Connectivity Indices and Ranking of Reef Nodes

All the connectivity index scores significantly covary between organism networks. The urchin and grouper networks have the most similar index scores as indicated by the highest r^2-values for each index (**Table 2**). Among the connectivity indices, betweenness centrality scores are weakly associated between the coral and urchin and the coral and grouper networks. Overall, the three organism networks have quite similar rankings for node importance, except for betweenness centrality.

When connectivity indices were compared, most of the organism-specific pairwise correlations were either not significant or weak (**Table 3**) and the spread of the index scores were high (**Supplementary Figure 1**). Only source diversity and sink diversity had a strong positive correlation ($r = 0.73–0.77$). Local retention had a strong negative correlation with both sink diversity and source diversity ($r = −0.59–−0.75$) and moderate negative correlation with source strength ($r = −0.29–−0.39$). Because of the significant negative correlation of local retention with the other indices, local retention was excluded in calculating the overall reef node rankings across organism networks.

Despite the between-organism and between-index variability in reef node rankings, there are reefs which consistently rank high in most connectivity indices (**Figure 2**). High ranking reef nodes tend to be located offshore or at major straits separating basins. The lowest ranking nodes indicate areas that are relatively isolated from the rest of the network. These were found at embayments and mostly at the eastern side of the Philippines. Furthermore, the overall top 10% mean ranking nodes have the lowest range of standard deviation rankings (**Figure 3A**). When inspecting the characteristics of the organism-specific index rankings of the top 25% of reef nodes (**Figure 4A**), these nodes consistently rank high in source diversity and sink diversity. The top nodes rank moderately high in betweenness centrality and source strength but most of the top nodes rank low in local retention.

Half of the reef nodes (128 out of 252) had at least one associated MPA (**Figure 3B**). Most of the MPAs are concentrated in a few reef nodes in the central Philippines. Only 16 of the 63 overall top 25% reef nodes based on connectivity features

TABLE 3 | Pairwise comparison between connectivity indices for each organism network.

Indices compared	Branching coral	Sea urchin	Grouper
Betweenness centrality vs. Source strength (+SSI)	−0.06	−0.22*	−0.28*
Betweenness centrality vs. Source diversity	0.10	0.00	−0.01
Betweenness centrality vs. Sink diversity	−0.03	−0.19*	−0.17*
Source diversity vs. Sink diversity	0.73*	0.75*	0.77*
Source strength vs. Source diversity	−0.26	−0.12	−0.09
Source strength vs. Sink diversity	0.23*	0.33*	0.31*
Betweenness centrality vs. Local retention	−0.02	0.07	0.09
Source strength vs. Local retention	−0.29*	−0.39*	−0.36*
Source diversity vs. Local retention	−0.59*	−0.64*	−0.61*
Sink diversity vs. Local retention	−0.75*	−0.73*	−0.69*

*The values are Pearson correlation coefficients (r) and * denotes $p < 0.001$.*

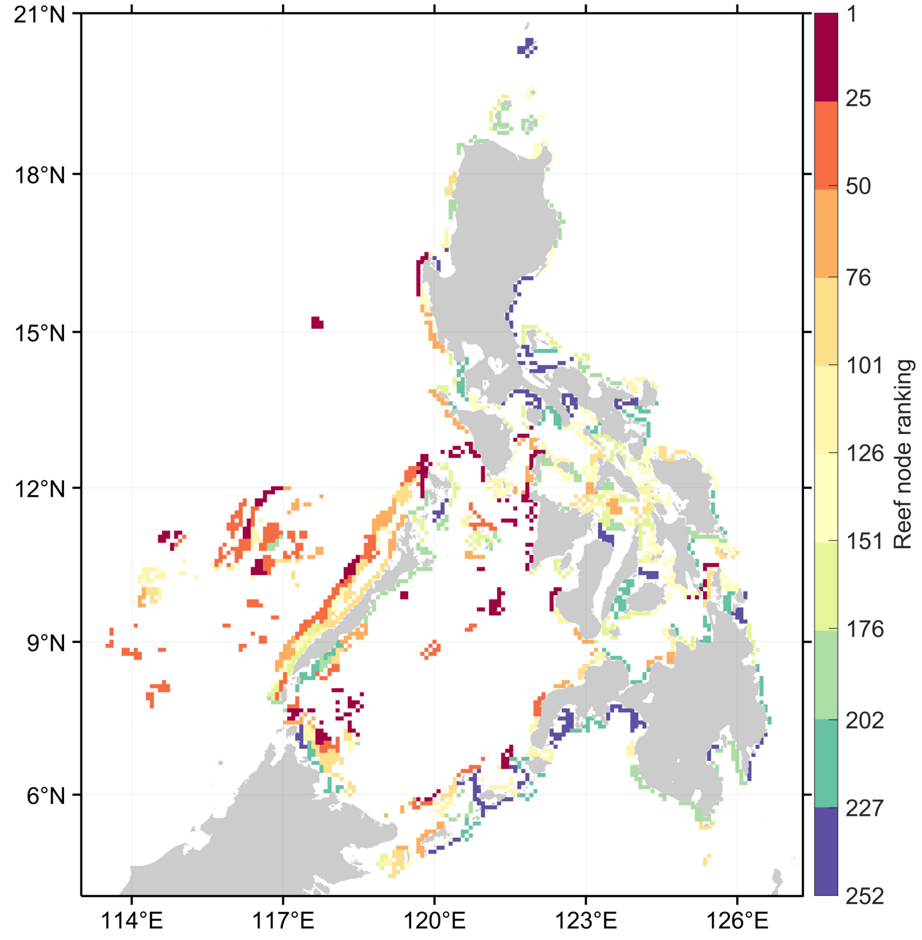

FIGURE 2 | Overall ranking of reef nodes based on the average ranking across organisms and four connectivity indices. Warm colors represent the top reef nodes that generally ranked high in most connectivity indices. Reef nodes in red are the top 10% while in purple are the bottom 10%.

have associated MPAs (**Figure 3A**). Of the 1,060 MPAs analyzed, around half are in nodes with high betweenness centrality and high source strength (**Figure 4B**). Majority of the established MPAs are found in nodes ranking the lowest in terms of source diversity and sink diversity and conversely, highest in local retention.

Philippine Reef Subnetworks

A sensitivity analysis of the multiplex partitioning of the three organism networks (**Supplementary Figure 2**) suggested that the local optimal resolution parameter values resulting in stable subnetworks are 0.0004 and 0.004. These represent the broad-scale and medium-scale subnetwork partitioning (**Figure 5**). The sensitivity analysis also demonstrated that the local optima are consistent, and the resolution parameters chosen were appropriate for the multiplex network and all the organism-specific networks. For the broad-scale subnetworks, subnetwork A consists of reefs from the West Philippine Sea, Sulu Sea, and Celebes Sea, while subnetwork B consists of reefs in the central Philippines (**Figure 5A**). Subnetwork C are reefs at the northeastern Philippines while subnetwork D are reefs at the southeastern Philippines.

The medium-scale subnetworks resulted in a partitioning that matches the major basins and reveals a latitudinal divide for the West Philippine Sea and Sulu Sea reefs (**Figure 5B**). Subnetwork A was divided into 6 medium-scale subnetworks while subnetwork B was divided into 4. Subnetwork C was divided into two medium-scale subnetworks, although subnetwork C1 representing reefs of the northern Philippines have nodes that are shared between networks A and C. At the medium-scale partitioning, subnetwork D remains the same. Within subnetwork A, two single-node subnetworks emerged (subnetwork A5 and A6) which suggests that these reefs are not as strongly interconnected to the nearby reefs despite being located at areas with high reef node density. This may be a limitation of the network partitioning method rather than an actual pattern given that these nodes are found between the opposite edges of the two largest subnetworks and that, at a higher resolution parameter value, these nodes would belong to a fine-scale subnetwork (**Supplementary Figure 3**). The fine-scale partitioning would double the

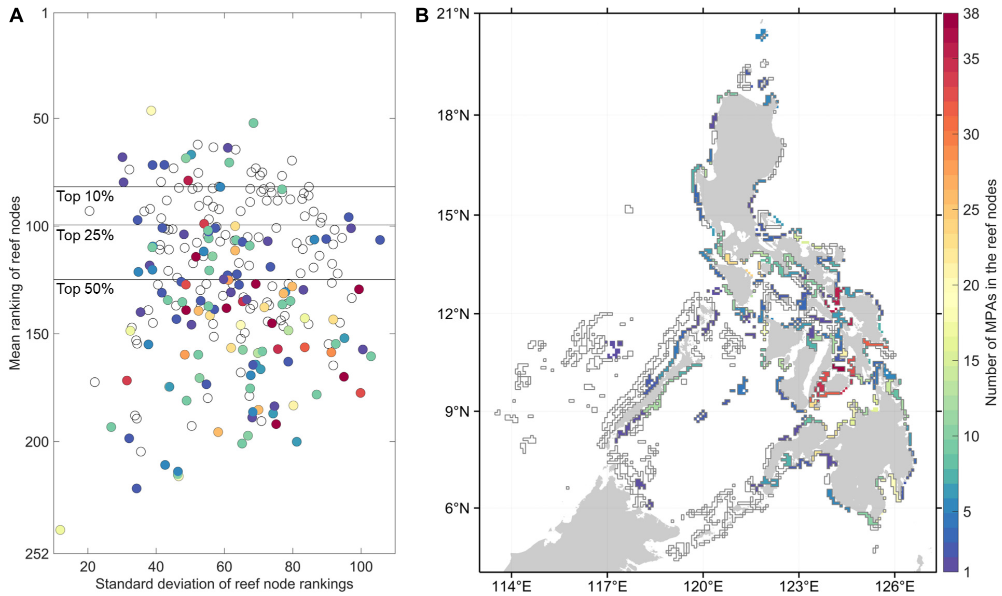

FIGURE 3 | Characteristics of the reef nodes relative to the 1,060 marine protected areas (MPAs). **(A)** The distribution of the overall mean rankings and their standard deviations of each reef node across indices and organisms. The horizontal lines mark the top 10, 25, and 50% mean ranking nodes. **(B)** Map of the reef nodes as polygons in the connectivity model. The colors in both **(A,B)** indicate the number of MPAs located in the reef nodes. Empty polygons indicate that there is no MPA geographic coordinate information for these reef nodes.

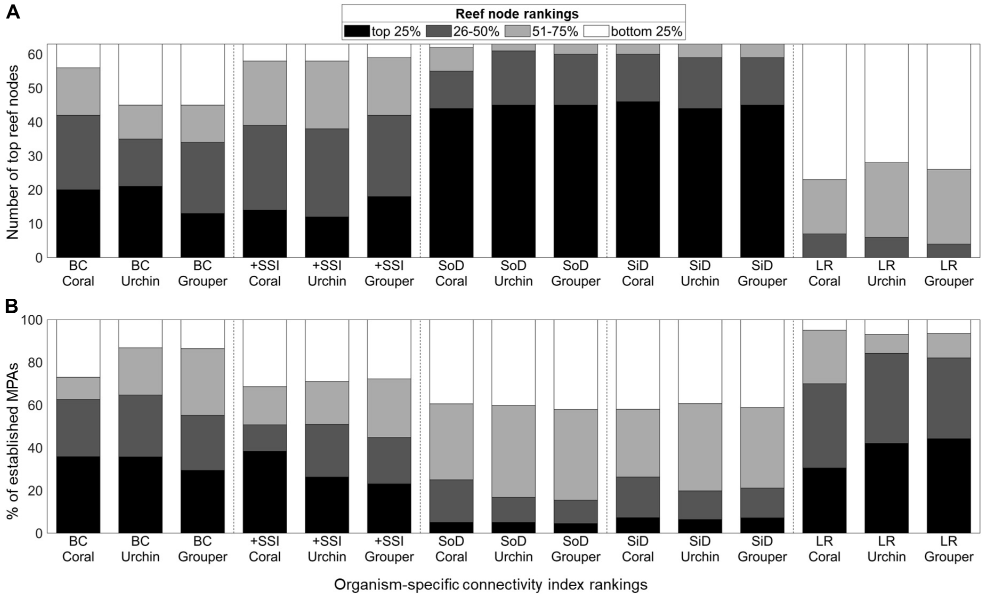

FIGURE 4 | Distribution of the organism-specific connectivity index rankings of the **(A)** overall top 25% of reef nodes and **(B)** 1,060 established MPAs **(B)**. The scale indicates the quartile ranking of the reef node or MPA. BC, Betweenness Centrality; +SSI, Source-Sink Index; SoD, Source Diversity; SiD, Sink Diversity; LR, Local Retention.

number of subnetworks and show more local structures of interconnectivity.

Analysis of the network topology of each subnetwork resulted in almost all subnetworks being strongly interconnected with a single SCC and short mean shortest paths and diameters (**Table 4**). This excluded subnetwork D which has 3 SCCs. Enumerating the number of MPAs found in each subnetwork revealed a highly uneven distribution across subnetworks (**Table 4**). At the broad-scale, subnetwork B has twice as many MPAs compared to subnetwork A, which is more than three times larger in terms of the number of reef nodes and four times as large in terms of reef area. Subnetworks C and D have similar numbers of MPAs despite subnetwork C being larger. At the medium-scale subnetworks, the disproportionate distribution of MPAs is more

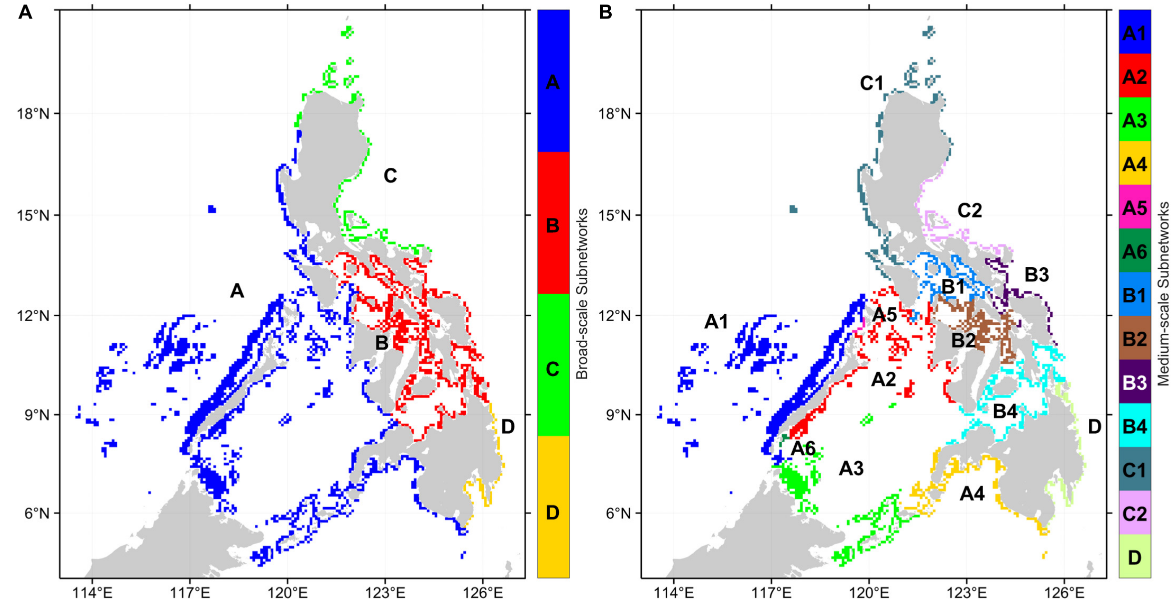

FIGURE 5 | Regional subnetworks based on the multiplex partitioning of the three organism networks. **(A)** Broad-scale subnetworks were partitioned with a resolution parameter of 0.0004. **(B)** Medium-scale subnetworks were partitioned with a resolution parameter of 0.004.

apparent with around 40% of the MPAs in B4, which is the 4th largest subnetwork. The 1st and 3rd largest subnetworks (A1 and A3) hold 1.5 and 0.4%, respectively, of the MPAs.

DISCUSSION

The interconnectedness of all reef nodes suggests that there is a single Philippine coral reef network that is regionally linked through the multi-generational dispersal of larvae. In contrast, a network analysis of corals in the Tropical Pacific identified several SCCs, isolated islands, and much longer connection paths (Treml et al., 2008). The Tropical Pacific covers a wider area with reefs distributed in distant islands compared to the Philippine reefs. This points to distance as a determinant of interconnectedness. In comparison to the regional-scale network of Caribbean reefs (Holstein et al., 2014), the Philippine network similarly has an SCC of 1 but has a longer mean shortest path and diameter. This suggests that it takes longer to traverse the Philippine network despite it covering a smaller area than the Caribbean network. Thus, in addition to distance, the complexity of the geomorphology also contributes to interconnectedness given that the Philippine network is composed of multiple embayments and basins that are connected through narrow straits (Pata and Yñiguez, 2019). The subnetworks we identified are often bordered by the major straits which are considered biodiversity corridors (Ong et al., 2002). The bifurcation of the North Equatorial Current into the strong western boundary Kuroshio and Mindanao currents (Gordon et al., 2014) also pose a dispersal barrier. This manifested as the second SCC in the sensitivity analysis scenarios and the emergence of the subnetworks C and D in the broad-scale partitioning. The multiple pathways within the Philippine coral reef network provide encouragement that extensive and effective management efforts could potentially yield connectivity benefits which would resonate beyond the local scale.

Coral reefs are diverse and three-dimensional ecosystems but our analysis was limited to three representative species and did not consider the vertical connectivity in mesophotic reefs (Kool and Nichol, 2015; Holstein et al., 2016). Previous studies have shown that connectivity dynamics are species-specific and are sensitive to larval characteristics, spatial location, and the temporal spawning period (Treml et al., 2008; Holstein et al., 2014; Thomas et al., 2014; Pata and Yñiguez, 2019). Larval connectivity is very complex and variable that even congeneric species found at the same area have contrasting observed larval dispersal patterns (Becker et al., 2007). The projection of reserve performance based on Marxan optimization scenarios has found that MPA network designs that incorporate a variety of connectivity patterns would not improve the biomass for all species (White et al., 2014). The three representative species we modeled captured a wide range of larval characteristics and yet we found between-organism similarity in network topology, connectivity index rankings, and subnetwork partitioning. Nonetheless, expanding the representation of coral reef species would improve the robustness of future connectivity analysis. This could be achieved after synthesizing databases and independent guild-specific studies on larval traits (Fisher et al., 2005; Macpherson and Raventós, 2006; Luiz et al., 2013; Green et al., 2015; Gumanao et al., 2016; Madin et al., 2016; Baird et al., 2021) and contextualizing these to the species found in the Philippine coral reefs.

Connectivity studies typically consider larval sources as ideal sites for reserve selection (Green et al., 2014; Kininmonth et al., 2019). Ideal sources would be populations with high genetic diversity (Jones et al., 2009) and have a wide range of sink

TABLE 4 | Reef area, MPAs, and topology of the subnetworks.

Sub-network	# Reef nodes	# Reef cells	Total reef area (km^2)	# MPAs	# SCCs			Mean shortest path			SD shortest paths			Longest shortest path		
					C	***U***	***G***	***C***	***U***	***G***	***C***	***U***	***G***	***C***	***U***	***G***
Broad-scale subnetworks																
A	159	1595	99.69	298	1	1	1	2.64	1.55	1.46	1.09	0.56	0.53	6	4	3
B	67	651	24.60	654	1	1	1	3.97	1.84	1.69	2.03	0.81	0.73	10	4	4
C	20	186	5.86	56	1	1	1	2.27	1.62	1.56	1.47	1.01	0.93	7	4	4
D	6	63	1.08	52	3	3	3	1.33	1.00	1.00	0.52	0.00	0.00	2	1	1
Medium-scale subnetworks																
A1	52	625	47.62	16	1	1	1	1.68	1.06	1.03	0.63	0.24	0.18	4	2	2
A2	33	290	15.29	108	1	1	1	1.65	1.12	1.09	0.64	0.33	0.29	3	2	2
A3	33	306	22.46	4	1	1	1	1.71	1.12	1.07	0.69	0.32	0.25	4	2	2
B4	25	238	10.23	400	2	1	1	2.32	1.43	1.37	1.42	0.78	0.68	7	4	4
B2	24	208	7.73	92	1	1	1	2.44	1.17	1.10	1.33	0.37	0.30	7	2	2
C1	23	218	8.75	109	1	1	1	2.04	1.30	1.28	1.22	0.50	0.48	6	3	3
A4	17	180	5.23	54	1	1	1	1.64	1.15	1.11	0.70	0.36	0.31	4	2	2
B1	16	146	4.04	102	1	1	1	1.91	1.09	1.05	0.95	0.29	0.23	5	2	2
C2	11	92	3.92	34	1	1	1	1.57	1.11	1.10	0.71	0.31	0.30	4	2	2
B3	8	91	2.48	65	1	1	1	1.61	1.09	1.09	0.71	0.29	0.29	3	2	2
D	8	85	2.31	74	3	3	3	1.50	1.08	1.08	0.67	0.29	0.29	3	2	2
A6	1	8	0.70	1	1	1	1									
A5	1	8	0.47	1	1	1	1									

The subnetwork names correspond to ***Figure 5*** *and are ordered by the number of reef nodes in each subnetwork. Network topology are organism-specific values:* ***C****, Branching coral;* ***U****, Sea urchin;* ***G****, Grouper. Shortest paths cannot be calculated for single-node SCCs.*

locations to spread out the connectivity benefits. Nodes with high source diversity on the other hand are suggested to more likely harbor resilient populations because of high population genetic diversity (Almany et al., 2009). Ensuring the persistence of populations across the network also involve intermediary sites that would connect the regional sources to the rest of the network nodes (Gaines et al., 2010). Additionally, protecting high local retention nodes would lead to faster population recovery (Hopf et al., 2016). Through considering various indices for the Philippine coral reef network, we found that the valuation of reef nodes is generally similar across different organisms given the covariation in index scores between networks. On the other hand, the limited strong correlations between indices indicate that each index captures different aspects of connectivity functioning. We did not identify any reef node which scored high in all indices but reefs which are important in most indices still emerged. Given the negative relationship between source strength and betweenness centrality, the top-ranking reef nodes are either (a) central reefs with diverse connections, or (b) important larval sources with diverse connections. The former includes reefs mostly located at straits and the latter are the exposed offshore reefs that can supply larvae at a long dispersal range. These reefs have previously been considered as national marine conservation priority areas (Ong et al., 2002). The negative correlation of the connectivity indices to local retention also suggests a trade-off that reflects how the relative exposure of shallow reefs and embayments affect dispersal and gene flow (Ackiss et al., 2018; Ravago-Gotanco and Kim, 2019; Torres et al., 2020). Further analysis should be done on balancing the representation of local retention and regional connectivity as these may address different management objectives (Krueck et al., 2017).

Many of the currently designated MPAs are found in moderate to high betweenness centrality, source strength, and local retention reefs. If these MPAs are well enforced and managed, they may partly account for regional connectivity benefits. Still, there is a need for MPAs located in reefs with more diverse connections. The presence of many MPAs in low-ranking reef nodes is explained by the primarily coastal distribution of MPAs resulting in the apparent mismatch between MPA distributions and the locations of the most important reefs for regional connectivity. This is especially relevant given that the MPAs are not evenly distributed among subnetworks and are concentrated in the central Philippines (Weeks et al., 2010). The subnetworks reveal the main barriers of larval dispersal and match the biogeographic regions identified for the Philippines (Aliño and Gomez, 1994; Nañola et al., 2011; Sutton et al., 2017). The strong interconnection within the subnetworks with shorter connection paths can be beneficial for systematically linking MPAs into fine-to-moderate scale governance networks (Horigue et al., 2015) which are likely to increase the size of protected area and improve the management of individual MPAs (Horigue et al., 2014). Additionally, spreading the potential benefits of MPAs also requires addressing the apparent geographic gap in distribution by expanding additional conservation efforts in underrepresented subnetworks.

Although connectivity is increasingly being considered in MPA design, there are of course other criteria that need to be considered in tandem with connectivity information (Balbar and Metaxas, 2019). Having a large area (>100 km^2) and isolation are key physical features of effective MPAs (Edgar et al., 2014). These may be addressed by protecting offshore reefs of the Philippines that have high betweenness centrality in the coral reef network.

Identifying reserves based on habitat extent and quality has been theorized to better fit fisheries objectives rather than connectivity (Cabral et al., 2016). Although this likely is the case for reef networks at the local scale, fisheries benefits may take decades to be noticeable (Abesamis and Russ, 2005; Hopf et al., 2016; McClanahan et al., 2016). Beyond the ecological characteristics, the allocation of funding, enforcement, and governance of MPAs determine the success of protection (Gill et al., 2017).

The effectiveness of an MPA is continuously threatened by marine pollution, sedimentation, thermal stress, coral bleaching, diseases, storms, destructive fishing, and overfishing (Arceo et al., 2001; Burke et al., 2012; Magdaong et al., 2014). Even a successful MPA which has seen recovery for three decades can be severely damaged by storms resulting in reduced fish densities (Abesamis et al., 2018). Furthermore, overfishing is the greatest threat in Philippine reefs (Burke et al., 2012) that a recent estimate quantified that reefs inside MPAs are greatly overfished, although not as bad as unprotected reefs (Muallil et al., 2019). In expanding the spatial extent of protection, the representation of different ecologically interconnected areas, replication of sites, and the consideration of less affected reefs would buffer the risks experienced in potential MPA networks (McLeod et al., 2009; Burke et al., 2012). Local threats can be addressed through integrated coastal management approaches (White et al., 2006). Active coral reef restoration tools like coral gardening and larval reseeding at the local level may also be beneficial (Abrina and Bennett, 2021). More importantly, the behavior of fishers should be considered in MPA establishment and MPA network simulations. A concurrent implementation of MPAs with fishing management strategies such as seasonal fishing closures were simulated to increase the effectiveness of reserves (Russo et al., 2019). Essentially, MPA networks are best deployed as part of a toolkit of management practices and broader frameworks that would respond to the variety of threats coral reefs face (McLeod et al., 2009).

In this study, we focused on the representation of connectivity to nominate potential areas for additional or expanded protection. Many of these potential areas for expansion have established MPAs, albeit with small coverage, and were also determined to be priority sites by other regional MPA assessment studies (Weeks et al., 2010; Beger et al., 2015; Horigue et al., 2015). This national-scale connectivity information can also help in the systematic planning of the timing of establishing MPAs (Kininmonth et al., 2019), and in using the level of connectivity between MPAs as an indicator of progress in marine protection (Roberts et al., 2018). Despite the potential benefits from MPAs as a management tool, it should be acknowledged that setting no-take reserves near coastal areas due to socioeconomic reasons (Crowder et al., 2000) may likely displace fisheries (Krueck et al., 2017) toward offshore areas which are regionally important based on many connectivity indices. We also stress that in addition to the empirical valuation and ranking of marine environments, connectivity and other biophysical criteria should fit into a systematic planning approach which takes into account local knowledge and stakeholder representation in establishing MPAs that would provide equitable benefits (Kockel et al., 2020).

DATA AVAILABILITY STATEMENT

The original connectivity data used in this study are openly available in Zenodo at https://doi.org/10.5281/zenodo.3236591. The subset connectivity data and MATLAB codes are available upon request from the corresponding author.

AUTHOR CONTRIBUTIONS

PRP conceptualization, data curation, formal analysis, visualization, and wrote the first draft. ATY conceptualization, formal analysis, project administration, and wrote sections of the manuscript. Both authors contributed to manuscript revision, read, and approved the submitted version.

FUNDING

PRP received an MSc scholarship through the Capturing Coral Reef and Related Ecosystem Services (CCRES) project (www.ccres.net), funded by the Global Environment Facility, the World Bank, and The University of Queensland. Additional funding was provided by the University of the Philippines, Office of the Vice Chancellor for Research & Development Outright Research Grant for the program "Enhancing coral reef management through tools assessing coral reef conditions and connections." The University of the Philippines, The Marine Science Institute provided partial support for the publication fee through the project entitled "Upgrading capacity, infrastructure, and assets for marine scientific research in the Philippines."

ACKNOWLEDGMENTS

We would like to thank Dr. Vera Horigue and Andrew Torres for constructive comments and suggestions during the early versions of this paper. We also thank the members of the Biological Oceanography and Modeling of Ecosystems (BiOME) Laboratory who assisted in running model simulations.

SUPPLEMENTARY MATERIAL

The Supplementary Material for this article can be found online at: https://www.frontiersin.org/articles/10.3389/fmars.2021.719691/full#supplementary-material

REFERENCES

Abesamis, R. A., and Russ, G. R. (2005). Density-dependent spillover from a marine reserve: long-term evidence. *Ecol. Appl.* 15, 1798–1812. doi: 10.1890/05-0174

Abesamis, R. A., Langlois, T., Birt, M., Thillainath, E., Bucol, A. A., Arceo, H. O., et al. (2018). Benthic habitat and fish assemblage structure from shallow to mesophotic depths in a storm-impacted marine protected area. *Coral Reefs* 37, 81–97. doi: 10.1007/s00338-017-1635-0

Abesamis, R. A., Stockwell, B. L., Bernardo, L. P., Villanoy, C. L., and Russ, G. R. (2016). Predicting reef fish connectivity from biogeographic patterns and larval dispersal modelling to inform the development of marine reserve networks. *Ecol. Indic.* 66, 534–544. doi: 10.1016/j.ecolind.2016.02.032

Abrina, T. A. S., and Bennett, J. (2021). A benefit-cost comparison of varying scales and methods of coral reef restoration in the Philippines. *Sci. Total Environ.* 799:149325. doi: 10.1016/j.scitotenv.2021.149325

Ackiss, A. S., Bird, C. E., Akita, Y., Santos, M. D., Tachihara, K., and Carpenter, K. E. (2018). Genetic patterns in peripheral marine populations of the fusilier fish *Caesio cuning* within the Kuroshio Current. *Ecol. Evol.* 8, 11875–11886. doi: 10.1002/ece3.4644

Aliño, P. M., and Gomez, E. D. (1994). "Philippine coral reef conservation: its significance to the South China Sea," in *Proceedings of the Regional Conference of the Development and Conservation in the Asia-Pacific Region*, eds K. Yamamoto, S. Ishijima, S. Sakihara, H. Taira, Z. Shimabukuro, F. Teruya, et al. (Honolulu, HI: East-West Center Association), 222–229.

Almany, G. R., Connolly, S. R., Heath, D. D., Hogan, J. D., Jones, G. P., McCook, L. J., et al. (2009). Connectivity, biodiversity conservation and the design of marine reserve networks for coral reefs. *Coral Reefs* 28, 339–351. doi: 10.1007/s00338-009-0484-x

Arceo, H. O., Quibilan, M. C., Aliño, P. M., Lim, G., and Licuanan, W. Y. (2001). Coral bleaching in Philippine reefs: coincident evidences with mesoscale thermal anomalies. *Bull. Mar. Sci.* 69, 579–593. doi: 10.1007/s00338-009-0502-z

Baird, A. H., Guest, J. R., Edwards, A. J., Bauman, A. G., Bouwmeester, J., Mera, H., et al. (2021). An Indo-Pacific coral spawning database. *Sci. Data* 8:35. doi: 10.1038/s41597-020-00793-8

Balbar, A. C., and Metaxas, A. (2019). The current application of ecological connectivity in the design of marine protected areas. *Glob. Ecol. Conserv.* 17:e00569. doi: 10.1016/j.gecco.2019.e00569

Becker, B. J., Levin, L. A., Fodrie, F. J., and McMillan, P. A. (2007). Complex larval connectivity patterns among marine invertebrate populations. *Proc. Natl. Acad. Sci. U.S.A.* 104, 3267–3272. doi: 10.1073/pnas.0611651104

Beger, M., McGowan, J., Treml, E. A., Green, A. L., White, A. T., Wolff, N. H., et al. (2015). Integrating regional conservation priorities for multiple objectives into national policy. *Nat. Commun.* 6, 1–8.

Berumen, M. L., Almany, G. R., Planes, S., Jones, G. P., Saenz-Agudelo, P., and Thorrold, S. R. (2012). Persistence of self-recruitment and patterns of larval connectivity in a marine protected area network. *Ecol. Evol.* 2, 444–452. doi: 10.1002/ece3.208

Betancur, R. R., Hines, A., Acero, P. A., Ortí, G., Wilbur, A. E., and Freshwater, D. W. (2011). Reconstructing the lionfish invasion: insights into Greater Caribbean biogeography: Reconstructing the lionfish invasion. *J. Biogeogr.* 38, 1281–1293. doi: 10.1111/j.1365-2699.2011.02496.x

Botsford, L. W., White, J. W., Coffroth, M.-A., Paris, C. B., Planes, S., Shearer, T. L., et al. (2009). Connectivity and resilience of coral reef metapopulations in marine protected areas: matching empirical efforts to predictive needs. *Coral reefs* 28, 327–337. doi: 10.1007/s00338-009-0466-z

Briggs, J. C. (2005). Coral reefs: conserving the evolutionary sources. *Biol. Conserv.* 126, 297–305. doi: 10.1016/j.biocon.2005.06.018

Burke, L., Reytar, K., Spalding, M., and Perry, A. (2012). *Reefs At Risk Revisited In The Coral Triangle*. Washington, DC: World Resources Institute.

Cabral, R. B., Aliño, P. M., Balingit, A. C. M., Alis, C. M., Arceo, H. O., Nañola, C. L. Jr., et al. (2014). The Philippine marine protected area (MPA) database. *Philipp. Sci. Lett.* 7, 300–308.

Cabral, R. B., Gaines, S. D., Lim, M. T., Atrigenio, M. P., Mamauag, S. S., Pedemonte, G. C., et al. (2016). Siting marine protected areas based on habitat quality and extent provides the greatest benefit to spatially structured metapopulations. *Ecosphere* 7:e01533.

Cabral, R. B., Mamauag, S. S., and Aliño, P. M. (2015). Designing a marine protected areas network in a data-limited situation. *Mar. Policy* 59, 64–76. doi: 10.1016/j.marpol.2015.04.013

Carpenter, K. E., and Springer, V. G. (2005). The center of the center of marine shore fish biodiversity: the Philippine Islands. *Environ. Biol. Fish.* 72, 467–480. doi: 10.1007/s10641-004-3154-4

CBD [Convention on Biological Diversity] (2010). *Strategic Plan for Biodiversity 2011–2020–COP 10, Decision X/2.* Montreal: Convention on Biological Diversity.

Chassignet, E. P., Hurlburt, H. E., Smedstad, O. M., Halliwell, G. R., Hogan, P. J., Wallcraft, A. J., et al. (2007). The HYCOM (hybrid coordinate ocean model) data assimilative system. *J. Mar. Syst.* 65, 60–83.

Cowen, R. K., and Sponaugle, S. (2009). Larval dispersal and marine population connectivity. *Annu. Rev. Mar. Sci.* 1, 443–466. doi: 10.1146/annurev.marine.010908.163757

Crowder, L. B., Lyman, S. J., Figueira, W. F., and Priddy, J. (2000). Source-sink population dynamics and the problem of siting marine reserves. *Bull. Mar. Sci.* 66, 799–820.

CTI-CFF [Coral Triangle Initiative on Coral reefs, Fisheries and Food Security] (2009). *National Plan Of Action For The Coral Triangle Initiative On Coral Reefs, Fisheries And Food Security*. Quezon City: Coral Triangle Initiative on Coral reefs, Fisheries and Food Security.

Deauna, J. D. L., Yatco, K. M. B., Villanoy, C. L., and Juinio-Meñez, M. A. (2021). Identification of priority sites to support management of commercially important sea cucumber species by applying infomap and habitat filters to larval dispersal data. *Front. Mar. Sci.* 7:571712. doi: 10.3389/fmars.2020.571712

DeVantier, L., and Turak, E. (2017). Species richness and relative abundance of reef-building corals in the indo-west pacific. *Diversity* 9:25. doi: 10.3390/d9030025

Dorman, J. G., Castruccio, F. S., Curchitser, E. N., Kleypas, J. A., and Powell, T. M. (2016). Modeled connectivity of *Acropora millepora* populations from reefs of the Spratly Islands and the greater South China Sea. *Coral Reefs* 35, 169–179. doi: 10.1007/s00338-015-1354-3

Edgar, G. J., Stuart-Smith, R. D., Willis, T. J., Kininmonth, S., Baker, S. C., Banks, S., et al. (2014). Global conservation outcomes depend on marine protected areas with five key features. *Nature* 506, 216–220. doi: 10.1038/nature13022

Ferrario, F., Beck, M. W., Storlazzi, C. D., Micheli, F., Shepard, C. C., and Airoldi, L. (2014). The effectiveness of coral reefs for coastal hazard risk reduction and adaptation. *Nat. Commun.* 5:3794.

Fisher, R., Leis, J. M., Clark, D. L., and Wilson, S. K. (2005). Critical swimming speeds of late-stage coral reef fish larvae: variation within species, among species and between locations. *Mar. Biol.* 147, 1201–1212. doi: 10.1007/s00227-005-0001-x

Flanders Marine Institute (2019). *Maritime Boundaries Geodatabase, Version 11*. Available online at: https://doi.org/10.14284/382 [Accessed May 9, 2021].

Gaines, S. D., White, C., Carr, M. H., and Palumbi, S. R. (2010). Designing marine reserve networks for both conservation and fisheries management. *Proc. Natl. Acad. Sci. U.S.A.* 107, 18286–18293. doi: 10.1073/pnas.0906473107

Gaither, M. R., and Rocha, L. A. (2013). Origins of species richness in the Indo-Malay-Philippine biodiversity hotspot: evidence for the centre of overlap hypothesis. *J. Biogeogr.* 40, 1638–1648. doi: 10.1111/jbi.12126

Gill, D. A., Mascia, M. B., Ahmadia, G. N., Glew, L., Lester, S. E., Barnes, M., et al. (2017). Capacity shortfalls hinder the performance of marine protected areas globally. *Nature* 543, 665–669. doi: 10.1038/nature21708

Gordon, A. L., Flament, P., Villanoy, C., and Centurioni, L. (2014). The nascent kuroshio of lamon bay. *J. Geophys. Res. Oceans* 119, 4251–4263. doi: 10.1002/2014jc009882

Green, A. L., Fernandes, L., Almany, G., Abesamis, R., McLeod, E., Aliño, P. M., et al. (2014). Designing marine reserves for fisheries management, biodiversity conservation, and climate change adaptation. *Coast. Manag.* 42, 143–159. doi: 10.1080/08920753.2014.877763

Green, A. L., Maypa, A. P., Almany, G. R., Rhodes, K. L., Weeks, R., Abesamis, R. A., et al. (2015). Larval dispersal and movement patterns of coral reef fishes, and implications for marine reserve network design. *Biol. Rev.* 90, 1215–1247. doi: 10.1111/brv.12155

Grorud-Colvert, K., Claudet, J., Tissot, B. N., Caselle, J. E., Carr, M. H., Day, J. C., et al. (2014). Marine protected area networks: assessing whether the whole is greater than the sum of its parts. *PLoS One* 9:e102298. doi: 10.1371/journal.pone.0102298

Gumanao, G. S., Saceda-Cardoza, M. M., Mueller, B., and Bos, A. R. (2016). Length–weight and length–length relationships of 139 Indo-Pacific fish species (Teleostei) from the Davao Gulf, Philippines. *J. Appl. Ichthyol.* 32, 377–385. doi: 10.1111/jai.12993

Harrison, H. B., Williamson, D. H., Evans, R. D., Almany, G. R., Thorrold, S. R., Russ, G. R., et al. (2012). Larval export from marine reserves and the recruitment benefit for fish and fisheries. *Curr. Biol.* 22, 1023–1028. doi: 10.1016/j.cub.2012.04.008

Hock, K., and Mumby, P. J. (2015). Quantifying the reliability of dispersal paths in connectivity networks. *J. R. Soc. Interface* 12:20150013. doi: 10.1098/rsif.2015.0013

Hock, K., Wolff, N. H., Ortiz, J. C., Condie, S. A., Anthony, K. R. N., Blackwell, P. G., et al. (2017). Connectivity and systemic resilience of the Great Barrier Reef. *PLoS Biol.* 15:e2003355. doi: 10.1371/journal.pbio.2003355

Holstein, D. M., Paris, C. B., and Mumby, P. J. (2014). Consistency and inconsistency in multispecies population network dynamics of coral reef ecosystems. *Mar. Ecol. Prog. Ser.* 499, 1–18. doi: 10.3354/meps10647

Holstein, D. M., Paris, C. B., Vaz, A. C., and Smith, T. B. (2016). Modeling vertical coral connectivity and mesophotic refugia. *Coral Reefs* 35, 23–37. doi: 10.1007/s00338-015-1339-2

Hopf, J. K., Jones, G. P., Williamson, D. H., and Connolly, S. R. (2016). Fishery consequences of marine reserves: short-term pain for longer-term gain. *Ecol. Appl.* 26, 818–829. doi: 10.1890/15-0348

Horigue, V., Aliño, P. M., and Pressey, R. L. (2014). Evaluating management performance of marine protected area networks in the Philippines. *Ocean Coast. Manag.* 95, 11–25. doi: 10.1016/j.ocecoaman.2014.03.023

Horigue, V., Aliño, P. M., White, A. T., and Pressey, R. L. (2012). Marine protected area networks in the Philippines: trends and challenges for establishment and governance. *Ocean Coast. Manag.* 64, 15–26. doi: 10.1016/j.ocecoaman.2012.04.012

Horigue, V., Pressey, R. L., Mills, M., Brotánková, J., Cabral, R., and Andréfouët, S. (2015). Benefits and challenges of scaling up expansion of marine protected area networks in the Verde Island Passage, Central Philippines. *PLoS One* 10:e0135789. doi: 10.1371/journal.pone.0135789

Jones, G. P., Almany, G. R., Russ, G. R., Sale, P. F., Steneck, R. S., Van Oppen, M. J. H., et al. (2009). Larval retention and connectivity among populations of corals and reef fishes: history, advances and challenges. *Coral Reefs* 28, 307–325. doi: 10.1007/s00338-009-0469-9

Kininmonth, S., Beger, M., Bode, M., Peterson, E., Adams, V. M., Dorfman, D., et al. (2011). Dispersal connectivity and reserve selection for marine conservation. *Ecol. Model.* 222, 1272–1282. doi: 10.1016/j.ecolmodel.2011.01.012

Kininmonth, S., Weeks, R., Abesamis, R. A., Bernardo, L. P. C., Beger, M., Treml, E. A., et al. (2019). Strategies in scheduling marine protected area establishment in a network system. *Ecol. Appl.* 29:e01820. doi: 10.1002/eap.1820

Kockel, A., Ban, N. C., Costa, M., and Dearden, P. (2020). Evaluating approaches for scaling-up community-based marine-protected areas into socially equitable and ecologically representative networks. *Conserv. Biol.* 34, 137–147. doi: 10.1111/cobi.13368

Kool, J. T., and Nichol, S. L. (2015). Four-dimensional connectivity modelling with application to Australia's north and northwest marine environments. *Environ. Model. Softw.* 65, 67–78. doi: 10.1016/j.envsoft.2014.11.022

Kough, A. S., and Paris, C. B. (2015). The influence of spawning periodicity on population connectivity. *Coral Reefs* 34, 753–757. doi: 10.1007/s00338-015-1311-1

Krueck, N. C., Ahmadia, G. N., Green, A., Jones, G. P., Possingham, H. P., Riginos, C., et al. (2017). Incorporating larval dispersal into MPA design for both conservation and fisheries. *Ecol. Appl.* 27, 925–941. doi: 10.1002/eap.1495

Licuanan, W. Y., Robles, R., and Reyes, M. (2019). Status and recent trends in coral reefs of the Philippines. *Mar. Pollut. Bull.* 142, 544–550. doi: 10.1016/j.marpolbul.2019.04.013

Luiz, O. J., Allen, A. P., Robertson, D. R., Floeter, S. R., Kulbicki, M., Vigliola, L., et al. (2013). Adult and larval traits as determinants of geographic range size among tropical reef fishes. *Proc. Natl. Acad. Sci. U.S.A.* 110, 16498–16502. doi: 10.1073/pnas.1304074110

Macpherson, E., and Raventós, N. (2006). Relationship between pelagic larval duration and geographic distribution of Mediterranean littoral fishes. *Mar. Ecol. Prog. Ser.* 327, 257–265. doi: 10.3354/meps327257

Madin, J. S., Anderson, K. D., Andreasen, M. H., Bridge, T. C., Cairns, S. D., Connolly, S. R., et al. (2016). The coral trait database, a curated database of trait information for coral species from the global oceans. *Sci. Data* 3, 1–22.

Magdaong, E. T., Yamano, H., and Fujii, M. (2014). "Development of a large-scale, long-term coral cover and disturbance database in the Philippines," in *Integrative Observations and Assessments*, eds S. Nakano, T. Yahara, and T. Nakashizuka (Cham: Springer), 83–109. doi: 10.1007/978-4-431-54783-9_5

McClanahan, T. R., Maina, J. M., Graham, N. A., and Jones, K. R. (2016). Modeling reef fish biomass, recovery potential, and management priorities in the Western Indian Ocean. *PLoS One* 11:e0154585. doi: 10.1371/journal.pone.0154585

McCook, L. J., Almany, G. R., Berumen, M. L., Day, J. C., Green, A. L., Jones, G. P., et al. (2009). Management under uncertainty: guide-lines for incorporating connectivity into the protection of coral reefs. *Coral Reefs* 28, 353–366. doi: 10.1007/s00338-008-0463-7

McLeod, E., Salm, R., Green, A., and Almany, J. (2009). Designing marine protected area networks to address the impacts of climate change. *Front. Ecol. Environ.* 7:362–370. doi: 10.1890/070211

McWilliam, M., Hoogenboom, M. O., Baird, A. H., Kuo, C.-Y., Madin, J. S., and Hughes, T. P. (2018). Biogeographical disparity in the functional diversity and redundancy of corals. *Proc. Natl. Acad. Sci. U.S.A.* 115, 3084–3089. doi: 10.1073/pnas.1716643115

Melbourne-Thomas, J., Johnson, C. R., Fung, T., Seymour, R. M., Chérubin, L. M., Arias-González, J. E., et al. (2011). Regional-scale scenario modeling for coral reefs: a decision support tool to inform management of a complex system. *Ecol. Appl.* 21, 1380–1398. doi: 10.1890/09-1564.1

MPAtlas (2021). *Global Marine Protection*. Available online at: https://mpatlas.org/ [Accessed May 9, 2021].

Muallil, R. N., Deocadez, M. R., Martinez, R. J. S., Campos, W. L., Mamauag, S. S., Nañola, C. L. Jr., et al. (2019). Effectiveness of small locally-managed marine protected areas for coral reef fisheries management in the Philippines. *Ocean Coast. Manag.* 179:104831. doi: 10.1016/j.ocecoaman.2019.104831

Mucha, P. J., Richardson, T., Macon, K., Porter, M. A., and Onnela, J.-P. (2010). Community structure in time-dependent, multiscale, and multiplex networks. *Science* 328, 876–878. doi: 10.1126/science.1184819

Munguia-Vega, A., Jackson, A., Marinone, S. G., Erisman, B., Moreno-Baez, M., Girón-Nava, A., et al. (2014). Asymmetric connectivity of spawning aggregations of a commercially important marine fish using a multidisciplinary approach. *PeerJ* 2:e511. doi: 10.7717/peerj.511

Nañola, C. L., Aliño, P. M., and Carpenter, K. E. (2011). Exploitation-related reef fish species richness depletion in the epicenter of marine biodiversity. *Environ. Biol. Fish* 90, 405–420. doi: 10.1007/s10641-010-9750-6

O'Leary, B. C., Winther-Janson, M., Bainbridge, J. M., Aitken, J., Hawkins, J. P., and Roberts, C. M. (2016). Effective coverage targets for ocean protection. *Conserv. Lett.* 9, 398–404. doi: 10.1111/conl.12247

O'Leary, J. K., Micheli, F., Airoldi, L., Boch, C., De Leo, G., Elahi, R., et al. (2017). The resilience of marine ecosystems to climatic disturbances. *BioScience* 67, 208–220. doi: 10.1093/biosci/biw161

Ong, P. S., Afuang, L. E., and Rosell-Ambal, R. G. (2002). *Philippine Biodiversity Conservation Priorities: A Second Iteration of the National Biodiversity and Action Plan*. Quezon City: DENR–PAWB, CI Philippines, UP CIDS, and FPE.

Parsons, E. C. M., Favaro, B., Aguirre, A. A., Bauer, A. L., Blight, L. K., Cigliano, J. A., et al. (2014). Seventy-one important questions for the conservation of marine biodiversity. *Conserv. Biol.* 28, 1206–1214. doi: 10.1111/cobi.12303

Pata, P. R., and Yñiguez, A. T. (2019). Larval connectivity patterns of the North Indo-West Pacific coral reefs. *PLoS One* 14:e0219913. doi: 10.1371/journal.pone.0219913

Peck, M. A., and Hufnagl, M. (2012). Can IBMs tell us why most larvae die in the sea? Model sensitivities and scenarios reveal research needs. *J. Mar. Syst.* 93, 77–93. doi: 10.1016/j.jmarsys.2011.08.005

Ravago-Gotanco, R., and Kim, K. M. (2019). Regional genetic structure of sandfish Holothuria (Metriatyla) scabra populations across the Philippine archipelago. *Fish. Res.* 209, 143–155. doi: 10.1016/j.fishres.2018.09.021

Roberts, K. E., Valkan, R. S., and Cook, C. N. (2018). Measuring progress in marine protection: a new set of metrics to evaluate the strength of marine protected area networks. *Biol. Conserv.* 219, 20–27. doi: 10.1016/j.biocon.2018.01.004

Russo, T., D'Andrea, L., Franceschini, S., Accadia, P., Cucco, A., Garofalo, G., et al. (2019). Simulating the effects of alternative management measures of trawl fisheries in the central Mediterranean Sea: application of a multi-species bio-economic modeling approach. *Front. Mar. Sci.* 6:542.

Spalding, M., Spalding, M. D., Ravilious, C., and Green, E. P. (2001). *World Atlas Of Coral Reefs*. Berkeley, CA: Univ of California Press.

Sutton, T. T., Clark, M. R., Dunn, D. C., Halpin, P. N., Rogers, A. D., Guinotte, J., et al. (2017). A global biogeographic classification of the mesopelagic zone. *Deep Sea Res. Part I* 126, 85–102. doi: 10.1016/j.dsr.2017.05.006

Thomas, C. J., Lambrechts, J., Wolanski, E., Traag, V. A., Blondel, V. D., Deleersnijder, E., et al. (2014). Numerical modelling and graph theory tools to study ecological connectivity in the Great Barrier Reef. *Ecol. Model.* 272, 160–174. doi: 10.1016/j.ecolmodel.2013.10.002

TNC-WWF-CI-WCS [The Nature Conservancy, World Wildlife Fund, Conservation International and Wildlife Conservation Society] (2008). *Marine Protected Area Networks In The Coral Triangle: Development And Lessons*. Cebu City: TNC, WWF, CI, WCS and the United States Agency for International Development.

Torres, A. F., Forsman, Z. H., and Ravago-Gotanco, R. (2020). Shifts in coral clonality along a gradient of disturbance: insights on reproduction and dispersal of *Pocillopora acuta*. *Mar. Biol.* 167:161. doi: 10.1007/s00227-020-03777-9

Traag, V. A., Krings, G., and Van Dooren, P. (2013). Significant scales in community structure. *Sci. Rep.* 3:2930. doi: 10.1038/srep02930

Traag, V., Waltman, L., and van Eck, N. J. (2018). *From Louvain to Leiden: Guaranteeing Well-Connected Communities. arXiv:1810.08473 [Physics]*. Available online at: http://arxiv.org/abs/1810.08473 [Accessed February 28, 2019].

Treml, E. A., Halpin, P. N., Urban, D. L., and Pratson, L. F. (2008). Modeling population connectivity by ocean currents, a graph-theoretic approach for marine conservation. *Landsc. Ecol.* 23, 19–36. doi: 10.1007/s10980-007-9138-y

Weeks, R., Russ, G. R., Alcala, A. C., and White, A. T. (2010). Effectiveness of marine protected areas in the Philippines for biodiversity conservation. *Conserv. Biol.* 24, 531–540. doi: 10.1111/j.1523-1739.2009.01340.x

Werner, F. E., Cowen, R. K., and Paris, C. B. (2007). Coupled biological and physical models: present capabilities and necessary developments for future studies of population connectivity. *Oceanography* 20, 54–69. doi: 10.5670/oceanog.2007.29

White, A. T., Aliño, P. M., and Meneses, A. B. T. (2006). *Creating and Managing Marine Protected Areas In The Philippines*. Cebu City: Fisheries Improved for Sustainable Harvest Project, Coastal Conservation and Education Foundation, Inc. and University of the Philippines Marine Science Institute.

White, J. W., Schroeger, J., Drake, P. T., and Edwards, C. A. (2014). The value of larval connectivity information in the static optimization of marine reserve design. *Conserv. Lett.* 7, 533–544. doi: 10.1111/conl.12097

Conflict of Interest: The authors declare that the research was conducted in the absence of any commercial or financial relationships that could be construed as a potential conflict of interest.

frontiers in Marine Science

ORIGINAL RESEARCH
published: 18 October 2021
doi: 10.3389/fmars.2021.756163

First Evidence of Cryptic Species Diversity and Population Structuring of *Selaroides leptolepis* in the Tropical Western Pacific

Lorenzo C. Halasan*[1], *Paul John L. Geraldino*[2] *and Hsiu-Chin Lin*[1,3]

[1] Department of Marine Biotechnology and Resources, National Sun Yat-sen University, Kaohsiung, Taiwan, [2] Department of Biology, University of San Carlos, Cebu, Philippines, [3] Doctoral Degree Program in Marine Biotechnology, National Sun Yat-sen University, Kaohsiung, Taiwan

The yellowstripe scad, *Selaroides leptolepis* (Carangidae), is an important fish commodity in the Tropical Western Pacific (TWP). It has a latitudinal Pacific range from south of Japan down to northern Australia, with the highest concentration in Southeast Asia. However, its TWP fishing grounds have long been a hotspot of unsustainable exploitations, thus threatening the remaining wild populations. Despite the species' commercial significance, there is limited understanding of its genetic structure and diversity. Herein, the genetic structure of *S. leptolepis* was examined using mitochondrial *COI* and *CytB* sequences. Both markers denoted significant genetic structuring based on high overall F_{ST} values. Hierarchical analysis of molecular variance (AMOVA), maximum likelihood (ML) phylogenetic trees, and median-joining (MJ) haplotype networks strongly supported the occurrence of two allopatrically distributed lineages. These comprised of a widespread Asian lineage and an isolated Australian lineage. Within-lineage distances were low (K2P $<$ 1%) whereas across-lineage distances were remarkably high (K2P $>$ 6%), already comparable to that of interspecific carangid divergences. Haplotype sequence memberships, high genetic variations, and the geographic correlation suggested that the Australian lineage was a putative cryptic species. Historical demographic inferences also revealed that the species experienced rapid expansion commencing on the late Pleistocene, most likely during the end of the Last Glacial Maximum (~20,000 years ago). The present study encouraged the application of lineage-specific management efforts, as the lineages are experiencing different evolutionary pressures. Overall, accurate knowledge of the species' genetic distribution is fundamental in protecting its diversity and assuring stock sustainability.

Keywords: yellowstripe scad, Carangidae, mitochondrial DNA, haplotype, COI (cytochrome oxidase I), cytochrome B (CytB)

Edited by:
Yehuda Benayahu,
Tel Aviv University, Israel

Reviewed by:
Claudio Oliveira,
São Paulo State University, Brazil
Marie Nydam,
Soka University of America,
United States

****Correspondence:***
Hsiu-Chin Lin
hsiuchinlin@mail.nsysu.edu.tw

Specialty section:
This article was submitted to
Marine Biology,
a section of the journal
Frontiers in Marine Science

Received: *10 August 2021*
Accepted: *28 September 2021*
Published: *18 October 2021*

Citation:
Halasan LC, Geraldino PJL and Lin H-C (2021) First Evidence of Cryptic Species Diversity and Population Structuring of Selaroides leptolepis in the Tropical Western Pacific.
Front. Mar. Sci. 8:756163.
doi: 10.3389/fmars.2021.756163

INTRODUCTION

The yellowstripe scad, *Selaroides leptolepis*, is an economically important fish commodity in the Tropical Western Pacific (TWP). This species is highly exploited in Southeast Asian countries, particularly Malaysia, Indonesia, the Philippines, and in the United Arab Emirates (Kempter, 2015; **Figure 1**). The *S. leptolepis* is commonly consumed fried, steamed, sun-dried, and even prepared as components of surimi and burger patties (Yu and Siah, 1998; Arfat and Benjakul, 2012). Aside from being a good source of dietary protein, it also contains other functional biomaterials such as protein hydrolyzates and histamine (Klompong et al., 2009; Huang et al., 2010). Since the market price of *S. leptolepis* is relatively more affordable than other fish groups (Kempter, 2015), it is highly patronized by local consumers. The species' commercial significance, however, also makes it a vulnerable target of extensive exploitations.

The *S. leptolepis* is the only representative of the genus *Selaroides* (Family Carangidae). Its closest relatives include *Selar*, *Alepes*, *Hemicaranx*, *Chloroscombrus*, and *Caranx* of the Tribe Carangini (Reed et al., 2002). Taxonomically, *S. leptolepis* is often misidentified as its Carangid relative—*Selar crumenophthalmus* (Bloch et al., 1793) due to morphological similarities. *S. leptolepis* differs by the absence of papilla on the lower pectoral girdle, absence of teeth on the upper jaw, and prominence of the longitudinal yellow stripe on its body (Nakabo, 2002). As a demersal species, *S. leptolepis* is commonly found in inshore waters shallower than 50 m (Allen and Erdmann, 2012). It is widely distributed throughout the tropical and subtropical Indian and Pacific waters (Abdussamad et al., 2013). In the TWP, it has a latitudinal distribution range from the south of Japan (Hata et al., 2017), down to the Indo-Malay-Philippine archipelagos (IMPA) (Mat Jaafar et al., 2012), and northern Australia (Dell et al., 2009).

Considered as one of the globally most important fishing regions, the TWP accounts for almost half of the world's marine fisheries production (Food and Agriculture Organization [FAO], 2020) and houses the top capture fish producers of the world, namely China, Indonesia, Vietnam, and Japan (Food and Agriculture Organization [FAO], 2020). Its IMPA region, in particular, is also considered a megadiverse area, with several studies documenting the presence of genetically distinct fish populations in the region (Rohfritsch and Borsa, 2005; Salini et al., 2006; Hubert et al., 2012; Thomas et al., 2014). The high biodiversity index of TWP had been attributed to its geologic history, oceanographic dynamics, capacity for biomass support, and vicariance histories (Carpenter and Springer, 2005; Gaither and Rocha, 2013). Unfortunately, some TWP fishing grounds have been experiencing high percentages of unsustainable fisheries. Stock depletions have already been reported in several fishing grounds within the TWP (Teh et al., 2007; Guanco et al., 2009; Tangke et al., 2018; Fauziyah et al., 2020). Records also revealed a steady decline in the global yield of *S. leptolepis* after reaching peak production in 2014 (Food and Agriculture Organization [FAO], 2021). The conservation of *S. leptolepis* and other demersal fishes is important since these groups constitute a significant portion of the TWP capture fisheries (Food and Agriculture Organization [FAO], 2020).

In fisheries management, the reduction of genetic diversity on the remaining natural populations remains a major problem. This loss of genetic diversity translates into reduced population fitness and its inability to adapt against evolutionary pressures (Kenchington, 2003). To address these problems, the incorporation of molecular techniques in conservation studies had been practiced. These techniques can reveal valuable genetic information, including a species' pattern of distribution and the demographic history of its populations. Clear information on the genetic structures allows us to define management zones and assess risks to overexploitation. Only a few records have documented the genetic distribution of *S leptolepis*, and all were done on small regional scales (Kempter, 2015; Mat Jaafar et al., 2020). There is no available information on its extant genetic structure and diversity in the TWP scale, hence this study.

The objective of this study was to investigate the intraspecies genetic diversity, structure, and demographic history of *S. leptolepis* in TWP. Sequence data from the mitochondrial DNA Cytochrome Oxidase I (COI) and Cytochrome B (CytB) regions were utilized to infer genetic structures. The mtDNA genome is conserved across animal lineages, contains few duplications, mutates rapidly, and is relatively easy to isolate—making it a good marker for intraspecies genetic studies (Desalle et al., 2017; Zhang et al., 2020). The COI and CytB have moderate evolutionary rates than other mtDNA genes (Kochzius et al., 2010; Kartavtsev, 2011) and their fragments contain adequate informative phylogenetic information (Liu et al., 2021). The coupled use of COI and CytB had not only been applied to barcode animal taxa and infer deep intraspecies divergences (Baker et al., 1995; Smith et al., 2011; Çiftçi et al., 2013; Joshi et al., 2019), but also to detect provisional cryptic populations awaiting thorough screenings (Asgharian et al., 2011; Hubert et al., 2012; Sienes et al., 2014; Thongtam Na Ayudhaya et al., 2017). Findings from this study serve as baseline information for the fishery management and sustainable utilization of *S. leptolepis* given its economic relevance and understudied status.

MATERIALS AND METHODS

Sampling and DNA Extraction

Selaroides leptolepis individuals were obtained from landing sites and wet markets from Central Philippines ($n = 132$) and Southern Taiwan ($n = 43$) between 2018 and 2021. Identification was based on morphological characters (i.e., longitudinal yellow stripe from upper part of eye to caudal peduncle, toothless upper jaw, and lower pectoral girdle absent of papilla; Nakabo, 2002; Motomura et al., 2017; Koeda and Ho, 2019). Approximately 1 g of muscle from the right caudal peduncle of each fish were stored in 2 ml tubes with 95% ethanol prior to genomic extraction. Donated muscle tissues from museum collections were also included and subjected to genomic extractions. These samples originated from Taiwan ($n = 6$), Philippines ($n = 1$), Malaysia ($n = 1$), and Australia ($n = 16$). More information regarding these samples can be found in **Supplementary Table 1**. Extraction was carried out using ReliaPrep^{TM} gDNA Tissue Miniprep System (Promega) or Genomic DNA Extraction Kit 2.0 (Yeastern Biotech) following manufacturers' protocols.

Polymerase Chain Reaction Amplification and Sequencing

The COI gene portion was amplified using published primers, namely, FishF1 (5′-TCA ACC AAC CAC AAA GAC ATT GGC AC-3′) and FishR1 (5′-TAG ACT TCT GGG TGG CCA AAG AAT CA-3′) (Ward et al., 2005); whereas the CytB regions were amplified using CytbF (5′-GGC TGA TTC GGA ATA TGC AYG

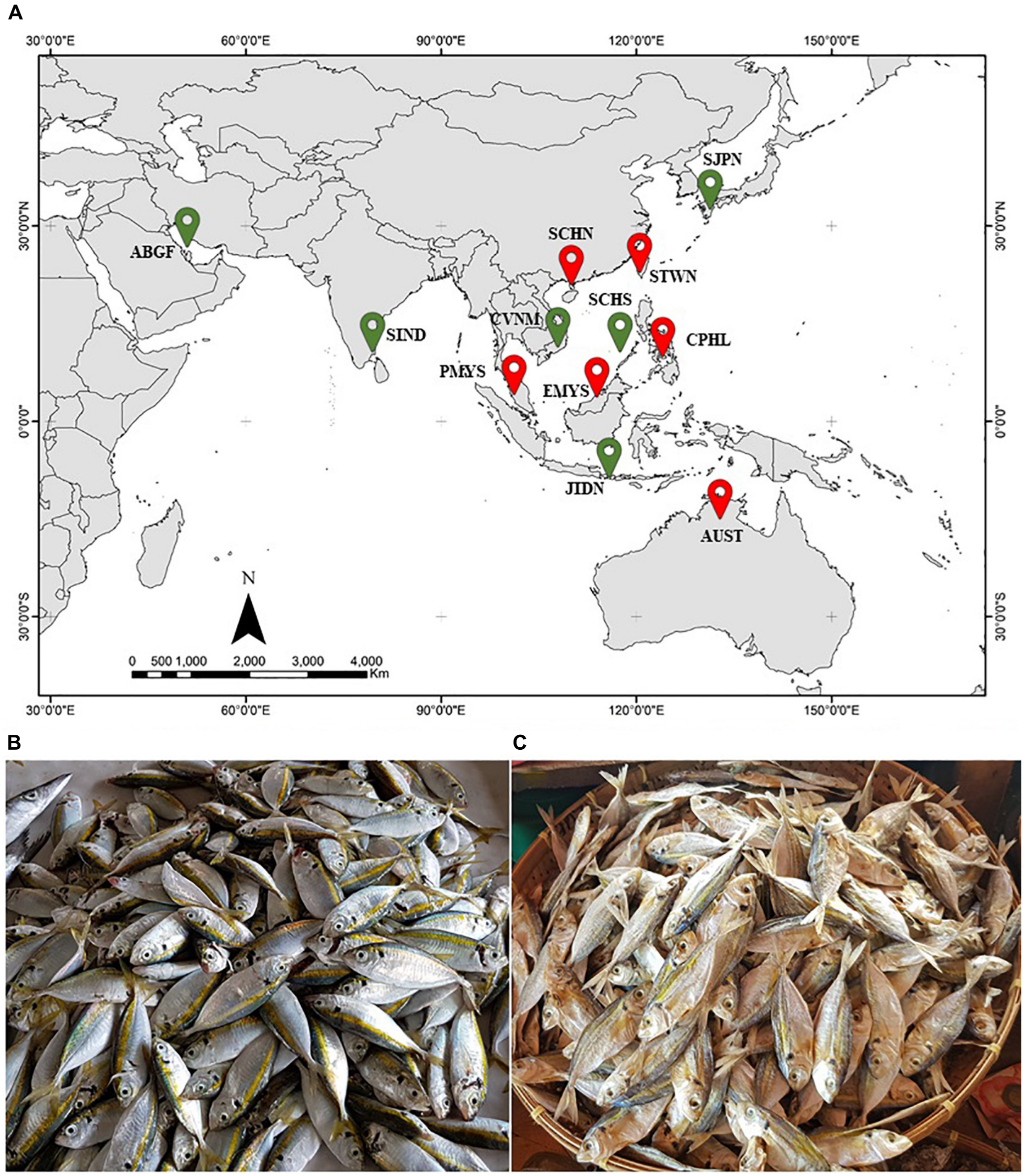

FIGURE 1 | (A) Major collection sites from this study indicated by 🔴 (*n* > 10 individuals) and 🟢 (*n* < 10 individuals). The map is courtesy of The World Bank Org (2021). **(B)** Fresh and **(C)** dried *S. leptolepis* sold at a local fish market in Central Philippines (CPHL).

CNA AYG G-3′) and CytbR (5′-GGG AAT GGA TCG TAG AAT TGC RTA NGC RAA-3′) (Kochzius et al., 2010). Amplifications were performed in 20 μl reaction volumes containing 10 μl Ampliqon Taq DNA Polymerase Master Mix, 1 μl of genomic DNA, 0.5 μl of each primer, and 8 μl of ultrapure water. Polymerase chain reaction (PCR) for both markers was carried out with an initial denaturation at 94°C for 2 min, followed by 35 cycles of 94°C denaturation for 30 s, 52°C annealing for 40 s, 72°C extension for 1 min, and final extension of 72°C for 10 min. The quality of the PCR products was evaluated in 1.5% agarose gel. PCR amplicons were either sent to Macrogen Inc. (Seoul, South Korea) or Genomics (New Taipei, Taiwan) for bidirectional sequencing using the mentioned respective PCR primers. Obtained sequences were quality checked and assembled in Sequencher 5.4.6 (Ann Arbor, MI, United States).

Data Analyses

Additional sequences publicly stored in GenBank were also incorporated in the analyses (**Supplementary Table 2**). COI sequences included the Malaysian dataset published by Mat Jaafar et al. (2020) (*n* = 70).

Genetic Diversity and Structuring

Sequences were aligned in BioEdit 7.2.5 (Hall, 1999) using Clustal W option with default settings and trimmed to 517- and 527-bp lengths, respectively, for COI and CytB. These were then exported to DnaSP 6.12 (Rozas et al., 2017) for clustering and haplotype generation. Sequences were grouped according to collection regions, namely: South Japan (SJPN), South Taiwan (STWN), Southeast China (SECH), Central Vietnam (CVNM), South China Sea (SCHS), Central Philippines (CPHL), Peninsular Malaysia (PMYS), East Malaysia (EMYS), Java Indonesia (JIDN), Southern Indian Peninsula (SIND), Arabian Gulf (ABGF), and Australia (AUST) (**Figure 1** and **Table 1**). Selection of the best-fit nucleotide substitution models through the Akaike information criteria (AIC) were carried out separately for COI and CytB using MEGA X (Kumar et al., 2018). Since some analyses were sensitive to the sample sizes, only groups with $n > 10$ sequences were included in the following calculations: estimations for genetic diversity (Hd), nucleotide diversity (π), and analysis of molecular variance (AMOVA)—which were carried out in Arlequin 3.5.2.2 (Excoffier and Lischer, 2010). K2P sequence divergence was calculated using MEGA X. For COI, the $n > 10$ groups included STWN, SECH, CPHL, PMYS, EMYS, and AUST, while CytB only included STWN, CPHL, and AUST (**Table 1**).

For phylogenetic trees and haplotype networks generations that were not sensitive to sample sizes, individuals from sparsely represented geographic regions ($n > 10$) were incorporated to explore the global relationship among all the available sequences. These regions included SJPN, SCHS, JIDN, SIND, and ABGF for COI, and SJPN, SCHN, CVNM, PMYS, and ABGF for CytB (**Table 1** and **Supplementary Table 2**). The inclusion of these sequences was relevant, as these regions represented individuals from the species' holotype collection site (i.e., JIDN, Cuvier and Valenciennes, 1833) and marginal distribution range (i.e., Southern Japan, Indian Ocean; Prabhu, 1956; Abdussamad et al., 2013; Hata et al., 2017). Maximum likelihood (ML) phylogenetic trees were created in MEGA X under substitution models K2P (COI) and K2P + G (CytB), with *S. crumenophthalmus* as the outgroup. PopART 1.7 (Leigh and Bryant, 2015) was used to generate the median-joining (MJ) haplotype networks.

TABLE 1 | Sampling region and abbreviations, sample size (N), and the number of haplotypes.

Sampling region	Abbreviation	N		No. of haplotypes	
		COI	*CytB*	*COI*	*CytB*
South Japan	SJPN	3	3	2	2
South Taiwan	STWN	49	49	7	11
Southeast China	SECH	14	1	2	1
Central Vietnam	CVNM	2	1	2	1
South China Sea	SCHS	2	–	2	1
Central Philippines	CPHL	135	133	21	29
Peninsular Malaysia	PMYS	42	1	10	1
East Malaysia	EMYS	28	–	5	–
Java Indonesia	JIDN	6	–	1	–
Southern Indian Peninsula	SIND	2	–	2	–
Arabian Gulf	ABGF	7	1	1	1
Australia	AUST	16	16	6	8
Overall		306	205	51	49

Demographic History

Neutrality tests and effective population size change estimations were done for the $n > 10$ sample groups. These were performed to infer historical demography and evolution neutrality. Deviation from the neutrality model was calculated using Tajima's D (Tajima, 1989) and Fu's Fs (Fu, 1997) in Arlequin 3.5.2.2. These indices indicate whether populations underwent expansions. Further inferences on historical demography were carried out with a mismatch distribution analysis. Demographic parameters such as tau (τ), θ_0, θ_1, sum of squared deviation (SSD), and Harpending's raggedness index (Hri) were also calculated in Arlequin 3.5.2.2. Graphical figures showing the pairwise comparison between the frequency of individuals (y-axis) with the corresponding number of pairwise differences (x-axis) were generated using DnaSP v6.12.

Changes in effective population size (N_e) across time were inferred using Bayesian skyline plot analysis (Drummond et al., 2005) implemented in BEAST 2.6.5 (Bouckaert et al., 2019). XML files were initially prepared with BEAUti 2.6.5 (Bouckaert et al., 2019). The HKY + G nucleotide substitution model was selected for both markers to take into account possible site-specific variations (Hill and Baele, 2019), and applied a strict clock mutation rate of 1×10^{-8} per site per year as suggested for reef fishes (Stewart Grant et al., 2012; Delrieu-Trottin et al., 2017). Independent Markov chain Monte Carlo (MCMC) analyses were ran for 100 million generations with a burn-in of 10 million and sampled every 1,000 iterations. If necessary, runs were repeated until combined ESS >200 values were attained, and consensus of these parameter values were visualized in Tracer 1.7.2 (Rambaut et al., 2018).

RESULTS

Genetic Diversity

A total of 306 and 205 sequences were generated for COI and CytB, respectively. Fifty-one haplotypes were identified from the 517-bp COI fragment (GenBank accession numbers: MZ520638–MZ520664), whereas 49 haplotypes were identified from the 527-bp CytB (GenBank accession numbers: MZ555658–MZ555703). Thirty-eight singletons were found for COI and 40 for CytB. Overall, 69 and 65 polymorphic sites were identified for COI and CytB, of which 45 and 40 were parsimony informative, and 22 and 25 were singleton variables, respectively. Global genetic diversities were high ($\text{COI}_{\text{global}}$ Hd = 0.7825; $\text{CytB}_{\text{global}}$ Hd = 0.7364) while nucleotide diversities were low ($\text{COI}_{\text{global}}$ π = 0.0119; $\text{CytB}_{\text{global}}$ π = 0.0106). Corresponding nucleotide composition for COI and CytB were 23.21 and 22.69% adenine, 29.15 and 28.63% thymine, 29.68 and 33.22% cytosine, and 17.96 and 15.46% guanine. The genetic indices for each group were presented in **Table 2**.

Genetic Structure and Phylogeographic Relationships

Overall, pairwise F_{ST} values for both markers showed significant genetic variation ($p < 0.05$) across populations. For COI, AUST, and CPHL significantly differed from the rest of the groups.

TABLE 2 | Polymorphic sites (PS), haplotype diversity (Hd), nucleotide diversity (π), and Tajima's D and Fu's Fs indices for cytochrome oxidase I (COI) and cytochrome B (CytB).

	PS	*Hd*	π	*Tajima's D*	*Fu's Fs*
COI					
STWN	8	0.4158	0.0010	−1.9214***	−4.4196***
SECH	1	0.1429	0.0003	−1.1552	−0.5948*
CPHL	23	0.6667	0.0031	−1.7569**	−12.9741***
PMYS	13	0.4878	0.0038	−1.0380	−2.2930
EMYS	10	0.3280	0.0021	−1.8258**	−0.4309
AUST/Australian lineage	5	0.5417	0.0014	−1.6917**	−3.6928***
Asian lineage	40	0.7446	0.0059	−1.5023**	−22.1143***
Overall	69	0.7825	0.0119	−1.2809*	−17.1323***
CytB					
STWN	12	0.4592	0.0012	−2.2610***	−10.1274***
CPHL	29	0.4984	0.0018	−2.4083***	−3.4e28***
AUST/Australian lineage	7	0.8417	0.0022	−1.5470*	−5.0042***
Asian lineage	36	0.6774	0.0021	−2.3779***	−29.3793***
Overall	65	0.7364	0.0106	−1.4956**	−22.5609***

*Significance values: ***p < 0.01; **p < 0.05; and *p < 0.1.*

TABLE 3 | Population pairwise distances using F_{ST}s (upper diagonals) and Kimura two-parameter (%K2P) (lower diagonals) for cytochrome oxidase I (COI) (upper table) and cytochrome B (CytB) (lower table).

		***COI* F_{ST}**					
		STWN	**SECH**	**CPHL**	**PMYS**	**EMYS**	**AUST**
***COI* %K2P**	STWN	–	0.0166	**0.7403**	**0.1036**	0.0381	**0.9834**
	SECH	0.0692	–	**0.7217**	0.0569	−0.0023	**0.9869**
	CPHL	0.9472	0.9274	–	**0.6203**	**0.6865**	**0.9515**
	PMYS	0.2745	0.2366	0.8930	–	0.0339	**0.9526**
	EMYS	0.1651	0.1252	0.9176	0.3163	–	**0.9721**
	AUST	7.2387	7.2271	6.3478	7.1601	7.1976	–

		***CytB* F_{ST}**		
		STWN	**CPHL**	**AUST**
***CytB* %K2P**	STWN	–	**0.4406**	**0.9747**
	CPHL	0.2831	–	**0.9688**
	AUST	6.1502	6.3129	–

Significant ($p < 0.05$) values for F_{ST}s are highlighted in bold.

AUST exhibited the highest pairwise differentiation ($F_{ST} > 0.95$) followed by CPHL ($F_{ST} > 0.62$). For CytB, all three sampling regions (STWN, CPHL, and AUST) significantly differed from each other. Pairwise F_{ST} values across each sampling group were presented in **Table 3**. Hierarchical AMOVA also showed the highest among-clusters F_{CT} variability when AUST was separated from the others (COI = 0.8847; CytB = 0.9491), though the variation was statistically insignificant at $p > 0.05$. Additional AMOVA results from other hypothetical combinations are shown in **Table 4**.

TABLE 4 | Analysis of molecular variance (AMOVA) results for hierarchical genetic subdivision for the percentage of variation and F-statistics of the cytochrome oxidase I (COI) and cytochrome B (CytB) genes.

Grouping		**Variance components**	**% variation**	**F-statistics**	***P*-value**
COI					
For all groups					
1	Cluster 1 (STWN, SECH, CPHL, PMYS, EMYS, AUST)	Among groups within total	84.07	F_{ST}: 0.8407	0.0000
Based on continental origins					
2	Cluster 1 (STWN, SECH, CPHL, PMYS, EMYS)	Among clusters	88.48	F_{CT}: 0.8847	0.1642
	Cluster 2 (AUST)	Among groups within cluster	7.57	F_{SC}: 0.6568	0.0000
		Within groups	3.96	F_{ST}: 0.9604	0.0000
Based on the significance of F_{ST}s					
3	Cluster 1 (STWN, SECH, PMYS, EMYS)	Among clusters	86.46	F_{CT}: 0.8646	0.2062
	Cluster 2 (CPHL)	Among groups within cluster	0.64	F_{SC}: 0.0473	0.0068
	Cluster 3 (AUST)	Within groups	12.90	F_{ST}: 0.8710	0.0000
4	Cluster 1 (SECH, PMYS, EMYS)	Among clusters	84.40	F_{CT}: 0.8440	0.2541
	Cluster 2 (STWN)	Among groups within cluster	0.68	F_{SC}: 0.0438	0.0860
	Cluster 3 (CPHL)	Within groups	14.91	F_{ST}: 0.8508	0.0000
	Cluster 4 (AUST)				
CytB					
For all groups					
1	Cluster 1 (STWN, SECH, AUST)	Among groups within total	91.63	F_{ST}: 0.9162	0.0000
Based on continental origins					
2	Cluster 1 (STWN, SECH)	Among clusters	94.91	F_{CT}: 0.9491	0.3480
	Cluster 2 (AUST)	Among groups within cluster	2.21	F_{SC}: 0.4338	0.0000
		Within groups	2.88	F_{ST}: 0.9712	0.0000

Combining all the other available sequences, the presence of two diverging lineages was detected from the network topologies (**Figure 2**) and phylogenetic trees (bootstrap > 75%) (**Figure 3**). Herein, these lineages were referred to as the Asian and Australian lineages. The Asian lineage covers all individuals excluding AUST, while the Australian lineage is comprised only of AUST individuals. The MJ haplotype networks for each marker showed a deep divergence on the Asian and Australian lineage in a reciprocally monophyletic network. Such type of network is characterized by the presence of more than one lineage, usually separated by numerous mutational steps (Jenkins et al., 2018). Pairwise K2P distances across the two lineages were COI = 6.77% and CytB = 6.64%. Within-lineage K2P differences were COI = 0.60% and CytB = 0.22% for the Asian lineage, and COI = 0.14% and CytB = 0.23% for the Australian lineage. Corresponding K2P differences across each collection region were presented in **Table 3**.

Further analyses without AUST were carried out to detect variations within the Asian lineage. F_{ST} values revealed significant differences across Asian populations (COI = 0.6511; CytB = 0.4406). Only the COI ML tree showed a further divergence of the Asian lineage into two main sublineages with 76% bootstrap support. The first sublineage consisted of STWN and most of CPHL individuals, as well as a few PMYS, EMYS, SIND, SJPN, and ABGF individuals. On the other hand, the second sublineage included STWN, SECH, CVNM, PMYS, EMYS, JIDN, and CPHL individuals. These two Asian sublineages had a pairwise difference of K2P = 0.99%. The COI network displayed the divergence by the separation of its two dominant haplotypes—H01 and H15. H01 includes individuals from STWN, SECH, CPHL, PMYS, EMYS, and the additional representatives from JIDN, SIND, SCHS, and CVNM. Meanwhile, H15 is composed exclusively of CPHL individuals. For CytB, the dominant haplotypes were H01 and H02. H01 is majorly represented by individuals from CPHL and with few samples from STWN and SJPN, while H02 is comprised mostly of STWN and few CPHL, PMYS, and CVNM individuals (**Figure 2** and **Supplementary Table 3**).

Demographic History

Overall Tajima's D were negative for COI ($D_{\text{global}} = -1.2809$; $p < 0.1$) and CytB ($D_{\text{global}} = -1.4956$; $p < 0.05$). Fu's Fs revealed highly significant negative values for both markers (COI$_{\text{global}}$ Fs = −17.1323, $p < 0.01$) (CytB$_{\text{global}}$ Fs = −22.5609,

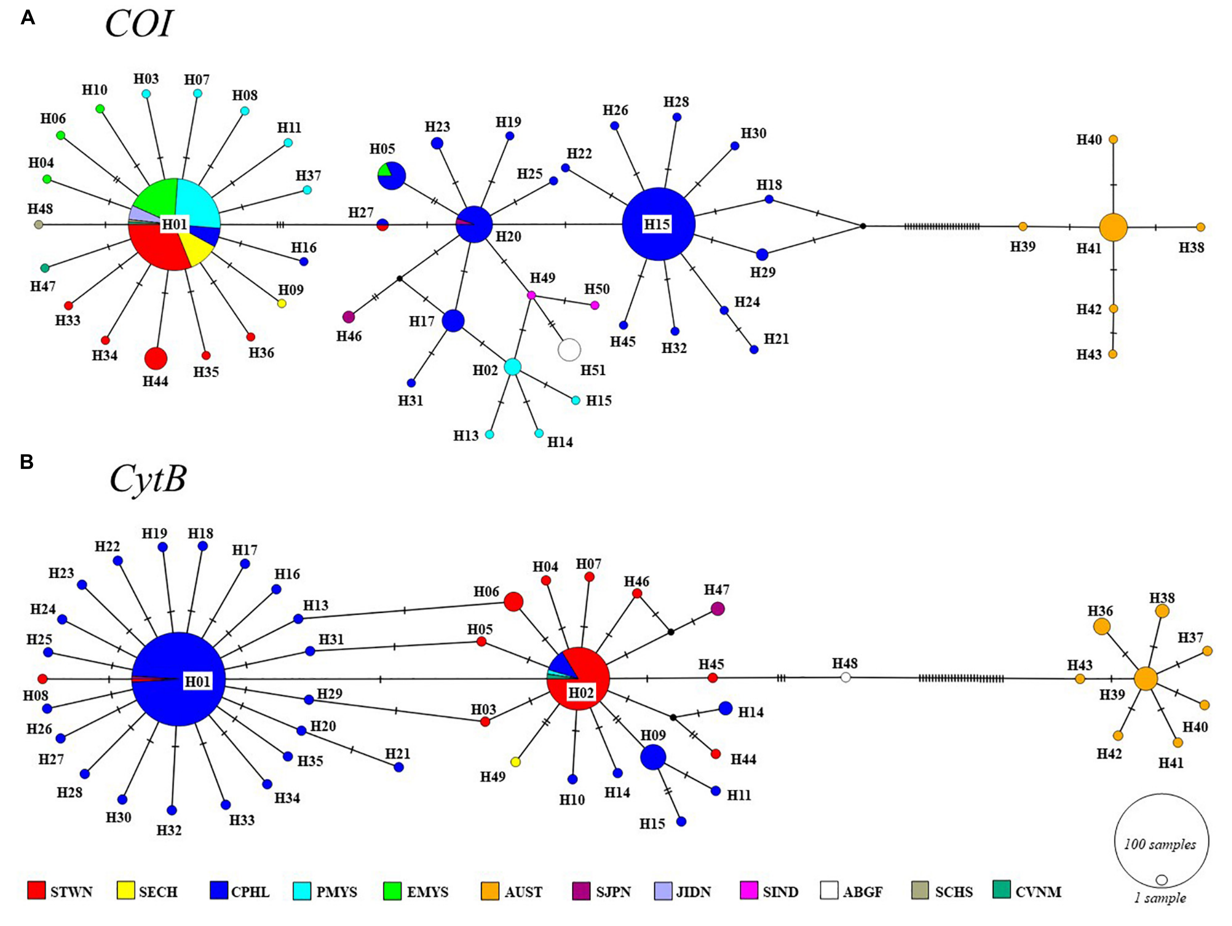

FIGURE 2 | Median-joining (MJ) networks of **(A)** cytochrome oxidase I (COI) and **(B)** cytochrome B (CytB) haplotypes of *S. leptolepis* Tropical Western Pacific (TWP) populations. The sizes of nodes (circles) are proportional to the number of individuals. Black dots represent median vectors (unsampled haplotypes).

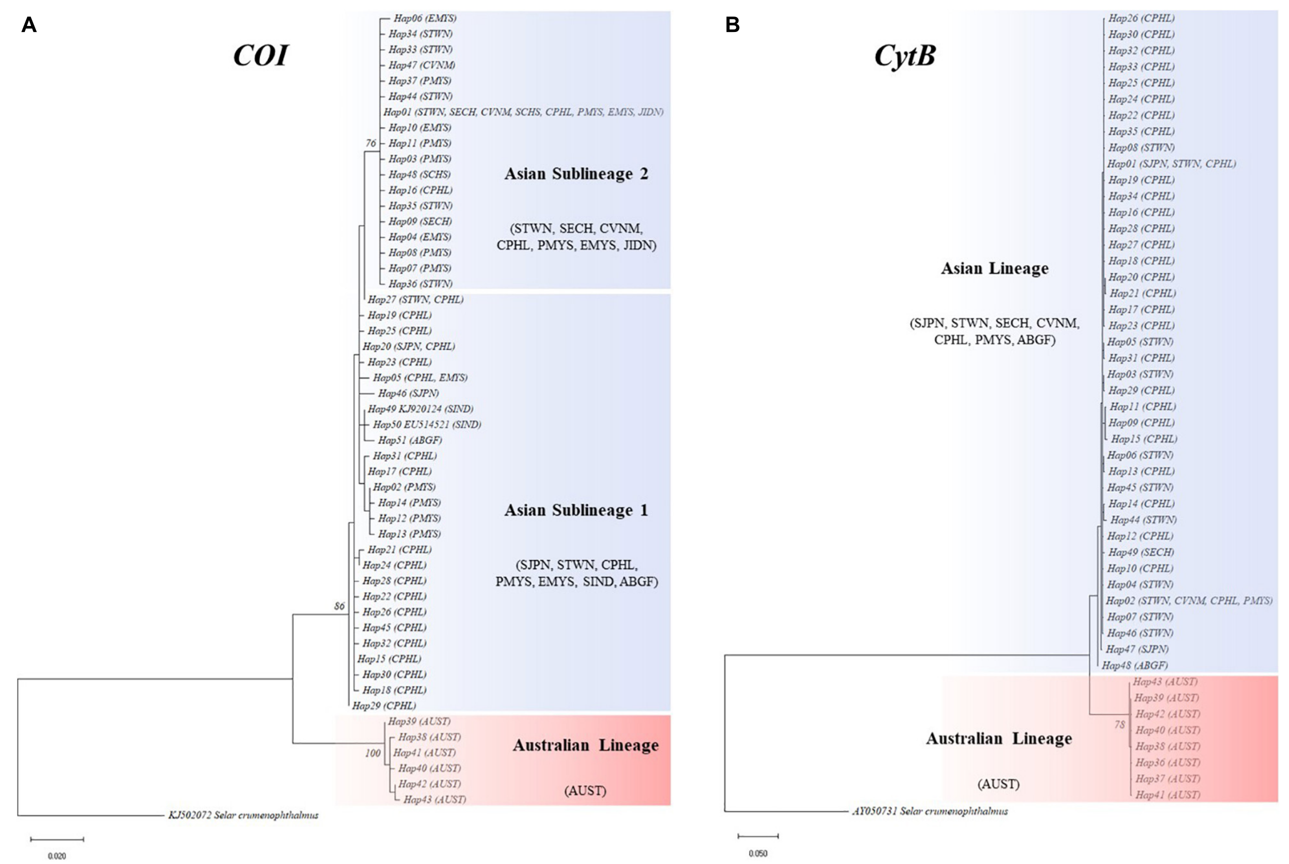

FIGURE 3 | (A) Cytochrome oxidase I (COI) and **(B)** cytochrome B (CytB) maximum likelihood (ML) trees of *S. leptolepis* rooted with *S. crumenophthalmus* (KJ502072, AY050731) from GenBank. Bootstrap consensus tree for the topology was inferred from 1,000 replicates and >75% support labels are retained at tree nodes.

$p < 0.01$) (**Table 2**). Total mismatch distribution for COI and CytB reflected different demographic signatures. COI showed a multimodal pattern whereas CytB was bimodal (**Figure 4**). SSD value for COI revealed an insignificant difference ($p > 0.05$) from a predicted growth expansion model. Raggedness values (Hri) for both markers also showed statistical insignificance ($p > 0.05$), implying the samples had a relatively good fit to a population expansion model. Corresponding mismatch indices for the lineages were shown in **Figure 4**. Using COI mismatch parameters θ_0 and θ_1 (Harpending, 1994; Marini et al., 2021), the estimated effective female population size for *S. leptolepis* after expansion (θ_1) was approximately 5,000 times higher than prior (θ_0).

Demographic scenarios supporting the recent population expansion of *S. leptolepis* were presented in the Bayesian skyline plots (**Figure 5**). Both COI and CytB revealed patterns of a long history of constant population size, followed by a slight decline (bottleneck), and a subsequent demographic expansion. The fastest increase of its effective population N_e happened between 21 and 10 thousand years ago (KYA). It showed a relatively stable effective population starting 2,000 years ago until the present. At the lineage level, the Asian lineage also displayed the rapid expansion signature, whereas the Australian lineage depicted slow population growths (**Supplementary Figure 1**).

DISCUSSION

Genetic Diversity

High overall haplotype and low nucleotide diversities were recorded for both markers, with numerous unique haplotypes or singletons present in the MJ haplotype networks. These singletons directly radiate from a largely shared haplotype, indicating few mutational step differences. On one hand, high haplotype diversity was detected when numerous unique sequences were present within the overall population. On the other hand, low nucleotide diversity was reflected when these nucleotide compositions were closely similar. This type of genetic pattern is usually attributed to a recently experienced expansion (Grant and Bowen, 1998), which is likewise supported by our historical demography findings. In such cases, individuals evolve into different haplotypes with minimal differences; and these haplotypes may either evolve directly or indirectly from an ancestral haplotype (Chanthran et al., 2020). This kind of genetic pattern has also been recorded in other TWP

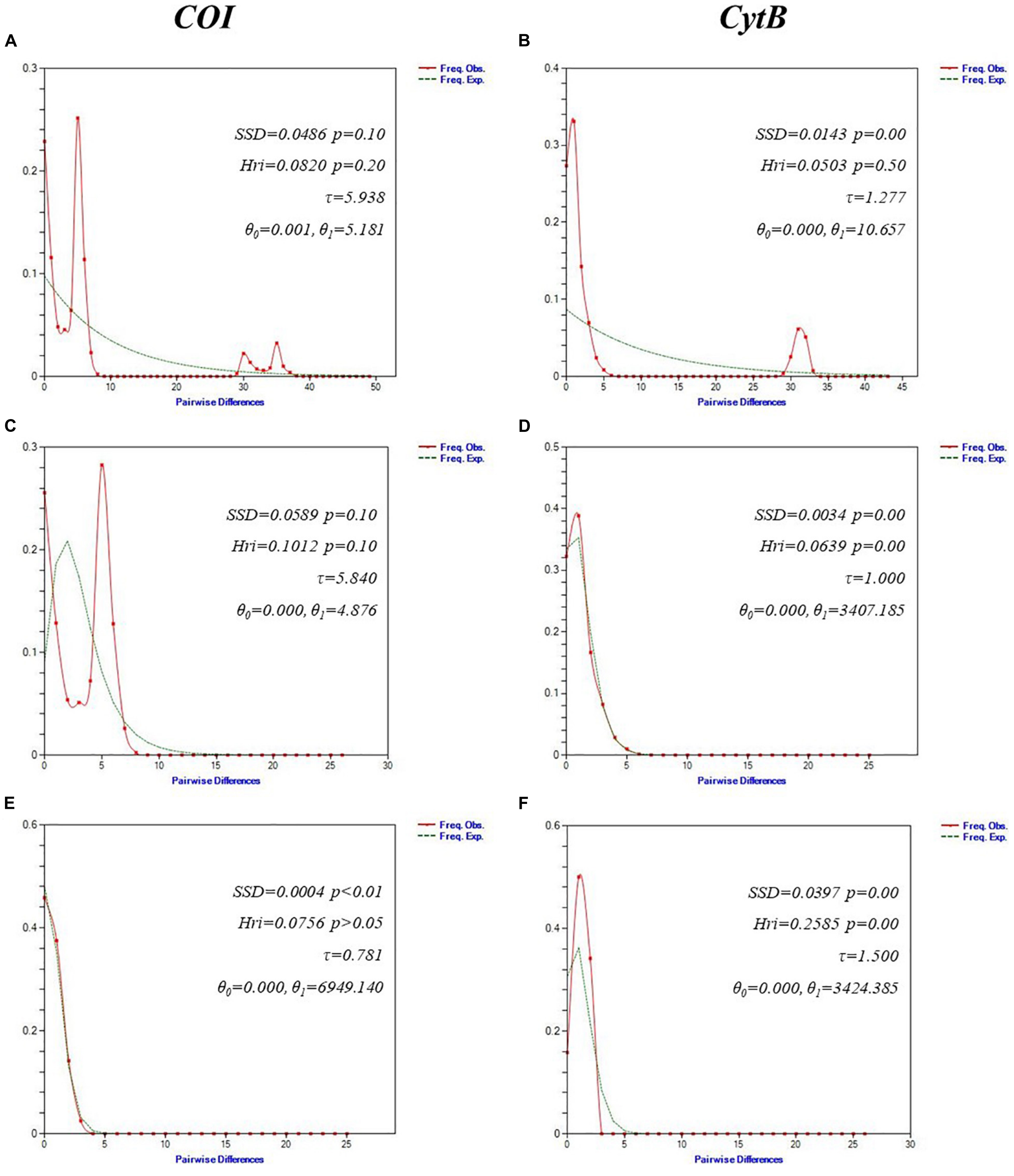

FIGURE 4 | Mismatch distribution analysis for *S. leptolepis* mtDNA cytochrome oxidase I (COI) (left) and cytochrome B (CytB) (right) using DnaSP v6.12. Graphs of the mismatch distributions of **(A,B)** overall populations; **(C,D)** Asian lineage; and **(E,F)** Australian lineage. The *X*-axis shows the observed distribution of pairwise nucleotide differences while *Y*-axis shows the frequencies. Solid lines represent the observed frequency of pairwise differences and broken lines show the expected values under the sudden expansion model. Sum of squared deviation (SSD) and Harpending's raggedness index (Hri) indices with corresponding *p*-values are also presented.

carangids (Rohfritsch and Borsa, 2005; Jamaludin et al., 2020; Mat Jaafar et al., 2020; Torres and Santos, 2020). The most recurrent and widespread haplotype is considered the oldest and most successful in traversing across sampling locations (Posada and Crandall, 2001; Mat Jaafar et al., 2012). This indicates that the second Asian sublineage might be the ancestral

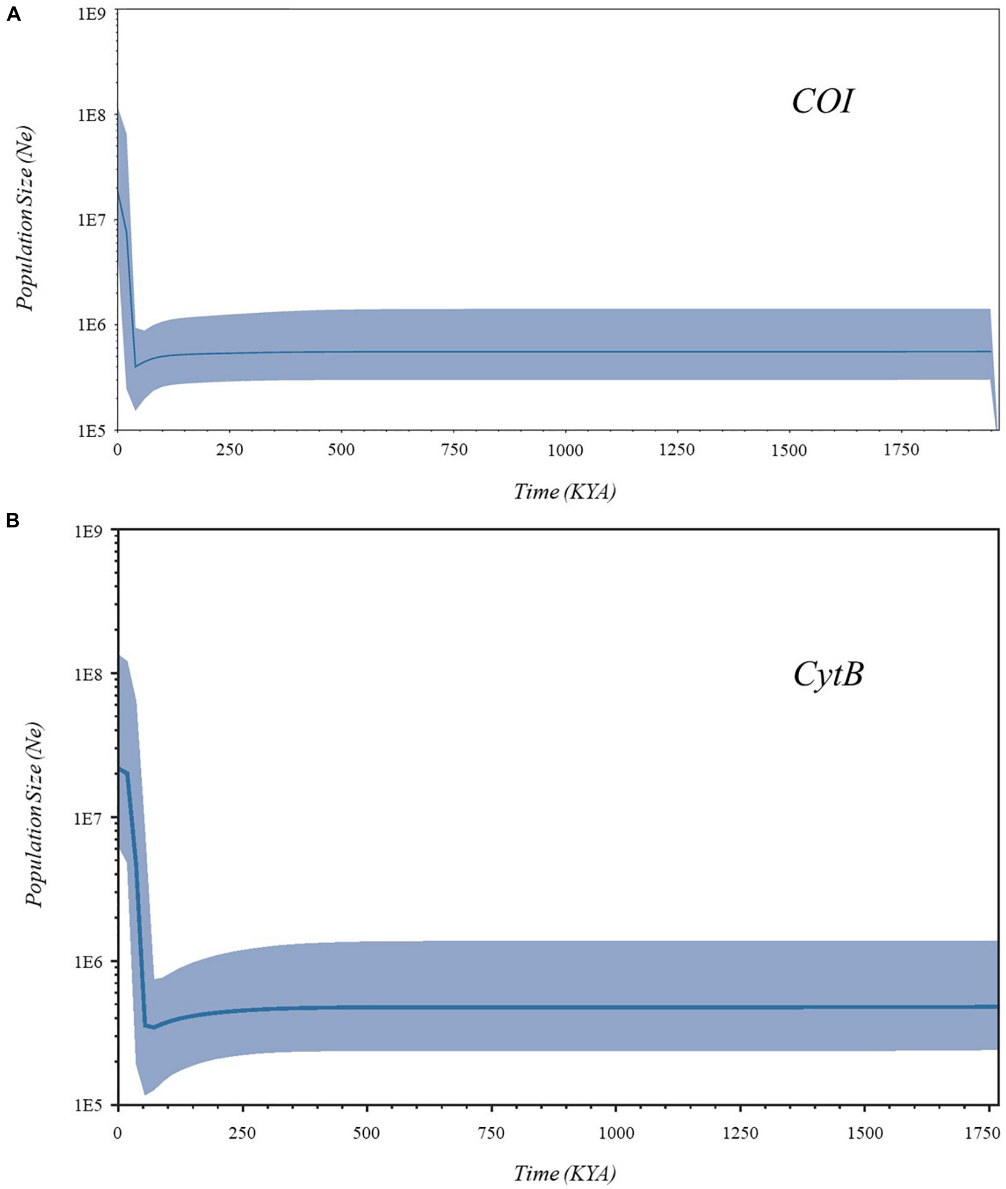

FIGURE 5 | Bayesian skyline plot based on **(A)** cytochrome oxidase I (COI) and **(B)** cytochrome B (CytB) for the effective population size changes throughout time. *X*-axes represent time in thousand years ago (KYA), while *Y*-axes show the effective population size (N_e). The blue line represents the median, while the thick blue band represents 95% highest posterior density (HPD) intervals.

S. leptolepis lineage and, the IMPA waters could be its potential geographic origin.

Genetic Structuring

Differentiation of Asia and Australia Groups

Our findings coherently supported the distinction of the Australian group. The high, significant genetic variations and correlation with geography supported an allopatric separation. The lineages' pairwise K2P divergences (COI = 6.77%; CytB = 6.64%) were higher than intraspecific variances on carangids with detected cryptic populations: *Atule mate* COI < 4.82%; *S. crumenophthalmus* COI < 4.66%; *Seriolina nigrofasciata* COI < 4.32% (Mat Jaafar et al., 2012); *Decapterus maruadsi* CytB < 5.0% (Jamaludin et al., 2020). These values were also more than 10× higher than the mean intraspecific divergences of barcoded fishes: COI = 0.39% (Ward et al., 2005); COI = 0.34% (Thu et al., 2019); COI = 0.32% (Zhang, 2011); COI = 0.59% and CytB = 0.57% (Kochzius et al., 2010); and CytB < 1.0% (Li et al., 2018). Herein, it is suggested that the two lineages represented different putative species in an *S. leptolepis* complex. This magnitude of divergence was at comparable values with the interspecific differentiation in the confamilial *Pseudocaranx dentex* complex (Bearham et al., 2020).

The separation of the two lineages can probably be related to habitat discontinuity, oceanographic barriers, the species' dispersal capacity, and past geologic events. For instance, additional collections from Eastern Java, Indonesia corresponded with the widely distributed Asian haplotype—H01. This sampling locality is known to exhibit continuous coral and rocky reef bottoms that extend to the Nusa Tenggara region (Fahmi et al., 2021). The Eastern Indian Ocean and the Timor Sea separate Eastern Java, Indonesia from North Australia, which is the southernmost range of the species in TWP. These two regions have a proximate distance of ∼1,400 km and reach a maximum depth of ∼3,300 m through the Timor Trough, implying that water dynamics between the two neighboring localities might have acted as barriers which prohibited their genetic exchange. The small islands in the area are also known to serve as a gateway for the strong intrusive Pacific waters flowing westwards to the Indian Ocean (Gordon, 2005). Being an inshore, demersal fish, these suggest that *S. leptolepis* has a weak migration capability to overcome deep water and strong current conditions despite proximity. In contrast, genetic homogeneity was displayed within the Australian group (K2P $\leq$ 0.2%), which consisted of individuals collected from Queensland and Western Australia (**Supplementary Table 1**). Found on opposite sides of the continent, this reflects an extant gene flow and signifies a high dispersal capability for *S. leptolepis* in shallow coastal regions. All in all, oceanographic hindrances and physical limitations explained the separation of Asian and Australian lineages. Other examples of fishes showing homogenous North Australian groupings with sharp discontinuities along the Timor Sea include *Lutjanus erythropterus* (Salini et al., 2006), *Decapterus russelli* (Rohfritsch and Borsa, 2005), and *Pristipomoides multidens* (Ovenden et al., 2002). Additional samples from the Lesser Sunda and nearby island localities will be ideal to establish a more comprehensive narrative of the *S. leptolepis* distribution.

Shallow Structuring Across Asia

A broadscale geographic homogeneity was observed in the Asian samples. Within this lineage, K2P divergences were <1% on both markers. However, despite the evident genetic differences in our findings, the magnitude of these differences was low and inadequately supported (i.e., insignificant F_{ST}s, low bootstrap support on CytB, and mixed haplotype and sublineage memberships). The discrepancy between the phylogenetic results of COI and CytB, where further substructuring was apparent in COI, might be an artifact of the level of sensitivity of the mtDNA marker. This undetected sub-clustering implies that such divergence is shallow. Moreover, the limited inference on phylogenetic trees is complemented with the use of networks. Since genetic diversity is usually low at the population level, this leads to indecisive tree resolutions and further overlooks other important evolutionary information. To effectively visualize reticulated relationships such as hybridization and recombination, networks are used. The implicit, sequence-based MJ haplotype network may suggest the possible occurrence of extant unsampled sequences or extinct sequences through median vectors (Bandelt et al., 1999; Kong et al., 2016; **Figure 2**). The mixed memberships of the dominant Asian haplotypes imply sympatric distribution and the absence of a clear genetic structure in the Asian lineage.

The absence of genetic structuring may partly be explained by the spawning patterns and pelagic larval duration of *S. leptolepis*, as well as the hydrogeographic features of the SCHS. *S. leptolepis* exhibits two annual spawning events succeeded by recruitment pulses which usually peak from March to June when the temperature is warmer (Prabhu, 1956; Guanco et al., 2009). In addition, observations from its close relative, *S. crumenophthalmus*, reveal an 18-day post-hatching time before reaching a nursing flexion stage (Welch et al., 2013), which supports the notion that the pelagic larval time of *S. leptolepis* might be close to 2–3 weeks. Our *S. leptolepis* Asian collection grounds also lie on the periphery of the SCHS, which is bounded to its adjacent areas by shallow waters and straits. The water movement of the SCHS's top layer is mainly influenced by seasonal monsoons, with its water circulation directly affected by two oppositely headed winds that sweep over the area at different times of the year (Huang et al., 1994). Consequently, the spawning times *S. leptolepis* temporally coincide with the timings of the opposing monsoons. With all these being said, the buoyancy of its ichthyoplankton, assisted with oceanographic circulators and ample pelagic larval durations, could be key factors in the successful genetic dispersal in the region.

Other notable clusterings of some haplotypes are shown in the ML trees and MJ networks. For instance, majority of the Malaysian haplogroup of Mat Jaafar et al. (2020) is now recognized as part of the widespread second Asian sublineage. This implies that most of the Malaysian *S. leptolepis* stocks are mainly comprised of direct ancient lineage descendants and thus support its IMPA origination. Additionally, SJPN sequences, which are collected from the northern-most TWP range of the species, appear to be more closely related to CPHL. This suggests a possible influence of the upward-moving Kuroshio current in dispersing the *S. leptolepis* to this northmost distribution. Also, the COI haplotype network showed that SIND (H49, H50) and ABGF (H51) samples formed a unique, close cluster. This suggests that *S. leptolepis* from the Indian Peninsula and ABGF region probably is a genetically distinct cluster. These samples are linked closely to the Peninsular Malaysian samples of Mat Jaafar et al. (2020), denoting that *S. leptolepis* from localities near the Malacca Strait might be genetically closer to its Indian Ocean conspecifics than those from the majority of IMPA. Additional samples are necessary to quantify their degree of genetic variability. This type of delineation was also observed in *Seriola nigrofasciata* (Mat Jaafar et al., 2012), *Lutjanus lutjanus* (Bakar et al., 2018), *Uranoscopus cognatus* (Mohd Yusoff et al., 2021), and *Penaeus semisulcatus* (Halim et al., 2021).

Demographic History

The negative Tajima's D and Fu's Fs indicated the presence of excessively rare haplotypes and imply a recent population expansion, thus rejecting the neutral evolution hypothesis. Fu's Fs has been considered as a more superior test, giving more reliability in inferring population growth (Ramos-Onsins and Rozas, 2002). A multi/bi-modal mismatch distribution suggested that the *S. leptolepis* populations are in equilibrium. However, relying solely on this graphical inference does not automatically warrant its respective history. Multiple and bimodality in mismatch analysis also happen in the presence of genetically distinct lineage in the samples. Its first peak in the graph represented the close intra-clade pairwise differences, and the next successive peaks illustrated a more ancient inter-clade pairwise difference. Therefore, lineages were suggested to be prior segregated to avoid possible violations in coalescent theory assumptions (Jenkins et al., 2018). In contrast, the unimodal patterns in each lineage depicted recent demographic expansion on the populations. Statistically insignificant values for SSD and Hri support such population expansion.

The Bayesian skyline plots suggested recent population expansion for *S. leptolepis* that initiated around the late Pleistocene era. The species recorded the most rapid increase in its effective population size during the Late Pleistocene (20 KYA) up to the early Holocene (10 KYA). During the Pleistocene, the TWP region, historically known as Sundaland, experienced glaciation and deglaciation processes which caused sea-level and temperature fluctuations that configured ocean dynamics. A contraction of the *S. leptolepis* effective populations was detected to coincide during these fluctuating periods (200–40 KYA). The formation of ice on continents and poles lowered sea levels, thus reducing the available space and ocean food supply for marine populations, and probably leading to depopulation. The abrupt rise in effective population size synchronously commenced during the Last Glacial Maximum's deglaciation timetable (∼20 KYA). This deglaciation caused a rapid rise in sea level which opened expansion opportunities. Once habitat conditions became acceptable, ancient *S. leptolepis* populations could have moved to these newly filled coastal regions. With the help of its high dispersal abilities in shallow environments, rapid population expansion, and new habitat colonization could have been easily achieved by the species. Overall, these collective circumstances might have influenced the present-day distribution patterns of *S. leptolepis* in the TWP coastal margins. Other relative carangids that exhibited similar expansion timelines in the region include *D. maruadsi* (Niu et al., 2019; Jamaludin et al., 2020), *D. macrosoma*, and *D. macarellus* (Arnaud et al., 1999).

Implications for Management and Conservation

The occurrence of two geographically isolated *S. leptolepis* lineages in TWP suggested at least two genetically distinct stocks were present in its waters. Their high level of K2P divergences was already at comparable levels for interspecies differentiation in Carangidae. The type locality for the original description of *S. leptolepis* was Java, Indonesia (Cuvier and Valenciennes, 1833). Specimens from Eastern Java grouped with the widespread Asian haplogroup suggested that this lineage might be the originally described *S. leptolepis*, and the Australian lineage is another putative species. Species complexes were considered recently diverged; therefore, their morphological differentiation is believed to have develop later due to new environment adaptations (Fahmi et al., 2021). A comprehensive and adequate collection on the *S. leptolepis* full range would also help us understand its global structure and detect the presence of any possible intermediate populations.

Selaroides leptolepis is of economic importance particularly in regions of Southeast Asia. However, this is also often coupled with a high exploitation rate. These Asian genetic stocks experience high fishery pressures driven by human consumption demands, which lead to localized fishery depletions. On the other hand, its Australian counterpart experiences relatively lesser pressures, as this species is not a top targeted fish commodity in the Australian region (Gunn, 1990). This species is usually documented as part of bycatch by fishery reports in this region (Blaber, 1993; Dell et al., 2009). Reports have indicated that >85% of Australia's fish stocks are well-managed and are at sustainable levels (Mobsby and Curtotti, 2018; Piddocke et al., 2020). This suggests that the two newly uncovered *S. leptolepis* lineages are experiencing different levels of fishery-induced pressures. Moreover, persisting localized unsustainable exploitations on the Asian stocks can cause fragmented isolation of small *S. leptolepis* populations. A lowered genetic diversity in these small *S. leptolepis* populations also means reduced fitness and higher risks against genetic degradation and drift. Small, isolated populations are also highly vulnerable to inbreeding, which reduces offspring number and viability. The *S. leptolepis* populations' ability in adapting to their constantly changing environment will also be restricted if genetic diversity is persistently decreased. If the highly targeted Asian lineage ultimately depletes, chances of replenishing its gene pool through migration will be unlikely due to the discussed isolating mechanisms.

Delimiting the *S. leptolepis* cryptic species complex will not only provide an advantage for its taxonomic recognition but can also aid in the formulation of better conservation measures. The challenge to fully delimit this *S. leptolepis* complex might rely on the combinatory use of genetic and non-genetic approaches. Exclusively associated characters in the morphology, reproductive traits, or habitat preferences will be helpful features for the species' field-based diagnostics. Otherwise, the absence of strong characters will make field-based differentiation impossible and even further complicate its management. Separating them into different units will foster more suitable stock-specific management approaches, especially since these groups are experiencing different exploitation pressures. Subdividing them will define their stock geographic boundaries, which can lead to more precise estimates on its fishery indices (e.g., recruitment, growth, and mortality) (Ovenden et al., 2009).

This study defined the genetic structure and the presence of a cryptic species of *S. leptolepis* in the TWP, wherein this species is of economic importance. Their isolated distribution, demographic history, and absence of in-between populations warrant the clear separation; and this signifies the need for other diagnostic characters, whether morphological, habitat or behavioral, to disintegrate the species complex. A full distributional range survey coupled with robust genetic approaches [e.g., single nucleotide polymorphisms (SNP)] will reveal the global structuring and evolutionary history of this taxon. Regarding management and conservation, we recommend a lineage-specific approach since stocks face different environmental and fishery pressures.

A transnational management scheme can be designed for the widely distributed lineage. Most importantly, the integration of insights from genetic studies and other scientific information can foster the best management plan for this species in the future.

DATA AVAILABILITY STATEMENT

The datasets presented in this study can be found in online repositories. The names of the repository/repositories and accession number(s) can be found below: NCBI (accession: MZ520638–MZ520664 and MZ555658–MZ555703).

ETHICS STATEMENT

Ethical review and approval was not required for the animal study because no live samples were used in the study. All specimens were acquired from local fish markets.

AUTHOR CONTRIBUTIONS

LCH performed the experiments and data analyses. H-CL helped to supervise the study. LCH and H-CL drafted the manuscript. All authors conceived and designed the study, reviewed the drafts, and approved the final version of the manuscript.

FUNDING

This work was supported by the Department of Science and Technology–Science Education Institute, Philippines and Ministry of Science and Technology, Taiwan (Grant No. 109-2611-M-110-003).

ACKNOWLEDGMENTS

We would like to thank our following contacts, especially for providing tissue sample collections: A. Graham (CSIRO National Research Collections, Australia), H. Motomura (Kagoshima University Museum, Japan), M. Nakae (National Museum of Nature and Science, Japan), A. Murase (University of Miyazaki, Japan), and S. P. Huang (Academia Sinica, Taiwan). We also thank A. C. J. Hurboda, T. A. B. Itong, P. H. T. Apag, O. P. C. Halasan, T. N. A. Mat Jaafar, Y. H. Guo, S. Yo, and J. W. Kuo for rendering technical assistance.

SUPPLEMENTARY MATERIAL

The Supplementary Material for this article can be found online at: https://www.frontiersin.org/articles/10.3389/fmars.2021.756163/full#supplementary-material

REFERENCES

Abdussamad, E. M., Rohit, P., Koya, S. K. P., Habeeb Mohamed, O. M. M. J., and Jeyabalan, K. (2013). Carangids (Family: Carangidae) in the seas around Indian subcontinent with description of macro-taxonomic characters for the field identification of genera and species. *Indian J. Fish.* 60, 21–36.

Allen, G. R., and Erdmann, M. V. (2012). *Reef Fishes of the East Indies: Volumes I-III, Tropical Reef Research*. Perth: Universitiy of Hawai'i Press.

Arfat, Y. A., and Benjakul, S. (2012). Gelling characteristics of surimi from yellow stripe trevally (*Selaroides leptolepis*). *Int. Aquat. Res.* 4:5. doi: 10.1186/2008-6970-4-5

Arnaud, S., Bonhomme, F., and Borsa, P. (1999). Mitochondrial DNA analysis of the genetic relationships among populations of scad mackerel (*Decapterus macarellus*, *D. macrosoma*, and *D. russelli*) in South-East Asia. *Mar. Biol.* 135, 699–707. doi: 10.1007/s002270050671

Asgharian, H., Sahafi, H. H., Ardalan, A. A., Shekarriz, S., and Elahi, E. (2011). Cytochrome c oxidase subunit 1 barcode data of fish of the Nayband National Park in the Persian Gulf and analysis using meta-data flag several cryptic species. *Mol. Ecol. Resour.* 11, 461–472. doi: 10.1111/j.1755-0998.2011.02989.x

Bakar, A. A., Adamson, E. A. S., Juliana, L. H., Nor Mohd, S. A., Chen, W. J., Man, A., et al. (2018). DNA barcoding of Malaysian commercial snapper reveals an unrecognized species of the yellow-lined *Lutjanus* (Pisces:Lutjanidae). *PLoS One* 13:e0202945. doi: 10.1371/journal.pone.0202945

Baker, C. S., Perry, A., Chambers, G. K., and Smith, P. J. (1995). Population variation in the mitochondrial cytochrome b gene of the orange roughy *Hoplostethus atlanticus* and the hoki *Macruronus novaezelandiae*. *Mar. Biol.* 122, 503–509. doi: 10.1007/BF00350673

Bandelt, H. J., Forster, P., and Röhl, A. (1999). Median-joining networks for inferring intraspecific phylogenies. *Mol. Biol. Evol.* 16, 37–48. doi: 10.1093/oxfordjournals.molbev.a026036

Bearham, D., Robert, M., Chaplin, J. A., Moore, G. I., Fairclough, D. V., and Bertram, A. (2020). Molecular evidence of three species in the *Pseudocaranx dentex* complex (Carangidae) in Australian waters. *Mar. Freshw. Res.* 71, 518–531. doi: 10.1071/mf18445

Blaber, S. J. M. (1993). *The Fish Resources of Tropical Northeastern Australian Waters*. Canberra: CSIRO.

Bloch, M. E., Berger, D., Berger, F. G., Bodenehr, G., Darchow, C., Gursch, C. F., et al. (1793). *D. Marcus Elieser Bloch's, AusÃijbenden Arztes zu Berlin ... Oeconomische Naturgeschichte der Fische Deutschlands*. Berlin: Auf Kosten des Verfassers und in Commission bei dem Buchhändler Hr. Hesse.

Bouckaert, R., Vaughan, T. G., Barido-Sottani, J., Duchêne, S., Fourment, M., Gavryushkina, A., et al. (2019). BEAST 2.5: an advanced software platform for Bayesian evolutionary analysis. *PLoS Comput. Biol.* 15:e1006650. doi: 10.1371/journal.pcbi.1006650

Carpenter, K. E., and Springer, V. G. (2005). The center of the center of marine shore fish biodiversity: the Philippine Islands. *Environ. Biol. Fish.* 72, 467–480. doi: 10.1007/s10641-004-3154-4

Chanthran, S. S. D., Lim, P. E., Li, Y., Liao, T. Y., Poong, S. W., Du, J., et al. (2020). Genetic diversity and population structure of *Terapon jarbua* (Forskal, 1775) (Teleostei, Terapontidae) in Malaysian waters. *Zookeys* 911, 139–160. doi: 10.3897/zookeys.911.39222

Çiftçi, Y., Eroğlu, O., and Firidin, S. (2013). Mitochondrial cytochrome b sequence variation in three sturgeon species (*A. stellatus* Pallas, 1771, *A. gueldenstaedtii* Brandt, 1833, *H. huso* Linnaeus, 1758) from the Black Sea coasts of Turkey. *Turkish J. Fish. Aquat. Sci.* 13, 291–303. doi: 10.4194/1303-2712-v13_2_11

Cuvier, G., and Valenciennes, M. (1833). *Histoire Naturelle Des Poissons*. Paris: Chez FG Levrault.

Dell, Q., Brewer, D. T., Griffiths, S. P., Heales, D. S., and Tonks, M. L. (2009). Bycatch in a tropical schooling - penaeid fishery and comparisons with a related, specialised trawl regime. *Fish. Manag. Ecol.* 16, 191–201. doi: 10.1111/j.1365-2400.2009.00655.x

Delrieu-Trottin, E., Mona, S., Maynard, J., Neglia, V., Veuille, M., and Planes, S. (2017). Population expansions dominate demographic histories of endemic and widespread Pacific reef fishes. *Sci. Rep.* 7:40519. doi: 10.1038/srep40519

Desalle, R., Schierwater, B., and Hadrys, H. (2017). MtDNA: the small workhorse of evolutionary studies. *Front. Biosci.* 22, 873–887. doi: 10.2741/4522

Drummond, A. J., Rambaut, A., Shapiro, B., and Pybus, O. G. (2005). Bayesian coalescent inference of past population dynamics from molecular sequences. *Mol. Biol. Evol.* 22, 1185–1192. doi: 10.1093/molbev/msi103

Excoffier, L., and Lischer, H. E. L. (2010). Arlequin suite ver 3.5: a new series of programs to perform population genetics analyses under Linux and Windows. *Mol. Ecol. Resour.* 10, 564–567. doi: 10.1111/j.1755-0998.2010.02847.x

Fahmi, Tibbetts, I. R., Bennett, M. B., and Dudgeon, C. L. (2021). Delimiting cryptic species within the brown-banded bamboo shark, *Chiloscyllium punctatum* in the Indo-Australian region with mitochondrial DNA and genome-wide SNP approaches. *BMC Ecol. Evol.* 21:121. doi: 10.1186/s12862-021-01852-3

Fauziyah, Putri, W. A. E., Purwiyanto, A. I. S., Agustriani, F., Ermatita, and Putra, A. (2020). The stock status of the pelagic fishes in Banyuasin coastal waters, Indonesia. *J. Fish.* 8, 798–807.

Food and Agriculture Organization [FAO] (2020). *The State of World Fisheries and Aquaculture 2020*. Rome: Food and Agriculture Organization of the United Nations.

Food and Agriculture Organization [FAO] (2021). *Species Fact Sheet. Selaroides leptolepis (Cuvier, 1833)*. Available online at: http://www.fao.org/fishery/species/3126/en (accessed July 21, 2021).

Fu, Y. X. (1997). Statistical tests of neutrality of mutations against population growth, hitchhiking and background selection. *Genetics* 147, 915–925. doi: 10.1093/genetics/147.2.915

Gaither, M. R., and Rocha, L. A. (2013). Origins of species richness in the Indo-Malay-Philippine biodiversity hotspot: evidence for the centre of overlap hypothesis. *J. Biogeogr.* 40, 1638–1648. doi: 10.1111/jbi.12126

Gordon, A. L. (2005). Oceanography of the Indonesian seas and their throughflow. *Oceanography* 18, 14–27. doi: 10.5670/oceanog.2005.01

Grant, W., and Bowen, B. (1998). Shallow population histories in deep evolutionary lineages of marine fishes: insights from sardines and anchovies and lessons for conservation. *J. Hered.* 89, 415–426. doi: 10.1093/jhered/89.5.415

Guanco, M. R., Mesa, S. V., Belga, P. B., and Nunal, D. R. M. (2009). Assessment of the commercial fisheries of Western and Central Visayan Sea. *BFAR NFRDI Techn. Pap. Ser.* 12, 1–44.

Gunn, J. S. (1990). A revision of selected genera of the family Carangidae (Pisces) from Australian waters. *Rec. Aust. Mus.* 12, 1–77. doi: 10.3853/j.0812-7387.12.1990.92

Halim, S. A. A. A., Othman, A. S., Akib, N. A. M., Jamaludin, N. A., Esa, Y., and Nor, S. A. M. (2021). Mitochondrial markers identify a genetic boundary of the Green Tiger Prawn (*Penaeus semisulcatus*) in the Indo-Pacific Ocean. *Zool. Stud.* 60:e8. doi: 10.6620/ZS.2021.60-08

Hall, T. (1999). BioEdit: a user-friendly biological sequence alignment editor and analysis program for Windows 95/98/NT. *Nucleic Acids Symp. Ser.* 41, 95–98.

Harpending, H. C. (1994). Signature of ancient population growth in a low-resolution mitochondrial DNA mismatch distribution. *Hum. Biol.* 66, 591–600.

Hata, H., Maekawa, T., Nakae, M., and Motomura, H. (2017). Records of three species of carangids (Perciformes: Carangidae), *Caranx tille*, *Megalaspis cordyla*, and *Selaroides leptolepis*, from Amima-oshima island, Amami Islands, Kagoshima Prefecture, southern Japan. *Nat. Kagoshima* 44, 27–35.

Hill, V., and Baele, G. (2019). Bayesian estimation of past population dynamics in BEAST 1.10 using the skygrid coalescent model. *Mol. Biol. Evol.* 36, 2620–2628. doi: 10.1093/molbev/msz172

Huang, Q. Z., Wang, W. Z., Li, Y. S., and Li, C. W. (1994). "Current characteristics of the South China Sea," in *Oceanology of China Seas*, eds D. Zhou, Y. B. Liang, and C. K. Tseng (Dordrecht: Kluwer Academic Publishers), 39–47. doi: 10.1007/978-94-011-0862-1_5

Huang, Y. R., Liu, K. J., Hsieh, H. S., Hsieh, C. H., Hwang, D. F., and Tsai, Y. H. (2010). Histamine level and histamine-forming bacteria in dried fish products sold in Penghu Island of Taiwan. *Food Control* 21, 1234–1239. doi: 10.1016/j.foodcont.2010.02.008

Hubert, N., Meyer, C. P., Bruggemann, H. J., Guerin, F., Komeno, R. J., Espiau, B., et al. (2012). Cryptic diversity in Indo-Pacific coral-reef fishes revealed by DNA-barcoding provides new support to the centre-of-overlap hypothesis. *PLoS One* 7:e28987. doi: 10.1371/journal.pone.0028987

Jamaludin, N. A., Mohd-Arshaad, W., Mohd Akib, N. A., Zainal Abidin, D. H., Nghia, N. V., and Nor, S. M. (2020). Phylogeography of the Japanese scad, *Decapterus maruadsi* (Teleostei; Carangidae) across the Central Indo-West Pacific: evidence of strong regional structure and cryptic diversity. *Mitochond. DNA A DNA Mapp. Seq. Anal.* 31, 298–310. doi: 10.1080/24701394.2020.1799996

Jenkins, T. L., Castilho, R., and Stevens, J. R. (2018). Meta-analysis of northeast Atlantic marine taxa shows contrasting phylogeographic patterns following post-LGM expansions. *PeerJ* 6:e5684. doi: 10.7717/peerj.5684

Joshi, B. D., Johnson, J. A., Negi, T., Singh, A., Goyal, S. P., and Negi, R. K. (2019). Understanding genetic diversity and population genetic structure of three Cyprinidae fishes occupying the same habitat from Uttarakhand. *India. Mitochond. DNA B: Resour.* 4, 2956–2961. doi: 10.1080/23802359.2019.1662740

Kartavtsev, Y. P. (2011). Divergence at Cyt-b and Co-1 mtDNA genes on different taxonomic levels and genetics of speciation in animals. *Mitochond. DNA A DNA Mapp. Seq. Anal.* 22, 55–65. doi: 10.3109/19401736.2011.588215

Kempter, J. M. (2015). Genetic traceability of selected populations of the yellowstripe scad, *Selaroides leptolepis* (Actinopterygii: Perciformes: Carangidae), based on the analysis of microsatellite DNA—CELFISH Project—Part 3. *Acta Ichthyol. Piscat.* 45, 299–305. doi: 10.3750/aip2015.45.3.08

Kenchington, E. (2003). "The effects of fishing on species and genetic diversity," in *Responsible Fisheries in the Marine Ecosystem*, eds M. Sinclair and G. Valdimarsson (Wallingford: CAB International), 235–253. doi: 10.1079/9780851996332.0235

Klompong, V., Benjakul, S., Yachai, M., Visessanguan, W., Shahidi, F., and Hayes, K. D. (2009). Amino acid composition and antioxidative peptides from protein hydrolysates of yellow stripe trevally (*Selaroides leptolepis*). *J. Food Sci.* 74, C126–C133. doi: 10.1111/j.1750-3841.2009.01047.x

Kochzius, M., Seidel, C., Antoniou, A., Botla, S. K., Campo, D., Cariani, A., et al. (2010). Identifying fishes through DNA barcodes and microarrays. *PLoS One* 5:e12620. doi: 10.1371/journal.pone.0012620

Koeda, K., and Ho, H. C. (2019). *Fishes of Southern Taiwan*. Pingtung: National Museum of Marine Biology & Aquarium.

Kong, S., Sánchez-Pacheco, S. J., and Murphy, R. W. (2016). On the use of median-joining networks in evolutionary biology. *Cladistics* 32, 691–699. doi: 10.1111/cla.12147

Kumar, S., Stecher, G., Li, M., Knyaz, C., and Tamura, K. (2018). MEGA X: molecular evolutionary genetics analysis across computing platforms. *Mol. Biol. Evol.* 35:1547. doi: 10.1093/molbev/msy096

Leigh, J. W., and Bryant, D. (2015). POPART: full-feature software for haplotype network construction. *Methods Ecol. Evol.* 6, 1110–1116. doi: 10.1111/2041-210X.12410

Li, X., Shen, X., Chen, X., Xiang, D., Murphy, R. W., and Shen, Y. (2018). Detection of potential problematic Cytb gene sequences of fishes in GenBank. *Front. Genet.* 9:30. doi: 10.3389/fgene.2018.00030

Liu, Y., Yao, L., Ci, Y., Cao, X., Zhao, M., Li, Y., et al. (2021). Genetic differentiation of geographic populations of *Rattus tanezumi* based on the mitochondrial Cytb gene. *PLoS One* 16:e0248102. doi: 10.1371/journal.pone.0248102

Marini, M., Pedrosa-Gerasmio, I. R., Santos, M. D., Shibuno, T., Daryani, A., Romana-Eguia, M. R. R., et al. (2021). Genetic diversity, population structure and demographic history of the tropical eel *Anguilla bicolor pacifica* in Southeast Asia using mitochondrial DNA control region sequences. *Glob. Ecol. Conserv.* 26:e01493. doi: 10.1016/j.gecco.2021.e01493

Mat Jaafar, T. N. A., Taylor, M. I., Mohd Nor, S. A., Bruyn, M., and Carvalho, G. R. (2020). Comparative genetic stock structure in three species of commercially exploited Indo-Malay Carangidae (Teleosteii, Perciformes). *J. Fish Biol.* 96, 337–349. doi: 10.1111/jfb.14202

Mat Jaafar, T. N. A., Taylor, M. I., Mohd Nor, S. A., De Bruyn, M., and Carvalho, G. R. (2012). DNA barcoding reveals cryptic diversity within commercially exploited Indo-Malay Carangidae (Teleosteii: Perciformes). *PLoS One* 7:e49623. doi: 10.1371/journal.pone.0049623

Mobsby, D., and Curtotti, R. (2018). *Snapshot of Australia's Commercial Fisheries and Aquaculture in ABARES Insights*. Canberra, ACT: Australian Bureau of Agricultural and Resource Economics and Sciences. doi: 10.25814/5c10f672bff77

Mohd Yusoff, N. I. S., Mat Jaafar, T. N. A., Vilasri, V., Mohd Nor, S. A., Seah, Y. G., Habib, A., et al. (2021). Genetic diversity, population structure and historical demography of the two-spined yellowtail stargazer (*Uranoscopus cognatus*). *Sci. Rep.* 11:13357. doi: 10.1038/s41598-021-92905-6

Motomura, H., Alama, U. B., Muto, N., Babaran, P., and Ishikawa, S. (2017). *Commercial and Bycatch Market Fishes of Panay Island, Republic of the Philippines*. Kagoshima: Kagoshima University Museum.

Nakabo, T. (2002). *Fishes of Japan: With Pictorial Keys to the Species*. Tokyo: Tokai University Press.

Niu, S. F., Wu, R. X., Zhai, Y., Zhang, H. R., Li, Z. L., Liang, Z. B., et al. (2019). Demographic history and population genetic analysis of *Decapterus maruadsi* from the northern South China Sea based on mitochondrial control region sequence. *PeerJ* 7:e7953. doi: 10.7717/peerj.7953

Ovenden, J. R., Kashiwagi, T., Broderick, D., Giles, J., and Salini, J. (2009). The extent of population genetic subdivision differs among four co-distributed shark species in the Indo-Australian archipelago. *BMC Evol. Biol.* 9:40. doi: 10.1186/1471-2148-9-40

Ovenden, J. R., Lloyd, J., Newman, S. J., Keenan, C. P., and Slater, L. S. (2002). Spatial genetic subdivision between northern Australian and southeast Asian populations of *Pristipomoides multidens*: a tropical marine reef fish species. *Fish. Res.* 59, 57–69. doi: 10.1016/S0165-7836(01)00415-5

Piddocke, T., Ashby, C., Hartmann, K., Hesp, A., Hone, P., Klemke, J., et al. (2020). *Status of Australian Fish Stocks Reports 2020*, 5 Edn, Canberra: Fisheries Research and Development Corporation.

Posada, D., and Crandall, K. A. (2001). Intraspecific gene genealogies: trees grafting into networks. *Trends Ecol. Evol.* 16, 37–45. doi: 10.1016/s0169-5347(00)02026-7

Prabhu, M. S. (1956). Maturation of intra-ovarian eggs and spawning periodicities in some fishes. *J. Fish.* 3, 51–90.

Rambaut, A., Drummond, A. J., Xie, D., Baele, G., and Suchard, M. A. (2018). Posterior summarization in Bayesian phylogenetics using Tracer 1.7. *Syst. Biol.* 67, 901–904. doi: 10.1093/sysbio/syy032

Ramos-Onsins, S. E., and Rozas, J. (2002). Statistical properties of new neutrality tests against population growth. *Mol. Biol. Evol.* 19, 2092–2100. doi: 10.1093/oxfordjournals.molbev.a004034

Reed, D. L., Carpenter, K. E., and Degravelle, M. J. (2002). Molecular systematics of the Jacks (Perciformes: Carangidae) based on mitochondrial cytochrome b sequences using parsimony, likelihood, and Bayesian approaches. *Mol. Phylogenet. Evol.* 23, 513–524. doi: 10.1016/S1055-7903(02)00036-2

Rohfritsch, A., and Borsa, P. (2005). Genetic structure of Indian scad mackerel *Decapterus russelli*: pleistocene vicariance and secondary contact in the Central Indo-West Pacific Seas. *Heredity* 95, 315–326. doi: 10.1038/sj.hdy.6800727

Rozas, J., Ferrer-Mata, A., Sánchez-Delbarrio, J. C., Guirao-Rico, S., Librado, P., Ramos-Onsins, S. E., et al. (2017). DnaSP 6: DNA sequence polymorphism analysis of large data sets. *Mol. Biol. Evol.* 34, 3299–3302. doi: 10.1093/molbev/msx248

Salini, J. P., Ovenden, J. R., Street, R., Pendrey, R., Haryanti, O., and Ngurah, T. (2006). Genetic population structure of red snappers (*Lutjanus malabaricus* Bloch & Schneider, 1801 and *Lutjanus erythropterus* Bloch, 1790) in central and eastern Indonesia and northern Australia. *J. Fish Biol.* 68, 217–234. doi: 10.1111/j.0022-1112.2006.001060.x

Sienes, P. M. Q., Willette, D. A., Romena, L. R., Alvior, C. G., and Estacion, J. S. (2014). Genetic diversity and the discovery of a putative cryptic species within a valued crab fishery, *Portunus pelagicus* (Linnaeus 1758), in the Philippines. *Philipp. Sci. Lett.* 7, 317–323.

Smith, P. J., Steinke, D., Mcmillan, P., Stewart, A., and Ward, R. D. (2011). DNA barcoding of morid cods reveals deep divergence in the antitropical *Halargyreus johnsoni* but little distinction between *Antimora rostrata* and *Antimora microlepis*. *Mitochond. DNA A DNA Mapp. Seq. Anal.* 22(Suppl. 1), 21–26. doi: 10.3109/19401736.2010.532329

Stewart Grant, W., Liu, M., Gao, T. X., and Yanagimoto, T. (2012). Limits of Bayesian skyline plot analysis of mtDNA sequences to infer historical demographies in Pacific herring (and other species). *Mol. Phylogenet. Evol.* 65, 203–212. doi: 10.1016/j.ympev.2012.06.006

Tajima, F. (1989). Statistical method for testing the neutral mutation hypothesis by DNA polymorphism. *Genetics* 123, 585–595. doi: 10.1093/genetics/123.3.585

Tangke, U., Sangadji, I., Rochmady, R., and Susiana, S. (2018). A population dynamic aspect of *Selaroides leptolepis* in the coastal waters of South Ternate Island, Indonesia. *Aquac. Aquar. Conserv. Legis.* 11, 1334–1342.

Teh, L. S. L., Zeller, D., Cabanban, A., Teh, L. C. L., and Sumaila, U. R. (2007). Seasonality and historic trends in the reef fisheries of Pulau Banggi, Sabah, Malaysia. *Coral Reefs* 26, 251–263. doi: 10.1007/s00338-006-0182-x

The World Bank Org (2021). *World Bank Official Boundaries*. Available online at: https://datacatalog.worldbank.org/dataset/world-bank-official-boundaries (accessed July 07, 2021).

Thomas, R. C. Jr., Willette, D. A., Carpenter, K. E., and Santos, M. D. (2014). Hidden diversity in sardines: genetic and morphological evidence for cryptic species in the goldstripe sardinella, *Sardinella gibbosa* (Bleeker, 1849). *PLoS One* 9:e84719. doi: 10.1371/journal.pone.0084719

Thongtam Na Ayudhaya, P., Muangmai, N., Banjongsat, N., Singchat, W., Janekitkarn, S., Peyachoknagul, S., et al. (2017). Unveiling cryptic diversity of the anemonefish genera *Amphiprion* and *Premnas* (Perciformes: Pomacentridae) in Thailand with mitochondrial DNA barcodes. *Agric. Nat. Resour.* 51, 198–205. doi: 10.1016/j.anres.2017.07.001

Thu, P. T., Huang, W. C., Chou, T. K., Van Quan, N., Van Chien, P., Li, F., et al. (2019). DNA barcoding of coastal ray-finned fishes in Vietnam. *PLoS One* 14:e0222631. doi: 10.1371/journal.pone.0222631

Torres, S. K. M., and Santos, B. S. (2020). Genetic diversity and population structure of three caranx species from Batangas Province. *Phillip. J. Sci.* 150, 223–236.

Ward, R. D., Zemlak, T. S., Innes, B. H., Last, P. R., and Hebert, P. D. (2005). DNA barcoding Australia's fish species. *Philos. Trans. R. Soc. Lond. B, Biol. Sci.* 360, 1847–1857. doi: 10.1098/rstb.2005.1716

Welch, A., Hoenig, R., Stieglitz, J., Daugherty, Z., Sardenberg, B., Miralao, S., et al. (2013). Growth rates of larval and juvenile bigeye scad *Selar crumenophthalmus* in captivity. *Springerplus* 2, 634–634. doi: 10.1186/2193-1801-2-634

Yu, S. Y., and Siah, W. M. (1998). Development and acceptability of burgers made from *Selaroides leptoleps* and *Aristichthys nobilis*. *Asian Fish. Sci.* 10, 329–337.

Zhang, J. (2011). Species identification of marine fishes in china with DNA barcoding. *Evid. Based Complement. Alternat. Med.* 2011:978253. doi: 10.1155/2011/978253

Zhang, Q., Sun, C., Zhu, Y., Xu, N., and Liu, H. (2020). Genetic diversity and structure of the round-tailed paradise fish (*Macropodus ocellatus*): implications for population management. *Glob. Ecol. Conserv.* 21:e00876. doi: 10.1016/j.gecco.2019.e00876

Conflict of Interest: The authors declare that the research was conducted in the absence of any commercial or financial relationships that could be construed as a potential conflict of interest.

frontiers
in Marine Science

ORIGINAL RESEARCH
published: 20 October 2021
doi: 10.3389/fmars.2021.731023

Zooxanthellae Diversity and Coral-Symbiont Associations in the Philippine Archipelago: Specificity and Adaptability Across Thermal Gradients

Andrew F. Torres[1,2], Darryl Anthony M. Valino[1] and Rachel Ravago-Gotanco[1]*

[1] Marine Science Institute, University of the Philippines Diliman, Quezon City, Philippines, [2] Department of Earth Sciences, Natural History Museum, London, United Kingdom

Prolonged thermal stress and high levels of solar irradiance can disrupt the coral-algal symbiosis and cause bleaching and lowered overall fitness that lead to the likely death of the cnidarian host. Adaptive bleaching and acclimatization of corals, which posits bleaching as an opportunity for the coral host to switch its currently susceptible endosymbionts to more stress-tolerant taxa, offers hope for survival of reefs amid rapidly warming oceans. In this study, we explored the diversity and distribution of coral-zooxanthellae associations in the context of geospatial patterns of sea surface temperature (SST) and thermal anomalies across the Philippine archipelago. Thermal clusters based on annual sea surface temperature means and each site's frequency of exposure to heat stress were described using three-decade (1985–2018) remotely sensed data. Haphazard sampling of 628 coral fragments was conducted in 14 reef sites over 3 years (2015–2018). Using polymerase chain reaction-denaturing gradient gel electrophoresis (PCR-DGGE) fingerprinting and sequencing of the zooxanthellae ITS2 region, we characterized endosymbiont diversity within four reef-building coral families across archipelagic thermal regimes. Consistency in dominant Symbiodiniaceae taxon was observed in *Acropora* spp., *Porites* spp., and *Heliopora coerulea*. In contrast, the family Pocilloporidae (*Pocillopora* spp., *Seriatopora* spp., and *Stylophora pistillata*) exhibited biogeographic variability in zooxanthellae composition, concordant with inferred occurrences of sustained thermal stress. Multivariate analyses identify two broad Pocilloporidae clusters that correspond with mean SST ranges and frequency of exposure to bleaching-level thermal stress which are largely supported by ANOSIM. Differences in zooxanthellae assemblages may reflect host-specific responses to ecological or environmental gradients across biogeographic regions. Such patterns of variability provide insight and support for the adaptability and potential resilience of coral communities in geographically and oceanographically complex regions, especially amidst the increasing severity of global and local-scale stressors.

Keywords: coral-algal symbiosis, Symbiodiniaceae, coral bleaching, thermal stress, PCR-DGGE fingerprinting, Coral Triangle

Edited by:
Yehuda Benayahu,
Tel Aviv University, Israel

Reviewed by:
Leïla Ezzat,
École Polytechnique Fédérale de Lausanne, Switzerland
Rafael A. Cabral-Tena,
Center for Scientific Research and Higher Education at Ensenada (CICESE), Mexico

***Correspondence:**
Andrew F. Torres
a.torres@nhm.ac.uk

Specialty section:
This article was submitted to Coral Reef Research, a section of the journal Frontiers in Marine Science

Received: 25 June 2021
Accepted: 28 September 2021
Published: 20 October 2021

Citation:
Torres AF, Valino DAM and Ravago-Gotanco R (2021) Zooxanthellae Diversity and Coral-Symbiont Associations in the Philippine Archipelago: Specificity and Adaptability Across Thermal Gradients. Front. Mar. Sci. 8:731023. doi: 10.3389/fmars.2021.731023

INTRODUCTION

Protozoan dinoflagellates of the family Symbiodiniaceae, colloquially known as zooxanthellae, are a diverse taxon of mostly endosymbiotic unicellular algae in marine invertebrates like corals, mollusks, and sponges (Trench et al., 1981; Berkelmans and van Oppen, 2006; Weisz et al., 2010). Formerly under the genus *Symbiodinium* and classified into nine clades (A–I; Coffroth and Santos, 2005; Pochon and Gates, 2010), the taxonomy of zooxanthellae was eventually revised into at least seven genera, six of which are novel and largely congruent with their predecessor clades (LaJeunesse et al., 2018). In corals, the symbiotic relationship involves the host providing shelter and inorganic nutrients for the photoautotrophic zooxanthellae which assimilate and export back to the host high concentrations of oxygen for respiration and calcification and other photosynthates like glycerol, glucose, amino acids, and lipids, supplying more than 90% of the host's metabolic requirements (Muscatine, 1990; Yellowlees et al., 2008; Davy et al., 2012; Fransolet et al., 2012). However, thermal stress and high levels of solar irradiance could disrupt the mutualistic relationship and cause bleaching and reduced fitness that lead to the likely death of the cnidarian host (Hoegh-Guldberg, 1999; Douglas, 2003; Weis, 2008; Wooldridge, 2013). While bleaching is a normal sign of coral stress, the rapid increase in mean global ocean temperatures due to anthropogenic climate change (Peñaflor et al., 2009; Lough et al., 2018), when compounded with prolonged periods of positive thermal anomalies brought by the El Niño Southern Oscillation (ENSO), indisputably leads to mass coral bleaching events that have been more widespread and more intense through the years (Eakin et al., 2016, 2017, 2019; Hughes et al., 2017) and that have ultimately degraded coral reefs around the world (Hoegh-Guldberg et al., 2007; Carpenter et al., 2008). The minor El Niño event in 2014 (with Oceanic Niño Index, or ONI, peaking at 0.66) and the subsequent year's severe El Niño (peaking at ONI 2.64) kicked off an unprecedented multi-year global coral bleaching which lasted 3 years and affected at least half of the world's coral reefs (Heron et al., 2016; Bahr et al., 2017; Couch et al., 2017; DeCarlo et al., 2017; Hughes et al., 2017; Le Nohaïc et al., 2017; NOAA, 2021). Although coral populations may respond variably to heat stress due to differences in local conditions (e.g., water flow, turbidity, sedimentation, etc.) and phenotypic plasticity, thermal stress is still predicted to be the major factor that will cause massive coral mortality in the foreseeable future (Guest et al., 2012; McManus et al., 2020; Quimpo et al., 2020; Valino et al., 2021).

Recurring bleaching events have been correlated with signs of acclimatization (i.e., increased tolerance to thermal stress) and lower mortality rates in several coral taxa, even in species expected to be more susceptible to bleaching (e.g., *Acropora* and *Pocillopora* spp.; Maynard et al., 2008; Guest et al., 2012). For over two decades, this "natural acclimatization" of corals to thermal stress has offered hope for the survival of reefs amid rapidly warming oceans (Buddemeier and Fautin, 1993; Berkelmans and van Oppen, 2006; Thompson and Van Woesik, 2009; Brown and Cossins, 2011). This has motivated research in identifying potentially resilient coral taxa to gain evolutionary insights, with the end goal of accelerating selection for climate-resistant traits in the holobiont (i.e., the assemblage of coral host and associated microbiota), which will then be useful for coral restoration efforts and engineering reef resilience (van Oppen et al., 2015).

The overall adaptive response of the coral holobiont to high temperatures has been shown to depend on the complex interactions between host- and symbiont-related factors (Abrego et al., 2008; Mieog et al., 2009a; Putnam et al., 2012; Parkinson et al., 2015; Bay et al., 2016). One prominent hypothesis for coral acclimatization centers on the algal endosymbiont and posits coral bleaching as an opportunity for the host to switch its currently susceptible symbionts with more stress-tolerant taxa like *Durusdinium* (formerly *Symbiodinium* clade D; LaJeunesse et al., 2018), ending up with a resilient holobiont geared for the conditions that caused the bleaching in the first place (Fautin and Buddemeier, 2004; Berkelmans and van Oppen, 2006). *Durusdinium glynnii* and *D. trenchii* zooxanthellae can tolerate a wider range of water temperatures (Mostafavi et al., 2007; Lajeunesse et al., 2014; Silverstein et al., 2017; Wham et al., 2017) and are hypothesized to contribute to the resilience of the coral holobiont (Stat and Gates, 2011; Guest et al., 2016). In many studies, these thermally tolerant zooxanthellae have been reported to reproduce from background concentrations within coral tissues (i.e., "rare biosphere"; Boulotte et al., 2016), eventually overtaking its bleaching-susceptible predecessor, and dominating the coral colony post-bleaching (Jones et al., 2008; Silverstein et al., 2015; Bay et al., 2016; Cunning et al., 2018; Davies et al., 2018). This is demonstrated among surveyed natural populations and within particular coral species where the observed coral-symbiont associations often signify recent thermal regimes or anomalies. Brener-Raffalli et al. (2018), sampling *Pocillopora damicornis* sensu lato from four thermally variable sites across the Indo-Pacific, reported warmer-site corals (Djibouti and French Polynesia) hosting stress resistant species of zooxanthellae (clade D1) and cooler-site corals (Taiwan and New Caledonia) harboring a less tolerant clade (*Cladocopium goreaui*, formerly *Symbiodinium* subclade C1). This reinforces the results of previous studies which also investigated the diversity of coral zooxanthellae assemblages at finer spatial scales across different host species and thermal variabilities and revealed the occurrence of thermally tolerant symbiont lineages in warmer or historically thermally stressed sites (Baker et al., 2013; Stat et al., 2013; Zhou et al., 2017; Baumann et al., 2018). Moreover, it has been demonstrated that certain host-symbiont associations can be more labile than others (e.g., *Pocillopora* spp. are likelier to be shuffled with a tolerant species than the more stable *Porites* spp.) (Baker et al., 2013).

The Philippines, an archipelago located at the northern apex of the Coral Triangle, has surrounding waters governed by thermal regimes characterized into four clusters (Peñaflor et al., 2009) largely shaped by variabilities in latitudinal heating and circulation patterns. Philippine reefs have a history of mass coral mortality during previous bleaching events. First documented during the 1997–1998 ENSO (ONI peaking at a 2.40 and crashing to −1.57; NOAA, 2021), a bleaching event was estimated to have caused ∼ 8% coral loss across the country

(Licuanan and Gomez, 2000; Arceo et al., 2001; Magdaong et al., 2014). The Bolinao-Anda Reef Complex, a diverse marine ecosystem and vital center for fisheries and aquaculture in northwestern Philippines (Cruz-Trinidad et al., 2011), was one of the worst hit areas in the region where about 80% of corals bleached. Mass coral bleaching incidents were again reported in the Philippines and neighboring Southeast Asian reefs during another significant ENSO event (ONI peaking at 1.56 and down to −1.64) in 2009–2010 (Tun et al., 2010). For 6 months, the region experienced elevated sea surface temperatures (SST) that resulted in an estimated coral mortality of 18%. Recently, Licuanan et al. (2019) reiterated the long-term decline in hard coral cover and health of Philippine reefs and estimated that 30% of shallow-water corals have died over the recent decades, but also reported the limited impact of the 2016–2017 mass bleaching event (based on non-significant change in hard coral cover in most of 101 reef sites from 2015 to 2018). Low bleaching rates that have led to minimal changes in community structure were observed in a few Philippine reefs during the 2016–2017 event which, in conjunction with the interaction of different local environmental factors (Quimpo et al., 2020; Valino et al., 2021), could be a sign that reef response to severe bleaching events can potentially improve.

Corals being exposed to more intense heating anomalies and subjected to shorter recovery periods (Burke et al., 2011; Muñiz-Castillo et al., 2019) have underscored further the importance of understanding the coral holobiont's adaptability. In this study, we characterized the diversity of Symbiodiniaceae in several coral families across local regions and explored their association with existing thermal gradients and theoretical bleaching occurrences in the Philippine archipelago. Examining the differentiation of coral-zooxanthellae associations across regions allows us to infer how each site's thermal history may have shaped the symbioses through prolonged exposures to thermal stress (Gierz et al., 2020; Keshavmurthy et al., 2020) and provide insights on the adaptive capacity of coral reefs.

MATERIALS AND METHODS

Collection of Coral Fragments

Haphazard sampling was conducted in 14 reef sites across the archipelago from July 2015 to May 2018 (**Figure 1A**). Study sites represent the spatial gradients of SST means sensu Peñaflor et al. (2009) and cover the northern Philippine Sea and Luzon Strait, the West Philippine Sea (the Philippines' exclusive economic zone in the South China Sea), Sulu Sea, Bohol Sea, and Celebes Sea (**Table 1** and **Supplementary Table 1**). Non-bleached coral fragments (i.e., live and with color; $N = 628$) from targeted families of varied thermal stress tolerance were collected at 2–10 m depths, except for samples from the off-shore reefs in Bicol Shelf (13–24 m) where no shallow reef was found. The families Acroporidae, Pocilloporidae, Poritidae, and Helioporidae were found to be abundant or potentially resilient (as defined by Walker et al., 2004) in the Bolinao-Anda Reef Complex, northwestern Philippines and, among others were considered candidate taxa for propagation in reef restoration initiatives in the country (Levy et al., 2010; Shaish et al., 2010a,b). As such, these four families were selected for this study. An arbitrary minimum distance of 2 m between colonies was set to minimize sampling clonal ramets. From the center of each adult colony (>5 cm diameter), a 2–4 cm coral nubbin was cut, immediately preserved in salt-saturated DMSO buffer (Gaither et al., 2011), and stored at 4°C. Due to the opportunistic nature of sampling and differences in field campaign objectives, not all species were collected in all of the study sites. Only the genus *Pocillopora* (*Pocillopora acuta* and *P. verrucosa*) was collected from all 14 sites. Two other pocilloporid genera (*Seriatopora* and *Stylophora*), poritids (*Porites cylindrica* or *P. lutea*) and *Heliopora coerulea* were collected from six sites, while acroporids (*Acropora digitifera*, *A. millepora*, or *A. tenuis*) were sampled from four (**Table 2**). All collections were covered by research permits (DA-BFAR Gratuitous Permit Nos. 0102-15, 0150-18, 0153-18, and PCSD Permit Nos. 2015-08 and 2017-09).

PCR-DGGE Fingerprinting

Holobiont DNA was extracted using a modified organic DNA extraction method (Mieog et al., 2009b) employing overnight digestion of coral tissue in CTAB and proteinase K, phase separation using 24:1 chloroform/isoamyl alcohol, precipitation with isopropanol, washing with 70% ethanol, and resuspension with nuclease-free water. GeneJET Genomic DNA purification kits (Thermo Fisher Scientific) were also used following manufacturer's protocols.

Following the touchdown thermal cycle protocol of LaJeunesse (2002), the zooxanthella-specific primers *ITSintfor2* and the GC-attached *ITS2clamp* were used to amplify the internal transcribed spacer 2 region (ITS2, ∼ 350 bp) for downstream DGGE fingerprinting. PCR amplification of the ITS2 was performed in 15 μL reactions using 0.7 μM of both primers, 1 × PCR buffer, 0.45 μM dNTPs, 1.8 mM $MgCl_2$, 0.23 units of Taq polymerase (Invitrogen), and ∼ 10 ng of template DNA. Thermal cycling protocol had an initial denaturation of 3 min at 92°C; 20 cycles of denaturation for 30 s at 92°C, annealing for 40 s at 62°C (with a drop of 0.5°C per cycle), and extension for 30 s at 72°C; followed by another 20 cycles with a fixed annealing temperature of 52°C and a final extension of 5 min at 72°C.

All ITS2 PCR products were loaded 1:1 with 0.05% bromophenol blue-xylene cyanol solution into an 8% polyacrylamide (37.5:1 acrylamide/bis) denaturing gel with an internal gradient (30–60%) of denaturants (urea and formamide) and were separated by electrophoresis using DCode Universal Mutation Detection System (Bio-Rad) for 18 h at 100 V with a constant tank buffer temperature of 60°C. The acrylamide gels were post-stained with 1 × SYBR Green (Thermo Fisher Scientific) in 1 × TAE buffer for 30 min and photographed under UV illumination.

A subset of prominent bands and heteroduplexes from five initial sites BOL, ELN, SIQ, IPL, and TWI (**Table 1**) were excised and incubated overnight with 500 μL nuclease-free water. Eluates were used as template for re-amplification of the ITS2 using the oligonucleotide primers *ITSintfor2* and *ITS2reverse* following a similar thermal cycling protocol but without the touchdown cycles (LaJeunesse, 2002). Bidirectional DNA

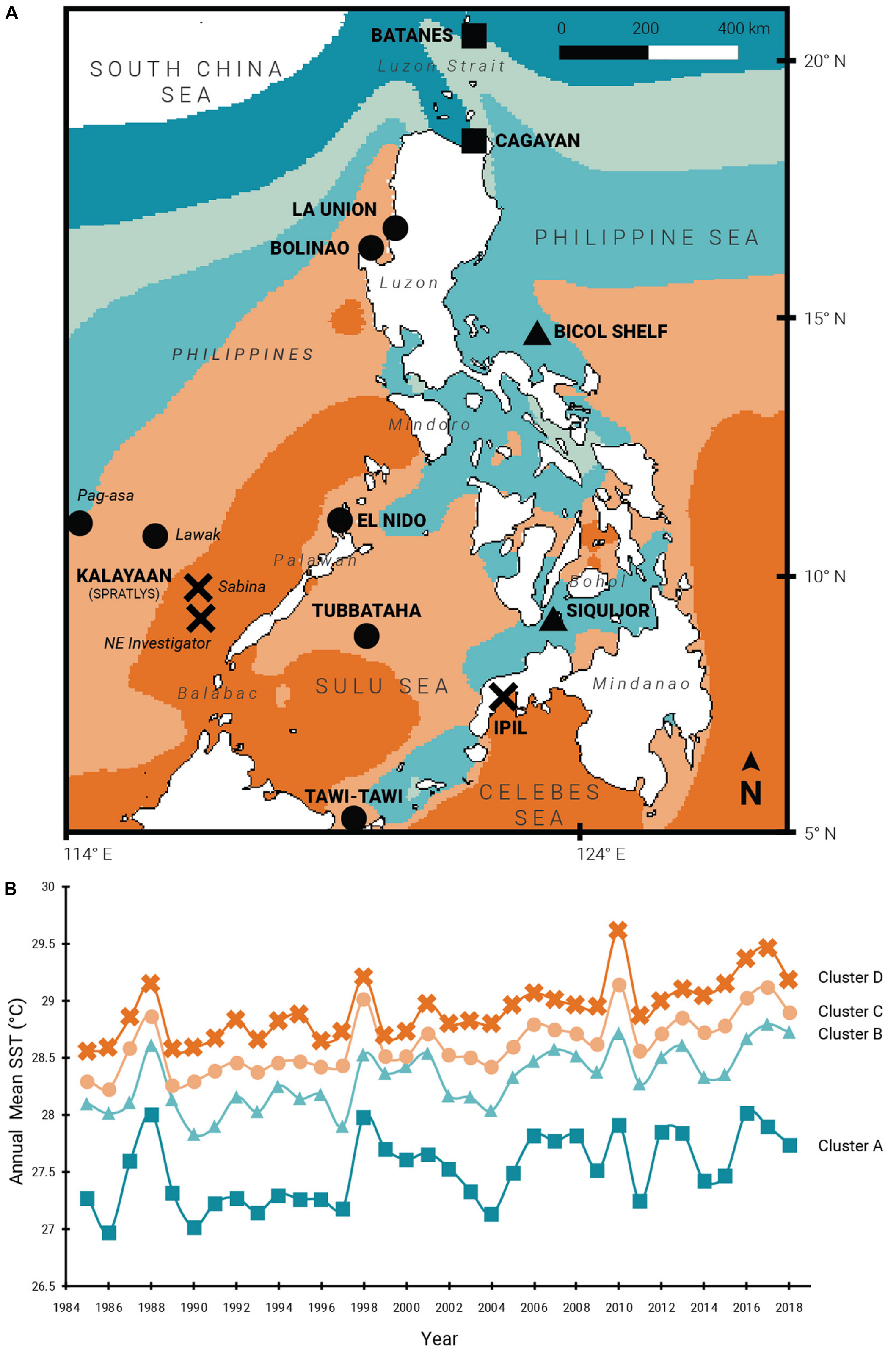

FIGURE 1 | Thermal regimes across the Philippine archipelago. **(A)** 14 study sites representing four thermal regions clustered using SST data obtained from 1985 to 2018; **(B)** Annual mean SSTs of clusters A–D from 1985 to 2018. Site symbols correspond to thermal cluster membership: square (cluster A), triangle (B), circle (C), and cross (D).

TABLE 1 | Sampling sites, dates of collection, and mean SST per thermal cluster.

Thermal cluster	Mean SST (std dev)	Sampling site	Site code	Latitude, Longitude	Project/s	Date of collection
A	27.31°C (0.26)	Batan, Batanes	BAT	20.370°N, 121.974°E	4	October 2017
		Gonzaga, Cagayan	CAG	18.377°N, 122.097°E	2	May 2016
B	28.30°C (0.18)	Bicol Shelf	BIC	14.627°N, 123.206°E	5	May 2018
		San Juan, Siquijor	SIQ	9.143°N, 123.507°E	1	October 2015; August 2016
C	28.63°C (0.13)	San Fernando, La Union	LAU	16.577°N, 120.303°E	2	April 2016
		Bolinao, Pangasinan	BOL	16.436°N, 119.941°E	1,2	June–August, November 2015; February, July, November 2016; June 2017
		El Nido, Palawan	ELN	11.114°N, 119.328°E	1	May 2016
		Kalayaan (Spratly Islands), Palawan				
		- Pag-asa Island	ASA	11.065°N, 114.279°E	4	May 2017
		- Lawak Island	LWK	10.729°N, 115.799°E	4	May 2017
		Tubbataha Reefs, Palawan	TUB	8.887°N, 119.894°E	3,4	April 2016; May 2017
		Bongao, Tawi-Tawi	TWI	5.050°N, 119.740°E	1	December 2015
D	28.87°C (0.14)	Kalayaan (Spratly Islands), Palawan				
		- Sabina Shoal	SAB	9.798°N, 116.414°E	2	May 2017
		- NE Investigator Shoal	NEI	9.184°N, 116.456°E	2	May 2017
		Ipil, Zamboanga Sibugay	IPL	7.685°N, 122.540°E	1	June 2016; February, August 2017

*Projects: **(1)** DOST-PCAARRD Coral Genomics Project 1; **(2)** DOST-PCAARRD Coral Genomics Project 3; **(3)** DOST-PCAARRD NACRE-PEARRL Project; **(4)** DENR-BMB WPS Project; **(5)** DENR-BMB SECURE Philippine Rise Project.*

TABLE 2 | Dominant zooxanthellae detected from four coral families across 14 sampling sites clustered according to thermal regime.

Thermal cluster	Site	Pocilloporidae			Acroporidae	Poritidae	Helioporidae
		Pocillopora	*Seriatopora*	*Stylophora*	*Acropora*	*Porites*	*Heliopora*
A	BAT	C (14); D (1)	–	–	–	–	–
	CAG	C + D (6); D (11)	–	–	–	–	–
B	BIC	C (28); C + D (1)	C (3)	C (12)	C (12)	C (7)	C (15)
	SIQ	**C1, C1t, C1d (12)**; C (6); D (3)	**C1, C1# (16)**; C (4)	**C1c.C45 (2)**; C (18)	–	**C15 (9)**	**Cspc (8)**
C	LAU	C + D (2), D (8)	–	–	–	–	–
	BOL	C (2); C + D (2); **D1 (15)**; D (29)	**D1, D1a (14)**	**C1c.C45 (10)**; **D1, D1a, D6 (3)**	**C3u (39)**	**C15 (25)**	**Cspc (22)**
	ELN	C (1); **D1 (19)**	**D1 (19)**	**C1 (11)**; **D1 (9)**	**C3u (13)**	**C15 (7)**	**Cspc (7)**
	ASA	D (10)	–	–	–	–	–
	LWK	C (3), D (1)	–	–	–	–	–
	TUB	C (21); C + D (4); D (2)	–	–	–	–	–
	TWI	**C1, C1c, C1d, C1e, C42a, C42-2 (11)**	**C1# (10)**	**C1c (4)**	–	**C15 (10), C55 (1)**	**Cspc (4), C1p (1)**
D	SAB	C (2), D (14)	–	–	–	–	–
	NEI	C (2)	–	–	–	–	–
	IPL	C + D (6), **D1 (4)**; D (9)	C (1); C + D (1); **D1a, D2.2 (9)**; D (8)	C (1); C + D (3); **D1a (9)**; D (6)	**C40 (5)**	**C15 (9)**; C (14)	**Cspc (9)**

Bold and underlined identities were validated through sequencing. Identities based on DGGE fingerprints are labeled as C or D (or C + D when found in mixed detections). Numbers of colonies that showed positive identifications are contained in parentheses. ("–" not sampled).

sequencing was performed (First Base Laboratories, Malaysia) and individual ITS2 sequences were manually trimmed, checked, and aligned using Geneious Prime v2020.0.3 (Kearse et al., 2012). For zooxanthellae clade/species identification, sequences were queried through BLAST in a custom database assembled from the curated GeoSymbio database of zooxanthellae taxa (Franklin et al., 2012) and additional unique sequences obtained from GenBank (query: "Symbiodiniaceae" "ITS2") that were not covered by the former. Genetically identified samples were used as diversity standards in subsequent DGGE runs for the other sites.

Sea Surface Temperatures Clustering and Inferring Stress Occurrences

Thermal regions in the Philippines were recharacterized to extend the dataset (Peñaflor et al., 2009) with more recent SSTs (1985–2018). The daily updated 5 km resolution SST product (CoralTemp) of Coral Reef Watch (CRW) produced from combining and blending geostationary and polar-orbiting environmental satellites (Liu et al., 2014) were averaged using SNAP v7.0.0[1] binning function. Clustering of similar-value pixels was done to the resulting three-decadal mean SSTs using SAGA k-means grid clustering tool (Peñaflor et al., 2009; Kleypas et al., 2015). Annual mean SSTs in all sites within each cluster were calculated.

Having limited empirical information on actual bleaching and mortality, possible past occurrences can be extrapolated from bleaching- and mortality-level degree-heating weeks (DHW, i.e., a thermal stress index based on the accumulation of SST anomalies) that have reached four to eight consecutive weeks (Liu et al., 2006; McClanahan et al., 2007). These metrics can proxy for sustained thermal stress especially during the ENSO years, when high levels of solar irradiance can be expected in the region (Muñiz-Castillo et al., 2019). Exposure to positive temperature anomalies and theoretical bleaching and mortality experienced by corals in all 14 sites were characterized by obtaining mean mortality-level degree-heating weeks ($8 \leq$ DHWs) and bleaching-level DHWs ($4 \leq$ DHWs < 8) during ENSO years (Muñiz-Castillo et al., 2019). The daily 5 km DHW product of CRW comes from positive heat anomalies or the accumulation of heat stress during a 12-week period derived from CoralTemp (Liu et al., 2014).

Statistical Analyses

Patterns for spatial distribution or association with thermal regimes were examined by performing multivariate analyses in the family Pocilloporidae where variability was observed. A dataset representing abundance information (i.e., colony counts for dominant or co-occurring symbiont genera) was produced. To quantify compositional differences of dominant zooxanthellae between populations, Bray-Curtis dissimilarity indices (BCD) were calculated based on both raw and square root-transformed abundance data. Non-metric multidimensional scaling (NMDS) was performed on BCD matrices for all-Pocilloporidae (combined *Pocillopora*, *Seriatopora*, and *Stylophora*) and *Pocillopora*-only datasets. Sites LWK and NEI were excluded from the analysis due to small sample sizes ($N < 5$ colonies). While square root transformation on abundance data returned lower BCD values versus non-transformed data, the clustering of populations did not change (**Supplementary Figure 2**). Likewise, performing NMDS on raw and transformed abundance data produced identical stress values and ordination, thus only the non-transformed data were used for subsequent analysis. Ordination plots were generated to visualize structuring of zooxanthellae diversity based on each of the site's thermal cluster membership and frequency of exposure to bleaching-level DHWs. Analysis of similarities (ANOSIM) was then used to test for significant differences in zooxanthellae species composition between emergent groupings from the NMDS analysis. All statistical analyses were conducted using the package "vegan" v2.5-7 (Oksanen et al., 2020) in R v4.0.2 (R Core Team, 2021).

RESULTS

Diversity of Dominant Coral Zooxanthellae

All coral samples were evaluated for zooxanthella clade/species/genus diversity using PCR-DGGE fingerprinting. Most profiles displayed the expected one or two prominent bands accompanied by background heteroduplexes (LaJeunesse, 2002). ITS2 sequences from a subset of these bands ($N = 217$) returned homology to 18 Symbiodiniaceae taxa (**Table 2**): *Cladocopium goreaui* (C1), 13 other *Cladocopium* lineages (C1c, C1c.C45, C1d, C1e, C1p, C1t, C1#, C3u, C15, C40, C42a, C42-2, and Cspc), *Durusdinium glynnii* (D1), *D. trenchii* (D1a), and two more *Durusdinium* clades (D2.2 and D6) (GenBank Accession Nos. MW024153–MW024369).

Sea Surface Temperatures Clustering and Thermal Stress

Geospatial clustering analysis shows five distinct marine SST regions surrounding the Philippines (**Figure 1A**). Four of these clusters (A–D) cover most circumjacent waters of the Philippines and are described in this study. Over the last three decades, most of the sites experienced above-average temperatures that peak during years with confirmed mass bleaching events (1998, 2010, 2015–2017; **Figure 1B** and **Supplementary Table 2**). Clusters A and B recorded lower annual SST means (ranging 26.98–28.02°C and 27.83–28.80°C, respectively) and cover the waters of northern and eastern Luzon, the internal seas of central Philippines, and the Sulu archipelago in the south. Annual mean SST values in these clusters show less fluctuations during the initial 10 years which increased toward the recent decades. In contrast, clusters C and D exhibited higher mean SSTs (28.23–29.15°C and 28.57–29.62°C) with low annual temperature fluctuations (**Table 1**). Cluster C partially encompasses the western seaboard of Luzon in the West Philippine Sea, the Kalayaan Island Group (Spratly Islands), and the northern

---

[1] http://step.esa.int

section of the Sulu Sea. Cluster D exhibits the highest annual mean SSTs and covers mainly the western Palawan shelf, southwestern Sulu Sea, and the southern and eastern waters off Mindanao.

All collection sites, with the exception of SIQ and TWI, were exposed to bleaching-level DHWs ($\geq$4 DHWs) between 1 and 4 times during ENSO years within the span of the time series and are thus inferred to have experienced bleaching (**Figure 2A**). One site (ASA) was exposed to one bleaching DHW, seven sites (BOL, ELN, LWK, TUB, SAB, NEI, and IPL) to two, and three sites (BAT, CAG, and LAU) were exposed to three. BIC with an exposure frequency of four had the most frequent bleaching DHWs. Only four sites reached mortality-level DHWs ($\geq$8 DHWs): BIC, SAB, and NEI with one exposure, and CAG with two exposures. No site in Cluster C was exposed to mortality-level DHWs. Coincident with mean SST fluctuations, sites from the cooler clusters A and B have been exposed more frequently to positive heat anomalies compared with the warmer clusters C and D (**Figures 1B**, **2A**).

Distribution of Coral-Symbiont Associations

Regional consistency in dominant zooxanthella species was observed in Acroporidae, Poritidae, and Helioporidae where each family was dominated by 1–2 clades of *Cladocopium* (**Figure 2B** and **Table 2**). Poritidae samples, regardless of species or site of collection, hosted *Cladocopium* clade C15. Most Helioporidae samples from five of six sites harbored *Cladocopium* clade Cspc with one colony detected with clade C1p. Acroporidae from two sites along the western Philippine seaboard hosted *Cladocopium* clade C3u (BOL and ELN), while colonies sampled from the Celebes Sea (IPL) hosted clade C40.

Pocilloporidae exhibited variation in zooxanthellae composition across sites (**Table 2** and **Supplementary Table 3**), with an emergent pattern of community composition broadly concordant with thermal clusters (**Figure 2B**). Pocilloporids from SIQ and TWI, falling within SST clusters B and C, respectively, and which have had neither bleaching nor mortality-level DHWs, predominantly host *Cladocopium* species (e.g., *C. goreaui*) and clades (e.g., C1c, C1d, C1t, C1#, and C42a). *Pocillopora* samples from BAT and TUB and all three pocilloporid genera from BIC, likewise, predominantly hosted *Cladocopium* zooxanthellae. Conversely, pocilloporid communities in BOL, ELN, and IPL were composed of colonies mainly dominated by *Durusdinium glynnii* or *D. trenchii* or mixed with *Cladocopium* symbionts (C + D; **Supplementary Figure 1**), except for the *Stylophora* colonies of BOL and ELN where slightly more than half of the colonies were detected only with *Cladocopium.* Within thermal cluster A, *Pocillopora* samples from BAT and CAG exhibit contrasting patterns, with colonies from CAG predominantly harboring *Durusdinium* or a mix of *Cladocopium* and *Durusdinium* while all colonies from BAT harbor predominantly *Cladocopium,* with the exception of one colony which harbors predominantly *Durusdinium*. Other sites within the West Philippine Sea, all falling under thermal clusters C and D and all having experienced bleaching-level DHWs, consisted of colonies hosting differential proportions of *Cladocopium* and *Durusdinium*. Sites LWK and NEI harbored predominantly *Cladocopium,* while LAU, ASA, and SAB colonies were dominated by *Durusdinium*.

Multivariate analysis of zooxanthellae composition for the Pocilloporidae reveal two broad groupings largely coinciding with SST rankings (**Figure 3**). Bray-Curtis dissimilarity indices between populations range from 0.143 (raw) and 0.136 (square root-transformed) to 1 (**Supplementary Table 4**). Stress values for both *Pocillopora*-only (0.069) and all-Pocilloporidae (0.012) ordinations are below the recommended threshold value of 0.2, indicating good fit to the original distance matrices (Dexter et al., 2018). The NMDS plots for all Pocilloporidae and for *Pocillopora* spp. present comparable ordinations differing only in the ordination of 1 site (BOL). NMDS axis 1 delineates two groups reflecting the predominance of *Durusdinium* (Group 1) and *Cladocopium* (Group 2). Group 1 consists of sites mostly from thermal clusters C and D (except for CAG from thermal cluster A) while Group 2 consists of sites mostly from thermal clusters A and B (except for TWI from thermal cluster C). Considering both NMDS axes, the ordination plot for all Pocilloporidae delineates four clusters based on clade composition: Subgroup 1A (CAG-LAU-IPL-BOL) predominantly hosting *Durusdinium* and C + D, Subgroup 1B (ASA-ELN-SAB) predominantly *Durusdinium* with a lower proportion of *Cladocopium*, Subgroup 2A (TUB-BIC) predominantly *Cladocopium* with C + D, and Subgroup 2B (BAT-SIQ-TWI) with predominantly *Cladocopium* and a lower proportion of *Durusdinium*. Considering *Pocillopora* only, the minor difference in subgrouping composition is the ordination of BOL intermediate between all-Pocilloporidae Subgroups 1A and 1B.

The difference in zooxanthellae species composition between the two NMDS groups is statistically significant (ANOSIM, R = 0.656, p = 0.007). When divided into four subgroups, the differentiation in species composition remains significant (R = 0.499; p = 0.025). Species composition does not vary significantly when sites are grouped by thermal cluster (R = 0.023; p = 0.372). Grouping according to frequency of exposure to bleaching-level DHWs likewise does not reveal statistically significant differences, although the R value is an order of magnitude higher than when grouping sites according to thermal cluster and the p-value is close to the threshold for significance (R = 0.2912, p = 0.075).

DISCUSSION

Understanding determinants underlying the adaptability of corals can provide valuable insight toward inferring potential responses to climate change-induced environmental stress. Having baseline information on the contemporary diversity and distribution of coral zooxanthellae provides important context regarding the flexibility and specificity of the symbiosis, as well as the potential of corals for acclimatization or

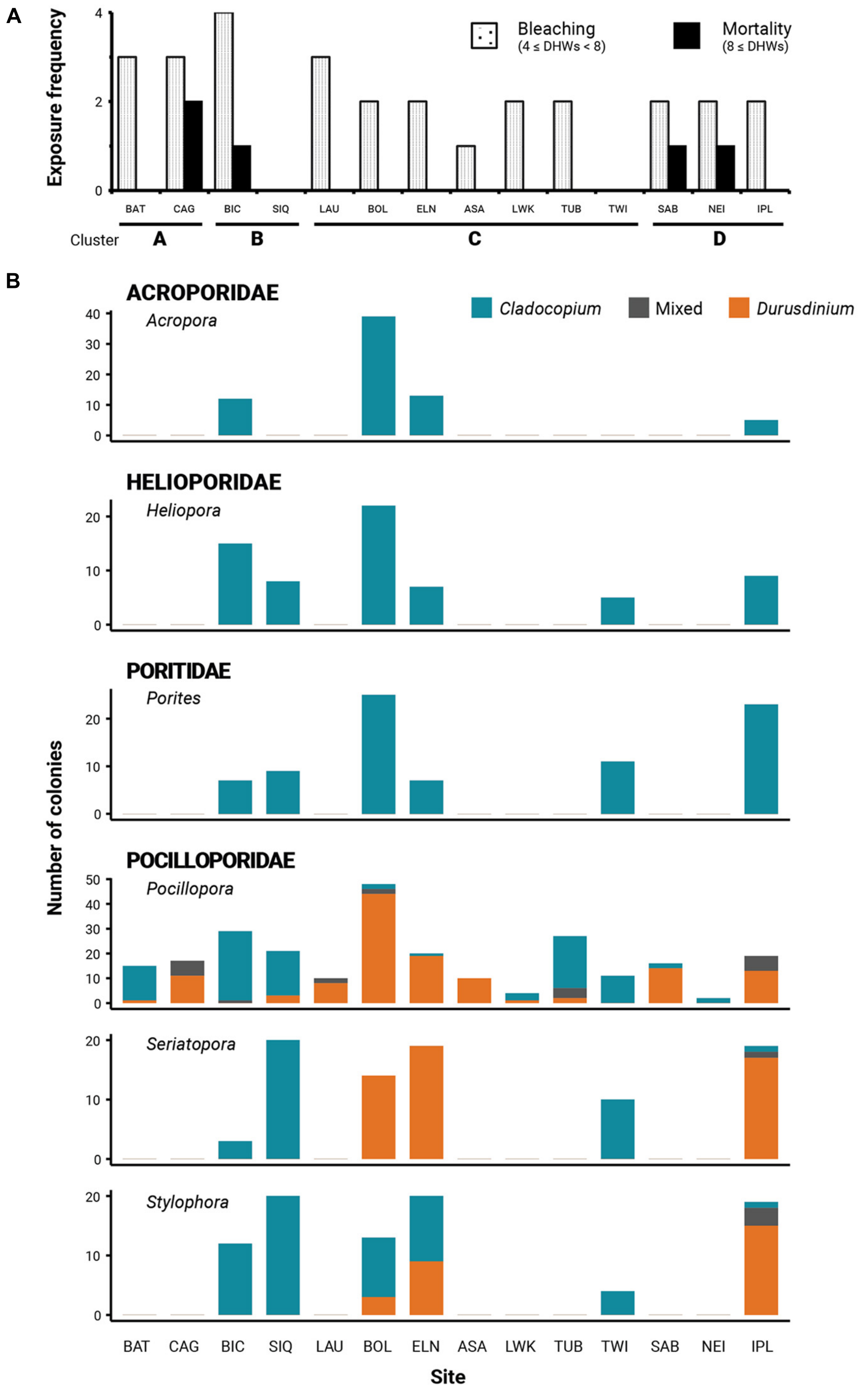

FIGURE 2 | (A) Frequency of site exposure to at least four and at least eight degree-heating weeks (DHW) indicative of prolonged thermal stress and respectively, predictive of coral bleaching and mortality; **(B)** Relative *Cladocopium*, *Durusdinium*, and mixed zooxanthellae occurrences across sites of different thermal histories and coral genera.

adaptability through periods of environmental fluctuations and sustained thermal stress. This study characterized zooxanthellae diversity and coral-endosymbiont associations in several coral taxa across the biogeographic regions of the Philippine archipelago at the northern region of the Coral Triangle, which exhibit varying thermal histories based on analysis of sea surface temperature data covering the past 34 years.

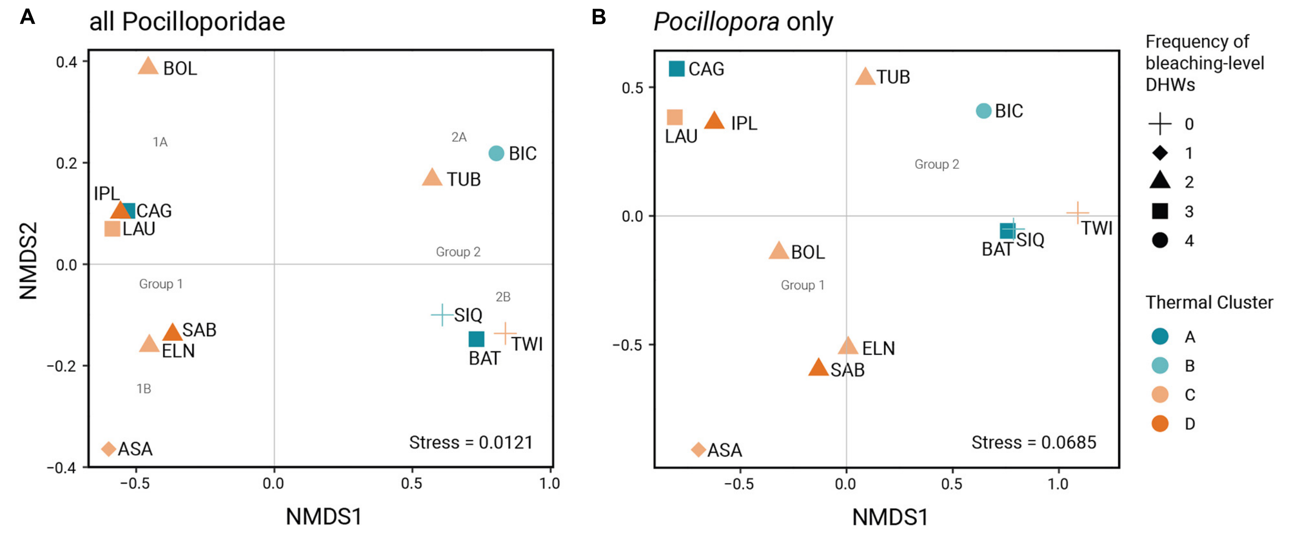

FIGURE 3 | Ordination plots from the non-metric multidimensional scaling analysis for **(A)** all-Pocilloporidae and **(B)** *Pocillopora*-only datasets, which suggest two broad groupings that coincide with thermal cluster and four subgroupings according to symbiont composition.

Three-Decadal Thermal History of Philippine Waters

Thermal stress that corals may have experienced can be inferred from historical SST data and recorded heating anomalies (Kayanne, 2016; McManus et al., 2020). The time-averaged thermal clusters described herein represent the net of the interactions of archipelagic and bathymetric complexity of the Philippines, a latitudinal heating gradient, and oceanic-atmospheric systems like the East Asian monsoons. Despite having different spatial resolutions, we observed resemblance of the five thermal regions found in this study with the SST sections identified by Peñaflor et al. (2009) and Kleypas et al. (2015). Thermal clusters A and B, characterized by lower means of daily SSTs (27.3–28.1°C), are largely influenced by the Pacific waters streaming through San Bernardino and Surigao Straits into the relatively shallow basins of central Philippines (Qu et al., 2009; Hurlburt et al., 2011; Lermusiaux et al., 2011) and by the intrusion of Kuroshio waters through the Luzon Strait. These systems, in conjunction with the cooling mechanisms of frequent precipitation (David et al., 2015), high riverine input, bathymetric features (e.g., Sulu archipelago; Han et al., 2009), and the existence of wind-driven upwelling (e.g., Zamboanga Peninsula, Bohol Sea; Cabrera et al., 2011; Villanoy et al., 2011) may have lowered SST signatures in these subregions, possibly buffering extreme warmings especially at local scales (Riegl et al., 2019). On the other hand, clusters C and D are characterized by slightly warmer SST means (28.6–28.9°C). These warmer clusters comprise most of the western and southern Philippines which are largely influenced by the mixed water masses, circulated in the larger South China Sea and which seasonally flow into the Sulu Sea through Mindoro and Balabac Straits (Sprintall et al., 2012), and by the Mindanao Current flowing south of the archipelago toward the Makassar Strait in Indonesia (Gordon et al., 1999). The Mindanao Current and its associated anticyclonic eddy to its north ultimately downwell the surface waters in the relatively shallow Moro Gulf, further warming the northern Celebes (Masumoto et al., 2001). Aggravated by an ENSO event, these existing oceanographic systems could be easily tipped toward conditions that can be too stressful for corals.

Specificity and Adaptability Across Thermal Gradients

All corals evaluated in this study either exclusively or predominantly hosted zooxanthellae taxa of *Cladocopium* or *Durusdinium*. This is consistent with previous studies that show *Cladocopium* and *Durusdinium* spp. as the main zooxanthellae in hard corals throughout the South China basin using DGGE (Chen et al., 2005; Zhou and Huang, 2011) and more recent approaches using high-throughput sequencing (Chen et al., 2019).

The homogeneity or variability observed among coral family-zooxanthella associations in the present study demonstrates the differential levels of host specificity to certain symbiont taxa (Baker, 2003; Thornhill et al., 2006). While Pocilloporidae were found to host either *Cladocopium, Durusdinium,* or a mix of both, *Acropora* and *Heliopora coerulea* displayed specificity, with each coral species detected with only one or two clades of *Cladocopium* regardless of the thermal regime or history of sampling location. The widespread Poritidae corals (*Porites cylindrica* and *P. lutea*) also exhibited strict preference to *Cladocopium* C15, a zooxanthella clade previously observed to be relatively stable under thermal stress (LaJeunesse et al., 2003). *Porites* corals mainly associating with C15 have also been observed in the Gulf of Thailand (Chankong et al., 2020) and across a wide latitudinal range in the South China

Sea (Ng and Ang, 2016; Chen et al., 2019; Gong et al., 2019). Previous transcriptomic studies that performed simulated bleaching (Barshis et al., 2013, 2014; Kenkel et al., 2013; Dixon et al., 2015) and transplantation experiments (Palumbi et al., 2014) have demonstrated potential molecular mechanisms for climate resiliency of the coral host itself. Thus, specific host-symbiotic associations suggest successful molecular mechanisms in the coral host that are independent of the symbiont (Drury, 2020). Host genotype has also been shown to positively play a role in tolerance to multiple and simultaneous stressors in *Acropora millepora* (Wright et al., 2019). However, further research can be done on specifically partnered symbioses, especially on the coral hosts' and zooxanthellae's physiological limits to wider ranges of stress conditions. It is also important to note that the symbiont composition presented here likely does not reflect low-abundance (<5–10%) zooxanthellae due to the limits of detection of DGGE-based assays (Thornhill et al., 2006; LaJeunesse et al., 2008; Baker et al., 2013). This limitation could result in an underestimation of the potential contribution of rare biosphere species like *Durusdinium* spp. (Boulotte et al., 2016) and underscores the advantages of methods like high-throughput sequencing which offer greater sensitivity and resolution in elucidating endosymbiont diversity. For example, multiple *Porites* lineages along the Saudi Arabian Red Sea have shown exceptionally diverse endosymbionts, following a north-south *Cladocopium-Durusdinium* gradient (Terraneo et al., 2019), not observed in most other DGGE-only studies.

The geographic variability of zooxanthellae hosted by pocilloporids (*Pocillopora*, *Seriatopora*, and *Stylophora*), in contrast to the consistency of symbionts hosted by *Acropora*, *Heliopora* and *Porites,* provides an interesting model to examine symbiont diversity in the context of varying environmental conditions. Sequencing of sampled DGGE bands from pocilloporids revealed *Cladocopium goreaui*, *Durusdinium glynnii*, *D. trenchii*, and other *Cladocopium* and *Durusdinium* clades, which all vary in thermal stress tolerance. Zooxanthellae composition is significantly different among sites, with two broad groups coincident with mean SST ranges and frequency of exposure to bleaching-level thermal stress. Pocilloporids in warmer thermal clusters C and D and the less warm clusters A and B generally differ in the predominance of the thermally tolerant *Durusdinium* and less tolerant *Cladocopium*, respectively. There are, however, a few exceptions. For instance, pocilloporids in TWI, despite experiencing higher mean SSTs, were shown to host thermally sensitive *Cladocopium* symbionts. That TWI had not experienced more-than-four continuous DHWs during the 34-year period (**Figure 2A**) may account for the observed dominance of *Cladocopium* instead of *Durusdinium*. Similarly, the dominance of *Cladocopium* symbionts in pocilloporids from TUB amidst relatively warmer temperatures, and in BIC which had the most frequent exposure to bleaching-level thermal stress, suggest the influence of other factors (e.g., clouds, reef health) not captured by mean SSTs and thermal anomalies. The highly protected Tubbataha Reefs Natural Park is situated in the middle of Sulu Sea away from anthropogenic stress and is known to host some of the most pristine and healthiest coral reefs in the world (Licuanan et al., 2017). While protection in itself cannot negate the impact of high temperatures to coral reef health, the compounded support by the immense biomass of herbivores, lower levels of localized stress, robust supply of larvae (i.e., connectivity), ample cloud cover, and geographic isolation could have facilitated recovery of stressed reefs in TUB (Selig et al., 2012; Gilmour et al., 2013; Peñaflor, 2015; Licuanan et al., 2019; McManus et al., 2020). Moreover, our findings in BIC imply the potential importance of deep or even turbid reef systems in providing refuge for future climate change scenarios in this specific region (Bongaerts et al., 2010; Sully and van Woesik, 2020). The depth of the sampled reefs in BIC ($\sim$ 26 m) may have prevented surface thermal anomalies to reach the reef, providing more stable ambient temperatures for corals. Additionally, as *Cladocopium* symbionts are more photosynthetically efficient than *Durusdinium* spp. (i.e., higher F_v/F_m) in lower temperatures (Silverstein et al., 2017), it might be expected for the former to thrive in deeper reef systems where irradiance levels are much reduced, as was observed in *Montastraea cavernosa* colonies along a depth gradient in Belize (Eckert et al., 2020). For all these cases, incorporating additional *in situ* and smaller-scale observations of other environmental factors is essential and should be considered for future studies.

The dominance of *Durusdinium* zooxanthellae (or their presence in mixed detections) in sites that were previously under thermal stress could indicate a switch to thermally tolerant endosymbionts from a thermally sensitive species like *C. goreaui* (C1). The observed *Durusdinium* dominance in historically stressed pocilloporids complements the findings of Baker et al. (2013); Brener-Raffalli et al. (2018), Qin et al. (2019); Chankong et al. (2020), and Poquita-Du et al. (2020) which report *Pocillopora*'s flexibility and tendency to harbor *Durusdinium* symbionts with increasing temperatures or recent thermal anomalies. In addition, mixing of zooxanthellae genera was exclusively observed in pocilloporid species. This mixing in conjunction with the geographically varied coral-zooxanthellae associations found in Pocilloporidae could suggest the occurrence of symbiont shuffling or a transition toward the dominance of more thermally tolerant zooxanthellae. The significant difference in zooxanthellae composition between the four NMDS subgroupings, which also correlate with frequency of bleaching-level DHWs, may imply incidences of coral acclimatization among pocilloporids. However, the haphazard sampling in this study does not allow us to fully capture possible fine-scale temporal changes in the zooxanthellae assemblage which may have already transpired within days, weeks, or months after peak stress levels (Claar and Baum, 2019). It is therefore not possible to conclude with certainty whether the co-occurrence or dominance of *Durusdinium* spp. is a transient switch from *Cladocopium* spp. or a snapshot of an enduring symbiosis with its coral host.

Implications for the Future of Coral Reefs

Identifying resilient coral communities will be vital in prioritizing areas for conservation (Hoegh-Guldberg et al., 2018) and augmenting levels of protection of such sites against other possible stressors such as overfishing that contribute to the decline of reef health, which will ultimately benefit coastal communities who extensively rely on these critical reef ecosystems. While several studies have predicted that neither level of protection nor bleaching history nor coral taxon may save coral reefs from extremely severe stress as what occurred at the Great Barrier Reef during the 2014–2017 event (Hughes et al., 2017; Eakin et al., 2019), it is also still possible that geographically and oceanographically more complex regions such as archipelagos may shed light on their biogeographic variability as a means for reef adaptability and resilience. Observations on the limited impact of the recent global bleaching event to Philippine reefs (Licuanan et al., 2019) provide interesting avenues for further research on the underlying basis of reef recovery and resilience. The Coral Triangle, a still understudied hotspot of reef biodiversity and geographic and oceanographic complexity will be proven valuable in understanding the potential resilience of coral reefs.

The diversity of symbionts and the flexibility of coral zooxanthellae associations observed in this study, particularly of pocilloporids, suggest that acclimatization of corals through symbiont shuffling is plausible in natural coral communities and could be a sign of hope for the persistence of reefs in the face of global change and uncertainty. The thermally tolerant *Durusdinium*, however, are known opportunists and harboring them has its trade-offs for the coral host (Little et al., 2004; Jones and Berkelmans, 2010, 2011; Stat and Gates, 2011; Lesser et al., 2013; Sproles et al., 2020). An established coral-*Durusdinium* symbiosis also does not guarantee bleaching resistance, as prolonged exposure to thermal stress can still result in the death the coral (Claar et al., 2020). Promising new results (Abbott et al., 2021) suggest that a near-equal relative proportion (co-dominance) of *Cladocopium* and *Durusdinium* symbionts elevates expression of genes related with productivity (i.e., translation and photosynthesis) in the zooxanthellae and at the same time promotes cellular growth for the coral host. This highlights the potential significance of co-occurring symbiont genera in corals and has important implications for predicting the health of the holobiont and of coral reefs in general.

Only a few studies have conducted long-term monitoring of the recovery and zooxanthella assemblage dynamics in corals and none has captured the net effect of *D. trenchii* or *D. glynnii* dominance to the long-term overall health of the coral. Loya et al. (2001) and van Woesik et al. (2011), for example, categorized species found in Okinawa, Japan as bleaching winners or losers in a 14-year interval, classifying all pocilloporid genera (that were considered in this study) as long-term losers due to lack of signs of recovery after two mass bleaching events. On the contrary, Guest et al. (2012) demonstrated a likely adaptive response from the usually susceptible corals *Pocillopora* and *Acropora* in Singapore, showing highly improved performance during the same mass bleaching events (1998 and 2010) and indicating what might be holobiont adaptability that is geographically variable. Both studies were not able to consider the diversity of endosymbionts and would have helped explain the difference in the two regions' post-bleaching performance. Whether *Durusdinium* can persist to be the dominant symbiont in the coral colony or coral populations years after shuffling also remains in question. Reversion from *D. glynnii*/*D. trenchii* back to the coral host's original symbiont assemblage has been observed in *Orbicella annularis* and *O. franksi* in the Florida Keys (Thornhill et al., 2006). *Durusdinium* symbionts among clonal ramets of *O. faveolata* have been recently detected, suggesting an intergenerational transmission of bleaching resistance (Manzello et al., 2019). Likewise, vertical transmission of endosymbiotic algae is known for the pocilloporid genera *Pocillopora*, *Seriatopora*, and *Stylophora* (Isomura and Nishihira, 2001), whose brooded larvae have also been shown to exhibit "environmental hardening" and pre-adaptability to thermal stress and acidic environmental conditions (Jiang et al., 2020; Kitchen et al., 2020). Other species like *Montipora digitata* in the Great Barrier Reef pass on shuffled endosymbionts through spawned gametes as well (Quigley et al., 2019). All these examples and their effect on the overall coral mortality or recovery rates in a population would be interesting to explore in the Philippines or the wider Coral Triangle region, which have been documented to have experienced frequent thermal stress occurrences in the past 30 years. In the broader context, the ability of reefs in the region to withstand future projections of global warming, to be a temporary refuge for genetic resources, or to naturally supply propagules for replenishing impacted reefs can only be predicted and realized with systematic and consistent monitoring of coral survival, investigating its underlying mechanisms, and effectively translating science into policy. Limited information on the factors underlying adaptability of the coral holobiont in the face of a changing environment emphasizes the need for more studies focusing on the Coral Triangle, while equally highlighting the need to act on mitigating anthropogenic stressors negatively impacting ecosystem function, whether global or local, with a heightened sense of urgency and resolve.

DATA AVAILABILITY STATEMENT

The datasets presented in this study can be found in the supplementary material and in online repositories. The names of the repository/repositories and accession number(s) can be found below: NCBI (GenBank Accession Nos. MW024153–MW024369).

AUTHOR CONTRIBUTIONS

AT, DV, and RR-G contributed to the conception and design of the study. AT conducted sample collection, laboratory work, all zooxanthellae-related analyses, and wrote the first draft of the manuscript. DV assisted in sampling and performed all SST-related methods. DV and RR-G wrote sections of the manuscript. All authors contributed to manuscript revision, read, and approved the submitted version.

FUNDING

This study was supported by the Philippine Department of Science and Technology – Philippine Council for Agriculture, Aquatic, and Natural Resources Research and Development (DOST-PCAARRD Project Numbers QSR-MR-COR.02.01 and QSR-MR-COR.02.03), Department of Environment and Natural Resources – Biodiversity Management Bureau (DENR-BMB), and University of the Philippines – Marine Science Institute.

ACKNOWLEDGMENTS

This paper is dedicated to the late Ronald D. Villanueva whose contribution to the project during its inception has been invaluable. The authors thank Patrick R. Pata and the reviewers LE and RC-T for their helpful comments and suggestions, and acknowledge Hazel O. Arceo, Cesar L. Villanoy, and Maria Lourdes San Diego-McGlone for their support of this study. Eileen Peñaflor and Mariana Soppa shared key knowledge in processing satellite products. Mikhael Tañedo, Romer Albino, Emmeline Jamodiong, David Siquioco, Lovely Heyres, Rhea Luciano, Joey Cabasan, Frederico Sabban, Geminne Manzano, Clairecynth Yu, Joyce Velos, Joseph Garcia, Robert Casauay, Maryjune Cabiguin, Macy Añonuevo-Arcega, Ariel Loja, Jerome Genilan, Amabelle Go, Jamie Dichaves, Elaine Saniel, and Miledel Quibilan assisted with field collections. Supporting hard coral data were provided by the DOST-PCAARRD NACRE Program and the DENR-BMB WPS and SECURE Philippine Rise Projects. This is MSI contribution number 486.

SUPPLEMENTARY MATERIAL

The Supplementary Material for this article can be found online at: https://www.frontiersin.org/articles/10.3389/fmars.2021.731023/full#supplementary-material

REFERENCES

Abbott, E., Dixon, G., and Matz, M. (2021). Codominance of two symbiont genera within the same coral host is associated with elevated symbiont productivity and lower host susceptibility to thermal stress. *bioRxiv* [Preprint]. doi: 10.1101/2021.01.20.427463

Abrego, D., Ulstrup, K. E., Willis, B. L., and van Oppen, M. J. H. (2008). Species-specific interactions between algal endosymbionts and coral hosts define their bleaching response to heat and light stress. *Proc. R. Soc. B Biol. Sci.* 275, 2273–2282. doi: 10.1098/rspb.2008.0180

Arceo, H. O., Quibilan, M. C., Aliño, P. M., Lim, G., and Licuanan, W. Y. (2001). Coral bleaching in Philippine reefs: coincident evidences with mesoscale thermal anomalies. *Bull. Mar. Sci.* 69, 579–593.

Bahr, K. D., Rodgers, K. S., and Jokiel, P. L. (2017). Impact of three bleaching events on the reef resiliency of Kāne'ohe Bay, Hawai'i. *Front. Mar. Sci.* 4:398. doi: 10.3389/fmars.2017.00398

Baker, A. C. (2003). Flexibility and specificity in coral-algal symbiosis: diversity, ecology, and biogeography of *Symbiodinium*. *Annu. Rev. Ecol. Evol. Syst.* 34, 661–689. doi: 10.1146/annurev.ecolsys.34.011802.132417

Baker, A. C., McClanahan, T. R., Starger, C. J., and Boonstra, R. K. (2013). Long-term monitoring of algal symbiont communities in corals reveals stability is taxon dependent and driven by site-specific thermal regime. *Mar. Ecol. Prog. Ser.* 479, 85–97. doi: 10.3354/meps10102

Barshis, D. J., Ladner, J. T., Oliver, T. A., and Palumbi, S. R. (2014). Lineage-specific transcriptional profiles of *Symbiodinium* spp. Unaltered by heat stress in a coral host. *Mol. Biol. Evol.* 31, 1343–1352. doi: 10.1093/molbev/msu107

Barshis, D. J., Ladner, J. T., Oliver, T. A., Seneca, F. O., Traylor-Knowles, N., and Palumbi, S. R. (2013). Genomic basis for coral resilience to climate change. *Proc. Natl. Acad. Sci. U.S.A.* 110, 1387–1392. doi: 10.1073/pnas.1210224110

Baumann, J. H., Davies, S. W., Aichelman, H. E., and Castillo, K. D. (2018). Coral *Symbiodinium* community composition across the belize mesoamerican barrier reef system is influenced by host species and thermal variability. *Microb. Ecol.* 75, 903–915. doi: 10.1007/s00248-017-1096-6

Bay, L. K., Doyle, J., Logan, M., and Berkelmans, R. (2016). Recovery from bleaching is mediated by threshold densities of background thermo-tolerant symbiont types in a reef-building coral. *R. Soc. Open Sci.* 3:160322. doi: 10.1098/rsos.160322

Berkelmans, R., and van Oppen, M. J. H. (2006). The role of zooxanthellae in the thermal tolerance of corals: a "nugget of hope" for coral reefs in an era of climate change. *Proc. R. Soc. B Biol. Sci.* 273, 2305–2312. doi: 10.1098/rspb.2006.3567

Bongaerts, P., Ridgway, T., Sampayo, E. M., and Hoegh-Guldberg, O. (2010). Assessing the 'deep reef refugia' hypothesis: focus on Caribbean reefs. *Coral Reefs* 29, 309–327. doi: 10.1007/s00338-009-0581-x

Boulotte, N. M., Dalton, S. J., Carroll, A. G., Harrison, P. L., Putnam, H. M., Peplow, L. M., et al. (2016). Exploring the *Symbiodinium* rare biosphere provides evidence for symbiont switching in reef-building corals. *ISME J.* 10, 2693–2701. doi: 10.1038/ismej.2016.54

Brener-Raffalli, K., Clerissi, C., Vidal-Dupiol, J., Adjeroud, M., Bonhomme, F., Pratlong, M., et al. (2018). Thermal regime and host clade, rather than geography, drive *Symbiodinium* and bacterial assemblages in the scleractinian coral *Pocillopora damicornis* sensu lato. *Microbiome* 6:39. doi: 10.1186/s40168-018-0423-6

Brown, B. E., and Cossins, A. R. (2011). "The potential for temperature Acclimatisation of reef corals in the face of climate change," in *Coral Reefs: An Ecosystem in Transition*, eds Z. Dubinsky and N. Stambler (Dordrecht: Springer), 421–433. doi: 10.1007/978-94-007-0114-4

Buddemeier, R. W., and Fautin, D. G. (1993). Coral bleaching as an adaptive mechanism. *Bioscience* 43, 320–326. doi: 10.2307/1312064

Burke, L., Reytar, K., Spalding, M., and Perry, A. (2011). *Reefs at Risk Revisited*. Washington, DC: World Resources Institute.

Cabrera, O. C., Villanoy, C. L., David, L. T., and Gordon, A. L. (2011). Barrier layer control of entraitnment and upwelling in the Bohol Sea, Philippines. *Oceanography* 24, 130–141. doi: 10.5670/oceanog.2011.10

Carpenter, K. E., Abrar, M., Aeby, G., Aronson, R. B., Banks, S., Bruckner, A., et al. (2008). One-third of reef-building corals face elevated extinction risk from climate change and local impacts. *Science* 321, 560–563. doi: 10.1126/science.1159196

Chankong, A., Kongjandtre, N., Senanan, W., and Manthachitra, V. (2020). Community composition of Symbiodiniaceae among four scleractinian corals in the eastern Gulf of Thailand. *Region. Stud. Mar. Sci.* 33:100918. doi: 10.1016/j.rsma.2019.100918

Chen, B., Yu, K., Liang, J., Huang, W., Wang, G., Su, H., et al. (2019). Latitudinal variation in the molecular diversity and community composition of Symbiodiniaceae in Coral From the South China Sea. *Front. Microbiol.* 10:1278. doi: 10.3389/fmicb.2019.01278

Chen, C. A., Yang, Y. W., Wei, N. V., Tsai, W. S., and Fang, L. S. (2005). Symbiont diversity in scleractinian corals from tropical reefs and subtropical non-reef communities in Taiwan. *Coral Reefs* 24, 11–22. doi: 10.1007/s00338-004-0389-7

Claar, D. C., and Baum, J. K. (2019). Timing matters: survey timing during extended heat stress can influence perceptions of coral susceptibility to bleaching. *Coral Reefs* 38, 559–565. doi: 10.1007/s00338-018-01756-7

Claar, D. C., Starko, S., Tietjen, K. L., Epstein, H. E., Cunning, R., Cobb, K. M., et al. (2020). Dynamic symbioses reveal pathways to coral survival through prolonged heatwaves. *Nat. Commun.* 11:6097. doi: 10.1038/s41467-020-19169-y

Coffroth, M. A., and Santos, S. R. (2005). Genetic diversity of symbiotic dinoflagellates in the genus *Symbiodinium*. *Protist* 156, 19–34. doi: 10.1016/j.protis.2005.02.004

Couch, C. S., Burns, J. H. R., Liu, G., Steward, K., Gutlay, T. N., Kenyon, J., et al. (2017). Mass coral bleaching due to unprecedented marine heatwave in Papahānaumokuākea Marine National Monument (Northwestern Hawaiian Islands). *PLoS One* 12:e0185121. doi: 10.1371/journal.pone.0185121

Cruz-Trinidad, A., Geronimo, R. C., Cabral, R. B., and Aliño, P. M. (2011). How much are the Bolinao-Anda coral reefs worth? *Ocean Coast. Manage.* 54, 696–705. doi: 10.1016/j.ocecoaman.2011.07.002

Cunning, R., Silverstein, R. N., and Baker, A. C. (2018). Symbiont shuffling linked to differential photochemical dynamics of *Symbiodinium* in three Caribbean reef corals. *Coral Reefs* 37, 145–152. doi: 10.1007/s00338-017-1640-3

David, L. T., Borja-Del Rosario, R., Peñaflor, E. L., Cordero-Bailey, K., Villanoy, C. L., Aliño, P. M., et al. (2015). "Developing a Philippine climate-ocean typology as input to national vulnerability assessments," in *Proceedings of the 36th 2015 Asian Conference on Remote Sensing*, Quezon, 34–38.

Davies, S. W., Ries, J. B., Marchetti, A., and Castillo, K. D. (2018). *Symbiodinium* functional diversity in the Coral *Siderastrea siderea* Is influenced by thermal stress and reef environment, but not ocean acidification. *Front. Mar. Sci.* 5:150. doi: 10.3389/fmars.2018.00150

Davy, S. K., Allemand, D., and Weis, V. M. (2012). Cell biology of Cnidarian-Dinoflagellate symbiosis. *Microbiol. Mol. Biol. Rev.* 76, 229–261. doi: 10.1128/mmbr.05014-11

DeCarlo, T. M., Cohen, A. L., Wong, G. T. F., Davis, K. A., Lohmann, P., and Soong, K. (2017). Mass coral mortality under local amplification of 2°c ocean warming. *Sci. Rep.* 7:44586. doi: 10.1038/srep44586

Dexter, E., Rollwagen-Bollens, G., and Bollens, S. M. (2018). The trouble with stress: a flexible method for the evaluation of nonmetric multidimensional scaling. *Limnol. Oceanogr. Methods* 16, 434–443. doi: 10.1002/lom3.10257

Dixon, G. B., Davies, S. W., Aglyamova, G. A., Meyer, E., Bay, L. K., and Matz, M. V. (2015). Genomic determinants of coral heat tolerance across latitudes. *Science* 348, 1460–1462. doi: 10.1126/science.1261224

Douglas, A. E. (2003). Coral bleaching - How and why? *Mar. Pollut. Bull.* 46, 385–392. doi: 10.1016/S0025-326X(03)00037-7

Drury, C. (2020). Resilience in reef-building corals: the ecological and evolutionary importance of the host response to thermal stress. *Mol. Ecol.* 29, 448–465. doi: 10.1111/mec.15337

Eakin, C. M., Liu, G., Gomez, A. M., De La Cour, J. L., Heron, S. F., Skirving, W. J., et al. (2016). Global coral bleaching 2014–2017: status and an appeal for observations. *Reef Encount.* 31, 20–26.

Eakin, C. M., Liu, G., Gomez, A. M., De La Cour, J. L., Heron, S. F., Skirving, W. J., et al. (2017). Ding, dong, the witch is dead (?)—three years of global coral bleaching 2014–2017. *Reef Encount.* 32, 33–38.

Eakin, C. M., Sweatman, H., and Brainard, R. E. (2019). The 2014–2017 global-scale coral bleaching event: insights and impacts. *Coral Reefs* 38, 539–545. doi: 10.1007/s00338-019-01844-2

Eckert, R. J., Reaume, A. M., Sturm, A. B., Studivan, M. S., and Voss, J. D. (2020). Depth Influences Symbiodiniaceae associations among *Montastraea cavernosa* corals on the belize barrier reef. *Front. Microbiol.* 11:518. doi: 10.3389/fmicb.2020.00518

Fautin, D. G., and Buddemeier, R. W. (2004). Adaptive bleaching: a general phenomenon. *Hydrobiologia* 530-531, 459–467. doi: 10.1007/s10750-004-2642-z

Franklin, E. C., Stat, M., Pochon, X., Putnam, H. M., and Gates, R. D. (2012). GeoSymbio: a hybrid, cloud-based web application of global geospatial bioinformatics and ecoinformatics for *Symbiodinium*–host symbioses. *Mol. Ecol. Resour.* 12, 369–373. doi: 10.1111/j.1755-0998.2011.03081.x

Fransolet, D., Roberty, S., and Plumier, J. C. (2012). Establishment of endosymbiosis: the case of cnidarians and *Symbiodinium*. *J. Exp. Mar. Biol. Ecol.* 420-421, 1–7. doi: 10.1016/j.jembe.2012.03.015

Gaither, M. R., Szabó, Z., Crepeau, M. W., Bird, C. E., and Toonen, R. J. (2011). Preservation of corals in salt-saturated DMSO buffer is superior to ethanol for PCR experiments. *Coral Reefs* 30, 329–333. doi: 10.1007/s00338-010-0687-1

Gierz, S., Ainsworth, T. D., and Leggat, W. (2020). Diverse symbiont bleaching responses are evident from 2-degree heating week bleaching conditions as thermal stress intensifies in coral. *Mar. Freshw. Res.* 71, 1149–1160. doi: 10.1071/mf19220

Gilmour, J. P., Smith, L. D., Heyward, A. J., Baird, A. H., and Pratchett, M. S. (2013). Recovery of an isolated coral reef system following severe disturbance. *Science* 340, 69–71. doi: 10.1126/science.1232310

Gong, S., Xu, L., Yu, K., Zhang, F., and Li, Z. (2019). Differences in Symbiodiniaceae communities and photosynthesis following thermal bleaching of massive corals in the northern part of the South China Sea. *Mar. Pollut. Bull.* 144, 196–204. doi: 10.1016/j.marpolbul.2019.04.069

Gordon, A. L., Susanto, R. D., and Ffield, A. (1999). Throughflow within Makassar Strait. *Geophys. Res. Lett.* 26, 3325–3328. doi: 10.1029/1999GL002340

Guest, J. R., Baird, A. H., Maynard, J. A., Muttaqin, E., Edwards, A. J., Campbell, S. J., et al. (2012). Contrasting patterns of coral bleaching susceptibility in 2010 suggest an adaptive response to thermal stress. *PLoS One* 7:e33353. doi: 10.1371/journal.pone.0033353

Guest, J. R., Low, J., Tun, K., Wilson, B., Ng, C. S. L., Raingeard, D., et al. (2016). Coral community response to bleaching on a highly disturbed reef. *Sci. Rep.* 6:20717. doi: 10.1038/srep20717

Han, W., Moore, A. M., Levin, J., Zhang, B., Arango, H. G., Curchitser, E., et al. (2009). Seasonal surface ocean circulation and dynamics in the Philippine Archipelago region during 2004-2008. *Dyn. Atmos. Oceans* 47, 114–137. doi: 10.1016/j.dynatmoce.2008.10.007

Heron, S. F., Johnston, L., Liu, G., Geiger, E. F., Maynard, J. A., De La Cour, J. L., et al. (2016). Validation of reef-scale thermal stress satellite products for coral bleaching monitoring. *Remote Sens.* 8, 1–16. doi: 10.3390/rs8010059

Hoegh-Guldberg, O. (1999). Climate Change, coral bleaching and the future of the world' s coral reefs. *Mar. Freshw. Res.* 50, 839–866. doi: 10.1071/MF99078

Hoegh-Guldberg, O., Kennedy, E. V., Beyer, H. L., McClennen, C., and Possingham, H. P. (2018). Securing a long-term future for coral reefs. *Trends Ecol. Evol.* 33, 936–944. doi: 10.1016/j.tree.2018.09.006

Hoegh-Guldberg, O., Mumby, P. J., Hooten, A. J., Steneck, R. S., Greenfield, P., Gomez, E. D., et al. (2007). Coral reefs under rapid climate change and ocean acidification. *Science* 318, 1737–1742. doi: 10.1126/science.1152509

Hughes, T. P., Kerry, J. T., Álvarez-Noriega, M., Álvarez-Romero, J. G., Anderson, K. D., Baird, A. H., et al. (2017). Global warming and recurrent mass bleaching of corals. *Nature* 543, 373–377. doi: 10.1038/nature21707

Hurlburt, H. E., Metzger, J. E., and Sprintall, J. (2011). Circulation in the Philippine Archipelago Simulated by 1/12° and 1/25° Global HYCOM and EAS NCOM. *Oceanography* 24, 28–47. doi: 10.5670/oceanog.2011.02

Isomura, N., and Nishihira, M. (2001). Size variation of planulae and its effect on the lifetime of planulae in three pocilloporid corals. *Coral Reefs* 20, 309–315. doi: 10.1007/s003380100180

Jiang, L., Guo, M.-L., Zhang, F., Zhang, Y.-Y., Zhou, G.-W., Lei, X.-M., et al. (2020). Impacts of elevated temperature and pCO2 on the brooded larvae of *Pocillopora damicornis* from Luhuitou Reef, China: evidence for local acclimatization. *Coral Reefs* 39, 331–344. doi: 10.1007/s00338-020-01894-x

Jones, A. M., and Berkelmans, R. (2010). Potential costs of acclimatization to a warmer climate: growth of a reef coral with heat tolerant vs. sensitive symbiont types. *PLoS One* 5:e10437. doi: 10.1371/journal.pone.0010437

Jones, A. M., and Berkelmans, R. (2011). Tradeoffs to thermal acclimation: energetics and reproduction of a reef coral with heat tolerant *Symbiodinium* Type-D. *J. Mar. Biol.* 2011:185890. doi: 10.1155/2011/185890

Jones, A. M., Berkelmans, R., van Oppen, M. J. H., Mieog, J. C., and Sinclair, W. (2008). A community change in the algal endosymbionts of a scleractinian coral following a natural bleaching event: field evidence of acclimatization. *Proc. R. Soc. B Biol. Sci.* 275, 1359–1365. doi: 10.1098/rspb.2008.0069

Kayanne, H. (2016). Validation of degree heating weeks as a coral bleaching index in the northwestern Pacific. *Coral Reefs* 36, 63–70. doi: 10.1007/s00338-016-1524-y

Kearse, M., Moir, R., Wilson, A., Stones-Havas, S., Cheung, M., Sturrock, S., et al. (2012). Geneious Basic: an integrated and extendable desktop software platform for the organization and analysis of sequence data. *Bioinformatics* 28, 1647–1649. doi: 10.1093/bioinformatics/bts199

Kenkel, C. D., Goodbody-Gringley, G., Caillaud, D., Davies, S. W., Bartels, E., and Matz, M. V. (2013). Evidence for a host role in thermotolerance divergence between populations of the mustard hill coral (*Porites astreoides*) from different reef environments. *Mol. Ecol.* 22, 4335–4348. doi: 10.1111/mec.12391

Keshavmurthy, S., Tee, H. S., Kao, K.-W., Wang, J.-T., and Chen, C. A. (2020). Specificity trumps flexibility—location-based stable associations between *Symbiodiniaceae genera* and *Platygyra verweyi* (Scleractinia; Merulinidae). *PeerJ* 8:e8791. doi: 10.7717/peerj.8791

Kitchen, R. M., Piscetta, M., de Souza, M. R., Lenz, E. A., Schar, D. W. H., Gates, R. D., et al. (2020). Symbiont transmission and reproductive mode influence responses of three Hawaiian coral larvae to elevated temperature and nutrients. *Coral Reefs* 39, 419–431. doi: 10.1007/s00338-020-01905-x

Kleypas, J. A., Castruccio, F. S., Curchitser, E. N., and Mcleod, E. (2015). The impact of ENSO on coral heat stress in the western equatorial Pacific. *Glob. Change Biol.* 21, 2525–2539. doi: 10.1111/gcb.12881

LaJeunesse, T. C. (2002). Diversity and community structure of symbiotic dinoflagellates from Caribbean coral reefs. *Mar. Biol.* 141, 387–400. doi: 10.1007/s00227-002-0829-2

LaJeunesse, T. C., Loh, W. K. W., Van Woesik, R., Hoegh-Guldberg, O., Schmidt, G. W., and Fitt, W. K. (2003). Low symbiont diversity in southern Great Barrier Reef corals, relative to those of the Caribbean. *Limnol. Oceanogr.* 48, 2046–2054. doi: 10.4319/lo.2003.48.5.2046

LaJeunesse, T. C., Parkinson, J. E., Gabrielson, P. W., Jeong, H. J., Reimer, J. D., Voolstra, C. R., et al. (2018). Systematic revision of Symbiodiniaceae highlights the antiquity and diversity of coral endosymbionts. *Curr. Biol.* 28, 2570–2580.e6. doi: 10.1016/j.cub.2018.07.008

LaJeunesse, T. C., Reyes-Bonilla, H., Warner, M. E., Wills, M., Schmidt, G. W., and Fitt, W. K. (2008). Specificity and stability in high latitude eastern Pacific coral-algal symbioses. *Limnol. Oceanogr.* 53, 719–727. doi: 10.4319/lo.2008.53.2.0719

Lajeunesse, T. C., Wham, D. C., Pettay, D. T., Parkinson, J. E., Keshavmurthy, S., and Chen, C. A. (2014). Ecologically differentiated stress-tolerant endosymbionts in the dinoflagellate genus *Symbiodinium* (Dinophyceae) Clade D are different species. *Phycologia* 53, 305–319. doi: 10.2216/13-186.1

Le Nohaïc, M., Ross, C. L., Cornwall, C. E., Comeau, S., Lowe, R. J., McCulloch, M. T., et al. (2017). Marine heatwave causes unprecedented regional mass bleaching of thermally resistant corals in northwestern Australia. *Sci. Rep.* 7:14999. doi: 10.1038/s41598-017-14794-y

Lermusiaux, P. F. J., HaLey, P. J. Jr., Leslie, W. G., Agarwal, A., Logutov, O. G., and Burton, L. J. (2011). Multiscale physical and biological dynamics in the Philippine Archipelago: predictions and processes. *Oceanography* 24, 70–89. doi: 10.5670/oceanog.2011.05

Lesser, M. P., Stat, M., and Gates, R. D. (2013). The endosymbiotic dinoflagellates (*Symbiodinium* sp.) of corals are parasites and mutualists. *Coral Reefs* 32, 603–611. doi: 10.1007/s00338-013-1051-z

Levy, G., Shaish, L., Haim, A., and Rinkevich, B. (2010). Mid-water rope nursery—Testing design and performance of a novel reef restoration instrument. *Ecol. Eng.* 36, 560–569. doi: 10.1016/j.ecoleng.2009.12.003

Licuanan, W. Y., and Gomez, E. D. (2000). "Philippine coral reefs: status and the role of the academe to improve their management," in *Proceedings of the Ninth International Coral Reef Symposium,* Bali, 835–840.

Licuanan, W. Y., Robles, R., and Reyes, M. (2019). Status and recent trends in coral reefs of the Philippines. *Mar. Pollut. Bull.* 142, 544–550. doi: 10.1016/j.marpolbul.2019.04.013

Licuanan, W. Y., Robles, R., Dygico, M., Songco, A., and van Woesik, R. (2017). Coral benchmarks in the center of biodiversity. *Mar. Pollut. Bull.* 114, 1135–1140. doi: 10.1016/j.marpolbul.2016.10.017

Little, A. F., van Oppen, M. J. H., and Willis, B. L. (2004). Flexibility in algal endosymbioses shapes growth in reef corals. *Science* 304, 1492–1494. doi: 10.1126/science.1095733

Liu, G., Heron, S. F., Eakin, C. M., Muller-Karger, F. E., Vega-Rodriguez, M., Guild, L. S., et al. (2014). Reef-scale thermal stress monitoring of coral ecosystems: new 5-km global products from NOAA Coral Reef Watch. *Remote Sens.* 6, 11579–11606. doi: 10.3390/rs61111579

Liu, G., Strong, A. E., Skirving, W., and Arzayus, L. F. (2006). *Overview of NOAA Coral Reef Watch Program's Near-Real Time Satellite Global Coral Bleaching Monitoring Activities*. (Washington, DC: NOAA), 1783–1793.

Lough, J. M., Anderson, K. D., and Hughes, T. P. (2018). Increasing thermal stress for tropical coral reefs: 1871-2017. *Sci. Rep.* 8:6079. doi: 10.1038/s41598-018-24530-9

Loya, Y., Sakai, K., Yamazato, K., Nakano, Y., Sambali, H., and Van Woesik, R. (2001). Coral bleaching: the winners and the losers. *Ecol. Lett.* 4, 122–131. doi: 10.1046/j.1461-0248.2001.00203.x

Magdaong, E. T., Fujii, M., Yamano, H., Licuanan, W. Y., Maypa, A., Campos, W. L., et al. (2014). Long-term change in coral cover and the effectiveness of marine protected areas in the Philippines: a meta-analysis. *Hydrobiologia* 733, 5–17. doi: 10.1007/s10750-013-1720-5

Manzello, D. P., Matz, M. V., Enochs, I. C., Valentino, L., Carlton, R. D., Kolodziej, G., et al. (2019). Role of host genetics and heat-tolerant algal symbionts in sustaining populations of the endangered coral *Orbicella faveolata* in the Florida Keys with ocean warming. *Glob. Change Biol.* 25, 1016–1031. doi: 10.1111/gcb.14545

Masumoto, Y., Kagimoto, T., Yoshida, M., Fukuda, M., Hirose, N., and Yamagata, T. (2001). Intraseasonal eddies in the Sulawesi Sea simulated in an ocean General Circulation Model. *Geophys. Res. Lett.* 28, 1631–1634. doi: 10.1029/2000GL011835

Maynard, J. A., Anthony, K. R. N., Marshall, P. A., and Masiri, I. (2008). Major bleaching events can lead to increased thermal tolerance in corals. *Mar. Biol.* 155, 173–182. doi: 10.1007/s00227-008-1015-y

McClanahan, T. R., Ateweberhan, M., Ruiz Sebastián, C., Graham, N. A. J., Wilson, S. K., Bruggemann, J. H., et al. (2007). Predictability of coral bleaching from synoptic satellite and in situ temperature observations. *Coral Reefs* 26, 695–701. doi: 10.1007/s00338-006-0193-7

McManus, L. C., Vasconcelos, V. V., Levin, S. A., Thompson, D. M., Kleypas, J. A., Castruccio, F. S., et al. (2020). Extreme temperature events will drive coral decline in the Coral Triangle. *Glob. Change Biol.* 26, 2120–2133. doi: 10.1111/gcb.14972

Mieog, J. C., Olsen, J. L., Berkelmans, R., Bleuler-Martinez, S. A., Willis, B. L., and van Oppen, M. J. H. (2009a). The roles and interactions of symbiont, host and environment in defining coral fitness. *PLoS One* 4:e6364. doi: 10.1371/journal.pone.0006364

Mieog, J. C., van Oppen, M. J. H., Berkelmans, R., Stam, W. T., and Olsen, J. L. (2009b). Quantification of algal endosymbionts (*Symbiodinium*) in coral tissue using real-time PCR. *Mol. Ecol. Resour.* 9, 74–82. doi: 10.1111/j.1755-0998.2008.02222.x

Mostafavi, P. G., Fatemi, S. M. R., Shahhosseiny, M. H., Hoegh-Guldberg, O., and Loh, W. K. W. (2007). Predominance of clade D *Symbiodinium* in shallow-water reef-building corals off Kish and Larak Islands (Persian Gulf, Iran). *Mar. Biol.* 153, 25–34. doi: 10.1007/s00227-007-0796-8

Muñiz-Castillo, A. I., Rivera-Sosa, A., Chollett, I., Eakin, C. M., Andrade-Gómez, L., McField, M., et al. (2019). Three decades of heat stress exposure in Caribbean coral reefs: a new regional delineation to enhance conservation. *Sci. Rep.* 9:11013. doi: 10.1038/s41598-019-47307-0

Muscatine, L. (1990). "The role of symbiotic algae in carbon and energy flux in reef corals," in *Ecosystems of the world 25: Coral Reefs*, ed. Z. Dubinsky (Amsterdam: Elsevier), 75–87.

Ng, T. Y., and Ang, P. (2016). Low symbiont diversity as a potential adaptive strategy in a marginal non-reefal environment: a case study of corals in Hong Kong. *Coral Reefs* 35, 941–957. doi: 10.1007/s00338-016-1458-4

NOAA (2021). *Cold & Warm Episodes by Season*. Available online at: https://origin.cpc.ncep.noaa.gov/products/analysis_monitoring/ensostuff/ONI_v5.php (accessed August 17, 2021).

Oksanen, J., Blanchet, F. G., Friendly, M., Kindt, R., Legendre, P., McGlinn, D., et al. (2020). *vegan: Community Ecology Package*. Available online at: https://CRAN.R-project.org/package=vegan (accessed August 02, 2021).

Palumbi, S. R., Barshis, D. J., Traylor-Knowles, N., and Bay, R. A. (2014). Mechanisms of reef coral resistance to future climate change. *Science* 344, 895–898. doi: 10.1126/science.1251336

Parkinson, J. E., Banaszak, A. T., Altman, N. S., LaJeunesse, T. C., and Baums, I. B. (2015). Intraspecific diversity among partners drives functional variation in coral symbioses. *Sci. Rep.* 5:15567. doi: 10.1038/srep15667

Peñaflor, E. L. (2015). Investigating physical parameters associated with massive coral bleaching events in the Coral Triangle. [dissertation]. (Quezon City, Philippines: University of the Philippines Diliman).

Peñaflor, E. L., Skirving, W. J., Strong, A. E., Heron, S. F., and David, L. T. (2009). Sea-surface temperature and thermal stress in the Coral Triangle over the past two decades. *Coral Reefs* 28, 841–850. doi: 10.1007/s00338-009-0522-8

Pochon, X., and Gates, R. D. (2010). A new *Symbiodinium* clade (Dinophyceae) from soritid foraminifera in Hawai'i. *Mol. Phylogenet. Evol.* 56, 492–497. doi: 10.1016/j.ympev.2010.03.040

Poquita-Du, R. C., Huang, D., Chou, L. M., and Todd, P. A. (2020). The contribution of stress-tolerant endosymbiotic dinoflagellate Durusdinium to *Pocillopora acuta* survival in a highly urbanized reef system. *Coral Reefs* 39, 745–755. doi: 10.1007/s00338-020-01902-0

Putnam, H. M., Stat, M., Pochon, X., and Gates, R. D. (2012). Endosymbiotic flexibility associates with environmental sensitivity in scleractinian corals. *Proc. R. Soc. B Biol. Sci.* 279, 4352–4361. doi: 10.1098/rspb.2012.1454

Qin, Z., Yu, K., Chen, B., Wang, Y., Liang, J., Luo, W., et al. (2019). Diversity of Symbiodiniaceae in 15 Coral Species From the Southern South China Sea: potential relationship with coral thermal adaptability. *Front. Microbiol.* 10:2343. doi: 10.3389/fmicb.2019.02343

Qu, T., Song, Y. T., and Yamagata, T. (2009). An introduction to the South China Sea throughflow: its dynamics, variability, and application for climate. *Dyn. Atmos. Oceans* 47, 3–14. doi: 10.1016/j.dynatmoce.2008.05.001

Quigley, K. M., Willis, B. L., and Kenkel, C. D. (2019). Transgenerational inheritance of shuffled symbiont communities in the coral *Montipora digitata*. *Sci. Rep.* 9:13328. doi: 10.1038/s41598-019-50045-y

Quimpo, T. J. R., Requilme, J. N. C., Gomez, E. J., Sayco, S. L. G., Tolentino, M. P. S., and Cabaitan, P. C. (2020). Low coral bleaching prevalence at the Bolinao-Anda Reef Complex, northwestern Philippines during the 2016 thermal stress event. *Mar. Pollut. Bull.* 160:111567. doi: 10.1016/j.marpolbul.2020.111567

R Core Team (2021). *R: A Language and Environment for Statistical Computing*. Vienna: R Foundation for Statistical Computing.

Riegl, B., Glynn, P. W., Banks, S., Keith, I., Rivera, F., Vera-Zambrano, M., et al. (2019). Heat attenuation and nutrient delivery by localized upwelling avoided coral bleaching mortality in northern Galapagos during 2015/2016 ENSO. *Coral Reefs* 38, 773–785. doi: 10.1007/s00338-019-01787-8

Selig, E. R., Casey, K. S., and Bruno, J. F. (2012). Temperature-driven coral decline: the role of marine protected areas. *Glob. Change Biol.* 18, 1561–1570. doi: 10.1111/j.1365-2486.2012.02658.x

Shaish, L., Levy, G., Katzir, G., and Rinkevich, B. (2010a). Coral reef restoration (Bolinao, Philippines) in the face of frequent natural catastrophes. *Restor. Ecol.* 18, 285–299. doi: 10.1111/j.1526-100X.2009.00647.x

Shaish, L., Levy, G., Katzir, G., and Rinkevich, B. (2010b). Employing a highly fragmented, weedy coral species in reef restoration. *Ecol. Eng.* 36, 1424–1432. doi: 10.1016/j.ecoleng.2010.06.022

Silverstein, R. N., Cunning, R., and Baker, A. C. (2015). Change in algal symbiont communities after bleaching, not prior heat exposure, increases heat tolerance of reef corals. *Glob. Change Biol.* 21, 236–249. doi: 10.1111/gcb.12706

Silverstein, R. N., Cunning, R., and Baker, A. C. (2017). Tenacious D: *Symbiodinium* in clade D remain in reef corals at both high and low temperature extremes despite impairment. *J. Exp. Biol.* 220, 1192–1196. doi: 10.1242/jeb.148239

Sprintall, J., Gordon, A. L., Flament, P., and Villanoy, C. L. (2012). Observations of exchange between the South China Sea and the Sulu Sea. *J. Geophys. Res. Oceans* 117, 1–18. doi: 10.1029/2011JC007610

Sproles, A. E., Oakley, C. A., Krueger, T., Grossman, A. R., Weis, V. M., Meibom, A., et al. (2020). Sub-cellular imaging shows reduced photosynthetic carbon and increased nitrogen assimilation by the non-native endosymbiont *Durusdinium trenchii* in the model cnidarian Aiptasia. *Environ. Microbiol.* 22, 3741–3753. doi: 10.1111/1462-2920.15142

Stat, M., and Gates, R. D. (2011). Clade D *Symbiodinium* in Scleractinian Corals: A "Nugget" of hope, a selfish opportunist, an ominous sign, or all of the above? *J. Mar. Biol.* 2011:730715. doi: 10.1155/2011/730715

Stat, M., Pochon, X., Franklin, E. C., Bruno, J. F., Casey, K. S., Selig, E. R., et al. (2013). The distribution of the thermally tolerant symbiont lineage (*Symbiodinium* clade D) in corals from Hawaii: correlations with host and the history of ocean thermal stress. *Ecol. Evol.* 3, 1317–1329. doi: 10.1002/ece3.556

Sully, S., and van Woesik, R. (2020). Turbid reefs moderate coral bleaching under climate-related temperature stress. *Glob. Change Biol.* 26, 1367–1373. doi: 10.1111/gcb.14948

Terraneo, T. I., Fusi, M., Hume, B. C. C., Arrigoni, R., Voolstra, C. R., Benzoni, F., et al. (2019). Environmental latitudinal gradients and host-specificity shape Symbiodiniaceae distribution in Red Sea Porites corals. *J. Biogeogr.* 46, 2323–2335. doi: 10.1111/jbi.13672

Thompson, D. M., and Van Woesik, R. (2009). Corals escape bleaching in regions that recently and historically experienced frequent thermal stress. *Proc. R. Soc. B Biol. Sci.* 276, 2893–2901. doi: 10.1098/rspb.2009.0591

Thornhill, D. J., LaJeunesse, T. C., Kemp, D. W., Fitt, W. K., and Schmidt, G. W. (2006). Multi-year, seasonal genotypic surveys of coral-algal symbioses reveal prevalent stability or post-bleaching reversion. *Mar. Biol.* 148, 711–722. doi: 10.1007/s00227-005-0114-2

Trench, R. K., Wethey, D. S., and Porter, J. W. (1981). Observations on the symbiosis with zooxanthellae among the tridacnidae (mollusca, bivalvia). *Biol. Bull.* 161, 180–198. doi: 10.2307/1541117

Tun, K., Chou, L. M., Low, J., Teemin, T., Phongsuwan, N., Setiashi, N., et al. (2010). "A regional overview on the 2010 coral bleaching event in Southeast Asia," in *Status of Coral Reefs in East Asian Seas Region: 2010*, (Sumida City: Japan Wildlife Research Center), 9–26.

Valino, D. A. M., Baria-Rodriguez, M. V., Dizon, R. M., and Aliño, P. M. (2021). Responses of Buluan Island turbid fringing reefs, southern Philippines to the 2016 thermal anomaly. *Region. Stud. Mar. Sci.* 43:101704. doi: 10.1016/j.rsma.2021.101704

van Oppen, M. J. H., Oliver, J. K., Putnam, H. M., and Gates, R. D. (2015). Building coral reef resilience through assisted evolution. *Proc. Natl. Acad. Sci. U.S.A.* 112, 2307–2313. doi: 10.1073/pnas.1422301112

van Woesik, R., Sakai, K., Ganase, A., and Loya, Y. (2011). Revisiting the winners and the losers a decade after coral bleaching. *Mar. Ecol. Prog. Ser.* 434, 67–76. doi: 10.3354/meps09203

Villanoy, C. L., Cabrera, O. C., Yñiguez, A., Camoying, M., de Guzman, A., David, L. T., et al. (2011). Monsoon-driven coastal upwelling off Zamboanga peninsula, Philippines. *Oceanography* 24, 156–165. doi: 10.5670/oceanog.2011.12

Walker, B., Holling, C. S., Carpenter, S., and Kinzig, A. (2004). Resilience, Adaptability and Transformability in Social–ecological Systems. *Ecol. Soc.* 9:5.

Weis, V. M. (2008). Cellular mechanisms of Cnidarian bleaching: stress causes the collapse of symbiosis. *J. Exp. Biol.* 211, 3059–3066. doi: 10.1242/jeb.009597

Weisz, J. B., Massaro, A. J., Ramsby, B. D., and Hill, M. S. (2010). Zooxanthellar Symbionts shape host sponge trophic status through translocation of carbon. *Biol. Bull.* 219, 189–197.

Wham, D. C., Ning, G., and LaJeunesse, T. C. (2017). *Symbiodinium glynnii* sp. nov., a species of stress-tolerant symbiotic dinoflagellates from pocilloporid and montiporid corals in the Pacific Ocean. *Phycologia* 56, 396–409. doi: 10.2216/16-86.1

Wooldridge, S. A. (2013). Breakdown of the coral-algae symbiosis: towards formalising a linkage between warm-water bleaching thresholds and the growth rate of the intracellular zooxanthellae. *Biogeosciences* 10, 1647–1658. doi: 10.5194/bg-10-1647-2013

Wright, R. M., Mera, H., Kenkel, C. D., Nayfa, M., Bay, L. K., and Matz, M. V. (2019). Positive genetic associations among fitness traits support evolvability of a reef-building coral under multiple stressors. *Glob. Change Biol.* 25, 3294–3304. doi: 10.1111/gcb.14764

Yellowlees, D., Rees, T. A. V., and Leggat, W. (2008). Metabolic interactions between algal symbionts and invertebrate hosts. *Plant Cell Environ.* 31, 679–694. doi: 10.1111/j.1365-3040.2008.01802.x

Zhou, G.-W., and Huang, H. (2011). Low genetic diversity of symbiotic dinoflagellates (*Symbiodinium*) in scleractinian corals from tropical reefs in southern Hainan Island, China. *J. Syst. Evol.* 49, 598–605. doi: 10.1111/j.1759-6831.2011.00161.x

Zhou, G.-W., Cai, L., Li, Y., Tong, H., Jiang, L., Zhang, Y.-Y., et al. (2017). Temperature-driven local acclimatization of Symbiodnium hosted by the coral *Galaxea fascicularis* at Hainan Island, China. *Front. Microbiol.* 8:2487. doi: 10.3389/fmicb.2017.02487

Conflict of Interest: The authors declare that the research was conducted in the absence of any commercial or financial relationships that could be construed as a potential conflict of interest.

frontiers in Marine Science

ORIGINAL RESEARCH
published: 26 October 2021
doi: 10.3389/fmars.2021.731675

Implications of Community-Based Management of Marine Reserves in the Philippines for Reef Fish Communities and Biodiversity

Sara E. Marriott[1]*, Courtney Cox[2], Rizaller C. Amolo[2], Dean Apistar[2], Roquelito H. Mancao[2] and Kim de Mutsert[1]

[1] Division of Coastal Sciences, School of Ocean Science and Engineering, The University of Southern Mississippi, Ocean Springs, MS, United States, [2] Rare, Arlington, VA, United States, [3] Rare Philippines, Cebu City, Philippines

Edited by:
Yehuda Benayahu,
Tel Aviv University, Israel

Reviewed by:
Jan Vanaverbeke,
Royal Belgian Institute of Natural Sciences, Belgium
Maria Gabriela Palomo,
Independent Researcher, Buenos Aires, Argentina

***Correspondence:**
Sara E. Marriott
sara.marriott@usm.edu;
saraeisler91@gmail.com

Specialty section:
This article was submitted to Marine Ecosystem Ecology, a section of the journal Frontiers in Marine Science

Received: *28 June 2021*
Accepted: *04 October 2021*
Published: *26 October 2021*

Citation:
Marriott SE, Cox C, Amolo RC, Apistar D, Mancao RH and de Mutsert K (2021) Implications of Community-Based Management of Marine Reserves in the Philippines for Reef Fish Communities and Biodiversity. Front. Mar. Sci. 8:731675. doi: 10.3389/fmars.2021.731675

Overfishing and destructive fishing practices are major threats to marine biodiversity in the Philippines, where over 1.9 million small-scale fishers are supported by these biodiverse marine communities. Nearly 50% of all marine fish capture in the Philippines is from artisanal fisheries, with much of it not reported or under-reported. Marine reserves, where fishing is prohibited have been created in many local government units to help restore and preserve this biodiversity. The success of these marine reserves is still under serious debate with effective management still representing a significant challenge. The lack of a governance system to centrally managed marine reserves has resulted in non-governmental organizations developing community-based management schemes. Using independent fisheries data from Rare's Fish Forever program, we applied PERMANOVA, SIMPER and biodiversity index analyses to evaluate the community structure of reef fish in 20 sites within the Philippines. We analyzed the differences in fish assemblage inside and outside of these marine reserves, before and after community-based management had been implemented. We provide evidence that: (i) fish community structure changes within marine reserves after community-based management strategies are implemented; and (ii) community-based management of marine fisheries resources protects and promotes biodiversity inside, and in some cases, outside marine reserves. Variability across sites suggests that other social or ecological factors may be influencing the ability of marine reserves to fully protect biodiversity and marine resources. Small-scale fishers in the Philippines participate in mixed-catch harvests and depend on biodiversity and reef community structure for their livelihoods. Thus, this work has implications on how community-based management strategies for marine reserves and adjacent waters may be beneficial for the sustainability of small-scale fishers.

Keywords: marine reserve, small scale fisheries, biodiversity, community-based management (CBM), community structure

INTRODUCTION

Destructive fishing habits, overfishing, and pollution have impacted coral reef systems and fisheries (Pastorok and Bilyard, 1985; McManus and Reyes, 1997; Wenger et al., 2015; Graham et al., 2017). Unsustainable fishing techniques as well as sediment and nutrient pollution can transition coral reef ecosystems from oligotrophic complex living coral reef structures with high biodiversity to eutrophic, macro-algae algae covered structures with reduced biodiversity (Mumby et al., 2007). Overfishing or destructive fishing practices exist in commercial or industrial fishing fleets as well as small-scale fishing (SSF) (Mora, 2008; Alfaro-Shigueto et al., 2010; Shester and Micheli, 2011; Selgrath et al., 2018; Muallil et al., 2019). Small-scale fishing, generally defined by small, man- or low-powered vessels, makes up at least 30% of global catch (Pauly and Zeller, 2016). In the Philippines, approximately 50% of catch is harvested by over 1.9 million small-scale fishers (FAO, 2014) and 68% of fisheries have been found to be unsustainable (Muallil et al., 2014b). Additionally, small-scale fishers are growing in number in the Philippines, increasing the total annual fishing pressure (Selgrath et al., 2018). Rural coastal communities, where much of small-scale fishing occurs, rely on subsistence fishing and are uniquely vulnerable to fishery collapse and environmental changes, such as sea-level rise or ocean acidification (World Bank, 2012). Thus, it continues to be important to focus on sustainable management strategies for small-scale fishing.

In many parts of the world, top-down management approaches, such as catch limits and gear restrictions, are the most common type of commercial fisheries management (Hilborn and Ovando, 2014). For these traditional approaches to be successful, they typically rely on centralized governance, limited targeted species and large quantities of biological data. In emergent countries with a high proportion of small-scale fishing, these top-down approaches are challenging due to lack of infrastructure for monitoring and enforcement (Brownman et al., 2004). In order to overcome these challenges, governments and non-governmental organizations (NGOs) have been focusing on management methods to create more sustainable fishing practices for small-scale fishers and create resilience for fishing communities (FAO, 2018).

Rare, one such international NGO, has been working with local communities in the Philippines to address overfishing. Rare, with the Environmental Defense Fund and University of California Santa Barbara, developed the Fish Forever Program using Pride Campaigns to inspire behavior change to reduce illegal fishing in marine reserves and increase effectiveness. Beginning in 2011, the program paired managed access with marine reserves hypothesizing that the combination would provide benefits to both fish, fishers, and the broader marine ecosystem (Rare, 2018). Importantly, local communities manage both the marine reserves and the managed access areas to reduce illegal fishing of the marine reserve and reduce destructive fishing habits outside the reserves.

Marine reserve areas, where fishing is prohibited, can be a powerful management tool for protection of an essential habitat and also benefit fishers through increased catch (Guidetti, 2006; Kerwath et al., 2013; Strain et al., 2019). However, marine reserves will only be beneficial to both if they are effectively managed (Mora, 2008; Strain et al., 2019). The Philippines is often cited as a success story for marine reserves because of how early they were implemented (since the 1970s) and how many were delineated (1,800 as of 2014) (Cabral et al., 2014). However, only 2% of reefs are under protection, many of them small, and only 10–30% are effectively managed (Campos and Aliño, 2008; Weeks et al., 2010; Arceo et al., 2013). As a part of the Convention on Biological Diversity, the Philippines had agreed to protect 10% of the country's marine resources by 2020 (Cabral et al., 2014), a target that was not achieved (Marine Conservation Institute, 2021).

One way to potentially increase effectiveness of marine reserves is to implement or strengthen community-based management (CBM) of those areas, which addresses the need for multi-species management and enforcement or compliance of fishing regulations (Smallhorn-West et al., 2019). Community-based management of natural resources has been a way for users to self-enforce and monitor those resources (Pinkerton, 1989; Pomeroy, 1995; Ostrom, 2000; Kearney et al., 2007). The Philippines government has decentralized fishery regulations, moving toward participatory approaches through the Local Government Code in 1991 and Fisheries code in 1998, which allow local governments or municipalities to manage fishery resources (Pomeroy and Courtney, 2018). Since then, the Philippines has used CBM in marine reserves with varying success (Aliño et al., 2000; Campos and Aliño, 2008; Arceo et al., 2013; Rohrer, 2017). Notably, Apo Island, one of the best studied marine reserves, has demonstrated that important fish species increase in both biomass and catch (Russ and Alcala, 1996; Maypa et al., 2002; Russ et al., 2003). Other studies have found that CBM marine reserves maintain fish abundance and diversity within the reserves, but not in the surrounding reefs (Christie et al., 2002).

Many of the existing marine reserves already established in the Philippines were "paper parks," protected in name only (Campos and Aliño, 2008). One of the issues with small-scale fishing is that top-down governance structures frequently lack enforcement and therefore are ineffective at reducing fishing pressure (Brownman et al., 2004). Managing these fisheries on a local level may increase enforcement and compliance of the marine reserves (McClanahan et al., 2006). Depending on the location and ecosystem, designation of a no-take marine reserves is not enough to protect the ecosystem and does not show significant regeneration of coral reef habitat or fishes, such as in parrotfish in Belize (Cox et al., 2017). Community-based management has been identified as a key component of effective marine reserves where increases in biomass of fished species is observed (Kearney et al., 2007; Guidetti and Claudet, 2010; Smallhorn-West et al., 2019).

In the Philippines, biomass of fish has increased both inside and outside CBM marine reserves (Russ et al., 2003; Rare, 2018). While fish biomass is higher in marine reserves, the stocks themselves are generally overfished (Muallil et al., 2019). In addition to biomass for evaluating management strategies, fish community structure is also needed because total biomass does not account for the diversity of species contributing to that biomass. Additionally, the increase of one species may not be as ecologically significant as the increase of all species across the community.

Researchers have repeatedly concluded that marine reserves will not lead to an increase in fishery resources if they are not effectively managed or designed (Mora, 2008; Gaines et al., 2010; Rife et al., 2013; Muallil et al., 2019). Here we investigated the impact of implementing community-based management on fish community structure and biodiversity in marine reserves and open access areas across the Philippines.

MATERIALS AND METHODS

Data Description

Fisheries independent data, such as species name, abundance, and estimated length were collected from 20 sites in the Philippines between the years of 2011 and 2017 as part of Rare's Fish Forever Program (**Figure 1**). The data were collected using five 50 m transects and two swimmers at each site, who would visually identify species, count, and estimate total lengths of each

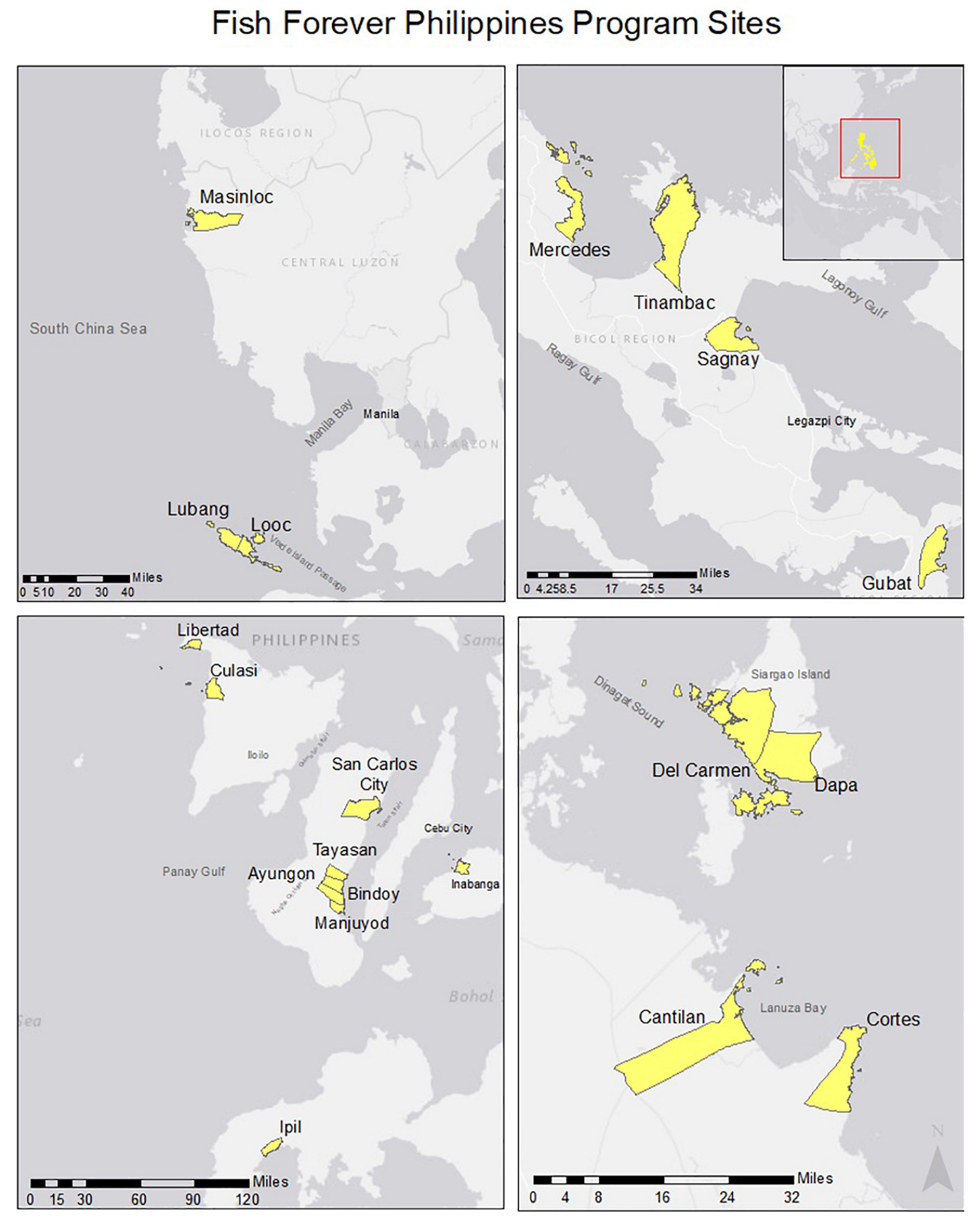

FIGURE 1 | Site Map of the 20 Fish Forever program sites where marine reserves are located. Data Source: GADM, Spatial Reference: GCS WGS 1984.

TABLE 1 | Description of marine reserve area, dates of establishment, and range of dates for data collection for each site.

Site name	Municipal waters (ha)	Marine reserve (ha)	% Protected	Reserve Est. date	Data dates	Protected habitat
Ayungon	9,399	237	2.5	2008*	2012–2017	Coral reef
Bindoy	10,230	332	3.2	2006*	2012–2017	Coral reef
Cantila	41,830	250	0.6	2006	2011–2017	Coral reef
Cortes	56,000	307	0.5	2007	2011–2017	Coral reef
Culasi	151,506	146	0.1	1991	2015–2017	Coral reef
Dapa	17,174	152	0.9	2006	2015–2017	Coral reef
Del Carmen	44,816	38	0.1	2015	2015–2017	Coral reef, seagrass beds
Gubat	8,244	35	0.4	2012*	2011–2017	Coral reef
Inabanga	14,837	100	0.6	2000	2011–2017	Coral reef
Ipil	20,270	1923	9.5	2004*	2012–2017	Coral reef, seagrass beds
Libertad	35,657	16	0.04	1998	2015–2017	Coral reef
Looc	138,304	913	0.7	2010	2015–2017	Coral reef
Lubang	109,886	581	0.5	2010	2015–2017	Coral reef
Manjuyod	12,158	83	0.7	1994	2015–2017	Coral reef
Masinloc	11,080	128	1.2	1989*	2015–2017	Coral reef
Mercedes	53,850	22	0.04	2002	2015–2017	Coral reef
Sagnay	13,566	475	3.5	1993	2012–2017	Coral reef
San Carlos	27,868	108	0.4	2005	2015–2017	Coral reef
Tayasan	6,552	6	0.1	1993	2015–2017	Coral reef
Tinambac	20,900	182	0.9	2006	2011–2017	Coral reef

Dates retrieved from Muallil et al. (2019).

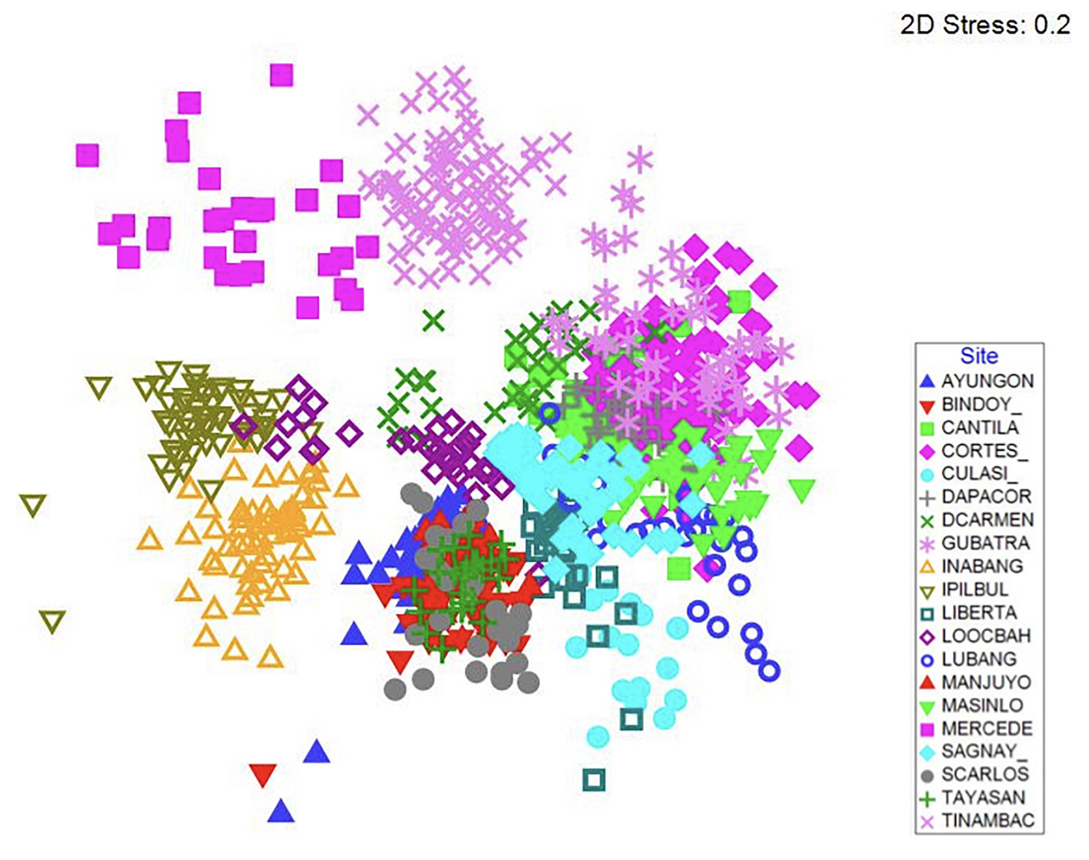

FIGURE 2 | Non-metric multidimensional scaling (nMDS) plot of fish species community structure of all sites. Symbols indicate site.

TABLE 2 | Results from PERMANOVA pair-wise test at each site for each combination factor.

Site	Interaction group	Pair-wise t	*P*	Permutations
Ayungon	Insidebefore, Insideafter	1.1924	0.018*	9822
	Insidebefore, Outsidebefore	1.3709	0.0022*	9362
	Insideafter, Outsideafter	1.5592	0.0001*	9854
	Outsidebefore, Outsideafter	1.0102	0.3938	9842
Bindoy	Insidebefore, Insideafter	0.93102	0.6620	9837
	Insidebefore, Outsidebefore	1.6926	0.0001*	9318
	Insideafter, Outsideafter	2.0107	0.0001*	9846
	Outsidebefore, Outsideafter	1.1027	0.1224	9762
Cantila	Insidebefore, Insideafter	1.4291	0.0002*	9829
	Insidebefore, Outsidebefore	1.4887	0.0001*	9825
	Insideafter, Outsideafter	1.3999	0.0001*	9809
	Outsidebefore, Outsideafter	1.5028	0.0001*	9806
Cortes	Insidebefore, Insideafter	1.4745	0.0001*	9825
	Insidebefore, Outsidebefore	1.4769	0.0002*	9824
	Insideafter, Outsideafter	1.6373	0.0001*	9816
	Outsidebefore, Outsideafter	1.2704	0.0021*	9798
Culasi	Insidebefore, Insideafter	1.0789	0.2735	15
	Insidebefore, Outsidebefore	1.1831	0.0629	15
	Insideafter, Outsideafter	1.6225	0.0015*	494
	Outsidebefore, Outsideafter	0.99826	0.4280	495
Dapa	Insidebefore, Insideafter	1.0265	0.3477	2900
	Insidebefore, Outsidebefore	1.1623	0.0462*	126
	Insideafter, Outsideafter	1.2076	0.0248*	9350
	Outsidebefore, Outsideafter	0.96393	0.6181	2896
Del carmen	Insidebefore, Insideafter	1.0611	0.2562	1000
	Insidebefore, Outsidebefore	0.94441	0.5870	210
	Insideafter, Outsideafter	1.1169	0.1488	9351
	Outsidebefore, Outsideafter	1.0597	0.2534	5701
Gubat	Insidebefore, Insideafter	2.0684	0.0001*	9851
	Insidebefore, Outsidebefore	0.98791	0.4782	9557
	Insideafter, Outsideafter	1.8759	0.0001*	9805
	Outsidebefore, Outsideafter	1.4304	0.0002*	9808
Inabanga	Insidebefore, Insideafter	1.0853	0.1543	8777
	Insidebefore, Outsidebefore	1.5218	0.0001*	9833
	Insideafter, Outsideafter	1.2544	0.0271*	2871
	Outsidebefore, Outsideafter	1.4027	0.001*	9872
Ipil	Insidebefore, Insideafter	1.1123	0.0976	9781
	Insidebefore, Outsidebefore	1.24	0.0081*	9312
	Insideafter, Outsideafter	1.4839	0.0001*	9850
	Outsidebefore, Outsideafter	1.2109	0.0248*	9842
Libertad	Insidebefore, Insideafter	1.2152	0.0157*	2869
	Insidebefore, Outsidebefore	0.90107	0.9045	126
	Insideafter, Outsideafter	1.1161	0.0572	9301
	Outsidebefore, Outsideafter	1.3003	0.0003*	2870
Looc	Insidebefore, Insideafter	1.0598	0.2423	2877
	Insidebefore, Outsidebefore	1.3194	0.033*	126
	Insideafter, Outsideafter	1.7291	0.0002*	9366
	Outsidebefore, Outsideafter	0.9031	0.7444	2878
Lubang	Insidebefore, Insideafter	1.0165	0.3559	2884
	Insidebefore, Outsidebefore	1.6057	0.0081*	126
	Insideafter, Outsideafter	2.0124	0.0001*	9338
	Outsidebefore, Outsideafter	0.96575	0.6228	2881
Manjuyod	Insidebefore, Insideafter	1.1161	0.0733	2872
	Insidebefore, Outsidebefore	1.0104	0.4004	126
	Insideafter, Outsideafter	1.1652	0.045*	9318
	Outsidebefore, Outsideafter	1.044	0.2695	1978
Masinloc	Insidebefore, Insideafter	1.1679	0.0374*	2880
	Insidebefore, Outsidebefore	1.2292	0.0243*	126
	Insideafter, Outsideafter	1.4242	0.0027*	9325
	Outsidebefore, Outsideafter	0.94929	0.6460	1983
Mercedes	Insidebefore, Insideafter	1.0241	0.3733	2871
	Insidebefore, Outsidebefore	1.2486	0.0477*	126
	Insideafter, Outsideafter	1.1981	0.0418*	9310
	Outsidebefore, Outsideafter	1.0515	0.2696	2879
Sagnay	Insidebefore, Insideafter	1.12	0.1367	9843
	Insidebefore, Outsidebefore	1.1131	0.1329	9307
	Insideafter, Outsideafter	1.1321	0.0808	9834
	Outsidebefore, Outsideafter	1.0552	0.2312	9763
San Carlos	Insidebefore, Insideafter	1.3202	0.0026*	7658
	Insidebefore, Outsidebefore	1.4902	0.0053*	210
	Insideafter, Outsideafter	2.0183	0.0001*	9473
	Outsidebefore, Outsideafter	1.1381	0.1010	494
Tayasan	Insidebefore, Insideafter	1.0722	0.2491	495
	Insidebefore, Outsidebefore	1.1236	0.0629	35
	Insideafter, Outsideafter	1.2372	0.0147*	5097
	Outsidebefore, Outsideafter	1.096	0.1524	495
Tinambac	Insidebefore, Insideafter	1.3424	0.0017*	9865
	Insidebefore, Outsidebefore	1.3688	0.0006*	9841
	Insideafter, Outsideafter	1.4386	0.0001*	9813
	Outsidebefore, Outsideafter	1.3806	0.0002*	9828

**Indicates significance.*

fish. In each of the sites, abundance data were collected inside and outside the marine reserve. Reserve implementation occurred as early as 1989 and as late as 2012 (**Table 1**). Rare facilitated the implementation of community based management in 2014 at all of these sites.

Analysis

To determine the reef fish communities inside and outside the marine reserves before and after CBM was implemented, one-way PERMANOVA and SIMPER analyses were run using PRIMER-e (Clarke and Gorley, 2006). Both analyses were completed on a combination factor of whether the samples were inside or outside the marine reserve and if they were before or after CBM. Of all the combinations we used pair-wise tests within the PERMANOVA to compare four of the combinations: (1) "inside before" and "inside after" (2) "outside before" and "outside after" (3) "inside before" and "outside before" and (4) "inside after" and "outside after". Fish abundance data were transformed using a 4th-root transformation and then a Hellinger similarity matrix was applied. Fish community structure was then visualized using non-metric multidimensional scaling (nMDS). The nMDS allows us to see similarities of species composition between treatment groups. PERMANOVAs were performed on each site to test the significance of difference between fish community structures, using the interaction of marine reserves status and before and after implementation of CBM. The PERMANOVAs ran up to 10,000 permutations. Where significant differences were found, SIMPER analyses, using the same combinations, were conducted to determine which fish families and species were the main contributors to the differences between treatment groups. Special attention was given to important fishery families jacks (*Carangidae*), fusiliers (*Caesionidae*), wrasses (*Labridae*), breams (*Lethrinidae* and *Nemipteridae*), rabbitfish (*Siganidae*), snapper (*Lutjanidae*), goatfish (*Mullidae*), grunts (*Haemulidae*), hogfish (*Bodianinae*), grouper (*Serranidae*, specifically *Epinephelinae*), parrotfish (*Scaridae*), surgeonfish (*Acanthuridae*), and ponyfish (*Leiognathidae*) (Muallil et al., 2014a; Fish Forever, 2020). We investigated CBM implementation effects on all sites aggregated as well as each site separately to observe overall patterns of fish community change and site level dynamics.

Biodiversity was assessed by calculating a Shannon Index on each transect and testing the interactions at the site, reserve status, and CBM level. The Shannon Index calculates both the species richness and evenness in an area, giving weight to rarer species. This type of diversity index is useful for areas where overexploitation of fishing resources may have resulted in more rare species, and accounting for the differences in abundance of these rare species is relevant to the study. Kruskal-Wallis tests were then performed on the Shannon Index values to test if CBM implementation resulted in significant differences. Biodiversity analyses were performed using the R package vegan and rstatix (R Core Team, 2013; Kassambara, 2020; Oksanen et al., 2020).

RESULTS

Community Structure

When all site data were aggregated, there is no clear clustering of fish communities between those inside marine reserves and outside marine reserves, but instead a strong clustering by site (**Figure 2**). However, when each site was analyzed separately, the percent of sites that had significant differences between fish community structure inside and outside marine reserves increased from 65% of sites to 85% of sites after the implementation of CBM (**Table 2**). Additionally, shifts in fish community structures were observed after CBM was implemented both inside marine reserves (40% of sites had a significant difference) and outside marine reserves (35% of sites had a significant difference). Due to the large total number of fish species observed (over 600), no single species makes up a large percentage of the dissimilarity between factors (inside versus outside the marine reserve before CBM, and inside versus outside the marine reserve after CBM) for any site in the SIMPER analyses. The SIMPER analyses performed after aggregating the data to the family level revealed that increases of abundance of many important fishery families contributed to the differences seen in community composition after the CBM was implemented.

Some sites, such as Lubang, San Carlos City, Bindoy, and Looc, had clearly defined clusters ($P < 0.05$) for fish communities inside and outside the marine reserve, but no significant differences for changes before and after the implementation of CBM (**Figure 3** and **Supplementary Figures 1–4**). For example, in Bindoy an increase of important fishery families (snappers, wrasses, jacks, goatfish, groupers, parrotfish, and breams) made up 25.9% of dissimilarity between inside and outside the marine reserves before CBM (**Figure 4**). However, not every important fishery family increased uniformly at each site. For the same location (Bindoy) and treatment (inside and outside reserve before CBM implementation), a decrease in fusiliers, rabbitfish, hogfish, and surgeonfish was responsible for 12.3% of the dissimilarity. Additionally, when comparing the differences inside and outside the marine reserves after CBM was implemented the increase of important families (snappers, wrasses, jacks, goatfish, groupers, parrotfish, breams, fusiliers, surgeonfish, and rabbitfish) contributed to 34.5% of the dissimilarity. Notably, there were increases in fusiliers and rabbitfish contributing to 6.8% of dissimilarity between inside and outside marine reserves after CBM was implemented.

Other sites, such as Cantilan, Tinambac, and Cortes, had significant clusters ($P < 0.05$) for each interaction of reserve and CBM status (**Figure 5** and **Supplementary Figures 5, 6**). For these three sites, the general effect of CBM implementation for both inside and outside the reserve was increasing abundances of most important fishery families. Tinambac outside the reserves after CBM was implemented was an exception, where a decrease in abundance of fusiliers, rabbitfish, wrasses, and parrotfish were responsible for 23% of dissimilarity (**Figure 6**). For Tinambac, both outside and inside the marine reserve after CBM was implemented, fusiliers decreased in abundance.

Four sites, Manjuyod, Culasi, Tayasan, and Gubat, had no difference in fish community structure before CBM inside and outside marine reserves, however, after CBM was implemented, there was a significant shift in community structure inside marine reserves (**Figure 7** and **Supplementary Figures 7–10**). This was also accounted for in the SIMPER analysis for species where prior to CBM there was a lower dissimilarity (56.68) between inside the marine reserve and outside the marine reserve. However, after CBM implementation the average dissimilarity increased both within the reserve (69.71) and in comparison, to outside the reserve (64.63). The SIMPER analysis of Gubat revealed that an increase of snappers, goatfish wrasse, fusiliers, hogfish, and rabbitfish contributed to 23% of the dissimilarity between inside the marine reserve before and after CBM was implemented, indicating the application of CBM marine reserves for fisheries, not just conservation (**Figure 8**). Similarly to the previous sites, not all important fishery species had an increase of relative abundance after CBM, approximately 8% of the dissimilarity inside the reserves after CBM was due to the decrease of surgeonfish and parrotfish. Finally, two sites, Del Carmen and Sagnay had no community structure changes after CBM was implemented either inside or outside the marine reserve.

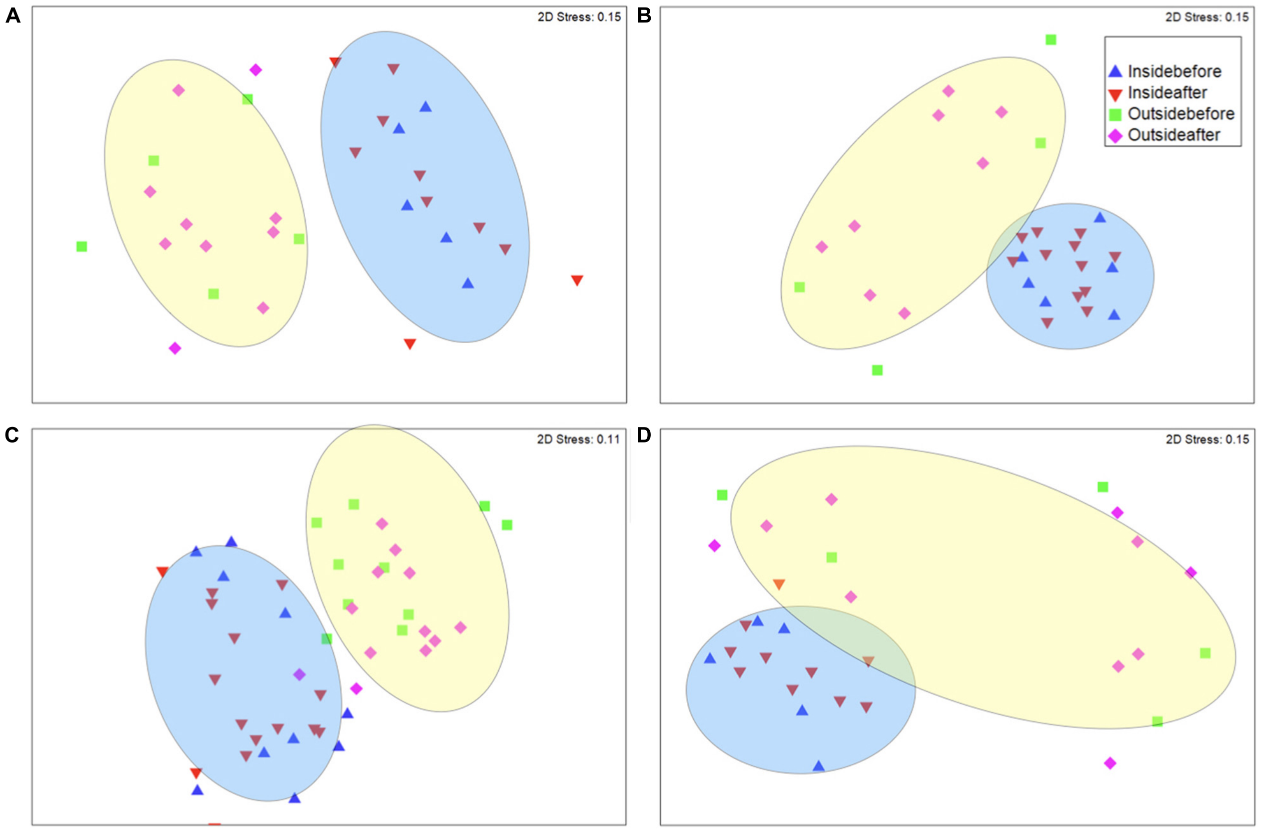

FIGURE 3 | Non-metric multidimensional scaling plot of fish species community structure similarities of **(A)** Lubang, **(B)** San Carlos City, **(C)** Bindoy, and **(D)** Looc. Triangles denote the community structure inside marine reserve [blue indicates before and red indicates after community-based management (CBM) implementation], and squares and diamonds outside of marine reserves, with squares indicating before, and diamonds indicating after CBM implementation. The ellipses indicate significant clusters ($P < 0.05$).

Biodiversity

At the site level, six sites (30%) had significant differences in biodiversity inside or outside marine reserves and five (25%) had differences before and after community-based management. Cortes and Libertad had similar biodiversity inside and outside marine reserves, but after CBM was implemented were significantly different, with high diversity inside the reserve than outside after implementation (**Figure 9**). Additionally, while some sites (Cantila, Masinloc, and Tinambac) had no significant differences in biodiversity inside and outside the marine reserves, biodiversity significantly increased in both areas after CBM was implemented. One site, Del Carmen, decreased in biodiversity overall after CBM, though the remaining sites increased in biodiversity. While there is some overlap between sites that had significant community structure changes and biodiversity changes there is no overall pattern.

DISCUSSION

Well-managed marine reserves in the Philippines have the potential to increase abundance of important species and biodiversity. Typically when evaluating the indicators of success for marine reserves, age and size of the reserve are important (Halpern, 2003; Vandeperre et al., 2011). While many of the marine reserves at our study sites have been established for many years ($x = 18$ years; SD = 7.5), it is possible they had little enforcement and were considered "paper parks" (Campos and Aliño, 2008). It is likely that there was little effect on fish and fisheries from the marine reserves prior to the implementation of managed access and CBM governance structure in 2014. Other studies have demonstrated that reduction of fishing pressure can result in changes in fish communities, such as an increase of high trophic level fish after fishing effort was reduced (Graham et al., 2017). Our study found that when looking at site-specific community composition, shifts in community structure occurred inside the marine reserve after community-based management was implemented.

There are large numbers of reef fish that are important for small-scale fisheries in the Philippines contributing to differences in communities after CBM was implemented. Fishers rely on a wide variety of fish species, but fusiliers (*Casionidae.*), rabbitfish (*Siganidae*), and groupers (*Serranidae*) make up the top ten fished species at these sites (Fish Forever, 2020). Because of this, their increased abundance after CBM implementation, as was seen in our study, is significant to the communities who depend on

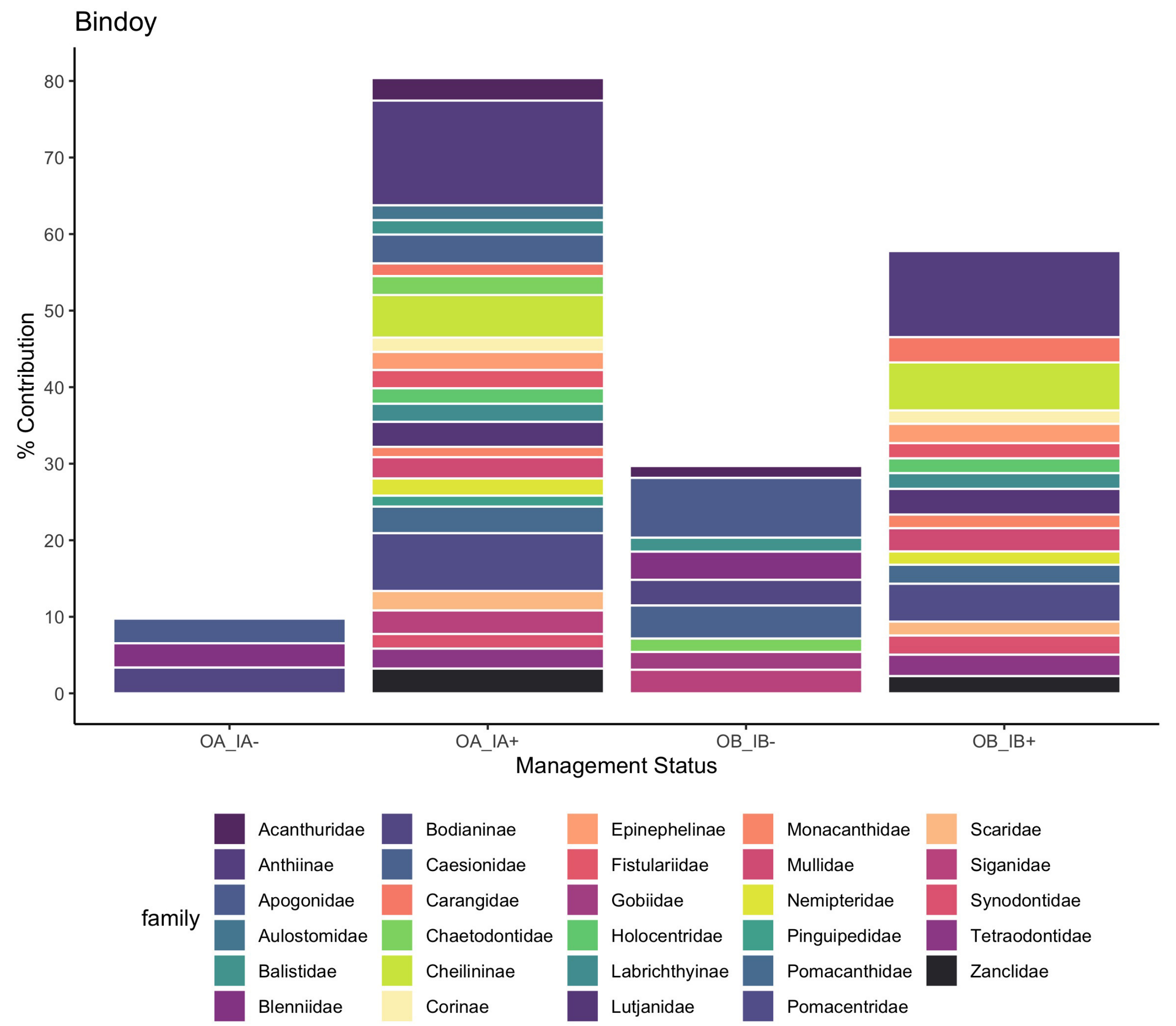

FIGURE 4 | Percent contribution to the dissimilarity between inside and outside before (average dissimilarity 30.36) and after (average dissimilarity 34.82) CBM implementation in Bindoy, aggregated by family. OA, outside marine reserve; after CBM implementation; OB, outside marine reserve; before CBM implementation; IA, inside marine reserve; after CBM implementation; IB, inside marine reserve; before CBM implementation. + means that there was higher abundance after CBM, – means there was lower abundance after CBM.

them. One target species, the leopard coral grouper (*Plectropomus leopardus)*, was previously listed as "Near-Threatened" by the International Union for Conservation of Nature (IUCN), citing population declines in the Philippines (Choat and Samoilys, 2018). In our study, the leopard coral grouper did contribute to the dissimilarity between communities inside marine reserves before and after community-based management, though with mixed results. In Bindoy, groupers, such as *P. leopardus*, decreased in relative abundance inside marine reserves after CBM (0.55% contribution to dissimilarity), but in Looc, they increased in abundance (0.56% contribution to dissimilarity). *Plectropomus leopardus* increased in abundance inside marine reserves after CBM in other sites such as Cantilan and Tinambac as well (contributing to 0.61 and 1.12%, respectively). Though the IUCN status has recently been updated to "Least Concern", populations are still declining and effectively managed marine reserves may be key to their continued recovery, especially since groupers have smaller home ranges and their populations generally respond well to marine reserves (Kramer and Chapman, 1999; Lowe et al., 2003).

In addition to groupers increasing in abundance inside the marine reserve after CBM implementation, other families of fishes displayed interesting movements. For example, in Tinambac rabbitfish (*Siganidae*) and parrotfish (*Scaridae*) decreased in abundance outside of the reserve but showed relative increases inside the reserves. One explanation for this is that

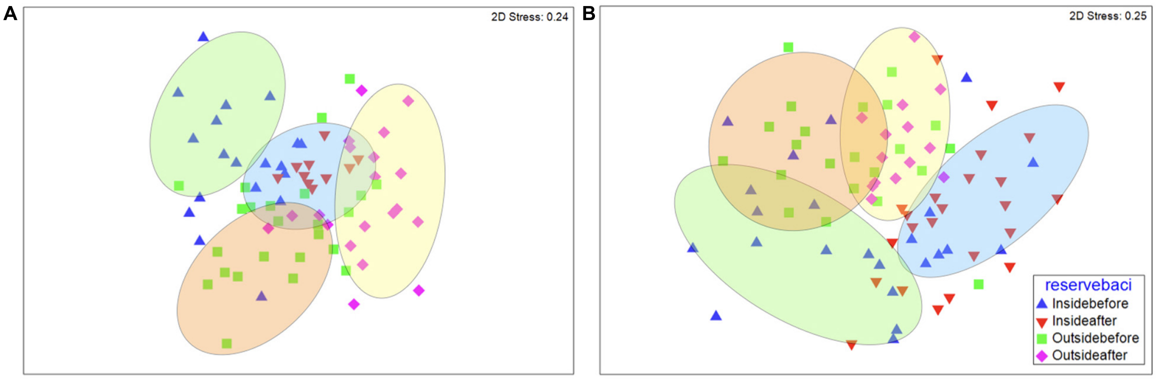

FIGURE 5 | Non-metric multidimensional scaling plot of fish species community structure similarities of **(A)** Cantila and **(B)** Cortes. Triangles denote the community structure inside marine reserve (blue indicates before and red indicates after CBM implementation), and squares and diamonds outside of marine reserves, with squares indicating before, and diamonds indicating after CBM implementation. The ellipses indicate significant clusters ($P < 0.05$).

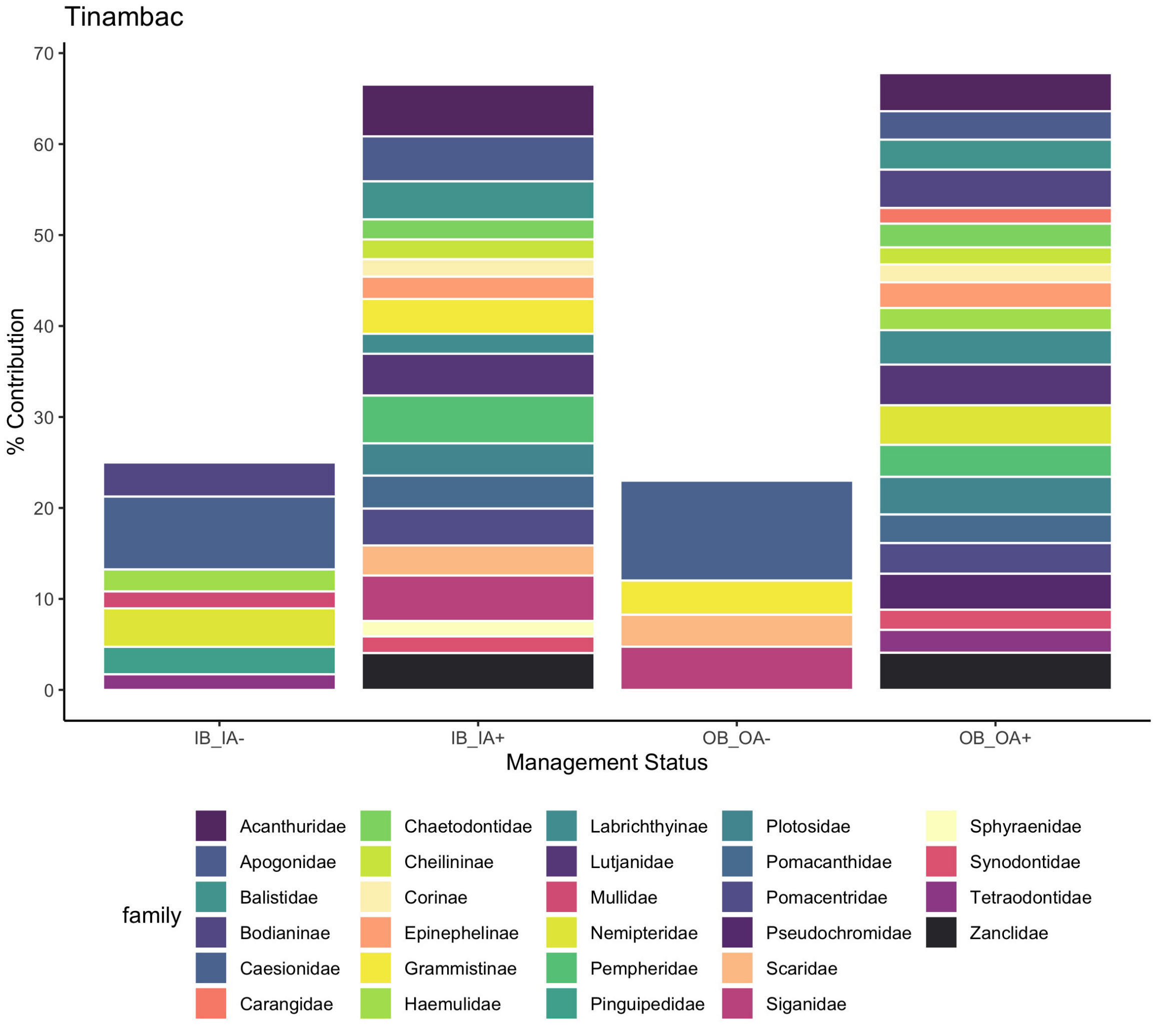

FIGURE 6 | Percent contribution to the dissimilarity between inside before and after (average dissimilarity 31.86) and outside marine reserves before and after (average dissimilarity 31.80) CBM in Tinambac, aggregated by family. OA, outside marine reserve; after CBM implementation; OB, outside marine reserve; before CBM implementation; IA, inside marine reserve; after CBM implementation; IB, inside marine reserve; before CBM implementation. + means that there was higher abundance after CBM, – means there was lower abundance after CBM.

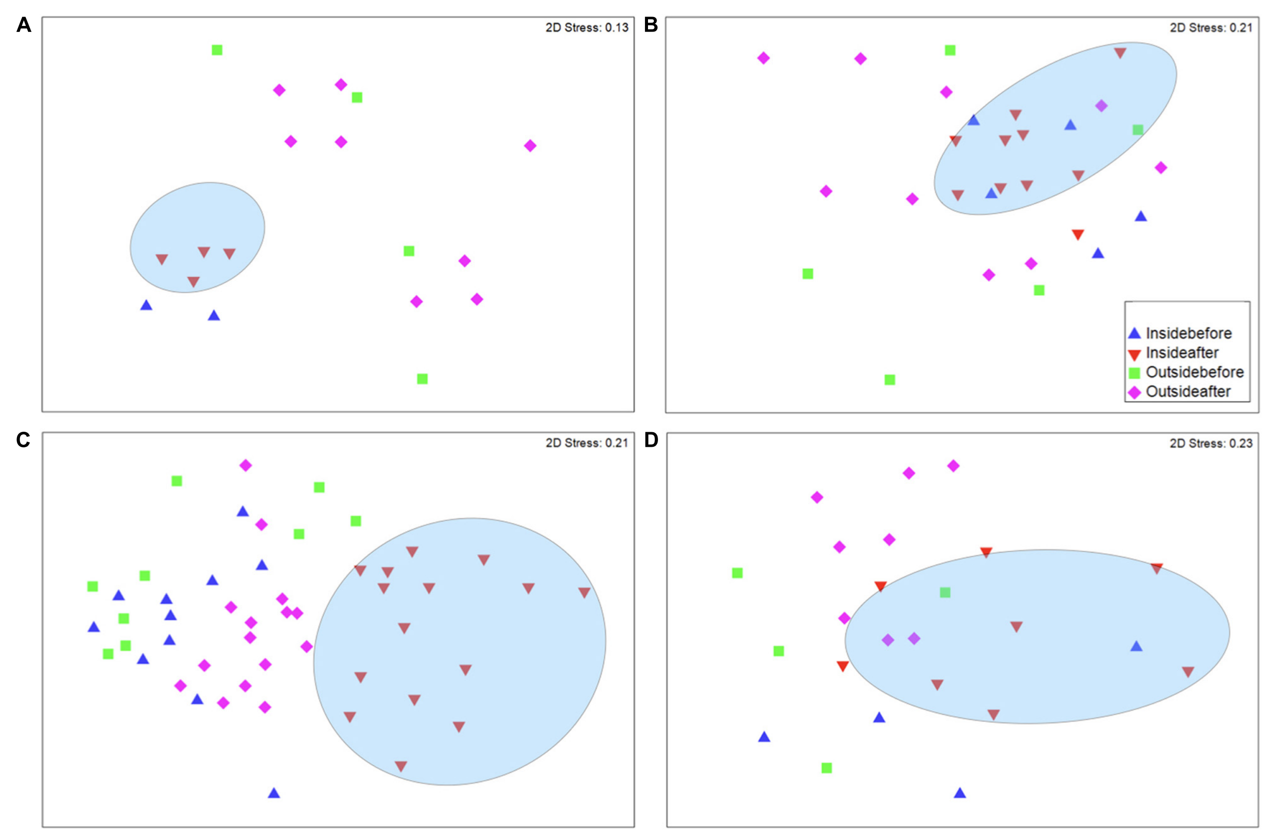

FIGURE 7 | Non-metric multidimensional scaling of community structure similarities for **(A)** Culasi, **(B)** Manjuyod, **(C)** Gubat, and **(D)** Tayasan. Triangles denote the community structure inside marine reserve and squares and diamonds outside of marine reserves. Triangles denote the community structure inside marine reserve (blue indicates before and red indicates after CBM implementation), and squares and diamonds outside of marine reserves, with squares indicating before, and diamonds indicating after CBM implementation. The ellipses indicate significant clusters ($P < 0.05$).

these fish are fished more heavily outside the reserve after CBM implementation. Another explanation is that fish leave fished areas and move into protected areas (Pittman et al., 2014). While this would appear as an increase of abundance inside the marine reserves, fish movement as opposed to fish reproduction is not a net increase of fish for the fishery. Though, the ability for fish to have refuge from fishing gives them a better chance for growth and reproduction in the future.

Biodiversity is typically used as an indicator of ecosystem health in relation to conservation, additionally, biodiversity is also correlated with higher catch and biomass, which is vital to small-scale fishers (Micheli et al., 2014). Marine reserves can assist in achieving both conservation and fishery goals if designed and enforced effectively (Cinner et al., 2020). While previous studies at the Fish Forever sites could not link the presence of the Fish Forever Pride Campaigns to increased biodiversity in marine reserves (Veríssimo et al., 2018), the implementation of community-based management investigated in this study does affect biodiversity in Philippine reefs. Overall, biodiversity increased after the implementation of CBM across all aggregated sites, which is a change from previous studies that did not find significant differences in biodiversity inside and outside marine reserves (Muallil et al., 2015). CBM at the sites in this study increased the effectiveness of the reserves and fostered higher biodiversity. A reason for this may be that Muallil et al. (2015) used 1 year of data (2012–2013), while our study uses a time series that allows for more time for populations to grow after fishing ceases. Additionally, our study tests biodiversity inside and outside marine reserves after CBM implementation, which occurred in 2014. Though, following the trends of the community structure analyses in this study, not all biodiversity indices increased significantly after the implementation of CBM for all sites. Our analyses reveal that sites do not all follow the same patterns, which leads to additional questions about why these fish communities differ.

In the Philippines, there are still instances of fishing occurring within marine reserves, which counteracts the ecological protections for the fish resulting in a lack of sustainability of the fishery (Muallil et al., 2014b). To increase the ecological function and protection of the reserves some suggest that marine reserves need to be larger (Muallil et al., 2014b). If community-based management does lead to reduced fishing pressure inside the marine reserves and more thoughtful fishing outside the marine reserves, we should expect greater biodiversity, abundance, and different fish communities. Our results suggest some sites performed better after CBM was implemented but not uniformly,

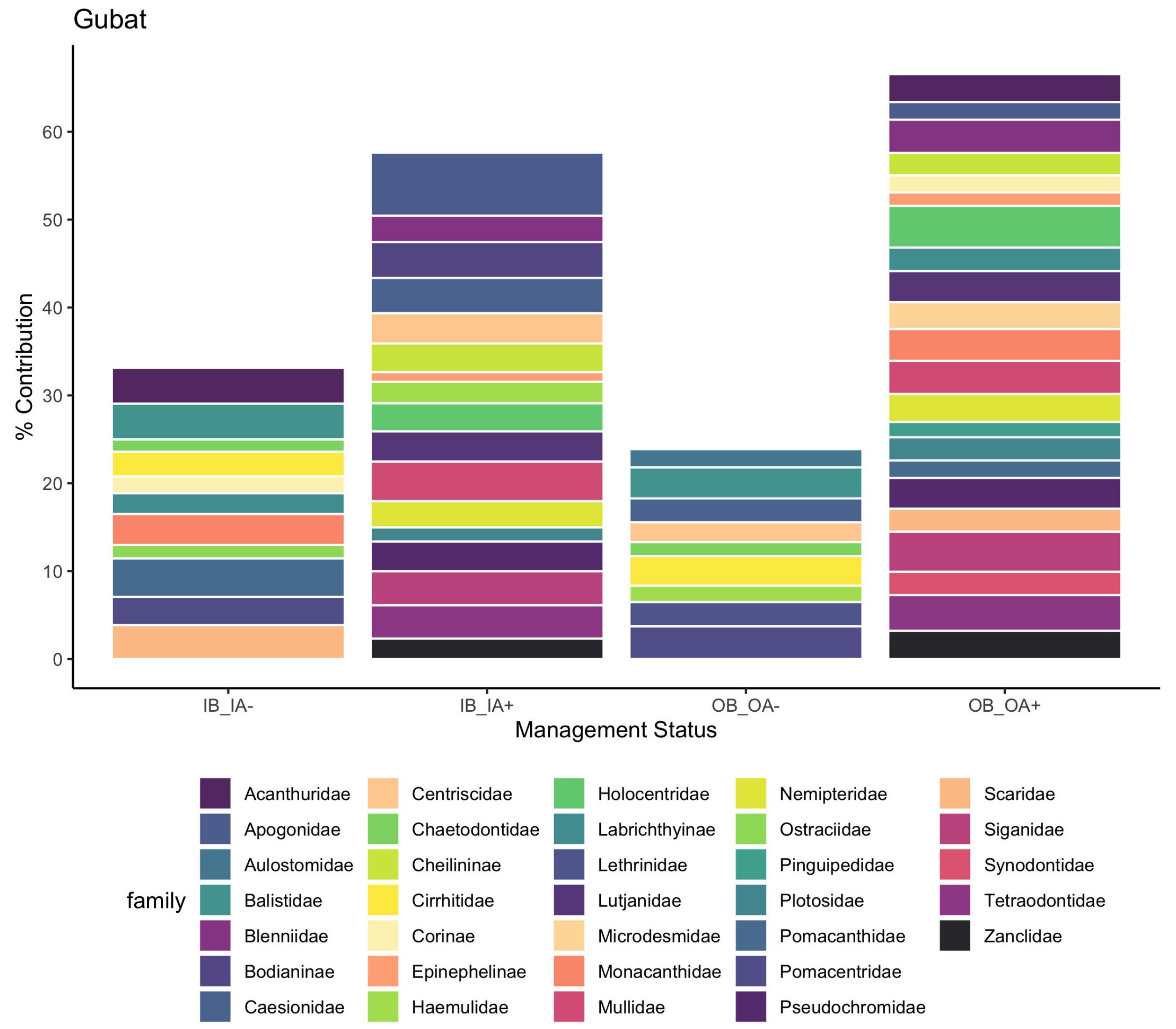

FIGURE 8 | Percent contribution to the dissimilarity between inside the marine reserves before and after CBM, inside and outside marine reserves before CBM, and inside and outside after CBM. OA, outside marine reserve; after CBM implementation; OB, outside marine reserve; before CBM implementation; IA, inside marine reserve; after CBM implementation; IB, inside marine reserve; before CBM implementation. + means that there was higher abundance inside the reserve or after CBM, – means there was lower abundance inside the reserve or after CBM.

approximately 30%. Some hypothesize that small marine reserves do not offer enough protection to impact fish community changes or biodiversity differences (Halpern, 2003; Friedlander et al., 2017), though the sites in our study that did show evidence of increase of biodiversity and abundance after community-based management were smaller reserves under 100 ha. The sites that had a significant difference in biodiversity in the interaction between reserves and CBM ranged from 16 to 307 ha in size. Even Tayasan, the smallest of the marine reserves at six hectares, and Gubat, a recently established marine reserve (in 2015), showed a significant change in community structure, showing increases of important fishery species, after CBM, which indicates that even small and recently established well-managed reserves can positively affect community structure for fisheries. It is also possible that some sites that did not show differences after CBM was implemented were already functioning and managed well prior to CBM. Of the sites where there were no community structure differences inside and outside reserves before CBM, 57% of them had differences after CBM. These sites indicate there is promise in well-designed CBM programs. Even though, the "after" dataset only encompassed 3 years, previous studies have shown that marine reserve impacts are seen within 1–3 years of implementation (Halpern and Warner, 2002; Micheli et al., 2004). Longer timeframes of data may allow for representation in the data of fish reproduction, spill-over, and growth, as well as for rules to be fully established and enforced, which may result in future changes to community structure and biodiversity (Russ and Alcala, 1996; Halpern et al., 2009; Friedlander et al., 2017).

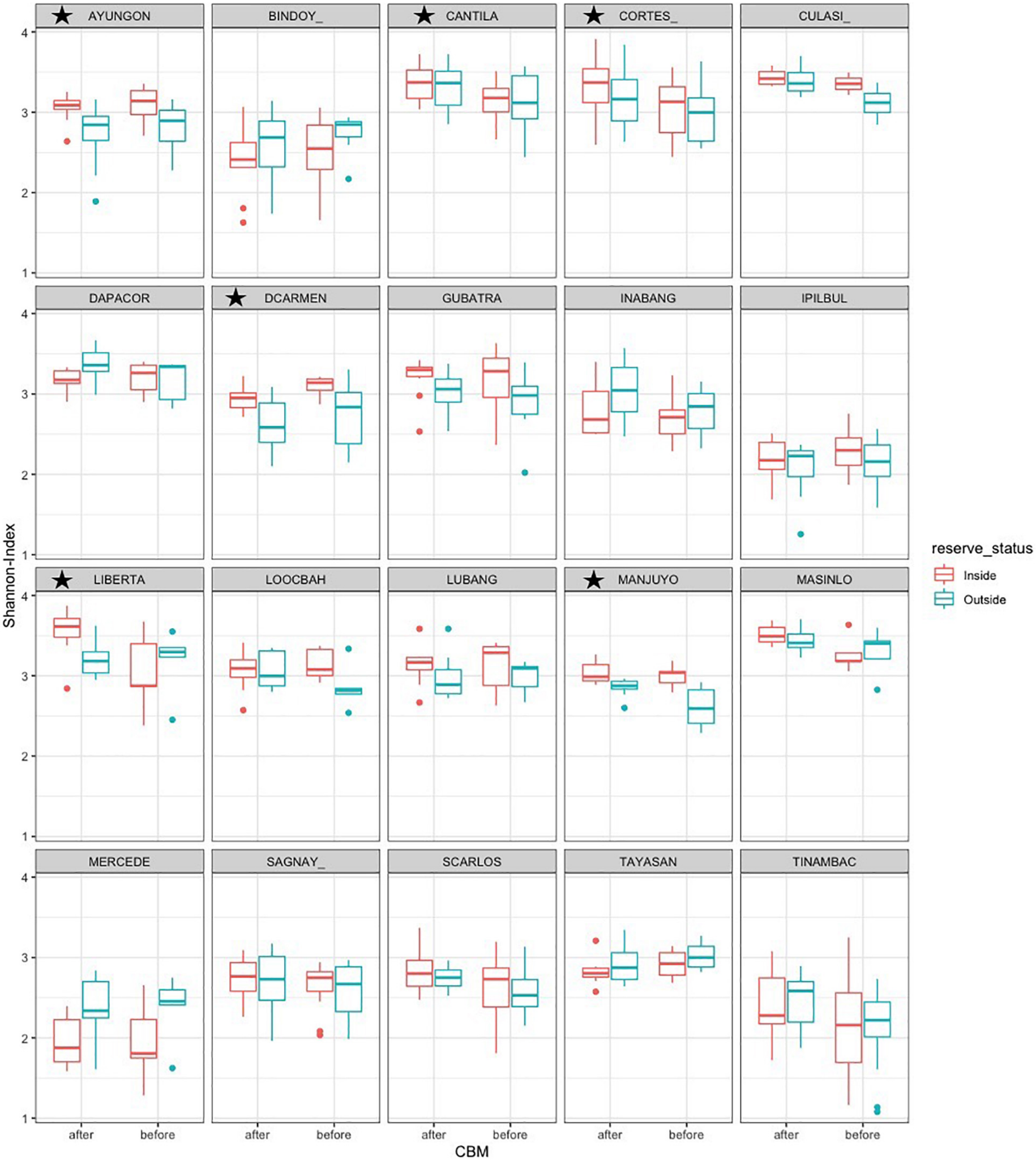

FIGURE 9 | Biodiversity index inside and outside marine reserves before and after CBM. * Indicates the interaction between CBM and reserve status at each site is $P < 0.05$.

Coastal fisheries exist in a complex socio-ecological system that involves many factors that determine the success of a particular management regime, but two major factors are compliance with fishery regulations and availability of nursery habitat. We provide evidence that community-based management leads to ecological changes that could benefit fisheries in the Philippines. However, our study is limited in answering "why" communities respond differently to CBM. We intend to further explore precise reasons why CBM may not be effective across all communities and address other impacts on fish communities, abundance, and biodiversity to improve the function of CBM of marine reserves. For example, marine reserves tend to be more effective when there is higher compliance within CBM (Pollnac et al., 2010). Though, there are many other indicators that also lead to increases in abundance of fish and biodiversity in CBM marine reserves such as residential community size, individual perceptions of fish populations, alternative livelihoods, trust in the marine reserve, and high participation in decision making (Pollnac et al., 2001; Quintana et al., 2021). These socio-ecological factors are dynamic, each heavily linked to the next, creating challenges in identifying a singular predictor for CBM marine reserve success. Negative perceptions on fish populations may result in the belief that the marine reserve is failing, thus that CBM is not working and create a feedback loop resulting in fewer rules for the marine reserves (Quintana et al., 2021). Additionally, external actors, such as fishers from other communities, may influence resources within the community fishing boundaries. Many municipalities in the Philippines have reported commercial fishers illegally fishing in municipal waters, who may have no regard nor knowledge of local regulations (Muallil, 2014). The presence of the commercial fishers may be impacting the success of these marine reserves to no fault of the local communities managing them. Future research will include interviewing fishers to clarify levels of compliance of regulations and what types of effects external commercial fishers have on the resources where CBM has not shown to have significant effects on fish biodiversity and community structure.

This study examined the fishery independent data in the context of marine reserves and the implementation of community-based management of those reserves. The implementation of these strategies does not necessarily result in compliance of the regulations. Additionally, marine reserves assessed in this study protect the near-shore reef, but not adjoining habitats. Many species of fish in this region, especially parrotfish and snappers, which are both commercially important species, undergo ontogenetic migration from nursery habitats onto the reef (Nagelkerken et al., 2000; Mumby, 2006; Unsworth et al., 2008; Jones et al., 2010). Mangroves and seagrasses provide much of that nursery habitat that many fish depend on (Honda et al., 2013). Mangroves have declined rapidly, with 80% percent loss in the Philippines in the last 100 years (Primavera, 2000). The loss of mangrove habitat has been linked to declines in fishery stock (Melana et al., 2005; Tran and Fischer, 2017), which may occur regardless of protection of reefs. Decline of mangroves may also negatively impact corals by the increase of turbidity and sedimentation on reefs (Manson et al., 2005). When the reef structure and nursery habitat is threatened, continued production of important fishery species can also be vulnerable (Manson et al., 2005). Additional research will examine the habitat availability and quality at these sites as part of the suite of variables that may contribute to why sites responded differently to CBM implementation.

Protecting coastal coral reef areas and managing fishing access through marine reserves are important steps in sustainability of fishery resources, however, if critical nursery habitat or habitat that provides ecological functions for corals is not protected, then the efforts of marine reserves may be in vain. Thus, small-scale fishery management through community-based management needs to fit into a broader social-ecological systems model, considering both the compliance of the fishing communities and the relationship of nursery habitats.

CONCLUSION

Fish communities have a high site fidelity, supporting the notion that marine reserves and fishery management strategies need to be evaluated by site. Our study highlights the importance of site level dynamics in the success of community-based management. While CBM implementation resulted in positive changes of biodiversity in 25% of the sites and fish community structure increasing from 65 to 85% of the sites, further research is needed to investigate the reasons why some sites successfully increased fish biodiversity and abundance and others did not. Understanding the variability across sites, enabling conditions, and drivers of success will promote better design and implementation of CBM marine reserves. We suggest that resource managers explore interactions occurring between social and ecological factors within reef fishing communities to tailor interventions for each locality and increase potential for success when implementing community-based management.

DATA AVAILABILITY STATEMENT

The raw data supporting the conclusion of this article will be made available by the authors, without undue reservation.

AUTHOR CONTRIBUTIONS

SM conceived the presented idea, performed analysis, and wrote the manuscript. CC, RA, RM, and DA coordinated the data collection and management. KM contributed to the design and implementation of research as well as meaningful contributions to the manuscript. All authors provided critical feedback and helped shape the research and manuscript.

FUNDING

Funding for data collection was provided by Rare.

ACKNOWLEDGMENTS

The authors want to acknowledge Rare and the partners in the Philippines for collecting and providing the data, which without this research would not be possible. S. Sanghera for advisement and thoughtful feedback on data analysis.

SUPPLEMENTARY MATERIAL

The Supplementary Material for this article can be found online at: https://www.frontiersin.org/articles/10.3389/fmars.2021.731675/full#supplementary-material

REFERENCES

Alfaro-Shigueto, J., Mangel, J. C., Pajuelo, M., Dutton, P. H., Seminoff, J. A., and Godley, B. J. (2010). Where small can have a large impact: structure and characterization of small-scale fisheries in Peru. *Fish. Res.* 106, 8–17. doi: 10.1016/j.fishres.2010.06.004

Aliño, P. M., Palomar, N. E., Arceo, H. O., and Uychiaoco, A. T. (2000). Challenges and opportunities for Marine Protected Area (MPA) management in the Philippines. *Proc. Coral Reef Symp.* 2, 635–640.

Arceo, H. O., Cazalet, B., Aliño, P. M., Mangialajo, L., and Francour, P. (2013). Moving beyond a Top-down fisheries management approach in the Northwestern Mediterranean: some lessons from the Philippines. *Mar. Policy* 39, 29–42. doi: 10.1016/j.marpol.2012.10.006

Brownman, H., Cury, P. M., Lotze, H. K., Jennings, S., Hilborn, R., Mace, P., et al. (2004). Perspectives on ecosystem-based approaches to the management of marine resources. *Mar. Ecol. Prog. Ser.* 274, 269–303. doi: 10.3354/meps274269

Cabral, R. B., Aliño, P. M., Balingit, A. C. M., Alis, C. M., Arceo, H. O., Nañola Jr, C. L., et al. (2014). The Philippine marine protected area (MPA) database. *Philipp. Sci. Lett.* 7, 300–308.

Campos, W. L., and Aliño, P. M. (2008). Recent advances in the management of marine protected areas in the Philippines. *Kuroshio Sci.* 2, 29–34.

Christie, P., White, A., and Deguit, E. (2002). Starting point or solution? Community-based marine protected areas in the Philippines. *J. Environ. Manag.* 66, 441–454. doi: 10.1006/jema.2002.0595

Choat, J. H., and Samoilys, M. (2018). *Plectropomusleopardus. The IUCN Red List of Threatened Species 2018: e.T44684A100462709.* doi: 10.2305/IUCN.UK.2018-2.RLTS.T44684A100462709.en

Cinner, J. E., Zamborain-Mason, J., Gurney, G. G., Graham, N. A. J., MacNeil, M. A., Hoey, A. S., et al. (2020). Meeting fisheries, ecosystem function, and biodiversity goals in a human-dominated World. *Science* 368, 307–311. doi: 10.1126/science.aax9412

Clarke, K. R., and Gorley, R. N. (2006). *PRIMER v6: User Manual/Tutorial.* Plymouth: PRIMER-E, 1–190.

Cox, C., Valdivia, A., McField, M., Castillo, K., and Bruno, J. F. (2017). Establishment of marine protected areas alone does not restore coral reef communities in Belize. *Mar. Ecol. Prog. Ser.* 563, 65–79. doi: 10.3354/meps11984

FAO (2014). *Fishery and Aquaculture Country Profiles. Philippines. Country Profile Fact Sheets. In: FAO Fisheries and Aquaculture Department [online]. Rome.* Available Online at: http://www.fao.org/fishery/

FAO (2018). *State of the World's Fisheries and Aquaculture: Meeting Sustainable Development Goals.* Rome: FAO.

Fish Forever (2020). *Philippines Fisheries Data. Rare.* Avaialable Online at: https://portal.rare.org/en/tools-and-data/fisheries-data/[Accessed: 06/05/2021].

Friedlander, A. M., Golbuu, Y., Ballesteros, E., Caselle, J. E., Gouezo, M., Olsudong, D., et al. (2017). Size, age, and habitat determine effectiveness of Palau's marine protected areas. *PloS One* 12:e0174787. doi: 10.1371/journal.pone.0174787

Gaines, S. D., White, C., Carr, M. H., and Palumbi, S. R. (2010). Designing marine reserve networks for both conservation and fisheries management. *Proc. Natl. Acad. Sci.* 107, 18286–18293. doi: 10.1073/pnas.0906473107

Graham, N. A. J., McClanahan, T. R., MacNeil, M. A., Wilson, S. K., Cinner, J. E., Huchery, C., et al. (2017). Human disruption of coral reef trophic structure. *Curr. Biol.* 27, 231–236. doi: 10.1016/j.cub.2016.10.062

Guidetti, P. (2006). Marine reserves reestablish lost predatory interactions and cause community changes in rocky reefs. *Ecol. Appl.* 16, 963–976. doi: 10.1890/1051-0761(2006)016[0963:MRRLPI]2.0.CO;2

Guidetti, P., and Claudet, J. (2010). Comanagement practices enhance fisheries in marine protected areas. *Conserv. Biol.* 24, 312–318. doi: 10.1111/j.1523-1739.2009.01358.x

Halpern, B. S. (2003). The impact of marine reserves: Do reserves work and does reserve size matter? *Ecol. Appl.* 13, 117–137. doi: 10.1890/1051-0761(2003)013[0117:TIOMRD]2.0.CO;2

Halpern, B. S., Lester, S. E., and Kellner, J. B. (2009). Spillover from marine reserves and the replenishment of fished stocks. *Environ. Conserv.* 36, 268–276. doi: 10.1017/S0376892910000032

Halpern, B. S., and Warner, R. R. (2002). Marine reserves have rapid and lasting effects. *Ecol. Lett.* 5, 361–366. doi: 10.1046/j.1461-0248.2002.00326.x

Hilborn, R., and Ovando, D. (2014). Reflections on the success of traditional fisheries management. *ICES J. Mar. Sci.* 71, 1040–1046. doi: 10.1093/icesjms/fsu034

Honda, K., Nakamura, Y., Nakaoka, M., Uy, W. H., and Fortes, M. D. (2013). Habitat use by fishes in coral reefs, seagrass beds and mangrove habitats in the Philippines. *PLoS ONE* 8:e65735. doi: 10.1371/journal.pone.0065735

Jones, D. L., Walter, J. F., Brooks, E. N., and Serafy, J. E. (2010). Connectivity through Ontogeny: fish population linkages among mangrove and coral reef habitats. *Mar. Ecol. Prog. Ser.* 401, 245–258. doi: 10.3354/meps08404

Kassambara, A. (2020). *rstatix: Pipe-Friendly Framework for Basic Statistical Tests. R package version 0.6.0.* Available Online at: https://CRAN.R-project.org/package=rstatix.

Kearney, J., Berkes, F., Charles, A., Pinkerton, E., and Wiber, W. (2007). The role of participatory governance and community-based management in integrated coastal and ocean management in Canada. *Coastal Manage.* 35, 79–104. doi: 10.1080/10.1080/08920750600970511

Kerwath, S. E., Winker, H., Götz, A., and Attwood, C. G. (2013). Marine protected area improves yield without disadvantaging fishers. *Nat. Commun.* 4:2347. doi: 10.1038/ncomms3347

Kramer, D. L., and Chapman, M. R. (1999). Implications of fish home range size and relocation for marine reserve function. *Environ. Biol. Fishes* 55, 65–79. doi: 10.1023/A:1007481206399

Lowe, C. G., Topping, D. T., Cartamil, D. P., and Papastamatiou, Y. P. (2003). Movement patterns, home range, and habitat utilization of adult kelp bass paralabrax clathratus in a temperate no-take marine reserve. *Mar. Ecol. Prog. Ser.* 256, 205–216. doi: 10.3354/meps256205

Manson, F. J., Loneragan, N. R., Skilleter, G. A., and Phinn, S. R. (2005). An evaluation of the evidence for linkages between mangroves and fisheries: A synthesis of the literature and identification of research directions. *Oceanogr. Mar. Biol.* 43, 493–524.

Marine Conservation Institute (2021). *Marine Protection Atlas: Philippines.* Avaialable Online at: https://mpatlas.org/countries/PHL[Retrieved February 28, 2021].

Maypa, A. P., Russ, G. R., Alcala, A. C., and Calumpong, H. P. (2002). Long-term trends in yield and catch rates of the coral reef fishery at Apo Island, Central Philippines. *Mar. Freshwater Res.* 53:207. doi: 10.1071/MF01134

McClanahan, T. R., Marnane, M. J., Cinner, J. E., and Kiene, W. E. (2006). A comparison of marine protected areas and alternative approaches to coral-reef management. *Curr. Biol.* 16, 1408–1413. doi: 10.1016/j.cub.2006.05.062

McManus, J. W., and Reyes, R. B. Jr. (1997). Effects of some destructive fishing methods on coral cover and potential rates of recovery. *Environ. Manage.* 21, 69–78. doi: 10.1007/s002679900006

Melana, D. M., Melana, E. E., and Mapalo, A. M. (2005). *Mangroves Management and Development in the Philippines. [Book chapter].* Aquaculture Department, Southeast Asian Fisheries Development Center. Available online at: http://hdl.handle.net/10862/712

Micheli, F., Halpern, B. S., Botsford, L. W., and Warner, R. R. (2004). Trajectories and correlates of community change in No-Take marine reserves. *Ecol. Appl.* 14, 1709–1723. doi: 10.1890/03-5260

Micheli, F., Mumby, P. J., Brumbaugh, D. R., Broad, K., Dahlgren, C. P., Harborne, A. R., et al. (2014). High vulnerability of ecosystem function and services to diversity loss in caribbean coral reefs. *Biol. Conserv.* 171, 186–194. doi: 10.1016/j.biocon.2013.12.029

Mora, C. (2008). A clear human footprint in the coral reefs of the Caribbean. *Proc. R. Soc. B Biol. Sci.* 275, 767–773. doi: 10.1098/rspb.2007.1472

Muallil, R. N., Deocadez, M. R., Martinez, R. J. S., Mamauag, S. S., Nañola, C. L., and Aliño, P. M. (2015). Community assemblages of commercially important coral reef fishes inside and outside marine protected areas in the Philippines. *Reg. Stud. Mar. Sci.* 1, 47–54. doi: 10.1016/j.rsma.2015.03.004

Muallil, R. N., Deocadez, M. R., Martinez, R. J. S., Campos, W. L., Mamauag, S. S., Nañola, C. L., et al. (2019). Effectiveness of small locally-managed marine protected areas for coral reef fisheries management in the Philippines. *Ocean Coastal Manage.* 179:104831. doi: 10.1016/j.ocecoaman.2019.104831

Muallil, R. N., Mamauag, S. S., Cababaro, J. T., Arceo, H. O., and Aliño, P. M. (2014a). Catch trends in Philippine small-scale fisheries over the last five decades: The Fishers× Perspectives. *Mar. Policy* 47, 110–117. doi: 10.1016/j.marpol.2014.02.008

Muallil, R. N., Mamauag, S. S., Cabral, R. B., Celeste-Dizon, E. O., and Aliño, P. M. (2014b). Status, trends and challenges in the sustainability of small-scale fisheries in the Philippines: Insights from FISHDA (Fishing Industries' Support in Handling Decisions Application) model. *Mar. Policy* 44, 212–221. doi: 10.1016/j.marpol.2013.08.026

Mumby, P. J. (2006). Connectivity of reef fish between mangroves and coral reefs: algorithms for the design of marine reserves at seascape scales. *Biol. Conserv.* 128, 215–222. doi: 10.1016/j.biocon.2005.09.042

Mumby, P. J., Harborne, A. R., Williams, J., Kappel, C. V., Brumbaugh, D. R., Micheli, F., et al. (2007). Trophic cascade facilitates coral recruitment in a marine reserve. *Proc. Natl. Acad. Sci.* 104, 8362–8367. doi: 10.1073/pnas.0702602104

Nagelkerken, I., van der Velde, G., Gorissen, M. W., Meijer, G. J., Van't Hof, T., and den Hartog, C. (2000). Importance of mangroves, seagrass beds and the shallow coral reef as a nursery for important coral reef fishes, using a visual census technique. *Estuar. Coast. Shelf Sci.* 51, 31–44. doi: 10.1006/ecss.2000.0617

Oksanen, J., Blanchet, F. G., Friendly, M., Kindt, R., Legendre, P., McGlinn, D., et al. (2020). *vegan: Community Ecology Package. R package version 2.5-7*. Available Online at: https://CRAN.R-project.org/package=vegan.

Ostrom, E. (2000). Collective action and the evolution of social norms. *J. Econ. Perspec.* 14, 137–158. doi: 10.1257/jep.14.3.137

Pastorok, R. A., and Bilyard, G. R. (1985). Effects of sewage pollution on coral-reef communities. *Mar. Ecol. Prog. Ser.* 21, 175–189. doi: 10.3354/meps021175

Pauly, D., and Zeller, D. (2016). Catch reconstructions reveal that global marine fisheries catches are higher than reported and declining. *Nat. Commun.* 7:10244. doi: 10.1038/ncomms10244

Pinkerton, E. (1989). "Introduction: attaining better fisheries management through co-management-prospects, problems and propositions," in *Cooperative Management of Local Fisheries*, ed. E. Pinkerton (Vancouver, Canada: University of British Columbia Press).

Pittman, S. J., Monaco, M. E., Friedlander, A. M., Legare, B., Nemeth, R. S., Kendall, M. S., et al. (2014). Fish with chips: tracking reef fish movements to evaluate size and connectivity of caribbean marine protected areas. *PLoS One* 9:e96028. doi: 10.1371/journal.pone.0096028

Pollnac, R., Christie, P., Cinner, J. E., Dalton, T., Daw, T. M., Forrester, G. E., et al. (2010). Marine reserves as linked social-ecological systems. *Proc. Natl. Acad. Sci.* 107, 18262–18265. doi: 10.1073/pnas.0908266107

Pollnac, R. B., Crawford, B. R., and Gorospe, M. L. G. (2001). Discovering factors that influence the success of community-based marine protected areas in the Visayas, Philippines. *Ocean Coastal Manage.* 44, 683–710. doi: 10.1016/S0964-5691(01)00075-8

Pomeroy, R., and Courtney, C. A. (2018). The Philippines context for marine tenure and small-scale fisheries. *Mar. Policy* 95, 283–293. doi: 10.1016/j.marpol.2018.05.030

Pomeroy, R. S. (1995). Community-based and Co-management institutions for sustainable coastal fisheries management in Southeast Asia. *Ocean Coastal Manage.* 27, 143–162. doi: 10.1016/0964-5691(95)00042-9

Primavera, J. H. (2000). Development and conservation of Philippine Mangroves: institutional issues. *Ecol. Econ.* 35, 91–106. doi: 10.1016/S0921-8009(00)00170-1

Quintana, A. C. E., Giron-Nava, A., Urmy, S., Cramer, A. N., Domínguez-Sánchez, S., Rodríguez Van Dyck, S., et al. (2021). Positive social-ecological feedbacks in community-based conservation. *Front. Mar. Sci.* 8:652318. doi: 10.3389/fmars.2021.652318

R Core Team (2013). *R: A language and environment for statistical computing*. Vienna, Austria: R Foundation for Statistical Computing.

Rare (2018). *Stemming the Tide of Coastal Overfishing Fish Forever Program Results 2012–2017*. Arlington, VA: Rare, 1–64.

Rife, A. N., Erisman, B., Sanchez, A., and Aburto-Oropeza, O. (2013). When good intentions are not enough Insights on Networks of 'Paper Park' marine protected areas: Concerns regarding marine 'Paper Parks. *Conserv. Lett.* 6, 200–212. doi: 10.1111/j.1755-263X.2012.00303.x

Rohrer, J. M. (2017). *Effectiveness of Locally Managed Marine Protected Areas in the Visayas, Negros Oriental Province, Philippines. Master's thesis*. Lisboa: Instituto Universitário de Ciências Psicológicas, Sociais e da Vida (ISPA).

Russ, G. R., and Alcala, A. C. (1996). Do marine reserves export adult fish biomass? Evidence from Apo Island, Central Philippines. *Mar. Ecol. Prog. Ser.* 132, 1–9. doi: 10.3354/meps132001

Russ, G. R., Alcala, A. C., and Maypa, A. P. (2003). Spillover from marine reserves: The Case of *Naso Vlamingii* at Apo Island, the Philippines. *Mar. Ecol. Prog. Ser.* 264, 15–20. doi: 10.3354/meps264015

Selgrath, J. C., Gergel, S. E., and Vincent, A. C. J. (2018). Shifting gears: diversification, intensification, and effort increases in small-scale fisheries (1950-2010). *PLoS One* 13:e0190232. doi: 10.1371/journal.pone.0190232

Shester, G. G., and Micheli, F. (2011). Conservation challenges for small-scale fisheries: bycatch and habitat impacts of traps and gillnets. *Biol. Conserv.* 144, 1673–1681. doi: 10.1016/j.biocon.2011.02.023

Smallhorn-West, P. F., Bridge, T. C. L., Malimali, S., Pressey, R. L., and Jones, G. P. (2019). Predicting impact to assess the efficacy of community-based marine reserve design. *Conserv. Lett.* 12:e12602. doi: 10.1111/conl.12602

Strain, E. M. A., Edgar, G. J., Ceccarelli, D., Stuart-Smith, R. D., Hosack, G. R., and Thomson, R. J. (2019). A global assessment of the direct and indirect benefits of marine protected areas for coral reef conservation. *Diver. Distrib.* 25, 9–20. doi: 10.1111/ddi.12838

Tran, L. X., and Fischer, A. (2017). Spatiotemporal changes and fragmentation of mangroves and its effects on fish diversity in Ca Mau province (Vietnam). *J. Coastal Conserv.* 21, 355–368. doi: 10.1007/s11852-017-0513-9

Unsworth, R. K. F., De León, P. S., Garrard, S. L., Jompa, J., Smith, D. J., and Bell, J. J. (2008). High connectivity of indo-pacific seagrass fish assemblages with mangrove and coral reef habitats. *Mar. Ecol. Prog. Se.* 353, 213–224. doi: 10.3354/meps07199

Vandeperre, F., Higgins, R. H., Sánchez-Meca, J., Maynou, F., Goñi, R., Martín-Sosa, P., et al. (2011). Effects of No-Take area size and age of marine protected areas on fisheries yields: A meta-analytical approach: MPA size and age: effects on fisheries. *Fish Fish.* 12, 412–426. doi: 10.1111/j.1467-2979.2010.00401.x

Veríssimo, D., Bianchessi, A., Arrivillaga, A., Cadiz, F. C., Mancao, R., and Green, K. (2018). Does it work for biodiversity? Experiences and challenges in the evaluation of social marketing campaigns. *Soc. Market. Q.* 24, 18–34. doi: 10.1177/1524500417734806

Weeks, R., Russ, G. R., Alcala, A. C., and White, A. T. (2010). Effectiveness of marine protected areas in the Philippines for biodiversity conservation. *Conserv. Biol.* 24, 531–540. doi: 10.1111/j.1523-1739.2009.01340.x

Wenger, A., Fabricius, K., Jones, G., and Brodie, J. (2015). "Effects of Sedimentation, Eutrophication, and Chemical Pollution on Coral Reef Fishes," in *Ecology of Fishes on Coral Reefs*, ed. C. Mora (Cambridge, England: Cambridge University Press), 145–153. doi: 10.1017/CBO9781316105412.017

World Bank (2012). *Hidden Harvest: The Global Contribution of Capture Fisheries (English)*. Washington, D.C: World Bank Group.

Conflict of Interest: CC, RA, RM, and DA work for Rare, which facilitated the implementation of the community-based management at these sites in the Philippines. To minimize the potential for a conflict of interest, Rare colleagues did not participate in the data analysis or interpretation used for this manuscript.

The remaining authors declare that the research was conducted in the absence of any commercial or financial relationships that could be construed as a potential conflict of interest.

frontiers
in Marine Science

ORIGINAL RESEARCH
published: 06 January 2022
doi: 10.3389/fmars.2021.782977

Spatial and Short-Term Temporal Patterns of Octocoral Assemblages in the West Philippine Sea

Jue Alef A. Lalas[1], Romina Therese S. Lim[1], Joey P. Cabasan[1], Christine S. Segumalian[1], Rhea Mae A. Luciano[1], Darryl Anthony M. Valino[1], Melchor R. Jacinto[1], Hazel O. Arceo[2] and Maria Vanessa Baria-Rodriguez[1]*

[1] The Marine Science Institute, University of the Philippines Diliman, Quezon City, Philippines, [2] Department of Biology and Environmental Science, College of Science, University of the Philippines Cebu, Cebu City, Philippines

Octocorals are relatively understudied than other coral reef organisms despite their ecological and economic values. The Philippines is known to have high marine biodiversity, but information on octocorals is lacking. This study investigated spatial and temporal variations in the assemblage of octocorals in selected reef sites in the West Philippine Sea (WPS)- the Kalayaan Island Group (i.e., Pag-asa, Sabina, Lawak, and Northeast Investigator) and Ulugan in 2017 and 2019. Results showed high octocoral taxonomic richness (at least 10 families) in the study sites. Mean percent octocoral cover in WPS was 5.35% SE ± 0.55, with Sabina having the highest octocoral cover in both years. Significant differences in octocoral cover were observed among sites in both years, but among-station differences were only observed in 2017. Octocoral assemblage also differed among sites in both years (ANOSIM: $R > 0.5$, $p < 0.05$), wherein different octocoral taxa dominated in different sites. In particular, variations were driven by high cover of holaxonians, nephtheids, and coelogorgiids in Sabina, and clavulariids, tubiporiids, and xeniids in Northeast Investigator in 2017. In 2019, significant variations were driven by high cover of helioporiids in Pag-asa, while Sabina had higher abundance of holaxonians, nephtheids, alcyoniids, and xeniids. Short-term temporal variation on octocoral cover in monitoring stations in Pag-asa was not observed (Kruskal-Wallis, $p > 0.05$), although the overall mean octocoral cover increased from 1.23% ± SE 0.47 in 2017 to 2.09% SE ± 0.37 in 2019. Further, there was no significant change in the octocoral assemblage in Pag-asa between years (ANOSIM, $R = 0.11$, $p = 0.07$). This study highlights high octocoral taxonomic richness in the WPS relative to other sites in the Indo-Pacific Region and provides baseline information on the octocoral assemblages, which can be useful for future ecological studies and marine biodiversity conservation efforts.

Keywords: octocorallia, soft corals, gorgonians, coral reef, Philippines, South China Sea, Spratly Islands

Edited by:
Susana Carvalho,
King Abdullah University of Science and Technology, Saudi Arabia

Reviewed by:
Erik Cordes,
Temple University, United States
Hin Boo Wee,
National University of Malaysia, Malaysia
Yuka Kushida,
Kagoshima University, Japan

Correspondence:
Maria Vanessa Baria-Rodriguez
vrodriguez@msi.upd.edu.ph

Specialty section:
This article was submitted to Marine Ecosystem Ecology, a section of the journal Frontiers in Marine Science

Received: *25 September 2021*
Accepted: *06 December 2021*
Published: *06 January 2022*

Citation:
Lalas JAA, Lim RTS, Cabasan JP, Segumalian CS, Luciano RMA, Valino DAM, Jacinto MR, Arceo HO and Baria-Rodriguez MV (2022) Spatial and Short-Term Temporal Patterns of Octocoral Assemblages in the West Philippine Sea. Front. Mar. Sci. 8:782977. doi: 10.3389/fmars.2021.782977

INTRODUCTION

Octocorals are benthic marine organisms characterized by the presence of polyps bearing eight pinnate tentacles and have evolved a wide range of biomineralization strategies, including the production of skeletal structures composed of different calcium carbonate polymorphs (Fabricius and Alderslade, 2001; Aharonovich and Benayahu, 2012; Conci et al., 2021). Octocorals belong to the subclass Octocorallia, which comprises orders Helioporacea (blue corals), Pennatulacea (sea pens), and Alcyonacea (soft corals and gorgonians) that represents one of the most diverse macrobenthic group in tropical and subtropical shallow coral reefs and deep-sea environments (Lau et al., 2020). In addition, Octocorallia represents 64% of all extant coral species in the world (Williams and Cairns, 2018), providing a wide array of ecological benefits including coral reef development and structural complexity (Jones et al., 1994; Edmunds et al., 2016; Shoham et al., 2019), nutrition (Etnoyer et al., 2016; Garra et al., 2020), and refuge for reef organisms (Carvalho et al., 2014; Cúrdia et al., 2015; Dias et al., 2015; Epstein and Kingsford, 2019). As major macrobenthic components, octocorals play a significant role in coral reef community dynamics and may serve as indicators of water quality in reefs affected by various disturbances including climate change and pollution (Nörstrom et al., 2009; De'ath and Fabricius, 2010; Edmunds and Lasker, 2019). Apart from their ecological importance, octocorals are known to be valuable sources of natural products, which are utilized in the pharmaceutical industry (Zubair et al., 2018). In fact, aquaculture studies in soft corals are currently gaining attention due to their biomedical potential (Sella and Benayahu, 2010).

Studies on shallow water octocorals began in the Indo-Pacific (Red Sea) about 250 years ago (Benayahu et al., 2019). While octocoral distribution across the Red Sea, Great Barrier Reef (Australia), and Hong Kong has been widely documented, only limited octocoral taxonomic and distribution studies have been conducted in the Philippines, with majority from the early twentieth century (Lalas et al., 2021). Most recent octocoral studies in the archipelago have focused on the distribution of blue corals (e.g., Licuanan et al., 2019; Atrigenio et al., 2020) while information on other octocorals is limited (Lalas et al., 2021). Unlike scleractinians, octocoral assemblage dynamics have been overlooked and actual diversity and abundance analyses are often underestimated (Shoham and Benayahu, 2016; Benayahu et al., 2019; Lasker et al., 2020). This results in an overall lack of information relative to other taxa, such as scleractinians. Knowing overall biodiversity in an area can have great benefits on biogeography and conservation (Benayahu et al., 2004; Huang et al., 2014), especially in understudied regions, which are hotspots of biodiversity and of multiple disturbances.

The Philippines is located within the Coral Triangle, the epicenter of marine biodiversity (Sanciangco et al., 2013). One of the major biogeographic regions in the Philippines is the West Philippine Sea (WPS) (Aliño and Gomez, 1994) located in the South China Sea. This area accounts for approximately 30% of the total reef area in the Philippines. Considered to have the highest species richness and biomass of reef-associated fauna among the marine biogeographic regions of the Philippines, the WPS supports a great diversity of fish and invertebrate species including corals, gastropods, and bivalves (Huang et al., 2014).

Located within the WPS is the Kalayaan Island Group (KIG), a part of the Spratly Islands consisting of several islets, shoals, and reefs covering an area of 3,257.70 km^2 (Asian Development Bank, 2014). Fisheries production and diversity in the WPS is relatively high, with the KIG potentially producing 3–5% of the total annual marine capture fisheries of the Philippines (Aliño et al., 1998; Arceo et al., 2020). Hypothesized to be a critical support system to reefs in nations bordering the South China Sea, KIG reefs serve as a potential source of pelagic propagules, replenishing populations of marine organisms such as fish and invertebrates (Aliño et al., 1998; Carpenter and Springer, 2005; Pata and Yñiguez, 2019). However, due to the geopolitical situation and remote distance of the KIG, conducting reef surveys and regular monitoring in the area is challenging (McManus, 1994; Aliño et al., 1998; Arceo et al., 2020). Most published studies in the KIG have focused on hard corals (i.e., Quibilan and Aliño, 2006; Quimpo et al., 2019). In fact, only the study of Dai and Fan (1996) on coral communities in Taiping Island has included a more detailed analysis of octocoral assemblages, leaving the ecological importance of these taxa underestimated (Epstein and Kingsford, 2019). This, and their major ecological and economic benefits on reefs, provide an impetus to conduct studies concerning this key taxon.

This study investigated the octocoral assemblage in shallow coral reefs in the West Philippine Sea (i.e., KIG: Pag-asa, Sabina, Lawak, and Northeast Investigator, and Ulugan). Through this study, (1) spatial differences among octocoral assemblages in this part of the WPS at different spatial scales were assessed and (2) changes in octocoral assemblage in selected stations in Pag-asa were evaluated through time. The results of this study will serve as baseline information on the octocoral assemblage of coral reefs in the Philippines and in the Indo-Pacific Region, which will highly benefit future coral reef monitoring and management efforts.

MATERIALS AND METHODS

Study Area

Scientific expeditions to the West Philippine Sea were carried out in 2017 and 2019 to conduct octocoral assemblage surveys (**Figure 1**). In 2017, twelve stations in four sites located in the Kalayaan Island Group (KIG), which were Pag-asa (*n* = 7) (N 114.3 E 11.0), Sabina (*n* = 3) (N 116.4 E 9.8), Lawak (*n* = 1) (N 115.8 E 10.7), and Northeast Investigator (*n* = 1) (N 116.5 E 9.2) were surveyed. In 2019, surveys were conducted in Pag-asa (*n* = 5) and Sabina (*n* = 2), with the addition of stations in Ulugan (*n* = 3) on the western coast of mainland Palawan. In Pag-asa, four stations were established as monitoring stations in 2017 and re-surveyed in 2019 to determine temporal changes in octocoral assemblages.

Octocoral Assemblage Survey

Two permanent 50-m transect lines were laid and established at a constant depth of 8–10 m in each survey station. Octocoral assemblage surveys were carried out using the photoquadrat method wherein a photograph was taken at every meter of the transect line using a digital camera (Sony RX100) with an underwater housing (Ikelite for Sony RX100) attached to a tetrapod covering a surface area of 1 m^2. The photos were analyzed using the Coral Point Count with Excel extensions (CPCe) program (Kohler and Gill, 2006). Through the area analysis feature of the CPCe, the circumference of each octocoral

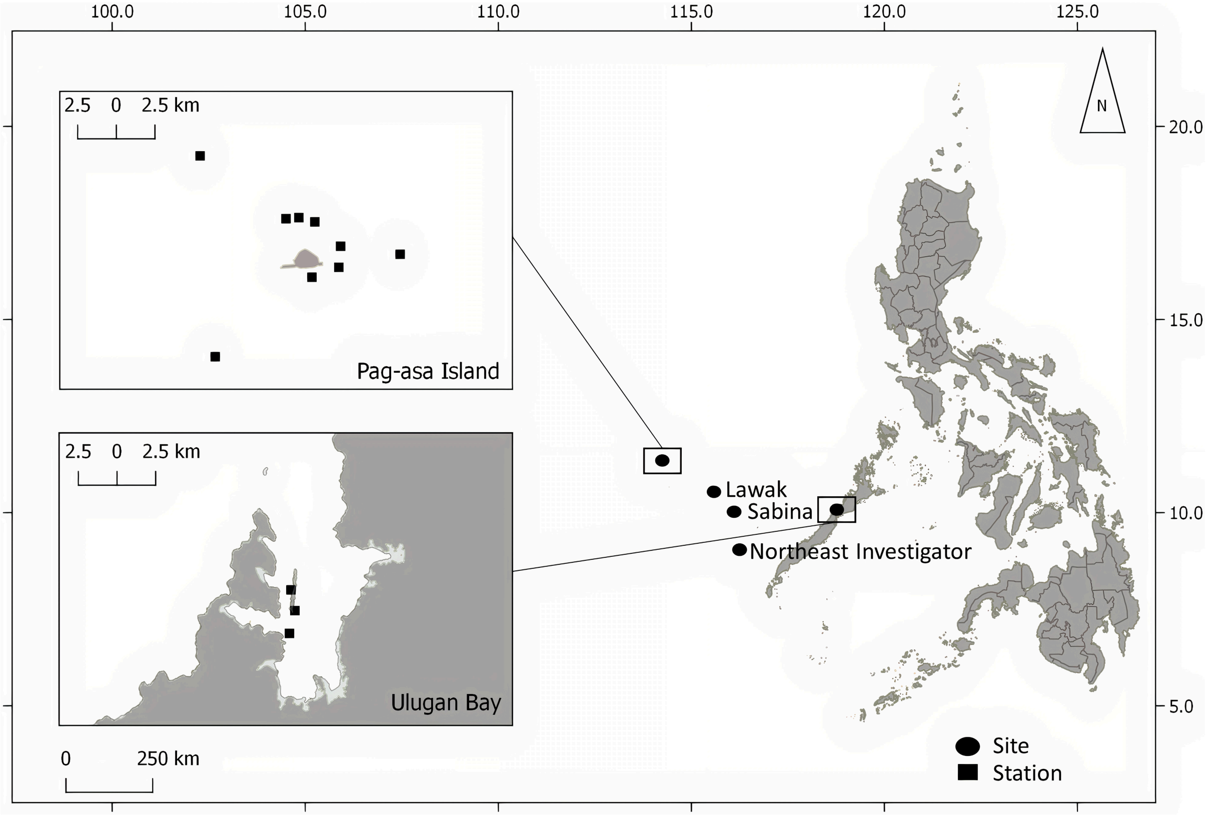

FIGURE 1 | Study sites and stations in the Kalayaan Island Group (Pag-asa, Sabina, Lawak and Northeast Investigator) and Ulugan in the West Philippine Sea surveyed in 2017 and 2019. Insets show stations in Pag-asa and Ulugan.

colony was traced to obtain the total area (cm^2) covered per transect. Percentage octocoral cover of each taxonomic group per transect was then computed.

Each octocoral colony was identified using coral taxonomic amalgamation units (TAUs) since it was not possible to differentiate the colonies to higher taxonomic resolutions. Coral TAUs are used to represent different closely related species that are hard to differentiate (Zvuloni et al., 2010). Given the current general taxonomic uncertainties among octocorals even at the generic level (Lau et al., 2020), the use of TAUs was necessary. The TAUs used in this study were generated based on the initial identification of inventories of octocoral specimens, which were systematically collected in the study stations in 2019. Soft coral TAUs used were mostly families, while gorgonians, which were colonies with obvious presence of axial skeleton, were identified as members of the suborder Holaxonia. Due to the difficulty in identifying these colonies to higher taxonomic resolutions basing on the photoquadrats, a Holaxonia TAU was created to represent colonies with such morphologies.

Data Analyses

A nested analysis was carried out to compare the mean octocoral cover (dependent variable) at different spatial scales (independent variable): among sites (250–500 km), among-stations (1–500 km), and within sites (1–10 km) in 2017 and 2019 (**Figure 1**). Each site was represented by the mean of the values representing the stations within the site, and a station was represented by the mean of the values representing each transect within the station. In 2017, Lawak and Northeast Investigator were not included in the among-sites and within-site analysis due to lack of replicate stations. Thus, the two sites, each represented by one station, were only compared at the among-stations analysis. Assumptions for normality and homogeneity of variance were tested using Shapiro-Wilk's test and Levene's test, respectively. One-way analysis of variance (ANOVA) was then used to compare variations in percent octocoral cover at different spatial scales. For datasets that were not normal or non-homogenous, the non-parametric Kruskal-Wallis test was performed. The Tukey's HSD *post hoc* (parametric) test and the Mann-Whitney pairwise comparisons (non-parametric) were then used to determine which pairs of stations or sites were significantly different. All tests were performed using the Paleontological Statistics v3 software (PAST) (Hammer et al., 2001).

Differences of the octocoral assemblage at different spatial scales were determined through the analysis of similarity (ANOSIM) using the Bray-Curtis similarity index. However, at the among-sites analysis, Lawak and Northeast Investigator were only represented by percentage cover per TAU from one station, unlike the rest of the sites, which were represented by the means of cover per TAU of multiple stations. The lack of station replicates for Lawak and Northeast Investigator prevented us from doing a within-site analysis for the two sites. A pairwise ANOSIM, using Bonferroni-corrected values, was then carried out for spatial scales (i.e., among sites, within site, among stations) with significant overall differences. Prior to the analyses, percentage cover datasets were square root-transformed. The similarity of percentages (SIMPER) analysis was then carried out to determine which taxonomic groups contributed to the differences and similarities in the octocoral assemblage among sites. However, in the SIMPER analysis, Lawak and Northeast Investigator were represented by one station only, unlike the other sites that were represented by multiple stations. To visualize the similarities and differences among stations, a non-metric multidimensional scaling (nMDS) and cluster analysis was done. The ANOSIM, SIMPER analysis, and nMDS were performed using PRIMER-E v6.0 statistical software (Clarke and Gorley, 2006). Short-term temporal changes in the octocoral cover and assemblage in Pag-asa were also determined. The Kruskal-Wallis test was used to determine differences in the mean octocoral cover of four monitoring stations in 2017 and 2019. ANOSIM was then used to determine changes in octocoral assemblage in Pag-asa between years.

RESULTS

A total of 5 sites, 18 stations, 44 transects, and 2,200 photoquadrats were analyzed in this study. Overall, the mean percent octocoral cover in the West Philippine Sea was 5.35% SE ± 0.55 with a total of 10 taxonomic groups observed: Alcyoniidae, Briareidae, Clavulariidae, Coelogorgiidae, Nephtheidae, Helioporiidae, Nidaliidae, Tubiporiidae, Xeniidae, and Holaxonians. To compare values with recent studies that did not pool Helioporiidae cover with other octocorals (e.g., soft corals and gorgonians) (e.g., Licuanan et al., 2019), an overall average value was also computed without helioporiids, which resulted to an overall mean percent cover of 4.74% SE ± 0.18.

Octocoral Cover

Among the sites surveyed in 2017, Sabina had the highest mean octocoral cover (8.43% SE ± 1.61), followed by Northeast Investigator (8.2% SE ± 2.18), Lawak (2.18% SE ± 0.89) and Pag-asa (1.12% SE ± 0.27) (**Figure 2A**). The analysis of variance revealed a significant difference between Pag-asa and Sabina (Kruskal-Wallis, $p < 0.01$). Overall significant difference of mean octocoral cover was also observed at the station level (Kruskal-Wallis, $p = 0.03$) (**Figure 3A**). However, there were no significant within-site differences in Pag-asa (Kruskal-Wallis, $p = 0.07$) and Sabina (Kruskal-Wallis, $p = 0.28$).

In 2019, Sabina still had the highest mean octocoral cover (11.76% SE ± 0.09) among the sites, while Ulugan, which was not surveyed in 2017, had the lowest (0.33% SE ± 0.05) (**Figure 2B**). Analysis of variance revealed significant differences among the three sites (ANOVA, $p < 0.001$). However, no significant difference was observed among the stations (Kruskal-Wallis, $p = 0.05$) and within the stations (Kruskal-Wallis, $p > 0.05$) (**Figure 3B**). Similar to the results in the 2017 surveys, this revealed greater among-site than within-site differences in terms of mean octocoral cover.

Octocoral Assemblage

Overall difference in the octocoral assemblage among the sites was observed in 2017 (ANOSIM: $R = 0.57$, $p = 0.001$) (**Table 1**). The pairwise comparisons between sites showed variations in the octocoral assemblage (ANOSIM: $R > 0.50$) except between Lawak and Pag-asa (ANOSIM: $R = -0.14$). Differences and similarities in the octocoral assemblage among the stations were also evident in the non-metric multidimensional scaling ordination (**Figure 4A**) and cluster analysis dendrogram (**Figure 5A**). Specifically, most stations from the same site grouped together while stations from different sites showed distinct separations in the nMDS and clusters analysis except for Lawak, which clustered together with stations in Pag-asa. The ANOSIM revealed overall significant difference (ANOSIM: $R = 0.84$, $p = 0.001$) among all the stations in terms of octocoral assemblage (**Table 1**). However, the stations within Pag-asa differed (ANOSIM: $R = 0.67$, $p = 0.001$), while stations within Sabina did not (ANOSIM: $R = 0.83$, $p = 0.067$). The similarity of percentages (SIMPER) analysis revealed that different octocoral taxa dominated the different survey sites (**Table 2**). In particular, alcyoniids dominated the octocoral assemblage in Pag-asa (Similarity contribution: 46.51%), Holaxonians in Sabina and Lawak (Similarity contribution: > 50.00%), and clavulariids in Northeast Investigator (Similarity contribution: 60.50%). Meanwhile, the dissimilarity percentages revealed which taxa contributed to the variations observed between sites (**Table 3**). Sabina mainly differed from Pag-asa and Lawak due to its higher holaxonian cover (Dissimilarity contribution: 43.93 and 36.64%, respectively). Northeast Investigator differed from the other sites due to higher presence of clavulariids [Dissimilarity contribution: Pag-asa (48.99%); Sabina (31.34%); Lawak (44.30%)]. Lastly, Lawak differed from Pag-asa due to higher abundance of Holaxonians (Dissimilarity contribution: 45.62%).

Significant overall among-site differences in the octocoral assemblage were also observed in 2019 (ANOSIM: $R = 0.87$, $p = 0.001$) (**Table 1**). Pairwise comparisons showed variations in the octocoral assemblage in all pairings (ANOSIM: $R > 0.80$). Among stations, overall significant differences were also observed (ANOSIM: $R = 0.79$, $p = 0.001$). Comparisons of the stations within each site showed no significant difference (ANOSIM: $p > 0.05$). The nMDS ordination (**Figure 4B**) and cluster analysis dendrogram (**Figure 5B**) also showed distinct clustering and separation of the different stations of the three sites surveyed in 2019. The SIMPER analysis revealed similar dominant octocoral taxa (i.e., holaxonians and alcyoniids) in the stations surveyed in Sabina in 2017 (**Table 2**) and 2019 (**Table 4**). Similar to results in 2017, holaxonians (Similarity contribution: 33.09%), alcyoniids (Similarity contribution: 29.73%), and helioporiids (Similarity contribution: 27.98%) also dominated the assemblage in Pag-asa in 2019. Ulugan, which was only surveyed in 2019, was dominated by holaxonians (Similarity contribution: 43.07%) and alcyoniids (Similarity contribution: 24.81%). Sabina differed

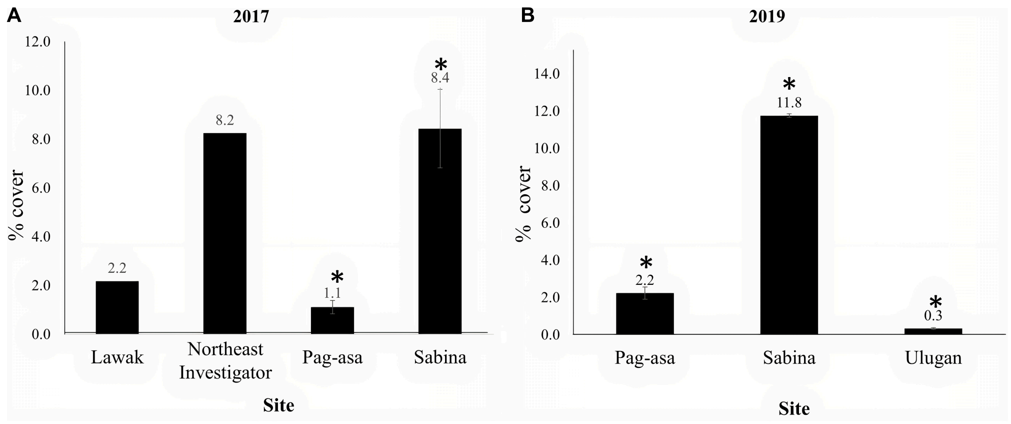

FIGURE 2 | Octocoral cover (mean ± SE) of the sites in the Kalayaan Island Group (Pag-asa, Sabina, Lawak and Northeast Investigator) and Ulugan surveyed in **(A)** 2017 and **(B)** 2019. Asterisks (*) indicate significant difference (p-value < 0.05). Lawak and Northeast Investigator were not included in the among-sites analyses due to lack of replicates.

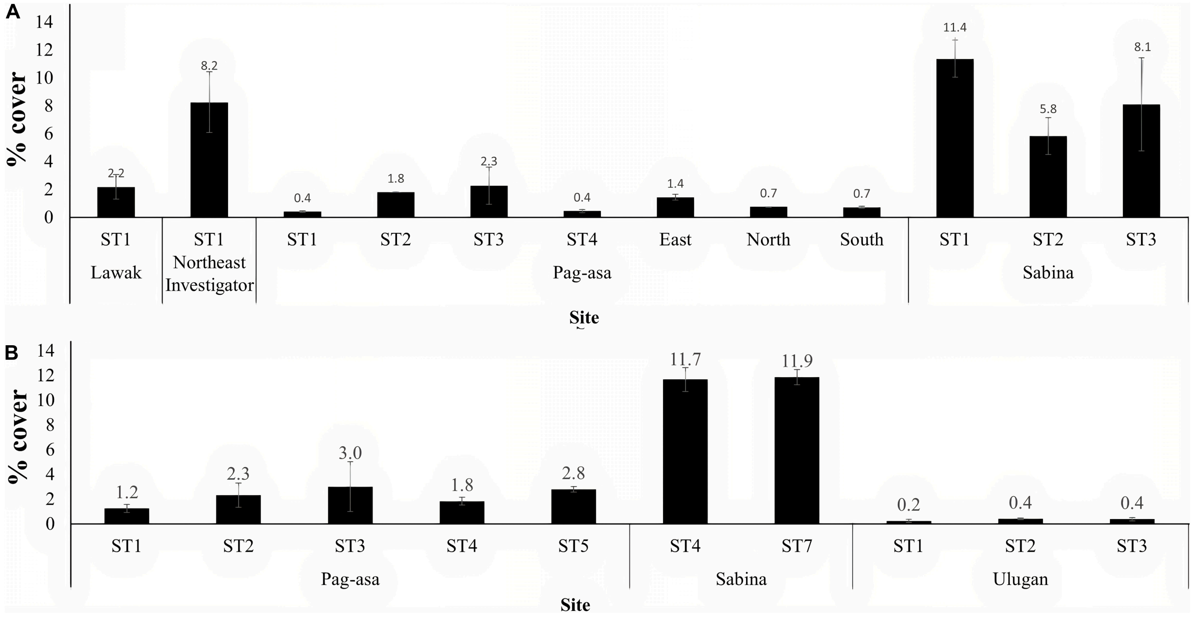

FIGURE 3 | Octocoral cover (mean ± SE) of the stations in the Kalayaan Island Group (Pag-asa, Sabina, Lawak and Northeast Investigator) and Ulugan surveyed in **(A)** 2017 and **(B)** 2019. ST denotes station.

from the other sites due to higher abundance of nephtheids and holaxonians (dissimilarity contribution:>20.00%), whereas Pag-asa differed from Ulugan due to higher abundance of helioporiids (dissimilarity contribution: 26.85%) (**Table 5**).

Temporal Patterns of Octocoral Assemblage in Pag-asa

Mean octocoral cover of all monitoring stations in Pag-asa increased in 2019 (**Figure 6**). This resulted to an increase in the overall mean octocoral cover in Pag-asa from 1.23% SE ± 0.47 in 2017 to 2.09% SE ± 0.37 in 2019, although the difference was not significant (Kruskal-Wallis, $p > 0.05$). The ANOSIM revealed no significant change in the octocoral assemblage in Pag-asa between years (ANOSIM, $R = 0.11$, $p = 0.07$).

DISCUSSION

This study is one of the few studies focused on the octocoral assemblage in reefs in the South China Sea (SCS) and one of the first in the Philippines. The overall mean octocoral cover of the area (5.35% with helioporiids, 4.74% without helioporiids) is slightly higher than the 3.2% overall octocoral cover (excluding helioporiids) of the coastal fringing reefs of northwestern Philippines (Lalas et al., 2021) and the national

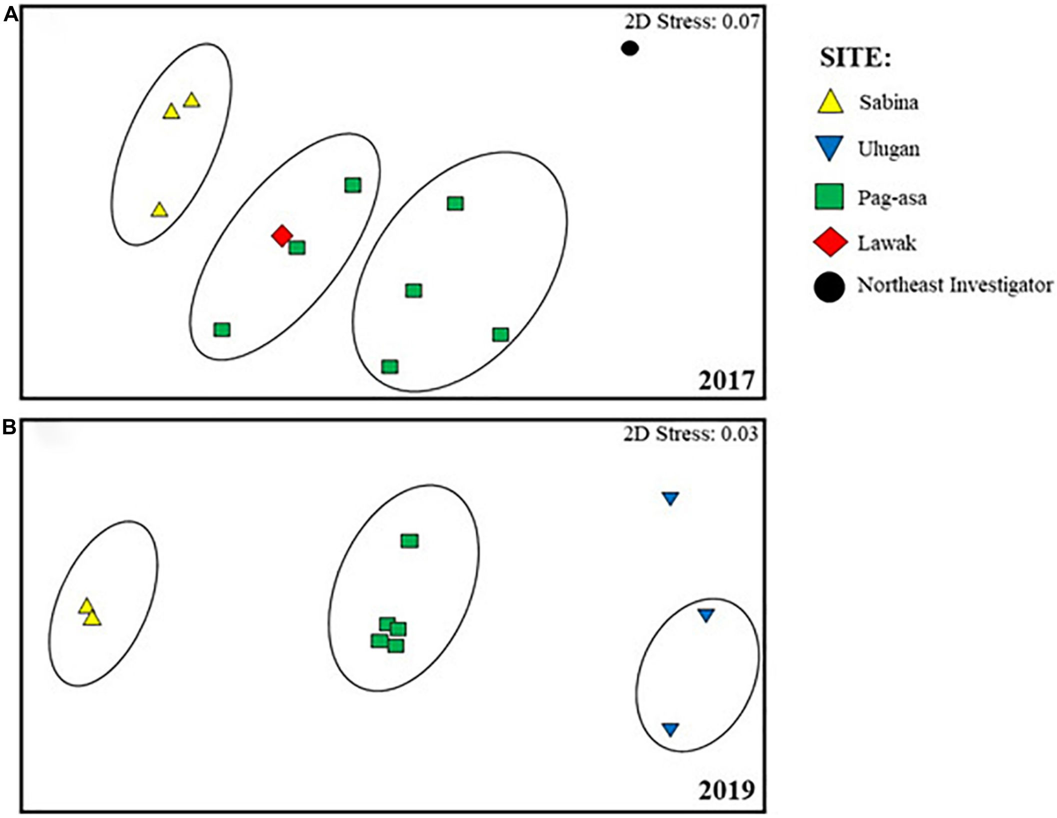

FIGURE 4 | Non-multidimensional scaling ordination based on the Bray-Curtis similarity index, showing differences in the octocoral assemblages in different stations in Kalayaan Island Group (Pag-asa, Sabina, Lawak and Northeast Investigator) and Ulugan, surveyed in **(A)** 2017 and **(B)** 2019. Eclipses indicate stations with more than 40% similarity.

mean soft coral cover (3.2% excluding helioporiids) reported by Licuanan et al. (2019). However, it is generally lower compared with covers recorded from other regions, with some reaching up to 50% soft coral cover (e.g., Red Sea: Benayahu and Loya, 1977, 1981; Great Barrier Reef, Australia: Dinesesn, 1983; Papua New Guinea: Tursch and Tursch, 1982). Most of the studies in other regions that measured octocoral cover using the similar techniques as the present study, however, were conducted decades ago. Revisiting these areas will benefit comparisons at a global scale.

Several factors may influence the living coverage of octocorals in a reef. In this study, reefs located near coastal communities (i.e., Pag-asa, Ulugan) and inside an embayment, which had limited water movement (i.e., Ulugan), tended to have lower octocoral cover compared with offshore reefs that had relatively high wave exposure (i.e., Sabina, Lawak, Northeast Investigator). This might be attributed to poor water quality due to anthropogenic disturbances, which is also consistent with findings of studies in other regions. Remotely sensed data show that among the sites, Ulugan has the higher chlorophyll *a* content and the lowest Secchi depth (**Supplementary Table 1**), both of which are proxies for water quality (Hughes et al., 2017). Low water quality in Ulugan can be explained by its proximity to a river mouth (**Supplementary Table 1**). Yeung et al. (2014) reported that limited water movement and poor water quality due to anthropogenic disturbances contributed to low abundance of octocorals in Hong Kong. This pattern in octocoral cover is similar to earlier studies in other regions (e.g., Dinesesn, 1983; Great Barrier Reef, Australia) where it was reported that increased octocoral cover in offshore more than nearshore reefs was likely due to clearer waters and stronger currents.

The results also highlight the variable spatial patterns in octocoral coverage and assemblage in the SCS. Significant variation observed in the octocoral assemblage among sites but not within sites may indicate higher variation in the environmental conditions at the site scale than at the station scale. This is in contrast with earlier observations in northwestern Philippines wherein variations in octocoral assemblage were observed within sites but not among sites (Lalas et al., 2021). This may indicate variabilities in different factors, both biological (e.g., interactions with other benthic organisms) and environmental (e.g., water quality, exposure monsoons). However, the lack of information on the different prevailing factors in this study limits the inferences on the causality of the observed variations. This warrants the need to include environmental data collection during reef surveys to elucidate octocoral-environment relationships.

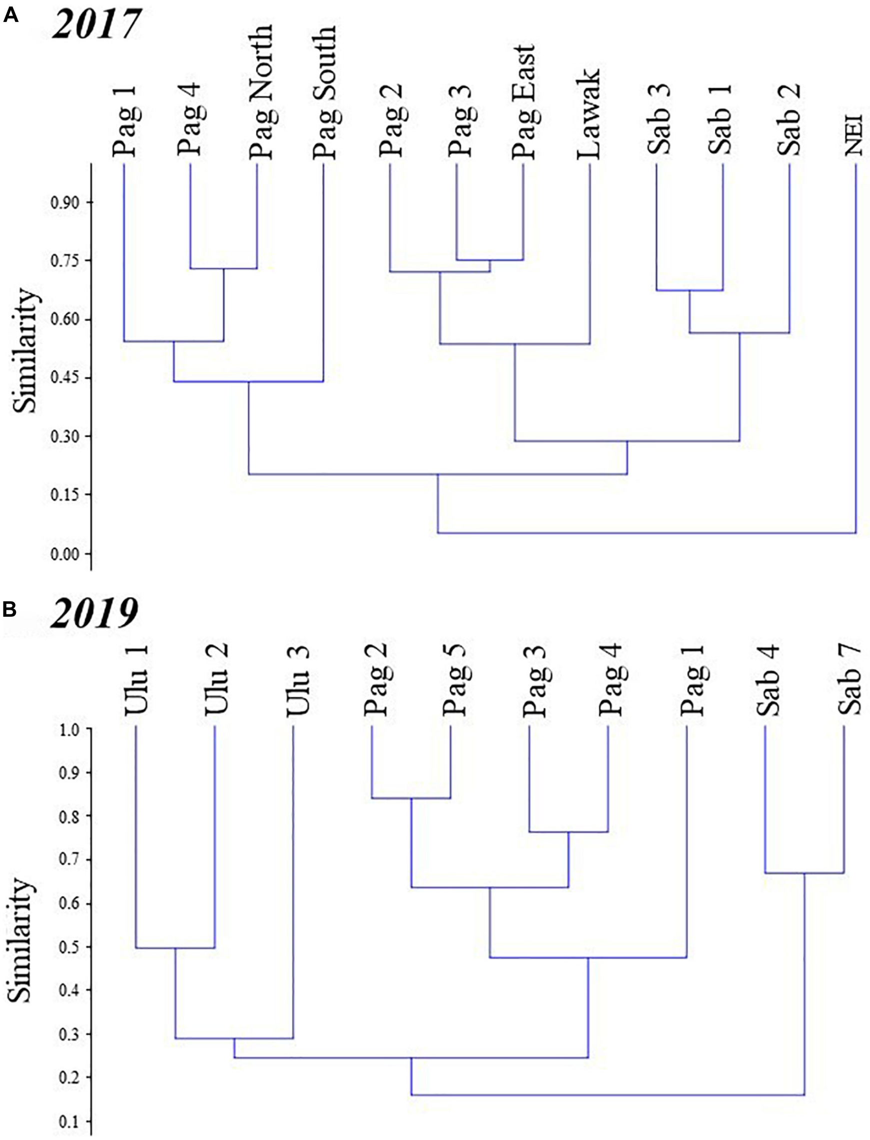

FIGURE 5 | Cluster analysis dendrogram based on the Bray-Curtis similarity index, showing differences in the octocoral assemblages in different stations in the Kalayaan Island Group [Pag-asa (Pag), Sabina (Sab), Lawak, and Northeast Investigator (NEI)] and Ulugan (Ulu), surveyed in **(A)** 2017 and **(B)** 2019.

Overall, octocoral assemblages in the study sites were dominated by holaxonians. Initial identification of collected samples, through analysis of morphological characters, indicate the presence of colonies belonging to the genera *Isis* and *Pinnigorgia* (**Supplementary Material**), which are both zooxanthellate and are usually abundant in flow-exposed areas (Fabricius and Alderslade, 2001). Northeast Investigator was dominated by clavulariids and xeniids. In the study of Lalas et al. (2021), clavulariids were positively correlated with water clarity and wave exposure. The relatively higher dominance of xeniids may also be an indication of a current-exposed and well-lit environment, similar to what was observed in inshore reefs of the central Great Barrier Reef (Dinesesn, 1983). Such inference may explain their abundance in our study sites, which are all exposed and non-inshore, except for Ulugan. Thus, the dominance of these taxa in the area may indicate generally high current conditions, which is a characteristic of offshore reefs.

The octocoral taxonomic composition in the study area is similar to observations in other areas in the SCS and in the Indo-Pacific. For example, all of the taxonomic groups reported here were also observed from Palau (Fabricius et al., 2007; McFadden et al., 2014) to as far as the Red Sea (Benayahu and Loya, 1977). The presence of these taxa was also reported in the Great Barrier Reef, Australia (Dinesesn, 1983). Many taxonomic groups reported in the present study were also reported in other areas such as in Southern Japan (Benayahu, 2002), Taiwan (Benayahu et al., 2004, 2012), and East Africa (Benayahu et al., 2003). Despite the taxonomic identification limitations of this study,

TABLE 1 | Summary result of the ANOSIM comparing octocoral assemblages at different spatial scales (among sites, stations and within site) in the Kalayaan Island Group and Ulugan and short-term temporal variation in Pag-asa in 2017 and 2019.

	Main effect	*R*	*P*
2017	Among sites	0.572	0.001
	Pag-asa × Sabina	0.656	0.001
	Pag-asa × Northeast Investigator	0.932	0.008
	Pag-asa × Lawak	−0.139	0.758
	Sabina × Northeast Investigator	1.000	0.036
	Sabina × Lawak	0.510	0.071
	Northeast Investigator × Lawak	1.000	0.333
	Among all stations	0.842	0.001
	Within Pag-asa	0.670	0.001
	Within Sabina	0.830	0.067
2019	Among sites	0.869	0.001
	Ulugan × Sabina	0.937	0.005
	Ulugan × Pag-asa	0.829	0.001
	Sabina × Pag-asa	0.967	0.001
	Among stations of all sites	0.793	0.001
	Within Pag-asa	−0.063	0.583
	Within Sabina	1.000	0.333
	Within Ulugan	0.722	0.067
Temporal (Pag-asa stations 1–4)	2017 × 2019	0.114	0.077

TABLE 2 | Summary result of the Similarity of Percentages (SIMPER) analysis among the sites in the Kalayaan Island Group in 2017.

Taxonomic group	Average abundance	Average similarity	Contribution (%)
Pag-asa			
Alcyoniidae	0.56	25.40	46.51
Holaxonia	0.52	13.40	‘24.54
Helioporiidae	0.30	10.67	19.54
Sabina			
Holaxonia	2.30	37.35	55.56
Nephtheidae	0.96	11.70	17.40
Alcyoniidae	0.74	9.25	13.76
Coelogorgiidae	0.63	4.20	6.24
Northeast investigator			
Clavulariidae	2.54	46.49	60.50
Xeniidae	1.14	23.64	30.77
Lawak			
Holaxonia	1.22	35.38	52.61
Alcyoniidae	0.58	20.36	30.28
Nephtheidae	0.39	6.46	9.61

TABLE 3 | Dissimilarity percentages among sites from the SIMPER analysis among sites in the Kalayaan Island Group in 2017.

Taxonomic group	Average abundance		Ave. dis.	Ratio	Cont. (%)
	Pag-asa	**Sabina**			
Holaxonia	0.52	2.30	27.22	2.04	43.93
Nephtheidae	0.11	0.96	11.35	1.86	18.31
Coelogorgiidae	0.02	0.63	8.26	1.15	13.33
Alcyoniidae	0.56	0.74	5.39	1.52	8.70
Helioporiidae	0.30	0.32	3.58	1.44	5.78
	Pag-asa	**Northeast Investigator**			
Clavulariidae	0.17	2.54	38.39	3.94	48.99
Xeniidae	0.03	1.14	17.96	7.01	22.92
Holaxonia	0.52	0.00	7.88	1.25	10.05
Alcyoniidae	0.56	0.36	5.25	1.40	6.70
Helioporiidae	0.3	0.09	3.21	1.20	4.10
	Sabina	**Northeast investigator**			
Clavulariidae	0.04	2.54	26.18	4.47	31.34
Holaxonia	2.30	0.00	23.89	3.44	28.59
Xeniidae	0.12	1.14	10.8	4.15	12.92
Nephtheidae	0.96	0.19	7.38	1.58	8.84
Coelogorgiidae	0.63	0.00	6.02	1.09	7.20
	Pag-asa	**Lawak**			
Holaxonia	0.52	1.22	18.83	1.53	45.62
Nephtheidae	0.11	0.39	6.94	1.30	16.82
Alcyoniidae	0.56	0.58	5.12	1.27	12.40
Helioporiidae	0.30	0.18	3.80	1.25	9.20
Clavulariidae	0.17	0.05	3.64	0.89	8.82
	Sabina	**Lawak**			
Holaxonia	2.30	1.22	15.49	1.85	36.64
Nephtheidae	0.96	0.39	8.40	1.86	19.87
Coelogorgiidae	0.63	0.00	7.53	1.10	17.81
Alcyoniidae	0.74	0.58	4.20	1.94	9.94
Helioporidae	0.32	0.18	2.81	1.55	6.65
	Northeast investigator	**Lawak**			
Clavulariidae	2.54	0.05	35.44	6.16	44.30
Holaxonia	0.00	1.22	17.18	3.61	21.48
Xeniidae	1.14	0.06	15.51	30.13	19.39
Alcyoniidae	0.36	0.58	3.78	1.13	4.73
Nephtheidae	0.19	0.39	3.72	1.31	4.65

information gained here may improve our knowledge on the biogeography of octocorals.

The taxonomic richness (at least 10 families) is relatively higher in this study compared with other quantitative studies in other regions (3–5 families) that assessed octocoral assemblages. In Thailand waters, only 4 families were reported by Chanmethakul et al. (2010) despite the larger study area covered. In the southern islands of Singapore, Goh et al. (2009) and Seah et al. (2015) reported genera from a total of 3 families only (i.e., Alcyoniidae, Nephtheidae, and Clavulariidae). In Hong Kong, which is generally characterized by turbid waters, only 5 of the 9 soft coral families observed in the present study were documented (Yeung et al., 2014). All taxonomic groups observed in the present study were also observed in northwestern Philippines (Lalas et al., 2021). This suggests that octocoral diversity may be higher in Philippine waters compared with other areas surrounding the South China Sea. It is also likely that patterns in octocoral diversity in the region is similar to patterns in scleractinian diversity, where species richness tends to be higher in the western Philippines (Huang et al., 2014).

TABLE 4 | Summary result of the Similarity of Percentages (SIMPER) analysis among sites in the Kalayaan Island Group and Ulugan in 2019.

Taxonomic group	Average abundance	Average similarity	Contribution (%)
Ulugan			
Holaxonia	0.36	22.75	43.07
Alcyoniidae	0.26	13.10	24.81
Nephtheidae	0.10	5.54	10.49
Xeniidae	0.11	5.47	10.35
Clavulariidae	0.10	5.07	9.60
Sabina			
Holaxonia	2.06	25.41	30.48
Nephtheidae	1.80	24.28	29.12
Alcyoniidae	1.59	16.50	19.79
Xeniidae	0.94	12.18	14.61
Pag-asa			
Holaxonia	0.79	22.01	33.09
Alcyoniidae	0.72	19.78	29.73
Helioporiidae	0.62	18.62	27.98

TABLE 5 | Dissimilarity percentages among sites from the SIMPER analysis among sites in the Kalayaan Island Group and Ulugan in 2019.

Taxonomic group	Average abundance		Average dissimilarity	Ratio	Contribution (%)
	Ulugan	**Sabina**			
Nephtheidae	0.10	1.80	21.54	7.32	28.01
Holaxonia	0.36	2.06	21.39	3.67	27.82
Alcyoniidae	0.26	1.59	16.71	1.97	21.73
Xeniidae	0.11	0.94	10.34	5.54	13.44
	Ulugan	**Pag-asa**			
Helioporiidae	0.04	0.62	15.94	2.24	26.85
Alcyoniidae	0.26	0.72	12.84	1.79	21.63
Holaxonia	0.36	0.79	11.44	1.73	19.27
Clavulariidae	0.10	0.44	10.06	1.04	16.95
Nephtheidae	0.10	0.11	3.11	1.22	5.24
Xeniidae	0.11	0.04	2.68	1.15	4.52
	Sabina	**Pag-asa**			
Nephtheidae	1.80	0.11	17.6	5.77	30.52
Holaxonia	2.06	0.79	13.44	2.31	23.30
Alcyoniidae	1.59	0.72	9.54	1.35	16.54
Xeniidae	0.94	0.04	9.28	5.53	16.10
Clavulariidae	0.08	0.44	4.15	0.91	7.19

In an earlier study in adjacent reefs in the Spratly Islands, Dai and Fan (1996) reported only three families of soft corals that were limited to depths below 15 m. Dai and Fan (1996) also reported four gorgonian families. However, gorgonians in the present study were pooled into one taxonomic unit, thus, preventing comparisons of gorgonian taxonomic richness to other studies. It should be noted that the present study is not directly comparable with studies that generated taxonomic inventories of octocoral species (e.g., Benayahu et al., 2012; McFadden et al., 2014). Thus, identifying octocoral species at the highest possible taxonomic identification (i.e., genus, species) merits attention and is expected to provide better understanding of the diversity and assemblage of octocorals in the Philippines and in the Indo-Pacific.

In the context of the Coral Triangle, information on octocorals is still very poor (Pérez et al., 2016). Studies on octocorals in Indonesia (e.g., Janes, 2013; McFadden et al., 2014; Rowley, 2018), Malaysia (e.g., Mohammad et al., 2016), and Papua New Guinea (e.g., Tursch and Tursch, 1982; Mana, 2011) focused on establishing taxonomic inventories and information on the contribution of different taxa to benthic assemblages is lacking. In general, the lack of data on the abundance of different octocoral taxa in coral reef studies is common among nations in the Coral Triangle (e.g., Asian Development Bank, 2014). Janes (2013) highlighted that the Philippines has the highest diversity of xeniids, which may indicate high octocoral diversity. The lack of a finer taxonomic resolution used in this study limits comparisons in terms of diversity. However, taxonomic richness observed in this study and a study by Lalas et al. (2021) in the northwestern Philippines (using similar methodologies and taxonomic resolutions) was higher compared to other areas in the Coral Triangle (e.g., Verseveldt and Tursch, 1979; Tursch and Tursch, 1982). This may indicate high octocoral diversity in the Philippines. However, the very limited number of areas studied and different methods employed make it difficult to identify spatial patterns in diversity within the Coral Triangle. This highlights the need to incorporate taxonomic inventories with abundance surveys to improve our understanding on coral reef communities in the Coral Triangle.

Increasing trend in the mean octocoral cover was observed in Pag-asa from 2017 to 2019, suggesting possible shifts in the coral community structure due to changing environmental conditions (Nörstrom et al., 2009). In the Caribbean, increase in gorgonian abundance in the last decade has been associated with increasing sea surface temperature (Edmunds and Lasker, 2019). In Indonesia, rapid dominance of soft corals has been associated with degradation caused by destructive fishing practices (Fox et al., 2003). Hence, an alternative state is hypothesized wherein octocorals dominate coral reefs after a disturbance (Nörstrom et al., 2009), although this may not always be the case. For example, soft corals did not dominate a reef in the Great Barrier Reef, which had available substrate space following a crown-of-thorns starfish outbreak (Fabricius, 1995). Such case is possible as responses of octocorals to disturbances may be taxon- or site- specific. In areas where octocorals dominated after a disturbance, octocoral assemblage would usually be composed of fast-growing species (e.g., xeniids, nephtheids) (Fox et al., 2003). This highlights the need for long-term monitoring to observe how octocorals can affect community structure of reefs in the future.

The Spratly Islands harbor ecologically and economically important reef systems to countries bordering the South China Sea (SCS) (McManus and Meñez, 1997; Ablan et al., 2002). Through simulated particle dispersal models, the islands have been inferred to be important sources of larvae that can replenish populations of different coral reef organisms in the SCS and in the Coral Triangle Region (Kool et al., 2011). However, the reefs of the SCS are generally threatened by habitat degradation caused

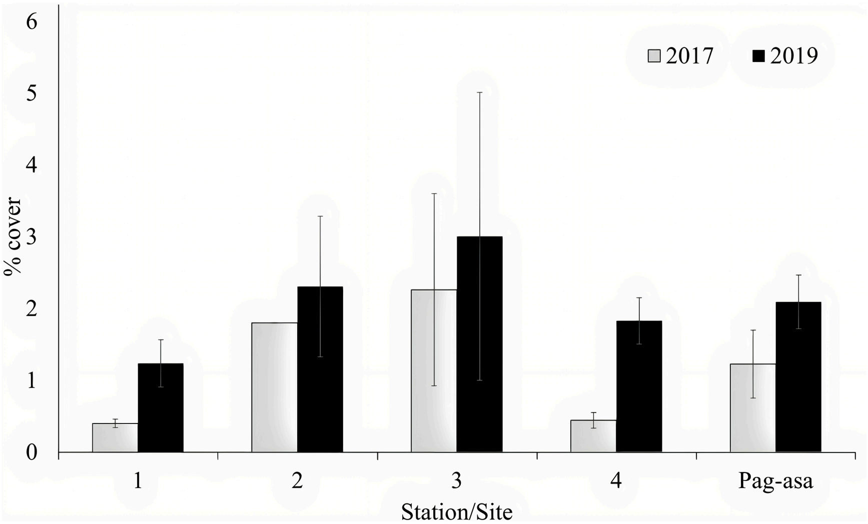

FIGURE 6 | Octocoral cover (mean ± SE) of the sampling stations in Pag-asa (n = 4) monitored in 2017 and 2019. The last two bars represent means of the means (mean ± SE) of the four monitoring stations in different years.

by anthropogenic factors (Rosenberg, 1999; Vo et al., 2013) such as military activities (Song, 2008; Asner et al., 2017), reclamation (Larson, 2015; Mora et al., 2016), unsustainable fishing practices (McManus, 1994), and oil and gas exploration (Song, 2008).

Natural perturbations (e.g., monsoons, typhoons; Quibilan and Aliño, 2006) and climate change-driven disturbances such as coral bleaching (Li et al., 2011; Tkachenko et al., 2020) may also have an influence on the structuring of coral reef communities. Although monitoring of environmental parameters was not done, remotely sensed data show that Sabina has the highest exposure to positive thermal anomaly events that causes bleaching and mass morality (**Supplementary Table 1**). In the Carribean, increased SST and the occurrence of bleaching events have been attributed to cause the decline of hard corals while gorgonian abundance increased (Edmunds and Lasker, 2019). Arceo et al. (2001) conducted one of the earliest comprehensive records of mass coral bleaching events in the Philippines and found that there were no significant changes in the soft coral cover in the Spratly Islands post bleaching. Although, it was emphasized that their report was not designed to detect small changes in the soft coral assemblages. Besides the 1998 bleaching event, coral reefs in the Philippines experienced sustained heat stress that led to mass bleaching in 2010, and 2016–2017 (Tun et al., 2010; Hughes et al., 2018; Licuanan et al., 2019). Unfortunately, due to geopolitical tensions and logistical constraints, studying the coral reef dynamics in the Spratly Islands has remained a challenge. This has resulted to patchy and sparse information on the area that limits our understanding on the changes or shifts of the octocoral assemblage brought about by climate change.

The ecological roles of octocorals remain greatly understudied. In areas where scleractinian corals do not dominate, such as in deep reefs, gorgonians may contribute to structural complexity providing potential habitats for other marine organisms (Slattery and Gochfeld, 2016). Conversely, increase in soft coral cover has been associated with degraded reefs (see Epstein and Kingsford, 2019). Soft corals are also considered non-reef builders, but some species, mostly from the genus *Sinularia,* are known to contribute to reef development through deposition of their sclerites (Jeng et al., 2011). Increased octocoral dominance has also been linked with by the decrease in diversity or biomass of associated organisms such as fishes and arthropods, but more recent studies report otherwise. For example, Syms and Jones (2001) reported lower coral reef fish biomass among soft coral-dominated areas compared to hard coral-dominated areas, but Epstein and Kingsford (2019) reported similar fish assemblages between hard coral- and soft coral-dominated reefs and an increase in fish species richness with increasing soft coral cover. Epstein and Kingsford (2019) suggested that the importance of soft corals as a habitat may have been underestimated. The contrasting results of different studies in different areas highlight the need to conduct more investigations related to the ecological roles of alternative state organisms.

This study has demonstrated the spatial patterns in the octocoral assemblage of an ecologically and economically important area in the South China Sea. Although factors that contributed to the variations were not identified, results of this study serve as baseline information on the contribution of octocorals in coral reefs. With the generally lacking information on octocoral assemblages in different marine regions, we recommend the inclusion of octocoral variables in the long-term monitoring of coral reef community structures, complemented with measurements of important environmental variables. This can further improve our knowledge on the mechanisms that affect coral reef community structure in the area, which will provide effective frameworks for the management of these ecologically and economically important habitats.

DATA AVAILABILITY STATEMENT

Data inquiries can be directed to the corresponding author.

ETHICS STATEMENT

The research expeditions in the West Philippine Sea were conducted with the approval of various national government departments and agencies in the Philippines thru Gratuitous Permits #2017-09 and #2019-09 issued by the Palawan Council for Sustainable Development.

AUTHOR CONTRIBUTIONS

MVBR and HOA secured the funding, designed the study, and provided supervision. JAAL, RTSL, JPC, CSS, RMAL, and DAMV conducted the fieldworks and analyzed the photoquadrats. JAAL, DAMV, and MRJ performed the data analysis. All authors contributed to the writing of this article.

FUNDING

This study was funded by the Biodiversity Management Bureau of the Department of Environment and Natural Resources (DENR-BMB) of the Philippines through the (1) Coastal Assessment for Rehabilitation Enhancement: Capability Development and Resiliency of Ecosystems (CARE-CaDRES) project and the (2) Predicting Responses between Ocean Transport and Ecological Connectivity of Threatened Ecosystems in the West Philippines Sea (PROTECT WPS) project, which were implemented by the Marine Science Institute of the University of the Philippines (UP MSI).

ACKNOWLEDGMENTS

We would like to thank the Department of Agriculture-Bureau of Fisheries and Aquatic Resources (DA-BFAR), Philippine Coast Guard (PCG), the Municipality of Kalayaan, and the Philippine Navy for their assistance and support during the research expeditions in the West Philippine Sea. We also thank Lovely Joy Heyres for assisting in the field collection and image analysis, and Kevin Yatco and Socorro Rodrigo for assisting in the satellite product processing. We also thank the valuable insights and suggestions given by the editor and reviewers of this journal that helped improve this manuscript.

SUPPLEMENTARY MATERIAL

The Supplementary Material for this article can be found online at: https://www.frontiersin.org/articles/10.3389/fmars.2021.782977/full#supplementary-material

REFERENCES

Ablan, M. C. A., McManus, J. W., Chen, C. A., Shao, K. T., Bell, J., Cabanban, A. S., et al. (2002). Meso-scale transboundary units for the management of coral reefs in the South China Sea. *Naga World Fish Center Q.* 25, 3–4.

Aharonovich, D., and Benayahu, B. (2012). Microstructures of octocoral sclerites for diagnosis. *Mar. Biodivers.* 42, 173–177. doi: 10.1038/s41598-018-37696-z

Aliño, P. M., and Gomez, E. D. (1994). "Philippine coral reef conservation: its significance to the South China Sea," in *Proceedings of Regional Conference of the Development and Conservation in the Asia-Pacific Region*, eds K. Yamamoto, S. Ishijima, S. Sakihara, H. Taira, Z. Shimabukuro, F. Teruya, et al. (Honolulu, HI: East West Center Association), 222–229.

Aliño, P. M., Nañola, C. L. Jr., Ochavillo, D. G., and Rañola, M. C. (1998). "The fisheries potential of the Kalayaan Island group, South China Sea," in *Proceedings of the International Conference on the Marine Biology of the South China Sea; 1996 Oct 28 – Nov 1*, (Hong Kong: Hong Kong University Press), 219–226.

Arceo, H. O., Cabasan, J. P., Luciano, R. M. A., Heyres, L. J. D., Mamauag, S. S., and Aliño, P. M. (2020). Estimating the potential fisheries production of three offshore reefs in the West Philippine Sea, Philippines. *Philipp. J. Sci.* 149, 647–658.

Arceo, H. O., Quibilan, M. C., Aliño, P. M., Lim, G., and Licuanan, W. Y. (2001). Coral bleaching in Philippine reefs: coincident evidences with mesoscale thermal anomalies. *Bull. Mar. Sci.* 69, 579–593.

Asian Development Bank (2014). *State of the Coral Triangle: Philippines*. Mandaluyong: Asian Development Bank.

Asner, G. P., Martin, R. E., and Mascaro, J. (2017). C66oral reef atoll assessment in the South China Sea using Planet Dove satellites. *Remote Sens. Ecol. Conserv.* 3, 57–65.

Atrigenio, M. P., Conaco, C., Guzman, C., Yap, H. T., and Aliño, P. M. (2020). Distribution and abundance of *Heliopora coerulea* (Cnidaria: Coenothecalia) and notes on its aggressive behavior against scleractinian corals: temperature mediated? *Reg. Stud. Mar. Sci.* 40:101502. doi: 10.1016/j.rsma.2020.101502

Benayahu, Y. (2002). Soft Corals (Octocorallia:Alcyonacea) of southern Ryuku Archipelago: the families Tubiporiidae, Clavulariidae, Alctoniidae, and Briareidae. Galaxae. *JCRS* 4, 11–32.

Benayahu, Y., and Loya, Y. (1977). Space partitioning by stony corals, soft corals, and benthic algae in the coral reefs of the northern Gulf of Eilat (Red Sea). Helgol˜inder wiss. *Meeresunters* 30, 362–382.

Benayahu, Y., and Loya, Y. (1981). Competition for space among coral-reef sessile organisms at Eilat, Red Sea. *Bull. Mar. Sci.* 31, 514–522.

Benayahu, Y., Bridge, T. C., Colin, P. L., Liberman, R., McFadden, C. S., Pizarro, O., et al. (2019). "Octocorals of the Indo-Pacific," in *Mesophotic Coral Ecosystems*, eds Y. Loya, K. Puglise, and T. Bridge (Cham: Springer), 709–728. doi: 10.11646/zootaxa.3617.1.1

Benayahu, Y., Jeng, M. S., Perkol-Finkel, S., and Dai, C. F. (2004). Soft coral (Octocorallia: Alcyonacea) from southern Taiwan. II. Species diversity and distributional patterns. *Zool. Stud.* 45, 548–560.

Benayahu, Y., Shlagman, A., and Schleyer, M. H. (2003). Corals of the south-west Indian Ocean: VI. The Alcyonacea (Octocorallia) of Mozambique, with a discussion on soft coral distribution on south equatorial east African reefs. *Zool. Verh. Leiden* 345, 49–57.

Benayahu, Y., van Ofwegen, L. P., Dai, C., Jeng, M., Soong, K., Shlagman, A., et al. (2012). Diversity, distribution, and molecular systematics of octocorals (Coelenterata: Anthozao) of the Penghu Archipelago, Taiwan. *Zool. Stud.* 51, 1529–1548.

Carpenter, K. E., and Springer, V. G. (2005). The center of the center of marine shore fish biodiversity: the Philippine Islands. *Environ. Biol. Fishes* 72, 467–480. doi: 10.1007/s10641-004-3154-4

Carvalho, S., Cúrdia, J., Pereira, F., Guerra-García, J. M., Santos, M. N., and Cunha, M. R. (2014). Biodiversity patterns of epifaunal assemblages associated with gorgonians *Eunicella gazella* and *Leptogorgia lusitanica* in response to host, space and time. *J. Sea Res.* 85, 37–47. doi: 10.1016/j.seares.2013.10.001

Chanmethakul, T., Chansang, H., and Watanasit, S. (2010). Soft coral (Cnidaria: Alcyonacea) distribution patterns in Thai waters. *Zool. Stud.* 49, 72–84.

Clarke, K. R., and Gorley, R. N. (2006). *PRIMER v6: User Manual/Tutorial (Plymouth Routines in Multivariate Ecological Research)*. Plymouth: PRIMER-E.

Conci, N., Vargas, S., and Wörheide, G. (2021). The biology and evolution of calcite and aragonite mineralization in *Octocorallia*. *Front. Ecol. Evol.* 9:623774. doi: 10.3389/fevo.2021.623774

Cúrdia, J., Carvalho, S., Fabio, P., Guerra-Garcia, J. M., Santos, M. N., and Cunha, M. R. (2015). Diversity and abundance of invertebrate epifaunal assemblages with gorgonians are driven by colony attributes. *Coral Reefs* 34, 611–624. doi: 10.1007/s00338-015-1283-1

Dai, C., and Fan, T. (1996). Coral fauna of Taiping island (Itu Aba island) in the Spratly's of the South China Sea. *Atoll Res. Bull.* 436, 1–21. doi: 10.1163/9789004323445_002

De'ath, G., and Fabricius, K. (2010). Water quality as a regional driver of coral biodiversity and macroalgae on the Great Barrier Reef. *Ecol. Appl.* 20, 840–850. doi: 10.1890/08-2023.1

Dias, I. M., Cúrdia, J., Cunha, M. R., Santos, M. N., and Carvalho, S. (2015). Temporal variability in epifaunal assemblages associated with gorgonian gardens. *Mar. Environ. Res.* 112, 140–151. doi: 10.1016/j.marenvres.2015.10.006

Dinesesn, Z. D. (1983). Patterns in the distribution of soft corals across the central Great Barrier Reef. *Coral Reefs* 1, 229–236. doi: 10.1007/bf00304420

Edmunds, P. J., and Lasker, H. R. (2019). Regulation of population size of arborescent octocorals on shallow Caribbean reefs. *Mar. Ecol. Prog. Ser.* 615, 1–14. doi: 10.3354/meps12907

Edmunds, P. J., Tsounis, G., and Lasker, H. R. (2016). Differential distribution of octocorals and scleractinians around St. John and St. Thomas, US Virgin Islands. *Hydrobiologia* 767, 347–360. doi: 10.1007/s10750-015-2555-z

Epstein, H. E., and Kingsford, M. J. (2019). Are soft coral habitats unfavourable? A closer look at the association between reef fishes and their habitat. *Environ. Biol. Fishes* 102, 479–497. doi: 10.1007/s10641-019-0845-4

Etnoyer, P. J., Wickes, L. N., Silva, M., Dubick, J. D., Balthis, L., Salgado, E., et al. (2016). Decline in condition of gorgonian octocorals on mesophotic reefs in the northern Gulf of Mexico: before and after the Deepwater Horizon oil spill. *Coral Reefs* 35, 77–90. doi: 10.1007/s00338-015-1363-2

Fabricius, K. E. (1995). Slow population turnover in the soft coral genera *Sinularia* and *Sarcophyton* on mid- and outer-shelf reefs of the Great Barrier Reef. *Mar. Ecol. Prog. Ser.* 126, 145–152. doi: 10.3354/meps126145

Fabricius, K. E., Alderslade, P., Williams, G. C., Colin, P. L., and Golbuu, Y. (2007). Octocorallia in Palau, Micronesia: effects of biogeography and coastal influences on local and regional biodiversity. *Palau Int. Coral Reef Centre* 7, 79–92.

Fabricius, K., and Alderslade, P. (2001). *Soft Corals and Sea Fans: A Comprehensive Guide to the Tropical Shallow Water Genera of the Central-West Pacific, the Indian Ocean and the Red Sea*. Townsville, QLD: Australian Institute of Marine Science.

Fox, H. E., Pet, J. S., Dahuri, R., and Caldwell, R. L. (2003). Recovery in rubble fields: long-term impacts of blast fishing. *Mar. Pollut. Bull.* 46, 1024–1031. doi: 10.1016/S0025-326X(03)00246-7

Garra, S., Hall, A., and Kingsford, M. J. (2020). The effects of predation on the condition of soft corals. *Coral Reefs* 39, 1329–1343. doi: 10.1007/s00338-020-01967-x

Goh, B. P. L., Tan, G. E., and Tan, L. T. (2009). Diversity, distribution and biological activity of soft corals (Octocorallia, Alcyonacea) in Singapore. *J. Coast. Dev.* 12, 89–98.

Hammer, O., Harper, D. A. T., and Ryan, P. D. (2001). PAST: paleontological statistics software package for education and data analysis. *Palaeontol. Electron.* 4:9.

Huang, D., Licuanan, W. Y., Hoeksema, B. W., Chen, C. A., Ang, P. O., Huang, H., et al. (2014). Extraordinary diversity of reef corals in the South China Sea. *Mar. Biodivers.* 45, 157–168. doi: 10.1038/s41597-020-00793-8

Hughes, T. P., Andesron, K. D., Connolly, S. R., Heron, S. F., Kerry, J. T., Lough, J. M., et al. (2018). Spatial and temporal patterns of mass coral bleaching of corals in the Anthropocene. *Science* 359, 80–83. doi: 10.1126/science.aan8048

Hughes, T. P., Kerry, J. T., and Alvarex-Noriega, M. (2017). Global warming and recurrent mass bleaching of corals. *Nature* 543, 373–385. doi: 10.1038/nature21707

Janes, M. P. (2013). Distribution and diversity of the soft coral family Xeniidae (Coelenterata: Octocorallia) in Lembeh Strait, Indonesia. *Galaxea J. Coral Reef Stud.* 15, 195–200. doi: 10.3755/galaxea.15.195

Jeng, M. S., Huang, H. D., Dai, C. F., Hsiao, Y. C., and Benayahu, Y. (2011). Sclerite calcification and reef-building in the fleshy octocoral genus Sinularia (Octocorallia: Alcyonacea). *Coral Reefs* 30, 925–933. doi: 10.1007/s00338-011-0765-z

Jones, C. G., Lawton, J. H., and Shachak, M. (1994). "Organisms as ecosystem engineers," in *Ecosystem Management* (New York, NY: Springer). doi: 10.1007/978-1-4612-4018-1_14

Kohler, K. E., and Gill, S. M. (2006). Coral point count with excel extensions (CPCe): a visual basic program for the determination of coral and substrate coverage using random point count methodology. *Comput. Geosci.* 32, 1259–1269. doi: 10.1016/j.cageo.2005.11.009

Kool, J. T., Paris, C. B., Barber, P. H., and Cowen, R. K. (2011). Connectivity and the development of population genetic structure in Indo-West Pacific coral reef communities. *Glob. Ecol. Biogeogr.* 20, 695–706. doi: 10.1111/j.1466-8238.2010.00637.x

Lalas, J. A. A., Benayahu, Y., and Baria-Rodriguez, M. V. (2021). Community structure and size-frequency distribution of soft corals in a heavily disturbed reef system in northwestern Philippines. *Mar. Pollut. Bull.* 162:111871. doi: 10.1016/j.marpolbul.2020.111871

Larson, C. (2015). China's island building is destroying reefs. *Science* 349:1434. doi: 10.1126/science.349.6255.1434

Lasker, H. R., Martinez-Quintana, A., and Edmunds, P. J. (2020). Resilience of octocoral forests to catastrophic storms. *Sci. Rep.* 10:4286. doi: 10.1038/s41598-020-61238-1

Lau, W. Y., Poliseno, A., Kushida, Y., Quere, G., and Reimer, J. D. (2020). The classification, diversity and ecology of shallow water octocorals. *Encycl. World's Biomes* 4, 597–611. doi: 10.1016/B978-0-12-409548-9.12109-8

Li, S., Yu, K., Chen, T., Shi, Q., and Zhang, H. (2011). Assessment of coral bleaching using symbiotic zooxanthellae density and satellite remote sensing data in the Nansha Islands, South China Sea. *Chin. Sci. Bull.* 56, 1031–1037. doi: 10.1007/s11434-011-4390-6

Licuanan, W. Y., Robles, R., and Reyes, M. (2019). Status and recent trends in coral reefs of the Philippines. *Mar. Pollut. Bull.* 142, 544–550. doi: 10.1016/j.marpolbul.2019.04.013

Mana, R. R. (2011). *BIOPAPUA Cruise: Highlighting the Deep-Sea Benthic Biodiversity of Papua New Guinea. A Report Submitted to School of Natural and Physical Sciences*. Port Moresby, PG: University of Papua New Guinea.

McFadden, C. S., Brown, A. S., Brayron, C., Hunt, C. B., and van Ofwagen, L. P. (2014). Application of DNA barcoding in biodiversity studies of shallow-water octocorals: molecular proxies agree with morphological estimates of species richness in Palau. *Coral Reefs* 33, 275–286. doi: 10.1007/s00338-013-1123-0

McManus, J. (1994). The Spratly islands: a marine park? *Ambio J. Hum. Environ.* 23, 181–186.

McManus, J. W., and Meñez, L. A. B. (1997). "The proposed international Spratly island marine park: ecological considerations," in *Proceedings of the 8th Coral Reef Symposium*, Vol. 2, (Panama: Smithsonian Tropical Research Institute), 1943–1948.

Mohammad, M., Apandi, Z. N., Marican, H. A. W., Kamphol, N., Mubin, N. A. A. A., Salleh, S., et al. (2016). The identification of octocorals from the northern regions of Straits of Malacca. *Trop. Life Sci. Res.* 27, 87–93. doi: 10.21315/tlsr2016.27.3.12

Mora, C., Caldwell, I. R., Birkeland, C., and McManus, J. W. (2016). Dredging in the Spratly Islands: gaining land but losing reefs. *PLoS Biol.* 14:e1002422. doi: 10.1371/journal.pbio.1002422

Nörstrom, A. V., Nyström, M., Lokrantz, J., and Folke, C. (2009). Alternative states on coral reefs: beyond coral-macroalgal phase shifts. *Mar. Ecol. Prog. Ser.* 376, 295–306. doi: 10.3354/meps07815

Pata, P. R., and Yñiguez, A. T. (2019). Larval connectivity patterns of the North Indo-West Pacific coral reefs. *PLoS One* 14:e0219913. doi: 10.1371/journal.pone.0219913

Pérez, C. D., de Moura Neves, B., Cordeiro, R. T., Williams, G. C., and Cairns, S. D. (2016). "Diversity and distribution of Octocorallia," in *The Cnidaria,* *Past, Present and Future*, eds S. Goffredo and Z. Dubinsky (Cham: Springer). doi: 10.1007/978-3-319-31305-4_8

Quibilan, M. C., and Aliño, P. M. (2006). "Coral community structure of western Philippine reefs I: spatial patterns," in *Proceedings of 10^{th} International Coral Reef Symposium*, (Okinawa), 341–350. doi: 10.1007/s10661-014-4089-7

Quimpo, T. J. R., Cabaitan, P. C., Go, K. T. B., Dumalagan, E. E. Jr., Villanoy, C. L., and Siringan, F. P. (2019). Similarity in benthic habitat and fish assemblages in the upper mesophotic and shallow water reefs in the West Philippine Sea. *J. Mar. Biol. Assoc. U. K.* 99, 1507–1517. doi: 10.1017/S0025315419000456

Rosenberg, D. (1999). Environmental pollution around the South China Sea: developing a regional response. *Contemp. Southeast Asia* 21, 119–145. doi: 10.1016/j.ecoenv.2019.01.116

Rowley, S. J. (2018). Environmental gradients structure gorgonian assemblages on coral reefs in SE Sulawesi, Indonesia. *Coral Reefs* 37, 609–630. doi: 10.1007/s00338-018-1685-y

Sanciangco, J. C., Carpenter, K. E., Etnoyer, P. J., and Moretzsohn, F. (2013). Habitat availability and heterogeneity and the Indo-Pacific warm pool as predictors of marine species richness in the tropical Indo-Pacific. *PLoS One* 8:e56245. doi: 10.1371/journal.pone.0056245

Seah, J. Z. S., Yap, N. W. L., Tan, L. T., and Goh, B. P. L. (2015). Distribution and abundance of octocoral (Octocorallia, Alcyonacea) communities at three southern islands of Singapore. *Ocean Sci. J.* 50, 299–306. doi: 10.1007/s12601-015-0027-z

Sella, I., and Benayahu, Y. (2010). Rearing cuttings of the soft coral *Sarcophyton glaucum* (Octocorallia, Alcyonacea): towards mass production in a closed seawater system. *Aquac. Res.* 41, 1748–1758. doi: 10.1111/j.1365-2109.2009.02475.x

Shoham, E., and Benayahu, Y. (2016). Higher species richness of octocorals in the upper mesophotic zone in Eilat (Gulf of Aqaba) compared to shallower reef zones. *Coral Reefs* 36, 71–81. doi: 10.1007/s00338-016-1528-7

Shoham, E., Prohaska, T., Barkay, Z., Zitek, A., and Benayahu, Y. (2019). Soft corals form aragonite-precipitated columnar spiculite in mesophotic reefs. *Sci. Rep.* 9:1241. doi: 10.1038/s41598-018-37696-z

Slattery, M., and Gochfeld, D. J. (2016). Butterflyfishes exhibit species-specific responses to changes in Pacific coral benthic communities. *Mar. Biol.* 163:246. doi: 10.1007/s00227-016-3025-5

Song, Y. (2008). The potential threat from oil and gas development activities in the disputed South China Sea/ Spratly Area: a role that Taiwan can play. *Ocean Dev. Int. Law* 39, 150–177. doi: 10.1080/00908320802013768

Syms, C., and Jones, G. P. (2001). Soft corals exert no direct effects on coral reef fish assemblages. *Ecologia* 127, 560–571. doi: 10.1007/s004420000617

Tkachenko, S., Hoang, D. T., and Dang, H. N. (2020). Ecological status of coral reefs in the Spratly Islands, South China Sea (East Sea) and its relation to thermal anomalies. *Estuarine Coast. Shelf Sci.* 238:106722. doi: 10.1016/j.ecss.2020.106722

Tun, K., Chou, L. M., Yeemin, T., Phongsuwan, N., Setiasih, N., Wilson, J., et al. (2010). "A regional overview on the 2010 coral bleaching event in Southeast Asia," in *Status of Coral Reefs in East Asian Seas Region: 2010* (Townsville, QLD: Global Coral Reef Monitoring Network), 9–27.

Tursch, B., and Tursch, A. (1982). The soft coral community on a sheltered reef quadrat at Laing Island (Papaua New Guinea). *Mar. Biol.* 68, 321–332. doi: 10.1007/bf00409597

Verseveldt, J., and Tursch, A. (1979). Octocorallia from the Bismarck Sea. *Zool. Meded.* 54, 133–148. doi: 10.11646/zootaxa.4652.2.1

Vo, S. T., Pernetta, J. C., and Paterson, C. J. (2013). Status and trends in coastal habitats of the South China Sea. *Ocean Coast. Manage.* 85, 153–163. doi: 10.1016/j.ocecoaman.2013.02.018

Williams, G. C., and Cairns, S. D. (2018). *Biodiversity Myth Busters*. Octocoral Research Center. Available online at: https://researcharchive.calacademy.org/research/izg/Biodiversity%20Myth%20Busters.html

Yeung, C. W., Cheang, C. C., Lee, M. W., Fung, H. L., Chow, W. K., and Ang, P. (2014). Environmental variabilities and the distribution of octocorals and black corals in Hongkong. *Mar. Pollut. Bull.* 85, 774–782. doi: 10.1016/j.marpolbul.2013.12.043

Zubair, M. S., Lallo, S., Rusmiyanti, R., Nugrahani, A. W., and Jantan, I. (2018). Screening of antibacterial and anticancer activity of soft corals from Togean Islands, Indonesia. *Indones. J. Pharm.* 29:173. doi: 10.14499/indonesianjpharm29iss4pp173

Zvuloni, A., van Woesik, R., and Loya, Y. (2010). Diversity partitioning of stony corals across multiple spatial scales around Zanzibar Island, Tanzania. *PLoS One* 5:e9941. doi: 10.1371/journal.pone.0009941

Conflict of Interest: The authors declare that the research was conducted in the absence of any commercial or financial relationships that could be construed as a potential conflict of interest.

frontiers in Marine Science

ORIGINAL RESEARCH
published: 25 January 2022
doi: 10.3389/fmars.2021.724504

Nearshore to Offshore Trends in Plankton Assemblage and Stable Isotopes in Reefs of the West Philippine Sea

Aletta T. Yñiguez[1], Gianina Cassandra May Apego[1], Norman Mendoza[2], Norchel Corcia Gomez[1] and Gil S. Jacinto[1]*

[1] Marine Science Institute, University of the Philippines Diliman, Quezon City, Philippines, [2] Philippine Nuclear Research Institute, Department of Science and Technology, Diliman, Quezon City, Philippines

OPEN ACCESS

Edited by:
Yehuda Benayahu,
Tel Aviv University, Israel

Reviewed by:
Kusum Komal Karati,
Centre for Marine Living Resources and Ecology (CMLRE), India
Vladimir G. Dvoretsky,
Murmansk Marine Biological Institute, Russia

****Correspondence:***
Aletta T. Yñiguez
atyniguez@msi.upd.edu.ph

Specialty section:
This article was submitted to Marine Ecosystem Ecology, a section of the journal Frontiers in Marine Science

Received: *13 June 2021*
Accepted: *27 December 2021*
Published: *25 January 2022*

Citation:
Yñiguez AT, Apego GCM, Mendoza N, Gomez NC and Jacinto GS (2022) Nearshore to Offshore Trends in Plankton Assemblage and Stable Isotopes in Reefs of the West Philippine Sea. Front. Mar. Sci. 8:724504. doi: 10.3389/fmars.2021.724504

Coral reefs are typified by their benthic components, and reef diversity and productivity are traditionally ascribed to the symbiotic association between corals and zooxanthellae, and other macroalgal forms. Less understood is the role of plankton and adjacent pelagic areas in contributing to reef productivity. Half of the reef benthos are filter or particle feeders, while a significant proportion of reef fishes are planktivorous. These organisms can serve as bridges between adjacent oceanic areas to the reef proper, and the pelagic and benthic realm. Here, we investigate the plankton trophic dynamics in two reef systems in the West Philippine Sea. Physico-chemical data, phytoplankton and mesozooplankton samples were collected from stations spanning offshore to reef areas per site. These were subjected to microscopic and stable isotope analysis to determine variability in plankton distribution, phytoplankton and zooplankton interactions, and gain insights into the trophic dynamics and productivity of reefs. Results showed distinct variations in plankton biomass and assemblage from offshore to reef areas, as well as between the reef systems. Phytoplankton distributions pointed toward filtering out of cells across the fore reef and reef flat areas, while mesozooplankton distributions could be mediated more by other factors. Isotopic signatures of δ^{13}C and δ^{15}N indicated the influence of different nutrient sources for phytoplankton and that mesozooplankton relied only partly on phytoplankton for food in most areas of the reefs. The mesozooplankton likely also obtain food from other sources such as the microbial and detrital pathways. More in-depth spatio-temporal studies on these bentho-pelagic interactions are recommended, which can provide more robust estimates of the trophic dynamics of these reefs that are situated in important fishing grounds and key biodiversity areas.

Keywords: benthic-pelagic coupling, plankton trophic dynamics, reef, stable isotope, West Philippine Sea

INTRODUCTION

Coral reefs are one of the most biologically diverse and productive coastal ecosystems. They are geographically located in shallow oligotrophic waters in the inter-tropical regions at 30°N–30°S, and these reefs occupy less than 0.1% of the world's oceans (Lesser, 2004). Within these restrictions, reefs are still able to support complex faunal and floral communities that are distinct in their taxonomic organization and spatial and temporal distribution. These marine ecosystems also play a role in the exchange of organic and non-organic matter with the adjacent ocean and lagoon (Hamner et al., 2007).

At the base of the marine food web, plankton support the functioning of the coral reef ecosystem by providing food for a wide array of coral reef-associated organisms. Half of the benthic fauna on coral reefs are estimated to be filter feeders or particle feeders; these animals feed on zooplankton and particulate organic matter (POM) (Yahel et al., 1998; Mayal et al., 2009). Many reef fish species larvae and juveniles rely on mesozooplankton and consequently the lower trophic levels for food. Despite occupying what is typically considered oligotrophic seas, the contribution of plankton to the productivity of coral reefs has long been recognized (Glynn, 1973; Hamner et al., 1998) though still less explored (Skinner et al., 2021). In one of the first studies to look into plankton on reefs, Glynn (1973) reported variations in plankton across a reef in Puerto Rico and estimated that over 91% of diatoms and 60% of zooplankton were removed from the water presumably by reef organisms. Hamner et al. (2007) illustrated the spatial variation of available zooplankton from the oceanic side to the lagoon in the barrier reef of Palau. This and other studies (Morales and Murillo, 1996; Gruber et al., 2018) also highlight the interaction between the open ocean and coral reefs through the import and export of plankton. More recent studies are demonstrating the significant contribution of oceanic processes to reef productivity (Genin et al., 2009; Wyatt et al., 2010, 2013; Leichter et al., 2013; McMahon et al., 2016; Morais and Bellwood, 2019; Fey et al., 2021). Wyatt et al. (2013) highlight that allochthonous oceanic particulate organic material (POM) comprised primarily of phytoplankton are important in providing nutrients at the fringing Ningaloo Reef. Morais and Bellwood (2019) estimated that 41% of the fish productivity in a windward reef on the Great Barrier Reef derived from pelagic subsidies, while McMahon et al. (2016) found that pelagic productivity can contribute greater than 70% to C consumed and assimilated by fish in oceanic reefs in the Red Sea.

Mesozooplankton are considered to be a key group bridging primary producers to benthos and fishes at the higher trophic levels in different marine ecosystems including coral reefs (Roman et al., 1990). This transfer of organic material through the mesozooplankton can occur through three possible pathways: grazing, microbial and detrital pathways (Gottfried and Roman, 1983; Morillo-Velarde et al., 2018). The grazing pathway is the classical concept of microphytoplankton as direct prey of zooplankton. The microbial pathway starts with heterotrophic bacteria which are consumed by nano- and microzooplankton such as protists which are then consumed by the mesozooplankton. In the detrital pathway, mesozooplankton consume non-living organic matter such as dead animals, plants, feces and other waste materials. The contribution of different trophic pathways in the system can vary depending on season (Nakajima et al., 2017) and location (McMahon et al., 2016; Skinner et al., 2021).

Measurement of stable isotopes has been widely used to provide insights on the trophic interactions both in freshwater and marine ecosystems (Fry and Sherr, 1984) specifically in a time-integrated manner (Vander Zanden and Rasmussen, 1999; Post, 2002). The pathways of energy flow through food webs can be traced and understood using carbon and nitrogen stable isotopes (Vander Zanden et al., 1999). The trophic positions of organisms, which reflect species' long-term diet, are estimated by using the δ^{13}C and δ^{15}N signatures of the primary producers (e.g., phytoplankton) and various consumers (e.g., zooplankton and fish) (Popp et al., 2007). Moreover, stable isotopes analyses have been used to better understand the trophic interactions between planktonic communities (Basedow et al., 2009, 2016; Giering et al., 2019) in pelagic zones to trace sources and transport of nutrients.

The input of allochthonous material into coral reef productivity is generally recognized yet relatively unexplored. Through these pelagic subsidies, larger-scale oceanographic variabilities can influence reef resilience and/or vulnerability. In this study, we contribute information on this process in reefs in the Philippines, an area that is a global biodiversity hotspot and within a key fisheries region but with limited data. We investigated the interaction between the pelagic and benthic areas through the plankton, and the potential trophic paths in reefs in the West Philippine Sea. Specifically, we examined the plankton composition, abundance, and stable isotope signatures and investigated the variations in the distribution of microphytoplankton and mesozooplankton across and between two tropical reefs in the West Philippine Sea, and assessed the potential trophic pathway between phytoplankton and mesozooplankton within these reefs.

MATERIALS AND METHODS

Study Sites

The Kalayaan Island Group (KIG) in the West Philippine Sea (WPS) is estimated to house approximately 30% of coral reefs in the Philippines and is recognized as a key biodiversity area (Ong et al., 2002; Arceo et al., 2020). These offshore reefs and surrounding pelagic areas also serve as important fishing grounds (Aliño and Quibilan, 2003). This area is embedded within the South China Sea (SCS) whose general circulation patterns are highly influenced by monsoonal wind systems (Wyrtki, 1961; Hu et al., 2000). During the northeast monsoon season (or winter time), overall circulation is cyclonic, with strong southward flows off the coast of Vietnam. During the southwest monsoon (summer), flow is primarily anticyclonic with weaker northward currents. Within the central area of the South China Sea, where the KIG is located, currents are weaker, and tides also have small amplitudes (Villanoy and Jacinto, 2017). The SCS is generally considered oligotrophic (Zhang and Yin, 2015), and the offshore and shelf waters of the WPS exhibit the Typical Tropical Structure with a thermocline, nutricline, a subsurface chlorophyll maximum found at around 40–75 m, and the peak primary production overlapping or just above the chlorophyll maximum (San Diego-McGlone et al., 1999). Previous work have focused on characterizing gross hydrodynamic features in the deeper waters of the WPS and SCS, and there are no studies that we are aware of specifically describing oceanographic patterns across time and space at a similar atoll scale featured in this study.

The research expedition in KIG was conducted from April 28, 2017 to May 18, 2017 on-board the BRP Velasquez. Two reef systems, Pag-asa (Thitu) Island and Sabina Shoal, within the KIG were the sites for this study (**Figure 1**). The samples were collected from at most six stations across two separate transects in Pag-asa Island on May 3 and 5, and one transect in Sabina Shoal on May 9. Small boats deployed from the ship were used to sample the reef areas. **Supplementary Table S1** documents the details for the sampling stations.

Pag-asa Island is at the eastern tip of an atoll in the northwestern portion of the KIG. It has an area of 37.2 hectares and is the largest Philippine-administered islands in the Kalayaan Island Group situated toward the west. It is occupied by military personnel and a civilian population of about 300. Transect 1 was located in the northwestern area, while Transect 2 was in the southwestern area. The first transect has a broad reef flat, a more pronounced spur and groove area, and a steeper reef slope than the second. Transect 2 is situated adjacent to the inhabited area of the island and the landing point for small boats is nearby. For both transects, Station 1 was in the lagoon area, Station 2

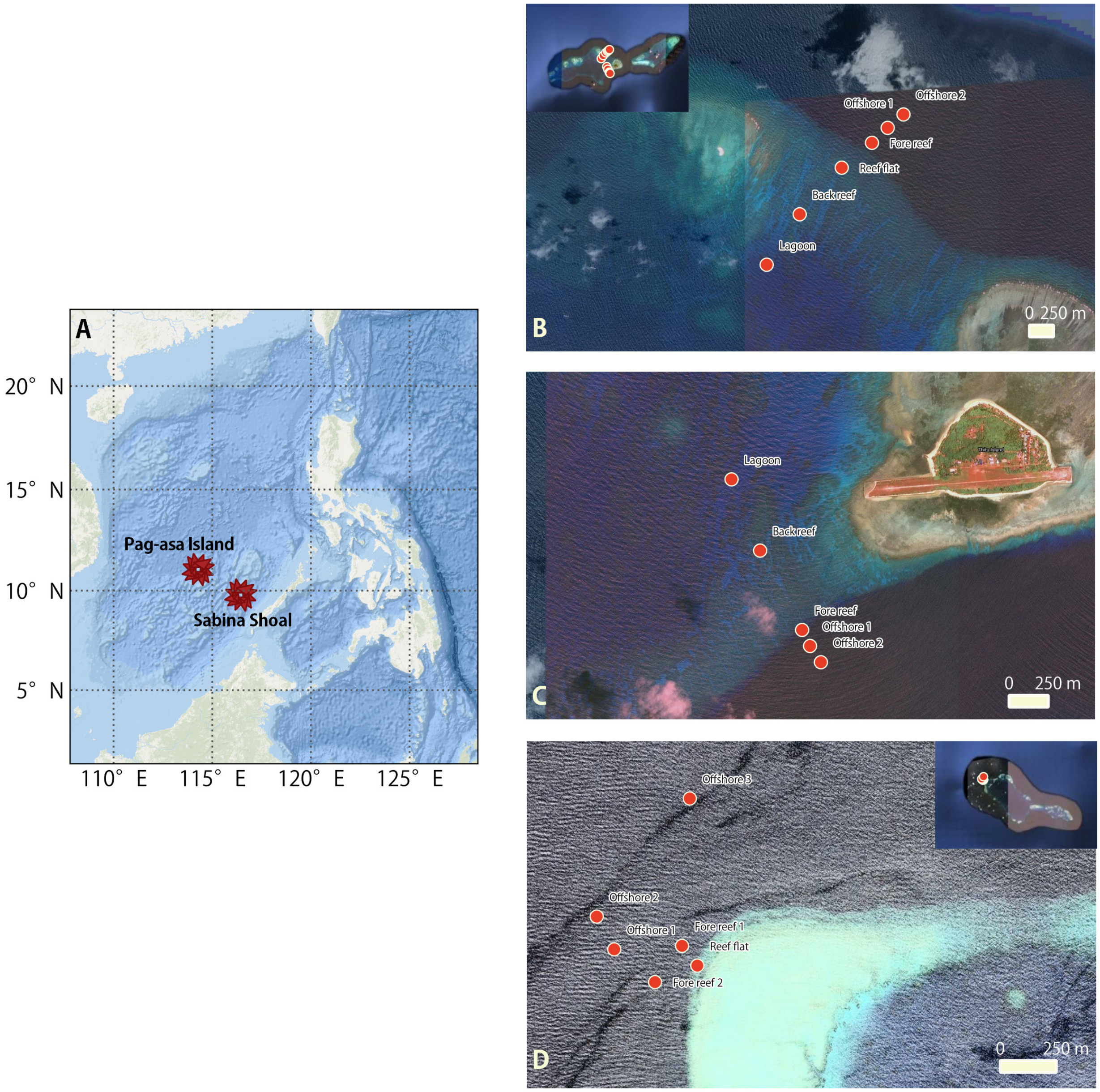

FIGURE 1 | Maps of the study sites in the Kalayaan Island Group. **(A)** Philippine map showing the West Philippine Sea and islands; **(B)** Pag-asa Island Transect 1 with the larger Pag-asa Island perspective showing the 2 transects as inset; **(C)** Pag-asa Island Transect 2; and, **(D)** Sabina Shoal Transect and the whole Sabina Shoal perspective as inset.

in the back reef, Station 3 in the reef flat (only for Transect 1), Station 4 on the fore reef slope and Stations 5 and 6 were offshore from the reef. We were unable to sample the targeted Station 3 at the reef flat area at Transect 2 due to a sudden squall and limited time at the island. In contrast to Pag-asa Island, Sabina Shoal is an uninhabited atoll at the eastern portion of the KIG. The transect is situated on the northwestern portion of the atoll and is characterized by a narrow and steep fore reef. Station 1 is in the reef flat area, while Station 2 is in the fore-reef area. Station 3 is in the fore-reef slope/deeper reef area. Stations 4 to 5 are sequentially further offshore from the reef. We were unable to access the lagoon here due to the extremely shallow and extensive reef flat.

Physico-Chemical Parameters

For each station, temperature, salinity, and density measurements were obtained using a CastAway CTD (YSI, United States) up to a maximum of 40 m or less, depending on the actual depth. A 5 L Niskin sampling bottle (General Oceanics Inc., United States) was deployed up to five depths per station to obtain samples for dissolved oxygen, nutrients, and chlorophyll *a*. Samples for dissolved oxygen were collected into BOD bottles and fixed with manganous chloride and alkali-iodide. Sub-samples for inorganic nutrients (phosphate, silicate, nitrite, and nitrate) were collected into 250 mL HDPE bottles, and water samples for chlorophyll *a* analysis were collected in 2.5 L book bottles. The inorganic nutrients and chlorophyll *a* samples were stored in an ice box until samples could be processed back on the ship.

On board the ship, samples for dissolved oxygen were immediately analyzed using a slight modification of the Winkler (1888) method by Carpenter (1965). Seawater samples for inorganic nutrients were transferred to centrifuge tubes and stored in a freezer at –20°C (4°C for silicate) before laboratory analyses on land. For chlorophyll *a*, 1000 mL of the sample was filtered through a 0.7 μm Whatman® GFF using a vacuum filter manifold. A few drops of magnesium carbonate ($MgCO_3$) solution were added to the filter paper prior to filtration to preserve the samples. After filtration, the filter papers were placed in aluminum foil sheets and stored in a freezer (−20°C) until analysis back on land.

Plankton Collection

Collection and Processing of Phytoplankton and Zooplankton for Microscopy

Niskin bottles were deployed at discrete depths per station ranging from subsurface to a maximum of 85 m to gather phytoplankton samples. The number and actual depths sampled depended on the actual bottom depth (**Supplementary Table S1**). A known volume, typically 1 L was collected from the Niskin bottles, which were subsequently filtered through a 20 μm sieve, decanted into amber bottles, and fixed with 5 ml formalin. These were used to characterize the type and abundance of phytoplankton per station. For zooplankton composition and abundance, a plankton net with 200 μm mesh size and a flowmeter were vertically deployed and lowered until about a meter above the bottom. Samples from these vertical tows were filtered using a 200 μm sieve and fixed with ethanol.

Collection and Processing of Phytoplankton and Zooplankton for Stable Isotope Analysis

Phytoplankton for stable isotope analysis were obtained using vertical net tows (20 μm mesh size) deployed near the bottom or a maximum of 50 m. Collected samples were filtered using a 20 μm sieve into amber bottles which were stored in an ice chest until they could be processed on the ship. Zooplankton samples were collected using horizontal and vertical (depth-permitting) tows using 200 μm mesh size nets and a flowmeter. Vertical tows were deployed near the bottom or a maximum of 50 m, while for horizontal tows, the net was lowered just below the water surface and towed for 3 min while the boat was circling immediately around the station. Samples from the tows were filtered through a 200 μm sieve into amber bottles and stored in an ice chest as well. On board the ship, both phytoplankton and zooplankton samples were directly filtered through a pre-combusted GF/F Whatman filter (47 mm diameter) using a filtration manifold with a vacuum pump. The filters were filtered to refusal, folded into half and placed in pre-combusted aluminum foils, and stored in a −80°C freezer until further analysis.

Chemical and Chlorophyll Analysis

Phosphate, silicate, and nitrite concentrations were determined colorimetrically using the methods from Strickland and Parsons (1972) and Jones (1984) with the use of a UV-Vis spectrometer (Shimadzu UV Mini 1240, Japan). NOx (nitrate and nitrite) concentrations were measured using a modified shaking technique to reduce nitrate to nitrite using cadmium granules from Jones (1984), and then detected using the colorimetric method. Chlorophyll *a* (chl *a*) samples were analyzed fluorometrically using a Trilogy® laboratory fluorometer following the Intergovernmental Oceanographic Commission (Protocols for the Joint Global Ocean Flux Study (JGOFS), 1994).

Microscopy

Phytoplankton samples were analyzed under the HPO of a Carl Zeiss Axiovert 25 inverted microscope. One ml aliquot from each sample bottle was obtained using a micropipette and decanted onto a Sedgewick Rafter slide. Initially, the slide was viewed under the scanner objective to have an overview of the cell density of the sample. The cell counts were performed thrice per sample bottle, and were averaged for data analysis and interpretation. Identification was made up to the genus level based on Tomas (1997). Data were expressed as cell density per liter. Phytoplankton counts were averaged across depths per station to obtain cross-reef profiles.

Before microscopy, the zooplankton samples from the vertical tows were diluted to a volume of 200 ml and split using a Folsom plankton splitter. The zooplankton to be subsampled was poured into the splitter and rotated slowly back and forth. Internal partitions divided the samples into equal fractions. One half of the sample portion, approximately 100 ml, was placed in a petri dish with grids etched on the bottom, and fully counted. Counting was done using a stereomicroscope. Identification was made up to the order level, except for the groups of fish larvae, nauplius, polychaete worms and unidentified eggs. Data were expressed as individuals per cubic meter.

Stable Isotope Analysis

The phytoplankton and mesozooplankton samples for stable isotope analysis were dried at 60°C, rinsed with dilute HCl and ultrapure water, then dried again at 60°C. The samples were recovered from GF/F filters by scraping and were ground into a fine powder using an agate mortar and pestle before analysis. These were weighed and wrapped in tin capsules.

Measurement of bulk carbon and nitrogen isotopes in both phytoplankton and mesozooplankton samples were performed using a continuous flow IRMS (Delta V Advantage, Thermoscientific) interfaced with an elemental analyzer (ECS 4010, Costech, Inc.). The relative abundance of carbon and nitrogen isotopes were calculated using pre-calibrated amino acid standards (Tayasu et al., 2011): Glycine ($\delta^{13}C = -34.92$) and L-Threonine ($\delta^{13}C = -9.45$) for carbon and DL-Alanine ($\delta^{15}N = -2.89$) and L-Alanine ($\delta^{15}N = 22.71$) for nitrogen.

Stable isotope ratios were reported as delta (δ) notation:

$$\delta^{15}\mathrm{N}\ and\ \delta^{13}\mathrm{C} = \left(\frac{R_{sample}}{R_{standard}} - 1\right) \times 1000$$

where R is $^{15}N/^{14}N$ or $^{13}C/^{12}C$. Isotope ratios are expressed in per mil (‰) relative to the ratio of international reference standards ($R_{standard}$) which are Atmospheric Nitrogen and Vienna PeeDee Belemnite (VPDB) for nitrogen and carbon, respectively (Perkins et al., 2014).

Statistical Analysis

Principal Coordinate Analysis (PCoA) was used to analyze the multivariate distribution of the phytoplankton and mesozooplankton compositions, while Canonical Correspondence Analysis (CCA) was used to analyze the influence of environmental variables on the phytoplankton and mesozooplankton assemblages. The data were first transformed into distance measures using the Bray-Curtis method for the PCoA (Legendre and Anderson, 1999; Legendre and Legendre, 2012). For the CCA, data were standardized using the Hellinger method (Legendre and Legendre, 2012). Spearman's correlation was employed to look at correlations and potential interactions between the phytoplankton and mesozooplankton taxa. Only taxa that were observed in at least half of the sampling stations per transect were included in the analysis. ANOVA was used to determine if there were any differences in the phytoplankton $\delta^{13}C$ and $\delta^{15}N$ between reef transects, followed by Tukey HSD to tease out specific differences. Data were assessed for conformity to the assumptions of normality and homogeneity of variances. The differences of the carbon and nitrogen isotopic values between the mesozooplankton and phytoplankton were calculated by obtaining the average $\delta^{13}C$ and $\delta^{15}N$ of the phytoplankton per transect or per reef zone, then subtracting the corresponding mesozooplankton average $\delta^{13}C$ and $\delta^{15}N$ for that transect or reef zone. All statistical analysis were done using R through the base package, as well as the *vegan* package.

RESULTS

Water Column Conditions

The physico-chemical section profiles for the Pag-asa Island and Sabina Shoal transects are shown in **Figure 2** in terms of temperature, salinity, density, chl *a*, phosphate (PO_4), silicate (SiO_3), and nitrate and nitrite (NOx). Generally, warm, stratified areas were evident in all transects with temperature values ranging from 28.76 to 31.70°C (**Figure 2** and **Supplementary Table S2**). Salinity ranged from 33.32 to 33.73 psu. The Sabina Shoal site, though, showed much stronger stratification across the transect due to very warm surface waters and sharp thermocline (**Figures 2C,F,I**).

Phytoplankton biomass is considered to be generally low in waters surrounding coral reef ecosystems, characterized by typical concentrations of chl *a* at approximately 0.2–0.6 μg/L (Nakajima et al., 2016) owing to a low concentration of inorganic nutrients (Hearn et al., 2001). San Diego-McGlone et al. (1999) observed a maximum of 0.66 in their South China Sea sites. In the present study, relatively lower chl *a* values were observed with a maximum of 0.13 μg/L, where the Pag-asa transects (PT1 and PT2) had slightly higher average concentrations, and larger areas with higher concentrations compared to Sabina Shoal (**Figures 2J,K,L** and **Supplementary Table S2**). These high chl *a* concentrations at PT1 and PT 2 were found in the subsurface to deeper waters at the forereef and offshore zones. Relatively high chl *a* concentrations were also observed in the lagoon of PT1. The high chl *a* levels in Sabina Shoal were observed near the surface at the forereef zone. In general, nutrient concentrations ranged from 0.12 to 0.59 μM for phosphate, 1.93 to 11.92 μM for silicate, and 0.17 to 8.65 μM for NOx. Overall, all three transects tended to be depleted in nutrients at the surface, which increased going deeper (**Figures 2M–U**). There were some specific differences, though, between the three. Pag-asa transect 1 and Sabina Shoal had relatively higher nutrient concentrations than Pag-asa transect 2. These were situated in deeper areas offshore and even extending toward shallower depths in some offshore areas as at the forereef slopes. In contrast, Pag-asa transect 2 had lower phosphate and NOx concentrations, and did not exhibit any distinct increase at the forereef zone (**Figure 2** and **Supplementary Table S2**). Silicate was also moderately high at the lagoon side of the two Pag-asa transects (**Figures 2S,T,U** and **Supplementary Table S2**).

Plankton Assemblages Across Reef Zones and Transects

A total of 48 phytoplankton genera belonging to 33 families were observed across the transects (**Supplementary Table S3**). Family Bacillariaceae was by far the most genera-abundant group, with four recorded genera each. Family Hemiaulaceae and Rhizosoleniaceae each had 3 genera, whereas families Chaetocerataceae, Dinophysaceae, Fragilariaceae, Skeletonemaceae, Thalassionemataceae, Thalassiosiraceae, and Triceratiaceae were represented by 2 genera each.

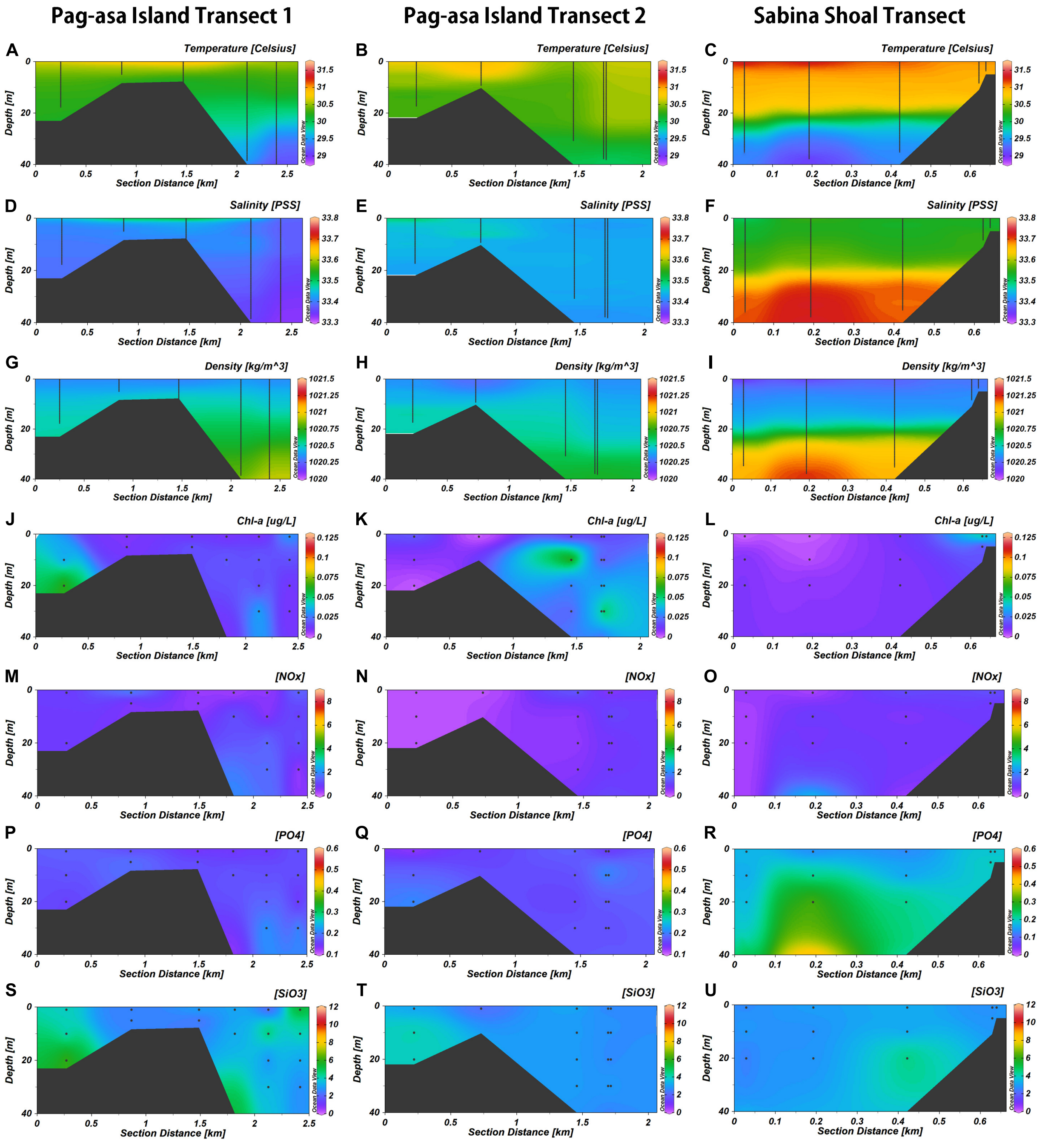

FIGURE 2 | Section plots of the three transects Pag-asa Transect 1 **(A,D,G,J,M,P,S)**, Pag-asa Transect 2 **(B,E,H,K,N,Q,T)**, and Sabina Transect **(C,F,I,L,O,R,U)** with contour plots for temperature, salinity, density, chlorophyll *a* (chl *a*), phosphate (PO_4), nitrate and nitrite (NOx), and silicate (SiO3) for each transect.

All other remaining phytoplankton families had one representative genus only.

Phytoplankton abundances and assemblages exhibited variations between reef zones as well as between the three transects (**Figures 3A**, **4A**, **5**). Back reef and reef flat areas tended to have decreased phytoplankton abundances while those in the lagoon and fore-reef zones had higher abundances (**Figure 5** and **Supplementary Table S3**). In Sabina Shoal, only the back reef and reef flat areas (Stations 1 and 2) were accessible, and these also had lower densities than fore-reef and deeper stations. The two Pag-asa Island transects had more similar phytoplankton compositions wherein diatoms of the Family Chaetoceraceae were the most abundant (dominated by the genus *Chaetoceros)*, followed by cyanobacteria of the Family Phormidiaceae (*Trichodesmium*), and then diatoms of the Thalassionemataceae family (*Thalassionema*). Sabina Shoal was distinct from Pag-asa

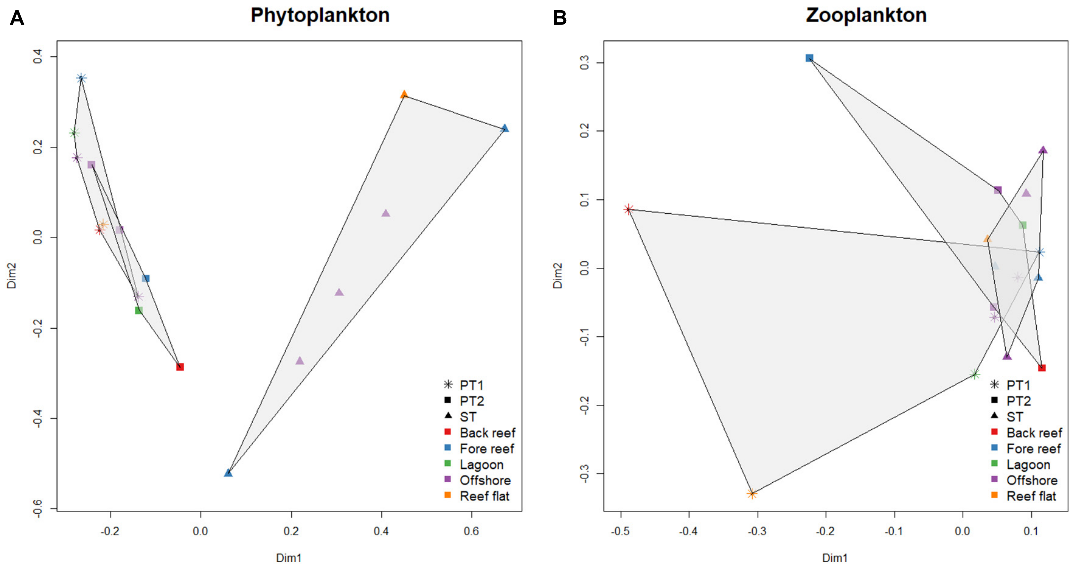

FIGURE 3 | Principal Coordinate Analysis of the stations based on phytoplankton **(A)** and zooplankton **(B)** assemblages. Transects are represented by different symbols, with the gray areas showing the dispersion of one transect. The colors of the symbols represent the reef zone.

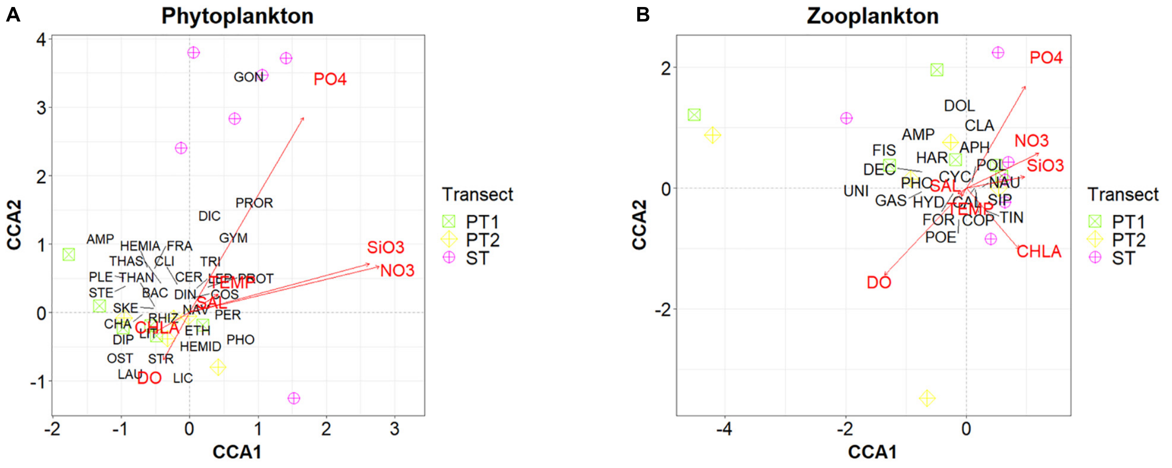

FIGURE 4 | Canonical Correspondence Analysis of the transects based on phytoplankton **(A)** and zooplankton **(B)** assemblages constrained by physico-chemical parameters. Transects are represented by different symbols. Text labels represent taxa. For phytoplankton taxa - AMP, Amphisoleniaceae; BAC, Bacillariaceae; CER, Ceratiaceae; CHA, Chaetocerotaceae; CLI, Climacospheniaceae; COS, Coscinodiscaceae; DIC, Dictyochaceae; DIN, Dinophysaceae; DIP, Diploneidaceae; ETH, Ethmodiscaceae; FRA, Fragilariaceae; GON, Gonyaulacaceae; GYM, Gymnodiniaceae; HEMIA, Hemiaulaceae; HEMID, Hemidiscaceae; LAU, Lauderiaceae; LEP, Leptocylindraceae; LIC, Licmophoraceae; LIT, Lithodesmiaceae; NAV, Naviculaceae; OST, Ostreopsidaceae; PER, Peridiniaceae; PHO, Phormidiaceae; PLE, Pleurosigmataceae; PROR, Prorocentraceae; PROT, Protoperidiniaceae; RHIZ, Rhizosoleniaceae; SKE, Skeletonemaceae; STE, Stephanopyxidaceae; STR, Striatellaceae; THAN, Thalassionemataceae; THAS, Thalassiosiraceae; TRI, Triceratiaceae. For zooplankton taxa - AMP, Amphipoda; APH, Aphragmophora; CAL, Calanoida; CLA, Cladocera; COP, Copelata; CYC, Cyclopoida; DEC, Decapoda; DOL, Doliolida; FIS, Fish larvae; FOR, Forcipulatida; GAS, Gastropoda; HAR, Harpacticoida; HYD, Hydrozoa; NAU, Nauplius; PHO, Phoronida; POE, Poecilomastoida; POL, Polychaete worm; SIP, Siphonophora; TIN, Tintinnida; UNI, Unidentified egg.

Island with much lower phytoplankton densities (except for the outer forereef), and its phytoplankton composition. The cyanobacteria *Trichodesmium* was the most dominant in Sabina Shoal, followed by the dinoflagellate *Prorocentrum* of family Prorocentraceae, and then diatoms of the Leptocylindraceae family (*Leptocylindrus*). The two axes of the CCA (**Figure 4A**) explained 47.42% of the variability in the phytoplankton. It highlighted the association of dinoflagellates from the Families Prorocentraceae and also Gonyaulacacea in Sabina Shoal, which exhibited low phytoplankton abundance, low chlorophyll, and higher nutrient concentrations, as also discussed above. Pagasa transects 1 and 2, on the other hand, clustered closer together and were associated more with higher chlorophyll, but relatively lower nutrient concentrations. Phytoplankton composition

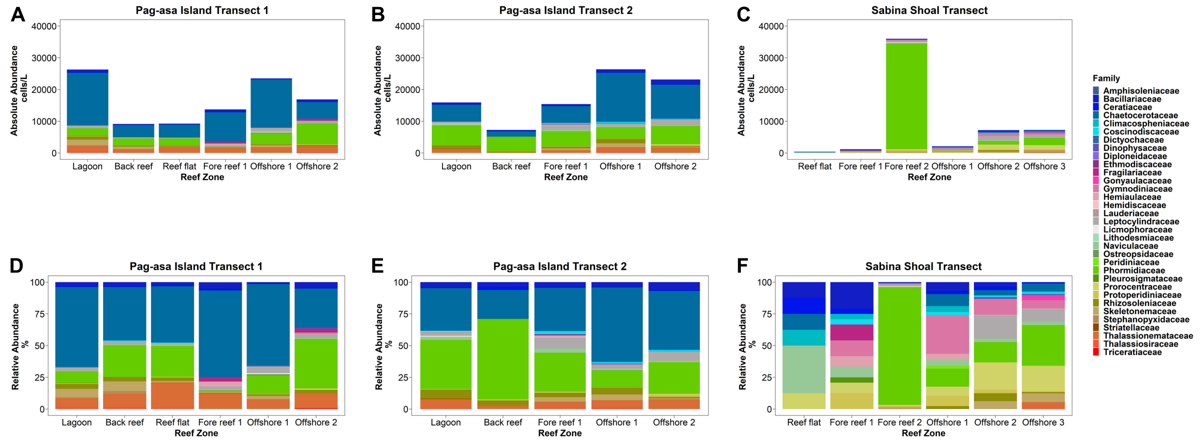

FIGURE 5 | Phytoplankton absolute **(A,B,C)** and relative **(D,E,F)** abundances across the reef systems of Pag-asa Island and Sabina Shoal.

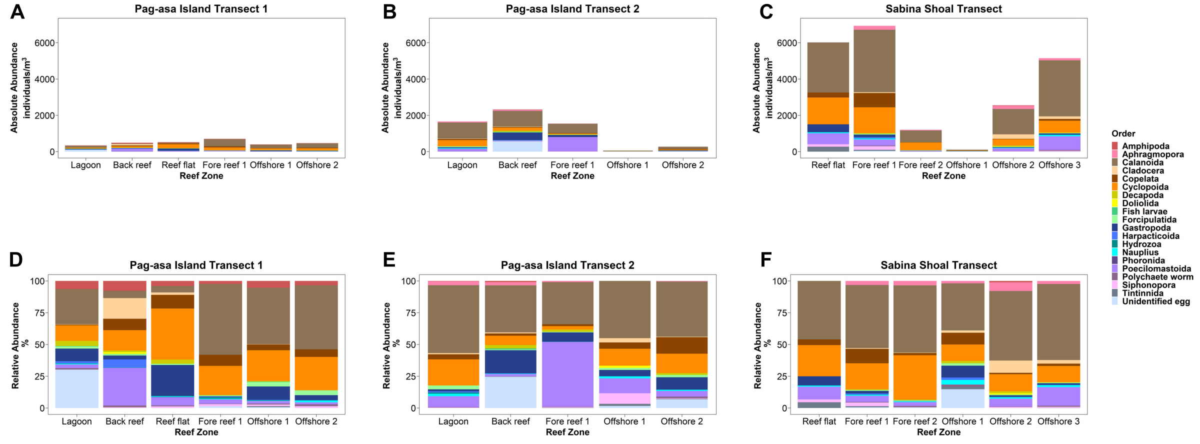

FIGURE 6 | Zooplankton absolute **(A,B,C)** and relative **(D,E,F)** abundances across the reef systems of Pag-asa Island and Sabina Shoal.

also appeared to have some variability within reef zones in a transect (**Figure 5** and **Supplementary Table S3**) driven mainly by shifts in the dominance of *Chaetoceros* and *Trichodesmium* and increases in the contribution of dinoflagellates like *Gymnodinium* sp., *Prorocentrum* sp., and *Protoperidinium* sp., and other diatom species such as *Thalassionema* sp., *Skeletonema* sp., and *Leptocylindrus* sp., particularly in the lagoon, fore reef and offshore zones.

A total of 20 zooplankton orders were observed across the transects. Zooplankton abundances exhibited more variability within and between transects (**Figures 3B**, **4B**, **6** and **Supplementary Table S4**) compared to phytoplankton. Zooplankton abundance tended to be higher in the inner reef areas compared to offshore, opposite the pattern observed for phytoplankton. Abundance was also the highest overall for Sabina Shoal and lowest for Pag-asa transect 1. Zooplankton composition had more overlaps between all three transects (**Figure 3B**) and was relatively more similar compared to patterns for the phytoplankton. The three transects were generally dominated by copepods (including their nauplii) under the orders Cyclopoida and Calanoida. Pag-asa Transect 2 and the Sabina transect had high abundances of copepods from the order Poecilostomatoida, while in Pag-asa transect 1 mesozooplankton under class Gastropoda were abundant. The CCA axes (**Figure 4B**) was able to explain 31.63% of the variance in zooplankton. It again highlighted the higher overlap in the mesozooplankton community composition across transects though there were variabilities in the environmental variables (**Figure 4B**). Though there are similarities between transects, the compositions still showed differences across reef zones where more types of mesozooplankton (e.g., fish larvae, Doliolida, Amphipoda, Hydrozoa) were found in the lagoon and/or back reef zones for the two Pag-asa transects, and offshore for Sabina transect (**Figure 6** and **Supplementary Table S4**).

The potential interactions between phytoplankton and mesozooplankton were evaluated per transect using Spearman correlation (**Figure 7**). There were only a few significant associations, and out of these, all showed a negative correlation between particular phytoplankton and mesozooplankton. In Pag-asa transect 1, four significant negative associations were observed: Cyclopoids and *Skeletonema*, Harpacticoids and *Thalassionema*, Poecilomastoida and *Protoperidinium*, and Siphonophore and *Skeletonema*. For Pag-asa transect 2, seven significant negative associations were observed, namely between Aphragmopora and *Coscinodiscus* as well as *Cylindrotheca*, Calanoida and *Chaetoceros* as well as *Cylindrotheca*, Decapoda and *Bacteriastrum*, Gastropoda and *Bacteriastrum*, and Polychaete worm and *Chaetoceros*. In the Sabina transect, only two significant negative associations were observed, namely between Cyclopoida and *Gymnodinium*, and Poecilomastoida and *Protoperidinium*.

Plankton Stable Isotope Analysis

The δ^{13}C values obtained for the phytoplankton ranged from −23.9 to −17.5‰ (**Table 1**). δ^{15}N values of phytoplankton were variable ranging from 3.1 to 11.4‰. There were no significant differences in the mean δ^{13}C between transects; however, there were significant differences for mean δ^{15}N. The two Pag-asa transects were significantly different from each other ($p = 0.0002$), as well as Pag-asa transect 2 and Sabina transect ($p = 0.0135$). There was no difference between Pag-asa transect 1 and Sabina transect ($p = 0.0988$) and both had higher δ^{15}N values than Pag-asa transect 2.

The mesozooplankton, on average in the Pag-asa transects, appeared to have relatively depleted ^{13}C compared to the phytoplankton within each transect, while the Sabina Shoal transect showed slight enrichment (**Table 1**). There can be large variability though across reef zones. Within the Sabina transect, the offshore zone were enriched, while ^{15}C values were slightly depleted in other zones. Within the Pag-asa transect 1, the enriched areas were the lagoon and back reef zones. All zones in Pag-asa transect 2 were consistently depleted. For δ^{15}N of mesozooplankton relative to the corresponding putative phytoplankton δ^{15}N per transect, only Pag-asa transect 2 on average appears to exhibit ^{15}N enrichment by 1.1‰ (**Table 1**). The Sabina transect mesozooplankton was only slightly depleted especially compared to the Pag-asa transect 1 mesozooplankton. There are also a few variabilities across reef zones, where the reef flat in the Sabina transect was slightly enriched. Conversely, only the back reef in Pag-asa transect 2 was depleted. The biplots with convex hulls for phytoplankton and mesozooplankton in **Figure 8** provide an indication of the breadth of their sources of nutrients and food. Pag-asa transect 1 and Sabina transect mesozooplankton potentially have other C sources apart from the phytoplankton in the transect. Pag-asa transect 2 mesozooplankton appears to have a less diverse source of food, which is more depleted than the phytoplankton. The larger range of δ^{15}N in Sabina followed by Pag-asa transect 2 suggests that mesozooplankton in these areas have a wide range of feeding types, especially compared to the smaller range of Pag-asa transect 1.

DISCUSSION

Variability of Plankton Across the Reefs

Coral reefs are dynamic environments influenced by tides and waves, yet distinct patterns in the plankton across the scale of the reef zones can be distinguished. The phytoplankton abundance and assemblage showed a distinct pattern of variation from offshore to the reef or lagoon side. Phytoplankton were abundant offshore, becomes depleted in the fore-reef and reef flat areas that harbor the most benthic and associated organisms, then increases again in the reefs with lagoons. This pattern was robust across the three reefs investigated. This supports the concept of the "wall of mouths" where plankton are removed from the water column by planktivores aggregated in the fore-reef area (Hamner et al., 1998; Morais and Bellwood, 2019). Benthic and suspension feeders are also potential consumers of phytoplankton in reefs in addition to planktivorous fish; these include bivalves (Klumpp et al., 1992), gastropods (Lesser et al., 1992), and polychaetes (Vedel and Riisgard, 1993). Previous observations such as by Glynn (1973) in a Caribbean coral reef, Moriarty et al. (1985) in Lizard Reef, GBR, Sorokin (1991) in Vietnam, and Wyatt et al. (2010) in Ningaloo Reef, highlight that the filtering out of phytoplankton and microbial communities from flowing water across reefs can be commonly seen. The lagoon areas typically have longer residence times, are deeper, and have fewer organisms, thus providing an environment where the phytoplankton can accumulate (Lowe and Falter, 2015; Pagano et al., 2017). This cross-reef pattern indicates that input of allochthonous phytoplankton from offshore can occur within different coral reefs, and can be one of the mechanisms by which reefs here in the West Philippine Sea obtain and retain nutrients in these low nutrient environments.

Interestingly, the mesozooplankton pattern was different from that of the phytoplankton. They were relatively more abundant in the fore reef and reef flat zones, but their distribution was also more variable. This can be due to differences in the planktivores and benthic suspension feeders present in the reefs. Different taxa feed on particular components of the plankton. Tunicates, sponges, and molluscs primarily incorporate dissolved organic matter (DOM), bacteria, and phytoplankton, whereas cnidarians also ingest zooplankton (Gili and Coma, 1998). Glynn (1973) also observed that diatoms were 31% more efficiently filtered out of the water column than zooplankton in a Puerto Rican reef. The distribution of mesozooplankton, particularly those of reef-associated or resident zooplankton, is also likely mediated by their swimming behavior (Emery, 1968; Ohlhorst, 1982). Increased abundances of zooplankton at the surface of a shallow back reef in Moorea, French Polynesia were attributed to their upward swimming behavior (Alldredge and King, 2009).

Potential Trophic Relationships Between Phytoplankton and Mesozooplankton

The C isotopic signature across the three reefs was similar even if there were differences in the phytoplankton assemblages between Sabina Shoal and Pag-asa Island. These differences were not enough to shift the δ^{13}C signatures, possibly since all three generally had abundant diatoms and cyanobacteria. There do appear to be variations in the nitrogen source for the reefs even within Pag-asa Island. Pag-asa Island transect 1 and Sabina Shoal have more enriched δ^{15}N that is potentially due to uptake of NOx from deeper upwelled waters (Loick et al., 2007; Michener and Kaufman, 2007; Henschke et al., 2015; Kürten et al., 2016). These

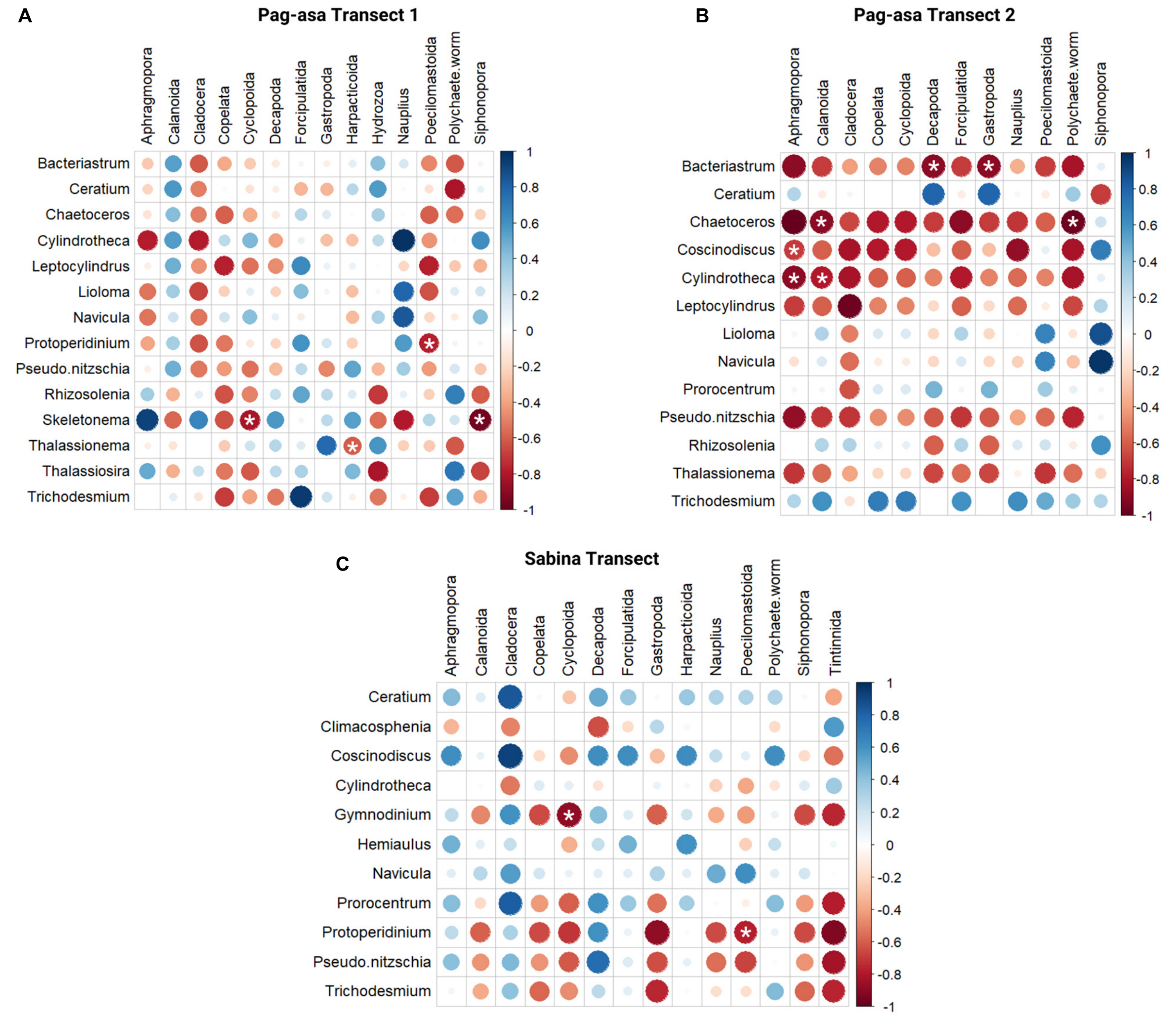

FIGURE 7 | Spearman's correlation between phytoplankton and zooplankton taxa per transect: **(A)** Pag-asa Transect 1, **(B)** Pag-asa Transect 2, and **(C)** Sabina Transect. Circles with a white asterisk are the only ones that are significant at $p < 0.05$.

transects had distinctly higher nutrient concentrations at the deeper portions up to the fore reef slope and mid-water column. Although for the Sabina Shoal transect, the stronger stratification possibly still limited the concentration, thus cell abundances were low. The more depleted δ^{15}N signature of Pag-asa transect 2 could then be due to the greater contribution of recycled nitrogen in the form of ammonium or urea under more oligotrophic conditions (Loick et al., 2007; Henschke et al., 2015).

There is a wide range of isotopic signatures observed in coral reefs even within the Pacific. For phytoplankton or POM, values from −22 to −18 δ^{13}C are measured on average (e.g., Yamamuro et al., 1995; Letourneur et al., 2013; Wyatt et al., 2013; Briand et al., 2015; and Fey et al., 2021), while for zooplankton values of −20.5 to −13 δ^{13}C on average (e.g., Yamamuro et al., 1995; Wyatt et al., 2013; and Fey et al., 2021). The δ^{15}N values are even wider at −0.14 for *Trichodesmium* at a New Caledonian reef (Briand et al., 2015) through 15 for phytoplankton at Marquesas (Fey et al., 2021). For zooplankton, δ^{15}N values ranging from about 5 to 17 on average have been observed on Pacific reefs (Yamamuro et al., 1995; Wyatt et al., 2013; Fey et al., 2021). The values obtained in this study lie within these typical observed values.

Mesozooplankton in the studied reefs likely have other food sources apart from phytoplankton since most of their δ^{13}C were depleted relative to the phytoplankton, and there were only a few signs of potential grazing interactions between them based on the correlations. The carbon isotopic composition of consumers is typically within ± 1‰ of their food source, with a small (about 0.5-1‰) enrichment (Peterson and Fry, 1987; Michener and Kaufman, 2007). Only three stations showed some level of ^{13}C enrichment where some areas in Pag-asa transect 1 and Sabina could have mesozooplankton

TABLE 1 | Phytoplankton and mesozooplankton isotope values of $\delta^{13}C$ and $\delta^{15}N$ (mean ± SD; ‰), sample size and average differences in $\delta^{13}C$ and $\delta^{15}N$ between mesozooplankton relative to phytoplankton per zone or transect.

Transect	Zone	Group	n	$\delta^{13}C$	$\delta^{15}N$	$\Delta\ \delta^{13}C$	$\Delta\ \delta^{15}N$
Pag-asa transect 1	Lagoon	Phytoplankton	1	−19.2	9.0		
		Mesozooplankton	1	−19.1	6.4	0.1	−2.5
	Back reef	Phytoplankton	1	−21.9	11.4		
		Mesozooplankton	1	−19.1	6.9	2.9	−4.5
	Reef flat	Phytoplankton	1	−20.1	9.6		
		Mesozooplankton	1	−21.2	6.5	−1.2	−3.1
	Fore reef	Phytoplankton	1	−23.9	5.6		
		Mesozooplankton	1	−34.7	2.8	−10.8	−2.9
	Offshore	Phytoplankton	2	−20.0 ± 0.7	8.7 ± 0.9		
		Mesozooplankton	4	−21.7 ± 6.6	4.2 ± 1.9	−1.7	−4.5
	Transect Average	Phytoplankton	6	−20.8 ± 1.8	8.8 ± 1.9		
		Mesozooplankton	8	−22.7 ± 6.9	4.8 ± 2.2	−1.8	−4.0
Pag-asa transect 2	Lagoon	Phytoplankton	1	−18.1	5.5		
		Mesozooplankton	1	−21.0	7.4	−2.9	1.9
	Back reef	Phytoplankton	1	−20.6	3.1		
		Mesozooplankton	1	−20.6	3.0	−0.1	−.1
	Fore reef	Phytoplankton	1	−17.5	5.3		
		Mesozooplankton	2	−20.6 ± 1.9	6.9 ± 2.9	−3.1	1.6
	Offshore	Phytoplankton	2	−19.2 ± 3.1	4.0 ± 0.2		
		Mesozooplankton	4	−21.1 ± 1.9	4.9 ± 2.4	−1.9	0.9
	Transect Average	Phytoplankton	5	−18.9 ± 2.0	4.4 ± 1.0		
		Mesozooplankton	8	−20.9 ± 1.9	5.5 ± 3.0	−2.0	1.1
Sabina transect	Reef flat	Phytoplankton	1	−22.1	7.4		
		Mesozooplankton	2	−22.5 ± 2.8	8.1 ± 4.2	−0.4	0.6
	Fore reef	Phytoplankton	2	−20.1 ± 2.5	7.7 ± 0.8		
		Mesozooplankton	4	−21.0 ± 2.8	7.0 ± 3.0	−0.9	−0.7
	Offshore	Phytoplankton	3	−20.5 ± 0.5	6.5 ± 0.5		
		Mesozooplankton	6	−18.9 ± 2.5	6.2 ± 3.8	1.5	−0.3
	Transect Average	Phytoplankton	6	−20.6 ± 1.4	7.1 ± 0.8		
		Mesozooplankton	12	−20.3 ± 2.9	6.8 ± 3.6	0.4	−0.3

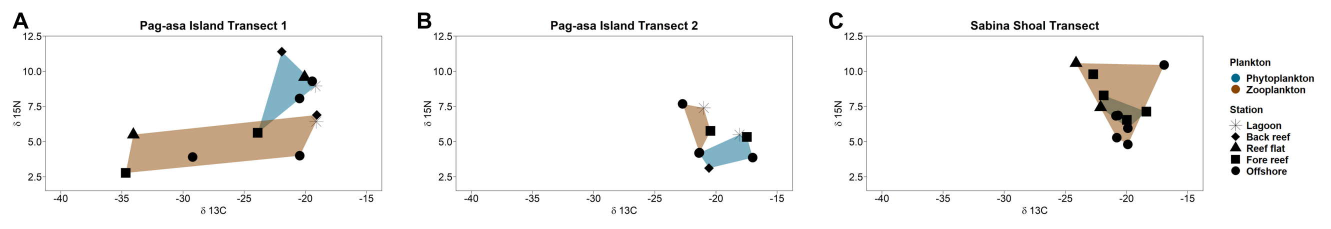

FIGURE 8 | $\delta^{15}N$: $\delta^{13}C$ biplot with convex hulls per transect: **(A)** Pag-asa Island Transect 1, **(B)** Pag-asa Island Transect 2, and **(C)** Sabina Shoal Transect. Symbols represent different reef zones. Blue-yellow hulls represent phytoplankton samples, while brown hulls represent mesozooplankton.

more directly linked to the phytoplankton through the grazing pathway. For the mesozooplankton in other areas and Pag-asa transect 2 in particular, the microbial and detrital pathways could be the main sources of food. Smaller components of the plankton (i.e., nanoplankton and picoplankton) have been found to significantly contribute to the productivity of coral reefs (Sorokin, 1995; Ferrier-Pagès and Gattuso, 1998; Wyatt et al., 2010). Mesozooplankton have broad and flexible feeding strategies. Picoplankton are grazed by mesozooplankton such as cladocerans (Lipej et al., 1997), rotifers (Sanders et al., 1989), barnacle larvae and larvaceans (Scheinberg et al., 2005; Vargas et al., 2006), and appendicularians (Gorsky et al., 1999). Pico-sized prey is generally viewed as inefficiently ingested by most mesozooplankton, including copepods, as exhibited by experiments using natural phytoplankton assemblages and culture set-ups (Frost, 1972), since they cannot be effectively retained by the grazer's feeding appendages (Kiørboe, 2011). However, field and laboratory studies have recently shown direct consumption of substantial concentrations of picoplankton by mesozooplankton (Wilson and Steinberg, 2010; Zhao et al., 2020). For instance, diet analysis exhibited the gut presence of *Synechococcus* in zooplankters, even in the presence of abundant alternative food sources (Motwani and Gorokhova, 2013). Picoplankton can form aggregates with detrital material and bacteria, thereby increasing accessibility to consumers (Heinle et al., 1977), and reports have now indicated that large zooplankton can also ingest relatively large quantities of picoplankton in the form of micro-colonies and loose agglomerates (Cruz and Neuer, 2019). Nanoplankton such as nanoflagellates are grazed on by marine cladocerans and veliger larvae (Katechakis and Stibor, 2004; Vargas et al., 2006). A mesocosm experiment by Uitto and Hällfors (1997) allowed the investigation of zooplankton grazing on nanoplankton. Meso- (copepods and cladocerans) and microzooplankton (mostly copepod nauplii) were able to ingest 3–70% and 1–6% of nanoplankton daily, with specific rates varying between 3 and 9% for mesozooplankton, and from 4 to 130% for microzooplankton. Increasing evidence from more recent research also revealed detrital remains of macrophytes and terrestrial plants can likewise contribute to organic matter and consequently subsidize the zooplankton diet (Harfmann et al., 2019; Tang et al., 2021). In this study, these smaller plankton were not sampled but could be contributing to the more depleted ^{13}C signature (Kukert and Riebesell, 1998; Rolff, 2000) as part of the microbial pathway. The other likely food source for zooplankton on these reefs is detrital material from dead plants, animals, feces, and other non-living organic material. The contribution of detritus to particulate organic carbon (POC) from different coral reefs in the Pacific range from 52 to 88% on average (Nakajima et al., 2017). In a coral reef in Okinawa, Japan, Nakajima et al. (2017) calculated the role of grazing and microbial food webs in sustaining the mesozooplankton community at an average of 38.7% and 37.2%, respectively, with the remaining amount filled in by detritus. These proportional contributions varied depending on the season, and in this study, the influence of these pathways could also shift depending on the reef zone and system.

The variations we have observed across and between reefs have been associated with the observed covariation in physico-chemical parameters, and possible biological interactions. However, other physical factors that we were unable to measure can also possibly influence the phytoplankton and mesozooplankton patterns. Local-scale circulation and the consequent advection of plankton can also contribute to their retention or dispersal in specific areas of the reef, and was, as mentioned above, one possible factor in the higher phytoplankton abundances observed in the lagoons (Lowe and Falter, 2015; Pagano et al., 2017). Tidal currents can impact the patterns of plankton abundances in reefs (Hamner et al., 2007). In this study though, we were unable to track the tides and sample across a spectrum of tides due to logistical constraints. We recommend that future work conduct longer observations, if possible, preferably with fixed stations across the reefs monitored for a variety of physico-chemical parameters, including hydrodynamic conditions. This would allow better resolution of the roles of different factors on the phytoplankton and zooplankton distributions and interactions.

Coral reefs are sentinel ecosystems that provide us with a slew of ecosystem services. Unfortunately, they are highly threatened by global and local stressors, most especially within the Coral Triangle biodiversity hotspot (Burke et al., 2012). Understanding the functioning and productivity of these ecosystems are important if we want to conserve better and manage them. Recent work has highlighted the significant role of pelagic subsidies in coral reef fish productivity (Skinner et al., 2021), despite declines in coral cover and lower topography (Morais and Bellwood, 2019). This also points to the potential influence of larger-scale oceanographic productivity variations on reefs. There has been very limited information in the Philippines, an archipelagic country, on the coupling of benthic reefs with the surrounding pelagic waters and tracing such trophic pathways. In this study, we present new information on the interaction of pelagic waters with offshore reefs through the phytoplankton and mesozooplankton communities. Spatially distinct patterns were apparent across reef zones and reef systems, likely mediated by water column conditions, filter-feeding of reef organisms as waters flow across the reefs, and mesozooplankton behavior. The phytoplankton on these reefs are also influenced by the different nutrient sources present. The trophic pathways for mesozooplankton in the reefs are possibly a combination of the grazing, microbial and detrital pathways, given that the stable isotope signatures and correlation analysis show limited signals from the direct grazing of the phytoplankton. More comprehensive sampling of different food web components and environmental conditions at different time points together with bulk and/or compound-specific stable isotopes (McMahon et al., 2016) would help provide a clearer picture of these trophic relationships. This first look into the interaction of pelagic plankton with coral reefs in the Philippines highlights the need to further explore the significance of pelagic contributions to the benthos across the different areas of the country, from offshore atolls to fringing reefs.

DATA AVAILABILITY STATEMENT

The raw data supporting the conclusions of this article will be made available by the authors, without undue reservation.

AUTHOR CONTRIBUTIONS

AY, GJ, and GA conceived of and designed the study. AY, GA, NG, and GJ conducted the field surveys. NM, GA, and NG conducted the laboratory analysis. AY, GA, NM, and NG analyzed the data and prepared the figures and tables. All authors contributed to writing and revising the manuscript.

FUNDING

This study was funded by the Philippine Department of Environment and Natural Resources through the program entitled "Coastal Assessment for Rehabilitation Enhancement: Capability Development and Resiliency of Ecosystems (CARE-CaDRES)". The Marine Science Institute, University of the Philippines provided partial support for the publication fee through the project entitled “Upgrading capacity, infrastructure, and assets for marine scientific research in the Philippines”.

ACKNOWLEDGMENTS

We thank Cesar Villanoy and the Physical Oceanography laboratory for organizing the research cruise, the Philippine Navy and the BRP Gregorio Velasquez (AGR 702) for the help in sample collection during the research expedition conducted in the Kalayaan Group of Islands in 2017. We also thank the Department of Science and Technology – Philippine Nuclear Research Institute for the collaboration in conducting the stable isotope analyses, John Kristoffer Q. Andres for identifying the zooplankton samples, and John Michael N. Aguilar for analyzing the samples for chemical parameters.

SUPPLEMENTARY MATERIAL

The Supplementary Material for this article can be found online at: https://www.frontiersin.org/articles/10.3389/fmars.2021.724504/full#supplementary-material

REFERENCES

Aliño, P. M., and Quibilan, M. C. C. (2003). *The Kalayaan Islands: Our Natural Heritage. Marine Science Institute*. Quezon City: University of the Philippines.

Alldredge, A. L., and King, J. M. (2009). Near-surface enrichment of zooplankton over a shallow back reef: implications for coral reef food webs. *Coral Reefs* 28, 895–908. doi: 10.1007/s00338-009-0534-4

Arceo, H. O., Cabasan, J. P., Luciano, R. M. A., Heyres, L. J. D., Mamauag, S. S., and Aliño, P. M. (2020). Estimating the potential fisheries production of three offshore reefs in the West Philippine Sea, Philippines. *Philipp. J. Sci.* 149, 647–658.

Basedow, S. L., De Silva, N. A. L., Bode, A., and Van Beusekorn, J. (2016). Trophic positions of mesozooplankton across the North Atlantic: estimates derived from biovolume spectrum theories and stable isotope analyses. *J. Plankton Res.* 38, 1364–1378. doi: 10.1093/plankt/fbw070

Basedow, S. L., Tande, K. S., and Zhou, M. (2009). Biovolume spectrum theories applied: spatial patterns of trophic levels within a mesozooplankton community at the polar front. *J. Plankton Res.* 32, 1105–1119. doi: 10.1093/plankt/fbp110

Briand, M. J., Bonnet, X., Goiran, C., Guillou, G., and Letourneur, Y. (2015). Major sources of organic matter in a complex coral reef lagoon: identification from isotopic signatures (δ13C and δ15N). *PLoS One* 10:e0131555. doi: 10.1371/journal.pone.0131555

Burke, L., Reytar, K., Spalding, M., and Perry, A. (2012). *Reefs At Risk Revisited in the Coral Triangle*. Washington, DC: World Resources Institute.

Carpenter, J. H. (1965). The chesapeake bay institute technique for the winkler dissolved oxygen method. *Limnol. Oceanogr.* 10, 141–143. doi: 10.4319/lo.1965.10.1.0141

Cruz, B. N., and Neuer, S. (2019). Heterotrophic bacteria enhance the aggregation of the marine picocyanobacteria *Prochlorococcus* and *Synechococcus*. *Front. Microbiol.* 10:1864. doi: 10.3389/fmicb.2019.01864

Emery, A. R. (1968). Preliminary observations on coral reef plankton 1. *Limnol. Oceanogr.* 13, 293–303.

Ferrier-Pagès, C., and Gattuso, J. P. (1998). Biomass, production and grazing rates of pico-and nanoplankton in coral reef waters (Miyako Island. Japan). *Microb. Ecol.* 35, 46–57. doi: 10.1007/s002489900059

Fey, P., Parravicini, V., Bãnaru, D., Dierking, J., Galzin, R., Lebreton, B., et al. (2021). Multi-trophic markers illuminate the understanding of the functioning of a remote, low coral cover Marquesan coral reef food web. *Sci. Rep.* 11, 1–14.

Frost, B. W. (1972). Effect of size and concentration of food particles on the feeding behavior of the marine planktonic copepod *Calanus finmarchicus*. *Limnol. Oceanogr.* 17, 805–815. doi: 10.4319/lo.1972.17.6.0805

Fry, B., and Sherr, E. B. (1984). δ13C Measurements as indicators of carbon flow in marine and freshwater ecosystems. *Contrib. Mar. Sci.* 27, 13–47.

Genin, A., Monismith, S. G., Reidenbach, M. A., Yahel, G., and Koseff, J. R. (2009). Intense benthic grazing of phytoplankton in a coral reef. *Limnol. Oceanogr.* 54, 938–951. doi: 10.4319/lo.2009.54.3.0938

Giering, S. L., Wells, S. R., Mayers, K. M. J., Schuster, H., Cornwell, L., Fileman, E. S., et al. (2019). Seasonal variation of zooplankton community structure and trophic position in the Celtic Sea: a stable isotope and biovolume spectrum approach. *Prog. Oceanogr.* 177:101943. doi: 10.1016/j.pocean.2018.03.012

Gili, J. M., and Coma, R. (1998). Benthic suspension feeders: their paramount role in littoral marine food webs. *Trends Ecol. Evol.* 13, 316–321. doi: 10.1016/s0169-5347(98)01365-2

Glynn, P. W. (1973). Ecology of a Caribbean Reef. The Porites reef flat biotope. II. Plankton community with evidence for depletion. *Mar. Biol.* 22, 1–21. doi: 10.1007/bf00388905

Gorsky, G., Chre ìtiennot-Dinet, M. J., Blanchot, J., and Palazzoli, I. (1999). Picoplankton and nanoplankton aggregation by appendicularians: Fecal pellet contents of *Megalocercus huxleyi* in the equatorial Pacific. *J. Geophys. Res. Oceans* 104, 3381–3390.

Gottfried, M., and Roman, M. R. (1983). Ingestion and incorporation of coral-mucus detritus by reef zooplankton. *Mar. Biol.* 72, 211–218. doi: 10.1007/bf00396825

Gruber, R. K., Lowe, R. J., and Falter, J. L. (2018). Benthic uptake of phytoplankton and ocean-reef exchange of particulate nutrients on a tide-dominated reef. *Limnol. Oceanogr.* 63, 1–17. doi: 10.1002/lno.10790

Hamner, W. M., Colin, P. L., and Hamner, P. P. (2007). Export-import dynamics of zooplankton on a coral reef in Palau. *Mar. Ecol. Prog. Ser.* 334, 83–92. doi: 10.3354/meps334083

Hamner, W. M., Jones, M. S., Carleton, J. H., Hauri, I. R., and Williams, D. (1998). Zooplankton, planktivorous fish, and water currents on a windward reef face: great Barrier Reef, Australia. *Bull. Mar. Sci.* 42, 459–479.

Harfmann, J., Kurobe, T., Bergamaschi, B., Teh, S., and Hernes, P. (2019). Plant detritus is selectively consumed by estuarine copepods and can augment their survival. *Sci. Rep.* 9:9076. doi: 10.1038/s41598-019-45503-6

Hearn, C., Atkinson, M., and Falter, J. (2001). A physical derivation of nutrient-uptake rates in coral reefs: effects of roughness and waves. *Coral Reefs* 20, 347–356.

Heinle, D. R., Harris, R. P., Ustach, J. F., and Flemer, D. A. (1977). Detritus as food for estuarine copepods. *Mar. Biol.* 40, 341–353. doi: 10.1007/bf00395727

Henschke, N., Everett, J. D., Suthers, I. M., Smith, J. A., Hunt, B. P. V., Doblin, M. A., et al. (2015). Zooplankton trophic niches respond to different water types of the western Tasman Sea: a stable isotope analysis. *Deep Sea Res. I* 104, 1–8. doi: 10.1016/j.dsr.2015.06.010

Hu, J., Kawamura, H., Hong, H., and Qi, Y. (2000). A review on the currents in the South China Sea: seasonal circulation, South China Sea warm current and Kuroshio intrusion. *J. Oceanogr.* 56, 607–624. doi: 10.1023/A:1011117531252

Jones, M. N. (1984). Nitrate reduction by shaking with cadmium: alternative to cadmium columns. *Water Re.* 18, 643–646. doi: 10.1016/0043-1354(84)90215-X

Katechakis, A., and Stibor, H. (2004). Feeding selectivities of the marine cladocerans Penilia avirostris, Podon intermedius and *Evadne nordmanni*. *Mar. Biol.* 145, 529–539.

Kiørboe, T. (2011). How zooplankton feed: mechanisms, traits and trade-offs. *Biol. Rev.* 86, 311–339. doi: 10.1111/j.1469-185X.2010.00148.x

Klumpp, D. W., Bayne, B. L., and Hawkins, A. J. S. (1992). Nutrition of the giant clam *Tridacna gigas* (L.). 1. Contribution of filter feeding and photosynthates to respiration and growth. *J. Exp. Mar. Biol. Ecol.* 155, 105–122.

Kukert, H., and Riebesell, U. (1998). Phytoplankton carbon isotope fractionation during a diatom spring bloom in a Norwegian fjord. *Mar. Ecol. Prog. Ser.* 173, 127–138.

Kürten, B., Al-Aidaroos, A. M., Kürten, S., El-Sherbiny, M. M., Devassy, R. P., Struck, U., et al. (2016). Carbon and nitrogen stable isotope ratios of pelagic zooplankton elucidate ecohydrographic features in the oligotrophic Red Sea. *Prog. Oceanogr.* 140, 69–90. doi: 10.1016/j.pocean.2015.11.003

Legendre, P., and Anderson, M. J. (1999). Distance-based redundancy analysis: testing multispecies responses in multifactorial ecological experiments. *Ecol. Monogr.* 69, 1–24.

Legendre, P., and Legendre, L. (2012). *Numerical Ecology*. Amsterdam: Elsevier.

Leichter, J. J., Alldredge, A. L., Bernardi, G., Brooks, A. J., Carlson, C. A., Carpenter, R. C., et al. (2013). Biological and physical interactions on a tropical island coral reef: transport and retention processes on Moorea, French Polynesia. *Oceanography* 26, 52–63. doi: 10.5670/oceanog.2013.45

Lesser, M. P. (2004). Experimental biology of coral reef systems. *J. Exp. Mar. Biol. Ecol.* 300, 217–252. doi: 10.1016/j.jembe.2003.12.027

Lesser, M. P., Shumway, S. E., Cucci, T., and Smith, J. (1992). Impact of fouling organisms on mussel rope culture: interspecific competition for food among suspension-feeding invertebrates. *J. Exp. Mar. Biol. Ecol.* 165, 91–102. doi: 10.1016/0022-0981(92)90291-h

Letourneur, Y., De Loma, T. L., Richard, P., Harmelin-Vivien, M. L., Cresson, P., Banaru, D., et al. (2013). Identifying carbon sources and trophic position of coral reef fishes using diet and stable isotope (δ 15 N and δ 13 C) analyses in two contrasted bays in Moorea, French Polynesia. *Coral Reefs* 32, 1091–1102.

Lipej, L., Mozetic, P., Turk, V., and Malej, A. (1997). The trophic role of the marine cladoceran *Penilia avirostris* in the Gulf of Trieste. *Hydrobiologia* 360, 197–203.

Loick, N., Dippner, J., Doan, H. N., Liskow, I., and Voss, M. (2007). Pelagic nitrogen dynamics in the Vietnamese upwelling area according to stable nitrogen and carbon isotope data. *Deep Sea Res. Part I* 54, 596–607. doi: 10.1016/j.dsr.2006.12.009

Lowe, R. J., and Falter, J. L. (2015). Oceanic forcing of coral reefs. *Annu. Rev. Mar. Sci.* 7, 43–66. doi: 10.1146/annurev-marine-010814-015834

Mayal, E. M., Neumann-Leitao, S., Feitosa, F., Schwamborn, R., Silva, T., and da Silva-Cunha, M. (2009). Hydrology, plankton, and corals of the Maracajaú reefs (Northeastern Brazil) - an ecosystem under severe thermal stress. *Braz. Arch. Biol. Technol.* 52, 665–678. doi: 10.1590/S1516-89132009000300019

McMahon, K. W., Thorrold, S. R., Houghton, L. A., and Berumen, M. L. (2016). Tracing carbon flow through coral reef food webs using a compound-specific stable isotope approach. *Oecologia* 180, 809–821. doi: 10.1007/s00442-015-3475-3

Michener, R. H., and Kaufman, L. (2007). Stable isotope ratios as tracers in marine food webs: an update. *Stable Isotopes Ecol. Environ. Sci.* 2, 238–282. doi: 10.1002/9780470691854.ch9

Morais, R. A., and Bellwood, D. R. (2019). Pelagic subsidies underpin fish productivity on a degraded coral reef. *Curr. Biol.*29, 1521–1527. doi: 10.1016/j.cub.2019.03.044

Morales, A. R., and Murillo, M. M. (1996). Distribution, abundance and composition of coral reef zooplankton, Cahuita National Park, Limon, Costa Rica. *Rev. Biol. Trop.* 44, 619–630.

Moriarty, D. J. W., Pollard, P. C., and Hunt, W. G. (1985). Temporal and spatial variation in bacterial production in the water column over a coral reef. *Mar. Biol.* 85, 285–292.

Morillo-Velarde, P. S., Briones-Fourzan, P., Alvarez-Filip, L., Aguiniga-Garcia, S., Sanchez-Gonzalez, A., and Lozano-Alvarez, E. (2018). Habitat degradation alters trophic pathways but not food chain length on shallow Caribbean coral reefs. *Nat. Sci. Rep.* 8, 1–12. doi: 10.1038/s41598-018-22463-x

Motwani, N. H., and Gorokhova, E. (2013). Mesozooplankton grazing on picocyanobacteria in the Baltic Sea as inferred from molecular diet analysis. *PLoS One* 8:e79230. doi: 10.1371/journal.pone.0079230

Nakajima, R., Nakatomi, N., Kurihara, H., Fox, M. D., Smith, J. E., and Okaji, K. (2016). Crown-of-thorns starfish larvae can feed on organic matter released from corals. *Diversity* 8:18.

Nakajima, R., Yamazaki, H., Lewis, L., Khen, A., Smith, J., Nakatomi, N., et al. (2017). Planktonic trophic structure in a coral reef ecosystem – grazing versus microbial food webs and the production of mesozooplankton. *Prog. Oceanogr.* 156, 104–120. doi: 10.1016/j.pocean.2017.06.007

Ohlhorst, S. L. (1982). Diel migration patterns of demersal reef zooplankton. *J. Exp. Mar. Biol. Ecol.* 60, 1–15. doi: 10.1016/0022-0981(81)90176-3

Ong, P. S., Afuang, L. E., and Rosell-Ambal, R.G. (eds.) (2002). *Philippine Biodiversity Conservation Priorities: A Second Iteration of the National Biodiversity Strategy and action Plan*. Quezon City: Department of Environment and Natural Resources, 113.

Pagano, M., Rodier, M., Guillaumot, C., Thomas, Y., Henry, K., and Andréfouët, S. (2017). Ocean-lagoon water and plankton exchanges in a semi-closed pearl farming atoll lagoon (Ahe, Tuamotu archipelago, French Polynesia). *Estuar. Coast. Shelf Sci.* 191, 60–73. doi: 10.1016/j.ecss.2017.04.017

Perkins, M. J., McDonald, R. A., van Veen, F. J. F., Kelley, S., Rees, G., and Bearhop, S. (2014). Application of nitrogen and carbon stable isotopes (δ 15N and δ 13C) to quantify food chain length and trophic structure. *PLoS One* 9:e0093281. doi: 10.1371/journal.pone.0093281

Peterson, B. J., and Fry, B. (1987). Stable isotopes in ecosystem studies. *Annu. Rev. Ecol. Syst.* 18, 293–320.

Popp, B. N., Graham, B. S., Olson, R. J., Hannides, C. C. S., Lott, M. J., Lopez-Ibarra, G. A., et al. (2007). "Insight into the trophic ecology of yellowfin tuna, *Thunnus albacares*, from compound-specific nitrogen isotope analysis of proteinaceous amino acids," in *Stable Isotopes as Indicators of Ecological Change*, eds T. Dawson and R. Siegwolf (Amsterdam: Elsevier Academic Press), 173–190. doi: 10.1016/s1936-7961(07)01012-3

Post, D. M. (2002). Using stable isotopes to estimate trophic position: models, methods, and assumptions. *Ecology* 83, 703–718. doi: 10.1111/j.1095-8649.2012.03251.x

Protocols for the Joint Global Ocean Flux Study (JGOFS) (1994). *Core Measurements. Intergovernmental Oceanographic Commission. Scientific Committee on Oceanic Research, Manual and Guides 29*. Paris: JGOFS, 97–100.

Rolff, C. (2000). Seasonal variation in δ13C and δ15N of size-fractionated plankton at a coastal station in the northern Baltic proper. *Mar. Ecol. Prog. Ser.* 203, 47–65.

Roman, M. R., Furnas, M. J., and Mullin, M. M. (1990). Zooplankton abundance and grazing at Davies Reef, Great Barrier Reef, Australia. *Mar. Biol.* 105, 73–82. doi: 10.1007/bf01344272

San Diego-McGlone, M. L., Jacinto, G. S., Dupra, V. C., Narcise, I. S., Padayao, D. O., and Velasquez, I. B. (1999). A comparison of nutrient characteristics and primary productivity in the Sulu Sea and South China Sea. *Acta Oceanogr. Taiwanica* 37, 219–229.

Sanders, R. W., Porter, K. G., Bennet, S. J., and DeBiase, A. E. (1989). Seasonal patterns of bacterivory by flagellates, ciliates, rotifers and cladocerans in a freshwater plankton community. *Limnol. Oceanogr.* 34, 673–687. doi: 10.4319/lo.1989.34.4.0673

Scheinberg, R. D., Landry, M. R., and Calbet, A. (2005). Grazing of two common appendicularians on the natural prey assemblage of a tropical coastal ecosystem. *Mar. Ecol. Prog. Ser.* 294, 201–212. doi: 10.3354/meps294201

Skinner, C., Mill, A. C., Fox, M. D., Newman, S. P., Zhu, Y., Kuhl, A., et al. (2021). Offshore pelagic subsidies dominate carbon inputs to coral reef predators. *Sci. Adv.* 7, 1–13. doi: 10.1126/sciadv.abf3792

Sorokin, Y. I. (1991). Parameters of productivity and metabolism of coral reef ecosystems off central Vietnam. *Est. Coast Shelf Sci.* 33, 259–280. doi: 10.1016/0272-7714(91)90056-H

Sorokin, Y. I. (1995). Role of plankton in the turnover of organic matter on the Great Barrier Reef, Australia. *Hydrobiologia* 308, 35–44. doi: 10.1007/bf00037785

Strickland, J. D. H., and Parsons, T. R. (1972). *A Practical Handbook of Seawater Analysis. Fisheries Research Board of Canada Bulletin 167*. Ottawa, ON: Fisheries Research Board of Canada.

Tang, Y., Zhou, D., Su, L., Liu, Z., Zhang, X., and Dumont, H. J. (2021). *Vallisneria natans* detritus supports *Daphnia magna* somatic growth and reproduction under addition of periphyton. *Aquat. Ecol.* 55, 579–588. doi: 10.1007/s10452-021-09846-5

Tayasu, I., Hirasawa, R., Ogawa, N. O., Ohkouchi, N., and Yamada, K. (2011). New organic reference materials for carbon-and nitrogen-stable isotope ratio measurements provided by Center for Ecological Research, Kyoto University, and Institute of Biogeosciences, Japan Agency for Marine-Earth Science and Technology. *Limnology* 12, 261–266. doi: 10.1007/s10201-011-0345-5

Tomas, C. R. (1997). *Identifying Marine Phytoplankton. Florida Department of Environmental Protection*. St. Petersburg, FL: Florida Marine Research Institute.

Uitto, A., and Hällfors, S. (1997). Grazing by mesozooplankton and metazoan microplankton on nanophytoplankton in a mesocosm experiment in the northern Baltic. *J. Plankton Res.* 19, 655–673. doi: 10.1093/plankt/19.6.655

Vander Zanden, M. J., Casselman, J. M., and Rasmussen, J. B. (1999). Stable isotope evidence for the food web consequences of species invasions in lakes. *Nature* 401, 464–467. doi: 10.1371/journal.pone.0211870

Vander Zanden, M. J., and Rasmussen, J. B. (1999). Primary consumer δ13C and δ15N and the trophic position of aquatic consumers. *Ecology* 80, 1395–1404. doi: 10.1890/0012-9658(1999)080[1395:pccana]2.0.co;2

Vargas, C. A., Manríquez, P. H., and Navarrete, S. A. (2006). Feeding by larvae of intertidal invertebrates: assessing their position in pelagic food webs. *Ecology* 87, 444–457. doi: 10.1890/05-0265

Vedel, A., and Riisgard, H. U. (1993). Filter-feeding in the polychaete *Nereis diversicolor*: growth and bioenergetics. *Mar. Ecol. Prog. Ser.* 100, 145–152. doi: 10.3354/meps100145

Villanoy, C. L., and Jacinto, G. S. (2017). *Component 1. Oceanography of KIG in Predicting Responses Between Ocean Transport and Ecological Connectivity of Threatened Ecosystems in the West Philippine Sea (PROTECT WPS) Terminal Report*. Quezon City: Marine Science Institute of the University of the Philippines (UP MSI), 137.

Wilson, S. E., and Steinberg, D. K. (2010). Autotrophic picoplankton in mesozooplankton guts: evidence of aggregate feeding in the mesopelagic zone and export of small phytoplankton. *Mar. Ecol. Prog. Ser.* 412, 11–27. doi: 10.3354/meps08648

Winkler, L. W. (1888). Die Bestimmung des in Wasser gelösten Sauerstoffen. *Berichte Deutschen Chem. Gesellschaft* 21, 2843–2855.

Wyatt, A. S., Lowe, R. J., Humphries, S., and Waite, A. M. (2010). Particulate nutrient fluxes over a fringing coral reef: relevant scales of phytoplankton production and mechanisms of supply. *Mar. Ecol. Prog. Ser.* 405, 113–130. doi: 10.3354/meps08508

Wyatt, A. S., Lowe, R. J., Humphries, S., and Waite, A. M. (2013). Particulate nutrient fluxes over a fringing coral reef: source-sink dynamics inferred from carbon to nitrogen ratios and stable isotopes. *Limnol. Oceanogr.* 58, 409–427. doi: 10.4319/lo.2013.58.1.0409

Wyrtki, K. (1961). The thermohaline circulation in relation to the general circulation in the oceans. *Deep Sea Res.* 8, 39–64. doi: 10.1016/0146-6313(61)90014-4

Yahel, G., Post, A. F., Fabricius, K. D. M., Vaulot, D., and Genin, A. (1998). Phytoplankton distribution and grazing near coral reefs. *Limnol. Oceanogr.* 43, 551–563. doi: 10.4319/lo.1998.43.4.0551

Yamamuro, M., Kayanne, H., and Minagawao, M. (1995). Carbon and nitrogen stable isotopes of primary producers in coral reef ecosystems. *Limnol. Oceanogr.* 40, 617–621.

Zhang, Y., and Yin, K. (2015). "Fish catch and nutrient limitation in the South China Sea," in *Proceedings of the International Conference on Plant, Marine and Environmental Sciences (PMES-2015) Jan. 1-2, 2015 Kuala Lumpur*, (Malaysia), doi: 10.15242/IICBE.C0115030

Zhao, Y., Dong, Y., Li, H., Shiquan, L., Huang, L., Xiao, T., et al. (2020). Grazing by microzooplankton and copepods on the microbial food web in spring in the Southern Yellow Sea, China. *Mar. Life Sci. Technol.* 2, 442–455. doi: 10.1007/s42995-020-00047-x

Conflict of Interest: The authors declare that the research was conducted in the absence of any commercial or financial relationships that could be construed as a potential conflict of interest.

frontiers in Marine Science

ORIGINAL RESEARCH
published: 04 February 2022
doi: 10.3389/fmars.2021.767024

Global Mass Spectrometric Analysis Reveals Chemical Diversity of Secondary Metabolites and 44-Methylgambierone Production in Philippine *Gambierdiscus* Strains

Zabrina Bernice L. Malto[1], Garry A. Benico[1,2], Jeremiah D. Batucan[1], James Dela Cruz[3], Marc Lawrence J. Romero[3], Rhodora V. Azanza[1] and Lilibeth A. Salvador-Reyes[1]*

[1] Marine Science Institute, University of the Philippines-Diliman, Quezon City, Philippines, [2] Department of Biological Sciences, Central Luzon State University, Science City of Muñoz, Philippines, [3] Bureau of Fisheries and Aquatic Resources, Quezon City, Philippines

Edited by:
Yehuda Benayahu,
Tel Aviv University, Israel

Reviewed by:
Richard J. Lewis,
The University of Queensland, Australia
Allan Patrick Macabeo,
University of Santo Tomas, Philippines

****Correspondence:***
Lilibeth A. Salvador-Reyes
lsreyes@msi.upd.edu.ph

Specialty section:
This article was submitted to Marine Biology, a section of the journal Frontiers in Marine Science

Received: *30 August 2021*
Accepted: *13 December 2021*
Published: *04 February 2022*

Citation:
Malto ZBL, Benico GA, Batucan JD, Dela Cruz J, Romero MLJ, Azanza RV and Salvador-Reyes LA (2022) Global Mass Spectrometric Analysis Reveals Chemical Diversity of Secondary Metabolites and 44-Methylgambierone Production in Philippine Gambierdiscus Strains. Front. Mar. Sci. 8:767024. doi: 10.3389/fmars.2021.767024

Surveillance and characterization of emerging marine toxins and toxigenic dinoflagellates are warranted to evaluate their associated health risks. Here, we report the occurrence of the ciguatera poisoning-causative dinoflagellate *Gambierdiscus balechii* in the Philippines. Toxin production and chemical diversity of secondary metabolites in *G. balechii* GtoxSAM092414, *G. balechii* Gtox112513, and the recently reported *Gambierdiscus carpenteri* Gam1BOL080513 were assessed using targeted and untargeted UPLC-MS/MS analysis and radioligand receptor-binding assay (RBA). 44-methylgambierone was produced by all three strains, *albeit* with different levels based on RBA and UPLC-HRMS/MS analysis. The fatty acid composition was similar in all strains, while subtle differences in monosaccharide content were observed, related to the collection site rather than the species. Molecular networking using the GNPS database identified 45 clusters belonging to at least ten compound classes, with terpene glycosides, carbohydrate conjugates, polyketides, and macrolides as major convergence points. Species-specific peptides and polyhydroxylated compounds were identified in *G. balechii* GtoxSAM092414 and *G. carpenteri* Gam1BOL080513, respectively. These provide a glimpse of the uncharacterized biosynthetic potential of benthic dinoflagellates and highlight the intricate and prolific machinery for secondary metabolites production in these organisms.

Keywords: *Gambierdiscus carpenteri*, *Gambierdiscus balechii*, ciguatera fish poisoning, marine toxins, dinoflagellates, secondary metabolites, 44-methylgambierone

INTRODUCTION

Ciguatera poisoning (CP) is one of the most common foodborne diseases associated with seafood consumption globally, having approximately 10,000–50,000 cases annually (Dickey and Plakas, 2010; Friedman et al., 2017; World Health Organization, 2020). Since 1988, 123 and 274 confirmed and suspected cases of CP, respectively, have been reported in the Philippines (Yñiguez et al., 2021).

A survey of reef fishes from the Visayan and Sibuyan Seas in the Philippines showed that 4.46% were positive for ciguatoxins based on a mouse bioassay (Montojo et al., 2020). The limited surveillance of CP-causative organisms and associated toxins may contribute to underreporting of CP cases in the Philippines.

Benthic dinoflagellates belonging to the genera *Gambierdiscus*, *Coolia*, and *Fukuyoa* are recognized as the toxin producers linked to CP (Berdalet and Tester, 2018; Murray et al., 2020). Grazing by invertebrates and herbivorous fishes allows the benthic dinoflagellates and toxins to enter the food chain (Munday et al., 2017; Holmes et al., 2021). While fishes are the main vectors of CP, mollusks, crustaceans, and echinoderms are also linked to CP (Munday et al., 2017; Holmes et al., 2021).

The associated symptoms of CP, such as gastrointestinal, neurological, and cardiovascular symptoms and paradoxical dysesthesia (temperature reversal) (Bagnis et al., 1979), can be traced to the cellular effects of ladder-shaped polyether toxins collectively called ciguatoxins (CTX). CTX are lipophilic molecules that biotransform and bioaccumulate in fish. To date, more than 50 CTX analogs have been identified from fishes and benthic dinoflagellates, grouped as Pacific (P-CTX), Caribbean (C-CTX), and Indian (I-CTX) (Soliño and Costa, 2018; Chinain et al., 2020). CTX are potent activators of voltage-gated sodium channels and show significant toxicity in mice when given orally (Holmes et al., 2021).

Another class of toxins in benthic dinoflagellates is the water-soluble maitotoxins (MTX) that accumulate in the fishes' digestive tract and liver. The presence of at least one sulfate moiety in the MTX backbone leads to significant hydrophilicity of these toxins and low bioaccumulation in fish flesh. MTX are the most potent marine toxins known to date, although MTX has lower toxicity compared to CTX via an oral route (Shmukler and Nikishin, 2017). The low oral bioavailability and bioaccumulation of MTX suggest that these compounds are not the main contributor to CP symptomatology (Holmes et al., 2021). To date, there are seven known MTX analogs, and their biological activity is varied (Estevez et al., 2020a, 2021). MTX-1, MTX-2, and MTX-4 cause massive Ca^{2+} influx leading to cell death (Estevez et al., 2020a). MTX-3 causes a similar phenotype to CTX, although with lower potency (Boente-Juncal et al., 2019).

Among the MTX congeners, only MTX-1 have an assigned structure based on mass spectrometry (MS) and nuclear magnetic resonance (NMR) spectroscopy. MTX-1 is the largest non-peptide toxin identified, with a molecular weight of 3425 Da, with 32 cyclic ether rings (Nonomura et al., 1996; Sasaki et al., 1996; Shmukler and Nikishin, 2017). Structural analysis of MTX-3 showed that it is smaller than MTX-1, with a mass of 1039 Da (Holmes and Lewis, 1994). Several groups undertook a targeted purification of MTX-3 to determine the structure. The purified material was analyzed by NMR and MS and indicated that MTX-3 is the 44-methyl analog of gambierone (Boente-Juncal et al., 2019; Murray et al., 2019). The difference in bioactivity, approximately 1,000-fold lower potency of 44-methylgambierone than the original data for partially purified MTX-3, may indicate a potential divergence in structure between MTX-3 and 44-methylgambierone (Holmes et al., 2021). Holmes and Lewis (1994) observed a potent toxic effect of partially purified MTX-3 when administered intraperitoneally in mice (Holmes and Lewis, 1994; Lewis et al., 1994). Purified 44-methylgambierone had lower toxicity, with LD_{50} of 20–38 mg/kg via intraperitoneal administration (Murray et al., 2020). Additional studies are necessary to ascertain the divergence in biological activity and structure between MTX-3 and 44-methylgambierone.

The complex structure of CTX and MTX and the limited biomass of dinoflagellate producers make the complete structural assignment and biological activity assessment of these toxins challenging. Several groups have implemented hyphenated liquid chromatography-mass spectrometry (LC-MS) to aid in toxin discovery. By using an LC-MS-based workflow, it is easier to screen extracts of benthic dinoflagellates for potential new congeners, and known CTX and MTX can be quantified and identified (Caillaud et al., 2010 and references cited therein; Chinain et al., 2010; Munday et al., 2017; Longo et al., 2019; Estevez et al., 2020a, 2021; Murray et al., 2020; Tibiriçá et al., 2020; Gago-Martínez et al., 2021 and references cited therein; Mudge et al., 2021). UPLC-HRMS profiling of 252 marine microalgae belonging to 32 genera showed that 44-methylgambierone production is ubiquitous in eight *Gambierdiscus* species (Murray et al., 2020). The benthic dinoflagellate *Coolia* and *Fukuyoa* were likewise producers of 44-methylgambierone (Murray et al., 2020), with a putative new analog likely to be present in *Coolia* (Tibiriçá et al., 2020). While 44-methylgambierone has low toxicity via the oral route, UPLC-HRMS quantitation showed significant amounts in the producer dinoflagellate and snappers, suggesting potential contributions to CP. The intracellular concentration of 44-methylgambierone in *Gambierdiscus* sp. is 5.8–74 pg MTX-1 eq $cell^{-1}$ (Longo et al., 2019), while bioaccumulation in snapper liver and muscles can increase the concentration (Kohli et al., 2014).

Apart from MTX and CTX, other compounds identified from CP-causative organisms include gambierone (Rodríguez et al., 2015), gambieroxide (Watanabe et al., 2013), gambierol (Satake et al., 1993), gambieric acids (Nagai et al., 1992), and the recently identified 29-methylgambierone (Mudge et al., 2021) and sulfo-gambierones (Yon et al., 2021). *Gambierdiscus* has the potential to produce compounds belonging to other molecular scaffolds, such as non-ribosomal peptide-polyketide hybrid compounds based on recent transcriptome profiling (Kohli et al., 2017; Van Dolah et al., 2020). The realization of the biosynthetic potential of *Gambierdiscus* has, however, yet to be established at the metabolome level.

Capitalizing on the improved methodology for mass spectrometry, untargeted metabolite analysis has become a mainstay tool to analyze chemical diversity in organisms. The Global Natural Products Social Molecular Networking Platform (GNPS) is based on spectral alignment to assess the similarities and relationships among molecules (Wang et al., 2016) and visualized using a molecular network. While GNPS is mainly used for biodiscovery of natural products (Teta et al., 2015; Naman et al., 2017; Ding et al., 2018; Via et al., 2018), it has been recently applied to dinoflagellate metabolites and demonstrated the unique metabolites from these organisms (Fiorini et al., 2020; Wu et al., 2020; Sibat et al., 2021). Molecular networking of five *Dinophysis* species identified the characteristic toxin profile for each strain and identified five new putative pectenotoxins (Sibat et al., 2021). Differences in the metabolites of *Pseudo-nitzchia* during the reproductive stages were evident from the GNPS-based analysis (Fiorini et al., 2020). Compounds with unprecedented chemical scaffolds in *Pseudo-nitzchia* extracts, not represented in reference databases, were observed (Fiorini et al., 2020). Improved qualitative and quantitative screening of okadaic acid and dinophysistoxins was achieved through molecular networking of extracts from *Prorocentrum lima* (Wu et al., 2020). New esters of okadaic acid and dinophysistoxins were also identified (Wu et al., 2020). A scientometric analysis on dinoflagellates research recommended using metabolite databases such as Dictionary of Natural Products, AntiBase, MassBank, and GNPS to share metabolites information to advance biomolecule discovery (Oliveira et al., 2020).

In this study, we looked at the biosynthetic potential of *Gambierdiscus carpenteri* and two *Gambierdiscus balechii* strains from the Philippines to produce toxins and other classes of secondary metabolites using high resolution mass spectrometry (HRMS) and the GNPS molecular networking platform. We probed the chemistry of the three *Gambierdiscus* strains and obtained insights into the production of ladder-shaped polyether toxins and other classes of compounds.

MATERIALS AND METHODS

Culture Condition and Morphological Observation

Three monoclonal cultures of *Gambierdiscus* spp. from The Marine Science Institute Red Tide Laboratory were used in this study (**Table 1**). Cultures were routinely maintained in filtered natural seawater (30 psu) supplemented with full strength IMK medium (WAKO, Tokyo, Japan) at 25 ± 2°C under 100 μmol photons m^{-2} s^{-1} of light using 40 W white fluorescent lamps, with a 12:12 h light:dark photoperiod. Large-scale 1-L cultures in Fernbach flasks were harvested after 21 days in the exponential phase by centrifugation at 4,000 × *g* for 15 min at 4°C (Thermo Fisher Scientific).

Cells of *G. balechii* GtoxSAM092414 and *G. balechii* Gtox112513 were observed with a Zeiss Axioskop 2 (Carl Zeiss, Göttingen, Germany) light microscope (LM). To visualize the thecal plates, cells were stained with Calcofluor white [5 μL, 10 × final concentration (Sigma-Aldrich)] and observed under a confocal laser scanning microscope (CLSM 710, Carl Zeiss, München Germany) at 420 nm wavelength. Autofluorescence of chloroplast was also observed using CLSM 710. Photos were taken with a Zeiss Axiocam MRm and processed using Zeiss Efficient Navigation (ZEN) software (Carl Zeiss, München Germany). Cell and thecal plate dimensions were measured from LM and CLSM micrographs. The modified Kofoidian tabulation system (Kofoid, 1909) described by Besada et al. (1982) was followed in naming the thecal plates of *Gambierdiscus*. These were compared to the previously identified *G. carpenteri* Gam1BOL080513 from Bolinao, Philippines (Vacarizas et al., 2018).

TABLE 1 | Cultures of *Gambierdiscus* used in this study.

Species	Strain	Location	Coordinates	Date of isolation	GenBank accession number
G. carpenteri	Gam1BOL 080513	Bolinao, Pangasinan	16°23′22″N 119°54′36 E	August 2013	MW658841
G. balechii	Gtox112513	Bolinao, Pangasinan	16°25′20″N 119°57′9″E	November 2013	OL437111
G. balechii	GtoxSAM 092414	Guiuan, Eastern Samar	11°1′26″N 125°43′34″E	September 2014	OL437112

Molecular Analyses

Genomic DNA was extracted from exponentially growing cultures using ISOLATE II Plant DNA Kit (Bioline, London, United Kingdom) following the manufacturer's procedure. The D8–D10 region of large subunit ribosomal DNA (LSU rDNA) gene was amplified using the primers D8F and D10R (Litaker et al., 2009). Amplification was conducted in 50 μL reaction mix containing 45 μL of PCR supermix (Invitrogen, California, United States), 2 μL of each primer and 1 μL of template DNA. The thermal condition of PCR was as follows: initial denaturation step at 95°C for 2 min, followed by 35 cycles of 94°C for 30 s, 60°C for 2 min, and 72°C for 60 min, and finally an elongation step of 72°C for 5 min. Reaction was performed in a T100 Thermal cycler (Biorad, California, United States). Amplicons were purified using QIAquick Gel Purification Kit (Qiagen) and sent to 1st Base (Malaysia) for sequencing.

DNA sequences were aligned using MAFFT v7.110 (Katoh and Standley, 2013) with taxa downloaded from GenBank. The multiple sequences were manually edited and/or trimmed using BioEdit Sequence Alignment Editor v7.2.5 (Hall, 1999) with 58 selected taxa of *Gambierdiscus* comprising 17 species. For outgroups, four *Fukuyoa* spp., two *Alexandrium* spp., *Akashiwo sanguinea* and *Prorocentrum micans* were used. Maximum likelihood (ML) analysis was performed using PhyML (Guindon et al., 2010) with 500 bootstrap replicates. The best fitting substitution model for the ML tree as selected by the Smart Model Selection (SMS) program (Lefort et al., 2017) was general time reversible (GTR) with gamma distribution ($G = 0.301$) plus proportion of invariable sites ($I = 0.881$). Bayesian inference (BI) was computed via MrBayes v3.1.2 (Ronquist and Huelsenbeck, 2003) using a Metropolis-coupled Markov chain Monte Carlo run for 10 million generations with sampling at every 100 iterations. The best-fit substitution model for the BI tree, selected by jModelTest 2.1.10 (Darriba et al., 2012), was TIM3 + G (0.899) + I (0.3000). GenBank accession numbers are provided in the phylogenetic trees.

Chemical Extraction

Gambierdiscus isolates were extracted according to the procedure of Murata et al. (1990). Lyophilized biomass from 1 L cultures were extracted using three volumes of acetone to yield the crude extracts. A portion of the crude extract (20.0 mg) was further fractionated on a Florisil® SPE-cartridge and eluted with 4:1 n-hexane:acetone (fraction A), 9:1 acetone:methanol (fraction B), and 1:1 acetone:methanol (fraction C). Fractions were dried and stored at −20°C until further analysis.

Toxicity Assessment

Dried crude extracts were resuspended in methanol and subjected to radioligand receptor-binding assay (RBA) based on the IAEA-Tecdoc-1729 for the detection of ciguatera toxins (IAEA, 2013). The test kit for RBA consisting of tritium-labeled brevetoxin-3 ([^{3}H]PbTx-3), unlabeled PbTx-3 and porcine brain membrane was acquired from American Radiolabeled Chemicals. A 15 nM working solution of [^{3}H]PbTx-3 was prepared by diluting with the assay buffer. Solutions of unlabeled PbTx-3, with final assay concentrations of 0.01 ng/mL to 1.0 μg/mL in half-log dilutions, were prepared for the CTX calibration curve. The assay was performed in a 96-well microtiter filter plate with FB glass fiber filter (0.65 μm pore size) by adding the following solutions in order: 35 μL assay buffer, 35 μL PbTx-3 standard solutions or extracts, 35 μL [^{3}H]PbTx-3 working solution, and 105 μL porcine membrane homogenates. Plates were covered and incubated at 4°C for 1 h, filtered using a vacuum manifold and washed with 200 μL ice-cold assay buffer (2 ×). A 50 μL aliquot of the scintillation cocktail (OptiPhase, PerkinElmer) was added to each well and the reaction plate was further incubated for 1 h at room temperature. Plates were counted using a microplate scintillation counter (MicroBeta®, PerkinElmer). Curve fitting of the PbTx-3 standards was performed using a four-parameter logistic fit (Sigmoidal, 4PL) with variable slope. Limit of detection for the assay was 2.0×10^{-5} g PbTx-3 eq./g. Results are presented as pg PbTx-3 eq./cell by normalizing the acquired RBA values to the total cell counts of the cultures.

Chemical Analyses

Carbohydrate Extraction and Analysis

Gambierdiscus biomass was subjected to a two-stage sulfuric acid extraction according to the method of Templeton et al. (2012) to yield the total carbohydrates. The hydrolyzed carbohydrates were identified and quantified using the method of Schulze et al. (2017) with modifications. Monosaccharides were separated using an Acquity UPLC BEH Amide column, 1.7 μm, 2.1 × 50 mm (Waters) by a gradient program of acetonitrile/5 mM ammonium formate in water (both with 0.1% formic acid modifier): 90–75% acetonitrile for 8.5 min, and 75% acetonitrile for 4 min. Detection was done by multiple reaction monitoring (MRM) analysis (Shimadzu LCMS-8040). The optimized transitions for each standard are provided in **Supplementary Table 1**.

Data analysis was performed through manual peak integration using LabSolution (Shimadzu). Individual monosaccharide standards (Sigma) were prepared (0.156 μg/mL to 0.0098 μg/mL) in two-fold serial dilutions and injected three times for repeatability to generate the external calibration curves. Results are presented as % w/w (mg sugar/mg biomass), based on two biological replicates with three technical replicates each.

Lipid Extraction and Analysis

Solid-liquid extraction of the *Gambierdiscus* biomass was done according to the method of Bligh and Dyer (1959) to yield the chloroform soluble lipid extract. Fatty acid methyl esters (FAMEs) were prepared based on the AOAC official method 969.33 (AOAC, 2000b). Resulting FAMEs were separated and analyzed using gas chromatography with flame ionization detector (Shimadzu GC-2010) through the AOAC Official Method 963.22 (AOAC, 2000a). Chromatographic separation was done on a Supelco SP-2560 capillary column (0.25 μm, 100 m × 0.20 mm). Retention times of the eluted FAMEs were compared with known amounts of mixed reference standards composed of C6, C8, C10, C12, C14, C16, C18, C18:1, C18:2, C18:3, C20, C22, and C24. Peak areas were integrated using GCSolution (Shimadzu), and the response factors were calculated from the ratio between the peak area of the individual FAME and the internal standard (heneicosanoic acid methyl ester). Analysis was done using two biological replicates with three technical replicates each. Results are presented as % w/w (mg fatty acid/mg biomass).

Secondary Metabolites Analysis Using Global Natural Products Social Molecular Networking Platform

UPLC-MS/MS analysis of all Florisil® fractions (1 mg/mL in acetonitrile) was performed using a Waters Acquity UPLC® H-Class System with a Xevo® G2-XS Quadrupole Time-of-Flight (QToF) high-resolution mass spectrometer. A 1 μL aliquot of each sample was injected in a Phenomenex Kinetex 2.6 μm C18 100Å column (50 × 2.1 mm) and eluted at 0.35 mL/min, using a gradient program of acetonitrile/water (0.1% formic acid modifier): 40–100% acetonitrile for 5.5 min, and 100% acetonitrile for 2 min. The mass spectrometer was set to observe at m/z 100–2,000 in positive ESI mode with an automated data dependent acquisition (DDA) MS/MS scan. Three DDA scans were acquired for each sample with increasing ramp collision energies: 15–25, 30–45, and 50–70 eV. DDA scan for the Pacific ciguatoxin 3C (P-CTX-3C, WAKO Chemicals) standard was acquired using the 15–25 eV ramp collision energy.

Chromatograms were converted to mzxml format using freely available MSConvert software[1]. A molecular network was created using the online workflow[2] on the GNPS website[3] (Wang et al., 2016). MS/MS data of the Florisil® fractions from each isolate were grouped to form the molecular network. The precursor ion mass tolerance was set to 2 Da and an MS/MS fragment ion tolerance of 0.1 Da. A network was created, with edges set to cosine score >0.7 and more than six matched peaks. Further, edges between two nodes were kept in the network if and only if each of the nodes appeared in each other's respective top 10 most similar nodes. Finally, the maximum size of a molecular family was set to 100, and the lowest scoring edges were removed from the molecular families until the molecular family size was below this threshold. The spectra in the network were searched against the GNPS spectral libraries. All matches kept between network spectra, and library spectra were required to have a score >0.7 and at least six matched peaks.

---

[1] www.proteowizard.sourceforge.net

[2] https://ccms-ucsd.github.io/GNPSDocumentation/

[3] http://gnps.ucsd.edu

RESULTS

Taxonomic Identification

Morphology

Morphological characters (**Figure 1**) of the two *Gambierdiscus* strains (Gtox112513 and GtoxSAM092414) were identical to *Gambierdiscus balechii* (Fraga et al., 2016; Azanza et al., 2017). Cells were anterio-posteriorly compressed, measuring 53.6–63.5 μm (57.7 ± 2.7, $n = 30$) in depth (dorsoventral diameter) and 56.7–63.0 μm (60.1 ± 1.9, $n = 30$) in width. Cell shape was round to ellipsoid in apical view (**Figures 1D,E**). The epithecal and hypothecal surfaces were heavily areolated (**Figures 1A,C, 2D**). The presence of small and large accumulation bodies was observed (**Figure 1B**). The nucleus was large and elongated (**Figure 1D**). Cells had a rod-shaped, golden-brown chloroplast evenly distributed throughout the cell (**Figure 1F**). Thecal plates of the two strains as observed with fluorescence microscopy, especially the taxonomically informative plates of the genus such as the shape of the second apical plate (2′), third precingular plate (3″), and second antapical plate (2⁗), support their identification as *G. balechii*. Thecal plate tabulation of the *Gambierdiscus* strain (Gtox112513) is only shown (**Figure 2**). The epitheca was composed of apical pore (Po), three apical plates and six precingular plates. In apical view, the first apical plate (1′) and sixth apical plate (6′) were barely visible (**Figure 2A**) but can be seen at ventral view (**Figure 2C**). Both plate 1′ and 6″ were the smallest among the apical and precingular plates, respectively. The second apical plate (2′) was the largest of the apical series and shaped like a hatchet, i.e., having a suture ratio of 2′/1″ and 2′/3″ = 0.60 ($n = 30$). The third precingular plate (3″) was asymmetrical (**Figure 2A**). The apical pore plate was oval with a fish-hook shaped slit (**Figures 1A,D**). The hypotheca was composed of two antapical plates (2⁗), five postcingular plates (5‴), and a posterior sulcal plate (Sp). Among the five postcingular plates, the plate 4‴ was the largest. The second antapical plate (2⁗) was narrow and pentagonal to trapezoidal (**Figure 2B**). Marginal borders of the plates in the epitheca and hypotheca were overlapping (**Figures 2A,B**).

Phylogeny

Two new LSU rDNA (D8–D10) sequences were obtained from *Gambierdiscus* cultures established from Bolinao, Pangasinan

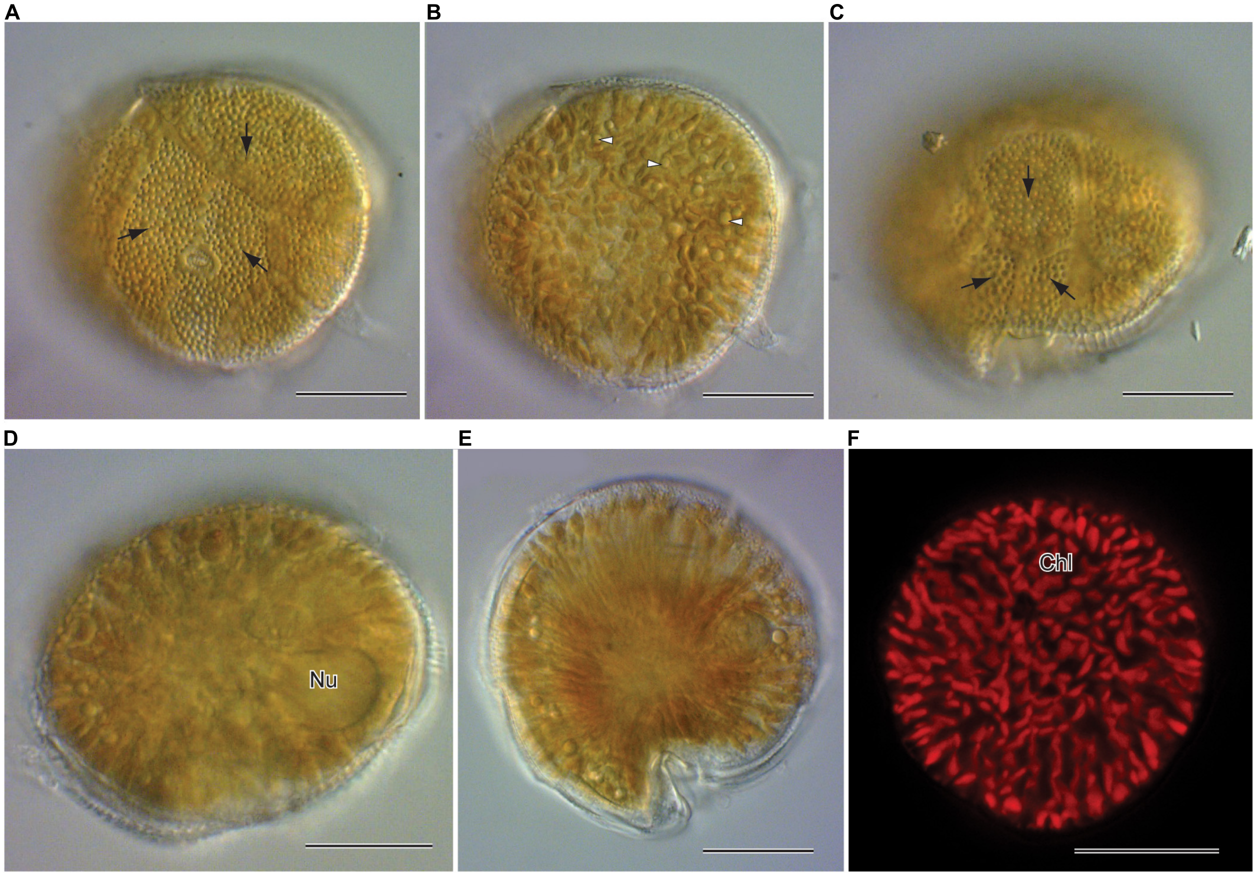

FIGURE 1 | Light and fluorescence microscopy of *Gambierdiscus balechii* **(A–D)**. Gtox112513; **(E,F)**. GtoxSAM092414. **(A)** Surface focus from apical view showing heavy areolations (black arrows) **(B)** deeper focus from apical view showing the chloroplast and accumulation bodies (white arrowheads) **(C)** surface focus from antapical view showing heavy areolations (black arrows) **(D)** deeper focus from antapical view showing nucleus (Nu) **(E)** deeper focus from apical view showing the shape of the cell **(F)** fluorescence microscopy showing the chloroplast (Chl). Scale = 20 μm **(A–F).**

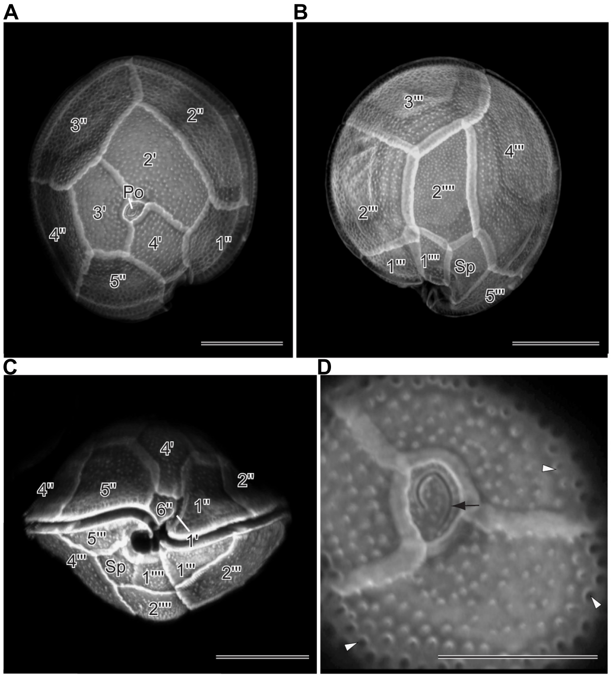

FIGURE 2 | Confocal Laser Scanning Microscopy of calcofluor stained *Gambierdiscus balechii* (Gtox112513) **(A)** apical view **(B)** antapical view **(C)** ventral view **(D)**. apical view. Apical pore plate showing the fishhook-shaped slit (black arrow) and pores (white arrow head). Scale = 20 μm **(A–C)**, 10 μm **(D)**. Apical pore plate (Po), apical plates (1′–4′), precingular plates (1″–6″), postcingular plates (1‴–5‴), and antapical plates (1⁗ and 2⁗).

(Gtox112513), and Guiuan, Eastern Samar, Philippines (GtoxSAM092414). The aligned sequences of 70 OTUs had 859 bps, of which 377 sites (43.9%) were variable, and 14 sites (1.6%) were parsimonious informative. Average base compositions were $A = 1.05$, $C = 0.250$, $G = 0.250$, and $T = 1.60$. The LSU sequences of the two strains differed at 14 positions (98.4% similarity). The maximum likelihood (ML) tree inferred from LSU rDNA is shown in **Figure 3**. Bootstrap support values derived from ML and posterior probability from Bayesian Inference (BI) analyses were given. The ML tree showed that Gtox112513 and GtoxSAM092414 clustered with previously reported *G. balechii* strains with strong support (BI/ML = 1.00/97%). This species formed a well-supported monophyletic clade (1.00/100%) comprising of *G. pacificus, G. toxicus, G. cheloniae, G. lewisii, G. lapillus, G. scabrosus, G. belizeanus, G. honu,* and two undescribed species. *Gambierdiscus carpenteri* (Gam1BOL080513) used in this study grouped with other reported *G. carpenteri* strains with strong support (0.96/94%) (**Figure 3**). This species formed a monophyletic clade composed of *G. caribaeus* and *G. jejuensis* with maximum support (1.00/100%).

Toxicity Assessment

The toxin content of the three *Gambierdiscus* strains was assessed via RBA using the IAEA-Tecdoc-1729 to detect ciguatera toxins (IAEA, 2013). *G. carpenteri* Gam1BOL080513 gave the highest toxicity with 12.36 ± 4.38 pg PbTx-3 eq./cell (**Figure 4**). The *G. balechii* strains GtoxSAM092414 (0.80 ± 1.13 pg PbTx-3 eq./cell), and Gtox112513 (0.14 ± 0.05 pg PbTx-3 eq./cell) showed comparable toxicities. The *G. balechii* toxin content was approximately 15–91-fold lower than *G. carpenteri* Gam1BOL080513.

Chemical Analysis

Carbohydrate Analysis

The total carbohydrate content of the three isolates was quantified using a colorimetric phenol-sulfuric acid assay (Masuko et al., 2005). *G. carpenteri* Gam1BOL080513 and *G. balechii* GtoxSAM092414 have comparable total carbohydrate content (**Figure 5A**). *G. balechii* Gtox112513 showed the highest total carbohydrate content with 12.66 ± 1.92% w/w.

Carbohydrates were hydrolyzed according to the method of Schulze et al. (2017). Multiple reaction monitoring of the monosaccharides facilitated the identification and quantitation of the sugars. Galactose, mannose, and glucose were the major monosaccharides in the hydrolysates of the three *Gambierdiscus* isolates, with glucose being the principal monosaccharide (**Figure 5A**). *G. balechii* GtoxSAM092414 and *G. balechii* Gtox112513 gave the highest glucose and galactose content, respectively (**Figure 5A**). The mannose content significantly varied across the three isolates, with the highest amount in *G. balechii* Gtox112513 (**Figure 5A**).

Lipid Analysis

Fatty acids from the biomass of the *Gambierdiscus* isolates were determined and quantified by converting the crude lipid extracts to fatty acid methyl esters (FAMEs) and detected using GC-FID based on the AOAC Official Method 963.22 (AOAC, 2000a). The total fatty acid content of the three *Gambierdiscus* strains was comparable (**Figure 5B**). The isolates also showed similar fatty acid profiles consisting of myristic (C14), palmitic (C16), stearic (C18), oleic (C18:1), linoleic (C18:2), arachidic (C20), and lignoceric (C24) acids (**Figure 5B**). Only *G. balechii* GtoxSAM092414 showed detectable levels of linolenic acid (C18:3) (**Figure 5B**). Principal fatty acids for all strains are C16 (2.53–4.55%), C18:1 (0.66–0.71%), and C24 (0.42–0.80%). The remaining fatty acids detected for all strains are saturated fatty acids, C14 (0.10–0.1%), and C20 (0.05–0.08%).

Secondary Metabolites Analysis

Untargeted metabolite profiling of the extracts was performed using reversed phase UPLC-MS and MSMS analysis and subsequently annotated using the GNPS database to identify the compounds and toxins produced by the three *Gambierdiscus* isolates. **Figure 6** shows the molecular network generated from the extracts of the three strains of *Gambierdiscus* and P-CTX-3C (in lavender) as a seed compound with a known identity. The entire molecular network consists of 541 nodes with 666 connections and 45 clusters with 271 single nodes. Cosine scores ranged from 0.70 to 0.96, suggesting that the putative hits from the GNPS database and the metabolites in the *Gambierdiscus* extracts may not be identical but would likely have the same chemical scaffold. Hence, clusters were annotated based on their

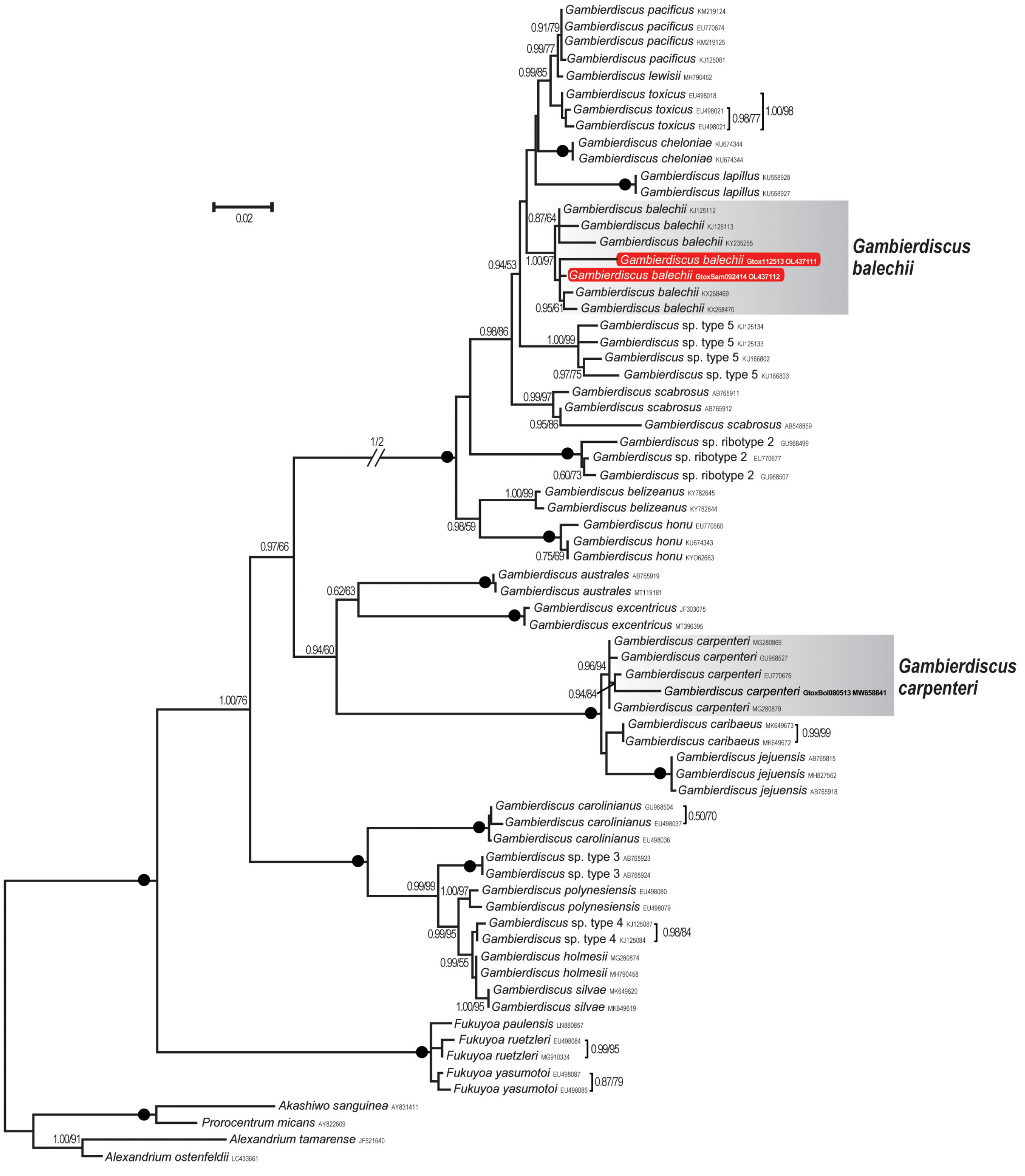

FIGURE 3 | Maximum likelihood (ML) phylogeny *of Gambierdiscus* species inferred from D8-D10 LSU rDNA (859 bp) based on the GTR + I + G model. Posterior probabilities (PP, ≥ 0.7) of Bayesian inference and bootstrap support (BS, ≥ 50%) values of ML were indicated, and black dots on nodes indicate maximum supports for both BI and ML (PP/BS = 1.00/100). New DNA sequences analyzed in this study are highlighted in red box. Strains used in this study are highlighted in bold.

common functional groups. Based on this, 45 clusters were generated belonging to at least ten compound classes (**Figure 6**).

The largest cluster contains the most convergence of the compounds from the three strains, mainly consisting of terpene glycosides (**2**, **3**), carbohydrate conjugates (**4–6**), polyketides, and macrolides (**7–10**) (**Figure 6**). Lipids and lipid-like molecules (**11–13**), fatty acids (**14–16**), and chlorophyll derivatives (**17, 18**) were present in all three strains. *G. balechii* strains also produced steroids and steroidal derivatives (**19, 20**). Strain-specific clusters were also observed, such as a peptide (**21**) cluster in the extract

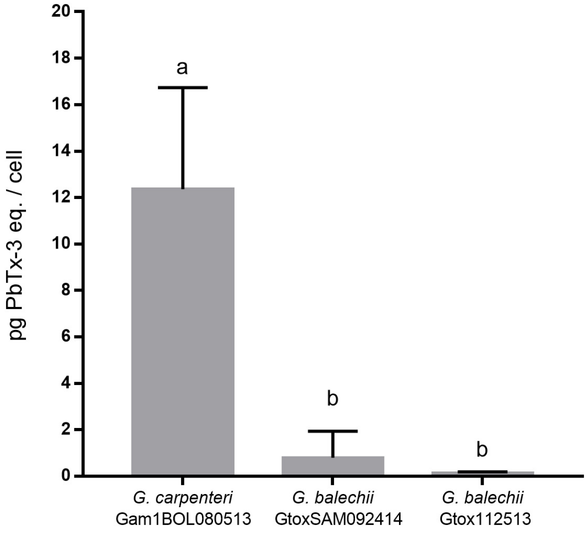

FIGURE 4 | Toxin content of crude acetone extracts of *G. carpenteri* Gam1BOL080513, *G. balechii* GtoxSAM092414, and *G. balechii* Gtox112513 shown in pg PbTx-3 eq./cell. The two *G. balechii* strains had ∼15 to ∼91-fold lower toxin content compared to *G. carpenteri*. Results are presented mean + SD ($n = 3$). Different letters indicate significant difference after one-way ANOVA analysis ($P < 0.05$).

of *G. balechii* GtoxSAM092414 and polyhydroxylated (**22**, **23**) compounds from *G. carpenteri* Gam1BOL080513 (**Figure 6**). The seed compound P-CTX-3C appears in the molecular network as a single node (**Figure 6** inset). Manual annotation of the single nodes in the molecular network revealed two precursor masses, 1021.65 and 1021.8 Da, in the three extracts (**Figure 6** inset) that clustered together. Examination of the chromatograms showed that these ions have identical retention times (**Figure 7A**) and MS^1 profiles (**Figure 7B**). The observed masses matched the pseudomolecular ion corresponding to a water loss $[M+H-H_2O]^+$ of 44-methylgambierone (**1**). Further, a comparison of the MS/MS spectra to the published data (Boente-Juncal et al., 2019; Estevez et al., 2020b) for 44-methylgambierone (**Table 2** and **Supplementary Figure 2**) showed similar fragmentation patterns, therefore, corroborating with the observed pseudomolecular ion. 44-methylgambierone was detected in fraction B of the *G. balechii* strains, and in fraction C of *G. carpenteri* Gam1BOL080513 (**Supplementary Figures 3–5**). The relative amount of 44-methylgambierone was semi-quantified by integrating the peak area corresponding to 44-methylgambierone (t_R = 0.78–0.90 min) along with the solvent blank (**Figure 7C**). *G. balechii* Gtox112513 showed the highest amount of 44-methylgambierone compared to *G. balechii* GtoxSAM092414 and *G. carpenteri* Gam1BOL080513.

DISCUSSION

Taxonomic Identification

Identification of *Gambierdiscus* mainly relies on cell size, thecal morphological features, and molecular genetic data (Chinain et al., 1999; Litaker et al., 2009; Kretzschmar et al., 2017). In this study, two *Gambierdiscus* strains (Gtox112513, GtoxSAM092414) from Bolinao, Pangasinan, and Guiuan, Eastern Samar were characterized based on cellular and thecal plate morphology, and phylogeny inferred from D8–D10 LSU rDNA (**Figures 1**, **2**). The morphology of these strains coincided with the key taxonomic features of *G. balechii*, as described by Fraga et al. (2016). Mainly, the cell size, thecal ornamentation, shape of second apical plate ($2'$), third precingular plate ($3''$) and second antapical plate ($2''''$) showed high resemblance to the original type material (Fraga et al., 2016). The Philippine strains possessed heavy areolation (reticulate-foveate) on their thecal plate surface, which is a character reported for *G. balechii, G. belizeanus*, *G. cheloniae*, *G. lapillus, G. lewisii*, *G. scabrosus* (Faust, 1995; Nishimura et al., 2014; Fraga et al., 2016; Smith et al., 2016; Kretzschmar et al., 2017, 2019). The shape of the taxonomically informative thecal plates i.e., hatchet shaped plate $2'$, asymmetrical plate $3''$ and narrow plate $2''''$ of our strains was similar to *G. balechii, G. cheloniae*, and *G. lewisii* (Fraga et al., 2016; Smith et al., 2016; Kretzschmar et al., 2019). Finally, the cell dimension of the Philippine strains is nearly identical to *Gambierdiscus balechii* compared to other closely species (**Supplementary Table 2**; Fraga et al., 2016; Dai et al., 2017).

With the analyses of phylogenetic position inferred from D8-D10 LSU rDNA sequences, the morphological identification of the two *Gambierdiscus* strains as *Gambierdiscus balechii* was further resolved by forming a well-supported clade that includes the sequence of the type material of *G. balechii* from Celebes Sea, Manado, Indonesia (KX268470). This clade is also composed of strains from Rawa Island, Malaysia (KY235255) and another strain originally identified as *Gamberidiscus* type 6 from Marakei, Kiribati (KJ125112, KJ125113) but now designated as *Gambierdiscus balechii* (Dai et al., 2017). The identification of *Gambierdiscus balechii* adds to the report of this species in the tropical Pacific (Fraga et al., 2016; Zhang et al., 2016; Dai et al., 2017; Tester et al., 2020).

Toxicity

The toxicity of *G. carpenteri* Gam1BOL080513 (12.36 ± 4.38 pg PbTx-3 eq./cell) was comparable to the highest toxin content reported by Vacarizas et al. (2018) at 7.48 ± 0.49 pg PbTx-3 eq./cell. The difference may be attributed to the extraction procedure performed in this study, using acetone instead of methanol. Compared to other *G. carpenteri* strains in literature (Litaker et al., 2017; Pisapia et al., 2017; Díaz-Asencio et al., 2019), the Philippine strain showed relatively higher toxin content. Several *Gambierdiscus* species associated with macrophytes identified in Cuba, including *G. carpenteri*, have toxin content below the RBA limits of quantitation (Díaz-Asencio et al., 2019). *G. carpenteri* strains isolated from Hawaii (Pisapia et al., 2017), the Caribbean (Litaker et al., 2017), and Mexico (Litaker et al., 2017) showed femtogram levels of CTX-3C eq./cell using cell-based neuro-2a assay (CBA-N2a).

The toxin content in the Philippine strains (0.13–0.79 pg PbTx-3 eq./cell) of *G. balechii* was also higher than the literature values. *G. balechii* strains from Marekei, Kiribati have toxin values ranging from 1.1 to 19.9 fg P-CTX-1 eq./cell (Dai et al., 2017),

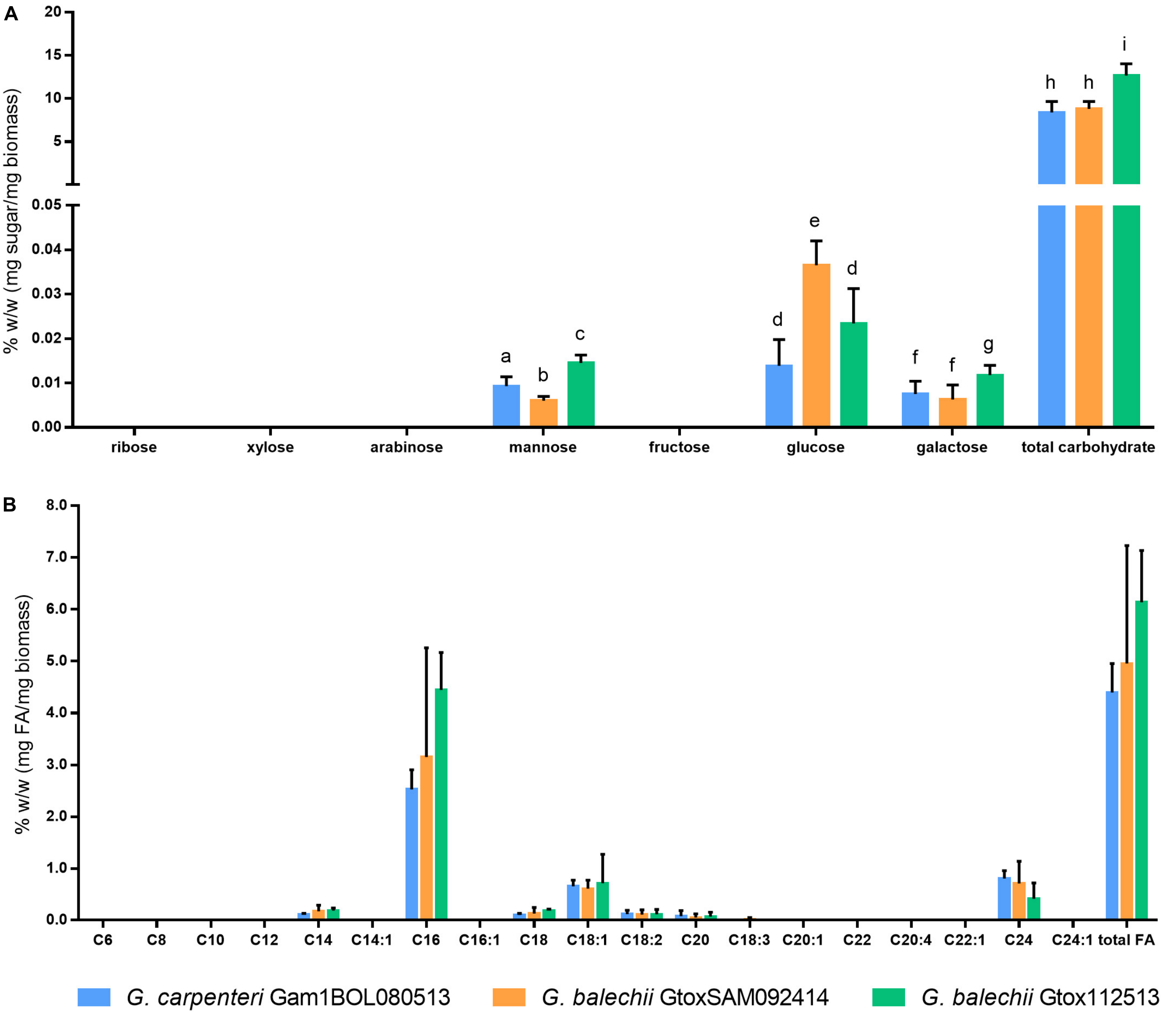

FIGURE 5 | Monosaccharide **(A)** and fatty acid **(B)** content of crude carbohydrate and lipid extracts of *G. carpenteri* Gam1BOL080513, *G. balechii* GtoxSAM092414, and *G. balechii* Gtox112513 biomass. The three strains showed significant difference in the monosaccharide content but not in the fatty acid composition. Results are presented as mean + SD from two biological replicates with three technical replicates each. Different letters indicate significant differences after one-way ANOVA analysis ($P < 0.05$).

while the Indonesian strain showed 3.4 ± 1.5 fg CTX-3C eq./cell (Pisapia et al., 2017) using CBA-N2a assay. However, a direct comparison cannot be established as the method for toxin determination, and the toxin standards used in these assays differed.

Chemical Analyses

An integrated targeted and untargeted metabolite profiling approach was done to comprehensively characterize the chemistry of the three *Gambierdiscus* strains from the Philippines. Monosaccharides and fatty acids were profiled and quantified directly using HPLC-MS/MS and GC-FID, respectively. Secondary metabolites were assessed using unbiased UPLC-MS and MS/MS techniques. Florisil® fractionation of the crude extracts was performed to improve the detection of compounds produced at low amounts and, therefore, allowed for higher metabolite coverage in the UPLC-MS analysis. We expand and report the first chemical analysis of *Gambierdiscus* spp. using the GNPS platform. We focused on molecular clusters with generated GNPS annotation and manually annotated toxin clusters.

Metabolites from *G. balechii* strains were concentrated in the more lipophilic Florisil® fractions A and B, while *G. carpenteri* Gam1BOL080513 metabolites showed higher richness in the hydrophilic Florisil® fraction C. The molecular network suggests that the *Gambierdiscus* strains produce metabolites with high chemical diversity, including carbohydrates, lipids, and polyketides. Exploration of the molecular network (**Figure 6**) identified strain-specific clusters. For example, a cluster of polyhydroxylated compounds (**22**, **23**, **38–42**) was only observed

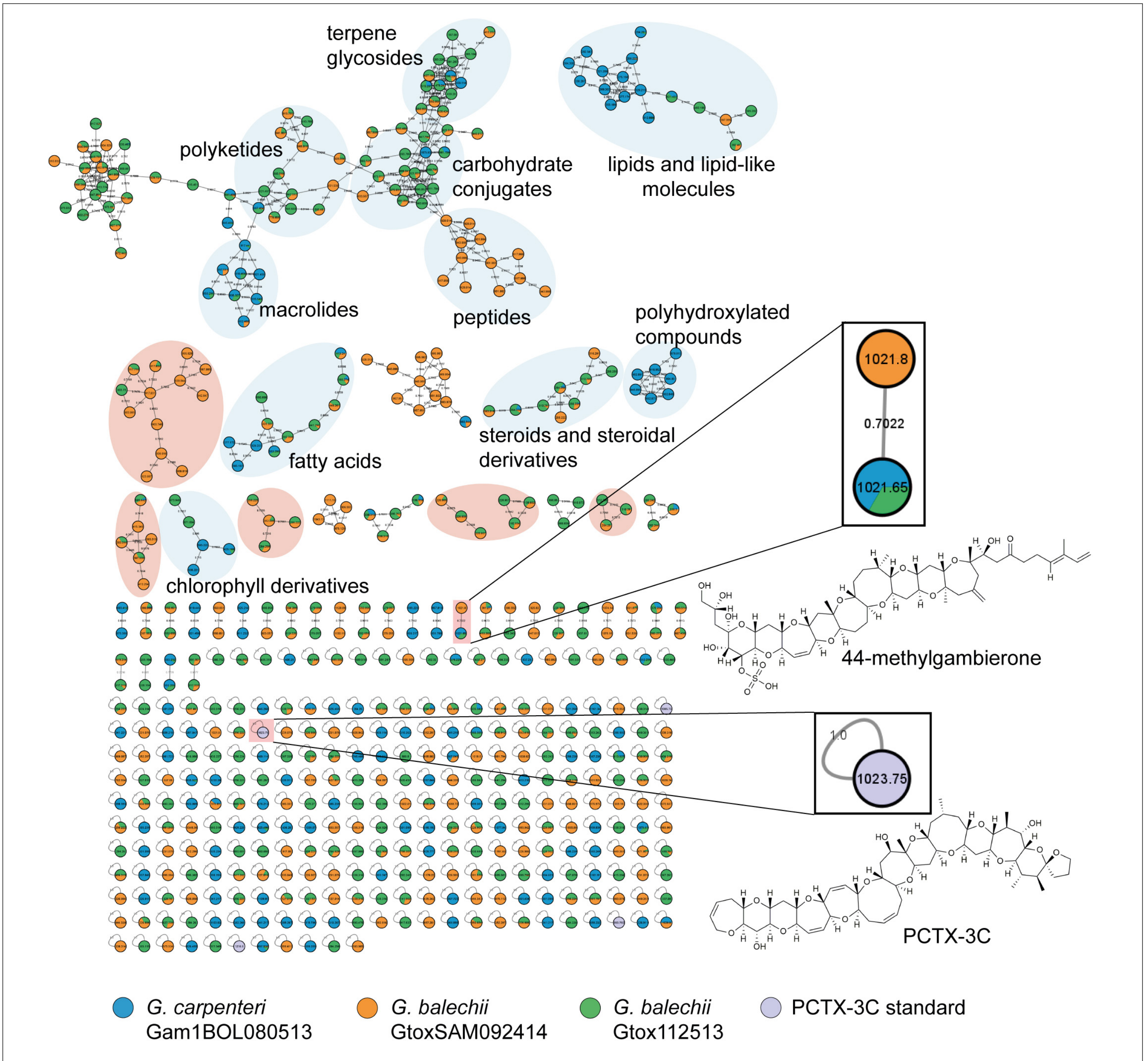

FIGURE 6 | Molecular network generated from HRMS/MS spectra from the Florisil® fractions of three *Gambierdiscus* strains, and P-CTX-3C standard using Global Natural Product Social Molecular Networking (GNPS) tool. Each node corresponds to a compound in the given strain (indicated by the color/s of the node). The nodes were color-coded according to the strains: *G. carpenteri* Gam1BOL080513 in blue, *G. balechii* GtoxSAM092414 in orange, *G. balechii* Gtox112513 in green, and the P-CTX-3C standard in lavender. Similarity between nodes is represented by the gray curves labeled by the cosine score. Annotation of compound class or family was performed through matching of fragmentation patterns of known compounds available in the GNPS server. Enlarged inset are manually annotated toxins, authentic standard (P-CTX-3C) and 44-methylgambierone with their chemical structures. The three *Gambierdiscus* strains contain 44-methylgambierone and chemically diverse secondary metabolites. A high-resolution image of the molecular network is provided in the **Supplementary Material** (**Supplementary Figure 1**).

in *G. carpenteri* Gam1BOL080513 (**Figure 6**). The two *G. balechii* strains showed related chemistries, evident from the clustering of their secondary metabolites (**Figure 6** highlighted in orange) and consequently, high convergence. These species- and strain-specific clusters may be potential chemotaxonomic markers for identifying particular *Gambierdiscus* isolates. Further studies toward identifying these compounds and spatiotemporal variations on the production are needed to define the potential utility as chemotaxonomic markers.

Carbohydrates and Derivatives

The central cluster in the molecular network, which is a convergence of the three strains, contained annotated compounds belonging to terpene glycosides (**2, 3**) and

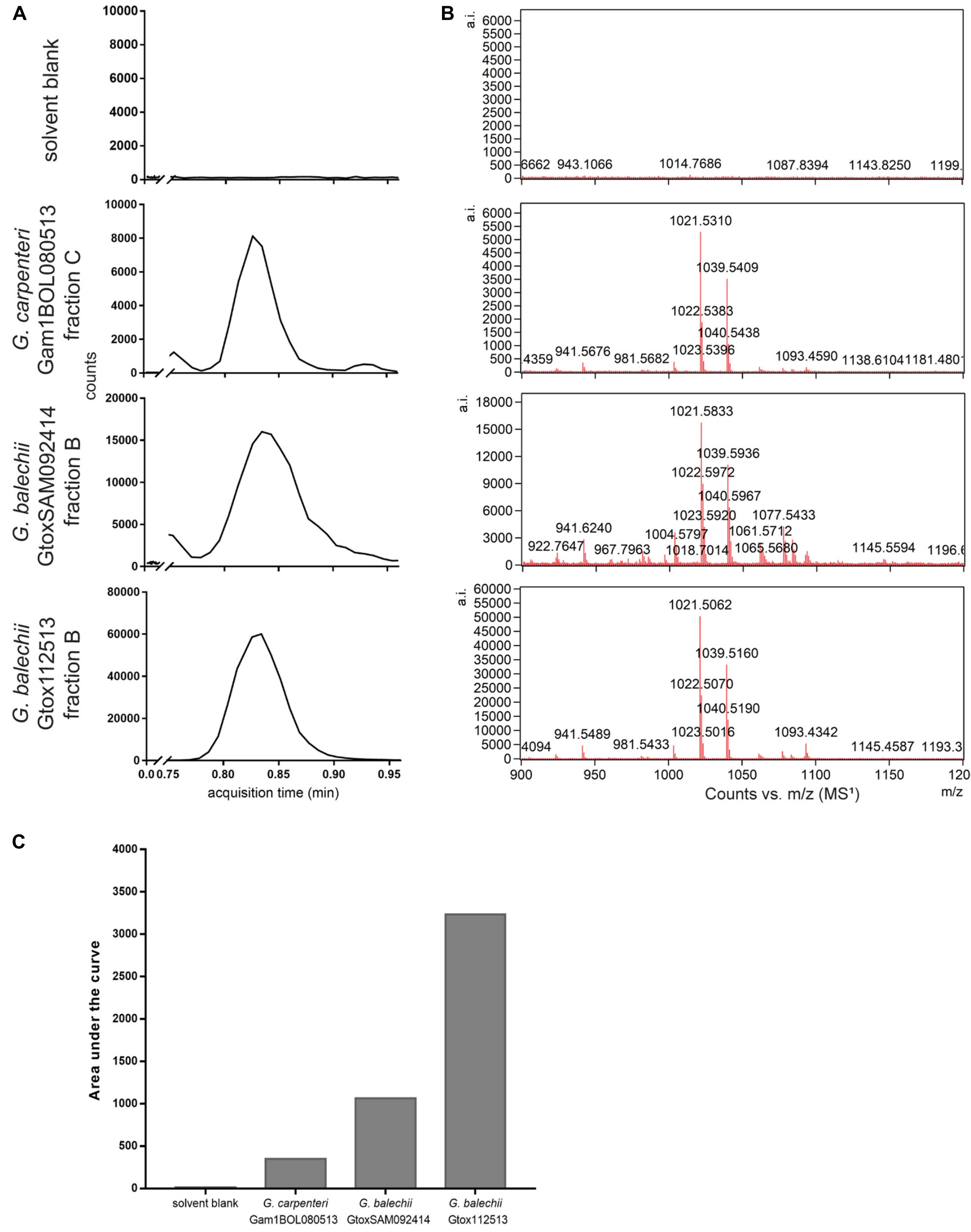

FIGURE 7 | LC-HRMS chromatograms **(A)** of the *Gambierdiscus* Florisil® fractions (t_R 0.75–0.95 min) and MS^1 spectra corresponding to 44-methylgambierone **(B)**. Relative amount of 44-methylgambierone was semi-quantified by integrating the area under the chromatogram peaks in **(A)** along with the solvent blank **(C)**. *G. balechii* Gtox112513 contained the highest amount of 44-methylgambierone.

carbohydrate conjugates (**4–6**). These are primarily carbohydrate-derived compounds connected to a lipophilic functional group. Based on the molecular network, these compounds are produced mainly by the two *G. balechii* strains.

Components of structural and storage polysaccharides were mainly detected through the targeted HPLC-MS-MRM approach (**Figure 5A**). The monosaccharides in the three *Gambierdiscus* strains are typical for microalgae (Templeton et al., 2012; Ortiz-Tena et al., 2016; Schulze et al., 2017). Glucose comprises the majority of the biomass since the main polysaccharide in dinoflagellate theca is cellulose (Okuda, 2002), and the primary storage polysaccharide for photosynthetic dinoflagellates is starch

TABLE 2 | Comparison between ions and fragments of 44-methylgambierone and MTX-3 from this study and literature values.

Peaks (m/z)	Ion species and fragments reported using mass spectrometry				
	***G. carpenteri* Gam1BOL080513 44-methylgambierone (this study)[a]**	***G. balechii* GtoxSAM092414 44-methylgambierone (this study)[a]**	***G. balechii* Gtox112513 44-methylgambierone (this study)[a]**	***G. belizeanus* CCMP401 44-methylgambierone (Boente-Juncal et al., 2019)[a]**	***G. toxicus* WC1/1 MTX-3 (Lewis et al., 1994)[b]**
1,099.5	[c]	[c]	[c]	[c]	$[M-H+2Na+K]^+$
1,083.5	[c]	$[M-H+2Na]^+$	$[M-H+2Na]^+$	$[M-H+2Na]^+$	$[M-2H+3Na]^+$
1,077.5	$[M+K]^+$	$[M+K]^+$	$[M+K]^+$	$[M+K]^+$	$[M-H+Na+K]^+$
1,061.5	$[M+Na]^+$	$[M+Na]^+$	$[M+Na]^+$	$[M+Na]^+$	$[M-H+2Na]^+$
1,056.5	[c]	[c]	[c]	$[M+NH_4]^+$	[c]
1,055.5	[c]	[c]	[c]	[c]	$[M+K]^+$
1,039.5	$[M+H]^+$	$[M+H]^+$	$[M+H]^+$	$[M+H]^+$	$[M+Na]^+$
1,021.5	$[M+H-H_2O]^+$	$[M+H-H_2O]^+$	$[M+H-H_2O]^+$	$[M+H-H_2O]^+$	$[M+Na-H_2O]^+$
1,003.5	$[M+H-2H_2O]^+$	$[M+H-2H_2O]^+$	$[M+H-2H_2O]^+$	$[M+H-2H_2O]^+$	$[M+Na-2H_2O]^+$
996.5	[c]	[c]	[c]	[c]	$[M-H+Na+K-SO_3]^+$
981.5	[c]	[c]	[c]	$[M+Na-SO_3]^+$	$[M-H+2Na-SO_3]^+$
963.5	[c]	[c]	[c]	[c]	$[M-H+2Na-H_2O-SO_3]^+$
959.5	$[M+H-SO_3]^+$	$[M+H-SO_3]^+$	$[M+H-SO_3]^+$	$[M+H-SO_3]^+$	$[M+Na-SO_3]^+$
941.5	$[M+H-H_2SO_4]^+$	$[M+H-H_2SO_4]^+$	$[M+H-H_2SO_4]^+$	$[M+H-H_2SO_4]^+$	$[M+Na-H_2O-SO_3]^+$
923.5	$[M+H-H_2O-H_2SO_4]^+$	$[M+H-H_2O-H_2SO_4]^+$	$[M+H-H_2O-H_2SO_4]^+$	$[M+H-H_2O-H_2SO_4]^+$	$[M+Na-2H_2O-SO_3]^+$
905.5	$[M+H-3H_2O-SO_3]^+$	$[M+H-3H_2O-SO_3]^+$	$[M+H-3H_2O-SO_3]^+$	$[M+H-3H_2O-SO_3]^+$	$[M+Na-3H_2O-SO_3]^+$
887.5	$[M+H-4H_2O-SO_3]^+$	$[M+H-4H_2O-SO_3]^+$	$[M+H-4H_2O-SO_3]^+$	$[M+H-4H_2O-SO_3]^+$	$[M+Na-4H_2O-SO_3]^+$

[a] *ESI(+): electrospray ionization positive mode.*
[b] *IS(+): ionspray mass spectrometry positive mode.*
[c] *Not detected.*

(Metting, 1996; Chen et al., 2013). Mannose and galactose were also reported as components of structural polysaccharides in dinoflagellates (Lewin et al., 1958; Brown, 1991). It is also the main organic component of mucilage found in the dinoflagellate *Gonyaulax hyalina* (MacKenzie et al., 2002) and a mixture of four phytoplanktonic taxa (Metaxatos et al., 2003). Benthic dinoflagellates, similar to *Gambierdiscus*, are known to produce mucilage as a means of attachment to their hosts (Heil et al., 1993; Rains and Parsons, 2015). In terms of the individual monosaccharide concentration, the glucose content was similar for the strains from Pangasinan, Philippines (Gam1BOL080513 and Gtox112513). A significant difference was observed for the strain from Eastern Samar, Philippines (GtoxSAM092414). In contrast, there was no evident relationship between the carbohydrate content and species suggesting spatial dependence. The carbohydrate content obtained in this study was significantly lower than other microalgae (Templeton et al., 2012; Ortiz-Tena et al., 2016; Schulze et al., 2017) and may be due to the partial hydrolysis of the complex carbohydrates using the sulfuric acid method.

Lipids

Lipids and sterols are utilized as chemotaxonomic guides among dinoflagellates and eukaryotic microalgae, respectively (Leblond et al., 2006; Mooney et al., 2007; Desmond and Gribaldo, 2009). In particular, the 4-methyl sterol, dinosterol, has been used as a biomarker in marine sediments to determine past dinoflagellate blooms (Boon et al., 1979). Marine-derived terpenes are also metabolites of particular interest because of their wide range of bioactivity and structural diversity (Gross and König, 2006). Though most studies for these terpenes were in sponges and corals, symbiotic dinoflagellates particularly *Symbiodinium* sp. were identified as the actual producers of some of these compounds (Mydlarz et al., 2003).

Three lipid clusters were observed in the extracts of *G. carpenteri* and *G. balechii* (**Figure 6**). Sterols and terpenes (**11–13**) were putatively identified in the lipid and lipid-like molecules cluster. These compounds are common in all three strains. Other steroidal derivatives, mainly steroidal ketones (**19, 20**), also clustered together and were specific to the two *G. balechii* strains. Steroidal ketones have been recognized as possible intermediates in the diagenesis of sterols in sedimenting particulate matter and marine sediments (Gagosian and Smith, 1979; Gagosian et al., 1982).

Free fatty acids clustered together for the three strains (**Figure 6**) and corroborated with the GC-FAME analysis. The hydrolyzed fatty acids from lipids were similar across the three isolates (**Figure 5B**). One of the primary fatty acids detected was C18:1, a precursor of docosahexaenoic acid (DHA) and eicosapentanoic acid (EPA). The C18:1 fatty acid was previously suggested as fatty acid biomarker for dinoflagellates and classified as essential fatty acids to grazers (Joseph, 1975; Parrish et al., 2000). PUFAs, characteristic of benthic dinoflagellates (Usup et al., 2008), were barely detected in the FAME analysis because of the lack of standards. GNPS was able to annotate PUFAs 20-hydroxy-eicosatetraenoic acid (**14**, cosine score 0.84), 9-hydroxy-octadecatrienoic acid (**15**, cosine score 0.84), and DHA (**16**, cosine score 0.78) in the fatty acid cluster. Detection of C24:0 in all strains may also indicate the presence of very long chain PUFAs, which is hypothesized to be the precursor of C28 fatty acids octacosaheptaenoic [28:7(n-6)] and octacosaoctaenoic acid [28:8(n-3)] found in dinoflagellates (Leblond and Chapman, 2000). Very long chain PUFAs serve as a distinguishing feature of marine algae from higher plants (Harwood, 1998).

Polyketides

Since GNPS molecular networking is based on similarities among molecules, we used P-CTX-3C as a seed compound to cluster other structurally related molecules belonging to the CTX and MTX families of compounds. Surprisingly, P-CTX-3C and 44-methylgambierone appeared as single nodes (**Figure 6** inset).

The 44-methylgambierone cluster (**Figure 6** inset) showed the pseudomolecular ion $[M+H-H_2O]^+$ with a mass of 1021 Da. *G. carpenteri* Gam1BOL080513 and *G. balechii* Gtox112513 formed a single node for 44-methylgambierone with precursor mass of 1021.65 Da. *G. balechii* GtoxSAM092414 clustered with a separate node with precursor mass 1021.8 Da. The mass difference between 44-methylgambierone in the three *Gambierdiscus* species may be attributed to the mass error from the instrument rather than structural variation. Manual inspection of the MS and MS/MS spectra corresponding to these nodes showed similar m/z peaks (**Figures 7A,B** and **Supplementary Figure 2**) and retention time, indicating that the 44-methylgambierone in the three species are identical. Since 44-methylgambierone has an equivalent mass to 2,3-dihydroxyCTX-3C, the presence of a sulfate moiety is important to verify the maitotoxin backbone. The MS/MS fragmentation (**Supplementary Figure 2**) confirmed the presence of a sulfate moiety. 44-methylgambierone is the main MTX detected in this study presumably due to the high intracellular concentration of this compound in the three *Gambierdiscus* species.

However, the amount of 44-methylgambierone did not fully account for the observed toxicity in the RBA assay (**Figure 7C**) for *G. carpenteri* Gam1BOL080513. Since 44-methylgambierone has a low potency, the high ciguatoxicity in the RBA assay for *G. carpenteri* Gam1BOL080513 may suggest the production of additional toxins. Accordingly, the low RBA activity observed for *G. balechii* Gtox112513 and *G. balechii* GtoxSAM092414 may imply that 44-methylgambierone is the principal marine biotoxin in these two strains.

Detection of other MTX and CTX in *G. carpenteri* Gam1BOL080513 was attempted using multiple reaction monitoring (**Supplementary Methods** and **Supplementary Table 3**), as adapted from Estevez et al. (2021). Apart from 44-methylgambierone, other MTX and CTX analogs were not detected in *G. carpenteri* Gam1BOL080513 (**Supplementary Figure 6**). The targeted monitoring also validated the results from the untargeted metabolite analysis.

Other MTX and CTX congeners are usually present in very low amounts, limiting the detection of the parent mass under positive ionization. Enrichment of *G. carpenteri* Gam1BOL080513 through column fractionation and subsequent targeted analysis for CTX and MTX may aid in the detection of other marine biotoxins produced by this species. More sensitive methods for mass spectrometry detection, such as multiple reaction monitoring, have proved to be successful in detecting minor CTX and MTX in benthic dinoflagellate extracts. Molecular networking in the negative ionization mode may improve the detection limit by capitalizing on the presence of a sulfate moiety in MTX.

Other Compound Classes

Pigments were also detected in the extracts of the three *Gambierdiscus* strains. Pheophorbide A (**18**) and pheophytin A (**17**), chlorophyll breakdown products, were putatively identified (cosine scores 0.80 and 0.87, respectively) in the chlorophyll derivatives cluster. Peridinin (**10**, cosine score 0.86) was also annotated in the polyketide cluster. Peridinin is an accessory pigment of several dinoflagellates, present as peridinin-chlorophyll-protein light harvesting complex used in photosynthesis (Song et al., 1976; Hofmann et al., 1996; Jiang et al., 2012). This pigment is also responsible for the characteristic orange to brown appearance of *Gambierdiscus* cells (Indelicato and Watson, 1986).

A cluster of polyhydroxylated compounds (**22, 23, 38–42**) specific to *G. carpenteri* Gam1BOL080513 was also observed. 26-(4′-carbamoyl-1,4′-bipiperidin-1′-yl)-2,15,17-trihydroxy-11-methoxy-3,7,12,14,16,18,22-heptamethyl-6,23,27,29-tetraoxo-8,30-dioxa-24-azatetracyclo[23.3.1.1^{4,7}.0^{5,28}]triaconta-1(28),2,4,9,19,21,25-heptaen-13-yl acetate (**22**, cosine score 0.79) was dereplicated from the GNPS spectral library. This putative compound is structurally related to linear polyhydroxylated compounds from dinoflagellates, such as the antifungal and hemolytic amphidinols, luteophanols, lingshuiol, and colopsinols produced by *Amphidinium* sp. (Echigoya et al., 2005). These compounds are cytotoxic through their membrane disrupting activity (Paul et al., 1997; Qi et al., 2007). Polyhydroxylated compounds are also highly valued because of their potent biological activity. Amphidinols, for example, are used as antifungal agents (Wakamiya et al., 2020). Related compounds may likewise have comparable bioactivity.

A strain-specific peptide cluster (**21, 43–49**) was putatively identified in the molecular network of *G. balechii* GtoxSAM092414. Peptide biosynthesis in dinoflagellates is understudied, principally due to the focused discovery of toxins synthesized by polyketide synthases (PKS). Non-ribosomal peptide synthetase (NRPS/PKS) are potentially widespread among dinoflagellates that are known producers of amine or amide-containing compounds such as *Karenia brevis* (Monroe and Van Dolah, 2008; López-Legentil et al., 2010; Van Dolah et al., 2017), and *Ostreopsis* spp. (Verma et al., 2019). NRPS/PKS hybrid sequences were also identified in the transcriptome of dinoflagellates which are not known producers of NRP-type metabolites, including *Alexandrium* (Vingiani et al., 2020) and *Gambierdiscus* (Kohli et al., 2017; Van Dolah et al., 2020). Brevisamide (Satake et al., 2008), ostreol A (Hwang et al., 2013), and alexandrolide (Satake et al., 2019) are NRPS-PKS hybrid compounds purified from dinoflagellates. Ostreol A is cytotoxic against brine shrimp at 0.9 μg/mL. Alexandrolide is cytotoxic against mouse lymphoid P388 cells at 4 μg/mL and inhibited the diatom *Skeletonema costatum* and *Chattonella antiqua*. NRPS-PKS hybrid compounds may serve as additional allelochemicals of dinoflagellates and could work in synergy with other toxins.

The targeted and untargeted chemical profiling and molecular networking of Philippine *Gambierdiscus* strains provided a glimpse of these organisms' biosynthetic potential and chemical diversity. At the same time, we gained insights into the similarities and differences in the metabolite production in the three *Gambierdiscus* strains. While the production of fatty acids, carbohydrates and 44-methylgambierone are common among the three strains, we observed species- and strain-specific compounds. There is much more to marine toxins in the extracts of *Gambierdiscus* sp. The putative identification of polyhydroxylated and peptide-based compounds may suggest additional allelochemicals and potentially high value compounds from *Gambierdiscus* species. The putative identification from untargeted chemical profiling can guide targeted purification and chemical characterization of *Gambierdiscus* extracts.

DATA AVAILABILITY STATEMENT

The datasets presented in this study can be found in online repositories. The names of the repository/repositories and accession number(s) can be found below: https://www.ncbi.nlm.nih.gov/genbank/, OL437111; OL437112 https://massive.ucsd.edu/ProteoSAFe/static/massive.jsp, MSV000088378.

AUTHOR CONTRIBUTIONS

ZM: conceptualization, methodology, software, formal analysis, investigation, visualization, writing – original draft, review, and editing. GB: methodology, formal analysis, writing – original draft, review, and editing. JDC: formal analysis, resources, writing – review, and editing. JB: methodology, formal analysis, writing – review, and editing. MR and RA: resources, writing – review, and editing. LS-R: conceptualization, methodology, writing – original draft, review and editing, supervision, resources, project, and funding acquisition. All authors have read and agreed to the published version of the manuscript.

FUNDING

This study was funded by the Department of Science and Technology—Philippine Council for Agriculture, Aquatic and Natural Resources Research and Development (DOST-PCAARRD) through the Hazard Detection and Mitigation Tools for Opportunistic Algal Blooms in a Changing Environment Research Program Project 3: Dynamics of Protein and Small Molecule Chemistry in HAB Causative Organisms (QMSR-MRRD-HAB-270-1275). Publication cost was supported by Upgrading Capacity, Infrastructure, and Assets for Marine Scientific Research in the Philippines (UPGRADE CIA) from the National Security Council.

ACKNOWLEDGMENTS

We would like to thank H. Junio and the Secondary Metabolites Profiling Laboratory of the Institute of Chemistry, University of the Philippines Diliman and K. B. Davis for assistance in the conduct of this study.

SUPPLEMENTARY MATERIAL

The Supplementary Material for this article can be found online at: https://www.frontiersin.org/articles/10.3389/fmars.2021.767024/full#supplementary-material

REFERENCES

AOAC (2000a). "Official method 963-22," in *Official Methods of Analysis of the Association of Official Analytical Chemists International*, ed. W. Horwitz (Gaithersburg, MD: AOAC), 2200.

AOAC (2000b). "Official method 969-33," in *Official Methods of Analysis of the Association of Official Analytical Chemists International*, ed. W. Horwitz (Gaithersburg, MD: AOAC), 2200.

Azanza, R. V., Benico, G. A., Iwataki, M., and Fukuyo, Y. (2017). *Harmful Marine Dinoflagellates in the Philippines*. Quezon City: The Marine Science Institute.

Bagnis, R., Kuberski, T., and Laugier, S. (1979). Clinical observations on 3,009 cases of ciguatera (fish poisoning) in the South Pacific. *Am. J. Trop. Med. Hyg.* 28, 1067–1073. doi: 10.4269/ajtmh.1979.28.1067

Berdalet, E., and Tester, P. A. (2018). "Key questions and recent research advances on harmful algal blooms in benthic systems," in *Global Ecology and Oceanography of Harmful Algal Blooms*, eds P. M. Glibert, M. A. Burford, G. C. Pitcher, and M. M. Caldwell (Cham: Springer Nature), 261–286.

Besada, E. G., Loeblich, L. A., and Loeblich, A. R. III (1982). Observations on tropical, benthic dinoflagellates from ciguatera-endemic areas: *Coolia, Gambierdiscus*, and *Ostreopsis*. *Bull. Mar. Sci.* 32, 723–735.

Bligh, E. G., and Dyer, W. J. (1959). A rapid method of total lipid extraction and purification. *Can. J. Biochem. Physiol* 37, 911–917. doi: 10.1139/cjz-2013-0052

Boente-Juncal, A., Álvarez, M., Antelo, Á, Rodríguez, I., Calabro, K., Vale, C., et al. (2019). Structure elucidation and biological evaluation of maitotoxin-3, a homologue of gambierone, from *Gambierdiscus belizeanus*. *Toxins* 11:79. doi: 10.3390/toxins11020079

Boon, J. J., Rijpstra, W. I. C., De Lange, F., De Leeuw, J. W., Yoshioka, M., and Shimizu, Y. (1979). Black Sea sterol—a molecular fossil for dinoflagellate blooms. *Nature* 277, 125–127. doi: 10.1038/277125a0

Brown, M. R. (1991). The amino-acid and sugar composition of 16 species of microalgae used in mariculture. *J. Exp. Mar. Bio. Ecol.* 145, 79–99. doi: 10.1016/0022-0981(91)90007-J

Caillaud, A., De La Iglesia, P., Darius, H. T., Pauillac, S., Aligizaki, K., Fraga, S., et al. (2010). Update on methodologies available for ciguatoxin determination: perspectives to confront the onset of ciguatera fish poisoning in Europe. *Mar. Drugs* 8, 1838–1907. doi: 10.3390/md8061838

Chen, C. Y., Zhao, X. Q., Yen, H. W., Ho, S. H., Cheng, C. L., Lee, D. J., et al. (2013). Microalgae-based carbohydrates for biofuel production. *Biochem. Eng. J.* 78, 1–10. doi: 10.1016/j.bej.2013.03.006

Chinain, M., Darius, H. T., Ung, A., Cruchet, P., Wang, Z., Ponton, D., et al. (2010). Growth and toxin production in the ciguatera-causing dinoflagellate *Gambierdiscus polynesiensis* (Dinophyceae) in culture. *Toxicon* 56, 739–750. doi: 10.1016/j.toxicon.2009.06.013

Chinain, M., Faust, M. A., and Pauillac, S. (1999). Morphology and molecular analyses of three toxic species of *Gambierdiscus* (Dinophyceae): *G. pacificus*, sp. nov., *G. australes*, sp. nov., and *G. polynesiensis*, sp. nov. *J. Phycol.* 35, 1282–1296. doi: 10.1046/j.1529-8817.1999.3561282.x

Chinain, M., Gatti, C. M., Roué, M., and Darius, H. T. (2020). "Ciguatera-causing dinoglagellates in the genera *Gambierdiscus* and *Fukuyoa*: distribution, ecophysiology and toxicology," in *Dinoflagellates: Morphology, Life History and Ecological Significance*, ed. D. S. Rao (New York, NY: Nova Science Publishers), 405–457.

Dai, X., Mak, Y. L., Lu, C. K., Mei, H. H., Wu, J. J., Lee, W. H., et al. (2017). Taxonomic assignment of the benthic toxigenic dinoflagellate *Gambierdiscus sp*. type 6 as *Gambierdiscus balechii* (Dinophyceae), including its distribution and ciguatoxicity. *Harmful Algae* 67, 107–118. doi: 10.1016/j.hal.2017.07.002

Darriba, D., Taboada, G. L., Doallo, R., and Posada, D. (2012). JModelTest 2: more models, new heuristics and parallel computing. *Nat. Methods* 9:772. doi: 10.1038/nmeth.2109

Desmond, E., and Gribaldo, S. (2009). Phylogenomics of sterol synthesis: insights into the origin, evolution, and diversity of a key eukaryotic feature. *Genome Biol. Evol.* 1, 364–381. doi: 10.1093/gbe/evp036

Díaz-Asencio, L., Vandersea, M., Chomérat, N., Fraga, S., Clausing, R. J., Litaker, R. W., et al. (2019). Morphology, toxicity and molecular characterization of *Gambierdiscus* spp. towards risk assessment of ciguatera in south central Cuba. *Harmful Algae* 86, 119–127. doi: 10.1016/j.hal.2019.05.007

Dickey, R. W., and Plakas, S. M. (2010). Ciguatera: a public health perspective. *Toxicon* 56, 123–136. doi: 10.1016/j.toxicon.2009.09.008

Ding, C. Y. G., Pang, L. M., Liang, Z. X., Goh, K. K. K., Glukhov, E., Gerwick, W. H., et al. (2018). MS/MS-based molecular networking approach for the detection of aplysiatoxin-related compounds in environmental marine cyanobacteria. *Mar. Drugs* 16:505. doi: 10.3390/md16120505

Echigoya, R., Rhodes, L., Oshima, Y., and Satake, M. (2005). The structures of five new antifungal and hemolytic amphidinol analogs from *Amphidinium carterae* collected in New Zealand. *Harmful Algae* 4, 383–389. doi: 10.1016/j.hal.2004.07.004

Estevez, P., Castro, D., Le, M., Sibat, M., Tud, A., Dickey, R., et al. (2021). Toxicity screening of a *Gambierdiscus australes* strain from the Western Mediterranean Sea and identification of a novel maitotoxin analogue. *Mar. Drugs* 19:460.

Estevez, P., Rambla-alegre, M., Aligizaki, K., Gago-martinez, A., and Hess, P. (2020a). Use of mass spectrometry to determine the diversity of toxins produced by *Gambierdiscus* and *Fukuyoa*. *Toxins* 12:305.

Estevez, P., Sibat, M., Leão-Martins, J. M., Costa, P. R., Gago-Martínez, A., and Hess, P. (2020b). Liquid chromatography coupled to high-resolution mass spectrometry for the confirmation of Caribbean ciguatoxin-1 as the main toxin responsible for ciguatera poisoning caused by fish from European Atlantic coasts. *Toxins* 12:267. doi: 10.3390/toxins12040267

Faust, M. A. (1995). Observation of sand-dwelling toxic dinoflagellates (Dinophyceae) from widely differing sites, including two new species. *J. Phycol.* 31, 996–1003.

Fiorini, F., Borgonuovo, C., Ferrante, M. I., and Brönstrup, M. (2020). A metabolomics exploration of the sexual phase in the marine diatom *Pseudo-nitzschia multistriata*. *Mar. Drugs* 18, 313. doi: 10.3390/md18060313

Fraga, S., Rodriguez, F., Riobo, P., and Bravo, I. (2016). *Gambierdiscus balechii* sp . nov (Dinophyceae), a new benthic toxic dinoflagellate from the Celebes Sea (SW Pacific Ocean). *Harmful Algae* 58, 93–105. doi: 10.1016/j.hal.2016.06.004

Friedman, M. A., Fernandez, M., Backer, L. C., Dickey, R. W., Bernstein, J., Schrank, K., et al. (2017). An updated review of ciguatera fish poisoning: clinical, epidemiological, environmental, and public health management. *Mar. Drugs* 15:72. doi: 10.3390/md15030072

Gago-Martínez, A., Estevez, P., Castro, D., Barrios, C., Hess, P., and Sibat, M. L. (2021). "Characterisation of ciguatoxins," in *EFSA Supporting Publication 2021:EN-6649* (Vigo: University of Vigo), doi: 10.2903/sp.efsa.2021.EN-6649

Gagosian, R. B., and Smith, S. O. (1979). Steroids ketones in surface sediments from the south-west African shelf. *Nature* 277, 287–289. doi: 10.1038/277287a0

Gagosian, R. B., Smith, S. O., and Nigrelli, G. E. (1982). Vertical transport of steroid alcohols and ketones measured in a sediment trap experiment in the equatorial Atlantic Ocean. *Geochim. Cosmochim. Acta* 46, 1163–1172. doi: 10.1016/0016-7037(82)90002-3

Gross, H., and König, G. M. (2006). Terpenoids from marine organisms: unique structures and their pharmacological potential. *Phytochem. Rev.* 5, 115–141. doi: 10.1007/s11101-005-5464-3

Guindon, S., Dufayard, J. F., Lefort, V., Anisimova, M., Hordijk, W., and Gascuel, O. (2010). New algorithms and methods to estimate maximum-likelihood phylogenies: assessing the performance of PhyML 3.0. *Syst. Biol.* 59, 307–321. doi: 10.1093/sysbio/syq010

Hall, T. A. (1999). BioEdit: a user-friendly biological sequence alignment editor and analysis program for Windows 95/98/NT. *Nucleic Acids Symp. Ser.* 41, 95–98.

Harwood, J. L. (1998). "Membrane lipids in algae," in *Lipids in Photosynthesis: Structure, Function and Genetics. Advances in Photosynthesis and Respiration*, eds S. Paul-André and M. Norio (Dordrecht: Springer), 53–64.

Heil, C. A., Maranda, L., and Shimizu, Y. (1993). "Mucus-associated dinoflagellates: large-scale culturing and estimation of growth rate," in *Toxic Phytoplankton Blooms in the Sea: Proceedings of the Fifth International Conference on Toxic Marine Phytoplankton*, eds T. J. Smayda and Y. Shimizu (Amsterdam: Elsevier), 501–506.

Hofmann, E., Wrench, P. M., Sharples, F. P., Hiller, R. G., Welte, W., and Diederichs, K. (1996). Structural basis of light harvesting by carotenoids: peridinin-chlorophyll-protein from *Amphidinium carterae*. *Science* 272, 1788–1791.

Holmes, M. J., and Lewis, R. J. (1994). Purification and characterisation of large and small maitotoxins from cultured *Gambierdiscus toxicus*. *Nat. Toxins* 2, 64–72. doi: 10.1002/nt.2620020204

Holmes, M. J., Venables, B., and Lewis, R. J. (2021). Critical review and conceptual and quantitative models for the transfer and depuration of ciguatoxins in fishes. *Toxins* 13:515. doi: 10.3390/toxins13080515

Hwang, B. S., Yoon, E. Y., Kim, H. S., Yih, W., Park, J. Y., Jeong, H. J., et al. (2013). Ostreol A: a new cytotoxic compound isolated from the epiphytic dinoflagellate *Ostreopsis* cf. *ovata* from the coastal waters of Jeju Island, Korea. *Bioorganic Med. Chem. Lett.* 23, 3023–3027. doi: 10.1016/j.bmcl.2013.03.020

IAEA (2013). *Detection of Harmful Algal Toxins Using the Radioligand Receptor Binding Assay A Manual of Methods*. Monaco: IAEA.

Indelicato, S. R., and Watson, D. A. (1986). Identification of the photosynthetic pigments of the tropical benthic dinoflagellate *Gambierdiscus toxicus*. *Mar. Fish. Rev.* 48, 44–47.

Jiang, J., Zhang, H., Kang, Y., Bina, D., Lo, C. S., and Blankenship, R. E. (2012). Characterization of the peridinin-chlorophyll a-protein complex in the dinoflagellate *Symbiodinium*. *Biochim. Biophys. Acta Bioenerg.* 1817, 983–989. doi: 10.1016/j.bbabio.2012.03.027

Joseph, J. D. (1975). Identification of 3, 6, 9, 12, 15-octadecapentaenoic acid in laboratory-cultured photosynthetic dinoflagellates. *Lipids* 10, 395–403. doi: 10.1007/BF02532443

Katoh, K., and Standley, D. M. (2013). MAFFT multiple sequence alignment software version 7: improvements in performance and usability. *Mol. Biol. Evol.* 30, 772–780. doi: 10.1093/molbev/mst010

Kofoid, C. A. (1909). On *Peridinium steini* Jörgensen, with a note on the nomenclature of the skeleton of the Peridinidae. *Arch. Für Protistenkd.* 16, 25–47.

Kohli, G. S., Campbell, K., John, U., Smith, K. F., Fraga, S., Rhodes, L. L., et al. (2017). Role of modular polyketide synthases in the production of polyether ladder compounds in ciguatoxin-producing *Gambierdiscus polynesiensis* and *G. excentricus* (Dinophyceae). *J. Eukaryot. Microbiol.* 64, 691–706. doi: 10.1111/jeu.12405

Kohli, G. S., Papiol, G. G., Rhodes, L. L., Harwood, D. T., Selwood, A., Jerrett, A., et al. (2014). A feeding study to probe the uptake of Maitotoxin by snapper (*Pagrus auratus*). *Harmful Algae* 37, 125–132. doi: 10.1016/j.hal.2014.05.018

Kretzschmar, A. L., Larsson, M. E., Hoppenrath, M., Doblin, M. A., and Murray, S. A. (2019). Characterisation of two toxic *Gambierdiscus spp*. (Gonyaulacales, Dinophyceae) from the Great Barrier Reef (Australia): *G. lewisii* sp. nov. and *G. holmesii* sp. nov. *Protist* 170:125699. doi: 10.1016/j.protis.2019.125699

Kretzschmar, A. L., Verma, A., Harwood, T., Hoppenrath, M., and Murray, S. (2017). Characterization of *Gambierdiscus lapillus* sp. nov. (Gonyaulacales, Dinophyceae): a new toxic dinoflagellate from the Great Barrier Reef (Australia). *J. Phycol.* 53, 283–297. doi: 10.1111/jpy.12496

Leblond, J. D., Anderson, B., Kofink, D., Logares, R., Rengefors, K., and Kremp, A. (2006). Fatty acid and sterol composition of two evolutionarily closely related dinoflagellate morphospecies from cold Scandinavian brackish and freshwaters. *Eur. J. Phycol.* 41, 303–311. doi: 10.1080/09670260600804843

Leblond, J. D., and Chapman, P. J. (2000). Lipid class distribution of highly unsaturated long chain fatty acids in marine dinoflagellates. *J. Phycol.* 36, 1103–1108.

Lefort, V., Longueville, J.-E., and Gascuel, O. (2017). SMS: smart model selection in PhyML. *Mol. Biol. Evol.* 34, 2422–2424. doi: 10.1093/molbev/msx149

Lewin, J. C., Lewin, R. A., and Philpott, D. E. (1958). Observations on *Phaeodactylum tricornutum*. *J. Gen. Microbiol.* 18, 418–426. doi: 10.1016/j.tig.2019.05.007

Lewis, R. J., Holmes, M. J., Alewood, P. F., and Jones, A. (1994). Ionspray mass spectrometry of ciguatoxin-1, maitotoxin-2 and -3, and related marine polyether toxins. *Nat. Toxins* 2, 56–63.

Litaker, R. W., Holland, W. C., Hardison, D. R., Pisapia, F., Hess, P., Kibler, S. R., et al. (2017). Ciguatoxicity of *Gambierdiscus* and *Fukuyoa* species from the Caribbean and Gulf of Mexico. *PLoS One* 12:e0185776. doi: 10.1371/journal.pone.0185776

Litaker, R. W., Vandersea, M. W., Faust, M. A., Kibler, S. R., Chinain, M., Holmes, M. J., et al. (2009). Taxonomy of *Gambierdiscus* including four new species, *Gambierdiscus caribaeus*, *Gambierdiscus carolinianus*, *Gambierdiscus carpenteri* and *Gambierdiscus ruetzleri* (Gonyaulacales, Dinophyceae). *Phycologia* 48, 344–390. doi: 10.2216/07-15.1

Longo, S., Sibat, M., Viallon, J., Darius, H. T., Hess, P., and Chinain, M. (2019). Intraspecific variability in the toxin production and toxin profiles of in vitro cultures of *Gambierdiscus polynesiensis* (Dinophyceae) from French Polynesia. *Toxins* 11:735. doi: 10.3390/toxins11120735

López-Legentil, S., Song, B., DeTure, M., and Baden, D. G. (2010). Characterization and localization of a hybrid non-ribosomal peptide synthetase and polyketide synthase gene from the toxic dinoflagellate *Karenia brevis*. *Mar. Biotechnol.* 12, 32–41. doi: 10.1007/s10126-009-9197-y

MacKenzie, L., Sims, I., Beuzenberg, V., and Gillespie, P. (2002). Mass accumulation of mucilage caused by dinoflagellate polysaccharide exudates in Tasman Bay, New Zealand. *Harmful Algae* 1, 69–83. doi: 10.1016/S1568-9883(02)00006-9

Masuko, T., Minami, A., Iwasaki, N., Majima, T., Nishimura, S. I., and Lee, Y. C. (2005). Carbohydrate analysis by a phenol-sulfuric acid method in microplate format. *Anal. Biochem.* 339, 69–72. doi: 10.1016/j.ab.2004.12.001

Metaxatos, A., Panagiotopoulos, C., and Ignatiades, L. (2003). Monosaccharide and amino acid composition of mucilage material produced from a mixture of four phytoplanktonic taxa. *J. Exp. Mar. Bio. Ecol.* 294, 203–217. doi: 10.1016/S0022-0981(03)00269-7

Metting, F. B. (1996). Biodiversity and application of microalgae. *J. Ind. Microbiol. Biotechnol.* 17, 477–489. doi: 10.1007/bf01574779

Monroe, E. A., and Van Dolah, F. M. (2008). The toxic dinoflagellate *Karenia brevis* encodes novel type I-like polyketide synthases containing discrete catalytic domains. *Protist* 159, 471–482. doi: 10.1016/j.protis.2008.02.004

Montojo, U., Tanyag, B., Perelonia, K. B., Cambia, F., and Oshiro, N. (2020). Ciguatera in the Philippines: examining reef fish vectors and its causative benthic dinoflagellates in Visayan and Sibuyan Seas. *Philipp. J. Fish.* 27, 19–29. doi: 10.31398/tpjf/27.1.2019a0015

Mooney, B. D., Nichols, P. D., De Salas, M. F., and Hallegraeff, G. M. (2007). Lipid, fatty acid, and sterol composition of eight species of Kareniaceae (Dinophyta): chemotaxonomy and putative lipid phycotoxins. *J. Phycol.* 43, 101–111. doi: 10.1111/j.1529-8817.2006.00312.x

Mudge, E. M., Robertson, A., Leynse, A. K., McCarron, P., and Miles, C. O. (2021). Selective extraction of gambierone and related metabolites in *Gambierdiscus silvae* using m-aminophenylboronic acid–agarose gel and liquid chromatography–high-resolution mass spectrometric detection. *J. Chromatogr. B* 1188:123014. doi: 10.1016/j.jchromb.2021.123014

Munday, R., Murray, S., Rhodes, L. L., Larsson, M. E., and Harwood, D. T. (2017). Ciguatoxins and maitotoxins in extracts of sixteen *Gambierdiscus* isolates and one *Fukuyoa* isolate from the South Pacific and their toxicity to mice by intraperitoneal and oral administration. *Mar. Drugs* 15:208. doi: 10.3390/md15070208

Murata, M., Legrand, A. M., Ishibashi, Y., Fukui, M., and Yasumoto, T. (1990). Structures and configurations of ciguatoxin from the moray eel *Gymnothorax javanicus*. *J. Am. Chem. Soc.* 112:4380–4386. doi: 10.1021/ja00167a040

Murray, J. S., Nishimura, T., Finch, S. C., Rhodes, L. L., Puddick, J., Harwood, D. T., et al. (2020). The role of 44-methylgambierone in ciguatera fish poisoning: acute toxicity, production by marine microalgae and its potential as a biomarker for *Gambierdiscus spp*. *Harmful Algae* 97:101853. doi: 10.1016/j.hal.2020.101853

Murray, J. S., Selwood, A. I., Harwood, D. T., van Ginkel, R., Puddick, J., Rhodes, L. L., et al. (2019). 44-Methylgambierone, a new gambierone analogue isolated from *Gambierdiscus australes*. *Tetrahedron Lett.* 60, 621–625. doi: 10.1016/j.tetlet.2019.01.043

Mydlarz, L. D., Jacobs, R. S., Boehnlein, J., and Kerr, R. G. (2003). Pseudopterosin biosynthesis in *Symbiodinium* sp., the dinoflagellate symbiont of *Pseudopterogorgia elisabethae*. *Chem. Biol.* 10, 1051–1056. doi: 10.1016/j

Nagai, H., Murata, M., Torigoe, K., Satake, M., and Yasumoto, T. (1992). Gambieric acids, new potent antifungal substances with unprecedented polyether structures from a marine dinoflagellate *Gambierdiscus toxicus*. *J. Org. Chem.* 57, 5448–5453. doi: 10.1021/jo00046a029

Naman, C. B., Rattan, R., Nikoulina, S. E., Lee, J., Miller, B. W., Moss, N. A., et al. (2017). Integrating molecular networking and biological assays to target the isolation of a cytotoxic cyclic octapeptide, samoamide A, from an American Samoan marine cyanobacterium. *J. Nat. Prod.* 80, 625–633. doi: 10.1021/acs.jnatprod.6b00907

Nishimura, T., Sato, S., Tawong, W., Sakanari, H., Yamaguchi, H., and Adachi, M. (2014). Morphology of *Gambierdiscus scabrosus* sp. nov. (Gonyaulacales): a new epiphytic toxic dinoflagellate from coastal areas of Japan. *J. Phycol.* 50, 506–514. doi: 10.1111/jpy.12175

Nonomura, T., Sasaki, M., Matsumori, N., Murata, M., Tachibana, K., and Yasumoto, T. (1996). The complete structure of maitotoxin, Part II: configuration of the C135-C142 side chain and absolute configuration of the entire molecule. *Angew. Chemie Int. Ed.* 35, 1675–1678.

Okuda, K. (2002). Structure and phylogeny of cell coverings. *J. Plant Res.* 115, 283–288. doi: 10.1007/s10265-002-0034-x

Oliveira, C. Y. B., Oliveira, C. D. L., Müller, M. N., Santos, E. P., Dantas, D. M. M., and Gálvez, A. O. (2020). A scientometric overview of global dinoflagellate research. *Publications* 8, 1–18. doi: 10.3390/publications8040052

Ortiz-Tena, J. G., Rühmann, B., Schieder, D., and Sieber, V. (2016). Revealing the diversity of algal monosaccharides: fast carbohydrate fingerprinting of microalgae using crude biomass and showcasing sugar distribution in *Chlorella vulgaris* by biomass fractionation. *Algal Res.* 17, 227–235. doi: 10.1016/j.algal.2016.05.008

Parrish, C. C., Abrajano, T. A., Budge, S. M., Helleur, R. J., Hudson, E. D., Pulchan, K., et al. (2000). "Lipid and phenolic biomarkers in marine ecosystems: analysis and applications," in *Marine Chemistry. The Handbook of Environmental Chemistry*, ed. P. J. Wangersky (Berlin: Springer), 193–223.

Paul, G. K., Matsumori, N., Konoki, K., Murata, M., and Tachibana, K. (1997). Chemical structures of amphidinols 5 and 6 isolated from marine dinoflagellate *Amphidinium klebsii* and their cholesterol-dependent membrane disruption. *J. Mar. Biotechnol.* 5, 124–128.

Pisapia, F., Holland, W. C., Hardison, D. R., Litaker, R. W., Fraga, S., Nishimura, T., et al. (2017). Toxicity screening of 13 *Gambierdiscus* strains using neuro-2a and erythrocyte lysis bioassays. *Harmful Algae* 63, 173–183. doi: 10.1016/j.hal.2017.02.005

Qi, X. M., Yu, B., Huang, X. C., Guo, Y. W., Zhai, Q., and Jin, R. (2007). The cytotoxicity of lingshuiol: a comparative study with amphidinol 2 on membrane permeabilizing activities. *Toxicon* 50, 278–282. doi: 10.1016/j.toxicon.2007.04.001

Rains, L. K., and Parsons, M. L. (2015). *Gambierdiscus* species exhibit different epiphytic behaviors toward a variety of macroalgal hosts. *Harmful Algae* 49, 29–39. doi: 10.1016/j.hal.2015.08.005

Rodríguez, I., Genta-Jouve, G., Alfonso, C., Calabro, K., Alonso, E., Sánchez, J. A., et al. (2015). Gambierone, a ladder-shaped polyether from the dinoflagellate *Gambierdiscus belizeanus*. *Org. Lett.* 17, 2392–2395. doi: 10.1021/acs.orglett.5b00902

Ronquist, F., and Huelsenbeck, J. P. (2003). MrBayes 3: bayesian phylogenetic inference under mixed models. *Bioinformatics* 19, 1572–1574. doi: 10.1093/bioinformatics/btg180

Sasaki, M., Matsumori, N., Nonomura, T., Murata, M., Tachibana, K., and Yasumoto, T. (1996). The complete structure of maitotoxin, Part I: configuration of the C1-C14 side chain. *Angew. Chemie Int. Ed.* 35, 1672–1675.

Satake, M., Bourdelais, A. J., Van Wagoner, R. M., Baden, D. G., and Wright, J. L. C. (2008). Brevisamide: an unprecedented monocyclic ether alkaloid from the dinoflagellate *Karenia brevis* that provides a potential model for ladder-frame initiation. *Org. Lett.* 10, 3465–3468. doi: 10.1021/ol801243n

Satake, M., Honma, D., Watanabe, R., and Oshima, Y. (2019). Alexandrolide, a diatom growth inhibitor isolated from the dinoflagellate *Alexandrium catenella*. *Tetrahedron Lett.* 60, 1341–1344. doi: 10.1016/j.tetlet.2019.04.019

Satake, M., Murata, M., and Yasumoto, T. (1993). Gambierol: a new toxic polyether compound isolated from the marine dinoflagellate *Gambierdiscus toxicus*. *J. Am. Chem. Soc.* 115, 361–362. doi: 10.1021/ja00054a061

Schulze, C., Strehle, A., Merdivan, S., and Mundt, S. (2017). Carbohydrates in microalgae: comparative determination by TLC, LC-MS without derivatization, and the photometric thymol-sulfuric acid method. *Algal Res.* 25, 372–380. doi: 10.1016/j.algal.2017.05.001

Shmukler, Y. B., and Nikishin, D. A. (2017). Ladder-shaped ion channel ligands: current state of knowledge. *Mar. Drugs* 15, 1–30. doi: 10.3390/md15070232

Sibat, M., Réveillon, D., Antoine, C., Carpentier, L., Rovillon, G. A., Sechet, V., et al. (2021). Molecular networking as a novel approach to unravel toxin diversity of four strains of the dominant *Dinophysis* species from French coastal waters. *Harmful Algae* 103:102026. doi: 10.1016/j.hal.2021.102026

Smith, K. F., Rhodes, L., Verma, A., Curley, B. G., Harwood, D. T., Kohli, G. S., et al. (2016). A new *Gambierdiscus* species (Dinophyceae) from Rarotonga, Cook Islands: *Gambierdiscus cheloniae* sp. nov. *Harmful Algae* 60, 45–56. doi: 10.1016/j.hal.2016.10.006

Soliño, L., and Costa, P. R. (2018). Differential toxin profiles of ciguatoxins in marine organisms: chemistry, fate and global distribution. *Toxicon* 150, 124–143. doi: 10.1016/j.toxicon.2018.05.005

Song, P.-S., Koka, P., Prézelin, B. B., and Haxo, F. T. (1976). Molecular topology of the photosynthetic light-harvesting pigment complex, peridinin-chlorophyll a-protein, from marine dinoflagellates. *Biochemistry* 15, 4422–4427. doi: 10.1021/bi00665a012

Templeton, D. W., Quinn, M., Van Wychen, S., Hyman, D., and Laurens, L. M. L. (2012). Separation and quantification of microalgal carbohydrates. *J. Chromatogr. A* 1270, 225–234. doi: 10.1016/j.chroma.2012.10.034

Tester, P., Wickliffe, L., Jossart, J., Rhodes, L., Enevoldsen, H., Adachi, M., et al. (2020). "Global distribution of genera *Gambierdiscus* and *Fukuyoa*," in *From Ecosystems to Socioecosystems. Proceedings of the 18th International Conference on Harmful Algae*, ed. P. Hess (Nantes: International Society for the Study of Harmful Algae), 138–143.

Teta, R., Della Sala, G., Glukhov, E., Gerwick, L., Gerwick, W. H., Mangoni, A., et al. (2015). Combined LC-MS/MS and molecular networking approach reveals new cyanotoxins from the 2014 cyanobacterial bloom in Green Lake, Seattle. *Environ. Sci. Technol.* 49, 14301–14310. doi: 10.1021/acs.est.5b04415

Tibiriçá, C. E. J. D. A., Sibat, M., Fernandes, L. F., Bilien, G., Chomérat, N., Hess, P., et al. (2020). Diversity and toxicity of the genus *Coolia* Meunier in Brazil, and detection of 44-methyl gambierone in *Coolia tropicalis*. *Toxins* 12:327. doi: 10.3390/toxins12050327

Usup, G., Hamid, S. Z., Chiet, P. K., Wah, C. K., and Ahmad, A. (2008). Marked differences in fatty acid profiles of some planktonic and benthic marine dinoflagellates from Malaysian waters. *Phycologia* 47, 105–111. doi: 10.2216/07-55.1

Vacarizas, J., Benico, G., Austero, N., and Azanza, R. (2018). Taxonomy and toxin production of *Gambierdiscus carpenteri* (Dinophyceae) in a tropical marine ecosystem: the first record from the Philippines. *Mar. Pollut. Bull.* 137, 430–443. doi: 10.1016/j.marpolbul.2018.10.034

Van Dolah, F. M., Kohli, G. S., Morey, J. S., and Murray, S. A. (2017). Both modular and single-domain Type I polyketide synthases are expressed in the brevetoxin-producing dinoflagellate, *Karenia brevis* (Dinophyceae). *J. Phycol.* 53, 1325–1339. doi: 10.1111/jpy.12586

Van Dolah, F. M., Morey, J. S., Milne, S., Ung, A., Anderson, P. E., and Chinain, M. (2020). Transcriptomic analysis of polyketide synthases in a highly ciguatoxic dinoflagellate, *Gambierdiscus polynesiensis* and low toxicity *Gambierdiscus pacificus*, from French Polynesia. *PLoS One* 15:e0231400. doi: 10.1371/journal.pone.0231400

Verma, A., Kohli, G. S., Harwood, D. T., Ralph, P. J., and Murray, S. A. (2019). Transcriptomic investigation into polyketide toxin synthesis in *Ostreopsis* (Dinophyceae) species. *Environ. Microbiol.* 21, 4196–4211. doi: 10.1111/1462-2920.14780

Via, C. W., Glukhov, E., Costa, S., Zimba, P. V., Moeller, P. D. R., Gerwick, W. H., et al. (2018). The metabolome of a cyanobacterial bloom visualized by MS/MS-based molecular networking reveals new neurotoxic smenamide analogs (C, D, and E). *Front. Chem.* 6:316. doi: 10.3389/fchem.2018.00316

Vingiani, G. M., Stalberga, D., De Luca, P., Ianora, A., De Luca, D., and Lauritano, C. (2020). De novo transcriptome of the non-saxitoxin producing *Alexandrium tamutum* reveals new insights on harmful dinoflagellates. *Mar. Drugs* 18:386. doi: 10.3390/MD18080386

Wakamiya, Y., Ebine, M., Matsumori, N., and Oishi, T. (2020). Total synthesis of amphidinol 3: a general strategy for synthesizing amphidinol analogues and structure-activity relationship study. *J. Am. Chem. Soc.* 142, 3472–3478. doi: 10.1021/jacs.9b11789

Wang, M., Carver, J. J., Phelan, V. V., Sanchez, L. M., Garg, N., Peng, Y., et al. (2016). Sharing and community curation of mass spectrometry data with global natural products social molecular networking. *Nat. Biotechnol.* 34, 828–837. doi: 10.1038/nbt.3597

Watanabe, R., Uchida, H., Suzuki, T., Matsushima, R., Nagae, M., Toyohara, Y., et al. (2013). Gambieroxide, a novel epoxy polyether compound from the dinoflagellate *Gambierdiscus toxicus* GTP2 strain. *Tetrahedron* 69, 10299–10303. doi: 10.1016/j.tet.2013.10.022

World Health Organization (2020). *World Health Organization Ciguatera Fish Poisoning*. Available online at: https://www.who.int/foodsafety/areas_work/chemical-risks/CFP/en/ (accessed February 2, 2020).

Wu, H., Chen, J., Peng, J., Zhong, Y., Zheng, G., Guo, M., et al. (2020). Nontarget screening and toxicity evaluation of diol esters of okadaic acid and dinophysistoxins reveal intraspecies difference of *Prorocentrum lima*. *Environ. Sci. Technol.* 54, 12366–12375. doi: 10.1021/acs.est.0c03691

Yñiguez, A. T., Lim, P. T., Leaw, C. P., Jipanin, S. J., Iwataki, M., Benico, G., et al. (2021). Over 30 years of HABs in the Philippines and Malaysia: what have we learned? *Harmful Algae* 102:101776. doi: 10.1016/j.hal.2020.101776

Yon, T., Sibat, M., Robert, E., Lhaute, K., Holland, W. C., Litaker, R. W., et al. (2021). Sulfo-Gambierones, two new analogs of gambierone produced by *Gambierdiscus excentricus*. *Mar. Drugs* 19:657.

Zhang, H., Wu, Z., Cen, J., Li, Y., Wang, H., and Lu, S. (2016). First report of three benthic dinoflagellates, *Gambierdiscus pacificus*, *G. australes* and *G. caribaeus* (Dinophyceae), from Hainan Island, South China Sea. *Phycol. Res.* 64, 259–273. doi: 10.1111/pre.12137

Conflict of Interest: The authors declare that the research was conducted in the absence of any commercial or financial relationships that could be construed as a potential conflict of interest.

frontiers in Marine Science

ORIGINAL RESEARCH
published: 17 February 2022
doi: 10.3389/fmars.2022.730518

A Snapshot on the Distribution of Coastal Phytoplankton Communities in Five HAB-Affected Bays in Eastern Visayas, Philippines

Stephanie Faith Ravelo[1], Leni G. Yap-Dejeto[1]*, Mark Leonard S. Silaras[1], Ma. Luningning L. Amparado[2], Jason A. Ocampo[2], Eugene G. Abria[1] and Marietta B. Albina[2]

[1] *Division of Natural Sciences and Mathematics, University of the Philippines Visayas Tacloban College, Tacloban City, Philippines,* [2] *College of Fisheries and Marine Sciences, Samar State University, Catbalogan City, Philippines*

In recent years, harmful algal blooms (HABs), commonly known as red tide, have started to occur year-round in the warm tropical marine waters of Eastern Visayas, Philippines. These are a threat to public safety and cause enormous loss in industries relying on marine resources. The first step in solving this problem is to establish the distribution and succession of phytoplankton communities and harmful microalgae that exist in the region. For the first time, simultaneous monthly monitoring of the phytoplankton community was conducted in five HAB-affected bays of Leyte and Samar islands. We observed spatial differences on the environmental profiles between the five bays in the two islands and these differences may, in part, influence the distribution and abundance of the phytoplankton community residing within these areas. Diatom associated groups were prevalent in all sampling sites, however, HAB causative species were abundant in the bays in Samar during the sampling period. Five (5) genera and nine (9) species that may cause HAB were identified in all five bays. These are potential vectors for paralytic shellfish poisoning, amnesic shellfish poisoning, diarrhetic shellfish poisoning, and fish kill due to hypoxia. The correlation analysis confirmed that the majority of potential HAB vectors correlated with temperature, dissolved oxygen, rainfall, nitrate, and phosphate. The abundance of *Pyrodinium bahamense* observed in October to November in Samar coincided with several red tide alerts announced by the region's fishery agency. This however, was never observed to dominate the phytoplankton community. Instead, the following diatoms dominated the five bays; *Skeletonema*, *Pseudo-nitzschia*, *Bacteriastrum*, *Chaetoceros*, *Rhizosolenia* and *Thalassionema*. This is a pioneering study that shows a simultaneous snapshot on the community structure and environmental profiles in these five bays in Eastern Visayas in 2020–2021. It discusses the effects of mariculture to its phytoplankton community and vice versa. Relationships between different phytoplankton species were further observed. This contributes to the knowledge of phytoplankton ecology in warm waters which is necessary to understand future phytoplankton ecosystems affected by sea temperature rise due to climate change.

Keywords: harmful algal blooms (HABs), surface phytoplankton, community composition, succession, Eastern Visayas, Philippines, climate change

Edited by:
Michael Yu Roleda,
University of the Philippines Diliman,
Philippines

Reviewed by:
Maria Paches,
Universitat Politècnica de València,
Spain
Arief Rachman,
Indonesian Institute of Sciences,
Indonesia

****Correspondence:***
Leni G. Yap-Dejeto
lgyapdejeto@up.edu.ph

Specialty section:
This article was submitted to
Marine Ecosystem Ecology,
a section of the journal
Frontiers in Marine Science

Received: *25 June 2021*
Accepted: *05 January 2022*
Published: *17 February 2022*

Citation:
Ravelo SF, Yap-Dejeto LG, Silaras MLS, Amparado MLL, Ocampo JA, Abria EG and Albina MB (2022) A Snapshot on the Distribution of Coastal Phytoplankton Communities in Five HAB-Affected Bays in Eastern Visayas, Philippines. Front. Mar. Sci. 9:730518. doi: 10.3389/fmars.2022.730518

INTRODUCTION

Phytoplankton are known as biological indicators of water and its ecological health status (Wu, 1993; Roelke et al., 2003). They contribute to almost half of the global net primary productivity and are responsible for sustaining the aquatic food webs in support of organisms in the higher trophic levels (Behrenfeld and Randerson, 1998). Phytoplankton respond quickly to different environmental parameters including physical (i.e., light, temperature, rainfall), chemical (inorganic carbon, nutrient, dissolved oxygen), and biological (competition and predation) factors (Maddux and Jones, 1964). These factors have implications in their growth, abundance, availability, and distribution. These understandings on phytoplankton ecology mostly come from studies in temperate areas. Knowing which of these aspects exert a greater influence to the behavior of phytoplankton species in tropical marine waters becomes exceedingly important in understanding the condition of the environment they proliferate, especially in the context of harmful algal blooms. This will also provide knowledge on what to anticipate when seawaters warm due to climate change.

Harmful algal blooms (HABs) are naturally occurring phenomenon that has exacerbated because of anthropogenic disturbances which results to proliferation of microalgae that exhibit a negative impact on aquaculture and aquatic ecosystem or toxic to human health and other aquatic organisms (Van Dolah, 2000; Wells et al., 2020). In Southeast Asia, for example, the Philippines is reported as one of the most impacted regions by HABs (Azanza and Max Taylor, 2001). The first reported case of HAB in the country was in Maqueda Bay, western Samar in 1983 (Maclean, 1989), and since then, the occurrences of these blooms have been increasing spatially and frequently, even diversifying into different HAB types in the recent years (Yñiguez et al., 2020). While many studies about HABs have been reported in the Philippines, most of these are primarily focused in the coastal towns of Bolinao and Anda in the Northern part of the Philippines. Blooms recorded here were caused by different phytoplankton species such as *Pyrodinium bahamense* (Azanza and Max Taylor, 2001), *Alexandrium minutum* (Azanza and Benico, 2013; Benico, 2015), *Prorocentrum cordatum* (Azanza et al., 2005; San Diego-McGlone et al., 2008), *Chattonella subsalsa* (Lum et al., 2019), *Skeletonema* sp. (Escobar et al., 2013), *Rhizosolenia* sp. (Azanza and Benico, 2013), *Takayama* sp. (Benico et al., 2018, 2019) and many others. Manila Bay, on the other hand, is the socio-economic center in the country draining Metro Manila and many surrounding watersheds also experienced blooms brought about by *P. bahamense* (Azanza and Max Taylor, 2001) and *A. minutum* (Benico, 2015). Unfortunately, there has been little published data on the primary hotspots of HAB in the Philippines, which is Eastern Visayas, where *Pyrodinium* blooms have been experienced frequently.

Region VIII, Eastern Visayas consist of three main islands, Leyte, Samar, and Biliran. This is the site of the first report of toxic *Pyrodinium* red tides in the Philippines in 1983. And while incidences of *Pyrodinium* blooms have been increasing in recent years with red tide bans imposed every month (Meniano, 2020; BFAR Region-8, 2021), there has been no phytoplankton ecological studies that have been comprehensively done in the area. This is disappointing as the islands primarily rely on fish, shellfish, and other marine resources as their food and livelihood. *P. bahamense* incidences of human deaths from mussel consumption have also been reported in recent years. Of the 3,800 PSP cases recorded worldwide during the 1985–2018 period, 2,555 cases of which occurred in the Philippines alone recording a total of 165 deaths (Hallegraeff et al., 2021) of which the majority of these cases originated from western Samar and Biliran Islands. While the Bureau of Fisheries and Aquatic Resources Regional Office 8 (BFAR-8) has been monitoring the HAB occurrences in the region, it has only been limited to HAB species, particularly *Pyrodinium bahamense* with no physico-chemical data. The successional dynamics of the phytoplankton species in this area has yet to be mapped out. This information can later be used as indicators for prediction of PSP events. This can also serve as seed data toward finding and building physical solutions of HABS in Region VIII. At the same time, we hope to contribute to the understanding of the ecology of not only *Pyrodinium,* but other phytoplankton species which may or may not cause harmful algal blooms in tropical marine waters.

To obtain the distribution of coast community phytoplankton in Leyte and Samar, a simultaneous monitoring activity was carried out in five major bays in the province of Samar, Leyte, and Biliran in Eastern Visayas from August 2020 to January 2021, which represents the Habagat (Southwest) to Amihan (Northeast) monsoons. The composition, abundance, and distribution of the entire phytoplankton community were determined with focus on microphytoplankton and HABs species. We also correlated the interaction between various physico-chemical parameters to the phytoplankton community and in particular on the toxic species.

MATERIALS AND METHODS

Sampling Site

The sites chosen in this study were among the bays in Eastern Visayas that experience recent year-round blooms of *P. bahamense*. In Samar, the three major bays are located within its mussel mariculture zone, namely Cambatutay Bay (11.900 N; 124.786 E), Irong-Irong Bay (11. 818 N; 124.825 E), and Villareal Bay (11.602 N; 124.913 E) were selected. All the bays exhibited a dark-muddy substrate as they received the sediment-rich water from different rivers and other waterway systems. Aside from being muddy, the sediment substrate in Villareal bay was also mixed with granular grains coming from crushed shells. On the other hand, the site in Leyte (Carigara Bay; 11.327 N; 124.693 E) and Biliran (Biliran Bay; 11.556 N; 124.605 E) were beside the coastal town community. There were two stations included in each site resulting in a total of 10 stations (**Figure 1**).

Phytoplankton Collection and Analysis

Surface water samples for qualitative analysis were collected monthly in triplicate in each station within 2-m depth using a 20-μm mesh size plankton net with a 30-cm diameter mouth opening. The plankton net was towed vertically and the

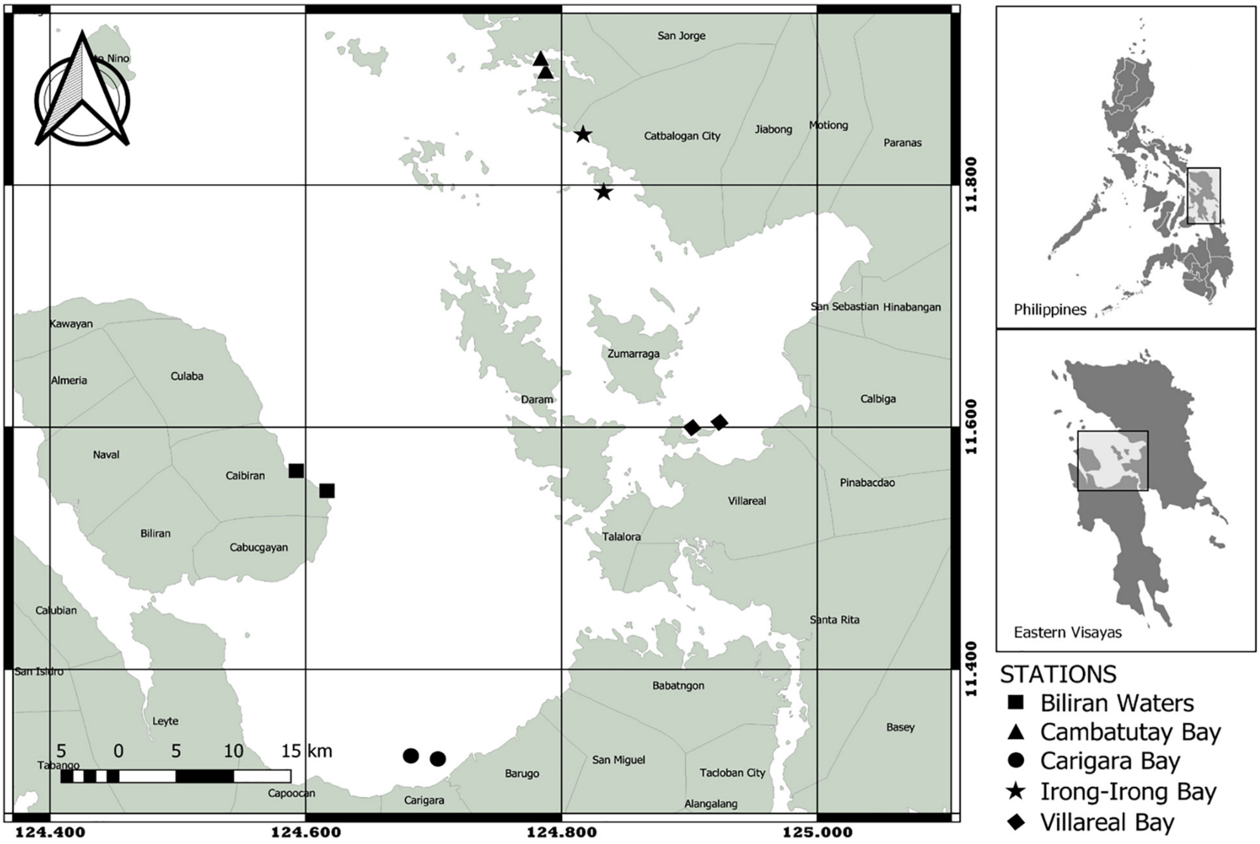

FIGURE 1 | The map of 10 stations surveyed for phytoplankton composition in Eastern Visayas, Philippines. Sampling sites are designated in different shapes.

concentrated 50-mL water was transferred in a translucent bottle and immediately fixed *in situ* with a 5-mL formalin solution. At the same time another set of surface water samples were collected by a bucket in triplicate in each station within 1-m depth and transferred into a 1-L straight bottle without corrugation to guarantee the settlement of all phytoplankton in the bottom. The samples were immediately fixed *in situ* using 1% formaldehyde solution and kept in a storage box until the arrival in the laboratory then left undisturbed for at least 24-h. The upper layer of water was carefully sucked out using a plastic capillary tubing and pump and the remaining 250-mL was transferred to a straight container with a relatively small diameter and settled again for another 24-h. The upper layer of water was discarded once again leaving the remaining 50-mL of seawater and the concentrated collected phytoplankton as the final samples. Phytoplankton were quantified using 1-mL aliquot from the final sample that was transferred to a gridded Sedgewick-Rafter counting chamber and allowed to settle for a few seconds before counting at least 300 cells. The densities (cells L^{-1}) were calculated by multiplying the concentrated volume with the cell counts. Counting was carried out in a 100X total magnification compound microscope in triplicate for every sampling bottle. Micrographs were taken and used in the identification of phytoplankton following the identification guides of Tomas (1997), Larink and Westheide (2006), Omura et al. (2012), and the AlgaeBase database (Guiry and Guiry, 2020). Identification of phytoplankton taxa were limited to diatoms and dinoflagellates.

Physico-Chemical Collection and Analysis

All phytoplankton sampling was accompanied by triplicate measurements of physical (surface water temperature, depth, turbidity, current velocity, and total suspended solids) and chemical (pH, salinity, dissolved oxygen, chlorophyll-*a*, phosphate, and nitrate) parameters. Temperature, pH, and dissolved oxygen were measured *in situ* using a calibrated HANNA multiparameter 1-m below the water surface layer. In the same way, salinity was measured using a handheld refractometer. Current velocity was estimated by drift method using a fabricated Holey Sock drogue attached to a 5-m thin rope. The drogue was deployed in the water and the time it traveled within 1-m distance was recorded. Both water depth and turbidity were estimated using a Secchi disc. The depth was obtained by submerging the disc up to the bottom of the water and recording the measurement using the calibration on the rope. Secchi Disk Transparency (SDT; turbidity of the water column) was measured by recording the depth where the disc disappeared from the view (A), and reappeared when hoisted (B), the formula as follows: limit of visibility = (A + B)/2. Data from

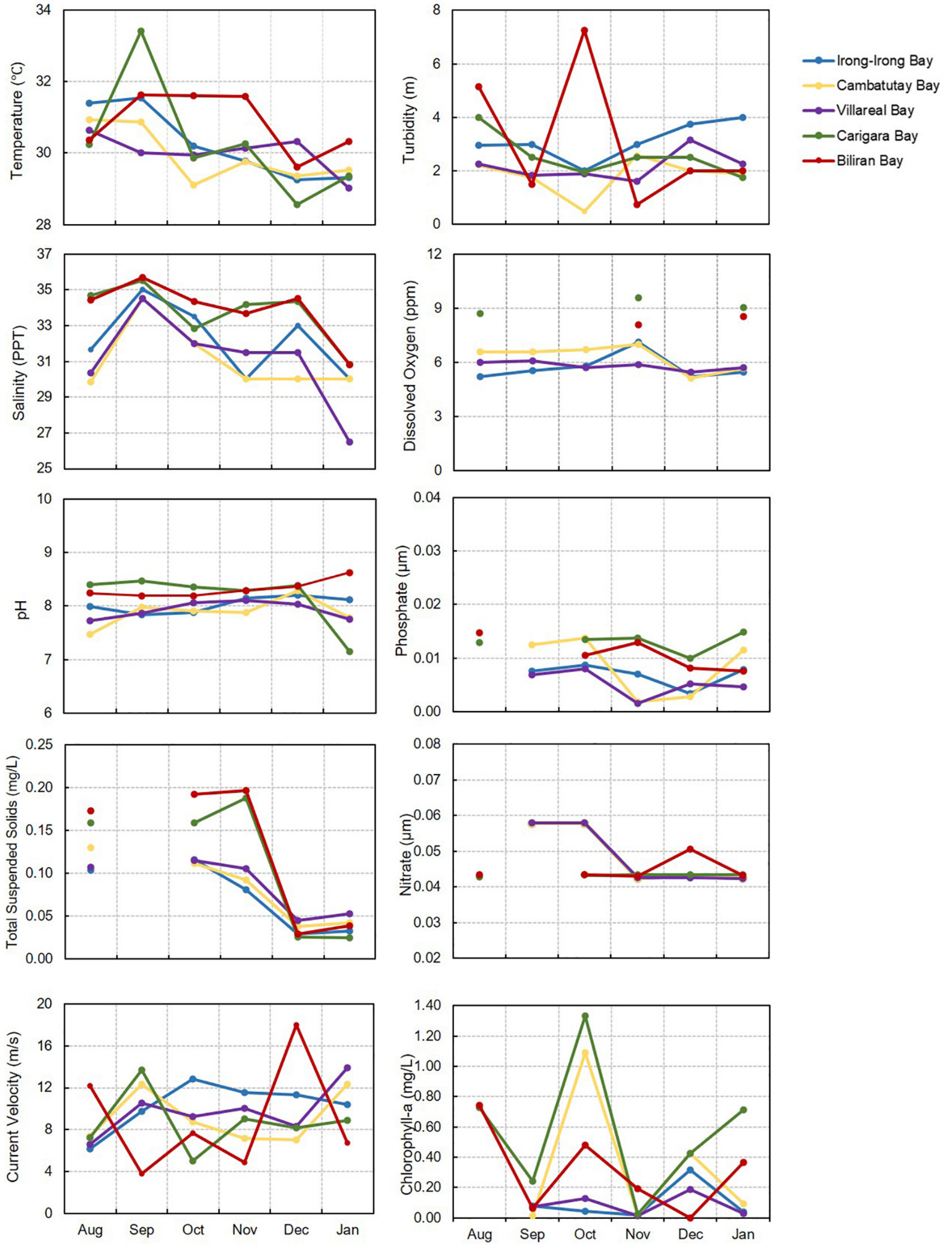

FIGURE 2 | Average measurement of physico-chemical parameters in the five HAB-affected bays in Eastern Visayas from August 2020-January 2021, including the inorganic nutrients (nitrates and phosphates). The number of parameters measured varied depending on the availability of the equipment during sampling and weather or sea condition.

rainfall was extracted from Philippine Atmospheric, Geophysical, and Astronomical Services Administration (PAG-ASA).

Analyses of water samples for Total Suspended Solids (TSS), chlorophyll-*a* (chl-*a*), and dissolved inorganic nutrients such as phosphate (PO_4^{-3}) and nitrate (NO_3^{-}) were collected in every sampling period using a 1-L pre-labeled polyethylene (PET) bottles and stored immediately in an icebox. All samples were filtered using 47-mm diameter Whatman® GF/C glass fiber filters in a motor-driver filtering set-up, while samples for chl-*a* were done in a low light environment to avoid photodegradation. TSS concentrations were measured following the American Public Health Association [APHA] (1992) method 2540D. Around 250-mL of the collected water was filtered in pre-weighed and pre-dried glass fiber filters. The filters were oven dried at 60°C

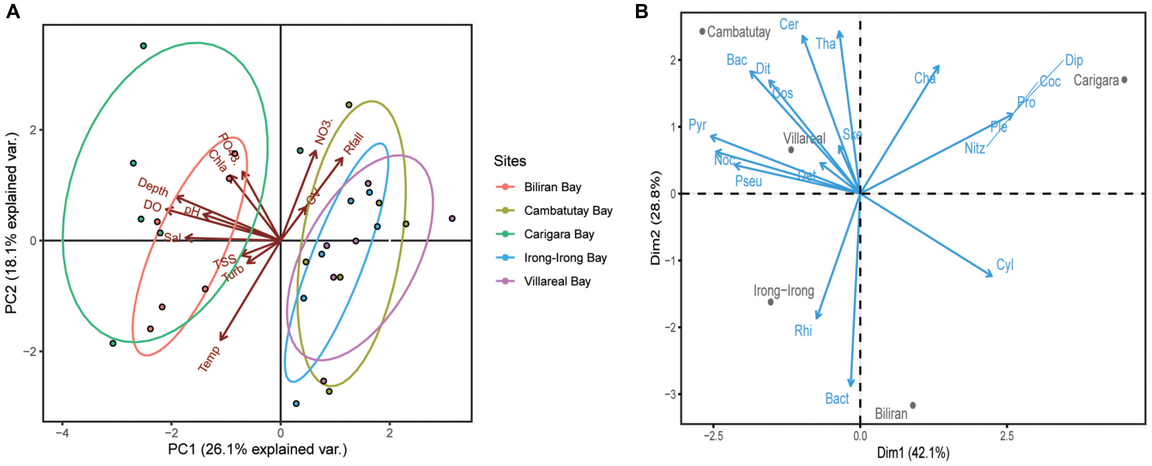

FIGURE 3 | Biplot of Principal Component Analysis (PCA). **(A)** PCA biplot for physico-chemical parameters of the five bays against different environmental gradients. The axis scores were shown for PCA 1 and PCA 2. There are five groups included during the PCA, represented by the five different bays designated by a specific color. Physico-chemical parameters legend: Sal (salinity), Turb (turbidity), Temp (temperature), Rfall (rainfall), CV (current velocity), TSS (total suspended solids), chla (chlorophyll-a), PO_4^{-3} (phosphate), NO_3^- (nitrate), and DO (dissolved oxygen). **(B)** PCA biplot of the phytoplankton abundance in five sampling sites. The blue arrows represent the phytoplankton genera. Phytoplankton legend: Ske (*Skeletonema*), Tha (*Thalassionema*), Pseu (*Pseudo-nitzschia*), Cha (*Chaetoceros*), Cos (*Coscinodiscus*), Bact (*Bacteriastrum*), Bac (*Bacillaria*), Dit (*Ditylum*), Cer (*Ceratium*), Noc (*Noctiluca*), Pyr (*Pyrodinium*), Det (*Detonula*), Rhi (*Rhizosolenia*), Cyl (*Cylindrotheca*), Ple (*Pleurosigma*), Dip (*Diploneis*), Nitz (*Nitzschia*), Coc (*Cocconeis*), and Pro (*Prorocentrum*).

for 24-h and the total suspended solids was calculated by the difference in initial and final constant weights. The same known volume of water was filtered in a new glass fiber filter for the measurement of chl-*a*. The filters were soaked in a 10-mL 90% acetone solution at 4°C for 24-h. The samples were then centrifuged for 20 min at 500-g and the absorbance at 750, 663, 645, and 630 nm were measured using a UV-VIS spectrophotometer. The samples were then treated with 100-μL of 0.1N hydrochloric acid (HCl) and the absorbance at 750 and 665 nm was measured once again. Chlorophyll-*a* concentration was evaluated using Environmental Sciences Section [ESS] (1991) method 150.1. All filtered water samples were then used for nutrient analyses. A volume of 250-mL was transferred in a 150-mL acid-washed beaker and the measurements were provided in full detail by United States Environmental Protection Agency [USEPA] (1978) methods 365.3 (1978) for PO_4^{-3} at 690 nm and PI® Reef Master Test Kit for NO_3^- at 540 nm using the spectrophotometer. The collection of water samples was done in triplicate in each station, and at least three replicate measurements were carried out in each analysis.

Statistics

Data for phytoplankton abundance and physico-chemical parameters were averaged monthly in each site to acquire mean semi-annual data. The mean abundance data were utilized to obtain biodiversity indices such as Shannon-Wiener diversity (H′), Margalef's richness index (D), and Pielou evenness (J′). using the Paleontological Statistics (PAST) software program version 4.13 (Hammer et al., 2001). The Principal Component Analysis (PCA) was carried out to evaluate the phytoplankton community and physico-chemical parameters at different bays and the extent to which the measured parameters could explain the distribution of the phytoplankton species. Before inputting into PCA, the mean data were centered and/or scaled to normalize data that were associated from different magnitudes followed by standardization for the physico-chemical parameters or pre-transformation using Helinger for the phytoplankton abundance. The PCA was carried out using the prcomp function. The scores for PCA 1 and 2 were extracted and used to visualize the PCA biplot of physico-chemical parameters using the ggbiplot2 (Wickham, 2016), phytoplankton taxa using factoextra (Kassambara and Mundt, 2017), and dominant phytoplankton species against the environmental parameters using Factoshiny package (Vaissie et al., 2021). To assess the correlation between the environmental drivers and dominant phytoplankton genera in each bay, the Pearson's correlation coefficient was performed using the corr function. We then performed a correlation test to know whether the correlation coefficient between variables is significantly different from 0 using the rcorr function. A correlogram was built using corrplot (Wei and Simko, 2021) to visualize correlation between all possible pairs present in the dataset, with a clear distinction for correlations that are different from 0. All multivariate analyses were performed in R.

RESULTS

Physico-Chemical Profiles in Eastern Visayas Sites

Monthly time-series for the physical and chemical environmental data recorded during the sampling period for the five HAB-affected bays in Eastern Visayas are presented in **Figure 2**. On the average, the surface water temperature in all the bays were collectively high at 29–32°C. The highest peak in temperature occurred in September in all the bays with the highest value recorded in Cambatutay Bay at 32°C, however, no obvious pattern is apparent in the temperature plot. The same is true in the pH values that were relatively alkaline (7∼8) and did not very much in between the five bays. Interestingly, the three bays in Samar seem to follow the same pattern compared to the bays in Leyte and Biliran in terms of turbidity, salinity, current velocity, dissolved oxygen, and TSS. The average depth in Cambatutay, Villareal, and Irong-Irong Bays were all shallow at 4-m, high in turbidity and current velocity, but low in salinity (Cambatutay = 30 ∼ 34 ppt; Irong-Irong = 31 ∼ 35 ppt; Villareal = 27 ∼ 34 ppt), dissolved oxygen (Cambatutay and Irong-Irong = 5 ∼ 7 ppm; Villareal = 5 ∼ 6 ppm), and TSS (Cambatutay, Irong-Irong, and Cambatutay = 0.3 ∼ 0.1 mg/L) compared to Carigara (salinity = 30–36 ppt; dissolved oxygen = 8 ∼ 9 ppm; TSS = 0.02 ∼ 0.2 mg/L) and Biliran (salinity = 30 ∼ 36 ppt; dissolved oxygen = 8 ∼ 9 ppm; TSS = 0.03 ∼ 0.02 mg/L) Bays. According to PAG-ASA, the highest rainfall during the sampling period starts in October in Leyte while in Samar, the increase in rainfall starts in December. Yet on the average, the rainfall concentration remains relatively high (Leyte = 162 ∼ 692 mm; Samar = 251 ∼ 556 mm) in Eastern Visayas. The alternate level on the concentration of chl-*a* was observed monthly for most of the bays, however, the average chl-*a* level in Carigara and Biliran Bays were a little high compared to Irong-Irong, Cambatutay, and Villareal bays. The PO_4^{-3} concentration was relatively the same in all of the bays at the mean of 0.01 μM. The nitrate concentrations in the three bays in Samar were slightly higher, at 0.06 μM than Carigara and Biliran Bays at 0.04 μM. Although starting in November, the NO_3^- concentration in Irong-Irong, Cambatutay, and Villareal Bays decreased to 0.04 μM.

Principal Component Analysis (PCA) using the physico-chemical parameters of the five bays used in this study separated the samples into two distinct clusters (**Figure 3A**), which explained 44.2% of total variance by the first two principal components (PCs): PC1 = 26.1%; eigenvalue = 3.13 and PC2 = 18.1%; eigenvalue = 2.17. The bays of Cambatutay, Irong-Irong, and Villareal clustered together and were separated against the bays of Carigara and Biliran. Looking at the axis, the bays for Biliran and Carigara were closely correlated on salinity, pH, dissolved oxygen, depth, chl-*a*, and PO_4^{-3} while Cambatutay Bay was closely correlated with rainfall and current velocity.

Phytoplankton Community in the Five Bays

A total of 43 phytoplankton genera were identified from the five bays in Eastern Visayas, mainly dominated by the taxa belonging to Bacillariophyceae (33 diatom genera), and nine Dinophyceae (dinoflagellates). The Samar bays had higher monthly total average phytoplankton densities at 55,000–73,000 cells/L compared with Leyte bays at 26,000–31,000 cells/L (**Figure 4**). For the whole sampling period, Irong-Irong Bay had the highest mean density of phytoplankton species (38,000 cells L^{-1}, H′ = 1.81, J′ = 0.32, D = 1.83) then followed by Villareal (37,000 cells L^{-1}, H′ = 0.155, J′ = 0.26, D = 1.83), Cambatutay (32,000 cells L^{-1}, H′ = 1.91, J′ = 1.78, D = 1.96), Carigara (25,000 cells L^{-1}, H′ = 1.67, J′ = 0.28, D = 1.92), and Biliran Bays (22,000 cells L^{-1}, H′ = 1.58, J′ = 0.27, D = 1.83), respectively. No clear spatial pattern can be discerned as to the evenness values of the five bays that remained low throughout the sampling period (0.2 to.4), yet the species diversity of these bays was fairly similar ranging from 1.6 to 1.9. Likewise, the Margalef's richness index of the five bays was similar with a range of 1.8 to 2.0.

The PCA showed that the first two principal components accounted for more than 71% of the variations (Dim1 = 42.1% with eigenvalue = 7.99 and Dim2 = 28.8% with eigenvalue = 5.47) in the species composition, with obvious pattern of species division between sites (**Figure 3B**). Top dominant genera, *Skeletonema*, *Pseudo-nitzschia*, and *Noctiluca scintillans* all exhibited positive linear correlation in Villareal Bay while *Pyrodinium bahamense* displayed positive correlation with Cambatutay and Villareal Bays. Most species with positive correlation in Carigara and Biliran Bays were non-HAB diatoms such as *Rhizosolenia*, *Bacteriastrum*, and *Chaetoceros*.

Based from the phytoplankton community composition, the relative abundances of diatoms, which accounted for up to 99% in Biliran Bay, 95% in Villarreal Bay, 94% in Carigara Bay, and 89% in Irong-Irong and Cambatutay Bays, remained high throughout the sampling period across all the five bays in contrast to dinoflagellates that was collectively < 11% in the population. Diatoms in the genus *Skeletonema*, *Bacteriastrum*, *Chaetoceros*, *Pseudo-nitzschia*, and *Thalassionema* were common and prevalent in all the bays during the sampling period (**Figure 4**). For dinoflagellates, genera which are HAB vectors such as genus *Ceratium*, *Pyrodinium bahamense,* and *Noctiluca scintillans* were common and prevalent in the three bays in Samar. In fact, we observed a spike in the density of *Pyrodinium* within September to November while the density on *N. scintillans* starts to increase in December. On the other hand, we observed the presence of other potential HAB vectors such as *Dinophysis*, *Alexandrium*, *Nitzschia*, *Prorocentrum*, and *Gymnodinium*, but all were collectively below 100 cells L^{-1}. Between the dominant genera, the most prevalent group belonged to *Skeletonema* with relative mean density of 10,000 cells L^{-1} but abundances of *Pseudo-nitzschia* species and *N. scintillans* were relatively high too, especially in the three bays in Samar, with mean densities of 4,000 and 600 cells L^{-1}, respectively.

Diatom Succession in the Five Bays

For Irong-Irong Bay in the Samar Seas, the diatoms *Skeletonema* and *Pseudo-nitzschia* dominated the phytoplankton community in August 2020, the start of the sampling period. *Skeletonema* then increased further and dominated in September, to be briefly replaced by *Bacteriastrum* the month after and *Rhizosolenia* by the next month, November. The profile in December changed with *Skeletonema*, *Bacteriastrum,* and a growing number of *Chaetoceros* as the most prevalent. *Pseudo-nitzschia* continued to decrease while *Chaetoceros* increased further by the end of the sampling period, in January 2021. In Cambatutay Bay, *Skeletonema* dominated the phytoplankton community except in December when *Ditylum*, *Bacteriastrum*, and *Chaetoceros* briefly dominated. *Chaetoceros* continued to increase in number in January. Villareal Bay was dominated by *Pseudo-nitzschia* sp. during August but they gradually decreased in the months after. Unlike *Pseudo-nitzschia* sp., the density of *Chaetoceros* increased monthly, with the highest increase in December and January. The abundance profile of *Bacteriastrum* was heterogeneous but they are mostly abundant in October and December. The density of *Skeletonema* spiked in September to November to abruptly decrease to low in December then increased by the next month, January.

In the Leyte side (**Figure 4**), more diatoms dominated in the two bays examined. In Carigara, *Chaetoceros* dominated the months of August and September. This was briefly replaced by *Thalassionema*. Then *Skeletonema* dominated the rest of the months. *Chaetoceros* also dominated the phytoplankton community of Biliran Bay except for the month of September when this was dominated by *Bacteriastum.*

Correlation of Harmful Algal Blooms Species and Environmental Drivers

Microscopic images of the HAB vectors identified in the sampling sites are shown in **Figure 5**. The relationship between the dominant phytoplankton groups with the physico-chemical parameters and potential HAB vectors in the five bays were further subjected to a correlation analysis through Pearson's correlation coefficient (**Figure 6**). In Villareal Bay, $PO_4{}^{-3}$ ($r = 0.47$; $p \geq 0.999$), NO_3^- ($r = 0.48$; $p \geq 0.999$), and rainfall ($r = 0.62$; $p \geq 0.999$) displayed positive correlation with *P. bahamense.* The same can be observed in Irong-Irong (PO_4^{-3}: $r = 0.61$; $p \geq 0.999$; NO_3^-: $r = 0.47$; $p \geq 0.999$; rainfall: $r = 0.13$; $p \geq 0.999$) and Cambatutay (PO_4^{-3}: $r = 0.4$; $p \geq 0.999$; NO_3^-: $r = 0.52$; $p \geq 0.999$; rainfall: $r = 0.47$; $p \geq 0.999$) Bays. Moreover, the relationship of temperature against dominant genera was highly heterogeneous with no clear spatial pattern, however, it displayed a positive correlation with *N. scintillans* in Villareal bay ($r = 0.55$; $p \geq 0.999$). *Pseudo-nitzschia* which was partly prevalent in the three bays in Samar displayed positive correlation with dissolved oxygen (Villareal: $r = 0.78$, $p \geq 0.999$; Irong-Irong: $r = 0.33$, $p \geq 0.999$; Cambatutay: $r = 0.95$, $p \geq 0.999$) but exhibited a negative correlation in Carigara ($r = 0.07$, $p \geq 0.999$) and Biliran ($r = -0.29$, $p \geq 0.999$) Bays. Between species interaction, *P. bahamense* displayed positive correlation with *N. scintillans* in Irong-Irong ($r = -0.59$, $p \geq 0.999$) and Cambatutay ($r = -0.68$, $p \geq 0.999$) Bays but exhibited a negative correlation in Villareal Bay. *Pseudo-nitzschia* that was prevalent in all the bays displayed a heterogenous relationship against other genera, except in Villareal ($r = -0.50$; $p \geq 0.999$) and Cambatutay ($r = -0.46$; $p \geq 0.999$) Bays where they exhibited a positive correlation with *P. bahamense*. Other diatom genera displayed a highly heterogeneous relationship between potential HAB vectors and non-HAB phytoplankton. Other correlations observed between the physico-chemical parameters, dominant phytoplankton taxa, and potential HAB-vectors were not significant.

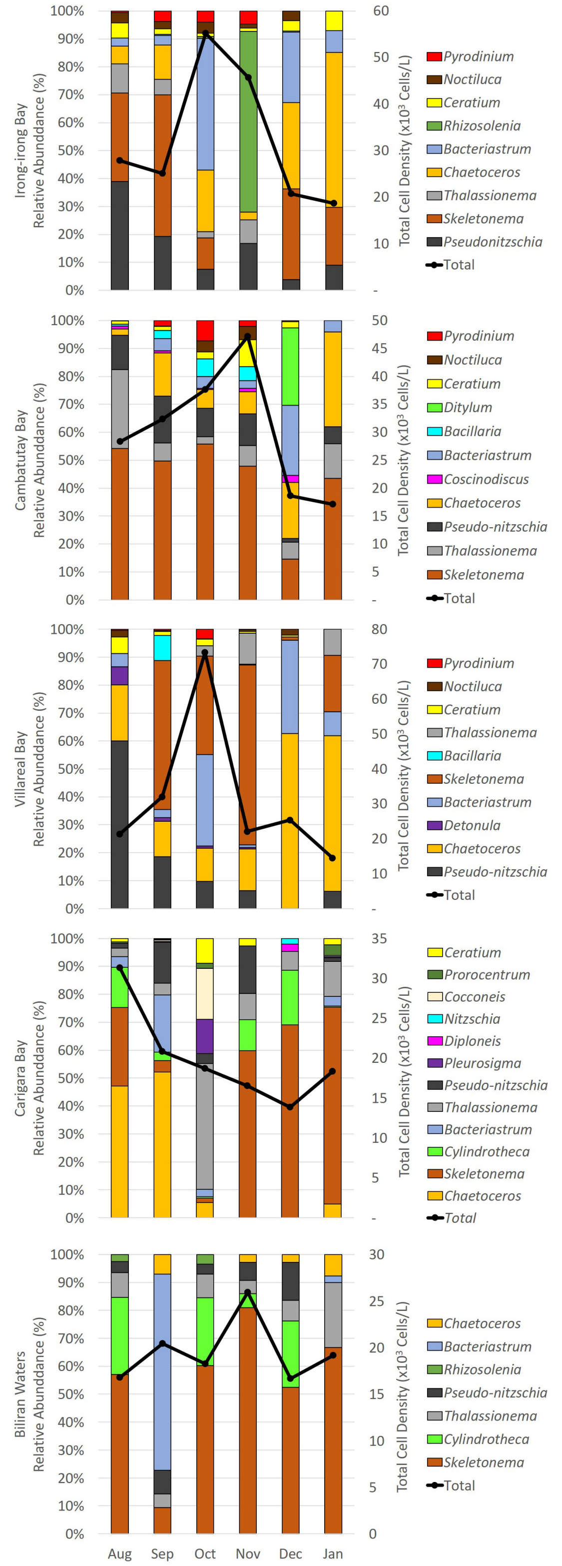

FIGURE 4 | Mean relative abundances (%) of the dominant phytoplankton taxonomic groups found in each sampling site in Eastern Visayas, Philippines from August 2020-January 2021 and the corresponding total average phytoplankton densities in 10^3 cells L^{-1}.

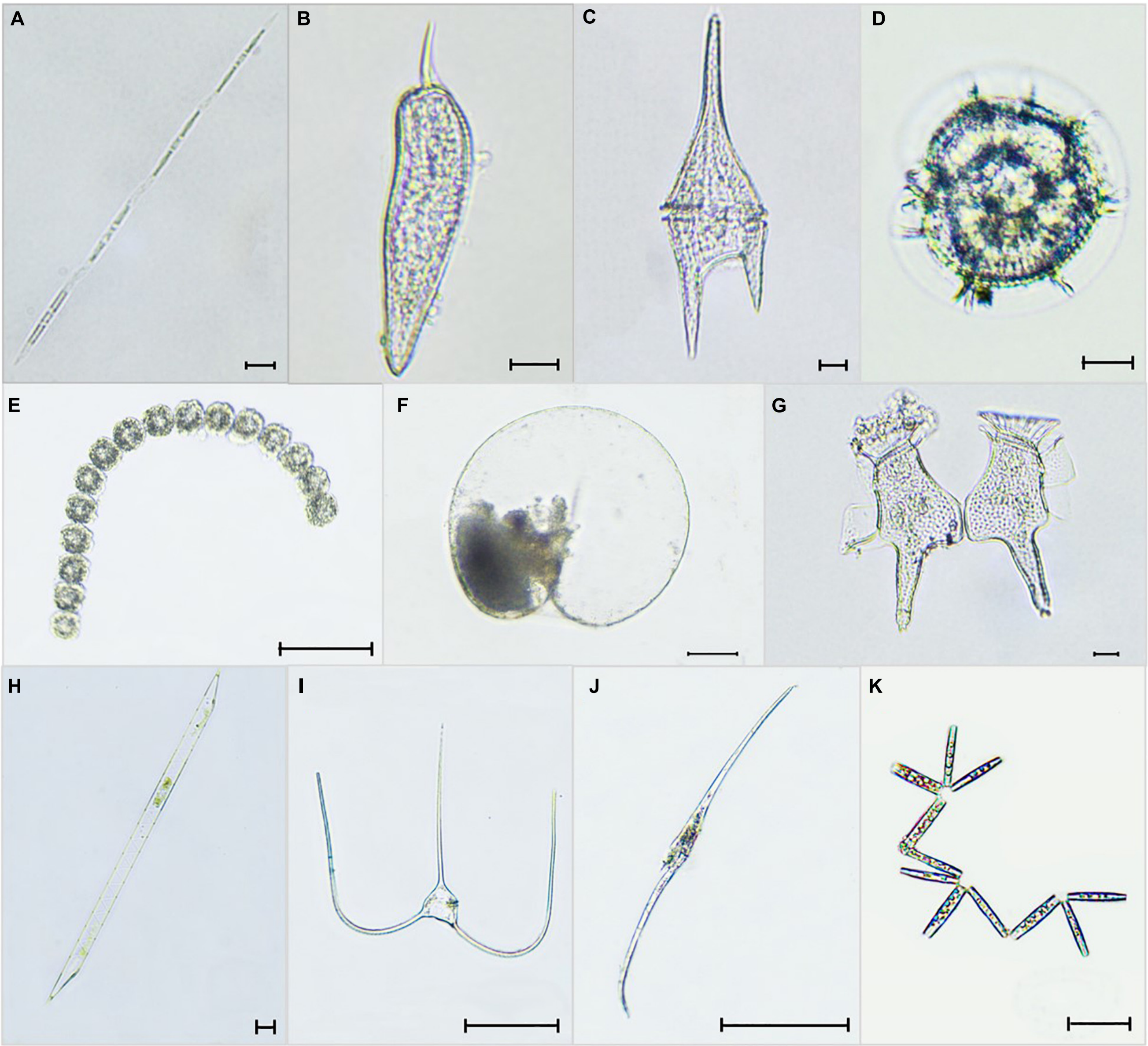

FIGURE 5 | Selected micrographs of the phytoplankton observed in the five bays of E. Visayas, 2020–2021: **(A)** *Pseudo-nitzschia* sp. **(B)** *Prorocentrum sigmoides*, **(C)** *Ceratium furca* (*Tripos furca*), **(D)** *Pyrodinium bahamense*, **(E)** *Gymnodinium catenatum*, **(F)** *Noctiluca scintillans*, **(G)** *Dinophysis caudata*, **(H)** *Rhizosolenia fallax*, **(I)** *Ceratium trichoceros* (*Tripos trichoceros*), **(J)** *Ceratium inflatum* (*Tripos inflatus*), and **(K)** *Thalassionema nitzschioides*. Scale Bars: **(A–D,F–H)** = 10 μm; **(E, I–K)** = 100 μm.

DISCUSSION

Spatial difference in terms of the physico-chemical profiles was observed between the five bays in Eastern Visayas. The bays located in Samar displayed a different profile than the bays in Leyte and Biliran. This is not surprising as Cambatutay, Irong-Irong, and Villareal Bays are sites of mussel mariculture zone near the river mouth in Samar unlike Carigara and Biliran Bays which are beside coastal communities. It is most likely that the differences observed in these bays will play a significant role in the abundance, distribution, and diversity of phytoplankton communities in these areas (Reynolds, 1984; Klausmeier and Litchman, 2001; Clegg et al., 2004).

The profiles we initially recorded in the bays in Samar were comparable to the study reported by Cebu and Orale (2017). The low concentration of dissolved oxygen and salinity can be attenuated due to heavy rainfalls and the possible volume of freshwater input from the rivers (Damotharan et al., 2010; Fatema et al., 2014; Cebu and Orale, 2017). Moreover, high levels of turbidity may have prevented the light from penetrating in the water column and may, in part, affect the chlorophyll-*a* concentrations. Since the three bays in Samar are located near the mussel farming area, the decline in concentration of dissolved oxygen may, in part, be associated with how mussels control the water chemistry within its habitat, maintaining an acidic (Martinez Rodriguez et al., 2015), anoxic (Nicklisch et al., 2016), and ionically sparse (Yu et al., 2011; Miller et al., 2015) environment to be able to keep producing byssal threads, a proteinaceous fiber that allows the mussel to adhere to surface underwater thereby preventing dislodgement (Bell and Gosline, 1996; Carrington et al., 2009). Furthermore, mussel farms in the area are extensive, and the farmers practiced the "staking" or "wigwam" method that uses bamboo that is stuck in the sediments. Most of the time these are left in the same area after harvest and thus contribute to the organic matter in the sea. Meanwhile, the concentrations of dissolved inorganic nutrients measured in all of the bays are generally low, an indication of impending or post bloom phase as several red tide outbreaks were announced throughout the duration of the sampling period.

Diatoms are a major component of the biological community, serving as one of the primary oxygen sources in aquatic environments. In Eastern Visayas, we observed the prevalence of diatom associated groups in its phytoplankton community. Among the diatom taxa, the genus *Skeletonema* was the most prevalent. This result was also observed by Azanza and Miranda (2001) in Manila Bay. The same group has caused fish kills in Bolinao, Pangasinan (Escobar et al., 2013). Other studies elsewhere, such as in the coastal and estuarine areas in China, found that *Skeletonema costatum* to be a cosmopolitan phytoplankton in the area (Huo and Shu, 2005). In the three bays in Samar, *Skeletonema* was positively correlated with temperature, salinity, and nitrates, and thus were abundant when these parameters were higher in these bays. This group is also the most prevalent in the waters of Biliran and Carigara Bays and was correlated to nitrate concentration. It has been shown both in the laboratory and in the field that *Skeletonema* blooms in higher temperatures (Shikata et al., 2008). Moreover, *S. costatum* has also been reported to uptake large concentrations of nitrate that results in chain elongation (Takabayashi et al., 2006). These results indicate that the waters in the five bays provide a suitable condition, at least with parameters such as temperature, salinity, and nutrients, for *Skeletonema* to grow in abundance (Zohdi and Abbaspour, 2019). Meanwhile, other diatom associated groups such as *Chaetoceros*, *Bacteriastrum*, *Pseudo-nitzschia*, and among others which are dominant in other parts of the Philippines (Yap-Dejeto et al., 2008; Yap-Dejeto et al., 2013; Yñiguez et al., 2020), were also abundant in all of the bays herein.

Aside from diatom groups, dinoflagellates such as *P. bahamense*, *N. scintillans*, and species of *Ceratium* co-dominated especially in the waters in Samar Sea. *N. scintillans* and species from genus *Ceratium* have been reported to cause fish kill (Mijares et al., 1985; Pullin et al., 1993; Orellana-Cepeda et al., 2004; Baek et al., 2008) while *P. bahamense* are STXs-producing causing Paralytic Shellfish Poisoning. The co-dominance of these dinoflagellate groups along with other diatoms in the three bays in Samar can be associated with the interplay of the environmental factors present in the area. The three bays both exhibited high rainfall and nitrate concentrations. Most of these species also displayed positive correlation with these parameters

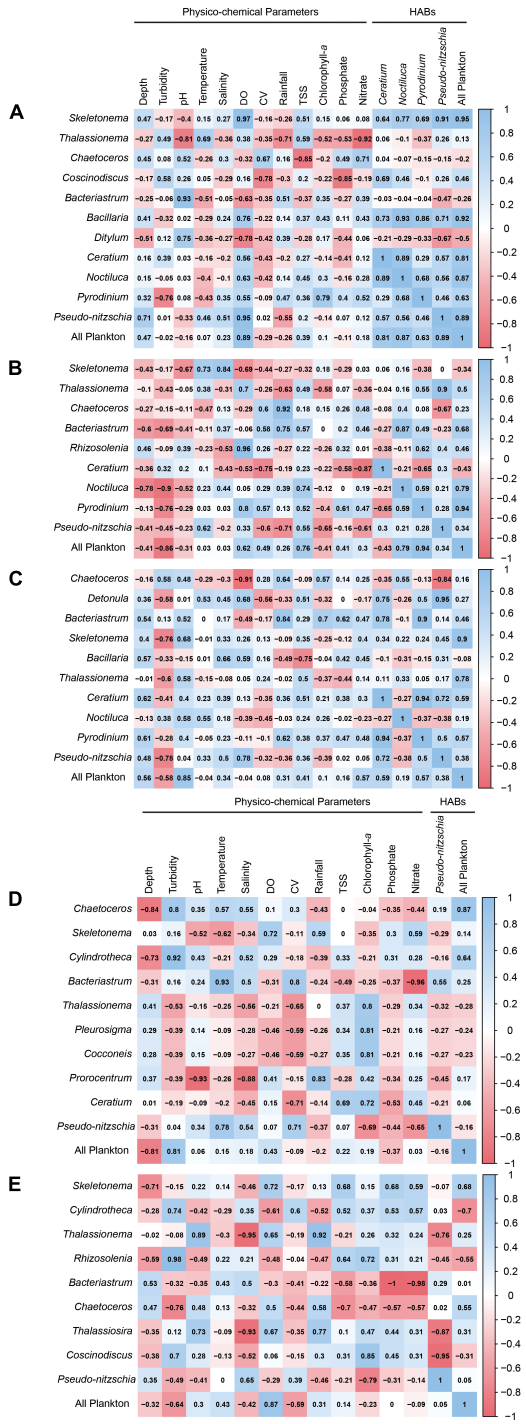

FIGURE 6 | Correlogram of the dominant phytoplankton groups, physico-chemical parameters, and dominant HAB-vectors in **(A)** Cambatutay, **(B)** Irong-Irong, **(C)** Villareal, **(D)** Carigara, and **(E)** Biliran Bays. The correlogram shows correlation coefficients for all pairs of variables. Positive correlations are displayed in blue and negative correlations in red. The intensity of the color is proportional to the correlation coefficient so the stronger the correlation (i.e., the closer to −1 or 1), the darker the boxes. The color legend on the right-hand side of the correlogram shows the correlation coefficients and the corresponding colors. The physico-chemical parameter legend: DO (dissolved oxygen), CV (current velocity), and TSS (total suspended solids).

in these bays. Since nitrate is the primary limiting nutrient for marine phytoplankton (Thomas, 1966, 1969) and heavy rainfall and winds are among other features contributing to HAB development (Mallin and Corbett, 2006), then rainfall-induced nutrient fluctuations is one of the key elements contributing in the co-dominance of HAB and non-HAB phytoplankton in the Samar Sea.

Moreover, the assemblages of potential HAB vectors such as *Pyrodinium*, *Noctiluca*, *Ceratium*, and *Pseudo-nitzschia* observed in the bays in Samar, of which the sites are mussel farming areas, were also observed by Albelda et al. (2019) in the areas near and within the fish farming site in Bolinao, Pangasinan. There is some evidence indicating that sites for mariculture or wild harvest of shellfish are hotspots of HAB events in the Philippines (Villanoy et al., 2006; Yñiguez et al., 2018). For example, *P. bahamense* is the causative agent of the red-tide outbreak in Samar. In fact, within September to November, a noticeable increase in the relative density of *P. bahamense* was observed in the three bays in Samar which also coincided with several red tide bans announced by BFAR 8 on the same duration in the province. In addition, mussels are naturally filter feeders and can accumulate high levels of STXs-producing phytoplankton. It could be that the feces and digestive tract of the mussels from the infected area can be loaded with viable *P. bahamense* cells and its resting cyst which, when transferred, can act as vector or inoculum to another mariculture site or to the neighboring waters (Bricelj et al., 1991; Hégaret et al., 2008). However, these hypotheses need to be confirmed.

Interestingly, we found a slight (statistically insignificant) positive correlation between *P. bahamense* and the unarmored dinoflagellate, *N. scintillans*, in Cambatutay, Irong-Irong, and Villareal Bays. The green *N. scintillans* was the cause of a fish kill event in Manila Bay in 1987. In 2010, Azanza et al. (2010) reported a prey-predator relationship between *P. bahamense* and *N. scintillans* using a feeding experiment in a laboratory setting. In 2017, Folio and Yap-Dejeto (2022) observed a decline of *P. bahamense* density with increasing *N. noctiluca* cells in Irong-Irong Bay. It is most likely that the abundance of *N. scintillans* in the Samar Sea can be associated with the presence of *P. bahamense* in its surrounding waters, however, enough evidence and a thorough study will be needed to unravel the complexity of this relationship.

In September, we detected an abrupt increase in the density of *Bacteriastrum* in Carigara and Biliran Bays while this observation occurred in October in Irong-Irong and Villareal Bays. The shifts in Irong-Irong and Villareal Bays must have been caused by elevated nitrates during that month in these bays. This is supported by positive correlations of nitrates with *Bacteriastrum* in all Samar bays. In Villareal Bay, elevation of nitrates supported other diatoms to bloom, and thus the bloom of *Bacteriastrum* is shared with *Skeletonema*. We can only surmise a similar occurrence in the bloom of *Bacteriastrum* in Carigara and Biliran Bays since nutrient data was not acquired during that time. Additionally, it may have been caused by peaks of temperature in September in both bays and a peak of current velocity in Carigara Bay. Bosak et al. (2016) also observed an abundance of *Bacteriastrum* at higher temperatures. Higher current velocity could have caused turbulence and water mixing increasing the availability of nutrients to chain forming *Bacteriastrum* causing these to multiply. Carigara Bay's *Bacteriastrum* bloom is only secondary to *Chaetoceros* bloom which is another chain forming diatom whose nutrient uptake is supported by turbulence (Dell'Aquila et al., 2017).

Chaetoceros dominated the bays of Irong-Irong and partly in Cambatutay Bays during the end of the sampling period (January 2021), while these were abundant during the beginning of the sampling period, in August and September, 2020 in Carigara Bay. In Villareal Bay, these dominated in both the end and the beginning of the sampling period and persisted during the whole of the sampling period. In the coastal area of northeastern Adriatic, slight increase of nutrients, mainly phosphate, influenced the *Chaetoceros* blooms (Bosak et al., 2016). In this study, *Chaetoceros* positively correlated with both phosphate and nitrate in the three bays in Samar. But the peaks of nutrients do not match the months when *Chaetoceros* increased. Current velocity which could affect turbulence is also correlated to *Chaetoceros* density in the bays where *Chaetoceros* bloomed. Thus, as Dell'Aquila et al. (2017) suggested, we hypothesize that the increasing densities of *Chaetoceros* could be an interplay of increased nutrients and turbulence during these months in these bays. The persistence of *Chaetoceros* in Villareal Bay for the whole sampling period indicates the existence of *Chaetoceros* resting spores (Ishii et al., 2011) in the area. The absence of these spores might also be the reason why this never bloomed in Biliran. This is just a hypothesis and will need to be verified by further research that will include searching for resting spores in sediments.

The dominance of the bloom forming diazotroph diatom (Villareal, 1992), *Rhizosolenia*, in Irong-Irong Bay in November must have caused an increase of dissolved oxygen as the data for these two components positively correlated. Other parameters showed only slight correlations and the bloom of this phytoplankton was not observed in any of the other four bays or in any other months during the study period. For example, Yoshimatsu et al. (2020) showed that maximum growth of *Rhizosolenia setigera* occurs in relatively warmer temperatures. Carstensen et al. (2004) also recorded summer blooms of *Rhizosolenia*. The temperatures in all five bays were relatively warm. Moreover, we also observed that there was a drop in salinity in Irong-Irong Bay during the time of the bloom. We hypothesize that the decrease in salinity in the month of November in this bay could have caused *Rhizosolenia* to dominate. Species of *Rhizosolenia* were noted to be stenohaline or even preferred lower salinities (Gnatiades and Smayda, 1970; Rijstenbil, 1987; Yoshimatsu et al., 2020). This then gave an advantage of *Rhizosolenia* to bloom over the rest of the other phytoplankton.

Thalassionema, on the other hand, must have provided for the high chlorophyll-*a* in October in Carigara Bay as both factors peaked during this month. Similar to *Rhizosolenia*, *Thalassionema* dominance was only observed once, and only in one bay, Carigara Bay. In our study, *Thalassionema* negatively correlated with current velocity. But in the study in India, *Thalassionema* bloomed together with other phytoplankton under turbulent conditions during the Southwest Monsoon (Retnamma et al., 2020). Seasonal change brought about by the Southwest Monsoon could also be the reason for the transient succession of *Thalassionema* in this study as October is the end month of the Southwest Monsoon in the Philippines. The effect of the monsoon conditions must have influenced the phytoplankton community in Carigara Bay during that time. Canini et al. (2013) also observed *Thalassionema* bloom during the Southwest Monsoon in Panguil Bay, Philippines.

In December, we detected a sudden increase of density between the three genera, *Skeletonema*, *Bacteriastrum*, and *Chaetoceros* in the Samar Sea. The prevalence of these species was accompanied by the increasing rainfall that started in the same month and subsequent decrease in the nitrate concentration by twofold. The dominance of these species was also evidenced by the increase of chlorophyll-*a* concentration in the three bays in Samar during December. These results are consistent with our observation from previous months showing that physical disturbances of the water column brought about by heavy rainfall indeed provides a favorable condition for phytoplankton species to grow, and sometimes, blooms. It seems that environmental factors, particularly rainfall, nitrate, and chlorophyll-*a* are likely associated with the structuring of these phytoplankton species in the Samar Sea. Interestingly, we observed a succession between *Chaetoceros* and *Pseudo-nitzschia* in the waters of Villareal, Irong-Irong, and Cambatutay Bays. In the three bays, *Pseudo-nitzschia* displayed a decreasing density in contrast with the increasing density of *Chaetoceros*. Unlike *Chaetoceros*, the *Pseudo-nitzschia* sp. in the three bays were correlated with decreasing temperature. This result indicates that the successional pattern discerned between the two diatoms might be governed by temperature as a factor driving the structuring of these species. This result is in line with previous observations showing temperature as one of the fundamental factors that influence the structuring of microalgal communities (Eppley, 1972; Karentz and Smayda, 1984; Bouman et al., 2003). Moreover, this data somewhat agrees with studies in the temperate regions that showed *Pseudo-nitzschia* to be temperature dependent (Lundholm et al., 1997).

Given these insights, we can say that the linkages of the phytoplankton groups displayed here provides a preview on the succession of phytoplankton communities in the waters of the five major HAB-affected bays in Eastern Visayas. The shifts of the phytoplankton composition observed in this study were governed by a myriad of complex interactions of many environmental factors (Barbosa et al., 2010; Pulina et al., 2012). However, there are other strategies that could also influence the turnover in the composition and abundance of phytoplankton such as stratification, grazing, predation, or allelopathy (Čalić et al., 2013). It is equally important to understand the impact of these biological drivers on the phytoplankton community structure and how this component relates to the HAB problem in Eastern Visayas. This emphasizes the need for a more comprehensive study involving many factors to better understand the dynamics in the change of phytoplankton community and determine which of these factors have influenced such changes. Furthermore, these results make the waters in Eastern Visayas a natural mesocosm to test fundamental questions related to tropical marine phytoplankton ecology and phytotoxins. Insights and answers will greatly benefit not only the ongoing problem of harmful algal bloom in the region where potential policy can be crafted and fine-tuned in the need of the area; but it provides a peak of what is to come when waters become warmer and more acidic due to climate change.

CONCLUSION

The present investigation explores the phytoplankton community structure and the physico-chemical profiles of five HAB-affected bays in Eastern Visayas from August 2020 to January 2021. Based on our initial results, the physico-chemical profiles of Irong-Irong, Cambatutay, and Villareal bays were different compared to the bays in Carigara and Biliran. The distinctness observed between these bays provides insights on the structure of the phytoplankton community present in these areas, especially on species that cause HAB. Trends of physico-chemical parameters as well as phytoplankton succession were documented and discussed. All five bays were diatom-dominated and succession between diatoms varied in the four bays. The diatoms that dominated in the bays were *Skeletonema*, *Pseudo-nitzschia*, *Bacteriastrum*. *Chaetoceros, Rhizosolenia* and *Thalassionema*. The following are the HAB causing species identified in the study; *Pseudo-nitzschia* spp., *Nitzschia* spp., *Alexandrium* sp., *Pyrodinium bahamense*, *Gymnodinium* sp., *Dinophysis caudata*, *Dinophysis miles*, *Prorocentrum lima*, *Skeletonema* spp., *Noctiluca scintillans*, *Prorocentrum sigmoides*, *Ceratium furca*, *Ceratium fusus*, *Ceratium inflatum*, and *Prorocentrum micans*. Overall, we see a snapshot on the phytoplankton ecology and HAB dynamics in the five HAB-affected bays in Eastern Visayas. These results will serve as a baseline information for future studies that aims to understand further the problem related to harmful algal blooms in the region.

DATA AVAILABILITY STATEMENT

The original contributions presented in the study are included in the article/**Supplementary Material**, further inquiries can be directed to the corresponding author/s.

AUTHOR CONTRIBUTIONS

LGYD, MLLA, and MBA conceptualized the study. SFR, MLSS, MLLA, JAO, and EGA conducted the data collection. SFR and LGYD conducted analysis and interpretation of the results. SFR, MLSS, and LGYD wrote the manuscript. All authors drafted, approved and agreed to be accountable for all aspects of the work in this article.

FUNDING

This work was supported by the DOST-GIA project of Department of Science and Technology—Philippine Council for Agriculture, Aquatic, and Natural Resources Research and Development (DOST-PCAARRD) entitled "WATCH HAB R8: Warning And Technology to Combat Hazards of Harmful Algal Blooms in Region 8" to LGYD.

ACKNOWLEDGMENTS

The authors would like to acknowledge the assistance of Alessandra M. Malacora in the phytoplankton identification and Clances Joanne Urmeneta in phytoplankton microscopy. The authors would also like to thank the Bureau of Fisheries and Aquatic Resources (BFAR) Region 8 for their assistance from the formulation of the study to the conduct and field experimentation. The authors also grateful to the reviewers who were instrumental in tremendously improving the manuscript.

SUPPLEMENTARY MATERIAL

The Supplementary Material for this article can be found online at: https://www.frontiersin.org/articles/10.3389/fmars.2022.730518/full#supplementary-material

REFERENCES

Albelda, R. L., Purganan, D. J. E., Gomez, N. C. F., Narvarte, C. D. V., Calalang, P. C., Genovia, T. G. T., et al. (2019). Summer phytoplankton community structure and distribution in a mariculture-affected coastal environment. *Phil. Sci. Lett.* 2, 157–166.

American Public Health Association [APHA] (1992). *Method 2540 D: Standard Methods for the Examination of Water and Waste Water*, 21st Edn. Washington, DC: American Public Health Association.

Azanza, R. V., and Benico, G. A. (2013). Toxic *Alexandrium* blooms in fish farming sites in Bolinao, Pangasinan. *J. Environ. Sci. Manag.* 16, 44–49.

Azanza, R. V., Cruz, L. J., Cariño, F. A., Blanco, A. G., and Butardo, V. M. (2010). Paralytic shellfish toxin concentration and cell density changes in *Pyrodinium bahamense - Noctiluca scintillans* feeding experiments. *Toxicon* 55, 1017–1023. doi: 10.1016/j.toxicon.2009.09.017

Azanza, R. V., Fukuyo, Y., Yap, L. G., and Takayama, H. (2005). *Prorocentrum minimum* bloom and its possible link to a massive fish kill in Bolinao, Pangasinan, Northern Philippines. *Harmful Algae* 4, 519–524. doi: 10.1016/j.hal.2004.08.006

Azanza, R. V., and Max Taylor, F. J. R. (2001). Are *Pyrodinium* blooms in the Southeast Asian region recurring and spreading? A view at the end of the millennium. *Ambio* 30, 356–364. doi: 10.1579/0044-7447-30.6.356

Azanza, R. V., and Miranda, L. N. (2001). Phytoplankton composition and *Pyrodinium bahamense* toxic blooms in Manila Bay, Philippines. *J. Shellfish Res.* 20, 1251–1255.

Baek, S. H., Shimode, S., Han, M. S., and Kikuchi, T. (2008). Growth of dinoflagellates, *Ceratium furca* and *Ceratium fusus* in Sagami Bay, Japan: the role of nutrients. *Harmful Algae* 7, 729–739. doi: 10.1016/j.hal.2008.02.007

Barbosa, A. B., Domingues, R. B., and Galvão, H. M. (2010). Environmental forcing of phytoplankton in a Mediterranean estuary (Guadiana estuary, south-western Iberia): a decadal study of anthropogenic and climatic influences. *Estuaries Coast.* 33, 324–341. doi: 10.1007/s12237-009-9200-x

Behrenfeld, M. J., and Randerson, J. T. (1998). Primary production of the biosphere: integrating terrestrial and oceanic components. *Science* 281, 237–240. doi: 10.1126/science.281.5374.237

Bell, E. C., and Gosline, J. M. (1996). Mechanical design of mussel byssus: material yield enhances attachment strength. *J. Exp. Biol.* 199, 1005–1017. doi: 10.1242/jeb.199.4.1005

Benico, G. A. (2015). *Taxonomy and toxicity of Alexandrium spp. Isolated from Northwestern and Western Philippines*. Master's thesis. Port Aransas, TX: Marine Science Institute.

Benico, G. A., Takahashi, K., Azanza, R. V., and Iwataki, M. (2018). "Morphology and phylogeny of harmful dinoflagellate *Takayama* sp. associated the recent fish kill events in the Philippines," in *Proceedings of the PICES 2018 Annual Meeting* (Yokohama: North Pacific Marine Science Organization).

Benico, G. A., Takahashi, K., Lum, W. M., Yñiguez, A. T., Azanza, R. V., Leong, S. C. Y., et al. (2019). First report of *Biecheleriopsis adriatica* in Bolinao, Northwestern Philippines and its wide distribution in Southeast Asia and adjacent waters. *Phil. J. Nat. Sci.* 24, 34–41.

BFAR Region-8 (2021). *Bureau of Fisheries and Aquatic Resources, Manila, Philippines*. Manila. Available online at: https://www.bfar.da.gov.ph/downloads

Bosak, S., Godrijan, J., and Šilović, T. (2016). Dynamics of the marine planktonic diatom family Chaetocerotaceae in a Mediterranean coastal zone. *Estuar. Coast. Shelf Sci.* 180, 69–81. doi: 10.1016/j.ecss.2016.06.026

Bouman, H. A., Platt, T., Sathyendranath, S., Li, W. K. W., Stuart, V., Fuentes-Yaco, C., et al. (2003). Temperature as indicator of optical properties and community structure of marine phytoplankton: implications for remote sensing. *Mar. Ecol. Prog. Ser.* 258, 19–30. doi: 10.3354/meps258019

Bricelj, V. M., Greene, M., Lee, J. H., and Cembella, A. D. (1991). "Growth response and fate of dinoflagellate cells and paralytic shellfish poisoning (PSP) toxins in mussels, *Mytilus edulis*," in *Proceedings of the Fifth International Conference on Toxic Marine Phytoplankton*, Newport.

Čalić, M., Carić, M., Kršinić, F., Jasprica, N., and Pećarević, M. (2013). Controlling factors of phytoplankton seasonal succession in oligotrophic Mali Ston Bay (south-eastern Adriatic). *Environ. Monit. Assess.* 185, 7543–7563. doi: 10.1007/s10661-013-3118-2

Canini, N. D., Metillo, E. B., and Azanza, R. V. (2013). Monsoon-influenced phytoplankton community structure in a Philippine mangrove estuary. *Trop. Ecol.* 54, 329–341.

Carrington, E., Moeser, G. M., Dimond, J., Mello, J. J., and Boller, M. L. (2009). Seasonal disturbance to mussel beds: field test of a mechanistic model predicting wave dislodgment. *Limnol. Oceanogr.* 54, 978–986.

Carstensen, J., Conley, D. J., and Henriksen, P. (2004). Frequency, composition, and causes of summer phytoplankton blooms in a shallow coastal ecosystem, the Kattegat. *Limnol. Oceanogr.* 49, 190–201.

Cebu, E. H., and Orale, R. L. (2017). Seawater physicochemical parameters in the green mussel belts in Samar Philippines. *J. Acad. Res.* 2, 1–15.

Clegg, M. R., Maberly, S. C., and Jones, R. I. (2004). Dominance and compromise in freshwater phytoplanktonic flagellates: the interaction of behavioural preferences for conflicting environmental gradients. *Funct. Ecol.* 18, 371–380. doi: 10.1111/j.0269-8463.2004.00834.x

Damotharan, P., Perumal, V. N., Arumugam, M., Vijayalakshmi, S., and Balasubramanian, T. (2010). Seasonal variation of physico-chemical characteristics in Point Calimere Coastal Waters (South East Coast of India). *Middle East J. Sci. Res.* 6, 333–339.

Dell'Aquila, G., Ferrante, M. I., Gherardi, M., Lagomarsino, M. C., D'Alcalà, M. R., Iudicone, D., et al. (2017). Nutrient consumption and chain tuning in diatoms exposed to storm-like turbulence. *Sci. Rep.* 7:1828. doi: 10.1038/s41598-017-02084-6

Environmental Sciences Section [ESS] (1991). *ESS Method 150.1.: Chlorophyll-Spectrophotometric*. Madison, WI: Inorganic Chemistry Unit.

Eppley, R. W. (1972). Temperature and phytoplankton growth in the sea. *Fish. Bull.* 70, 1063–1085.

Escobar, M. T. L., Sotto, L. P. A., Jacinto, G. S., Benico, G. A., San Diego-McGlone, M. L., and Azanza, R. V. (2013). Eutrophic conditions during the 2010 fish kill in Bolinao and Anda, Pangasinan, Philippines. *J. Environ. Sci. Manag.* 16, 29–35.

Fatema, K., Maznah, O. W. W., and Mat Isa, M. (2014). Spatial and temporal variation of physico-chemical parameters in the Merbok Estuary, Kedah, Malaysia. *Trop. Life Sci. Res* 25, 1–19.

Folio, F. M., and Yap-Dejeto, L. G. (2022). Phytoplankton diversity and abundance during a red tide ban in Irong-Irong Bay, Western Samar, Philippines. *Phil. J. Sci.* (in press).

Gnatiades, L., and Smayda, T. J. (1970). Autecological studies on the marine diatom *Rhizosolenia fragilissima* Bergon. II. Enrichment and dark viability experiments. *J. Phycol.* 6, 357–364.

Guiry, M. D., and Guiry, G. M. (2020). *AlgaeBase. World-Wide Electronic Publication*. Galway: National University of Ireland.

Hallegraeff, G. M., Anderson, D. M., Belin, C., Bottein, M.-Y. D., Bresnan, E., Chinain, M., et al. (2021). Perceived global increase in algal blooms is attributable to intensified monitoring and emerging bloom impacts. *Commun. Earth Environ.* 2:117. doi: 10.1038/s43247-021-00178-8

Hammer, Ø., Harper, D. A. T., and Ryan, P. D. (2001). PAST: paleontological Statistics Software package for education and data analysis. *Palaeontol. Electron.* 4, 1–9.

Hégaret, H., Shumway, S. E., Wikfors, G. H., Pate, S., and Burkholder, J. M. (2008). Potential transport of harmful algae via relocation of bivalve molluscs. *Mar. Ecol. Prog. Ser.* 361, 169–179. doi: 10.3354/meps07375

Huo, W. Y., and Shu, J. J. (2005). "Outbreak of *Skeletonema costatum* Bloom and its relations to environmental factors in Jiaozhou Bay, China," in *Proceedings of the WSEAS International Conference on Environment, Ecosystems and Development*, Venice, 205–210.

Ishii, K., Iwataki, M., Matsuoka, K., and Imai, I. (2011). Proposal of identification criteria for resting spores of *Chaetoceros* species (Bacillariophyceae) from a temperate coastal sea. *Phycologia* 50, 351–362. doi: 10.2216/10-36.1

Karentz, D., and Smayda, T. J. (1984). Temperature and seasonal occurrence patterns of 30 dominant phytoplankton species in Narragansett Bay over a 22-year period (1959-1980). *Mar. Ecol. Prog. Ser.* 18, 277–293. doi: 10.3354/meps018277

Kassambara, A., and Mundt, F. (2017). *Factoextra: Extract and Visualize the Results of Multivariate Data Analyses. R package*. Available online at: http://www.sthda.com/english/rpkgs/factoextra [accessed April 1, 2020].

Klausmeier, C. A., and Litchman, E. (2001). Algal games: the vertical distribution of phytoplankton in poorly mixed water columns. *Limnol. Oceanogr.* 46, 1998–2007. doi: 10.4319/lo.2001.46.8.1998

Larink, O., and Westheide, W. (2006). *Coastal Plankton: Photo Guide for European Seas*. München: Verlag Dr. Friedrich Pfeil.

Lum, W. M., Benico, G., Furio, E., Lim, P. T., Lim, H. C., Takahashi, K., et al. (2019). Morphology and molecular phylogeny of the harmful raphidophyte *Chattonella subsalsa* isolated from Bolinao, Philippines. *Phil. J. Nat. Sci.* 24, 50–56. doi: 10.13140/RG.2.2.34697.08801

Lundholm, N., Skov, J., Pocklington, R., and Moestrup, Ø. (1997). Studies on the marine planktonic diatom *Pseudo-nitzschia*. 2. Autecology of *P. pseudodelicatissima* based on isolates from Danish coastal waters. *Phycologia* 36, 381–388. doi: 10.2216/i0031-8884-36-5-381.1

Maclean, J. L. (1989). Indo-Pacific red tides, 1985-1988. *Mar. Pollut. Bull.* 20, 304–310. doi: 10.1016/0025-326X(89)90152-5

Maddux, W. S., and Jones, R. F. (1964). Some interactions of temperature, light intensity, and nutrient concentration during the continuous culture of *Nitzschia closterium* and *Tetraselmis* sp. *Limnol. Oceanogr.* 9, 79–86.

Mallin, M. A., and Corbett, C. A. (2006). How hurricane attributes determine the extent of environmental effects: multiple hurricanes and different coastal systems. *Estuaries Coast.* 29, 1046–1061. doi: 10.1007/BF02798667

Martinez Rodriguez, N. R., Das, S., Kaufman, Y., Israelachvili, J. N., and Waite, J. H. (2015). Interfacial pH during mussel adhesive plaque formation. *Biofouling* 31, 221–227. doi: 10.1080/08927014.2015.1026337.Interfacial

Meniano, S. (2020). *BFAR Warns Anew vs. red tide in Eastern Visayas*. Available online at: https://www.pna.gov.ph/articles/1119358 [accessed October 22, 2020].

Mijares, A. J., Sevcik, C., Barboz, C. A., and Saavedra, A. (1985). Ichthyotoxism by a paralytic toxin produced by marine dinoflagellates of the genus *Ceratium*: relationship to fraction b isolated from the sponge *Tedania ignis*. *Toxicology* 23, 221–233. doi: 10.1016/0041-0101(85)90145-x

Miller, D. R., Spahn, J. E., and Waite, J. H. (2015). The staying power of adhesion-associated antioxidant activity in *Mytilus californianus*. *J. R. Soc. Interface* 12:20150614. doi: 10.1098/rsif.2015.0614

Nicklisch, S. C. T., Spahn, J. E., Zhou, H., Gruian, C. M., and Waite, J. H. (2016). Redox capacity of an extracellular matrix protein associated with adhesion in *Mytilus californianus*. *Biochemistry* 55, 2022–2030. doi: 10.1021/acs.biochem.6b00044

Omura, T., Iwataki, M., Borja, V. M., Haruyoshi, T., and Fukuyo, Y. (2012). *Marine Phytoplankton of the Western Pacific*. Tokyo: Kouseisha Kouseikaku Co., Ltd.

Orellana-Cepeda, E., Granados-Machuca, C., and Serrano-Esquer, J. (2004). "*Ceratium furca*: one possible cause of mass mortality of cultured Blue-Fin tuna at Baja California, Mexico," in *Harmful Algae*, eds K. A. Steidinger, J. Landsberg, C. R. Tomas, and G. A. Vargo (St. Petersburg, FL: Florida Fish and Wildlife Conservation Commission), 514–516.

Pulina, S., Padedda, B. M., Satta, C. T., Sechi, N., and Lugliè, A. (2012). Long-term phytoplankton dynamics in a Mediterranean Eutrophic lagoon (Cabras Lagoon, Italy). *Plant Biosyst.* 146, 259–272. doi: 10.1080/11263504.2012.717545

Pullin, R., Rosenthal, H., and Maclean, J. L. (1993). "Environment and aquaculture in developing countries," in *Proceedings of the ICLARM Conference*, eds R. Pullin, H. Rosenthal, and J. L. Maclean (Manila: ICLARM), 359.

Retnamma, J., Chinnadurai, K., Loganathan, J., Nagarathinam, A., Singaram, P., and Jose, A. K. (2020). Ecological responses of autotrophic microplankton to the eutrophication of the coastal upwelling along the Southwest coast of India. *Environ. Sci. Pollut. Res.* 28, 11401–11414. doi: 10.1007/s11356-020-11354-2

Reynolds, C. S. (1984). *The Ecology of Freshwater Phytoplankton*. Cambridge: Cambridge University Press. doi: 10.4319/lo.1987.32.3.0779

Rijstenbil, J. W. (1987). Phytoplankton composition of stagnant and tidal ecosystems in relation to salinity, nutrients, light and turbulence. *Netherlands J. Sea Res.* 21, 113–123. doi: 10.1016/0077-7579(87)90027-5

Roelke, D., Augustine, S., and Buyukates, Y. (2003). Fundamental predictability in multispecies competition: the influence of large disturbance. *Am. Nat.* 162, 615–623. doi: 10.1086/378750

San Diego-McGlone, M. L., Azanza, R. V., Villanoy, C. L., and Jacinto, G. S. (2008). Eutrophic waters, algal bloom and fish kill in fish farming areas in Bolinao, Pangasinan, Philippines. *Mar. Pollut. Bull.* 57, 295–301. doi: 10.1016/j.marpolbul.2008.03.028

Shikata, T., Nagasoe, S., Matsubara, T., Yoshikawa, S., Yamasaki, Y., Shimasaki, Y., et al. (2008). Factors influencing the initiation of blooms of the raphidophyte *Heterosigma akashiwo* and the diatom *Skeletonema costatum* in a port in Japan. *Limnol. Oceanogr.* 53, 2503–2518. doi: 10.2307/40058340

Takabayashi, M., Lew, K., Johnson, A., Marchi, A., Dugdale, R., and Wilkerson, F. P. (2006). The effect of nutrient availability and temperature on chain length of the diatom, *Skeletonema costatum*. *J. Plankton Res.* 28, 831–840. doi: 10.1093/plankt/fbl018

Thomas, W. H. (1966). Surface nitrogenous nutrients and phytoplankton in the Northeastern tropical Pacific Ocean. *Limnol. Oceanogr.* 11, 393–400.

Thomas, W. H. (1969). Phytoplankton nutrient enrichment experiments off Baja California and in the eastern equatorial Pacific Ocean. *J. Fish. Res. Board Canada* 26, 1133–1145. doi: 10.1139/f69-104

Tomas, C. (1997). *Identification Marine Phytoplankton*. San Diego, CA: Academic Press, 859.

United States Environmental Protection Agency [USEPA] (1978). *Method 365.3: Phosphorous, All forms (Colorimetric, Ascorbic Acid, Two Reagent)*. Washington, DC: U.S. Environmental Protection Agency.

Vaissie, P., Monge, A., and Husson, F. (2021). *Factoshiny: Perform Factorial Analysis from 'FactoMineR' with a Shiny Application. R package version 2.4.* Available online at: https://CRAN.R-project.org/package=Factoshiny [accessed February 3, 2021].

Van Dolah, F. M. (2000). Marine algal toxins: origins, health effects, and their increased occurrence. *Environ. Health Perspect.* 108, 133–141. doi: 10.1289/ehp.00108s1133

Villanoy, C. L., Azanza, R. V., Altemerano, A., and Casil, A. L. (2006). Attempts to model the bloom dynamics of *Pyrodinium*, a tropical toxic dinoflagellate. *Harmful Algae* 5, 156–183. doi: 10.1016/j.hal.2005.07.001

Villareal, T. A. (1992). "Marine nitrogen-fixing diatom-cyanobacteria symbiosis," in *Marine Pelagic Cyanobacteria: Trichodesmium and Other Diazotrophs*, eds E. J. Carpenter, D. G. Capone, and J. G. Rueter (Berlin: Springer), 163–175. doi: 10.1007/978-94-015-7977-3

Wei, T., and Simko, V. (2021). *'corrplot': Visualization of a Correlation Matrix. R package version 0.92.* Available online at: https://github.com/taiyun/corrplot [accessed November 13, 2021].

Wells, M. L., Karlson, B., Wulff, A., Kudela, R., Trick, C., Asnaghi, V., et al. (2020). Future HAB science: directions and challenges in a changing climate. *Harmful Algae* 91:101632. doi: 10.1016/j.hal.2019.101632

Wickham, H. (2016). *ggplot2: Elegant Graphics for Data Analysis. R. Package*. New York, NY: Springer-Verlag.

Wu, J. T. (1993). "Use of phytoplankton community as indicator of water quality," in *Recent Advances in Botany: In Commemoration of the 30th Anniversary of the Restoration of the Institute of Botany*, eds C. Zhou and Y.-I. Hsing (Taipei: Academia Sinica).

Yap-Dejeto, L. G., Cobacha, M., and Cinco, G. (2008). The surface phytoplankton community in a mariculture zone and its adjacent waters of San Pedro Bay, Leyte Philippines during 2005-2006. *J. Nat. Stud.* 7, 123–128.

Yap-Dejeto, L. G., Omura, T., Cinco, G. F., Cobacha, M. M., and Fukuyo, Y. (2013). Species account of marine diatoms of the genus *Pseudo-nitzschia* in San Pedro Bay, Philippines. *Phil. J. Sci.* 142, 27–37.

Yñiguez, A. T., Lim, P. T., Leaw, C. P., Jipanin, S. J., Iwataki, M., Benico, G., et al. (2020). Over 30 years of HABs in the Philippines and Malaysia: what have we learned? *Harmful Algae* 102:101776. doi: 10.1016/j.hal.2020.101776

Yñiguez, A. T., Maister, J., Villanoy, C. L., Dianne, J. D., Peñaflor, E., Almo, A., et al. (2018). Insights into the dynamics of harmful algal blooms in a tropical estuary through an integrated hydrodynamic-*Pyrodinium*-shellfish model. *Harmful Algae* 80, 1–14. doi: 10.1016/j.hal.2018.08.010

Yoshimatsu, T., Yamaguchi, H., Iimura, A., Nishimura, T., Kadono, T., and Adachi, M. (2020). Effects of temperature, salinity, and light intensity on the growth of the diatom *Rhizosolenia setigera* in Japan. *Phycologia* 59, 551–555. doi: 10.1080/00318884.2020.1812260

Yu, J., Wei, W., Danner, E., Ashley, R. K., Israelachvili, J. N., and Waite, J. H. (2011). Mussel protein adhesion depends on interprotein thiol-mediated redox modulation. *Nat. Chem. Biol.* 7, 588–590. doi: 10.1038/nchembio.630

Zohdi, E., and Abbaspour, M. (2019). Harmful algal blooms (red tide): a review of causes, impacts and approaches to monitoring and prediction. *Int. J. Environ. Sci. Technol.* 16, 1789–1806. doi: 10.1007/s13762-018-2108-x

Conflict of Interest: The authors declare that the research was conducted in the absence of any commercial or financial relationships that could be construed as a potential conflict of interest.

frontiers
in Marine Science

ORIGINAL RESEARCH
published: 24 February 2022
doi: 10.3389/fmars.2022.766936

Restriction Site-Associated DNA Sequencing Reveals Local Adaptation Despite High Levels of Gene Flow in *Sardinella lemuru* (Bleeker, 1853) Along the Northern Coast of Mindanao, Philippines

Kevin Labrador[1,2]*, Joseph Dominic Palermo[1,3], Altair Agmata[1], Rachel Ravago-Gotanco[1] and Ma. Josefa Pante[1]

[1] The Marine Science Institute, University of the Philippines Diliman, Quezon City, Philippines, [2] Department of Biological Sciences and Environmental Studies, University of the Philippines Mindanao, Davao City, Philippines, [3] Institute of Environmental Science and Meteorology, University of the Philippines Diliman, Quezon City, Philippines

Edited by:
Sangeet Lamichhaney,
Uppsala University, Sweden

Reviewed by:
Hsiu-Chin Lin,
National Sun Yat-sen University,
Taiwan
Juha Merilä,
University of Helsinki, Finland

***Correspondence:**
Kevin Labrador
kllabrador@up.edu.ph

Specialty section:
This article was submitted to
Marine Biology,
a section of the journal
Frontiers in Marine Science

Received: *30 August 2021*
Accepted: *19 January 2022*
Published: *24 February 2022*

Citation:
Labrador K, Palermo JD, Agmata A, Ravago-Gotanco R and Pante MJ (2022) Restriction Site-Associated DNA Sequencing Reveals Local Adaptation Despite High Levels of Gene Flow in Sardinella lemuru (Bleeker, 1853) Along the Northern Coast of Mindanao, Philippines.
Front. Mar. Sci. 9:766936.
doi: 10.3389/fmars.2022.766936

Stock identification and delineation are important in the management and conservation of marine resources. These were highlighted as priority research areas for Bali sardinella (*Sardinella lemuru*) which is among the most commercially important fishery resources in the Philippines. Previous studies have already assessed the stocks of *S. lemuru* between Northern Mindanao Region (NMR) and Northern Zamboanga Peninsula (NZP), yielding conflicting results. Phenotypic variation suggests distinct stocks between the two regions, while mitochondrial DNA did not detect evidence of genetic differentiation for this high gene flow species. This paper tested the hypothesis of regional structuring using genome-wide single nucleotide polymorphisms (SNPs) acquired through restriction site-associated DNA sequencing (RADseq). We examined patterns of population genomic structure using a full panel of 3,573 loci, which was then partitioned into a neutral panel of 3,348 loci and an outlier panel of 31 loci. Similar inferences were obtained from the full and neutral panels, which were contrary to the inferences from the outlier panel. While the full and neutral panels suggested a panmictic population (global $F_{ST} \sim 0$, $p > 0.05$), the outlier panel revealed genetic differentiation between the two regions (global $F_{ST} = 0.161$, $p = 0.001$; $F_{CT} = 0.263$, $p < 0.05$). This indicated that while gene flow is apparent, selective forces due to environmental heterogeneity between the two regions play a role in maintaining adaptive variation. Annotation of the outlier loci returned five genes that were mostly involved in organismal development. Meanwhile, three unannotated loci had allele frequencies that correlated with sea surface temperature. Overall, our results provided support for local adaptation despite high levels of gene flow in *S. lemuru*. Management therefore should not only focus on demographic parameters (e.g., stock size and catch volume), but also consider the preservation of adaptive variation.

Keywords: Bali sardinella, population genomics, RADseq, sea surface temperature, SNPs, stock assessment

INTRODUCTION

Stocks are the basic unit of management in fisheries and identifying them is a prerequisite to fisheries assessment and other management measures (Kritzer and Liu, 2014). Stocks can be identified based on genetic variation inferred using molecular markers which may be neutral or non-neutral (i.e., adaptive or outliers) (Kirk and Freeland, 2011; Cadrin et al., 2014). Each marker type provides a different perspective on the evolutionary forces that shape populations. Neutral markers provide insight on the genome-wide effects of gene flow and genetic drift, whereas non-neutral markers are more likely to reveal locus-specific effects of natural selection and how these change local gene pools (Holderegger et al., 2006; Russello et al., 2012; Mariani and Bekkevold, 2014). These markers also have different functionality with regards to stock identification; while neutral markers are used to identify stocks based on the levels of gene flow and demographic independence, non-neutral markers are used to identify genetic groups based on adaptive genetic variation and patterns of local adaptation (Funk et al., 2012; Moore et al., 2014). Consequently, the hierarchical analysis of neutral and non-neutral markers was proposed as a more comprehensive approach to delineating conservation units (Funk et al., 2012). Within this framework, both neutral and non-neutral markers are initially used to delineate evolutionary significant units (ESU) – populations that are reproductively isolated and have adaptive differences. Afterward, neutral markers are used to delineate stocks or management units (MU), and non-neutral markers are used to identify adaptive groups. Previously, genetic assessment using non-neutral markers was difficult most especially for non-model organisms; however, with the advent of next-generation sequencing (NGS), these limitations had been largely overcome (Metzker, 2009; Davey and Blaxter, 2010; Willette et al., 2014; Andrews et al., 2016).

Identifying stocks and determining the extent to which they are connected across space and time are needed to better manage fisheries resources that are facing threats of overexploitation. These include the Bali sardinella (*Sardinella lemuru* Bleeker, 1853), an important small pelagic fishery resource in the Indo-West Pacific region (Gaughan and Mitchell, 2000; Jaya, 2002; Metillo et al., 2018). This species' distribution ranges from southern Japan, up to its southern limit in western Australia and westernmost limit in the Andaman Sea (Whitehead, 1985; Willette and Santos, 2013). As with most sardine species, *S. lemuru* forms shoals in coastal waters over continental shelves not exceeding depths of 200 m (Willette et al., 2011), and is often found in areas of upwelling and regions with high primary productivity (Sartimbul et al., 2010; Villanoy et al., 2011). The species is particularly important in Indonesia as it comprises more than 90% of the total catch in the pelagic fishery of Bali Strait (Sartimbul et al., 2010), where it provides livelihood for the local population (Jaya, 2002). It also constitutes a variable component of the small pelagic fishery in Western Australia, where it has been marketed as bait for the rock lobster fishery (Gaughan and Mitchell, 2000). In addition to its social and economic value, *S. lemuru* also plays key ecological roles, as substantial decline in its abundance was predicted to have serious consequences on the breeding success of organisms at higher trophic levels (e.g., seabirds; Gaughan and Mitchell, 2000).

In the Philippines, *S. lemuru*, previously misidentified as *Sardinella longiceps* (Willette and Santos, 2013), is the most abundant species in the small pelagic fishery and has significantly contributed to the country's economy by providing billions of pesos to the annual revenue (Willette et al., 2011), as well as serving as a source of food and livelihood (Willette and Santos, 2013; Narvaez, 2017). However, the country's sardine fishery is considered overexploited (Guanco et al., 2009; Olaño et al., 2009), with reports of age-at-maturity being attained as early as 3.7–6.3 months (Campos et al., 2015). *S. lemuru* dominates the small pelagic fishery along the northern coast of Mindanao, and efforts in understanding the dynamics and processes involved in the sardine fisheries were heavily focused along this area, covering both the Northern Zamboanga Peninsula (NZP) and Northern Mindanao Region (NMR). These include looking at the influence of oceanographic conditions (e.g., upwelling, primary productivity, temperature, and advection) to sardine productivity (Villanoy et al., 2011, 2015) and variability in larval recruitment (Pata et al., 2021); spatio-temporal patterns in fish catch composition, fishing effort, spawning, and recruitment (De Guzman et al., 2015); mortality at early life stages and sources of recruits (Campos et al., 2015); ontogenetic feeding shifts (Metillo et al., 2018); susceptibility to microplastic pollution (Palermo et al., 2020); and occurrence of endoparasites (Palermo, 2021). Stock connectivity within and between regions were also reported (Luceño et al., 2014; Campos et al., 2015; De Guzman et al., 2015; Pante et al., 2019; Labrador et al., 2021).

Previous stock assessments of *S. lemuru* suggested regional differentiation between the NZP and NMR despite their adjacent locations along a contiguous coastline spanning around 400 km. These included (1) variations in life history parameters, particularly the earlier onset of spawning in NZP and earlier maturation in NMR (De Guzman et al., 2015); and (2) differences in body shape based on geometric morphometrics (Luceño et al., 2014); while (3) different sardine endoparasites between regions suggest that these could serve as biological tags for source tracking (Palermo, 2021). Larval connectivity models further support the distinction between NZP and NMR, at least for coral reef-associated species of fish *(Epinephelus* sp.) and invertebrates (*Acropora millepora* and *Tripneustes gratilla*) (Pata and Yñiguez, 2019). These observed patterns of regional differentiation could be attributed to the spatiotemporal differences in the hydrographic processes between the two regions. The NZP, located at the eastern boundary of the Sulu Sea, experiences monsoon-driven coastal upwelling during the northeast monsoon (Villanoy et al., 2011), while the NMR, located at the southern boundary of the Bohol Sea System (BSS), exhibits a "double estuarine type" circulation with entrainment in the eastern basin and eddy formation in the southwestern basin (Cabrera et al., 2011). While both regions exhibit high primary productivity to support the sardine fishery, productivity in the NZP is mostly driven by the upwelling system, while productivity in NMR is mostly driven by the large nutrient input from major river systems to the Bohol Sea (De Guzman et al., 2015). Furthermore, the strong signature of upwelling in the NZP makes it more dynamic compared to the NMR. These different oceanographic features between regions could affect spawning and recruitment success (Campos et al., 2015; Metillo et al., 2018) and limit migration (Luceño et al., 2014), which in turn could drive regional adaptive variation. Previous reports have already shown how environmental parameters associated with ocean primary productivity (e.g., sea surface temperature and chlorophyll-a) affect variability in the catch (Sartimbul et al., 2010; Villanoy et al., 2011), distribution and migratory behavior (Sambah et al., 2012), as well as recruitment success (Pata et al., 2021) of *S. lemuru*.

A previous genetic stock assessment using the mitochondrial DNA (mtDNA) meanwhile reported contrasting patterns indicating the absence of regional genetic differentiation (Labrador et al., 2021). Although minimal yet significant genetic structuring was recovered, such signature was due to genetically distinct haplogroups which occurred in sympatry, with each haplogroup exhibiting panmixia over relatively large spatial scales (Pedrosa-Gerasmio et al., 2015; Labrador et al., 2021). This supports the idea that the sea systems in NMR and NZP are coupled despite the differences in their respective oceanographic features, and that recruits come from the same source (Campos et al., 2015). Such connectivity is expected for *S. lemuru* due to its high dispersal potential, as was reported for stocks around the Sulu-Celebes Sea (Pedrosa-Gerasmio et al., 2015) and along the coast of Western Australia (Gaughan and Mitchell, 2000). However, the absence of regional genetic differentiation could be attributed to the low resolving power of mtDNA. In general, mtDNA markers may perform poorly at detecting recent genetic divergence, especially in species with large effective population sizes and high dispersal potential (Corander et al., 2013; Pedrosa-Gerasmio et al., 2015; Sukumaran et al., 2016). Furthermore, mtDNA markers are often associated with historical processes and are thus unable to detect adaptive variation occurring at a more contemporary ecological timescale (Conover et al., 2006; Rocha et al., 2007). Genome-wide single nucleotide polymorphisms (SNPs) offer a better alternative in providing the resolving power needed to detect low levels of genetic divergence expected for organisms with high dispersal potential and large effective population sizes (Corander et al., 2013; Sukumaran et al., 2016). Moreover, since local adaptation can still occur despite high levels of genetic connectivity (Hemmer-Hansen et al., 2007a; Nielsen et al., 2009b), concurrent examination of both neutral and non-neutral genetic variation is needed to understand the relative contribution of gene flow, genetic drift, and selection in shaping the population (Funk et al., 2012; Yadav et al., 2019). In this regard, delineating conservation units as proposed by Funk et al. (2012) serves as a good framework in stock delineation of *S. lemuru* in the Philippines.

This study used genome-wide SNPs to assess *S. lemuru* populations along the northern coast of Mindanao. Given that phenotypic variation was observed between NMR and NZP despite the species' high dispersal potential, we tested the hypothesis of genetic differentiation between these two adjacent regions using both neutral and non-neutral (hereafter referred to as outlier) markers. We hypothesized that the former would reveal a panmictic stock, while the latter would show genetic structuring between regions due to adaptive variation. Given the differences in the signature of upwelling between the two regions, we further characterized the outliers to identify genes that drive regional variation and assess their possible association with the environment, focusing on parameters that are associated with primary productivity – sea surface temperature (SST), chlorophyll *a* (chl-*a*), and particulate organic carbon (POC).

MATERIALS AND METHODS

Sample Collection

A total of 48 *S. lemuru* samples were collected in November 2016 from seven bays representing two regions along the northern coast of Mindanao (**Figure 1**): NMR ($n = 21$) included Butuan (BUT), Gingoog (GIN), Macajalar (MAC), and Iligan (ILG); NZP ($n = 27$) included Dipolog (DIP), Sindangan (SIN), and Patawag (PAT). Identification was initially done using the count of pelvic fin rays (one unbranched, eight branched; Willette and Santos, 2013), and was confirmed using genetic sequences of the mtDNA markers, cytochrome oxidase I (COI) and control region (CR) (Labrador et al., 2021). Appropriate mass (10% w/v) of dorsal muscle tissues excised from freshly caught samples were placed in 1.5 mL microcentrifuge tube containing nucleotide stabilization solution (RNA/DNA Shield, ZymoResearch, United States). Preserved tissue samples were then shipped to Beijing Genomics Institute (BGI), China for DNA extraction, library preparation, and sequencing.

DNA Extraction, Library Preparation, and Sequencing

DNA extraction, preparation of RAD libraries, and sequencing was done following the protocol of Baird et al. (2008). Genomic DNA (gDNA) was extracted from the tissue samples, the quality and concentration of which were determined using agarose gel electrophoresis and fluorometric quantification (Qubit Fluorometer, Thermo Fisher Scientific, United States). gDNA (0.1–1.0 μg) was then digested using the restriction enzyme *EcoRI*. After digestion, P1 adaptor, containing the forward PCR primer, Illumina primer, and the sample-specific barcode sequences were ligated to the DNA fragments. The samples were pooled and then sheared using a sonicator. For size selection, sheared samples were electrophoresed on a gel, and fragments ranging from 300 to 500 bp were extracted. The ends were polished using a blunt enzyme and a 3′–dA overhang was added to the blunt end. This overhang was where P2 (Y) adaptors with divergent ends were ligated. Only the fragments containing both P1 and P2 adaptors were amplified in the PCR step, and the resulting amplicons were considered as the RAD library. The library was validated using 2100 Bioanalyzer (Agilent Technologies, United States) and ABI StepOnePlus Real-Time PCR (Thermo Fisher Scientific, United States). Paired-end sequencing was performed on HiSeq 4000 (Illumina, United States). The sequence data was then demultiplexed and assigned back to an individual using the sample-specific barcodes.

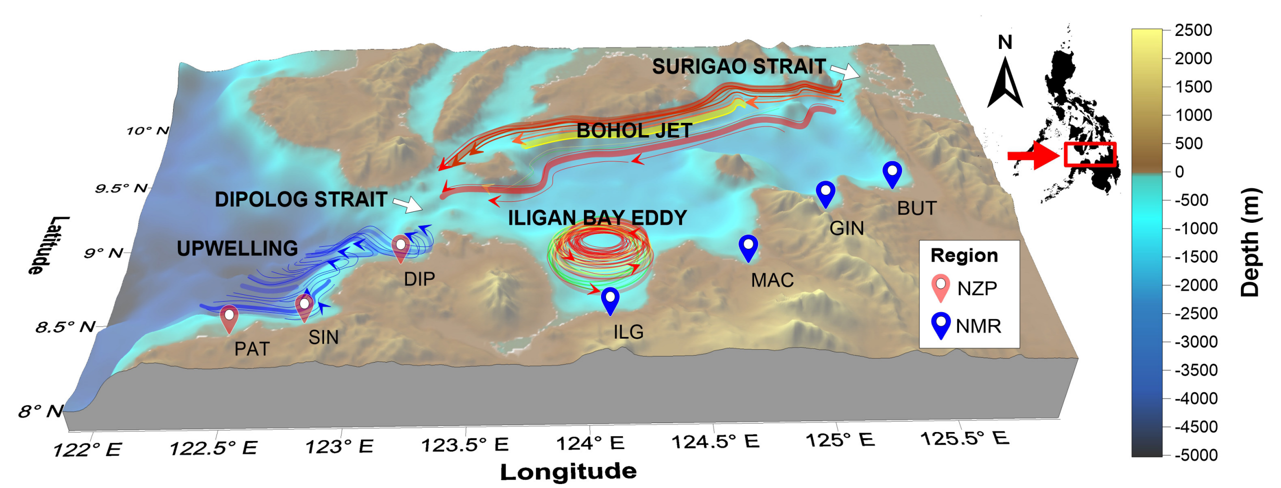

FIGURE 1 | Map of sampling locations. Colors of map markers indicate the geopolitical regions from where the sites belong (NMR, Northern Mindanao Region; BUT, Butuan; GIN, Gingoog; MAC, Macajalar; ILG, Iligan; NZP, Northern Zamboanga Peninsula; DIP, Dipolog; SIN, Sindangan; PAT, Patawag). The location relative to the Philippine archipelago is shown. Also shown are the general location and flow direction of the Bohol Jet and Iligan Eddy in the NMR (Cabrera et al., 2011), and the upwelling region in the NZP (Villanoy et al., 2011).

Quality Filtering and Parameter Optimization

Low quality reads were removed using the *process_radtags* module in Stacks v.1.46 (Catchen et al., 2011, 2013), and FastQC (Andrews, 2010) was used to further assess sequence quality. Samples with low read counts ($<1.6 \times 10^6$) were also removed since including them reduced the number of SNPs that can be genotyped. A reduced dataset for parameter optimization was generated by using the first five samples with the highest read count from each of the six bays ($n = 35$).

Optimization of the Stacks genotyping pipeline followed the recommendations of Mastretta-Yanes et al. (2014), Paris et al. (2017), and Rochette and Catchen (2017). Optimization was performed using the *denovo_map.pl* module and focused on the following core parameters: (1) the minimum number of identical filtered reads to create a stack (*m*; default: 3), (2) the number of mismatches allowed between loci within an individual (*M*; default: 2), and (3) the number of mismatches allowed between loci among individuals (*n*; default: 1). The following decision frameworks were implemented in selecting the optimal parameters: (1) the value of *m* was chosen when all samples had coverage depths ≥10 X, since coverage depths of <10 X for multiple samples lead to genotypes that may be unreliable and biased even after filtering (Rochette and Catchen, 2017); (2) the value of *M* was chosen when the number of polymorphic loci shared by ≥80% of the samples (i.e., *r80* loci) began to plateau; lastly, (3) the value of *n* was iterated among $n = M$, $n = M + 1$, and $n = M - 1$, and the value that generated the highest number of *r80* loci was selected. To do so, several runs were performed; we first iterated the value of *m* from 1 to 9, while keeping the value of $M = n = 2$. The *m* value that met our criteria on coverage depths was then fixed while the value of $M = n$ was iterated from 1 to 9. Afterward, the value of *M* that met the criteria on *r80* loci was fixed, while *n* was iterated. Output from each run was passed on to Stacks' *populations* module; here, we filtered loci that adhered to the following criteria: (1) they were present in all sampling locations ($p = 7$); and (2) they were found in ≥80% of the samples ($r = 0.80$). Meanwhile, (3) only the first SNP from each polymorphic locus (*write_single_snp*) with a minimum minor allele frequency of 5% (*min_maf* = 0.05) was retained; this is to minimize calling loci that are in linkage disequilibrium and alleles that are extremely rare. Using custom bash scripts, the following information from each run was extracted: (1) the coverage depth, and (2) the number of loci shared by 80% of the samples. Visual diagnostics were done by plotting the core assembly metrics in R v.4.0.4 (R Core Team, 2021).

Single Nucleotide Polymorphism Genotyping

Single nucleotide polymorphisms were genotyped from the full dataset using the optimal parameters in the *denovo_map.pl* pipeline. Correction was done using the *rxstacks* module with the following settings: (1) the non-biological haplotypes that were unlikely to occur in the population were pruned out (*prune_haplo*); and (2) the minimum log likelihood ratio to retain a catalog locus (*ln_lim*) was set to −10.0. The output of the *rxstacks* module was then passed on to the *populations* module using the same criteria during parameter optimization.

Further SNP filtering was performed in R v.4.0.4 (R Core Team, 2021) using the packages adegenet v.2.1.3 (Jombart, 2008; Jombart and Ahmed, 2011) and dartR v.1.8.3 (Gruber et al., 2018). First, loci metrics (e.g., call rates) were calculated. Second, the calculated metrics were used to remove missing data by filtering out (1) individuals with call rates <80%, and (2) loci with call rates <100%. Third, each locus was tested for Hardy–Weinberg Equilibrium (HWE) across all populations using the exact test by Wigginton et al. (2005), and those that showed significant departures from HWE expectations ($p < 0.05$)

after Bonferroni correction were removed. Fourth, to limit the influence of non-independent loci, all loci pairs were tested for Linkage Disequilibrium (LD) as implemented in genetics v.1.3.8.1.3 (Warnes et al., 2021; function called *via* dartR), and pairs that had $R^2 > 0.80$ were removed (Lee et al., 2018; Mendiola and Ravago-Gotanco, 2021). Finally, to eliminate loci exhibiting extremely high heterozygosity which could be due to false SNP calls or assembly errors, loci with observed heterozygosity (H_O) > 0.60 were removed from the dataset (Ackiss et al., 2018; Lee et al., 2018; Mendiola and Ravago-Gotanco, 2021). The SNP panel after post-processing is hereafter referred to as the "full panel."

Outlier Screening and Panel Preparation

The full panel was screened for loci that were putatively under selection. Five outlier detection methods were used, four of which were F_{ST}-based approaches, and one was an individual-based approach. F_{ST}-based outlier detection simulates a null distribution from the genetic differentiation between pre-defined groups, and loci that deviate from this distribution are tagged as outliers (Foll and Gaggiotti, 2008; Excoffier et al., 2009). Meanwhile, individual-based approaches no longer calculate F_{ST} indices to detect outliers; rather, these approaches utilize multivariate methods and detect outliers not based on how they drive differentiation between groups, but on how they drive genetic structure as a whole (Luu et al., 2017).

F_{ST}-based outlier detection included (1) Arlequin v.3.5.2.2 (Excoffier and Lischer, 2010); (2) BayeScan v.2.1 (Foll and Gaggiotti, 2008); and the R packages (3) fsthet (Flanagan and Jones, 2017); and (4) OutFLANK v 0.2 (Whitlock and Lotterhos, 2015). Arlequin utilizes an explicit hierarchical island model in generating the F_{ST} null distribution, thereby making outlier detection more robust to uncertainties on the exact number of groups and demes per group in the system (Excoffier et al., 2009). Detecting loci under selection utilized 10 simulated groups with 100 demes per group; this was run for 20,000 simulations, and loci that had p-values ≤ 0.01 beyond the 99% confidence interval were tagged as outliers. BayeScan utilizes a Bayesian approach to estimate the posterior probability that a given locus is under the effect of selection by comparing two alternative models based on the inclusion or exclusion of selection (Foll and Gaggiotti, 2008). Default chain parameters were used in the analysis (sample size = 5,000; thinning interval = 10; pilot runs = 20; pilot run length = 5,000, and additional burn-in = 50,000), and the convergence of the Markov Chain Monte Carlo (MCMC) simulation was assessed using the R package, coda (Plummer et al., 2006). Loci with false discovery rate (FDR) q-value < 0.05 were considered outliers. Fsthet v.1.0.1 (Flanagan and Jones, 2018) calculates smoothed quantiles from the dataset to identify putatively outlier loci with extreme F_{ST} values relative to heterozygosity (Flanagan and Jones, 2017). The F_{ST} analog, β, was used to calculate genetic differentiation, and loci with β values outside the 95% quantiles of the Fst-Heterozygosity distribution were tagged as outliers. OutFLANK generates the null distribution by trimming extreme F_{ST} values from the observed distribution and fitting a modified X^2 probability density distribution on the remaining values (Whitlock and Lotterhos, 2015). OutFLANK was executed using default parameters (left and right trim fraction = 0.05; minimum heterozygosity = 0.10), and loci were considered outliers when FDR q-value < 0.05.

The R package, pcadapt, was used as the individual-based outlier detection approach. The method utilizes principal components analysis (PCA) to infer population structure from the genomic dataset, and then uses this information to detect outlier loci. A preliminary screening was done by running PCA several times and determining the largest value of the number of principal components (K) before the screeplot plateaus. Afterward, Mahalanobis distance is calculated for each locus; this test statistic measures up to what extent a SNP is related to K that was used to infer structure (Luu et al., 2017). Loci with Mahalanobis distances that do not follow the distribution of the main bulk of points and have FDR q-value < 0.05 were considered as outliers.

Additional SNP panels were generated based on the results of outlier screening. The neutral panel was generated by removing all loci that were tagged as outliers from the full panel. Meanwhile, the outlier panel was generated by retaining only the loci that were identified as outliers by at least two detection methods.

Genetic Diversity and Population Structure

The following genetic diversity indices were calculated for all SNP panels using the summary function of adegenet: (1) number of alleles (N_A), (2) percentage of observed alleles (A_O), (3) observed heterozygosity (H_O), and (4) expected heterozygosity (H_E) under HWE. Calculations were done across various hierarchical groupings of individuals: global, regional, and embayment.

Spatial patterns of genetic structure for all SNP panels were examined using discriminant analysis of principal components (DAPC). This method first utilizes PCA to summarize the overall variation in the genomic dataset in as few dimensions as possible; the appropriate number PC axes is then subjected to discriminant analysis (DA) which maximizes between-group while minimizing within-group variation, thereby achieving the best discrimination of individuals (Jombart et al., 2010). The number of groups assigned as priors to DA was initially identified using K-means clustering, and the optimal number of PCs used for DA was determined using cross-validation with 1,000 iterations.

The magnitude of genetic differentiation was calculated using the F_{ST} analog, θ, by Weir and Cockerham (1984). Global F_{ST} was calculated using hierfstat v.0.5-7 (Goudet, 2005; Goudet and Jombart, 2020), the significance of which was tested with 1,000 permutations. Pairwise F_{ST} among bays were calculated as implemented in dartR; pairwise genetic variation was considered significant when the 95% confidence interval calculated after 1,000 bootstrap replicates did not include $F_{ST} \leq 0$. Meanwhile, the hypotheses of spatial genetic differentiation within and between regions, as well as those inferred from DAPC and pairwise F_{ST}, were tested using hierarchical analysis of molecular variance (AMOVA; Excoffier et al., 1992). This was done using the wrapper function of poppr v.2.9.0 (Kamvar et al., 2014, 2015), which in turn carries out AMOVA as implemented in ade4 v.1.7-16 (Dray and Dufour, 2007); calculation of variance within individuals was excluded from the analysis, and the significance of the calculated statistics was tested using 1,000 permutations.

Identifying Candidate Genes Under Selection

The associated RAD sequences of all loci under the outlier panel were extracted from the Stacks catalog and were identified using NCBI-Basic Local Alignment Search Tool (BLAST[1]). The sequences were queried in the nucleotide collection (nr/nt) database using only Actinopterygii sequences (taxid: 7898). The search was optimized for somewhat similar sequences (blastn) with the *E*-value set to 0.001. Functional annotation of the identified sequences was done using the UniProt database.[2]

Moreover, the association between the outlier loci and environmental parameters were elucidated by correlating allele frequencies with remotely sensed oceanographic parameters. Only the loci that had loadings which contributed greater than 75% to the explained variation along the first discriminant axis in the DAPC ordination of the outlier panel were considered. SST (°C), chl-*a* (mg m^{-3}), and POC (mg m^{-3}) from January 2014 to December 2016 were processed as described in Palermo (2021). All these remotely sensed parameters were downloaded and compiled on a 4-km grid scale from the NASA Goddard Space Flight Center Distributed Active Archive Center.[3] The gridded data were extracted and binned average in SeaDAS per demarcated sardine fishing ground. Spatial variation between NMR and NZP was assessed using *t*-test, with *p*-values adjusted for multiple comparisons using Bonferroni correction. Prior to *t*-test, environmental parameters were transformed using the ordered quantile normalization technique implemented in the bestNormalize package (Peterson and Cavanaugh, 2020). The mean values of the oceanographic parameters were then correlated with the mean focal allele frequencies using Spearman's rho (ρ), with *p*-values also adjusted using Bonferroni correction.

R Packages

In addition to R packages already mentioned, the following were used for data analyses. Data wrangling and other miscellaneous functions were from dplyr v.1.0.6 (Wickham et al., 2021), factoextra v.1.0.7 (Kassambara and Mundt, 2020), forcats v.0.5.1 (Wickham, 2021a), magrittr v.2.0.1 (Bache and Wickham, 2020), purrr v.0.3.4 (Henry and Wickham, 2020), reshape2 v.1.4.4 (Wickham, 2007), rstatix v.0.7.0 (Kassambara, 2021), tictoc v.1.0 (Izrailev, 2014), and tidyr v.1.1.3 (Wickham, 2021b). Plotting and visualization functions utilized cowplot v.1.1.1 (Wilke, 2020), ggplot2 v.3.3.3 (Wickham, 2016), ggpubr v.0.4.0 (Kassambara, 2020), ggrepel v.0.9.1 (Slowikowski, 2021), gridExtra v.2.3 (Auguie, 2017), and scales v.1.1.1 (Wickham and Seidel, 2020). Genomic analyses and formatting genomic dataset utilized ape v.5.5 (Paradis and Schliep, 2019), diveRsity v1.9.90 (Keenan et al., 2013), mmod v.1.3.3 (Winter, 2012), pegas v.0.14 (Paradis, 2010), poppr v.2.9.0 (Kamvar et al., 2014), and zvau v.0.27 (Lustrik and Skrbinsek, 2016).

RESULTS

De novo Assembly Parameter Optimization

From a total of 239,995,133 reads obtained from restriction site-associated DNA sequencing (RADseq), the *process_radtags* program removed 264,906 (0.11%) low quality reads. Based on the remaining reads, the RAD dataset had an average of 4,994,380 (±3,283,774 SD) reads ranging from 347,394 to 14,363,982 (**Figure 2A**), with read lengths ranging from 92 to 96 bases. Since samples with low number of reads tend to decrease the number of loci that can be genotyped from the dataset, we dropped six samples that had read counts $<1.6 \times 10^6$. The first five samples with the highest read count per bay were then used to optimize the parameters for Stacks *de novo* assembly (*denovo_map.pl*).

Iteration of the *m* parameter while holding *M* and *n* constant showed that increasing *m* values led to the overall increase in coverage depths (**Figure 2B**). We have selected $m = 6$ since this is the lowest parameter value with samples having coverage depths ≥10 X; at this value, the resulting average coverage depth was 20 X (± 7.58 SD). Meanwhile, increasing the value of *M* while holding *m* and *n* constant resulted in the increase in the number of *r80* loci. This peaked at $M = 5$ ($n_{loci} = 17{,}268$), and then decreased at succeeding parameter values (**Figure 2C**). Lastly, iterating *n* while holding the other two parameters constant showed that $n = 4$ further increased the number of r80 loci ($n_{loci} = 18{,}063$). Based on our criteria, the optimal parameters for *denovo_map.pl* were $m = 6$, $M = 5$, and $n = 4$.

Genotyping and Outlier Detection

Using the optimal *de novo* assembly parameters on the full dataset with 42 samples, a total of 11,075 SNPs were genotyped with Stacks. From these, five samples and 7,400 SNPs did not pass the thresholds for call rates and were thus removed. From the remaining 3,675 SNPs, 20 deviated from HWE, 74 showed high levels of LD, and eight had $H_O > 0.60$; these loci were thus consequently removed. The remaining 37 samples and 3,573 SNPs were used to generate the full panel.

Three of the five methods used were able to detect putatively outlier loci from the full panel. While BayeScan and OutFLANK were unable to detect any outliers, Arlequin detected 64 with F_{ST} values ranging from 0.12 to 0.27, fsthet detected 173 with β values ranging from −0.03 to 0.27, and pcadapt detected 21 with Mahalanobis distances ranging from 26.44 to 74.82 (**Figure 3A**). All 225 loci tagged as putative outliers were removed from the full panel to generate a neutral panel of 3,348 SNPs. Meanwhile, out of all the outlier loci, 31 were common to both Arlequin and fsthet, while pcadapt had no common outliers with the other two

---

[1] https://blast.ncbi.nlm.nih.gov/Blast.cgi

[2] https://www.uniprot.org/

[3] https://oceancolor.gsfc.nasa.gov/

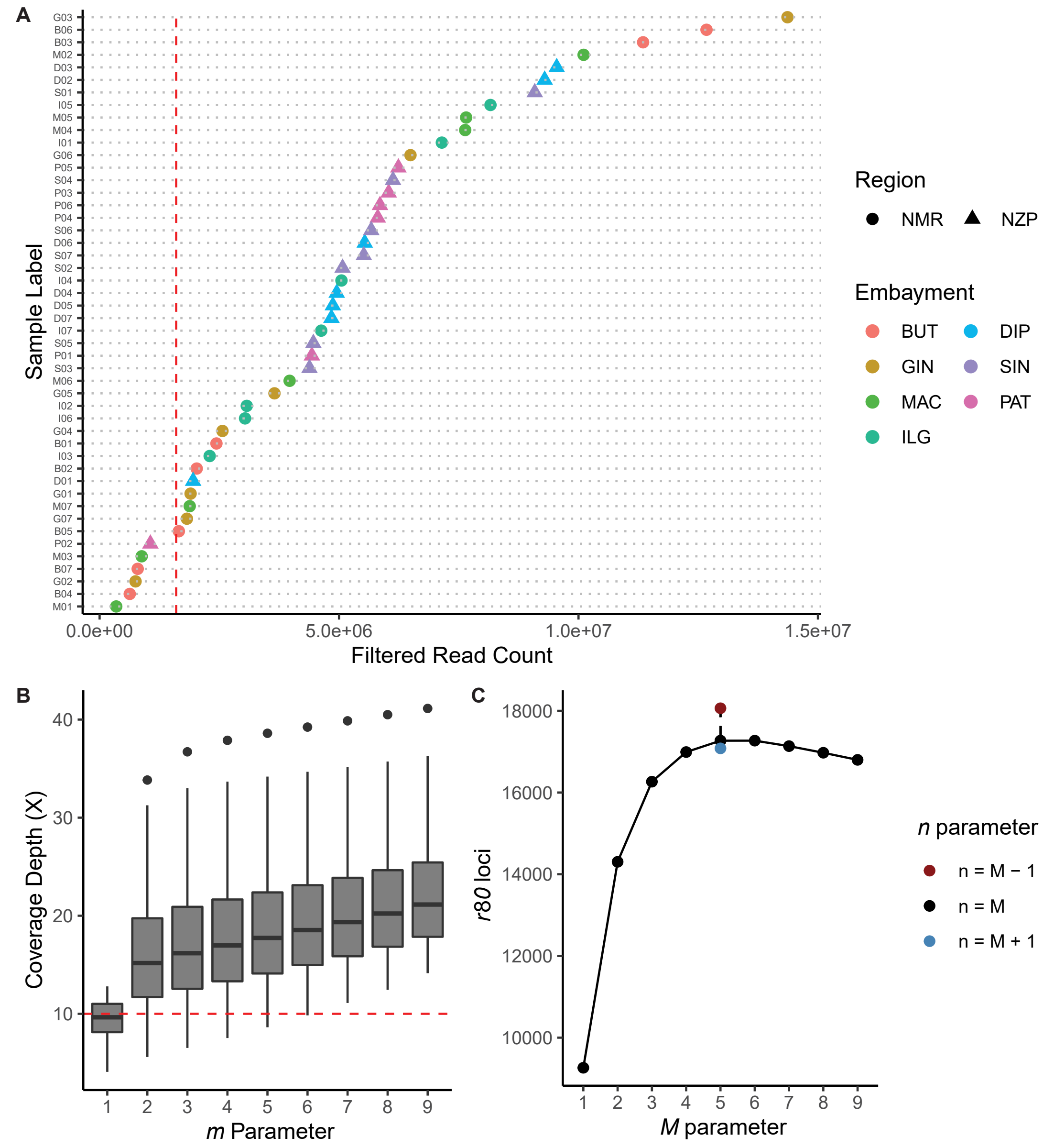

FIGURE 2 | Diagnostic plots for Stacks *de novo* assembly. **(A)** Filtered read count per sample. Shapes indicate the region, while colors indicate the bays from where the samples were collected. Samples with read count <1.6 × 10^6 (vertical red line) were removed from the analysis. **(B)** Coverage depth (X) for every iteration of the *m* parameter, while holding the other core parameters constant (*M* = *n* = 2). The lowest *m* value where all samples had X ≥ 10 (horizontal red line) was chosen. **(C)** Number of loci shared by ≥80% of the samples (i.e., *r80* loci) for every iteration of *M* and *n* core parameters, while holding *m* 6 constant. Parameter values that generated the highest number of r80 loci were selected.

methods (**Figure 3B**); these 31 loci were thus used to generate the outlier panel.

Genetic Diversity and Population Genetic Structure

All SNP panels consisted of 37 samples, 19 coming from NMR and 18 from NZP, with four to seven samples per bay (**Table 1**). The full and neutral panels had almost similar genetic diversity indices between regions. Specifically, both regions had $A_O > 99\%$, and although heterozygosity was slightly higher in NZP (full panel: $H_O = 0.226 \pm 0.034$ SE, $H_E = 0.233 \pm 0.031$; neutral panel: $H_O = 0.226 \pm 0.034$, $H_E = 0.232 \pm 0.031$) compared to NMR (full panel: $H_O = 0.211 \pm 0.032$, $H_E = 0.226 \pm 0.031$; neutral Panel: $H_O = 0.216 \pm 0.031$, $H_E = 0.232 \pm 0.030$), such variation was not significant (*t*-test Bonferroni-adjusted *p*-values > 0.05). In contrast, the outlier panel showed disparities between the two regions. All observed alleles were represented in NMR ($A_O = 100\%$), while only 93.55% were represented in NZP. Moreover, heterozygosity

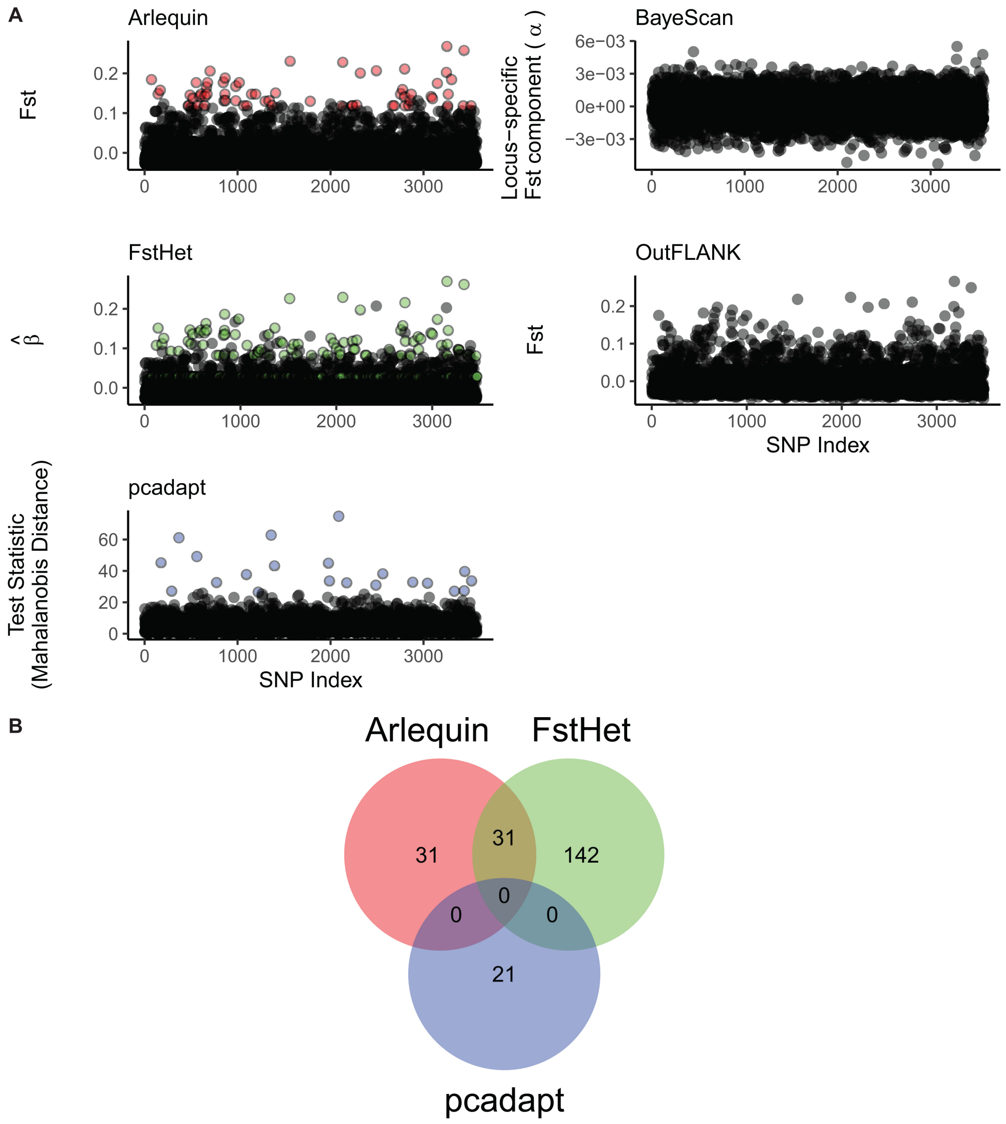

FIGURE 3 | Screening of putatively outlier loci from the genomic dataset. **(A)** Manhattan plots of the different outlier detection methods used. Arlequin, fsthet, and pcadapt were able to detect outliers (colored circles), while BayeScan and OutFLANK did not. **(B)** Venn diagram showing the number of loci flagged as outliers by the three outlier detection methods, and those that are common between them.

was significantly higher in NZP (H_O = 0.314 ± 0.042; H_E = 0.328 ± 0.040) than NMR (H_O = 0.219 ± 0.032; H_E = 0.241 ± 0.036) (*t*-test Bonferroni-adjusted *p*-values < 0.05 for both H_O and H_E).

Various analyses done on full and neutral SNP panels did not reveal evidence of genetic differentiation. PCA was unable to recover distinct clusters in the ordination, and *K*-means clustering recovered only one group for all samples (**Figures 4A,B**). Furthermore, genetic differentiation was negligible (global $F_{ST} \sim 0$; $p > 0.05$ pairwise $F_{ST} = -0.009$ to 0.007; **Figure 5**). Lastly, hierarchical AMOVA did not recover significant genetic variation among samples within region ($\leq$0.05% variance explained; $F_{SC} \sim 0$; $p > 0.05$) nor between regions ($\sim$ 0.00% variance explained; $F_{CT} \sim 0$; $p > 0.05$; **Table 2**).

In contrast, the outlier panel revealed regional genetic structure. PCA ordination was able to separate the different bays into their respective regions along the first axis (21.19% variance explained), while residual variance among samples within region was shown along the second axis (9.46% variance explained; **Figure 4C**). *K*-means clustering suggested $K = 2$ which corresponded to the two regions, and DAPC was able to assign the individuals from the different bays into their respective regions. Genetic differentiation was significant overall (global $F_{ST} = 0.161$, $p = 0.001$). Pairwise genetic differentiation was significant between regions (pairwise F_{ST} = 0.09–0.21), but not within regions (pairwise F_{ST} = −0.061 to 0.031; **Figure 5**). Lastly, hierarchical AMOVA recovered a significant partitioning of genetic variation between regions (26.29% variance explained,

TABLE 1 | Sampling information and genetic diversity indices of *Sardinella lemuru* along the northern coast of Mindanao.

Sampling location	Site code	*N*	Full panel				Neutral panel				Outlier panel			
			N_A	A_O (%)	$H_O \pm SE$	$H_E \pm SE$	N_A	A_O (%)	$H_O \pm SE$	$H_E \pm SE$	N_A	A_O (%)	$H_O \pm SE$	$H_E \pm SE$
Northern Mindanao Region	NMR	19	7,085	99.15	0.211 ± 0.032	0.226 ± 0.031	6,656	99.40	0.216 ± 0.031	0.232 ± 0.030	62	100.00	0.219 ± 0.032	0.241 ± 0.036
Butuan	BUT	4	5,765	80.67	0.205 ± 0.110	0.198 ± 0.089	5,437	81.20	0.209 ± 0.110	0.202 ± 0.089	51	82.26	0.218 ± 0.115	0.229 ± 0.099
Gingoog	GIN	4	5,787	80.98	0.206 ± 0.110	0.198 ± 0.088	5,464	81.60	0.211 ± 0.110	0.202 ± 0.089	54	87.10	0.274 ± 0.122	0.240 ± 0.088
Macajalar	MAC	4	5,836	81.67	0.224 ± 0.115	0.206 ± 0.089	5,525	82.51	0.230 ± 0.115	0.212 ± 0.089	49	79.03	0.194 ± 0.124	0.185 ± 0.092
Iligan	ILG	7	6,404	89.62	0.211 ± 0.068	0.216 ± 0.060	6,063	90.55	0.216 ± 0.068	0.222 ± 0.059	52	83.87	0.203 ± 0.072	0.224 ± 0.072
Northern Zamboanga Peninsula	NZP	18	7,090	99.22	0.226 ± 0.034	0.233 ± 0.031	6,654	99.37	0.226 ± 0.034	0.232 ± 0.031	58	93.55	0.314 ± 0.042	0.328 ± 0.040
Dipolog	DIP	6	6,294	88.08	0.223 ± 0.080	0.217 ± 0.066	5,890	87.96	0.223 ± 0.080	0.216 ± 0.066	55	88.71	0.312 ± 0.105	0.314 ± 0.079
Sindangan	SIN	7	6,484	90.74	0.228 ± 0.072	0.224 ± 0.059	6,075	90.73	0.229 ± 0.072	0.223 ± 0.059	57	91.94	0.323 ± 0.082	0.304 ± 0.066
Patawag	PAT	5	6,088	85.19	0.225 ± 0.096	0.213 ± 0.076	5,701	85.14	0.225 ± 0.096	0.213 ± 0.076	55	88.71	0.303 ± 0.095	0.305 ± 0.086
Global		37	7,146	100.00	0.218 ± 0.021	0.233 ± 0.021	6,696	100.00	0.221 ± 0.021	0.235 ± 0.021	62	100.00	0.265 ± 0.017	0.315 ± 0.017

Diversity indices for each SNP panel are shown.

N, sample size; N_A, number of alleles; A_O, percentage of observed alleles represented within site; H_O, observed heterozygosity; H_E, expected heterozygosity; SE, standard error.

F_{CT} = 0.263, p = 0.03) and within samples (74.60% variance explained, F_{ST} = 0.254, $p < 0.001$), but none among samples within region (−0.89% variance explained, F_{SC} = −0.012, $p > 0.05$; **Table 2**).

Candidate Genes Under Selection

Out of the 31 loci putatively under selection, nine were identified using BLAST, four of which were unannotated loci belonging to assembled genomes of various species under Actinopterygii. The remaining five were annotated genes that code for various predicted proteins which largely play roles in organismal development, with percent identities ranging from 87.50 to 93.75% (**Table 3**). With reference to DAPC, eight loci were found to greatly drive regional differentiation based on their respective loadings; seven of these loci were unidentified, while one (SNP_8118) was identified to be a fragment of the mRNA for the diphthamide biosynthesis 2 (dph2) protein.

The 36-month average of remotely sensed parameters highlighted the regional variability between NMR and NZP (**Figure 6A**). Bays in NZP had cooler waters compared to those in NMR, and regional variation in SST ($SST_{NZP} = 28.72 \pm 0.14$°C SE; $SST_{NMR} = 29.52 \pm 0.09$°C) was significant ($t_{215}^{SST} = 4.78$, p.adj < 0.001). Furthermore, the higher concentrations of chl-*a* and POC in NZP (chl-*a* = 1.93 ± 0.31 mg m^{-3}; POC = 228.11 ± 25.97 mg m^{-3}) compared to NMR (chl-*a* = 0.64 ± 0.07 mg m^{-3}; POC = 120.74 ± 6.52 mg m^{-3}) were also significant ($t_{185}^{chl-a} = -2.44$, p.adj < 0.05; $t_{183}^{POC} = -2.47$, p.adj < 0.05). Likewise, the mean frequencies of the focal allele of the shortlisted SNPs also varied at a regional scale (**Figure 6B**). Some of these SNPs had a focal allele that was absent in some bays of one region but was present in all bays of the other. Spearman correlation further showed three loci (SNP_1895, SNP_2472, and SNP_9403) that were strongly associated with SST ($\rho \geq 0.94$, p.adj < 0.05; **Table 4** and **Supplementary Figures 1–3**).

DISCUSSION

Sardinella lemuru Exhibits Local Adaptation Despite High Levels of Gene Flow

Contrasting inferences on genetic structure of *S. lemuru* along the northern coast of Mindanao were obtained from neutral and outlier loci. These reveal the potential inference of neutral and adaptive processes in shaping population structure (Kirk and Freeland, 2011; Funk et al., 2012). While neutral loci revealed genetic homogeneity suggestive of high levels of gene flow between the two regions, outlier loci revealed pronounced genetic structure and underscores how natural selection and local adaptation can shape regional genetic structure (Holderegger et al., 2006; Mariani and Bekkevold, 2014). This reflects the biological reality that local adaptation can still occur despite high levels of gene flow (Waples, 1998; Hemmer-Hansen et al., 2007b; Nielsen et al., 2009b; Corander et al., 2013; Yadav et al., 2019; Mendiola and Ravago-Gotanco, 2021).

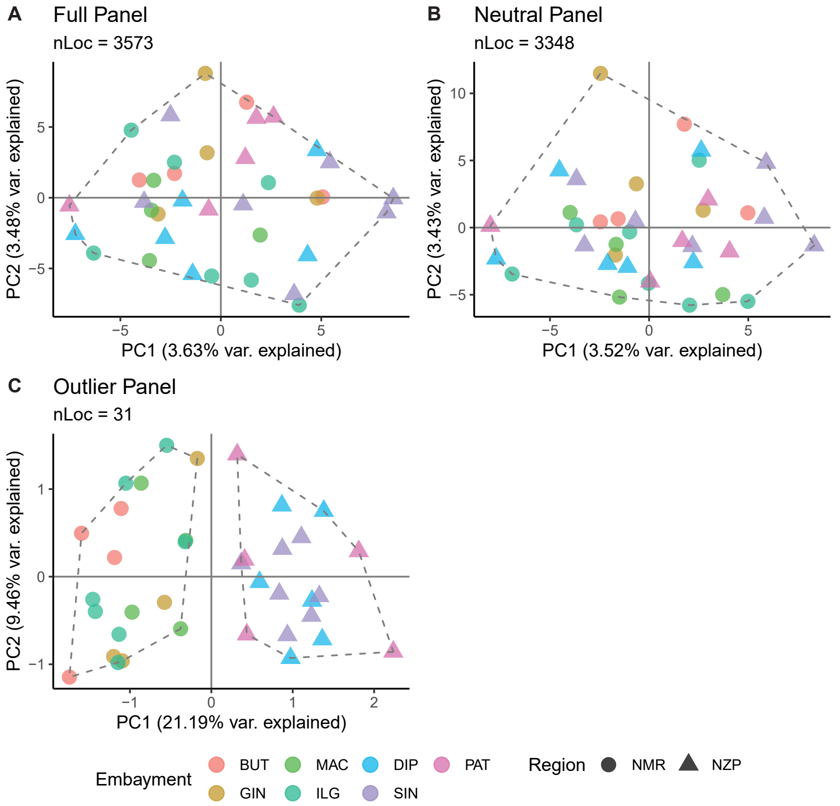

FIGURE 4 | Summary of the ordination analyses done on the **(A)** full, **(B)** neutral, and **(C)** outlier SNP panels. The number of loci (nLoc) for each panel is shown. Colors indicate the bays, while shapes indicate the regions. The ordination plot was projected using PCA scores, the dashed polygons indicate the optimal number of groups inferred from *K*-means clustering, and the points within the polygon depict the membership of samples inferred from DAPC.

Spatial genetic homogeneity of *S. lemuru* corroborates previous reports based on the mtDNA CR (Pedrosa-Gerasmio et al., 2015; Labrador et al., 2021). Most marine pelagic fishes, including this species, have large effective population sizes, are highly migratory, and have high dispersal capabilities at both larval and adult stages (Waples, 1998; Tinti et al., 2002; Lecomte et al., 2004; Ravago-Gotanco and Juinio-Meñez, 2004; Atarhouch et al., 2007; Nielsen et al., 2009b; Ruggeri et al., 2013; Pedrosa-Gerasmio et al., 2015; Sukumaran et al., 2016); all these biological properties increase the homogenizing effects of gene flow while minimizing the structuring effects of genetic drift. Moreover, agents that facilitate gene flow are not limited to biological characteristics, since oceanographic features such as the dynamic movement of water interconnecting the different geopolitical boundaries, ocean circulation shifts due to monsoon cycle, and tidal shifts are known to mediate larval dispersal and influence adult migration (Campos et al., 2015; Pedrosa-Gerasmio et al., 2015; Pata et al., 2021). Although spawning sites of *S. lemuru* were found to be localized in different bays within NMR and NZP (De Guzman et al., 2015; Pata et al., 2021), larvae are passively transported from one bay to another where they, along with recruits that are already present in the area, eventually make up the spawning pool (Campos et al., 2015). Dispersal models have shown how ocean currents facilitate larval transport along the northern coast of Mindanao (Pata et al., 2021). The Bohol Jet, a strong southwestward-flowing surface current from the Pacific Ocean to the Sulu Sea passing along the northern Bohol Sea (Cabrera et al., 2011), facilitates the importation of sardine larvae from the spawning grounds in NMR toward the NZP, essentially linking these regions; this was contrary to the conclusion of Luceño et al. (2014) who suggested that geographic isolation limits migration of *S. lemuru* between the two regions. Furthermore, there was a strong offshore transport of sardine larvae from the NZP during the northeast monsoon due to the intensified upwelling and northwestward direction of currents exiting the Dipolog Strait; this essentially facilitates the movement of sardine larvae from the northern coast of Mindanao toward other regions along the Sulu-Celebes Sea.

Meanwhile, putatively outlier SNPs revealed regional genetic differentiation, indicating that patterns of gene flow do not match patterns of adaptive divergence (Funk et al., 2012). The strong adaptive differentiation observed against a backdrop of high levels of gene flow indicates that the influence of natural selection overpowers genetic drift, a common occurrence in populations with large effective population size and inhabit heterogeneous environments (Hemmer-Hansen et al., 2007b; Funk et al., 2012; Limborg et al., 2012a,b; Moore et al., 2014; Sebastian et al., 2021). Remotely sensed parameters have shown

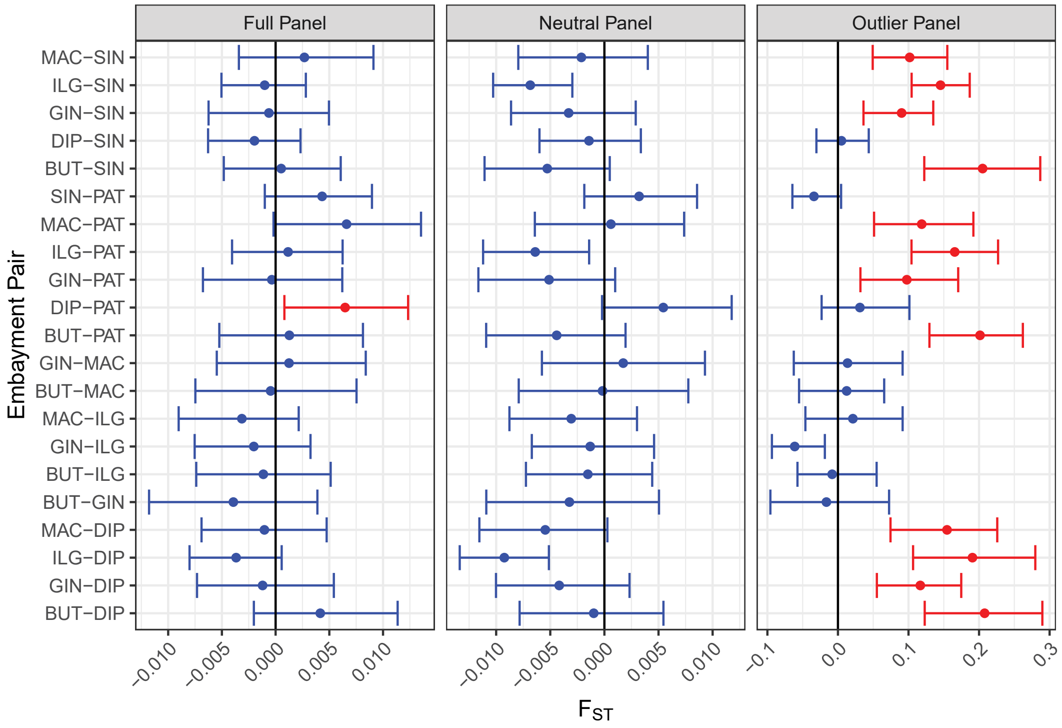

FIGURE 5 | Pairwise F_{ST} comparison among bays for all SNP panels. The F_{ST} analog by Weir and Cockerham (1984) was used in the calculation. The error bar indicates the 95% confidence interval of the estimate based on 1,000 iterations. Significant comparisons are shown in red.

TABLE 2 | Hierarchical analysis of molecular variance (AMOVA) testing the hypothesis of *Sardinella lemuru* genetic structure within and between Northern Mindanao Region (NMR) and Northern Zamboanga Peninsula (NZP).

SNP panel	Between regions			Among samples, within region			Within samples		
	d.f.	% var	F_{CT}	d.f.	% var	F_{SC}	d.f.	% var	F_{ST}
Full panel	1	−0.01	$-8.99e^{-5}$	5	0.05	$5.088e^{-4}$	30	99.96	$4.189e^{-4}$
Neutral panel	1	−1.06	−0.011	5	0.09	−0.001	30	100.97	−0.010
Outlier panel	1	26.29	0.263*	5	−0.89	−0.012	30	74.60	0.254***

Hypothesis was tested using the full, neutral, and outlier SNP panels. Shown are degrees of freedom (d.f.), percent variation (% var), and F-statistics.
**$p < 0.05$, ***$p < 0.001$.*

TABLE 3 | Loci putatively under selection that had predicted protein functions.

SNP ID	BLASTn ID	Query cover (%)	Identity (%)	Biological function	Reference accession no.
SNP_2470	*Clupea harengus*, EF-hand and coiled-coil domain-containing protein 1 (EFCC1)-like, mRNA	100	87.5	Function unknown	XM_012822564.2
SNP_2475	*Clupea harengus*, myelin transcription factor 1 (myt1)-like protein, mRNA	66	93.75	Cell differentiation, nervous system development	XM_031580484.1
SNP_2939	*Clupea harengus*, polyhomeotic homolog 3 (phc3), mRNA	45	90.91	Multicellular organism development	XM_031559940.1
SNP_8104	*Poecilia reticulata*, von Willebrand factor C domain containing protein 2 (vwc2), mRNA	46	86.67	Multicellular organism development	XM_008430062.2
SNP_8118	*Clupea harengus*, diphthamide biosynthesis 2 (dph2), mRNA	48	93.62	Transferase activity, peptidyl-diphthamide biosynthesis pathway	XM_031583972.1

BLAST hits (query length = 96 bp) were only from Actinopterygii (taxid: 7898). Biological functions were inferred from the UniProt database (https://www.uniprot.org/).

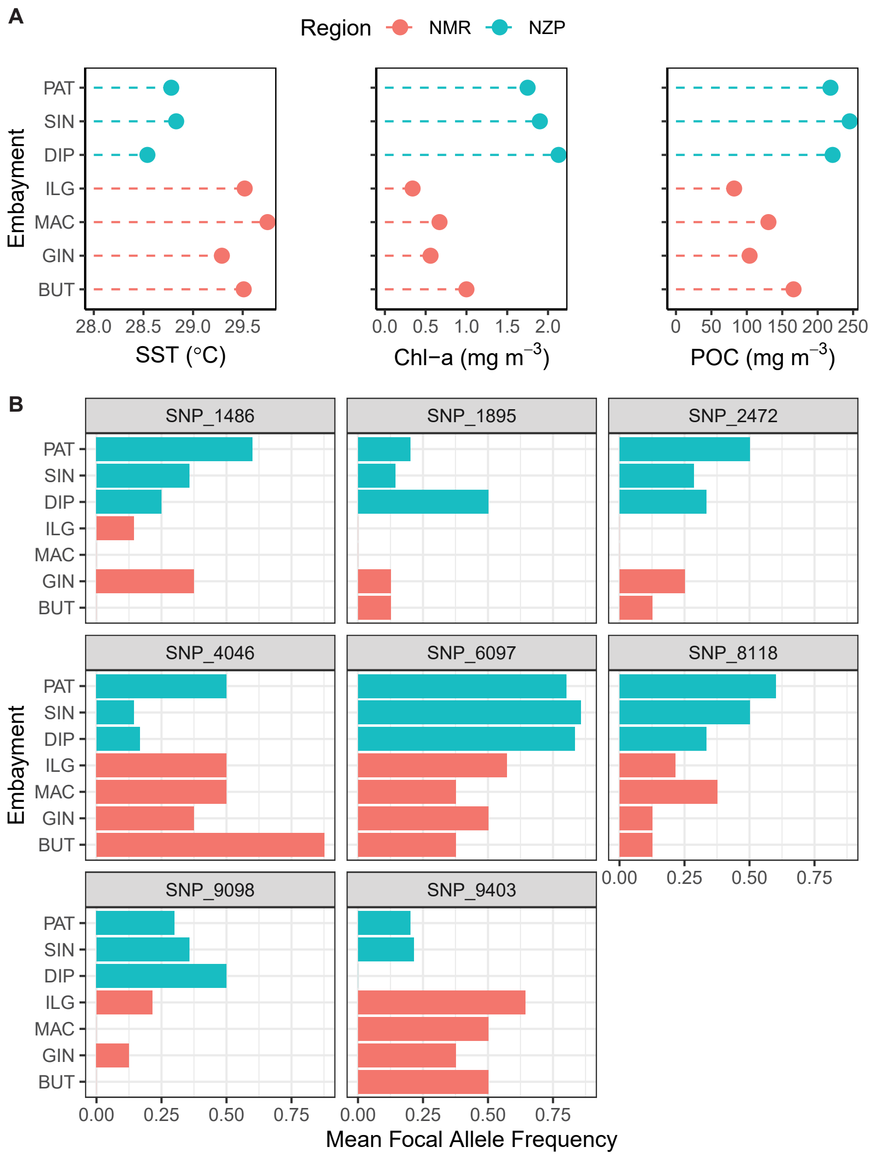

FIGURE 6 | Association between remotely sensed (RS) oceanographic parameters and focal allele frequencies. Colors indicate region (NMR, Northern Mindanao Region; NZP, Northern Zamboanga Peninsula). **(A)** Oceanographic parameters (SST, sea surface temperature; chl-*a*, chlorophyll *a*; POC, particulate organic carbon) averaged across a span of 3 years (2014–2016). **(B)** Mean focal allele frequencies of outlier loci that contributed greatly to the regional structuring observed in the ordination analyses. The sample sizes are: BUT = 4; GIN = 4; MAC = 4; ILG = 7; DIP = 6; SIN = 7; and PAT = 5.

that, at a temporal scale, the stronger signature of upwelling in NZP causes more pronounced fluctuation in SST, chl-*a*, and POC between monsoons, making it relatively more dynamic than NMR; meanwhile, at a spatial scale, NZP has, on average, cooler waters and higher concentrations of chl-*a* and POC than NMR. Even with high levels of gene flow between these two regions, larvae produced from spawning events passively drift toward areas with different environmental conditions where they are consequently subjected to the forces of selection (Nielsen et al., 2009a); this in turn heavily impacts their natural mortality and recruitment success since sardine larvae are highly vulnerable to variabilities in the environment (Pata et al., 2021). Larvae that exhibit greater fitness to prevailing environmental conditions would have a higher likelihood of survival to sexual maturity, and will eventually contribute to the gene pool, thereby resulting in a spawning population carrying specific adaptive genetic variants (Willette et al., 2014).

Signatures of genetic variation recovered using outlier loci have been reported for many fish species that exhibit high levels of gene flow, including *S. longiceps* (Sebastian et al., 2021), *Gadus morhua* (Westgaard and Fevolden, 2007; Nielsen et al., 2009b; Bradbury et al., 2010), *Platichthys flesus* (Hemmer-Hansen et al., 2007a,b), *Caesio cuning* (Ackiss et al., 2018), *Clupea harengus* (André et al., 2011; Lamichhaney et al., 2012;

TABLE 4 | Spearman correlation (ρ) between putatively outlier loci and remotely sensed environmental parameters.

SNP ID	Environmental Parameters		
	chl-*a* (mg m^{-3})	POC (mg m^{-3})	SST (°C)
SNP_1486	0.23	0.27	−0.68
SNP_1895	0.87	0.80	−0.98***
SNP_2472	0.76	0.72	−0.95**
SNP_4046	−0.48	−0.52	0.56
SNP_6097	0.63	0.67	−0.76
SNP_8118	0.50	0.58	−0.34
SNP_9098	0.67	0.63	−0.83
SNP_9403	−0.85	−0.77	0.94*

Shown here are the eight loci that greatly drove regional genetic differentiation based on their loadings in DAPC. The environmental parameters are sea surface temperature (SST), chlorophyll-a (chl-a), and particulate organic carbon (POC). p-Values were adjusted for multiple comparisons using Bonferroni correction.
**p < 0.05, **p < 0.01, ***p < 0.001.*

Limborg et al., 2012b; Corander et al., 2013), and *Oncorhynchus nerka* (Russello et al., 2012). In most cases, outlier loci identified additional genetic clusters and more complex admixture patterns compared to neutral loci, thereby increasing the overall statistical power in distinguishing the underlying genetic structure of these high gene flow species (Limborg et al., 2012b). Furthermore, several of these papers recommended that non-neutral markers could be used in differentiating stocks of high gene flow species, and that these stocks should be considered as separate MU to preserve adaptive variation.

Adaptive Divergence May Be Associated With Sea Surface Temperature

Identification of adaptively divergent fisheries populations have been conducted mostly on model organisms (e.g., *Danio rerio, Gasterosteus aculeatus*, and *G. morhua*; see Nielsen et al., 2009a). Genetic assessments were conducted using well-characterized candidate genes (*HSc70, PanI*, and *HbI*) associated with specific environmental stressors (e.g., temperature fluctuations, osmotic stress, and heavy metals; Nielsen et al., 2009a). With RADseq, we were able to perform a genome scan on a non-model organism and detected 31 loci that were putatively under selection; five of these loci were annotated to code for proteins, most of which are involved in organismal development, and three were found to be associated with the environment.

Environmental parameters linked to upwelling were previously reported to affect the population dynamics of *S. lemuru*. High primary productivity during upwelling, often characterized by high concentration of chl-*a* and relatively colder SST, correlated with higher sardine catches in Indonesia (Sartimbul et al., 2010; Sambah et al., 2012) and the Philippines (Villanoy et al., 2011). Moreover, Pata et al. (2021) posited that spawning strategies of *S. lemuru* in the Southern Philippines, the peak of which coincides with the upwelling event during the northeast monsoon, are adaptations to maximize sardine recruitment and lower natural mortality since the improved prey density and cooler temperatures during this time translate into more optimal growth conditions for the sardine larvae. Variability in primary productivity due to wind and ocean current was also hypothesized to influence recruitment success of *S. lemuru* along the coast of Western Australia (Gaughan and Mitchell, 2000). In this study, three unannotated loci that contributed greatly to the observed regional genetic differentiation correlated with SST, suggesting that this environmental parameter acts as a selective force putatively driving adaptive divergence on such genomic regions (Sebastian et al., 2021). Temperature is important for the proper functioning of proteins that affect physiological processes; it is therefore considered a primary selective agent involved in local adaptation in the marine environment, as was observed in many fishes (e.g., Hemmer-Hansen et al., 2007a; Dionne et al., 2008; Nielsen et al., 2009a,b; Limborg et al., 2012a,b; Sebastian et al., 2021). Conversely, we found no association between the candidate outlier loci and the parameters that are often used as proxies for ocean primary productivity and food availability, namely chl-*a* and POC. This contrasts with the findings of Sebastian et al. (2021) who reported that chl-*a* is among the environmental parameters that led to two adaptively divergent populations of *S. longiceps* in the Indian Ocean. While it is possible that chl-*a* and POC are not strong enough to drive adaptive divergence despite their differences between regions, it is more likely that loci associated with these parameters were neither genotyped nor screened with the outlier detection methods used.

It should be noted that inferences from this study were largely limited by the relatively few samples that were used for screening outliers. While some authors favored the use of larger sample sizes in population genetic studies (e.g., Kalinowski, 2005; Morin et al., 2009), others reported that increasing the number of markers would be more informative in estimating population genetic parameters (e.g., genetic differentiation and genetic diversity) rather than increasing the number of samples (Felsenstein, 2006; Landguth et al., 2012; Willing et al., 2012; Nazareno et al., 2017). Large number of SNPs can still provide reliable estimates even with small sample sizes (Willing et al., 2012; Nazareno et al., 2017); thus, reducing the sample size in favor of increasing the number of loci offered an alternative strategy. Furthermore, the estimator used for genetic differentiation was the FST analog by Weir and Cockerham (1984); based on simulations by Willing et al. (2012), this estimator is reliable even with small sample sizes ($n = 4$–6) if the number of biallelic loci is high ($n_{\text{loci}} > 1{,}000$) and the actual measure of genetic differentiation is low ($FST < 0.10$). While this provides confidence in the results inferred from both the full and neutral panels, there is a risk of bias in the estimates from the outlier panel since the number of loci was low ($n_{\text{loci}} = 31$) and genetic differentiation was high ($FST > 0.1$). Corander et al. (2013) also raised the possibility of underestimating the degree of divergence in *C. harengus* populations in Baltic Sea due to limited sampling. Furthermore, the outlier loci screened (0.87% of the full SNP panel) was fewer than those reported for other high gene flow species such as *C. harengus* (5.7%; Limborg et al., 2012b) and *G. morhua* (4.2%; Bradbury et al., 2010); this could be due to the small sample size of the current dataset which lacks sufficient power to detect outliers (Whitlock and Lotterhos, 2015). Ultimately, despite the valuable insights obtained from the small number of samples, further studies should either use a larger sample size per population (Corander et al., 2013) or increase the total number of sampled populations (Whitlock and Lotterhos, 2015) to get better estimates of the levels of genetic differentiation, including the number or relative proportion of putative outlier loci.

The absence of a reference genome for *Sardinella* also made it difficult to annotate the outlier loci. More comprehensive insights on local adaptation could have been obtained otherwise. We were unable to rule out the possibility that some loci driving regional genetic differentiation may not necessarily be adaptive genes nor are they directly associated with a phenotype, as they may be associated with coding or regulatory regions of functional genes subject to selection (Corander et al., 2013). Furthermore, with genetic hitchhiking, even neutral loci may appear to be under selection when it is linked to another gene that is influenced by selection (Gagnaire et al., 2015). It is also possible that these loci are found in genomic regions that are resistant to gene flow; these cold spots of recombination, where recombination rate is lower than average, include heterochromatic regions such as centromeres and telomeres (Tigano and Friesen, 2016). In the absence of an empirical observation regarding the link between the outlier loci and the associated phenotype with adaptive importance, our results must retain an element of speculation and must be considered as hypotheses to be tested (Nielsen et al., 2009a).

General Implications

Our results based on neutral loci suggest high levels of gene flow and likely demographic connectivity among *S. lemuru* populations along the northern coast of Mindanao. A null hypothesis of panmixia was not rejected, in contrast to previous reports that suggested otherwise. Following the framework by Funk et al. (2012), *S. lemuru* in these two regions can be considered as a single management unit. This is important to note since efforts in safeguarding the sardine fisheries, such as the implementation of a closed fishing season during peak spawning season in the northeast monsoon months (Pata et al., 2021), were more intensive in NZP compared to NMR. Improvements in the sardine fisheries in NZP (e.g., increased landed catch value and volume, increased production of bottled sardine, and increased monthly salary of fishing crew; Narvaez, 2017) would therefore be shared with NMR due to population connectivity.

However, even with high levels of gene flow, our results also provided evidence for regional genetic differentiation brought about by local adaptation. Further, results suggest that adaptive divergence could be driven by the differences in the SST between NMR and NZP as these introduce variability in the sardine's population dynamics (e.g., recruitment success and natural mortality; Pata et al., 2021). A locally adapted subpopulation has members that are more fit in the native habitat compared to immigrants (Kawecki and Ebert, 2004); thus, even if *S. lemuru* has high dispersal potential, there remains a possibility that non-native individuals will have lower fitness when entering a new environment (Nielsen et al., 2009a). Larvae that enter a particular habitat are subjected to selective forces which can remove unfit individuals even before they reach sexual maturity; this results in an adult population having a higher proportion of individuals with genetic variants matching the local environment (Willette et al., 2014). Even though there is continuous larval supply from NZP to NMR and vice versa, environmental differences between the two regions would still contribute to the larval mortality which will ultimately lower the number of successful recruits, and consequently, the population size. In extreme cases when locally adapted populations decline, replenishing them would still prove challenging due to non-matching habitats (Sebastian et al., 2021). This ultimately suggests the need to not only focus on demographic parameters (e.g., stock size and catch volume increase) in management measures, but to also consider preservation of adaptive variation and evolutionary potential that are present within regions (Funk et al., 2012; Sebastian et al., 2021), as well as consider the influence of the environment especially on recruitment success (Pata et al., 2021).

DATA AVAILABILITY STATEMENT

The datasets presented in this study can be found in online repositories. The names of the repository/repositories and their respective links are as follows: (1) sequence reads (NCBI, https://www.ncbi.nlm.nih.gov/bioproject/PRJNA752467) and (2) R script, SNP panels, and metadata (Dryad, https://doi.org/10.5061/dryad.4qrfj6qbx).

ETHICS STATEMENT

Ethical review and approval was not required for the animal in this study because Bali sardinella (*Sardinella lemuru*) is commercially available and is sold in markets all over the country.

AUTHOR CONTRIBUTIONS

KL, RR-G, and MJP conceptualized the project. KL, JDP, and AA collected the samples, conducted the laboratory work, and performed administrative and procurement tasks. KL and AA worked to generate the sequence data, while JDP processed the remote sensing data. KL performed the formal analysis, wrote the original draft of the manuscript, and along with JDP, prepared the figures for visualization; all these were done under the supervision of RR-G and MJP. MJP secured the funding for this project. All authors commented on the manuscript and agreed to its submission.

FUNDING

This work was funded by the Department of Science and Technology – Philippine Council for Agriculture, Aquatic and Natural Resources Research and Development (DOST-PCAARRD) through the project entitled "Molecular Technology-Based Assessment of the Sustainability of Sardine

Fisheries" under the program, "Development of Robust Tools in Support of the Sustainable Management of Sardine Fisheries in the Zamboanga Upwelling–Bohol Sea System (SarDyn)." Completion of the manuscript was made possible by the thesis writing grant awarded to KL by the University of the Philippines – Marine Science Institute (UP-MSI). Support for the publication fee was also provided by UP-MSI through the project entitled, "Upgrading Capacity, Infrastructure, and Assets for Marine Scientific Research in the Philippines."

ACKNOWLEDGMENTS

We would like to acknowledge the assistance provided by Ma. Rio Naguit, Asuncion De Guzman, Jerry Garcia, Jhunrey Follante, Joshep Mercene, and John Christopher Azcarraga in sample collection and initial processing. We also acknowledge the research staff of the Marine Molecular Ecology and Evolution Laboratory (MMEEL), as well as the Marine Genomics and Molecular Genetics Laboratory (MGMGL) and its head, Arturo Lluisma, for providing valuable input in the conduct of the experiment and analysis of the data. Finally, we extend our gratitude to Demian Willette, Laura David, and Jonas Quilang for their valuable feedback on the manuscript.

SUPPLEMENTARY MATERIAL

The Supplementary Material for this article can be found online at: https://www.frontiersin.org/articles/10.3389/fmars.2022.766936/full#supplementary-material

REFERENCES

Ackiss, A. S., Bird, C. E., Akita, Y., Santos, M. D., Tachihara, K., and Carpenter, K. E. (2018). Genetic patterns in peripheral marine populations of the fusilier fish *Caesio cuning* within the Kuroshio current. *Ecol. Evol.* 8, 11875–11886. doi: 10.1002/ece3.4644

André, C., Larsson, L. C., Laikre, L., Bekkevold, D., Brigham, J., Carvalho, G. R., et al. (2011). Detecting population structure in a high gene-flow species, Atlantic herring (*Clupea harengus*): direct, simultaneous evaluation of neutral vs putatively selected loci. *Heredity* 106, 270–280. doi: 10.1038/hdy.2010.71

Andrews, K. R., Good, J. M., Miller, M. R., Luikart, G., and Hohenlohe, P. A. (2016). Harnessing the power of RADseq for ecological and evolutionary genomics. *Nat. Rev. Genet.* 17, 81–92. doi: 10.1038/nrg.2015.28

Andrews, S. (2010). *FastQC: A Quality Control Tool for High Throughput Sequence Data*. Babraham: Babraham Institute.

Atarhouch, T., Rami, M., Naciri, M., and Dakkak, A. (2007). Genetic population structure of sardine (*Sardina pilchardus*) off Morocco detected with intron polymorphism (EPIC-PCR). *Mar. Biol.* 150, 521–528. doi: 10.1007/s00227-006-0371-8

Auguie, B. (2017). *gridExtra: Miscellaneous Functions for "Grid" Graphics*. Available online at: https://cran.r-project.org/package=gridExtra (accessed September 9, 2017).

Bache, S. M., and Wickham, H. (2020). *magrittr: A Forward-Pipe Operator for R*. Available online at: https://cran.r-project.org/package=magrittr (accessed November 17, 2020).

Baird, N. A., Etter, P. D., Atwood, T. S., Currey, M. C., Shiver, A. L., Lewis, Z. A., et al. (2008). Rapid SNP discovery and genetic mapping using sequenced RAD markers. *PLoS One* 3:e3376. doi: 10.1371/journal.pone.0003376

Bradbury, I. R., Hubert, S., Higgins, B., Borza, T., Bowman, S., Paterson, I. G., et al. (2010). Parallel adaptive evolution of Atlantic cod on both sides of the Atlantic Ocean in response to temperature. *Proc. R. Soc. B Biol. Sci.* 277, 3725–3734. doi: 10.1098/rspb.2010.0985

Cabrera, O. C., Villanoy, C. L., David, L. T., and Gordon, A. L. (2011). Barrier layer control of entrainment and upwelling in the Bohol sea, Philippines. *Oceanography* 24, 130–141. doi: 10.5670/oceanog.2011.10

Cadrin, S. X., Kerr, L. A., and Mariani, S. (2014). *Stock Identification Methods: Applications in Fishery Science*, 2nd Edn, eds S. X. Cadrin, L. A. Kerr, and S. Mariani (Amsterdam: Elsevier, Inc).

Campos, W., Acabado, C., Metillo, E., Naguit, M. R., Bagarinao, A., Almaquer, C. J., et al. (2015). *Estimating Early Life Stage Mortality and Sources of Recruits. Project 3 of Development of Robust Tools for Managing Sardine Fisheries in the Philippines: Zamboanga Upwelling – Bohol Sea System (SarDyn). Terminal Report*. Laguna: Department of Science and Technology – Philippine Council for Agriculture, Aquatic and Natural Resources Research and Development (DOST-PCAARRD), 77.

Catchen, J. M., Amores, A., Hohenlohe, P., Cresko, W., and Postlethwait, J. H. (2011). Stacks: building and genotyping loci de novo from short-read sequences. *G3 Genes Genomes Genetics* 1, 171–182. doi: 10.1534/g3.111.000240

Catchen, J., Hohenlohe, P. A., Bassham, S., Amores, A., and Cresko, W. A. (2013). Stacks: an analysis tool set for population genomics. *Mol. Ecol.* 22, 3124–3140. doi: 10.1111/mec.12354

Conover, D. O., Clarke, L. M., Munch, S. B., and Wagner, G. N. (2006). Spatial and temporal scales of adaptive divergence in marine fishes and the implications for conservation. *J. Fish. Biol.* 69, 21–47. doi: 10.1111/j.1095-8649.2006.01274.x

Corander, J., Majander, K. K., Cheng, L., and Merila, J. (2013). High degree of cryptic population differentiation in the Baltic Sea herring *Clupea harengus*. *Mol. Ecol.* 22, 2931–2940. doi: 10.1111/mec.12174

Davey, J. W., and Blaxter, M. L. (2010). RADSeq: next-generation population genetics. *Brief. Funct. Genomics* 9, 416–423. doi: 10.1093/bfgp/elq031

De Guzman, A., Jimenez, C. R., Abrea, R. A., Garcia, J. P., Recamara, D. B., Flores, M. H., et al. (2015). *Sustaining the Sardine Fisheries Industry Through Understanding Spatio-Temporal Dynamics in the Zamboanga Peninsula and Bohol Sea System. Project 2 of Development of Robust Tools for Managing Sardine Fisheries in the Philippines: Zamboanga Upwelling– Bohol Sea System (SarDyn). Terminal Report*. Laguna: Department of Science and Technology – Philippine Council for Agriculture, Aquatic and Natural Resources Research and Development (DOST-PCAARRD), 63.

Dionne, M., Caron, F., Dodson, J. J., and Bernatchez, L. (2008). Landscape genetics and hierarchical genetic structure in Atlantic salmon: the interaction of gene flow and local adaptation. *Mol. Ecol.* 17, 2382–2396. doi: 10.1111/j.1365-294X.2008.03771.x

Dray, S., and Dufour, A. B. (2007). The ade4 package: implementing the duality diagram for ecologists. *J. Stat. Softw.* 22, 1–20.

Excoffier, L., and Lischer, H. E. L. (2010). Arlequin suite ver 3.5: a new series of programs to perform population genetics analyses under Linux and Windows. *Mol. Ecol. Resour.* 10, 564–567. doi: 10.1111/j.1755-0998.2010.02847.x

Excoffier, L., Hofer, T., and Foll, M. (2009). Detecting loci under selection in a hierarchically structured population. *Heredity* 103, 285–298. doi: 10.1038/hdy.2009.74

Excoffier, L., Smouse, P. E., and Quattro, J. M. (1992). Analysis of molecular variance inferred from metric distances among DNA Haplotypes: application to human mitochondrial DNA restriction data. *Genetics* 131, 479–491. doi: 10.1093/genetics/131.2.479

Felsenstein, J. (2006). Accuracy of coalescent likelihood estimates: do we need more sites, more sequences, or more loci? *Mol. Biol. Evol.* 23, 691–700. doi: 10.1093/molbev/msj079

Flanagan, S. P., and Jones, A. G. (2017). Constraints on the FST–heterozygosity outlier approach. *J. Hered.* 108, 561–573. doi: 10.1093/jhered/esx048

Flanagan, S. P., and Jones, A. G. (2018). *fsthet: Fst-Heterozygosity Smoothed Quantiles*. Available online at: https://cran.r-project.org/package=fsthet (accessed March 20, 2018).

Foll, M., and Gaggiotti, O. (2008). A genome-scan method to identify selected loci appropriate for both dominant and codominant markers: a bayesian perspective. *Genetics* 180, 977–993. doi: 10.1534/genetics.108.092221

Funk, W. C., McKay, J. K., Hohenlohe, P. A., and Allendorf, F. W. (2012). Harnessing genomics for delineating conservation units. *Trends Ecol. Evol.* 27, 489–496. doi: 10.1016/j.tree.2012.05.012

Gagnaire, P. A., Broquet, T., Aurelle, D., Viard, F., Souissi, A., Bonhomme, F., et al. (2015). Using neutral, selected, and hitchhiker loci to assess connectivity of marine populations in the genomic era. *Evol. Appl.* 8, 769–786. doi: 10.1111/eva.12288

Gaughan, D. J., and Mitchell, R. W. D. (2000). *Final Report, FRDC Project 95/037: The Biology and Stock Assessment of the Tropical Sardine, Sardinella lemuru, off the Mid-West Coast of Western Australia*. Fisheries Research Report 119. Hillarys WA: WA Marine Research Laboratories.

Goudet, J. (2005). HIERFSTAT, a package for R to compute and test hierarchical F-statistics. *Mol. Ecol. Notes* 5, 184–186. doi: 10.1111/j.1471-8278

Goudet, J., and Jombart, T. (2020). *hierfstat: Estimation and Tests of Hierarchical F-Statistics*. Available online at: https://cran.r-project.org/package=hierfstat (accessed November 17, 2021).

Gruber, B., Unmack, P. J., Berry, O. F., and Georges, A. (2018). DARTR: an R package to facilitate analysis of SNP data generated from reduced representation genome sequencing. *Mol. Ecol. Resour.* 18, 691–699. doi: 10.1111/1755-0998.12745

Guanco, M. R., Mesa, S. V., Belga, P. B., and Nuñal, D. R. M. (2009). Assessment of the commercial fisheries of Western and Central Visayan Sea. *BFAR NFRDI Tech. Paper Ser.* 12, 1–44.

Hemmer-Hansen, J., Nielsen, E. E., Frydenberg, J., and Loeschcke, V. (2007a). Adaptive divergence in a high gene flow environment: Hsc70 variation in the European flounder (*Platichthys flesus* L.). *Heredity* 99, 592–600. doi: 10.1038/sj.hdy.6801055

Hemmer-Hansen, J., Nielsen, E. E., Grønkjær, P., and Loeschcke, V. (2007b). Evolutionary mechanisms shaping the genetic population structure of marine fishes; lessons from the European flounder (*Platichthys flesus* L.). *Mol. Ecol.* 16, 3104–3118. doi: 10.1111/j.1365-294X.2007.03367.x

Henry, L., and Wickham, H. (2020). *purrr: Functional Programming Tools*. Available online at: https://cran.r-project.org/package=purrr (accessed April 17, 2020).

Holderegger, R., Kamm, U., and Gugerli, F. (2006). Adaptive vs. neutral genetic diversity: implications for landscape genetics. *Landsc. Ecol.* 21, 797–807. doi: 10.1007/s10980-005-5245-9

Izrailev, S. (2014). *tictoc: Functions for Timing R Scripts, as Well as Implementations of Stack and List Structures*. Available online at: https://cran.r-project.org/package=tictoc (accessed April 19, 2021).

Jaya, I. (2002). Acoustical study of the schooling behavior of Lemuru (*Sardinella lemuru*). *Fish. Sci.* 68, 1881–1884.

Jombart, T. (2008). Adegenet: a R package for the multivariate analysis of genetic markers. *Bioinformatics* 24, 1403–1405. doi: 10.1093/bioinformatics/btn129

Jombart, T., and Ahmed, I. (2011). adegenet 1.3-1: new tools for the analysis of genome-wide SNP data. *Bioinformatics* 27, 3070–3071. doi: 10.1093/bioinformatics/btr521

Jombart, T., Devillard, S., and Balloux, F. (2010). Discriminant analysis of principal components: a new method for the analysis of genetically structured populations. *BMC Genet.* 11:94. doi: 10.1186/1471-2156-11-94

Kalinowski, S. T. (2005). Do polymorphic loci require large sample sizes to estimate genetic distances? *Heredity* 94, 33–36. doi: 10.1038/sj.hdy.6800548

Kamvar, Z. N., Brooks, J. C., and Grünwald, N. J. (2015). Novel R tools for analysis of genome-wide population genetic data with emphasis on clonality. *Front. Genet.* 6:208. doi: 10.3389/fgene.2015.00208

Kamvar, Z. N., Tabima, J. F., and Grünwald, N. J. (2014). Poppr: an R package for genetic analysis of populations with clonal, partially clonal, and/or sexual reproduction. *PeerJ* 2:e281. doi: 10.7717/peerj.281

Kassambara, A. (2020). *ggpubr: "ggplot2" Based Publication Ready Plots*. Available online at: https://cran.r-project.org/package=ggpubr (accessed June 27, 2020).

Kassambara, A. (2021). *rstatix: Pipe-Friendly Framework for Basic Statistical Tests*. Available online at: https://cran.r-project.org/package=rstatix (accessed February 13, 2021).

Kassambara, A., and Mundt, F. (2020). *factoextra: Extract and Visualize the Results of Multivariate Data Analyses*. Available online at: https://cran.r-project.org/package=factoextra (accessed April 1, 2020).

Kawecki, T. J., and Ebert, D. (2004). Conceptual issues in local adaptation. *Ecol. Lett.* 7, 1225–1241. doi: 10.1111/j.1461-0248.2004.00684.x

Keenan, K., Mcginnity, P., Cross, T. F., Crozier, W. W., and Prodöhl, P. A. (2013). diveRsity: an R package for the estimation and exploration of population genetics parameters and their associated errors. *Methods Ecol. Evol.* 4, 782–788. doi: 10.1111/2041-210X.12067

Kirk, H., and Freeland, J. R. (2011). Applications and implications of neutral versus non-neutral markers in molecular ecology. *Int. J. Mol. Sci.* 12, 3966–3988. doi: 10.3390/ijms12063966

Kritzer, J. P., and Liu, O. R. (2014). "Fishery management strategies for adressing complex spatial structure in marine fish stocks," in *Stock Identification Methods: Application in Fishery Science*, eds S. X. Cadrin, L. A. Kerr, and S. Mariani (Amsterdam: Elsevier, Inc), 29–53.

Labrador, K., Agmata, A., Palermo, J. D., Ravago-Gotanco, R., and Pante, M. J. (2021). Mitochondrial DNA reveals genetically structured haplogroups of Bali sardinella (*Sardinella lemuru*) in Philippine waters. *Reg. Stud. Mar. Sci.* 41:101588. doi: 10.1016/j.rsma.2020.101588

Lamichhaney, S., Barrio, A. M., Rafati, N., Sundstrom, G., Rubin, C.-J., Gilbert, E. R., et al. (2012). Population-scale sequencing reveals genetic differentiation due to local adaptation in Atlantic herring. *Proc. Natl. Acad. Sci.* 109, 19345–19350. doi: 10.1073/pnas.1216128109

Landguth, E. L., Fedy, B. C., Oyler-Mccance, S. J., Garey, A. L., Emel, S. L., Mumma, M., et al. (2012). Effects of sample size, number of markers, and allelic richness on the detection of spatial genetic pattern. *Mol. Ecol. Resour.* 12, 276–284. doi: 10.1111/j.1755-0998.2011.03077.x

Lecomte, F., Grant, W. S., Dodson, J. J., Rodríguez-Sánchez, R., and Bowen, B. W. (2004). Living with uncertainty: genetic imprints of climate shifts in East Pacific anchovy (Engraulis mordax) and sardine (*Sardinops sagax*). *Mol. Ecol.* 13, 2169–2182. doi: 10.1111/j.1365-294X.2004.02229.x

Lee, S. R., Jo, Y. S., Park, C. H., Friedman, J. M., and Olson, M. S. (2018). Population genomic analysis suggests strong influence of river network on spatial distribution of genetic variation in invasive saltcedar across the southwestern United States. *Mol. Ecol.* 27, 636–646. doi: 10.1111/mec.14468

Limborg, M. T., Blankenship, S. M., Young, S. F., Utter, F. M., Seeb, L. W., Hansen, M. H. H., et al. (2012a). Signatures of natural selection among lineages and habitats in *Oncorhynchus mykiss*. *Ecol. Evol.* 2, 1–18. doi: 10.1002/ece3.59

Limborg, M. T., Helyar, S. J., De Bruyn, M., Taylor, M. I., Nielsen, E. E., Ogden, R., et al. (2012b). Environmental selection on transcriptome-derived SNPs in a high gene flow marine fish, the Atlantic herring (*Clupea harengus*). *Mol. Ecol.* 21, 3686–3703. doi: 10.1111/j.1365-294X.2012.05639.x

Luceño, A. J. M., Torres, M. A. J., Tabugo, S. R. M., and Demayo, C. G. (2014). Describing the body shapes of three populations of *Sardinella lemuru* (Bleeker, 1853) from Mindanao Island, Philippines using relative warp analysis. *Int. Res. J. Biol. Sci.* 3, 6–17.

Lustrik, R., and Skrbinsek, T. (2016). *zvau: Misc Functions Used by Our Ecology Lab*. Available online at: https://github.com/romunov/zvau

Luu, K., Bazin, E., and Blum, M. G. B. (2017). pcadapt: an R package to perform genome scans for selection based on principal component analysis. *Mol. Ecol. Resour.* 17, 67–77. doi: 10.1111/1755-0998.12592

Mariani, S., and Bekkevold, D. (2014). "The nuclear genome: neutral and adaptive markers in fisheries science," in *Stock Identification Methods: Application in Fishery Science*, eds S. X. Cadrin, L. A. Kerr, and S. Mariani (Amsterdam: Elsevier Inc), 298–320.

Mastretta-Yanes, A., Arrigo, N., Alvarez, N., Jorgensen, T. H., Piñero, D., and Emerson, B. C. (2014). Restriction site-associated DNA sequencing, genotyping error estimation and de novo assembly optimization for population genetic inference. *Mol. Ecol. Resour.* 15, 28–41. doi: 10.1111/1755-0998.12291

Mendiola, M. J. R., and Ravago-Gotanco, R. (2021). Genetic differentiation and signatures of local adaptation revealed by RADseq for a highly dispersive mud crab *Scylla olivacea* (Herbst, 1796) in the Sulu Sea. *Ecol. Evol.* 11, 7951–7969. doi: 10.1002/ece3.7625

Metillo, E. B., Campos, W. L., Villanoy, C. L., Hayashizaki, K., Tsunoda, T., and Nishida, S. (2018). Ontogenetic feeding shift and size- based zooplanktivory in *Sardinella lemuru* (Pisces, Clupeidae) during an upwelling in southeastern Sulu Sea, The Philippines. *Fish. Manag. Ecol.* 25, 441–445. doi: 10.1111/fme.12319

Metzker, M. L. (2009). Sequencing technologies - the next generation. *Nat. Rev. Genet.* 11, 31–46. doi: 10.1038/nrg2626

Moore, J.-S., Bourret, V., Dionne, M., Bradbury, I., O'Reilly, P., Kent, M., et al. (2014). Conservation genomics of anadromous Atlantic salmon across its North

American range: outlier loci identify the same patterns of population structure as neutral loci. *Mol. Ecol.* 23, 5680–5697. doi: 10.1111/mec.12972

Morin, P. A., Martien, K. K., and Taylor, B. L. (2009). Assessing statistical power of SNPs for population structure and conservation studies. *Mol. Ecol. Resour.* 9, 66–73. doi: 10.1111/j.1755-0998.2008.02392.x

Narvaez, T. (2017). *Assessment of the Industry-Level Impacts of the Closed Fishing Season Policy for Sardines in Zamboanga Peninsula, Philippines*. Kawana: Food and Fertilizer Technology Center for the Asian and Pacific Region.

Nazareno, A. G., Bemmels, J. B., Dick, C. W., and Lohmann, L. G. (2017). Minimum sample sizes for population genomics: an empirical study from an Amazonian plant species. *Mol. Ecol. Resour.* 17, 1136–1147. doi: 10.1111/1755-0998.12654

Nielsen, E. E., Hemmer-Hansen, J., Larsen, P. F., and Bekkevold, D. (2009a). Population genomics of marine fishes: identifying adaptive variation in space and time. *Mol. Ecol.* 18, 3128–3150. doi: 10.1111/j.1365-294X.2009.04272.x

Nielsen, E. E., Hemmer-Hansen, J., Poulsen, N. A., Loeschcke, V., Moen, T., Johansen, T., et al. (2009b). Genomic signatures of local directional selection in a high gene flow marine organism; the Atlantic cod (*Gadus morhua*). *BMC Evol. Biol.* 9:276. doi: 10.1186/1471-2148-9-276

Olaño, V. L., Vergara, M. B., and Gonzales, F. L. (2009). Assessment of the Fisheries of Sorsogon Bay (Region 5). *BFAR NFRDI Tech. Paper Ser.* 12, 1–33.

Palermo, J. D. H. (2021). *Trophic Ecology of Sardines: Sardinella lemuru Feeding Strategies, Vulnerability to Marine Microplastic Pollution, and Endoparasitism in Northern Mindanao*. Ph.D. Dissertation. Quezon City: University of the Philippines-Diliman.

Palermo, J. D. H., Labrador, K. L., Follante, J. D., Agmata, A. B., Pante, M. J. R., Rollon, R. N., et al. (2020). Susceptibility of *Sardinella lemuru* to emerging marine microplastic pollution. *Glob. J. Environ. Sci. Manag.* 6, 373–384. doi: 10.22034/gjesm.2020.03.07

Pante, M. J. R., Palermo, J. D., Labrador, K. L., Agmata, A. A., and Follante, J. D. (2019). *Molecular Technology-Based Assessment of the Sustainability of Sardine Fisheries. Project 5 of Development of Robust Tools for Managing Sardine Fisheries in the Philippines: Zamboanga Upwelling – Bohol Sea System (SarDyn). Terminal Report*. Laguna: Department of Science and Technology – Philippine Council for Agriculture, Aquatic and Natural Resources Research and Development (DOST-PCAARRD), 84.

Paradis, E. (2010). Pegas: an R package for population genetics with an integrated-modular approach. *Bioinformatics* 26, 419–420. doi: 10.1093/bioinformatics/btp696

Paradis, E., and Schliep, K. (2019). ape 5.0: an environment for modern phylogenetics and evolutionary analyses in R. *Bioinformatics* 35, 526–528. doi: 10.1093/bioinformatics/bty633

Paris, J. R., Stevens, J. R., and Catchen, J. M. (2017). Lost in parameter space: a road map for stacks. *Methods Ecol. Evol.* 8, 1360–1373. doi: 10.1111/2041-210X.12775

Pata, P. R., and Yñiguez, A. T. (2019). Larval connectivity patterns of the North Indo-West Pacific coral reefs. *PLoS One* 14:e0219913. doi: 10.1371/journal.pone.0219913

Pata, P. R., Yñiguez, A. T., Deauna, J. D. L., De Guzman, A. B., Jimenez, C. R., Rosario, R. T. B., et al. (2021). Insights into the environmental conditions contributing to variability in the larval recruitment of the tropical sardine *Sardinella lemuru*. *Ecol. Model.* 451:109570. doi: 10.1016/j.ecolmodel.2021.109570

Pedrosa-Gerasmio, I. R., Agmata, A. B., and Santos, M. D. (2015). Genetic diversity, population genetic structure, and demographic history of *Auxis thazard* (Perciformes), *Selar crumenophthalmus* (Perciformes), *Rastrelliger kanagurta* (Perciformes) and *Sardinella lemuru* (Clupeiformes) in Sulu-Celebes Sea inferred by mitochondrial DNA sequences. *Fish. Res.* 162, 64–74. doi: 10.1016/j.fishres.2014.10.006

Peterson, R. A., and Cavanaugh, J. E. (2020). Ordered quantile normalization: a semiparametric transformation built for the cross-validation era. *J. Appl. Stat.* 47, 2312–2327. doi: 10.1080/02664763.2019.1630372

Plummer, M., Best, N., Cowles, K., and Vines, K. (2006). CODA: convergence diagnosis and output analysis for MCMC. *R. News* 6, 7–11.

R Core Team (2021). *R: A Language and Environment for Statistical Computing.* Vienna: R Foundation for Statistical Computing.

Ravago-Gotanco, R., and Juinio-Meñez, M. A. (2004). Population genetic structure of the milkfish, *Chanos chanos*, based on PCR-RFLP analysis of the mitochondrial control region. *Mar. Biol.* 145, 789–801. doi: 10.1007/s00227-004-1372-0

Rocha, L. A., Craig, M. T., and Bowen, B. W. (2007). Phylogeography and the conservation of coral reef fishes. *Coral Reefs* 26, 501–512. doi: 10.1007/s00338-007-0261-7

Rochette, N. C., and Catchen, J. M. (2017). Deriving genotypes from RAD-seq short-read data using Stacks. *Nat. Protoc.* 12, 2640–2659. doi: 10.1038/nprot.2017.123

Ruggeri, P., Splendiani, A., Bonanomi, S., Arneri, E., Cingolani, N., Santojanni, A., et al. (2013). Searching for a stock structure in *Sardina pilchardus* from the Adriatic and Ionian seas using a microsatellite DNA-based approach. *Sci. Mar.* 77, 565–574. doi: 10.3989/scimar.03843.26A

Russello, M. A., Kirk, S. L., Frazer, K. K., and Askey, P. J. (2012). Detection of outlier loci and their utility for fisheries management. *Evol. Appl.* 5, 39–52. doi: 10.1111/j.1752-4571.2011.00206.x

Sambah, A. B., Miura, F., Kadarisman, H. P., and Sartimbul, A. (2012). "Remote sensing application for *Sardinella lemuru* assessment: a case study of the south waters of Malang Regency, East Java, Indonesia," in *Proceedings of the SPIE, Remote Sensing of the Marine Environment II, 85250M*, Vol. 8525, Kyoto. doi: 10.1117/12.976284

Sartimbul, A., Nakata, H., Rohadi, R., Yusuf, B., and Kadarisman, H. P. (2010). Variations in chlorophyll-a concentration and the impact on *Sardinella lemuru* catches in Bali Strait, Indonesia. *Prog. Oceanogr.* 87, 168–174. doi: 10.1016/j.pocean.2010.09.002

Sebastian, W., Sukumaran, S., Abdul Azeez, S., Muraleedharan, K. R., Dinesh Kumar, P. K., Zacharia, P. U., et al. (2021). Genomic investigations provide insights into the mechanisms of resilience to heterogeneous habitats of the Indian Ocean in a pelagic fish. *Sci. Rep.* 11:20690. doi: 10.1038/s41598-021-00129-5

Slowikowski, K. (2021). *ggrepel: Automatically Position Non-Overlapping Text Labels with "ggplot2."*. Available online at: https://cran.r-project.org/package=ggrepel (accessed January 15, 2021).

Sukumaran, S., Sebastian, W., and Gopalakrishnan, A. (2016). Population genetic structure of Indian oil sardine, *Sardinella longiceps* along Indian coast. *Gene* 576, 372–378. doi: 10.1016/j.gene.2015.10.043

Tigano, A., and Friesen, V. L. (2016). Genomics of local adaptation with gene flow. *Mol. Ecol.* 25, 2144–2164. doi: 10.1111/mec.13606

Tinti, F., Di Nunno, C., Guarniero, I., Talenti, M., Tommasini, S., Fabbri, E., et al. (2002). Mitochondrial DNA Sequence variation suggests the lack of genetic heterogeneity in the Adriatic and Ionian Stocks of *Sardina pilchardus*. *Mar. Biotechnol.* 4, 163–172. doi: 10.1007/s10126-002-0003-3

Villanoy, C. L., Cabrera, O. C., Yniguez, A., Camoying, M., de Guzman, A., David, L. T., et al. (2011). Monsoon-driven coastal upwelling off Zamboanga Peninsula, Philippines. *Oceanography* 24, 156–165. doi: 10.5670/oceanog.2011.12

Villanoy, C., Yniguez, A., David, L., Deauna, J. D., Prado, J., Pata, P., et al. (2015). *Capturing the Dynamic Linkages Between Small Pelagic Fisheries and Primary Production Through Satellite Images and Models for Better Resource Management in the Bohol Sea and Zamboanga Peninsula. Project 1 of Development of Robust Tools for Managing Sardine Fisheries in the Philippines: Zamboanga Upwelling – Bohol Sea System (SarDyn). Terminal Report*. Laguna: Department of Science and Technology – Philippine Council for Agriculture, Aquatic and Natural Resources Research and Development (DOST-PCAARRD), 84.

Waples, R. S. (1998). Separating the wheat from the chaff: patterns of genetic differentiation in high gene flow species. *J. Hered.* 89, 438–450. doi: 10.1093/jhered/89.5.438

Warnes, G., Gorjanc, G., Leisch, F., and Man, M. (2021). *genetics: Population Genetics*. Available online at: https://cran.r-project.org/package=genetics (accessed March 1, 2021).

Weir, B. S., and Cockerham, C. C. (1984). Estimating F-statistics for the analysis of population structure. *Evolution* 38, 1358–1370. doi: 10.2307/2408641

Westgaard, J. I., and Fevolden, S. E. (2007). Atlantic cod (*Gadus morhua* L.) in inner and outer coastal zones of northern Norway display divergent genetic signature at non-neutral loci. *Fish. Res.* 85, 306–315. doi: 10.1016/j.fishres.2007.04.001

Whitehead, P. J. P. (1985). *FAO Species Catalogue. Vol. 7. Clupeoid fishes of the world: An Annotated and Illustrated Catalogue of the Herrings, Sardines, Pilchards, Sprats, Shads, Anchovies and Wolf-Herrings. Part 1 – Chirocentridae, Clupeidae and Pristigas- teridae*. FAO Fisheries Synopsis No. 125, Vol. 7. Rome: Food And Agriculture Organization Of The United Nations, 303.

Whitlock, M. C., and Lotterhos, K. E. (2015). Reliable detection of loci responsible for local adaptation: inference of a null model through trimming the distribution of FST. *Am. Nat.* 186, S24–S36. doi: 10.1086/682949

Wickham, H. (2007). Reshaping data with the {reshape} package. *J. Stat. Softw.* 21, 1–20.

Wickham, H. (2016). in *ggplot2: Elegant Graphics for Data Analysis*, 2nd Edn, eds R. Gentleman, K. Hornik, and G. Parmigiani (Cham: Springer).

Wickham, H. (2021a). *forcats: Tools for Working with Categorical Variables (Factors)*. Available online at: https://cran.r-project.org/package=forcats (accessed January 27, 2021).

Wickham, H. (2021b). *tidyr: Tidy Messy Data*. Available online at: https://cran.r-project.org/package=tidyr (accessed September 27, 2021).

Wickham, H., and Seidel, D. (2020). *scales: Scale Functions for Visualization*. Available online at: https://cran.r-project.org/package=scales (accessed May 11, 2020).

Wickham, H., François, R., Henry, L., and Müller, K. (2021). *dplyr: A Grammar of Data Manipulation*. Available online at: https://cran.r-project.org/package=dplyr (accessed June 18, 2021).

Wigginton, J. E., Cutler, D. J., and Abecasis, G. R. (2005). A note on exact tests of Hardy-Weinberg equilibrium. *Am. J. Hum. Genet.* 76, 887–893.

Wilke, C. O. (2020). *cowplot: Streamlined Plot Theme and Plot Annotations for "ggplot2."*. Available online at: https://cran.r-project.org/package=cowplot (accessed December 30, 2020).

Willette, D. A., and Santos, M. D. (2013). Correcting widespread misidentifications of the highly abundant and commercially important sardine species *Sardinella lemuru*, Bleeker, 1853 in the Philippines. *J. Appl. Ichthyol.* 29, 881–885. doi: 10.1111/jai.12051

Willette, D. A., Bognot, E., Mutia, M., and Santos, M. (2011). Biology and ecology of sardines in the Philippine: a review. *BFAR NFRDI Tech. Paper Ser.* 13, 1–22.

Willette, D., Allendorf, F., Barber, P., Barshis, D., Carpenter, K., Crandall, E., et al. (2014). So, you want to use next-generation sequencing in marine systems? Insight from the Pan-Pacific advanced studies institute. *Bull. Mar. Sci.* 90, 79–122. doi: 10.5343/bms.2013.1008

Willing, E. M., Dreyer, C., and van Oosterhout, C. (2012). Estimates of genetic differentiation measured by fst do not necessarily require large sample sizes when using many snp markers. *PLoS One* 7:e42649. doi: 10.1371/journal.pone.0042649

Winter, D. J. (2012). MMOD: an R library for the calculation of population differentiation statistics. *Mol. Ecol. Resour.* 12, 1158–1160. doi: 10.1111/j.1755-0998.2012.03174.x

Yadav, S., Stow, A. J., and Dudaniec, R. Y. (2019). Detection of environmental and morphological adaptation despite high landscape genetic connectivity in a pest grasshopper (*Phaulacridium vittatum*). *Mol. Ecol.* 28, 3395–3412. doi: 10.1111/mec.15146

Conflict of Interest: The authors declare that the research was conducted in the absence of any commercial or financial relationships that could be construed as a potential conflict of interest.

frontiers | Frontiers in Marine Science

TYPE Original Research
PUBLISHED 11 November 2022
DOI 10.3389/fmars.2022.858853

OPEN ACCESS

EDITED BY
Guang Gao,
Xiamen University, China

REVIEWED BY
Pablo P. Leal,
Instituto de Fomento Pesquero (IFOP),
Chile
Jacob Carstensen,
Aarhus University, Denmark
Kai Xu,
Jimei University, China

*CORRESPONDENCE
Raffi R. Isah
rrisah@up.edu.ph

SPECIALTY SECTION
This article was submitted to
Global Change and the Future Ocean,
a section of the journal
Frontiers in Marine Science

RECEIVED 20 January 2022
ACCEPTED 19 October 2022
PUBLISHED 11 November 2022

CITATION
Isah RR, Enochs IC
and San Diego-McGlone ML
(2022) Sea surface carbonate
dynamics at reefs of Bolinao,
Philippines: Seasonal variation and
fish mariculture-induced forcing.
Front. Mar. Sci. 9:858853.
doi: 10.3389/fmars.2022.858853

Sea surface carbonate dynamics at reefs of Bolinao, Philippines: Seasonal variation and fish mariculture-induced forcing

Raffi R. Isah[1]*, Ian C. Enochs[2]
and Maria Lourdes San Diego-McGlone[1]

[1]Marine Biogeochemistry Laboratory, Marine Science Institute, University of the Philippines Diliman, Quezon City, Philippines, [2]Atlantic Oceanographic and Meteorological Laboratory, Ocean Chemistry and Ecosystem Division, National Oceanic and Atmospheric Administration (NOAA), Miami, FL, United States

Coral reefs are vulnerable to global ocean acidification (OA) and local human activities will continue to exacerbate coastal OA. In Bolinao, Philippines, intense unregulated fish mariculture has resulted in regional eutrophication. In order to examine the coastal acidification associated with this activity and the impact on nearby coral reefs, water quality and carbonate chemistry parameters were measured at three reef sites, a mariculture site and an offshore, minimally impacted control site during both the wet and dry season. Additionally, benthic community composition was characterized at reef sites, and both autonomous carbonate chemistry sampling and high-frequency pH measurements were used to characterize fine-scale (diel) temporal variability. Water quality was found to be poorer at all reefs during the wet season, when there was stronger outflow of waters from the mariculture area. Carbonate chemistry parameters differed significantly across the reef flat and between seasons, with more acidic conditions occurring during the dry season and increased primary production suppressing further acidification during the wet season. Significant relationships of both total alkalinity (TA) and dissolved inorganic carbon (DIC) with salinity across all stations may imply outflow of acidified water originating from the mariculture area where pH values as low as 7.78 were measured. This apparent mariculture-induced coastal acidification was likely due to organic matter respiration as sustained mariculture will continue to deliver organic matter. While TA-DIC vector diagrams indicate greater contribution of net primary production, net calcification potential in the nearest reef to mariculture area may already be diminished. The two farther reefs, characterized by higher coral cover, indicates healthier ecosystem functioning. Here we show that unregulated fish mariculture activities can lead to localized acidification and impact reef health. As these conditions at times approximate those projected to occur globally due to OA, our results may provide insight into reef persistence potential worldwide. These results also underscore the importance of coastal acidification and indicate that actions taken to mitigate OA on coral reefs should address not only global CO_2 emissions but also local perturbations, in this case fish mariculture-induced eutrophication.

KEYWORDS

coastal acidification, coral reef, Bolinao, mariculture, eutrophication, carbonate chemistry dynamics, Philippine reefs

1 Introduction

Approximately 25% of anthropogenic CO_2 is absorbed by the oceans, resulting in global declines in seawater pH known as ocean acidification (OA) (Caldeira and Wickett, 2003; Orr et al., 2005; Doney et al., 2009; Friedlingstein et al., 2020). It is widely reported that many species of reef-building corals exhibit reduced calcification under OA, associated with the depressed saturation states (Ω) of calcium carbonate ($CaCO_3$) minerals (Kroeker et al., 2010; Chan and Connolly, 2013). Moreover, OA favors abiotic dissolution and biogenic $CaCO_3$ erosion (bioerosion), leading to the breakdown of important reef framework habitats (Enochs et al., 2016; Schönberg et al., 2017). Since the formation of reef structure *via* calcification must exceed dissolution and bioerosion in order for reefs to persist and grow, OA-induced alteration of these processes has strong negative implications on the future of coral reef ecosystems (Silverman et al., 2009; Eyre et al., 2018). Ultimately, in conjunction with local (e.g., eutrophication, overfishing) and global (e.g., seawater warming, sea level rise) stressors, OA will facilitate phase shifts towards ecosystem states dominated by macroalgae and seagrass that can persist or even thrive under high pCO_2 conditions (Koch et al., 2013; Johnson et al., 2014; Enochs et al., 2015).

Coastal conditions, however, are often more complex than those in the open ocean, where global OA projections are most often applied (Carstensen and Duarte, 2019; Sutton and Newton, 2020). Here, the interactions of land, inland waters, open ocean, and atmosphere create a complex and dynamic coastal carbon system (Aufdenkampe et al., 2011; Duarte et al., 2013). In addition, coastal carbonate chemistry can be strongly affected by anthropogenic activities (e.g., agriculture, mariculture, urban waste) that results in water poorly buffered and rich in CO_2, nutrients, and organic matter (Fabricius, 2005; Prouty et al., 2017; Carlson et al., 2019). While coastal eutrophication can enhance primary production that may partially mitigate OA (Borges and Gypens, 2010), the net effect of eutrophication over longer timescales is acidification due to excess organic matter respiration and the subsequent lowering of the seawater's buffering capacity (Cai et al., 2011; Cai et al., 2021).

In addition to coastal and anthropogenic processes, benthic communities (e.g., coral reefs, seagrass meadows, macroalgal beds) have the capacity to alter their physical and chemical environment (Gutiérrez et al., 2011). Coral reef communities, for example, can modulate the overlying carbonate chemistry through calcification and dissolution, as well as photosynthesis and respiration. Net community calcification (NCC), or the sum of calcification and dissolution, alters total alkalinity (TA) and dissolved inorganic carbon (DIC) in a ratio of 2:1 per mole of $CaCO_3$. Positive NCC (calcification) causes TA and DIC to decrease as well as pH and Ω. Net community production (NCP), or the sum of photosynthesis and respiration, alters DIC with positive NCP (photosynthesis) decreasing DIC and increasing pH and Ω. Using TA-DIC plots, the relative balance of community metabolism (NCP:NCC) can be determined (Suzuki and Kawahata, 2003; Cyronak et al., 2018). The extent to which these metabolic processes can alter carbonate chemistry relies on biological factors, including community composition and health (Kleypas et al., 2011; Albright et al., 2013; Anthony et al., 2013; Page et al., 2016), as well as environmental factors such as depth and light, residence time, waves, and tidal forcing (Falter et al., 2013). Provided that the latter is carefully considered or controlled, TA-DIC plots can serve as a useful tool for evaluating the former, especially within the context of acidification.

The Bolinao reef flat (Figure 1) is located in the municipality of Bolinao, along the western side (37 km of coastline) of the Lingayen Gulf and is part of the most extensive fringing reef (200 km^2) in the northwestern Philippines (Cruz-Trinidad et al., 2011). The reef system is characterized by seagrass beds in the reef flat zone, and patches of coral reefs in the reef crest and slope (McManus et al., 1992; Nañola, 2002). The Bolinao reefs are an important source of livelihood to coastal communities through fisheries, mariculture, and tourism (Cruz-Trinidad et al., 2009). In the same manner, the Philippines' dependence on coral reefs is derived from the reef's large geographic extent (Gomez et al.,

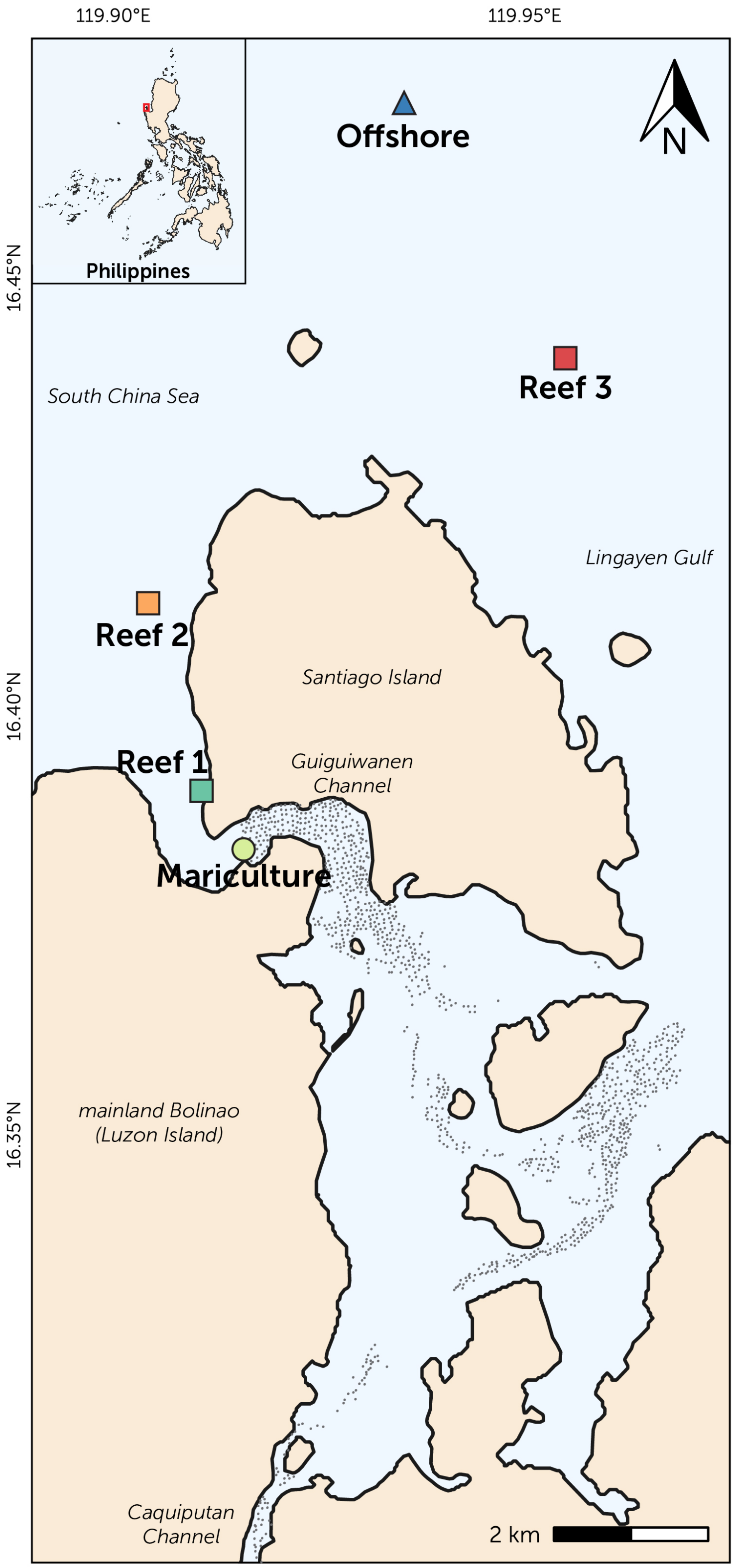

FIGURE 1
Map of Bolinao, Pangasinan showing the sampling locations: mariculture station (circle), three reefs (squares), and offshore station (triangle). Approximate location of mariculture structures (black dots) is also shown.

1994; Licuanan et al., 2019), high biodiversity (DeVantier and Turak, 2017), substantial role in food security (Cabral and Geronimo, 2018), and high economic value (Tamayo et al., 2018). Philippine reefs, including those in Bolinao (Lalas et al., 2020; Quimpo et al., 2020), are declining in coral cover (Licuanan et al., 2019) due to multiple disturbances such as pollution (Fabricius, 2005; Kaczmarsky and Richardson, 2011; Panga et al., 2021), overfishing (Hughes et al., 2007; Nañola et al., 2011), seawater warming (Arceo et al., 2001; Hoegh-Guldberg et al., 2007), and disease outbreaks (Harvell et al., 1999; Garren et al., 2009; Raymundo et al., 2009).

Adjacent to the Bolinao reef flat is an area of intensive fish mariculture activities, spanning from Guiguiwanen Channel in the north to Caquiputan Channel in the south (Figure 1). The industry generates approximately US$10.8 million annually and is a major source of cultured seafood for the country (David et al., 2014). Mariculture started in the 1970s with the construction of fish pens and cages along the embayment for raising milkfish (*Chanos chanos*) (Verceles et al., 2000). The number of fish structures, however, rapidly increased, reaching >1600 before a major 2002 fish mortality event (David et al., 2014), but is now below the maximum carrying capacity of 544 structures (San Diego-McGlone et al., 2008). In addition to the unsustainable size of this operation, poor farming practices such as excessive feeding and use of poor low-quality feeds contribute to poor water quality (Holmer et al., 2002; Ferrera et al., 2016). Nutrients and organic matter have accumulated due to wasted food, fish faecal production, and respiration (Wu, 1995; Holmer et al., 2002; Holmer et al., 2003; Holmer, 2010; White, 2013), coupled with restricted water flow due to the overcrowding of pens (San Diego-McGlone et al., 2008). Conditions of eutrophication and hypoxia (San Diego-McGlone et al., 2008; Ferrera et al., 2016) have resulted in fish kills and harmful algal blooms (HABs) (Azanza et al., 2005; Azanza and Benico, 2013; Escobar et al., 2013), with no sign of improvement based on recent monitoring of water quality conditions.

Bolinao has two seasons based on average temperature and rainfall: dry season from December to May and wet season from June to November (PAGASA, 2021). During the wet season there is higher freshwater discharge, primarily from the nearby Bani and Alaminos rivers with 17,000 ha and 21,100 ha of watershed areas, respectively (Rivera, 1997; Yoshikai et al., 2021). Offshore waters are brought in by the prevailing offshore shelf current (Northwest Luzon coastal current) that mix with the waters flowing out of the northeastern end of Guiguiwanen Channel (Altemerano and Villanoy, 2002; Ashikawa et al., 2013). Based on hydrodynamic models, the considerable outflow of eutrophic mariculture waters from Caquiputan and Guiguiwanen Channels reach the reef flat during the wet season (Yoshikai et al., 2016). Poor coral and seagrass health in Bolinao have previously been attributed to water quality issues (Villanueva et al., 2005; Villanueva et al., 2006; Tanaka et al., 2014; Watai et al., 2014). Little is known, however, about the local carbonate chemistry and the potential for mariculture activities to cause localized acidification in the nearby reefs. This study aims to characterize the link between mariculture-driven eutrophication and coastal acidification, describe the seawater carbonate chemistry at nearby reef sites, and ultimately assess the health of these reefs by quantifying the relative balance of metabolic processes (NCC and NCP) that underpin key reef function and relating them to benthic community structure.

2 Materials and methods

2.1 Study site

Three reef stations (Reef 1: Tomasa, Reef 2: Lucero, Reef 3: East Malilnep) were selected based on their proximity to the mariculture area, whereby Reef 1 is the closest upstream to the mariculture area and located near the open boundary of Guiguiwanen Channel (~1.3 km alongshore), followed by Reef 2 (~3.7 km) and Reef 3 (~10.5 km) (Figure 1). These three stations are located at the shallow reef crest at approximately 4 m depth. A strongly impacted mariculture station (23 m depth, surrounded by fish structures in the channel) and unimpacted distant offshore station (3.8 km northwest of Reef 3; 24 m depth) were sampled to determine the impact of mariculture and offshore oceanographic processes, respectively. Sampling was carried out seasonally in May 2019 (warm dry season; 146.9 mm average monthly rainfall), and August and September 2019 (cool wet season; 495.8 mm average monthly rainfall, data from Philippine Atmospheric, Geophysical and Astronomical Services Administration-PAGASA).

2.2 Water quality and carbonate chemistry measurements

Seasonal sampling for water quality and carbonate chemistry were conducted across all sites. Vertical profiles of *in situ* temperature (± 0.01 °C), salinity (± 0.003), dissolved oxygen (± 0.4 mg L^{-1}), and turbidity (± 0.3 FTU) were acquired during both seasons at each station using a water quality profiler (AAQ-RINKO, JFE Advantech). Water samples (n = 3-6 per site) for nutrients, chlorophyll-*a*, and carbonate chemistry were collected from the surface (1 m depth) using 5 L Niskin sampler (General Oceanics). All samples were collected during daytime, between 09:19 and 14:23, and timed to occur during the ebbing phase of neap tide (0.6 m tidal range). Samples for nutrients and chlorophyll-*a* were immediately stored and kept frozen until analysis. Samples for TA and pH analysis were carefully drawn from the Niskin sampler by attaching a silicone tube from the spigot of the sampler into the bottom of the 250 mL borosilicate glass bottle, minimizing introduction of bubbles and turbulent water movement. Samples were poisoned with 200 µL of saturated $HgCl_2$ (6 g $HgCl_2$/100 mL distilled water) to halt any biological activity. TA and pH samples were stored at room temperature and away from sunlight until analysis.

Sampling for diel variability of carbonate parameters was conducted during dry (1 day per site) and wet (2 days at Reef 1, 3 days at all other sites) seasons across the reef sites. Subsurface automated samplers (SAS) (Enochs et al., 2020) were deployed in each reef station at similar depths (~4 m). SAS were programmed to collect discrete water samples for TA and pH analyses at 3-hour intervals by pumping reef water into pre-poisoned (200 µL of saturated $HgCl_2$ solution) 1 L Tedlar gas sampling bags. The samplers were programmed to collect ~700 mL of seawater, enough to be transferred to a borosilicate glass bottle with rinsing while ensuring that sample bags were not overfilled in the field. An autonomous pH sensor (SeaFET V2 Ocean pH sensor, Sea-Bird Scientific) was co-deployed and set to record pH and temperature at 30-sec intervals throughout the deployment period. Spectrophotometric pH measurements from discrete SAS-collected samples were used to calibrate the SeaFET.

Dissolved inorganic nutrients nitrate (NO_3^-), nitrite (NO_2^-), ammonium (NH_4^+), phosphate (PO_4^{3-}), and silicate (SiO_4^{4-}) content were measured using spectrophotometric methods (Shimadzu UV Mini 1240) following Parsons et al. (1984). Nitrate samples were processed before analysis using a modified shaking technique to reduce nitrate to nitrite (Jones, 1984). Chlorophyll-*a* content was determined using fluorescence method (Trilogy® Laboratory Fluorometer, Turner Designs) following Parsons et al. (1984). Seawater pH (Total scale) at room temperature (~25°C) was measured spectrophotometrically (Shimadzu UV-1900i) with purified m-cresol purple (Byrne Labe, University of South Florida), following standard procedures (Dickson, 2007). The method was calibrated and periodically checked for accuracy and precision during each run with certified reference materials (CRMs) from the laboratory of A. Dickson (Scripps Institution of Oceanography). Seawater pH measurements were determined to have an accuracy of -0.002 ± 0.003 (n = 24), calculated as the average offset (± standard deviation) from the measured CRM pH. TA was measured using a closed-cell potentiometric titration system (Total Alkalinity Analyzer, ATT-05, Kimoto). Measurements were calibrated with CRMs and periodically checked for accuracy and precision during each run. TA measurements were determined to have an accuracy of 3.15 µmol kg^{-1} ± 3.56 (n = 15). DIC, *in situ* pH, aragonite saturation state (Ω_{Arag}), and partial pressure of CO_2 (pCO_2) were calculated using CO2SYS (Lewis and Wallace, 1998), taking measured values of *in situ* temperature, salinity, and nutrients (when nutrient samples were collected alongside TA and pH samples) into consideration. Calculations were made using the carbonic acid dissociation constants (K^*_1 and K^*_2) as defined by Mehrbach et al. (1973) and refit by Dickson and Millero (1987), the dissociation constants of bisulfate (K_{HSO4}) by Dickson (1990), and total boron by Uppström (1974).

2.3 Reef surveys

Benthic communities were characterized at each reef site using phototransects, following the methodologies of van Woesik et al. (2009). Reef surveys were conducted during wet (August 2019, all reef sites) and dry season (February 2021, except for Reef 3 due to rough weather conditions). Briefly, an area (75 m long and 25 m wide, maximum depth of 5 m) was demarcated at each reef and five 50-m transects were randomly placed within this area. The shallower, nearshore side of each transect was photographed at 1-m intervals using a digital camera (Olympus Tough TG-3) mounted on a PVC tetrapod. Photos were analyzed using Coral Point Count with Excel Extension (CPCe 4.1) (Kohler and Gill, 2006), whereby ten random points were overlaid on each photo and classified as one of the following: hard coral, crustose coralline algae (CCA), *Halimeda* spp., fleshy macroalgae, turf algae, dead coral, octocoral (soft corals and gorgonian corals), other lifeforms, and abiotic (rubble, sand, rock). Fleshy macroalgae are described as any macrophyte with thicker, fleshier appearance and with lamina visible to the naked eye. Turf algae, often growing on dead corals, are described as any filamentous algae, either single species or a multi-species assemblage, with little to no structure observable with the naked eye (Noonan et al., 2018).

2.4 Statistical analyses

Data are presented as mean ± standard deviation. Two-way ANOVAs were used for all physico-chemical parameters to test for differences between reef stations and differences between seasons. All variables, except for pH which is already on a log-scale, were log-transformed prior to ANOVA analysis in order to conform to the assumptions of the test. To examine the relationship of TA and DIC with salinity, two-way ANCOVA was conducted with season and all stations as factors, controlling for salinity.

To account for processes such as precipitation and evaporation, TA and DIC values were normalized (nTA and nDIC) to the annual average salinity (32.2), using a non-zero end member following Friis et al. (2003). To determine the net calcification potential of each reef station during each season, these salinity-normalized values were used to calculate nTA anomalies (ΔnTA, Cyronak et al., 2018). These were calculated by getting the difference between normalized reef and sourcewater TA (i.e., $nTA_{reef} - nTA_{sourcewater}$). As there are two potential sources of water incident upon each reef site, we calculate both, using an offshore source ($\Delta nTA_{offshore}$ = reef nTA − offshore nTA) and mariculture source ($\Delta nTA_{mariculture}$ = reef TA − mariculture nTA). Mean, range, and mean diurnal ranges (wet season) of pH and temperature were calculated from SeaFET pH measurements.

For diel data, linear relationship of nTA and nDIC were analyzed using Type II linear regressions which assume error for both y and x axes. The slopes produced by the major axis method were used to calculate the NCP:NCC ratios (NCP:NCC ratio = 2/ slope − 1) (Suzuki and Kawahata, 2003).

Differences in multivariate community composition were tested between reef sites using permutational multivariate analysis of variance (PERMANOVA) based on Bray-Curtis distances with 999 permutations performed. ANOVA was done to test for differences of the functional groups between the reef stations during the wet season when all reefs were surveyed. Percentage cover data were arcsine-transformed prior to the ANOVA analysis (Sokal and Rohlf, 1995). All analyses and data visualizations were generated using the R statistical software (R Core Team, 2021).

3 Results

3.1 Water quality

Differences in surface temperature and salinity were observed between the two seasons (Table S1; Figure 2). Averaged across all five stations, temperature and salinity were higher in dry season (31.2 ± 0.2°C and 33.4 ± 0.1) compared to wet season (29.7 ± 0.6°C and 30.7 ± 0.6). The two-way ANOVA (Table S2) yielded a significant effect of season on both parameters, and of reef site on salinity ($p < 0.0001$, F = 1435). Spatially, a distinguishable trend of increasing salinity from the mariculture station towards the reef flat was observed with

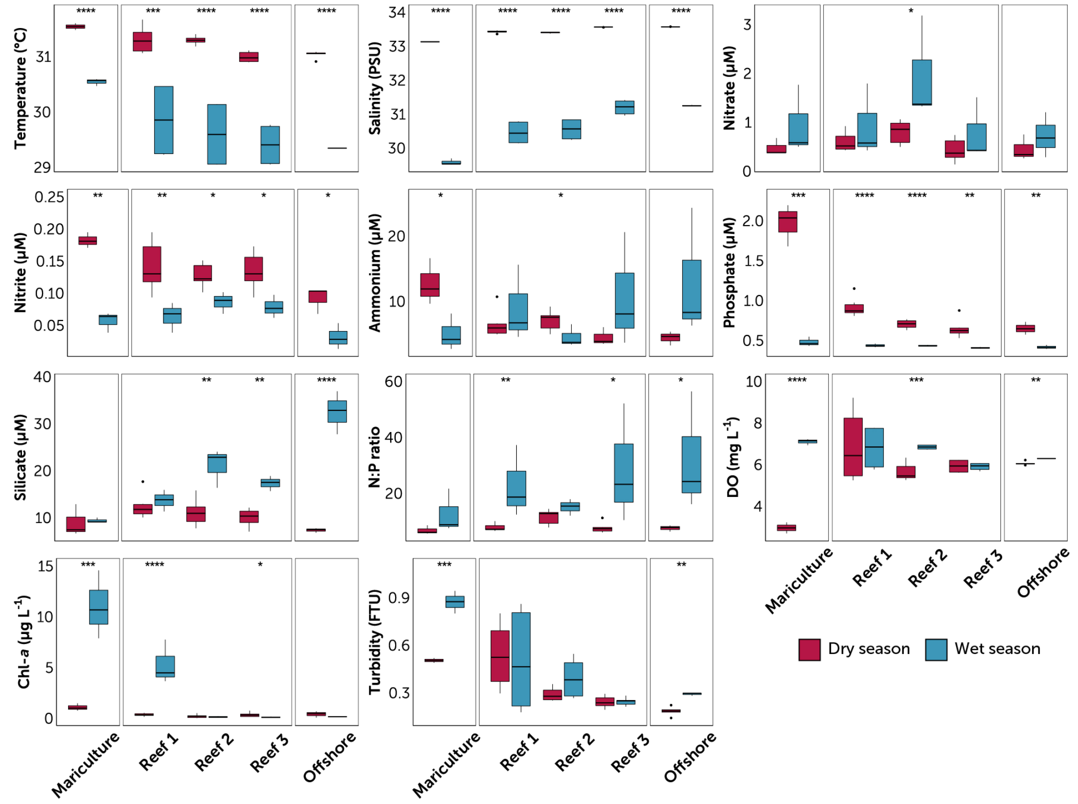

FIGURE 2
Water quality parameters at the sampled stations, grouped by station type (mariculture, three reefs, and offshore). Reefs are arranged from nearest (Reef 1) to farthest (Reef 3) from the mariculture station. Data are divided into dry (red) and wet season (blue) for each station. Value pairs within each station that share a symbol (*$p \le 0.05$; **$p \le 0.01$; ***$p \le 0.001$; ****$p \le 0.0001$) denote significant difference between seasons (t-test of log-transformed values). Circles are outliers > 1.5x the inter-quartile range.

lowest mean salinity in the mariculture station during both seasons, and the offshore and Reef 3 stations having the highest mean salinity (Table S1; Figure 2).

Seasonals trend in nutrients (Table S3; Figure 3) were characterized by, on average, higher phosphate (dry 0.90 ± 0.44 µM vs. wet 0.43 ± 0.04 µM) and nitrite (dry 0.14 ± 0.04 µM vs. wet 0.06 ± 0.03 µM) during the dry season, and higher nitrate (dry 0.57 ± 0.25 µM vs. wet 1.07 ± 0.79 µM), ammonium (dry 6.63 ± 3.14 µM vs. wet 8.45 ± 6.54 µM), and silicate (dry 10.45 ± 2.84 µM vs. wet 18.80 ± 8.54 µM) during the wet season. Overall, this resulted to higher N:P ratios during the wet season (dry 8.54 ± 2.52 vs. wet 22.28 ± 14.97). DO (dry 5.77 ± 1.39 mg L^{-1} vs. wet 6.56 ± 0.66 mg L^{-1}) was higher during the wet season, with the lowest value in the mariculture station during the dry season (2.96 mg L^{-1}, Table S3; Figure 3). Similarly, chlorophyll-*a* (dry 0.41 ± 0.34 µg L^{-1} vs. wet 3.35 ± 4.73 µg L^{-1}) was higher during the wet season, with the highest values obtained in the mariculture station and Reef 1 during the wet season. No clear trend in turbidity was observed between seasons (dry 0.34 ± 0.17 FTU vs. wet 0.43 ± 0.26 FTU). Significant seasonal differences in nutrient levels within the reefs were supported by ANOVA results ($p < 0.05$, Table S2), but between-reef differences were more nuanced.

3.2 Carbonate chemistry

3.2.1 Seasonal variability

Higher TA (dry 2181.8 ± 11.3 µmol kg^{-1} vs. wet 2147.5 ± 34.4 µg L^{-1}), DIC (dry 1920.2 ± 39.7 µmol kg^{-1} vs. wet 1886.4 ± 48.8 µmol kg^{-1}) and pCO_2 (dry 552 ± 153 µatm vs. wet 459 ± 72 µatm) and lower pH (dry 7.92 ± 0.08 units vs. wet 7.99 ± 0.05) were observed during the dry season (Table S1; Figure 4). ANOVA ($p < 0.05$) in reefs yielded season as a significant factor for all carbonate chemistry parameters except Ω_{Arag} (Table S2).

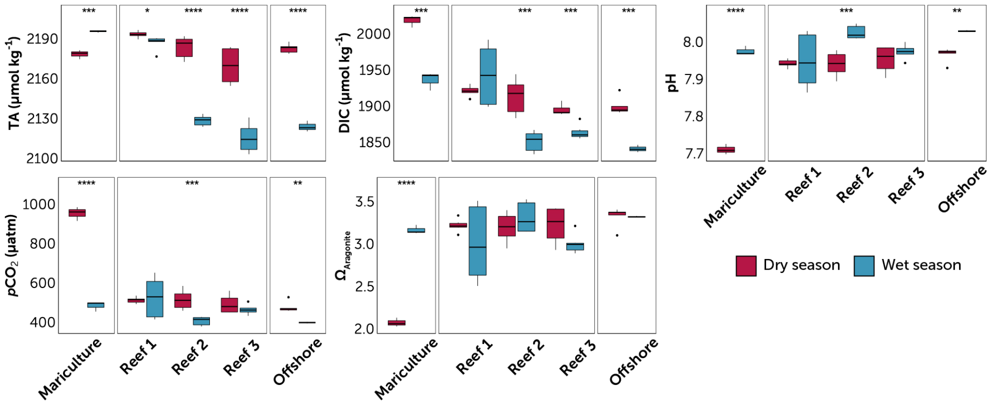

FIGURE 3
Carbonate chemistry parameters at the sampled stations, grouped by station type (mariculture, three reefs, and offshore). Reefs are arranged from nearest (Reef 1) to farthest (Reef 3) from the mariculture station. Data are divided into dry (red) and wet season (blue) for each station. Value pairs within each station that share a symbol (*$p \leq 0.05$; **$p \leq 0.01$; ***$p \leq 0.001$; ****$p \leq 0.0001$) denote significant difference between seasons (t-test of log-transformed values). Circles are outliers > 1.5x the inter-quartile range.

TABLE 1 Summary of analyses (two-way ANCOVA) comparing the effect of station and season to TA and DIC while accounting for salinity.

Variable	Effect	Df	Ss	F	*p*
DIC	Salinity	1	0.0001	6.896	*0.0120*
	Station	4	0.002	29.48	*< 0.0001*
	Season	1	7.36 10^{-6}	0.413	0.5240
	Station:Season	4	0.0009	12.406	*< 0.0001*
TA	Salinity	1	1.39 10^{-5}	6.758	*0.0130*
	Station	4	0.0003	41.833	< 0.0001
	Season	1	0.0002	110.637	*< 0.0001*
	Station:Season	4	0.0003	36.965	*< 0.0001*

Data from all five stations collected from seasonal sampling were used in this analysis. TA and DIC are log-transformed prior to analysis. *p*-values < 0.05 are italicized. Df, degrees of freedom; Ss, sum of squares.

TABLE 2 Net calcification potential (ΔnTA in µmol kg^{-1}) of each reef calculated per season and with either mariculture ($\Delta nTA_{mariculture}$) or offshore ($\Delta nTA_{offshore}$) considered as source water.

Reef	$\Delta nTA_{offshore,\ dry}$	$\Delta nTA_{offshore,\ wet}$	$\Delta nTA_{mariculture,\ dry}$	$\Delta nTA_{mariculture,\ wet}$
Reef 1	11.2	72.3	11.9	-18.1
Reef 2	2.1	10.0	2.9	-80.5
Reef 3	-12.4	-8.5	-11.7	-98.9

Reef location was a significant factor (ANOVA, $p < 0.05$) for all carbonate chemistry parameters, except for Ω_{Arag} and pH. This can be observed by a distinct trend of decreasing TA and DIC from Reef 1 to Reef 3 during both seasons (Figure 4). The mariculture station had the highest levels of TA and DIC (Table S1; Figure 4) and the most acidified waters (highest pCO_2 and lowest pH) were during the dry season (953 ± 35 µatm and 7.71 ± 0.01). While all three reefs have significant seasonal TA variations (Figure 4), TA at Reef 1 varied similarly with the mariculture station, while TA at Reefs 2 and 3 have large seasonal fluctuations, similar with the offshore station. ANCOVA results yielded statistically significant difference of all factors (except Season for DIC) for both DIC and TA (Table 1).

To determine net calcification potential (Table 2), $\Delta nTA_{offshore}$ was used for the dry season when mariculture outflow is weaker and offshore waters are a more likely source. At Reef 1, a positive ΔnTA ($\Delta nTA_{offshore,\ dry}$ = 11.2 µmol kg^{-1}) indicated net dissolution. At Reef 2, the ΔnTA value was closer to zero ($\Delta nTA_{offshore,\ dry}$ = 2.1 µmol kg^{-1}), which may indicate similar calcification and dissolution rates, and likely net accretionary stasis. In Reef 3, a decrease in TA ($\Delta nTA_{offshore,\ dry}$ = -12.4 µmol kg^{-1}) was observed, suggesting net calcification and potentially more-healthy reef growth. During the wet season when mariculture outflow is more extensive than during dry season, $\Delta nTA_{mariculture}$ was considered and all reefs displayed negative values, potentially indicating net calcification.

3.2.2 Diel carbonate chemistry

The diel range of pH (i.e., diel peak-to-trough amplitude) provided an estimate of the variability in pH at each reef site.

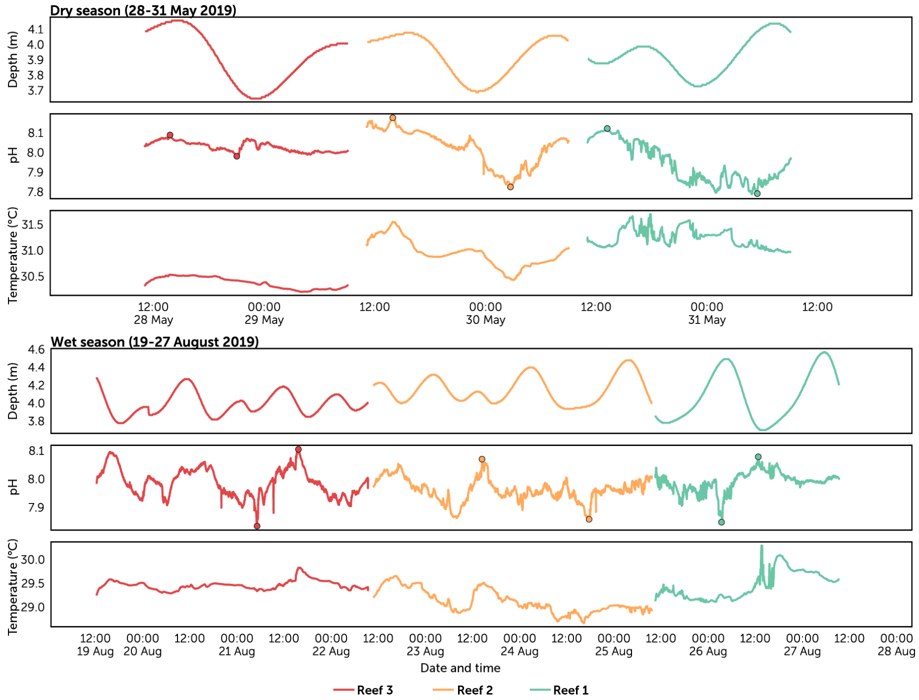

FIGURE 4
Predicted tide level, pH and temperature time series recorded in each reef per season. Circles represent the amplitude (lowest and highest) pH values for each reef per season.

The largest diel ranges were recorded during the dry season at Reef 2 (dry 0.35 vs. wet 0.18) and Reef 1 (dry 0.33 vs. wet 0.22), while the smallest range was at Reef 3 during the dry season (dry 0.09 vs. wet 0.22) (Table S4; Figure 5). The lowest pH (7.78) was recorded during nighttime at Reef 1 in the dry season, while the highest pH (8.18) was observed during daytime at Reef 2 also in the dry season. Diel fluctuations in pH and temperature coincided with each other, with the highest values occurring between midday and dusk, and the lowest values between midnight and dawn (Figure 5). Diel fluctuation and amplitudes of the other carbonate chemistry parameters (TA, DIC, $p\mathrm{CO}_2$, and Ω_{Arag}) were consistent with pH (Table S5; Figure S1). When pH was higher during the day, high Ω_{Arag} and low TA, DIC and $p\mathrm{CO}_2$ were observed, and at night when pH was depressed, low Ω_{Arag}, high TA, DIC and $p\mathrm{CO}_2$ were observed.

3.2.3 Relative balance of community metabolism

The plots of nTA-nDIC yielded significant relationships ($p <$ 0.05) in Reef 1 during the dry season (slope = 0.31), in Reef 2 both seasons (dry 0.29 and wet 0.32), and in Reef 3 during the wet season (0.24) (Table S6). These slope values were within a narrow range (0.24 – 0.32) corresponding to NCP:NCC ratio range of 5.42 to 7.37. Photosnythesis/respiration over calcification/dissolution were therefore the major contributors to reef metabolism across all Bolinao reefs.

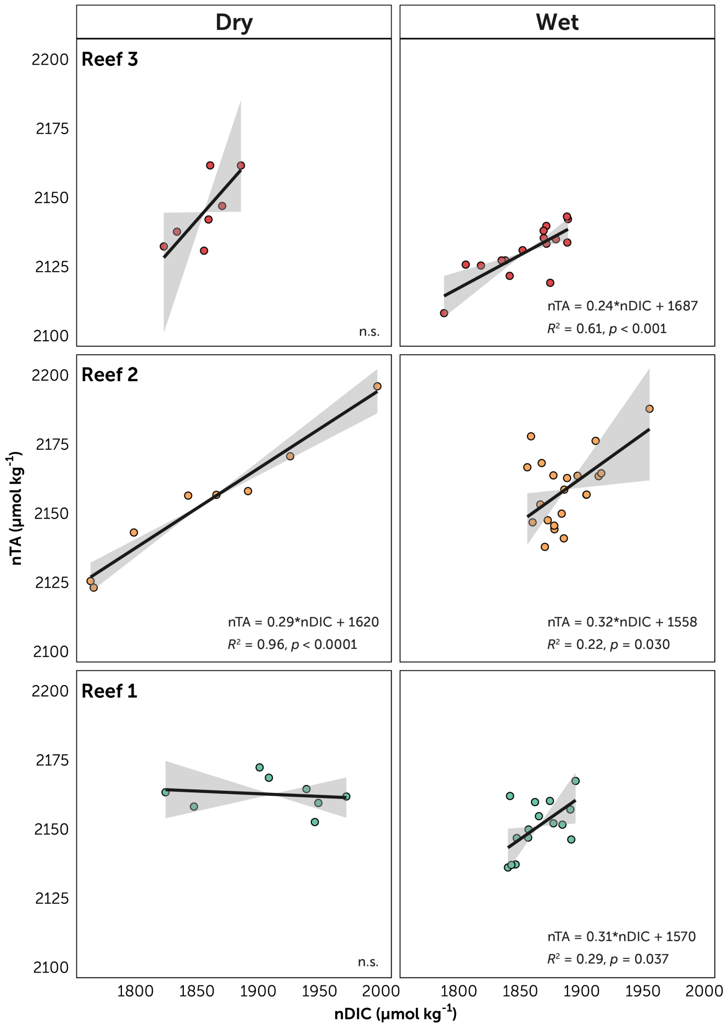

FIGURE 5
Relationships between salinity-normalized dissolved inorganic carbon (nDIC) and salinity-normalized total alkalinity (nTA) for the three reef stations, facetted by season. The solid line represents linear regression models (Model II, major axis method) with 95% confidence interval (gray area). Equation of the line, R^2 and p-values are given. Non-significant (p>0.05) are marked n.s.

3.3 Reef surveys

Benthic community composition (Table S7; Figure S2) was significantly different at the three reef stations (PERMANOVA, $p < 0.05$; Table S8). Some functional groups (hard coral, dead coral, turf algae, and coralline algae) were found to be significantly different between the reef stations during the wet season (ANOVA, $p < 0.05$) (Table S9). Differences in benthic cover were not tested during the dry season because only two reefs were surveyed. All reefs were dominated by turf algae or dead coral overgrown with algae (Reef 1: dry 58.90 ± 2.25% vs. wet 68.48 ± 12.78%, Reef 2: dry 50.12 ± 4.02% vs. wet 29.08 ± 5.79%, Reef 3: wet 39.08 ± 5.40%) (Table S7). The site furthest from the mariculture area (Reef 3) had the highest hard coral cover (wet 28.49 ± 6.62%) and there was a decrease in coral cover closer to the mariculture site, with Reef 2 having lower coral cover (dry 21.87 ± 3.96% vs. wet 18.96 ± 4.61%), and Reef 1 with no coral cover. In terms of coral community composition, Reef 3 consists of diverse coral morphologies (branching, encrusting, foliose, submassive) dominated by submassive corals, while encrusting corals were dominant at Reef 2.

4 Discussion

We utilized two approaches in characterizing the surface carbonate chemistry dynamics of the Bolinao reefs. Seasonal discrete sampling of water quality and carbonate chemistry allowed us to determine any heterogeneity of water chemistry between the reefs and calculate useful metrics (TA and DIC-salinity relationship and ΔnTA). Diel sampling results complemented the discrete sampling data to further evaluate how community metabolism on each reef act on the overlying carbonate chemistry. Here we first describe the environmental setting of Bolinao - the persisting eutrophication in the mariculture area and the significant carbonate chemistry trend among reefs. These observations reveal a water quality gradient, with eutrophied, more-acidic water reaching nearby reefs and influencing overall reef health and function, including community metabolism.

4.1 Regional water quality dynamics

Eutrophic conditions in the mariculture area of Bolinao have continued for years (San Diego-McGlone et al., 2008; Escobar et al., 2013; Ferrera et al., 2016), with poorest water quality in the vicinity of the mariculture area as also seen in this study (Figure 3). The elevated ammonium and phosphate and low DO measured during the dry season can be attributed to high organic matter respiration (Kemp et al., 1990; Slomp and Van Cappellen, 2007; Fennel and Testa, 2019). Aside from a decrease in DO during the dry season when temperatures are warmer (decrease in solubility), there is also a tendency for a temperature-driven increase in metabolic oxygen demand and respiration (Winder and Sommer, 2012; Altieri and Gedan, 2015).

In addition to biogeochemical oxygen consumption, the residence time of the water body contributes to occurrence of low DO conditions (Fennel and Testa, 2019). From hydrodynamic models (San Diego-McGlone et al., 2008; Gečck and Legović, 2010), the residence time in the mariculture embayment of Bolinao (12-18 days) is longer than at the open boundaries (< 6 days). Residence time tend to increase during the dry season due to weaker freshwater discharge, southward mass transport of surface currents from offshore (Rivera, 1997), and the direction of residual current flow in the embayment (Ferrera et al., 2016; Yoshikai et al., 2016). A longer residence time may lead to increased biogeochemical oxygen consumption, and consequently to lower DO and higher nutrients.

In addition to elevated phosphate and ammonium content in the water column, the sediments in the mariculture area are enriched with organic matter from fish wastes and uneaten feeds (Holmer et al., 2002; Holmer et al., 2003). When this material is respired by sediment-dwelling microbiota, DO and nitrate are consumed, ultimately resulting in a release of ammonium and phosphate (Holmer et al., 2002; Holmer et al., 2003). Higher nutrients and low DO from deeper layers can be introduced to surface waters during the dry season when vertical density stratification (Figure S3) is weaker due to less freshwater discharge (low precipitation rates, PAGASA, 2021) from rivers to the mariculture embayment (Rivera, 1997; Yoshikai et al., 2021). This is unlike other eutrophic river-dominated estuarine systems where coastal hypoxia occurs seasonally during density stratification from freshwater input that isolates bottom waters from oxygen supply in the surface (Testa and Kemp, 2014; Qian et al., 2018). During the wet season, there was more stratification from increased freshwater discharge driven by higher precipitation rates (PAGASA, 2021). Riverine waters, characterized by high DIN and high N:P ratio (Ferrera et al., 2016) can enhance primary production in the N-limited mariculture embayment as evidenced by the high chlorophyll-a and DO values (Table S3; Figure 3).

4.2 Implications for carbonate chemistry and regional acidification

The observed trend in carbonate chemistry is likely driven by the same prevailing biogeochemical and hydrodynamic conditions influencing water quality. Vertical mixing during the dry season could introduce low-O_2 and high-CO_2 bottom waters to the surface (Cai et al., 2010). During the wet season, increased primary production (seen as higher chlorophyll-*a* content) decreased the DIC, as CO_2 is consumed.

Simultaneously, the increased influence of freshwater discharge may decrease TA although initial TA measurements in the nearby rivers showed variable results, with the larger Alaminos River having lower values (1610 µmol kg^{-1}) than Bani River (2870 µmol kg^{-1}; unpublished). Nonetheless, TA and DIC in the mariculture area is greater than the reef flat, regardless of season. The mariculture area can therefore be a source of acidified waters (high TA and DIC) to the reef flat. Coastal and estuarine environments with high organic matter respiration such as salt marshes (Cai et al., 2000), seagrass meadows (Turk et al., 2015; Cyronak et al., 2018), mangrove forests (Ho et al., 2017) are also known to be high in DIC. Higher TA in these environments is generally caused by sulfate reduction and $CaCO_3$ dissolution (Wang and Van Cappellen, 1996; Cai et al., 2017). Holmer et al. (2003), for instance, reported that sediments in the Bolinao mariculture area are enriched in organic matter and undergo anaerobic respiration as oxygen is depleted, with consequent high sulfate reduction rates. The contribution of organic alkalinity may also be significant due to the input of dissolved organic matter (DOM) that can be derived from primary production (Kim and Lee, 2009), sediment porewater (Lukawska-Matuszewska et al., 2018), terrestrial input (Kuliński et al., 2014), and possibly from fish food and fecal matter.

4.3 Impacts to nearby reefs

Particle tracking simulations show that mariculture outflow, *via* the open boundaries, can reach the nearby reef flat extensively during the wet season (Yoshikai et al., 2016), which is also seen in the eastward mass transport of surface currents during the southwest monsoon (wet season) (Rivera, 1997). Seasonal circulation patterns can therefore explain why water quality conditions are poorer in the northern part of the reef flat (near Reef 3) during the wet season as also seen from the water quality monitoring in Bolinao, as well as the significant seasonal fluctuations of most nutrients across the reefs (Table S2, Figure 3**).** Other studies have reported presence of the eutrophication gradient in Bolinao that caused a decrease in seagrass species (Fortes et al., 2012; Tanaka et al., 2014), reduced growth and survivorship of hard corals (Villanueva et al., 2005; Villanueva et al., 2006), and decrease in coral recruitment (Quimpo et al., 2020).

The gradient observed across the reef flat (decreasing TA and DIC from Reefs 1 to 3) reflected the net effect of local biogeochemical processes affecting carbonate chemistry of a water parcel that flows across the reef flat (Page et al., 2018). Reef 1, being closest to the mariculture area (~1 km), received high-TA, high-DIC waters from the mariculture area and has the lowest pH. The reef community in turn can influence the carbonate chemistry through local metabolic processes. During the dry season, DIC decreased and pH increased compared to the mariculture area (Figure 4), indicating active photosynthesis that takes up CO_2 which could be driven by the dominant algal community in Reef 1 (Figure S2). Positive ΔnTA values (Table 2) for Reef 1 (except $\Delta nTA_{mariculture,\ wet}$ = -18.1 µmol kg^{-1}) suggest that it is net dissolving given the increase in reef TA relative to both potential source-water sites (mariculture and offshore). This result is supported by benthic surveys in Reef 1 where no visible hard coral cover was seen (Figure S2). Historically, hard coral cover at Reef 1 was 26.13% two decades ago (Nañola, 2002). What remains now are dead corals overgrown with algae, which are likely colonized by bioeroders and experiencing dissolution (de Orte et al., 2021). Nonetheless, considering the extensive outflow of mariculture waters during the wet season, the negative $\Delta nTA_{mariculture,\ wet}$ value suggests a net calcifying state, seen as the persistence of *Halimeda* spp. (and potentially other calcifying organisms not seen in reef surveys) during wet season. Some species of *Halimeda* spp. are reported to be tolerant to low-pH conditions (Vogel et al., 2015; Schubert et al., 2022). Reefs 2 and 3 which are further away from the mariculture site exhibited lower TA and DIC which may be due to local metabolic processes (calcification and photosynthesis). This seems to be reflected in the benthic community composition where there is higher cover of calcifying hard coral and CCA. ΔnTA values for Reef 3 were negative across all seasons and source-water indicating its net calcifying state. The negative $\Delta nTA_{mariculture,\ wet}$ value at Reef 2 (net calcifying state) is seen by the presence of hard corals and CCA across both seasons. However, the near-zero, positive ΔnTA values for Reef 2 (except $\Delta nTA_{mariculture,\ wet}$ = -80.5 µmol kg^{-1}) may indicate the reef's susceptibility towards net dissolution state and should be emphasized in management efforts since it is the next nearest reef to the mariculture area.

The diel range of pH and its amplitude, regardless of season, underscores the capacity of reef metabolism to drive short-term fluctuations in pH (Cyronak et al., 2019). Daytime photosynthesis increases pH and decreases DIC as inorganic carbon is converted to organic carbon. This means that NCP becomes the major contributor to community metabolism, as seen in coral reefs worldwide where net production rates are typically greater than net calcification rates (Davis et al., 2021). The large rhythmic diel patterns in Reefs 1 and 2 during the dry season suggest substantial influence of the reef community on local chemistry, particularly NCP driving changes in DIC, pH and pCO_2. Unlike Reef 2, the minor diel fluctuations of TA in Reef 1 during dry season may indicate relatively smaller influence of calcification and dissolution processes (NCC). This should be expected from the dominance of fleshy and turf algae and small cover of calcifying organisms in the benthos. On the other hand, the persistence of calcifying organisms (*Halimeda*) during wet season may allow for the diel fluctuation of TA to occur, and the negative $\Delta nTA_{mariculture,\ wet}$ may point to their capacity to thrive. In Reef 2 during the dry season, diel TA cycles were also consistent with DIC, suggesting calcification during the daytime and dissolution at night. The calcification of reef-building coral species is strongly dependent on light intensity, as calcification and photosynthesis enhance each other (Gattuso et al., 1999; Erez et al., 2011). Thus, during daytime, elevated saturation states (Ω_{Arag}) and NCP are suitable for calcification (Andersson and Gledhill, 2013). Recent studies that measured both NCC and NCP have shown their interactive relationship, with NCP strongly driving NCC (Albright et al., 2015; DeCarlo et al., 2017).

The magnitude of diel fluctuations in reef carbonate chemistry is dependent on the relative balance of community metabolism (NCP and NCC), metabolic rates, depth, and residence time (Takeshita et al., 2018). The extent to which community metabolism can influence carbonate chemistry is dependent on benthic community composition, organismal abundances, health of organisms, and individual metabolic rates, especially in shallow coral reefs where smaller water volumes lead to more pronounced carbonate chemistry alterations (Koweek et al., 2014; Page et al., 2016; Lantz et al., 2017). In Bolinao, benthic composition among the three reefs could potentially contribute to the observed differences in community metabolism, as implied in the diel variability of carbonate chemistry and further supported here by nTA-nDIC relationships. All reefs have slope values within a narrow range of 0.24 to 0.32, indicating greater contribution of NCP over NCC across all reefs, and within values found in most Indo-Pacific reefs (Cyronak et al., 2018). While these values may seem low for Reefs 2 and 3 where there is greater calcifying cover (> 25% combined hard coral and CCA cover) than Reef 1, non-calcifying cover still dominated these reefs. Nonetheless, other similar reefs with extensive coral cover and high NCC rates also yielded low slope values (McMahon et al., 2013; Albright et al., 2015). Such findings are consistent with previous studies that showed differential carbonate chemistry modifications by key reef benthic functional groups due to differences in their metabolic rates (Anthony et al., 2011; Anthony et al., 2013; Page et al., 2016; Page et al., 2017). Moreover, direct measurements of metabolic processes at different functional scales should be done to fully understand the contribution of the benthic community to carbonate chemistry variability. Within the scope of this study, potential metrics (ΔnTA and slope of nTA-nDIC relationships) serve as simple, but effective chemistry-based tools to assess reef health and metabolic state (Cyronak et al., 2018). It is noted that these metrics represent single measurements and may vary over time. Further observations should be collected in order to describe their variance and correlate with the continuing health decline of Bolinao reefs.

Aside from benthic community, the physical setting (e.g., depth, residence time, prevailing current, wave forcing, tides) can strongly influence the magnitude of carbonate chemistry changes. The influence of the mariculture outflow on the carbonate chemistry of nearby reefs is supported by the lowest average pH (7.94) and the lowest single pH value (7.78, dry season) recorded at nearby Reef 1. For reefs that are further away, the capacity of the community to alter the overlying carbonate chemistry may act to partially offset the localized acidification from the mariculture outflow (Anthony et al., 2011; Andersson et al., 2014; Page et al., 2016). For instance, the highest pH recorded (8.18) was on Reef 2 during the dry season, which could be a result of high primary production at this site during the daytime. However, this buffering capacity may be compromised by global OA, warming, and other anthropogenic stressors (Davis et al., 2021).

In addition, the extensive outflow of mariculture waters to the reef flat delivers organic matter and nutrients that can alter rates of NCP and NCC (Kawahata et al., 2000; Silverman et al., 2007; Silbiger et al., 2018). Elevated nutrients could suppress NCC rates as a direct physiological response by calcifying organisms and therefore facilitate transition to net dissolution state (Silbiger et al., 2018). Under future OA, it is likely that diel variability of coastal carbonate chemistry parameters will amplify due to the influence of anthropogenic activities (Cyronak et al., 2014; Torres et al., 2021).

4.4 Concluding remarks

This study reveals the impact of fish mariculture-induced eutrophication on the carbonate chemistry dynamics of Bolinao coral reefs. Extensive outflow of eutrophic and acidified waters has resulted in a decline in reef health and will continue to degrade nearby ecosystems. In Bolinao, although no previous studies have measured community metabolism, the continuing decline in coral cover mainly due to localized eutrophication has caused substantial changes in both net calcification and primary production. This is particularly evident in the reef site closest to the mariculture activity (Reef 1) where no hard coral cover was detected. This reef is likely already in a net erosional state, and a loss of essential reef framework habitat will follow (Eyre et al., 2018). The near-zero values of ΔnTA in Reef 2 may indicate that reefs further downstream will also continue to be affected as mariculture-induced eutrophication persist. Local reef disturbances should therefore be considered and given utmost attention in evaluating future OA conditions, and in developing potential mitigation strategies to locally combat OA in addition to reducing global CO_2 emissions. In Bolinao, it is imperative to reduce the number of fish mariculture structures to improve flushing rates and to observe best practices in fish feeding to reduce organic matter and nutrient input.

Data availability statement

The raw data supporting the conclusions of this article will be made available by the authors, without undue reservation.

Author contributions

RI and MSD-M conceptualized the study. All authors contributed to the design of the study. RI collected and analysed the data and wrote the first draft of the manuscript.

All authors contributed to the article and approved the submitted version.

Funding

This study was part of the research program entitled "Coastal Acidification: How it Affects the Marine Environment and Resources in the Philippines" under Project 1, "Spatio-temporal trends in pH, pCO_2, and related parameters" (Project Code QMSR-MRRD-MEC-295-1447). The program was funded by the Department of Science and Technology-Philippine Council for Agriculture, Aquatic and Natural Resources Research and Development (DOST-PCAARRD).

Acknowledgments

This paper is part of the master's thesis of RI supervised by MS-M entitled "Carbonate chemistry dynamics on the Bolinao reef flat". The authors are grateful to the Marine Biogeochemistry Laboratory and Bolinao Marine Laboratory of the Marine Science Institute, University of the Philippines for the valuable logistical and laboratory support provided. We thank Jay Burce, Ryan Carl Magyaya, Natasha Tamayo for their tremendous help in field activities and laboratory analyses. We thank Alice Webb for providing insights into improving the manuscript.

Conflict of interest

The authors declare that the research was conducted in the absence of any commercial or financial relationships that could be construed as a potential conflict of interest.

Publisher's note

Supplementary material

The Supplementary Material for this article can be found online at: https://www.frontiersin.org/articles/10.3389/fmars.2022.858853/full#supplementary-material

References

Albright, R., Benthuysen, J., Cantin, N., Caldeira, K., and Anthony, K. R. N. (2015). Coral reef metabolism and carbon chemistry dynamics of a coral reef flat. *Geophys. Res. Lett.* 42, 3980–3988. doi: 10.1002/2015GL063488

Albright, R., Langdon, C. J., and Anthony, K. R. N. (2013). Dynamics of seawater carbonate chemistry, production, and calcification of a coral reef flat, Central Great Barrier Reef. *Biogeosciences* 10, 6747–6758. doi: 10.5194/bg-10-6747-2013

Altemerano, A. M., and Villanoy, C. L. (2002). Influence of the Western Luzon Shelf Current on Larval dispersal in Lingayen Gulf based on numerical Lagrangian dispersal experiments. *UPV J. Nat. Sci.* 1, 103–119.

Altieri, A. H., and Gedan, K. B. (2015). Climate change and dead zones. *Glob. Change Biol.* 21, 1395–1406. doi: 10.1111/gcb.12754

Andersson, A. J., and Gledhill, D. (2013). Ocean acidification and coral reefs: Effects on breakdown, dissolution, and net ecosystem calcification. *Ann. Rev. Mar. Sci.* 5, 321–348. doi: 10.1146/annurev-marine-121211-172241

Andersson, A. J., Yeakel, K. L., Bates, N. R., and De Putron, S. J. (2014). Partial offsets in ocean acidification from changing coral reef biogeochemistry. *Nat. Clim. Change* 4, 56–61. doi: 10.1038/nclimate2050

Anthony, K. R. N., Diaz-Pulido, G., Verlinden, N., Tilbrook, B., and Andersson, A. J. (2013). Benthic buffers and boosters of ocean acidification on coral reefs. *Biogeosciences* 10, 4897–4909. doi: 10.5194/bg-10-4897-2013

Anthony, K. R. N., Kleypas, J. A., and Gattuso, J.-P. (2011). Coral reefs modify their seawater carbon chemistry – implications for impacts of ocean acidification. *Glob. Change Biol.* 17, 3655–3666. doi: 10.1111/j.1365-2486.2011.02510.x

Arceo, H. O., Quibilan, M. C., Aliño, P. M., Lim, G., and Licuanan, W. Y. (2001). Coral bleaching in Philippine reefs: Coincident evidences with mesoscale thermal anomalies. *Bull. Mar. Sci.* 69, 579–593. Availabe at:https://www.ingentaconnect.com/contentone/umrsmas/bullmar/2001/00000069/00000002/art00030

Ashikawa, K., Pokavanich, T., Kartadikaria, A., Nadaoka, K., Villanoy, C., and Herrera, E. (2013). Seasonal larval dispersal characteristics and sediment discharge impacts on the coral reefs in Lingayen Gulf, Philippines towards coastal ecosystem conservation. *Galaxea J. Coral Reef Stud.* 15, 295–299. doi: 10.3755/galaxea.15.295

Aufdenkampe, A. K., Mayorga, E., Raymond, P. A., Melack, J. M., Doney, S. C., Alin, S. R., et al. (2011). Riverine coupling of biogeochemical cycles between land, oceans, and atmosphere. *Front. Ecol. Environ.* 9, 53–60. doi: 10.1890/100014

Azanza, R. V., and Benico, G. A. (2013). Toxic alexandrium blooms in fish farming sites in Bolinao, Pangasinan. *J. Environ. Sci. Manage.* 1, 44–49.

Azanza, R. V., Fukuyo, Y., Yap, L. G., and Takayama, H. (2005). *Prorocentrum minimum* bloom and its possible link to a massive fish kill in Bolinao, Pangasinan, Northern Philippines. *Harmful Algae* 4, 519–524. doi: 10.1016/j.hal.2004.08.006

Borges, A. V., and Gypens, N. (2010). Carbonate chemistry in the coastal zone responds more strongly to eutrophication than ocean acidification. *Limnol. Oceanogr.* 55, 346–353. doi: 10.4319/lo.2010.55.1.0346

Cabral, R. B., and Geronimo, R. C. (2018). How important are coral reefs to food security in the philippines? diving deeper than national aggregates and averages. *Mar. Policy* 91, 136–141. doi: 10.1016/j.marpol.2018.02.007

Cai, W.-J., Feely, R. A., Testa, J. M., Li, M., Evans, W., Alin, S. R., et al. (2021). Natural and anthropogenic drivers of acidification in large estuaries. *Ann. Rev. Mar. Sci.* 13, 23–55. doi: 10.1146/annurev-marine-010419-011004

Cai, W.-J., Huang, W. J., Luther, G. W., Pierrot, D., Li, M., Testa, J., et al. (2017). Redox reactions and weak buffering capacity lead to acidification in the Chesapeake Bay. *Nat. Commun.* 8, 1–12. doi: 10.1038/s41467-017-00417-7

Cai, W.-J., Hu, X., Huang, W.-J., Murrell, M. C., Lehrter, J. C., Lohrenz, S. E., et al. (2011). Acidification of subsurface coastal waters enhanced by eutrophication. *Nat. Geosci.* 4, 766–770. doi: 10.1038/ngeo1297

Cai, W.-J., Luther, G. W., Cornwell, J. C., and Giblin, A. E. (2010). Carbon cycling and the coupling between proton and electron transfer reactions in aquatic sediments in Lake Champlain. *Aquat. Geochem* 16, 421–446. doi: 10.1007/s10498-010-9097-9

Cai, W.-J., Wiebe, W. J., Wang, Y., and Sheldon, J. E. (2000). Intertidal marsh as a source of dissolved inorganic carbon and a sink of nitrate in the Satilla River-estuarine complex in the southeastern U.S. *Limnol. Oceanogr.* 45, 1743–1752. doi: 10.4319/lo.2000.45.8.1743

Caldeira, K., and Wickett, M. E. (2003). Anthropogenic carbon and ocean pH. *Nature* 425, 365. doi: 10.1038/425365a

Carlson, R. R., Foo, S. A., and Asner, G. P. (2019). Land use impacts on coral reef health: A ridge-to-reef perspective. *Front. Mar. Sci.* 6. doi: 10.3389/fmars.2019.00562

Carstensen, J., and Duarte, C. M. (2019). Drivers of pH variability in coastal ecosystems. *Environ. Sci. Technol.* 53, 4020–4029. doi: 10.1021/acs.est.8b03655

Chan, N. C. S., and Connolly, S. R. (2013). Sensitivity of coral calcification to ocean acidification: A meta-analysis. *Glob. Change Biol.* 19, 282–290. doi: 10.1111/gcb.12011

Cruz-Trinidad, A., Geronimo, R. C., and Aliño, P. M. (2009). Development trajectories and impacts on coral reef use in Lingayen Gulf, Philippines. *Ocean Coast. Manage.* 52, 173–180. doi: 10.1016/j.ocecoaman.2008.12.002

Cruz-Trinidad, A., Geronimo, R. C., Cabral, R. B., and Aliño, P. M. (2011). How much are the Bolinao-Anda coral reefs worth? *Ocean Coast. Manage.* 54, 696–705. doi: 10.1016/j.ocecoaman.2011.07.002

Cyronak, T., Andersson, A. J., Langdon, C. J., Albright, R., Bates, N. R., Caldeira, K., et al. (2018). Taking the metabolic pulse of the world's coral reefs. *PloS One* 13, e0190872. doi: 10.1371/journal.pone.0190872

Cyronak, T., Schulz, K. G., Santos, I. R., and Eyre, B. D. (2014). Enhanced acidification of global coral reefs driven by regional biogeochemical feedbacks. *Geophys. Res. Lett.* 41, 5538–5546. doi: 10.1002/2014GL060849

Cyronak, T., Takeshita, Y., Courtney, T. A., DeCarlo, E. H., Eyre, B. D., Kline, D. I., et al. (2019). Diel temperature and pH variability scale with depth across diverse coral reef habitats. *Limnol. Oceanogr. Lett.* 5, 193–203. doi: 10.1002/lol2.10129

David, L. T., Pastor-Rengel, D., Talaue-McManus, L., Magdaong, E., Salalila-Aruelo, R., Bangi, H. G., et al. (2014). The saga of community learning: Mariculture and the Bolinao experience. *Aquat. Ecosyst. Heal. Manage.* 17, 196–204. doi: 10.1080/14634988.2014.910488

Davis, K. L., Colefax, A. P., Tucker, J. P., Kelaher, B. P., and Santos, I. R. (2021). Global coral reef ecosystems exhibit declining calcification and increasing primary productivity. *Commun. Earth Environ.* 2, 1–10. doi: 10.1038/s43247-021-00168-w

DeCarlo, T. M., Cohen, A. L., Wong, G. T. F., Shiah, F., Lentz, S. J., Davis, K. A., et al. (2017). Community production modulates coral reef pH and the sensitivity of ecosystem calcification to ocean acidification. *J. Geophys. Res. Ocean.* 122, 745–761. doi: 10.1002/2016JC012326.Received

de Orte, M. R., Koweek, D. A., Cyronak, T., Takeshita, Y., Griffin, A., Wolfe, K., et al. (2021). Unexpected role of communities colonizing dead coral substrate in the calcification of coral reefs. *Limnol. Oceanogr.* 66, 1793–1803. doi: 10.1002/lno.11722

De Vantier, L., and Turak, E. (2017). Species richness and relative abundance of reef-building corals in the indo-west pacific. *Diversity* 9 (3). doi: 10.3390/d9030025

Dickson, A. G. (1990). Thermodynamics of the dissociation of boric acid in potassium chloride solutions from 273.15 to 318.15 K. *J. Chem. Eng. Data* 35, 253–257. doi: 10.1021/je00061a009

Dickson, A. G. (2007). *Guide to best practices for ocean CO2 measurements.* Eds. A. G. Dickson, C. L. Sabine and J. R. Christian (Sidney, BC: North Pacific Marine Science Organization).

Dickson, A. G., and Millero, F. J. (1987). A comparison of the equilibrium constants for the dissociation of carbonic acid in seawater media. *Deep Sea Res. Part A Oceanogr. Res. Pap.* 34, 1733–1743. doi: 10.1016/0198-0149(87)90021-5

Doney, S. C., Fabry, V. J., Feely, R. A., and Kleypas, J. A. (2009). Ocean acidification: The other CO_2 problem. *Ann. Rev. Mar. Sci.* 1, 169–192. doi: 10.1146/annurev.marine.010908.163834

Duarte, C. M., Hendriks, I. E., Moore, T. S., Olsen, Y. S., Steckbauer, A., Ramajo, L., et al. (2013). Is ocean acidification an open-ocean syndrome? understanding anthropogenic impacts on seawater pH. *Estuaries Coasts* 36, 221–236. doi: 10.1007/s12237-013-9594-3

Enochs, I. C., Formel, N., Shea, L., Chomiak, L., Piggot, A., Kirkland, A., et al. (2020). Subsurface automated samplers (SAS) for ocean acidification research. *Bull. Mar. Sci.* 96, 735–752. doi: 10.5343/BMS.2020.0018

Enochs, I. C., Manzello, D. P., Donham, E. M., Kolodziej, G., Okano, R., Johnston, L., et al. (2015). Shift from coral to macroalgae dominance on a volcanically acidified reef. *Nat. Clim. Change* 5, 1083–1088. doi: 10.1038/nclimate2758

Enochs, I. C., Manzello, D. P., Kolodziej, G., Noonan, S. H. C., Valentino, L., and Fabricius, K. E. (2016). Enhanced macroboring and depressed calcification drive net dissolution at high-CO_2 coral reefs. *Proc. R. Soc B Biol. Sci.* 283, 1-8. doi: 10.1098/rspb.2016.1742

Erez, J., Reynaud, S., Silverman, J., Schneider, K., and Allemand, D. (2011). "Coral calcification under ocean acidification and global change," in *Coral reefs: An ecosystem in transition.* Eds. Z. Dubinsky and N. Stambler (London: Springer), 151–177.

Escobar, M. T. L., Sotto, L. P. A., Jacinto, G. S., Benico, G. A., San Diego-McGlone, M. L., and Azanza, R. V. (2013). Eutrophic conditions during the 2010 fish kill in Bolinao and Anda, Pangasinan, Philippines. *J. Environ. Sci. Manage.* 16 (Special Issue 1-2013), 29–35.

Eyre, B. D., Cyronak, T., Drupp, P., De Carlo, E. H., Sachs, J. P., Andersson, A. J., et al. (2018). Coral reefs will transition to net dissolving before end of century. *Science* 359, 908–911. doi: 10.1126/science.aao1118

Fabricius, K. E. (2005). Effects of terrestrial runoff on the ecology of corals and coral reefs: review and synthesis. *Mar. pollut. Bull.* 50, 125–146. doi: 10.1016/j.marpolbul.2004.11.028

Falter, J. L., Lowe, R. J., Zhang, Z., and McCulloch, M. (2013). Physical and biological controls on the carbonate chemistry of coral reef waters: Effects of metabolism, wave forcing, sea level, and geomorphology. *PloS One* 8, e53303. doi: 10.1371/journal.pone.0053303

Fennel, K., and Testa, J. M. (2019). Biogeochemical controls on coastal hypoxia. *Ann. Rev. Mar. Sci.* 11, 105–130. doi: 10.1146/annurev-marine-010318-095138

Ferrera, C. M., Watanabe, A., Miyajima, T., San Diego-McGlone, M. L., Morimoto, N., Umezawa, Y., et al. (2016). Phosphorus as a driver of nitrogen limitation and sustained eutrophic conditions in Bolinao and Anda, Philippines, a mariculture-impacted tropical coastal area. *Mar. pollut. Bull.* 105, 237–248. doi: 10.1016/j.marpolbul.2016.02.025

Fortes, M. D., Go, G., Bolisay, K., Nakaoka, M., Uy, W., Lopez, M., et al. (2012). "Seagrass response to mariculture-induced physico-chemical gradients in bolinao, northwestern Philippines," in *Proceedings 12th Int. Coral Reef Symp* (Cairns, Australia). 9–13. Available at: http://www.icrs2012.com/proceedings/manuscripts/ICRS2012_15B_3.pdf.

Friedlingstein, P., O'Sullivan, M., Jones, M. W., Andrew, R. M., Hauck, J., Olsen, A., et al. (2020). Global carbon budget 2021. *Earth Syst. Sci. Data* 12, 3269–3340. doi: 10.5194/essd-14-1917-2022

Friis, K., Körtzinger, A., and Wallace, D. W. R. (2003). The salinity normalization of marine inorganic carbon chemistry data. *Geophys. Res. Lett.* 30, 1–4. doi: 10.1029/2002GL015898

Garren, M., Raymundo, L., Guest, J., Harvell, C. D., and Azam, F. (2009). Resilience of coral-associated bacterial communities exposed to fish farm effluent. *PloS One* 4, 1-9. doi: 10.1371/journal.pone.0007319

Gattuso, J.-P., Allemand, D., and Frankignoulle, M. (1999). Photosynthesis and calcification at cellular, organismal and community levels in coral reefs: A review on interactions and control by carbonate chemistry. *Am. Zool.* 39, 160–183. doi: 10.1093/icb/39.1.160

Geček, S., and Legović, T. (2010). Towards carrying capacity assessment for aquaculture in the Bolinao Bay, Philippines: A numerical study of tidal circulation. *Ecol. Modell.* 221, 1394–1412. doi: 10.1016/j.ecolmodel.2010.02.005

Gomez, E., Aliño, P., Yap, H., and Licuanan, W. (1994). A review of the status of philippine reefs. *Mar. pollut. Bull.* 29 (1-3), 62–68. doi: 10.1016/0025-326X(94)90427-8

Gutiérrez, J. L., Jones, C. G., Byers, J. E., Arkema, K. K., Berkenbusch, K., Commito, A., et al. (2011). "Physical ecosystem engineers and the functioning of estuaries and coasts," in *Treatise on estuarine and coastal science* (UK: Elsevier Inc), 53–81. doi: 10.1016/B978-0-12-374711-2.00705-1

Harvell, C. D., Kim, K., Burkholder, J. M., Colwell, R. R., Epstein, P. R., Grimes, D. J., et al. (1999). Emerging marine diseases-climate links and anthropogenic factors. *Science* 285, 1505–1510. doi: 10.1126/science.285.5433.1505

Hoegh-Guldberg, O., Mumby, P. J., Hooten, A. J., Steneck, R. S., Greenfield, P., Gomez, E., et al. (2007). Coral reefs under rapid climate change and ocean acidification. *Science* 318, 1737–1742. doi: 10.1126/science.1152509

Ho, D. T., Ferrón, S., Engel, V. C., Anderson, W. T., Swart, P. K., Price, R. M., et al. (2017). Dissolved carbon biogeochemistry and export in mangrove-dominated rivers of the Florida Everglades. *Biogeosciences* 14, 2543–2559. doi: 10.5194/bg-14-2543-2017

Holmer, M. (2010). Environmental issues of fish farming in offshore waters: Perspectives, concerns and research needs. *Aquac. Environ. Interact.* 1, 57–70. doi: 10.3354/aei00007

Holmer, M., Duarte, C. M., Heilskov, A., Olesen, B., and Terrados, J. (2003). Biogeochemical conditions in sediments enriched by organic matter from net-pen fish farms in the bolinao area, Philippines. *Mar. pollut. Bull.* 46, 1470–1479. doi: 10.1016/S0025-326X(03)00281-9

Holmer, M., Marbá, N., Terrados, J., Duarte, C. M., and Fortes, M. D. (2002). Impacts of milkfish (*Chanos chanos*) aquaculture on carbon and nutrient fluxes in the Bolinao area, Philippines. *Mar. pollut. Bull.* 44, 685–696. doi: 10.1016/S0025-326X(02)00048-6

Hughes, T. P., Rodrigues, M. J., Bellwood, D. R., Ceccarelli, D., Hoegh-Guldberg, O., McCook, L., et al. (2007). Phase shifts, herbivory, and the resilience of coral reefs to climate change. *Curr. Biol.* 17, 360–365. doi: 10.1016/j.cub.2006.12.049

Johnson, M. D., Price, N. N., and Smith, J. E. (2014). Contrasting effects of ocean acidification on tropical fleshy and calcareous algae. *PeerJ* 2014, 1–28. doi: 10.7717/peerj.411

Jones, M. N. (1984). Nitrate reduction by shaking with cadmium: Alternative to cadmium columns. *Water Res.* 18, 643–646. doi: 10.1016/0043-1354(84)90215-X

Kaczmarsky, L., and Richardson, L. L. (2011). Do elevated nutrients and organic carbon on Philippine reefs increase the prevalence of coral disease? *Coral Reefs* 30, 253–257. doi: 10.1007/s00338-010-0686-2

Kawahata, H., Yukino, I., and Suzuki, A. (2000). Terrestrial influences on the Shiraho fringing reef, Ishigaki Island, Japan: High carbon input relative to phosphate. *Coral Reefs* 19, 172–178. doi: 10.1007/s003380000093

Kemp, W. M., Sampou, P., Caffrey, J., Mayer, M., Henriksen, K., and Boynton, W. R. (1990). Ammonium recycling versus denitrification in Chesapeake Bay sediments. *Limnol. Oceanogr.* 35, 1545–1563. doi: 10.4319/lo.1990.35.7.1545

Kim, H. C., and Lee, K. (2009). Significant contribution of dissolved organic matter to seawater alkalinity. *Geophys. Res. Lett.* 36, 1–5. doi: 10.1029/2009GL040271

Kleypas, J. A., Anthony, K. R. N., and Gattuso, J. P. (2011). Coral reefs modify their seawater carbon chemistry - case study from a barrier reef (Moorea, French Polynesia). *Glob. Change Biol.* 17, 3667–3678. doi: 10.1111/j.1365-2486.2011.02530.x

Koch, M., Bowes, G., Ross, C., and Zhang, X. H. (2013). Climate change and ocean acidification effects on seagrasses and marine macroalgae. *Glob. Change Biol.* 19, 103–132. doi: 10.1111/j.1365-2486.2012.02791.x

Kohler, K. E., and Gill, S. M. (2006). CCoral Point Count with Excel extensions (CPCe): A Visual Basic program for the determination of coral and substrate coverage using random point count methodology. *Comput. Geosci.* 32, 1259–1269. doi: 10.1016/j.cageo.2005.11.009

Koweek, D., Dunbar, R. B., Rogers, J. S., Williams, G. J., Price, N., Mucciarone, D., et al. (2014). Environmental and ecological controls of coral community metabolism on Palmyra Atoll. *Coral Reefs* 34, 339–351. doi: 10.1007/s00338-014-1217-3

Kroeker, K. J., Kordas, R. L., Crim, R. N., and Singh, G. G. (2010). Meta-analysis reveals negative yet variable effects of ocean acidification on marine organisms. *Ecol. Lett.* 13, 1419–1434. doi: 10.1111/j.1461-0248.2010.01518.x

Kuliński, K., Schneider, B., Hammer, K., Machulik, U., and Schulz-Bull, D. (2014). The influence of dissolved organic matter on the acid-base system of the Baltic Sea. *J. Mar. Syst.* 132, 106–115. doi: 10.1016/j.jmarsys.2014.01.011

Lalas, J. A. A., Benayahu, Y., and Baria-Rodriguez, M. V. (2020). Community structure and size-frequency distribution of soft corals in a heavily disturbed reef system in northwestern Philippines. *Mar. pollut. Bull.* 162, 111871. doi: 10.1016/j.marpolbul.2020.111871

Lantz, C. A., Carpenter, R. C., Comeau, S., and Edmunds, P. J. (2017). Organisms composing an experimental coral reef community from Mo'orea, French Polynesia, exhibit taxon-specific net production: Net calcification ratios. *Front. Mar. Sci.* 4. doi: 10.3389/fmars.2017.00298

Lewis, E., and Wallace, D. W. R. (1998). "Program developed for CO_2 system calculations," in *Carbon dioxide information analysis center* (Oak Ridge, TN: Oak Ridge National Laboratory, U.S. Department of Energy).

Licuanan, W. Y., Robles, R., and Reyes, M. (2019). Status and recent trends in coral reefs of the Philippines. *Mar. pollut. Bull.* 142, 544–550. doi: 10.1016/j.marpolbul.2019.04.013

Lukawska-Matuszewska, K., Grzybowski, W., Szewczun, A., and Tarasiewicz, P. (2018). Constituents of organic alkalinity in pore water of marine sediments. *Mar. Chem.* 200, 22–32. doi: 10.1016/j.marchem.2018.01.012

McMahon, A., Santos, I. R., Cyronak, T., and Eyre, B. D. (2013). Hysteresis between coral reef calcification and the seawater aragonite saturation state. *Geophys Res. Lett.* 40, 4675–4679. doi: 10.1002/GRL.50802

McManus, J. W., Nañola, C. L., Reyes, R. B., and Kesner, K. N. (1992) *Resource ecology of the bolinao coral reef system*. Manila: International Center for Living Aquatic Resources Management. Available at: http://pubs.iclarm.net/libinfo/Pdf/PubSR7622.pdf.

Mehrbach, C., Culberson, C. H., Hawley, J. E., and Pytkowicx, R. M. (1973). Measurement of the apparent dissociation constants of carbonic acid in seawater at atmospheric pressure. *Limnol. Oceanogr.* 18, 897–907. doi: 10.4319/lo.1973.18.6.0897

Nañola, C. J. L. (2002). "Bolinao," in *Atlas of Philippine coral reefs*. Eds. P. M. Aliño, E. F. B. Miclat, C. J. L. Nañola, H. A. Roa-Quiaoit and R. T. Campos (Quezon City: Goodwill Trading Co), 31–34.

Nañola, C. L., Aliño, P. M., and Carpenter, K. E. (2011). Exploitation-related reef fish species richness depletion in the epicenter of marine biodiversity. *Environ. Biol. Fishes* 90, 405–420. doi: 10.1007/s10641-010-9750-6

Noonan, S. H. C., Kluibenschedl, A., and Fabricius, K. E. (2018). Ocean acidification alters early successional coral reef communities and their rates of community metabolism. *PloS One* 13, e0197130. doi: 10.1371/journal.pone.0197130

Orr, J. C., Fabry, V. J., Aumont, O., Bopp, L., Doney, S. C., Feely, R. A., et al. (2005). Anthropogenic ocean acidification over the twenty-first century and its impact on calcifying organisms. *Nature* 437, 681–686. doi: 10.1038/nature04095

PAGASA (2021) *Climate of the Philippines*. Available at: https://www.pagasa.dost.gov.ph/information/climate-philippines.

Page, H. N., Andersson, A. J., Jokiel, P. L., Rodgers, K. S., Lebrato, M., Yeakel, K., et al. (2016). Differential modification of seawater carbonate chemistry by major coral reef benthic communities. *Coral Reefs* 35, 1311–1325. doi: 10.1007/s00338-016-1490-4

Page, H. N., Courtney, T. A., Collins, A., De Carlo, E. H., and Andersson, A. J. (2017). Net community metabolism and seawater carbonate chemistry scale non-intuitively with coral cover. *Front. Mar. Sci.* 4. doi: 10.3389/fmars.2017.00161

Page, H. N., Courtney, T. A., De Carlo, E. H., Howins, N. M., Koester, I., and Andersson, A. J. (2018). Spatiotemporal variability in seawater carbon chemistry for a coral reef flat in kāne'ohe Bay, hawai'i. *Limnol. Oceanogr.* 9999, 1–22. doi: 10.1002/lno.11084

Panga, F. M., Anticamara, J. A., Quibilan, M. C. C., Atrigenio, M. P., and Aliño, P. M. (2021). Through the boundaries: Environmental factors affecting reef benthic cover in marine protected areas in the Philippines. *Front. Mar. Sci.* 8. doi: 10.3389/fmars.2021.702071

Parsons, T. R., Maita, Y., and Lalli, C. M. (1984). *A manual of chemical and biological methods for seawater analysis*. doi: 10.1016/B978-0-08-030287-4.50004-9

Prouty, N. G., Cohen, A., Yates, K. K., Storlazzi, C. D., Swarzenski, P. W., and White, D. (2017). Vulnerability of coral reefs to bioerosion from land-based sources of pollution. *J. Geophys. Res. Ocean.* 122, 9319–9331. doi: 10.1002/2017JC013264

Qian, W., Gan, J., Liu, J., He, B., Lu, Z., Guo, X., et al. (2018). Current status of emerging hypoxia in a eutrophic estuary: The lower reach of the Pearl River Estuary, China. *Estuar. Coast. Shelf Sci.* 205, 58–67. doi: 10.1016/j.ecss.2018.03.004

Quimpo, T. J. R., Ligson, C. A., Manogan, D. P., Requilme, J. N. C., Albelda, R. L., Conaco, C., et al. (2020). Fish farm effluents alter reef benthic assemblages and reduce coral settlement. *Mar. pollut. Bull.* 153, 111025. doi: 10.1016/j.marpolbul.2020.111025

Raymundo, L. J., Halford, A. R., Maypa, A. P., and Kerr, A. M. (2009). Functionally diverse reef-fish communities ameliorate coral disease. *Proc. Natl. Acad. Sci.* 106, 17067–17070. doi: 10.1073/pnas.0900365106

R Core Team (2021) *R: A language and environment for statistical computing*. (Vienna, Austria). Available at: http://www.r-project.org/.

Rivera, P. C. (1997). *ydrodynamics, Sediment Transport and Light Extinction Off Cape Bolinao, Philippines (1st ed.)* (Boca Raton: CRC Press). doi: 10.1201/9781003073161

San Diego-McGlone, M. L., Azanza, R. V., Villanoy, C. L., and Jacinto, G. S. (2008). Eutrophic waters, algal bloom and fish kill in fish farming areas in Bolinao, Pangasinan, Philippines. *Mar. pollut. Bull.* 57, 295–301. doi: 10.1016/j.marpolbul.2008.03.028

Schönberg, C. H. L., Fang, J. K. H., Carreiro-Silva, M., Tribollet, A., and Wisshak, M. (2017). Bioerosion: The other ocean acidification problem. *ICES J. Mar. Sci.* 74, 895–925. doi: 10.1093/icesjms/fsw254

Schubert, N., Alvarez-Filip, L., and Hofmann, L. C. (2022). Systematic review and meta-analysis of ocean acidification effects in Halimeda: Implications for algal carbonate production. *Climate Change Ecol.* 4, 100059. doi: 10.1016/J.ECOCHG.2022.100059

Silbiger, N. J., Nelson, C. E., Remple, K., Sevilla, J. K., Quinlan, Z. A., Putnam, H. M., et al. (2018). Nutrient pollution disrupts key ecosystem functions on coral reefs. *Proc. R. Soc B Biol. Sci.* 285, 2–10. doi: 10.1098/rspb.2017.2718

Silverman, J., Lazar, B., Cao, L., Caldeira, K., and Erez, J. (2009). Coral reefs may start dissolving when atmospheric CO_2 doubles. *Geophys. Res. Lett.* 36, 1–5. doi: 10.1029/2008GL036282

Silverman, J., Lazar, B., and Erez, J. (2007). Community metabolism of a coral reef exposed to naturally varying dissolved inorganic nutrient loads. *Biogeochemistry* 84, 67–82. doi: 10.1007/s10533-007-9075-5

Slomp, C. P., and Van Cappellen, P. (2007). The global marine phosphorus cycle: Sensitivity to oceanic circulation. *Biogeosciences* 4, 155–171. doi: 10.5194/bg-4-155-2007

Sokal, R. R., and Rohlf, F. J. (1995). *Biometry: The principles and practices of statistics in biological research. 3rd ed* (New York: W. H. Freeman).

Sutton, A., and Newton, J. (2020). Reaching consensus on assessments of ocean acidification trends. *Eos (Washington DC)* 101. doi: 10.1029/2020EO150944

Suzuki, A., and Kawahata, H. (2003). Carbon budget of coral reef systems: an overview of observations in fringing reefs, barrier reefs and atolls in the indo-pacific regions. *Tellus B* 55, 428–444. doi: 10.3402/tellusb.v55i2.16761

Takeshita, Y., Cyronak, T., Martz, T. R., Kindeberg, T., and Andersson, A. J. (2018). Coral reef carbonate chemistry variability at different functional scales. *Front. Mar. Sci.* 5. doi: 10.3389/fmars.2018.00175

Tamayo, N. C. A., Anticamara, J. A., and Acosta-Michlik, L. (2018). National estimates of values of Philippine reefs' ecosystem services. *Ecol. Econ.* 146, 633–644. doi: 10.1016/j.ecolecon.2017.12.005

Tanaka, Y., Go, G. A., Watanabe, A., Miyajima, T., Nakaoka, M., Uy, W. H., et al. (2014). 17-year change in species composition of mixed seagrass beds around Santiago Island, Bolinao, the northwestern Philippines. *Mar. pollut. Bull.* 88, 81–85. doi: 10.1016/j.marpolbul.2014.09.024

Testa, J. M., and Kemp, W. M. (2014). Spatial and temporal patterns of winter–spring oxygen depletion in Chesapeake Bay bottom water. *Estuaries Coasts* 37, 1432–1448. doi: 10.1007/s12237-014-9775-8

Torres, O., Kwiatkowski, L., Sutton, A. J., Dorey, N., and Orr, J. C. (2021). Characterizing mean and extreme diurnal variability of ocean CO_2 system variables across marine environments. *Geophys. Res. Lett.* 48, 1–12. doi: 10.1029/2020GL090228

Turk, D., Yates, K. K., Vega-Rodriguez, M., Toro-Farmer, G., L'Esperance, C., Melo, N., et al. (2015). Community metabolism in shallow coral reef and seagrass ecosystems, lower Florida keys. *Mar. Ecol. Prog. Ser.* 538, 35–52. doi: 10.3354/meps11385

Uppström, L. R. (1974). The boron/chlorinity ratio of deep-sea water from the Pacific Ocean. *Deep. Res. Oceanogr. Abstr.* 21, 161–162. doi: 10.1016/0011-7471(74)90074-6

van Woesik, R., Gilner, J., and Hooten, A. J. (2009). *Standard Operating Procedures for Repeated Measures of Process and State Variables of Coral Reef Environments* (The University of Queensland, Melbourne: Coral Reef Targeted Research and Capacity Building for Management Program), 34.

Verceles, L. F., McManus, L. T., and Aliño, P. M. (2000). Participatory monitoring and feedback system: An important entry towards sustainable aquaculture in Bolinao, northern Philippines. *Sci. Diliman* 12, 78–87. Availabe at: https://journals.upd.edu.ph/index.php/sciencediliman/article/view/222

Villanueva, R. D., Yap, H. T., and Montaño, M. N. E. (2005). Survivorship of coral juveniles in a fish farm environment. *Mar. pollut. Bull.* 51, 580–589. doi: 10.1016/j.marpolbul.2005.04.033

Villanueva, R. D., Yap, H. T., and Montaño, M. N. E. (2006). Intensive fish farming in the Philippines is detrimental to the reef-building coral Pocillopora damicornis. *Mar. Ecol. Prog. Ser.* 316, 165–174. doi: 10.3354/meps316165

Vogel, N., Fabricius, K. E., Strahl, J., Noonan, S. H. C., Wild, C., and Uthicke, S. (2015). Calcareous green alga Halimeda tolerates ocean acidification conditions at tropical carbon dioxide seeps. *Limnol Oceanogr* 60, 263–275. doi: 10.1002/LNO.10021

Wang, Y., and Van Cappellen, P. (1996). A multicomponent reactive transport model of early diagenesis: Application to redox cycling in coastal marine sediments. *Geochim. Cosmochim. Acta* 60, 2993–3014. doi: 10.1016/0016-7037(96)00140-8

Watai, M., Nakamura, Y., Honda, K., Bolisay, K. O., Miyajima, T., Nakaoka, M., et al. (2014). Diet, growth, and abundance of two seagrass bed fishes along a pollution gradient caused by milkfish farming in Bolinao, northwestern Philippines. *Fish. Sci.* 81, 43–51. doi: 10.1007/s12562-014-0824-9

White, P. (2013). "Environmental consequences of poor feed quality and feed management," in *On-farm feeding and feed management in aquaculture*. Eds. M. R. Hasan and M. B. New (Rome: FAO), 553–564.

Winder, M., and Sommer, U. (2012). Phytoplankton response to a changing climate. *Hydrobiologia* 698, 5–16. doi: 10.1007/s10750-012-1149-2

Wu, R. S. S. (1995). The environmental impact of marine fish culture: Towards a sustainable future. *Mar. pollut. Bull.* 31, 159–166. doi: 10.1016/0025-326X(95)00100-2

Yoshikai, M., Herrera, E. C., Tsuchiya, T., Watanabe, A., Blanco, A. C., and Nadaoka, K. (2016). Numerical modeling analysis of tidal circulation and water quality dynamics in an intensive mariculture area in Bolinao and Anda, Philippines. *Prep.*

Yoshikai, M., Nakamura, T., Tanaka, Y., Nakaoka, M., Watanabe, A., Herrera, E. C., et al. (2021). Modeling seagrass bed dynamics under environmental impacts of intensive mariculture activities in bolinao and anda, the Philippines. *Estuar. Coast. Shelf Sci.* 250, 107152. doi: 10.1016/j.ecss.2020.107152

Frontiers in
Marine Science

Explores ocean-based solutions for emerging global challenges

The third most-cited marine and freshwater biology journal, advancing our understanding of marine systems and addressing global challenges including overfishing, pollution, and climate change.

Discover the latest Research Topics

See more →

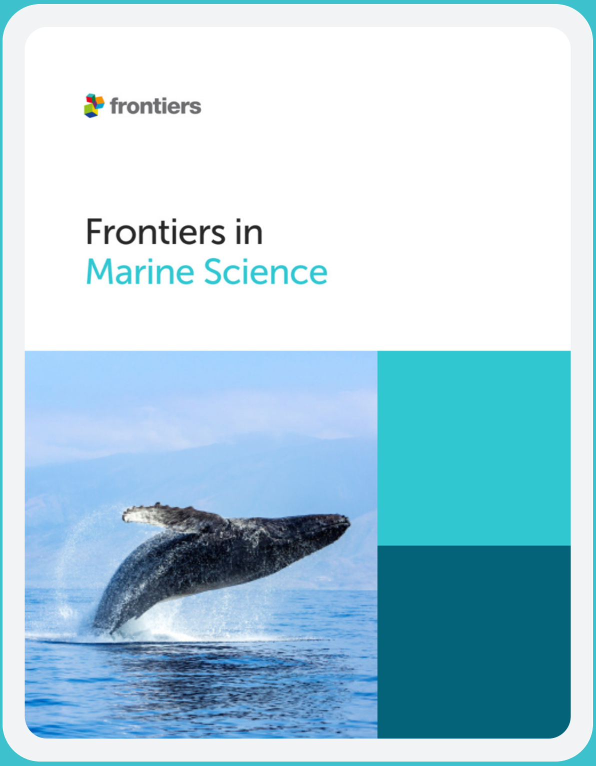

frontiers

Frontiers in
Marine Science

Frontiers

Avenue du Tribunal-Fédéral 34
1005 Lausanne, Switzerland
frontiersin.org

Contact us

+41 (0)21 510 17 00
frontiersin.org/about/contact